



Fisheries and Oceans
Canada

Pêches et Océans
Canada

Ecosystems and
Oceans Science

Sciences des écosystèmes
et des océans

Canadian Science Advisory Secretariat (CSAS)

Research Document 2025/021

Newfoundland and Labrador Region

Results of Comparative Fishing Between the CCGS *Teleost* and CCGS *Alfred Needler* with the CCGS *John Cabot* and CCGS *Capt. Jacques Cartier* in the Newfoundland and Labrador Region in 2021 and 2022

Trueman, S.¹, Wheeland, L.¹, Benoît, H.², Munro, H.¹, Nguyen, T.¹, Novaczek, E.¹, Skanes, K.¹, and Yin, Y.³

¹ Fisheries and Oceans Canada
Newfoundland and Labrador Region
PO Box 5667
St. John's, NL A1C 5X1

² Fisheries and Oceans Canada
Maurice Lamontagne Institute
Mont Joli, QC G5H 3Z4

³ Fisheries and Oceans Canada
Bedford Institute of Oceanography
Dartmouth, NS B2Y 4A2

Foreword

This series documents the scientific basis for the evaluation of aquatic resources and ecosystems in Canada. As such, it addresses the issues of the day in the time frames required and the documents it contains are not intended as definitive statements on the subjects addressed but rather as progress reports on ongoing investigations.

Published by:

Fisheries and Oceans Canada
Canadian Science Advisory Secretariat
200 Kent Street
Ottawa ON K1A 0E6

<http://www.dfo-mpo.gc.ca/csas-sccs/>
DFO.CSAS-SCAS.MPO@dfo-mpo.gc.ca



© His Majesty the King in Right of Canada, as represented by the Minister of the Department of Fisheries and Oceans, 2025

This report is published under the [Open Government Licence - Canada](#)

ISSN 1919-5044

ISBN 978-0-660-76391-0 Cat. No. Fs70-5/2025-021E-PDF

Correct citation for this publication:

Trueman, S., Wheeland, L., Benoît, H., Munro, H., Nguyen, T., Novaczek, E., Skanes, K., and Yin, Y. 2025. Results of Comparative Fishing Between the CCGS *Teleost* and CCGS *Alfred Needler* with the CCGS *John Cabot* and CCGS *Capt. Jacques Cartier* in the Newfoundland and Labrador Region in 2021 and 2022. DFO Can. Sci. Advis. Sec. Res. Doc. 2025/021. v + 237 p.

Aussi disponible en français :

Trueman, S., Wheeland, L., Benoît, H., Munro, H., Nguyen, T., Novaczek, E., Skanes, K. et Yin, Y. 2025. Résultats de la pêche comparative du NGCC *Teleost* et du NGCC *Alfred Needler* par rapport au NGCC *John Cabot* et au NGCC *Capt Jacques Cartier* dans la région de Terre-Neuve-et-Labrador en 2021 et 2022. Secr. can. des avis sci. du MPO. Doc. de rech. 2025/021. v + 241 p.

TABLE OF CONTENTS

ABSTRACT.....	v
1. INTRODUCTION	1
2. METHODS.....	1
2.1. COMPARATIVE FISHING PROGRAM.....	1
2.1.1. Gear Performance and Geometry.....	2
2.2. COMPARATIVE FISHING DATA ANALYSIS	3
2.2.1. Binomial Models	4
2.2.2. Beta-binomial Models	6
2.2.3. Tweedie Model for Biomass Data	7
2.2.4. Model Fitting, Selection and Validation	8
2.2.5. Interpretation of Analysis Results and Application of Conversion Factors	10
2.2.6. Biological Community Analysis	11
2.2.7. Habitat and Environmental Comparisons.....	12
3. SPATIAL CONSIDERATIONS	13
3.1. SEABED REPRESENTATION OF THE PAIRED SETS	13
3.2. AREA-VESSEL GROUPINGS FOR CONVERSION FACTOR ESTIMATION.....	14
4. RESULTS AND DISCUSSION.....	16
4.1. PRESENTATION OF CONVERSION FACTORS	16
4.1.1. Fall Conversions – CCGS <i>Teleost</i> (Div. 2HJ3KL).....	17
4.1.2. Spring Conversions – CCGS <i>Alfred Needler</i> (Div. 3Ps)	19
4.1.3. Spring Conversions – CCGS <i>Alfred Needler</i> (Div. 3LNO).....	19
4.1.4. Fall Conversions – CCGS <i>Alfred Needler</i> (For Use in Div. 3KL)	20
4.1.5. Fall Conversions – CCGS <i>Alfred Needler</i> (Grand Bank Stocks, 3LNO).....	22
4.1.6. Special Case – Yellowtail Flounder	22
4.2. DIVERSITY AND COMMUNITY COMPOSITION	22
4.3. BENTHIC HABITAT VARIABLES	24
5. CONCLUSIONS.....	24
6. ACKNOWLEDGEMENTS	25
7. REFERENCES CITED	25
8. FIGURES.....	28
9. TABLES	44
APPENDIX 1: LENGTH-BASED CONVERSIONS	56
FIGURES	56
TABLES	130
APPENDIX 2: SIZE AGGREGATED CONVERSIONS	140
FIGURES	140

APPENDIX 3: DIVERSITY, COMMUNITY COMPOSITION, AND BENTHIC HABITAT IN COMPARATIVE SETS.....	226
FIGURES	226

ABSTRACT

Multispecies bottom trawl surveys have been conducted annually in the spring and fall in the Newfoundland and Labrador Region using a Campelen 1800 survey trawl aboard the Canadian Coast Guard Ship (CCGS) *Teleost* and CCGS *Alfred Needler* since 1995. These surveys are used to estimate the distribution and abundance of many fish and invertebrate species, to determine species life history characteristics, and form the basis of a number of ecosystem indicators. The CCGS *Alfred Needler* and CCGS *Teleost* will no longer be used for these surveys after 2022 and 2023, respectively, and will be replaced by the CCGS *John Cabot* and CCGS Capt. *Jacques Cartier*. The Campelen 1800 survey trawl will continue to be used, with a few modifications. Comparative fishing has been ongoing since 2021 to determine differences in relative catchability between the outgoing vessels and the new vessels with the modified Campelen trawl. Data collected were sufficient to estimate conversion factors for the fall CCGS *Teleost* series, and for a portion of taxa within the fall CCGS *Alfred Needler* series. There were insufficient data to determine conversion factors for the spring CCGS *Alfred Needler* series, though a special case was made for Yellowtail Flounder (*Myxopsetta ferruginea*) where fall and spring data were combined to determine a conversion, given the species limited distribution across both seasons. Overall, for the CCGS *Teleost* fall time series, conversion factors were accepted for 14 taxa, with two species having a significant length effect, 18 taxa had no significant difference in catchability, and 9 taxa were deemed to have insufficient data to accurately determine a conversion. For the CCGS *Alfred Needler* fall time series, conversion factors were accepted for 15 taxa, including 6 taxa with a significant length effect, 17 taxa had no difference in catchability, and 12 were deemed to have insufficient data to accurately determine a conversion. Comparative fishing work will continue during 2023 to fill identified data gaps from the 2021–22 data set, including deep water (>1,000 m) and shallow water sets (<150 m).

1. INTRODUCTION

The Newfoundland and Labrador (NL) fall Multi-Species Survey (MSS) covers Northwest Atlantic Fisheries Organization (NAFO) Divisions (Div.) 2HJ3KLNO (Figure 2), extending from the Labrador Shelf in the North to the Grand Bank in the South. Data from these surveys are used to inform stock assessment and fisheries management, ecosystem assessments, species at risk, marine conservation monitoring, and a variety of research programs. These surveys have been completed with the Canadian Coast Guard Ship (CCGS) *Teleost* (Div. 2HJ3K + 3L strata ≥ 750 m) and CCGS *Alfred Needler* (Div. 3KLNO) (hereafter, the “*Teleost*” [TEL] and “*Needler*” [AN]) since the mid-1990s. The spring multispecies survey covers NAFO Div. 3LNOP and has been completed primarily with the *Needler* since the mid-1990s. The *Teleost* has been used in some divisions in some years when the *Needler* was unavailable to conduct the spring survey.

The *Teleost* and *Needler* are now being replaced with the CCGS Capt. *Jacques Cartier* and the CCGS *John Cabot* (hereafter, the “*Cartier* [CAR]” and “*Cabot* [CAB],” or collectively “CAX”). Comparative fishing was undertaken in order to ensure that data collected from these new vessels is comparable to that from the old vessels and can be used to extend existing data time series. This involves fishing old and new vessels side by side to quantify differences in catch size and composition (by species, size, etc.) and determine difference in relative fishing efficiency (also referred to as catchability) between the old and new vessels.

2. METHODS

2.1. COMPARATIVE FISHING PROGRAM

Comparative fishing occurred in the fall of 2021 (*Teleost* to *Cartier*; Figure 3), spring of 2022 (*Needler* to *Cabot*; Figure 4), and fall of 2022 (*Teleost* to *Cabot* and *Cartier*, *Needler* to *Cabot*; Figure 5). Full details of the comparative program are described in Wheeland et al. (2024) and a summary of successful tows by NAFO Divisions is provided in Table 1. In the fall of 2021 and the spring of 2022, comparative fishing was undertaken as a shadow survey, where regular survey stations were chosen according to the survey stratified random design, with locations within the survey determined by vessel availability. In the fall of 2022, a targeted program was designed. Stations were still chosen within normal survey strata following the same random set selection, but the number and distribution of strata was limited, and the number of sets within a stratum was adjusted to distribute set allocations across depth more consistently.

At each station, the vessels within a pair fished as close together in space and in time as operationally feasible. Most sets were done side by side, with vessels instructed to tow at the same time, 0.5 nautical miles (nM) apart, and complete parallel tows. If the amount of fishable bottom was limited (e.g., steep slope), then one of two alternative approaches was conducted:

1. vessels could complete a “single file/follow the leader” tow type, where both vessels tow at the same time with the trawl path of the rear vessel not overlapping that of the vessel in front; or
2. if both a side by side or single file tow could not be completed safely then a “one then the other” tow was done where one vessel completed its tow first, and the second vessel would immediately fish along the same ground, attempting to avoid the exact line of the previous vessel.

Distance between tows within a pair ranged from 0 to 1.9 nM, but was 0.59 ± 0.02 nM on average, with distance greater for single file tows than other pair types. Depth difference within a pair averaged 4.62 ± 0.32 (0–36 m range) (Wheeland et al. 2024).

Both vessels in any given pair fished standard tows targeting a tow time of 15 minutes at 3.0 knots following the standard tow protocol for the NL MSS. Tow durations of at least 10 minutes and up to 20 minutes were considered acceptable. Tow time was measured from the time the trawl was on bottom to the time it lifted off bottom, with trawl performance and geometry measured with SCANMAR sensors. The *Cabot* and *Cartier* are sister vessels and results from the present analysis indicate consistent fishing of the two vessels (see Section 2.1.1 and Appendix 4 for details). When included in conversion factor analysis collectively as “CAX”, there is no evidence to support a difference between the two vessels for any species assessed. Thus, the data from both vessels has been pooled together, and the vessels are considered to have equal catchability going forward.

Table 1. Summary of successful paired sets per vessel pair, year, and season, where AN represents the CCGS Alfred Needler, CAB represents the CCGS John Cabot, CAR represents the CCGS Capt. Jacques Cartier, and TEL represents the CCGS Teleost.

Vessel Pair	Year	Season	NAFO Div.	No. Paired Tows
TEL:CAR	2021	Fall	2H	14
TEL:CAR	2021	Fall	2J	18
TEL:CAR	2021	Fall	3K	8
TEL:CAR	2021	Fall	Total	40
AN:CAB	2022	Spring	3N	12
AN:CAB	2022	Spring	3P	25
AN:CAB	2022	Spring	Total	37
AN:CAB	2022	Fall	3K	71
AN:CAB	2022	Fall	3L	2
AN:CAB	2022	Fall	3N	17
AN:CAB	2022	Fall	3O	10
AN:CAB	2022	Fall	Total	100
TEL:CAR	2022	Fall	2H	20
TEL:CAR	2022	Fall	2J	38
TEL:CAR	2022	Fall	3K	82
TEL:CAR	2022	Fall	Total	140
TEL:CAB	2022	Fall	2J	5
TEL:CAB	2022	Fall	3K	8
TEL:CAB	2022	Fall	3L	4
TEL:CAB	2022	Fall	Total	17

2.1.1. Gear Performance and Geometry

In general, the trawl geometry and performance of the *Needler* showed considerable differences when compared to that of the other three vessels, *Teleost*, *Cabot*, and *Cartier*, as should be expected given the difference in vessel power and winch systems. The standard and modified Campelen trawl geometry were comparable among and between the *Teleost* and the new vessels (*Cabot*, and *Cartier*) and there were overall small differences in average tow speeds

and durations among all four vessels. Details on this will be provided in Nguyen & Walsh (in prep.)¹.

2.2. COMPARATIVE FISHING DATA ANALYSIS

The analytical approach described here has been adapted from Benoît et al. (2024).

The application of analytical approaches to the available paired data from the NL Region was determined following a decision tree framework based on spatial coverage, sample size, and the availability of length/count/weight data (Figure 1). This decision method was used as the baseline approach for all species, however there were some deviations made from this decision tree which are described in the applicable sections for where they occurred.

¹ Nguyen, T., and Walsh, S.J. In prep. Trawl Geometry and Performance During Comparative Fishing in the Newfoundland and Labrador Region. DFO Can. Sci. Advis. Sec. Res. Doc.

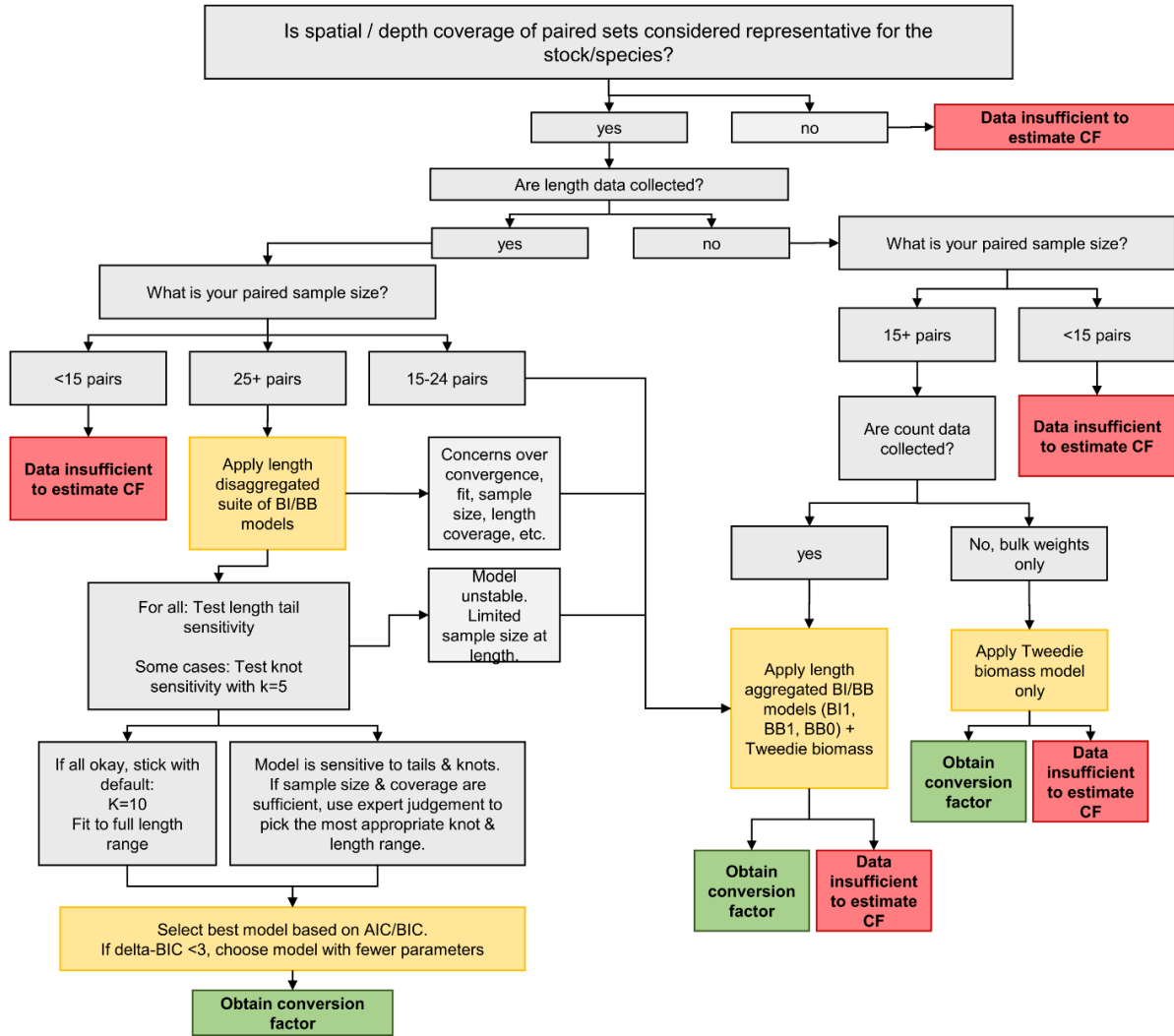


Figure 1. Model application decision tree for comparative fishing analysis in the Newfoundland and Labrador Region.

2.2.1. Binomial Models

In the analysis of comparative fishing data, the goal is to estimate the relative fishing efficiency between a pair of vessel-gear combinations (referred to as vessel in this section for simplicity). We assume the expected catch from vessel v ($v \in \{A, B\}$) at length l and at station i is:

$$E[C_{vi}(l)] = q_{vi}(l)D_{vi}(l)f_{vi}$$

where, $q_{vi}(l)$ is the catchability of vessel v , D_{vi} is the underlying population density sampled by vessel v , and f_{vi} is a standardization term which usually includes the swept area of a tow, and if applicable, the proportion of sub-sampling for size measurement on-board. In a binomial model (e.g., Miller 2013), the catch from vessel A at station i , conditioning on the combined catch from both vessels at this station, $C_i(l) = C_{Ai}(l) + C_{Bi}(l)$, is binomial-distributed:

$$C_{Ai}(l) \sim BI(C_i(l), p_{Ai}(l))$$

where $p_{Ai}(l)$ is the expected proportion of catch from vessel A . Tows in a pair are generally assumed to fish the same underlying densities at the station, as the paired vessels typically fish within a small distance (both spatial and temporal) of each other: $D_{Ai}(l) = D_{Bi}(l) = D_i(l)$. It follows that the logit-probability of catch by vessel A is then:

$$\text{logit}(p_{Ai}(l)) = \log\left(\frac{E[C_{Ai}(l)]}{E[C_{Bi}(l)]}\right) = \log(\rho_i(l)) + o_i$$

Where $\rho_i(l)$ is the ratio of catchabilities between vessels A and B at species length l and at station i , or the conversion factor, the quantity of interest:

$$\rho_i(l) = q_{Ai}(l)/q_{Bi}(l)$$

and $o_i = \log(f_{Ai}/f_{Bi})$ is an offset term derived from known standardization terms for swept area and subsampling.

For a length-based conversion factor, we consider a smooth length effect based on a general additive smooth function:

$$\log(\rho(l)) = \sum_{k=0}^K \beta_k X_k(l) = \mathbf{X}^T \boldsymbol{\beta},$$

where $\boldsymbol{\beta}$ are the coefficient parameters and are estimated, \mathbf{X} , or $\{X_k(l), k = 0, 1, \dots, K\}$, are a set of smoothing basis functions, and K is the dimension of the basis that controls the number of coefficient parameters and is usually pre-defined. Here a cubic spline smoother was used (Hastie et al. 2009), with the basis functions and penalty matrices generated by R (R Core Team 2021).

The estimation of a cubic spline smoother is based on the penalized sum of squares smoothing objective, but in practice, this is usually replaced by a penalized likelihood objective (Green and Silverman 1993):

$$\mathcal{L}(\boldsymbol{\beta}, \lambda) = f(\mathbf{Y}|\mathbf{X}, \boldsymbol{\beta}) e^{-\frac{\lambda}{2} \boldsymbol{\beta}^T \mathbf{S} \boldsymbol{\beta}}$$

\mathcal{L} denotes the likelihood objective function. $f(\mathbf{Y}|\mathbf{X}, \boldsymbol{\beta})$ is the joint probability function of the survey data \mathbf{Y} conditional on the basis functions and coefficient parameters. \mathbf{S} is the penalty matrix defined by the smoother and the dimension of the basis, and λ is the smoothness parameter. This smoothness parameter is estimated by maximum likelihood along with other model parameters but may be sensitive to the data. In such cases, it can be determined by other criteria such as generalized cross-validation (Wood 2000).

The penalized maximum likelihood smoother can also be re-parameterized into a mixed effects model (Verbyla et al. 1999; Wood 2017) to facilitate implementation as well as incorporation of additional random effects:

$$\log(\rho_i(l)) = \mathbf{X}_f^T \boldsymbol{\beta}_f + \mathbf{X}_r^T \mathbf{b}$$

where $\boldsymbol{\beta}_f$ are fixed effects and \mathbf{b} are random effects. \mathbf{X}_f and \mathbf{X}_r are transformed from the basis functions \mathbf{X} and an eigen-decomposition of the penalty matrix \mathbf{S} , $\mathbf{X}_f = \mathbf{U}_f^T \mathbf{X}$ and $\mathbf{X}_r = \mathbf{U}_r^T \mathbf{X}$, where \mathbf{U}_f and \mathbf{U}_r are the eigenvectors that correspond to the zero and positive eigenvalues of \mathbf{S} . The random effects $b \sim N(0, \mathbf{D}_+^{-1}/\lambda)$ where \mathbf{D}_+ is the diagonal matrix of the positive eigenvalues of \mathbf{S} . In the mixed effects model representation of the cubic spline smoother, the number of fixed effects is 2 and the number of random effects is bounded by $K - 2$. Smoothing effects are

transformed into shrinkage of random effects in the fitting of random deviations and can be integrated into complex mixed effects models commonly used in fisheries science (Thorson and Minto 2015).

Additional random effects can be incorporated into the mixed effects model to address variations in the relative catch efficiency related to each station,

$$\log(\rho_i(l)) = \mathbf{X}_f^T(\boldsymbol{\beta}_f + \boldsymbol{\delta}_i) + \mathbf{X}_r^T(\mathbf{b} + \boldsymbol{\epsilon}_i).$$

where $\boldsymbol{\delta}_i \sim N(\mathbf{0}, \boldsymbol{\Sigma})$ and $\boldsymbol{\epsilon}_i \sim N(\mathbf{0}, \mathbf{D}_+^{-1}/\xi)$. From a similar re-parameterization of the cubic spline smoother, these random effects allow for deviations of the length-based conversion at each station. $\boldsymbol{\Sigma}$ is the covariance matrix of the random effects corresponding to the random deviations and contains three parameters. ξ controls the degree of smoothness of the random smoothers and the smoother at each station can differ.

A summary of the above binomial mixed model is as follows,

$$\begin{aligned} C_i(l) &= C_{Ai}(l) + C_{Bi}(l) \\ C_{Ai}(l) &\sim BI(C_i(l), p_{Ai}(l)) \\ \text{logit}(p_{Ai}(l)) &= \log(\rho_i(l)) + o_i \\ \log(\rho_i(l)) &= \mathbf{X}_f^T(\boldsymbol{\beta}_f + \boldsymbol{\delta}_i) + \mathbf{X}_r^T(\mathbf{b} + \boldsymbol{\epsilon}_i) \end{aligned}$$

The model is estimated via maximum likelihood and the marginal likelihood integrating out random effects is:

$$\mathcal{L}(\boldsymbol{\beta}_f, \boldsymbol{\Sigma}, \lambda, \xi) = \int \left(\prod_{i=1}^m \int \int f(\mathbf{Y}_i | \mathbf{X}_f, \mathbf{X}_r, \boldsymbol{\beta}_f, \mathbf{b}, \boldsymbol{\delta}_i, \boldsymbol{\epsilon}_i) f(\boldsymbol{\delta}_i | \boldsymbol{\Sigma}) f(\boldsymbol{\epsilon}_i | \xi) d\boldsymbol{\delta}_i d\boldsymbol{\epsilon}_i \right) f(\mathbf{b} | \lambda) d\mathbf{b}$$

The binomial mixed model can be adapted for various assumptions on the smoother and potential station variation to accommodate different underlying density of a species and data limitations especially in length measurements. A set of binomial models considered in the present analyses is provided in Table 4.

2.2.2. Beta-binomial Models

The binomial assumption of the catch can be extended to a beta-binomial distribution to explain over-dispersion at the stations (Miller 2013):

$$C_{A,i}(l) \sim BB(C_i(l), p_{A,i}(l), \phi_i(l)).$$

The beta-binomial distribution is a compound of the binomial distribution and a beta distribution. More specifically, it assumes a beta-distributed random effect in the expected proportion of catch from vessel *A* across stations. As a result, the expected catch by vessel *A* has a variance of

$$\text{var}(C_{A,i}) = C_i p_i (1 - p_i) \frac{\phi_i + C_i}{\phi_i + 1}$$

where ϕ is the over-dispersion parameter that captures the extra-binomial variation.

The same smoothing length effect can be applied to the over-dispersion parameter,

$$\log(\phi_i(l)) = \mathbf{X}_f^T \boldsymbol{\gamma} + \mathbf{X}_r^T \mathbf{g}$$

where $\boldsymbol{\gamma}$ are fixed effects and \mathbf{g} are random effects, $\mathbf{g} \sim N(\mathbf{0}, \mathbf{D}_+^{-1}/\tau)$. This length effect models the variance heterogeneity and is particularly useful for projecting uncertainty to poorly sampled

lengths. However, estimation of a length-based variance parameter typically requires sufficient catch at length data, which is usually not available for less abundant species.

A summary of the beta-binomial mixed model is as follows,

$$\begin{aligned}
 C_i(l) &= C_{Ai}(l) + C_{Bi}(l) \\
 C_{Ai}(l) &\sim BB(C_i(l), p_{Ai}(l), \phi_i(l)) \\
 \text{logit}(p_{Ai}(l)) &= \text{log}(\rho_i(l)) + o_i \\
 \text{log}(\rho_i(l)) &= \mathbf{X}_f^T(\boldsymbol{\beta}_f + \boldsymbol{\delta}_i) + \mathbf{X}_r^T(\mathbf{b} + \boldsymbol{\epsilon}_i) \\
 \text{log}(\phi_i(l)) &= \mathbf{X}_f^T\boldsymbol{\gamma} + \mathbf{X}_r^T\mathbf{g}
 \end{aligned}$$

The marginal likelihood is:

$$\begin{aligned}
 &\mathcal{L}(\boldsymbol{\beta}_f, \boldsymbol{\gamma}, \boldsymbol{\Sigma}, \lambda, \xi, \tau) \\
 &= \int \int \left(\prod_{i=1}^m \int \int f(\mathbf{Y}_i | \mathbf{X}_f, \mathbf{X}_r, \boldsymbol{\beta}_f, \mathbf{b}, \boldsymbol{\gamma}, \mathbf{g}, \boldsymbol{\delta}_i, \boldsymbol{\epsilon}_i) f(\boldsymbol{\delta}_i | \boldsymbol{\Sigma}) f(\boldsymbol{\epsilon}_i | \xi) d\boldsymbol{\delta}_i d\boldsymbol{\epsilon}_i \right) f(\mathbf{b} | \lambda) f(\mathbf{g} | \tau) d\mathbf{b}
 \end{aligned}$$

Likewise, various smoothing assumptions can be applied to the variance parameter. The set of beta-binomial models considered in this analysis are presented in Table 5.

2.2.3. Tweedie Model for Biomass Data

The binomial and beta-binomial models are appropriate for data constituted of catch counts but are not appropriate for catch weight or biomass. Biomass indices are routinely derived from survey data for population trend monitoring. For taxa that are measured, biomass values adjusted for the change in relative catchability are most reliably derived by applying the results of the analyses described above to length specific catch numbers and to estimate a length-weight conversion. However, individual measurements are not made for numerous invertebrate taxa, and were not made for some years or some specific survey hauls for many of the remaining taxa. Estimates of relative catchabilities were therefore required for size-aggregated catch weights for all taxa.

The analysis of catch weights required a probability distribution with a frequent occurrence of zero, but that is otherwise continuous and can accommodate some overdispersion in catch weights. Unlike the models for catch counts, it was not possible to condition model estimates on the total catch. We employed the following model, which assumed Tweedie (TW) distributed error:

$$\begin{aligned}
 W_{i,v} &\sim TW(\mu_{i,v}, \varphi, \tau) \\
 E[W_{i,v}] &= \mu_{i,v} = \exp(v + \delta_i + o_{i,v}) \\
 \text{Var}[W_{i,v}] &= \varphi(\mu_{i,v})^\tau
 \end{aligned}$$

where $W_{i,v}$ is the catch weight at station i by vessel v , $\mu_{i,v}$ is the expected catch weight at station i for vessel v , φ is the dispersion parameter of the Tweedie distribution, τ is a power parameter, restricted to the interval $1 < \tau < 2$ (Dunn and Smyth 2005), v is the fixed vessel effect, where $\exp(v) = \rho$, δ_i is a random effect that accounts for the biomass at station i , and $o_{i,v}$ is the offset. Unlike the model for catch numbers in which the offset term was the log of the ratio of sampling effort (tow distance and catch sampling fraction), the offset term in the Tweedie model is the log of sampling effort at station i for vessel v , relative to the standard effort for that vessel.

This method differs from that employed in similar comparative fishing experiments with these vessels in the Gulf and Quebec Regions of DFO whereby station was considered a fixed effect in analysis due to undesirable behaviour of residuals and non-normal distribution of the random effect on the linear predictor. For the NL Region analysis the assumed normal distribution of the random effect residuals was met, thus station was treated as a random effect.

2.2.4. Model Fitting, Selection and Validation

The binomial and beta-binomial models in Table 4 and Table 5 for analyses of length-disaggregated catches were implemented using the Template Model Builder (TMB) package (Kristensen et al. 2016) in R. TMB uses the Laplace approximation to integrate the joint negative loglikelihood (nll) over the random effects to calculate the marginal nll (mnl). Optimization of the mnl is then undertaken in R using the *nminb()* function. The basis functions for the cubic smoothing spline and the corresponding penalty matrices were generated using the R package *mgcv* (Wood 2011) based on 10 equally-spaced knots ($K = 9$) within the pre-specified length range depending on the range of lengths observed proper to each taxon. TMB automatically calculates a standard error for the maximum likelihood estimation of the conversion factor via the delta method (Kristensen et al. 2016).

Analyses were also undertaken for size-aggregated catch numbers (i.e., abundance) and biomass (kg). There were three candidate models assessed for size-aggregated catch numbers and one for catch weights. Contrary to the analyses described above that treat the catch of a taxon at a given station and in a given length class as the basic datum, these size-aggregated analyses model the total catch numbers at each station. For simplicity, these analyses were implemented using the *glmmTMB* function from the homonymous R package (Brooks et al. 2017). Models BI1, BB0 and BB1 (Table 2 and 3) were fitted by specifying `family=binomial(link = "logit")` or `family=betabinomial(link = "logit")`, as appropriate. Note that conversion factor estimates for these models obtained from the length-disaggregated analyses are likely to differ from those obtained from the size-aggregated analyses when there are strong underlying length-dependent effects on relative catchability between the two vessels. Furthermore, because sample sizes are greater in the length-disaggregated analyses, standard errors on the correction factors are generally expected to be smaller. The analysis of catch weights was also implemented using the *glmmTMB* function, with the option `family = tweedie` specified.

Length-disaggregated models were fitted only for taxa for which there were data for at least 25 relevant set pairs (pairs with catch by at least one vessel). Size-aggregated models were only fitted for taxa for which there were data for at least 15 relevant set pairs. While these thresholds are somewhat arbitrary, they are reasonable in light of the complexity of the models (number of fixed and random parameters estimated) and are consistent with minimum requirements evident from the simulation study of Yin and Benoît (2022).

In total there were 13 candidate models used to assess length-disaggregated catches for estimating conversion factors. Poor convergence occurred for BI4, and BB6, and initial exploratory analysis demonstrated that convergence for BB7 was not possible for any species for any vessel pairings. Based on similar observations from comparative fishing projects in the Gulf and Quebec Regions of DFO comparative fishing analyses (Benoît et al. 2024) the decision was made to remove BB7 as a candidate model. The best model for each set of analyses was selected by BIC (Bayesian information criterion) to maximize model fitting, while avoiding over-fitting of more complicated models, especially in cases without adequate data. We also examined values for AIC (Akaike information criterion), which tends to select slightly more complex models compared to BIC, and report values alongside each other.

In most cases, final model selection was done using BIC values, and for those models where $\Delta\text{BIC} \leq 3$ between two candidate models for a given species-vessel pairing, then the model with fewer variables was selected (Figure 1). However, in cases where AIC/BIC values were in close contention between a constant conversion or a length-based conversion, consideration was given to both models and final model selection was determined based on the comparison of length composition calibration fits (i.e., Witch Flounder, Section 4.1.1.4 & 4.1.4.4), and results from the size aggregated analysis (i.e., a significant conversion for abundance and not biomass could indicate the potential of a length effect on catchability).

During the model selection process, it was observed in a few species that limited data in the extremes of the length distribution could be disproportionately influencing the shape of the length-dependent model conversion selected, leading to conversions that may not be biologically accurate. Sensitivity analysis was conducted by running the suite of length-dependent models on the data considering the full length range, 1 and 99 percentile lengths removed, and 2.5 and 97.5 percentile lengths removed (for example, see Figure 11). If the model selection remained consistent across all length ranges, then the best model from the full length range was selected for implementation of the conversion factor for that species. In one case (Redfish for *Needler & Cabot*) where removal of the 1 and 99 percentile resulted in a completely different model shape (Figure 12), and further sensitivity was conducted through reduction of specified knots in the model (full details provided in Section 4.1.4.7). For Northern Shrimp (Figure 13) the decision was made to use the model fit on the data trimmed at the 2.5 and 97.5 percentile lengths due to the limited observations in normal survey catches of the extreme lengths, sensitivity of the model to the tails of the data, and how length data is typically handled within the shrimp assessment framework. This decision was made in consultation with the shrimp assessment leads as the most appropriate conversion and applied for both vessel pairings.

In each length-disaggregated analysis, the estimated μ function (length-dependent expected proportion of catch by vessel A) from all converged models were compared along with the sample proportions (aggregated by stations and averaged for each length) to provide a more rigorous interpretation of the results. The estimated $\rho(l)$ (expected relative catch efficiency, or conversion factor function) and associated approximate 95% confidence interval from the best model is then shown over the range of lengths contained in the input data. Normalized quantile model residuals (Dunn and Smyth 1996) were produced and plotted using boxplots against length and survey station to visually assess the adequacy of model fit. Finally, we plotted model residuals against depth and the time at which a station was fished, two factors known to affect catchability (e.g., Benoît and Swain 2003), to evaluate whether these effects might interact with the vessel effect under study. To flag possible cases where these effects may have been influential we also fit the following gaussian models (presented using pseudo equations) to the normalized quantile model residuals (NQR):

1. $\text{NQR} \sim s(\text{depth}) + (1|\text{station})$
2. $\text{NQR} \sim s(\text{time}) + (1|\text{station})$
3. $\text{NQR} \sim \text{factor}(\text{day}) + (1|\text{station})$

where $s(x)$ denotes a smooth function of variable x (depth or time), $(1|\text{station})$ denotes a random effect for the station and $\text{factor}(\text{day})$ is a factor delineating day and night, where $\text{day} = 7:30 < \text{time} \leq 17:30$ in Newfoundland Standard Time (NST). Both smoothed and discrete effects of time were considered to flag cases of a possible diel effect on relative catchability (e.g., Benoît and Swain 2003). We examined the p-values associated with the effects of depth, time, and day, and further investigated the residuals patterns in cases with $p < 0.01$. For the

Teleost pairs with the *Cartier/Cabot*, the following additional Gaussian models were used to assess the effect of year and vessel:

1. $NQR \sim \text{factor}(\text{year}) + (1|\text{station})$
2. $NQR \sim \text{factor}(\text{vessel}) + (1|\text{station})$

where $\text{factor}(\text{year})$ denotes the factor for 2021 and 2022, and $\text{factor}(\text{vessel})$ for the *Cartier* and *Cabot*. These tests were not required for the *Needler* and *Cabot* pairs since the comparative fishing program for the *Needler* only spanned one year, and no paired sets were conducted with the *Cartier* during that time.

Lastly, a special case was made for Yellowtail Flounder, where data was combined across season for analysis, and thus the following was conducted:

1. $NQR \sim \text{factor}(\text{season}) + (1|\text{station})$

where $\text{factor}(\text{season})$ denotes the factor for spring and fall for the *Needler* and *Cabot* pairs in 2022. Details on the decision to combine these data for Yellowtail Flounder reflect consistency in distributions across seasons and are further detailed below (Section 4.1.6).

The fit of catch-aggregated analyses for counts and weights was assessed by plotting the conversion factor and associated approximate 95% confidence interval (CI) in biplots of the catch of one vessel over the other. Additionally, we examined the scaled quantile residuals obtained using the R package DHARMA (Hartig 2022). Unlike the normalized quantile residuals used in the length-disaggregated analyses above, which have an expected Gaussian distribution when model fit is adequate, the quantile residuals from DHARMA have an expected uniform distribution. Residuals for the size-aggregated analyses were examined for uniformity and possible overdispersion, and plotted as a function of the fitted values, station depth and time. The evaluation of residuals in size-aggregated analyses was limited to a visual inspection.

2.2.5. Interpretation of Analysis Results and Application of Conversion Factors

The estimated conversion factor from the best selected model is the estimate of relative catch efficiency (ρ) whereby $\rho < 1$ indicates the new vessel has a higher catch, and $\rho > 1$ indicates the old vessel has a higher catch. If the catchability between both vessels is $\rho = 1$, then no conversion is required.

During model selection and review of analysis, it became clear that in some cases additional screening criteria would be required to determine whether a conversion factor should be applied. In cases where the CIs for a length-dependent conversion factor function overlapped with a value of one for the majority of the estimated function, indicating no statistical difference with the case of equivalent vessel catchability across lengths, we then also examined the results for the non-length dependent analyses.

As noted above, the estimation of length-specific conversion factor functions can be sensitive to the sparseness of data in the tails of the length frequencies. We therefore adopted the following procedure. For taxa where a length dependant conversion was estimated, we identified the lengths that constituted the 0.5 and 99.5 percentiles of the taxon-specific total length frequency distribution for the 2021–22 experiments for taxa with ≥ 20 length classes and used the 2.5 and 97.5 percentiles for taxa with < 20 length classes. We then identified the conversion factor function values at these percentile length groups for each taxon and assumed these values as constants for lengths below and above these percentiles, respectively.

For size aggregated models (abundance and biomass), a conversion factor is considered significant when $p < 0.05$ and the CI does not overlap with one. For species where one of the

two conversions is significant, the corresponding metric is considered significant if $p < 0.1$ regardless of if the CIs overlapped with one, otherwise only the conversion significant at $p < 0.05$ is recommended to be applied.

Where a conversion factor has been estimated for a group of taxa, this conversion is applicable only at the grouped level and should not be applied to a single species within the group. Any taxa not specifically mentioned in these analyses were not present in the comparative fishing data set or did not meet the minimum sample size, and relative catch efficiency could not be evaluated.

2.2.6. Biological Community Analysis

To compare the biological community of paired sets three metrics of diversity were evaluated:

1. species richness,
2. Shannon-Weaver Diversity Index, and
3. Pielou's Evenness Index.

Due to variation in taxonomic level of identification possible at sea, the lowest taxonomic level of identification for some groups was done to the level of genus (e.g., *Lycodes*), family (e.g., *Myctophidae*) or even phylum (e.g., Porifera) in some cases. Taxonomic groups with fewer than seven records, or 0.05% of total records, were excluded as they were deemed too rare to support reliable and consistent results. All biological community analyses used catch weights standardized to tow length. Species richness and Shannon-Weaver diversity were calculated using the R package *vegan* (Oksanen et al. 2022). Pielou's evenness was calculated using Shannon-Weaver Diversity divided by the natural log of species richness.

All analyses were completed on the full dataset (i.e., all taxonomic groups including the non-commercial invertebrates, referred to from here on as "full community"), and repeated on a subset of the data including finfish and commercial shellfish (referred to from here on as "fish community"). Data from the non-commercial invertebrates are not widely used in the region and many of the species' identifications are at higher taxonomic levels than the fish community subset.

Comparisons between paired sets of the three diversity metrics were performed using a generalized linear mixed model using the R package *glmmTMB*. All models included station as a random factor and looked at differences between vessel group (old vs new vessels) and vessel pairs (*Needler* pairs vs *Teleost* pairs). The interaction between vessel and pair group was not found to be significant and was removed. Models examining the three metrics of diversity were built using different error distributions: species richness used a Tweedie, Shannon-Weaver diversity used a Gaussian, and Pielou's evenness used a beta error distribution. Residuals were examined using the *DHARMa* R package.

In addition to the above metrics, community composition was examined using Non-metric MultiDimensional Scaling (nMDS). Bray-Curtis distance matrix was calculated using square root transformed and Wisconsin standardized catch weights to reduce the impact of large catches. For both the full and fish communities three dimensions were calculated for the nMDS analysis. To determine if vessels were sampling the same community, permutational multivariate analysis of variance (PERMANOVA) was conducted. We included the relationship between vessel pair (TEL:CAX or AN:CAB) and vessel group (old vs. new), and the interaction term. PERMANOVA does not allow for random factors, so station was included as a non-random variable. We used 9,999 permutations to calculate significance. To determine which species were driving any patterns, a similarity percentages (SIMPER) analysis was conducted on the *Teleost* and

Needler paired sets separately and only looking at the impact of vessel group. We used 999 permutations to calculate which species were significantly contributing to the relationships. All analyses were conducted using the R package *vegan*.

2.2.7. Habitat and Environmental Comparisons

A suite of benthic and other environmental variables (Table 2) were examined to:

1. look at patterns in benthic habitat between sets and years, and
2. determine the representativeness of areas where paired tows were completed relative to the standard survey.

Variables examined were derived from measured conditions at the time of sampling or spatial models for the area.

Examination between sets (both vessel pairs) and years (*Teleost* only) was examined using nMDS, PERMANOVA, and SIMPER methods as described above for biological community analyses. A Gower distance matrix was calculated using the R package *vegan* with all variables scaled between 0 and 1, converting negative values and scaling large values.

Information on substrate type was not available for all sets. Analyses were partitioned so that results are presented for models that included all variables, but excluded sets that did not overlap with substrate data (*sets_rm*), and a second set of results are presented for models that included all sets but excluded substrate variables (*var_rm*).

Seabed characteristics of the survey strata completed by each retiring vessel during comparative fishing were compared to the characteristics of the fall survey area to assess the success of the shadow survey and targeted CF approaches in capturing the range of environmental conditions encountered by the NL Region MSS. Seabed characteristics included in this analysis are depth (GEBCO 2023); terrain attributes (slope, ruggedness, and benthic position index); bottom current velocity (Tyberghein et al. 2012; Assis et al. 2017); and modeled dominant substrate (E. Novaczek, unpublished data).

The General Bathymetric Chart of the Oceans (GEBCO) bathymetry data and Bio-Oracle current velocity data used are open access and were not modified for this analysis. Terrain attributes were derived from the GEBCO bathymetry using the Benthic Terrain Modeler toolbox in ArcGIS Pro (Walbridge et al. 2018). Slope was calculated in a 3x3 cell window and is presented in degrees. Terrain ruggedness is included here as a measure of seafloor complexity that captures variability in both slope and aspect in a 3x3 cell window ranging from 0 (no terrain variation) to 1 (complete terrain variation). Benthic Position Index (BPI) is the measure of where a referenced location lies relative to its surroundings; i.e., peak or valley. Positive BPI values indicate areas that are higher than their surroundings, while negative values indicate areas that are lower. BPI values over flat terrains will approach zero. Two BPI layers are presented here, defined by the neighborhood analysis. Fine BPI was generated using an inner radius of 3 cells and an outer radius of 9 cells. Broad BPI was generated using an inner analysis radius of 30 cells and an outer radius of 90 cells.

The substrate data are unpublished model results generated by E. Novaczek. Dominant substrate texture classifications (mud, sand, and gravel) from multiple sources, including geophysical surveys, sidescan interpretation, cores, and grab samples were provided by the Geological Survey of Canada. Boosted Regression Tree models were built to predict dominant sediment type, based on current, depth, geomorphometric variables, and distance from shore with high overall accuracy (0.74–0.78). The modeled layers represent predicted likelihood of occurrence (0–1) of mud, sand, and gravel as the dominant substrate type.

Results for the comparison of seabed characteristics between comparative areas and the standard survey are presented in Section 3.0.

Table 2. Benthic variables included in habitat and environmental characteristic analysis.

Category	Variable	Description	Source
Current velocity	Current	Bottom current at the Bio-oracle mean bottom depth for “present” time period. unit: m/second, resolution: 8,077 m	Bio-oracle; Tyberghein et al. 2012.
Substrate type	Mud	Probability of mud as the primary substrate type (0–1). Resolution: 75 m.	E. Novaczek unpublished models
Substrate type	Sand	Probability of sand as the primary substrate type (0–1). Resolution: 75 m.	E. Novaczek unpublished models
Substrate type	Grav	Probability of gravel as the primary substrate type (0–1). Resolution: 75 m.	E. Novaczek unpublished models
Bathymetry	Bathy	Depth in meters. Resolution: 415 m.	GEBCO
Geomorphometry	Slope	Slope in degrees. Resolution 415 m.	GEBCO, benthic terrain modeler toolbox
Geomorphometry	Rugg	Terrain ruggedness (0–1). Resolution 415 m.	GEBCO, benthic terrain modeler toolbox
Geomorphometry	bBPI	Broad scale Benthic Position Index (i.e., peak or valley); inner radius of 30 cells and outer radius of 90 cells. Resolution 415 m.	GEBCO, benthic terrain modeler toolbox
Geomorphometry	fBPI	Fine scale BPI; inner radius of 3 cells and outer radius of 9 cells. Resolution 415 m.	GEBCO, benthic terrain modeler toolbox
Latitude	Lat_start	Start latitude of trawl	Ship-mounted GPS
Temperature	bot_temp	Bottom temperature during trawl	Trawl-mounted CTD

3. SPATIAL CONSIDERATIONS

3.1. SEABED REPRESENTATION OF THE PAIRED SETS

Summary statistics were calculated for geomorphometric variables, bottom current velocity, and substrate for the following areas:

- NAFO Div. 2HJ3K Fall survey area of the *Teleost* (comparative fishing conducted in 2021–22),
- NAFO Div. 3LNO and 3K Fall survey areas of the *Alfred Needler* (comparative fishing in 2022), and;

-
- NAFO Div. 3Ps Spring survey area of the *Alfred Needler* (comparative fishing conducted in 2022).

The NAFO Div. 3LNO spring survey area of the *Needler* was excluded from this analysis due to insufficient data. Completed comparative fishing strata were defined as strata with two or more successful paired sets (TEL:CAX or AN:CAB) within a survey season.

It is also important to note that the quality of bathymetric data has improved significantly since the survey strata were originally developed. As a result, the GEBCO 2023 depth does not always match the listed strata depth. Maximum survey depth is 1,500 m for the *Teleost* and 732 m for the *Needler*. However, depths beyond these thresholds appear in the summary plots, reflecting the mismatch between strata boundaries and updated bathymetry.

Spring comparative fishing strata completed with the *Needler* in NAFO Div. 3Ps show severe truncation in the surveyed range of all geomorphometric variables (Figure 6), indicating an underrepresentation of deep and complex habitats in the comparative fishing program for this area. Current and substrate were omitted from these comparisons due to gaps in the data coverage.

Fall comparative fishing strata completed with the *Needler* in NAFO Div. 3LNO appear to be broadly representative of the average survey area (Figure 7). For almost all tested variables the comparative fishing strata mean values closely match the total survey area mean values. However, there is truncation of depth, slope, ruggedness, and BPI. Comparative fishing strata completed by the *Needler* under-represent deep, high slope, and complex habitats. Substrate was omitted from these comparisons due to gaps in the data coverage.

Fall comparative fishing strata completed with the *Needler* in NAFO Div. 3K appear to be broadly representative of the survey area (Figure 8). For bathymetry and the geomorphometric derivatives (depth, slope, ruggedness, BPI), the comparative fishing strata mean values closely match the total survey area mean values. However, there is minor truncation of maximum depth, slope, ruggedness, and BPI, indicating some underrepresentation of highly complex habitats. Substrate and current velocity of the survey area appear to be well represented by the comparative fishing strata.

Fall comparative fishing strata completed to date with the *Teleost* in NAFO Div. 2HJ3K appear to be representative of the survey area (Figure 9). For most of the tested variables (depth, slope, ruggedness, BPI, and current velocity) the comparative fishing strata mean values closely match the total survey area mean values in both 2021 and 2022. There is some truncation in range of depth, slope, and terrain ruggedness in comparative fishing strata completed by the *Teleost* to date (Figure 10). Overall, the substrate of the completed strata match the survey area well, and this is consistent for the targeted strata completed in 2022. When subset from the rest of the comparative fishing data, the shadow survey completed in 2021 may over-represent muddy habitats and underrepresent sandy and gravelly habitats.

3.2. AREA-VESSEL GROUPINGS FOR CONVERSION FACTOR ESTIMATION

To calculate conversion factors, data were first considered across Ecosystem Production Units (EPUs; Pepin et al. 2014) defined as: Labrador Shelf (Div. 2GH), Northeast Newfoundland Shelf (Div. 2J3K), The Grand Bank (Div. 3LNO), and Southern Newfoundland (Subdiv. 3Ps). A summary of these groupings and application of conversion factors are provided in Table 3.

Teleost

Div. 2H was grouped with the Northeast NL Shelf (Div. 2J3K) for the *Teleost*, given the broad continuity in environmental conditions of the area, and that the connectivity of stock boundaries

often straddle EPU boundaries in this area. In addition, four paired tows were completed with the *Teleost* in Div. 3L near the Bonavista corridor and have been included with the rest of the *Teleost* pairs. Conversion factors were therefore estimated using data from across Div. 2HJ3KL and are considered applicable across this area in the fall.

Needler

Data for paired sets with the *Needler* is more sparse and the application of the data is considered limited.

Fall: Fall paired sets have been pooled across Div. 3KLNO to capture the normal survey conditions in 3KL for this vessel (3NO sets used as a proxy for areas in 3L on top of the Bank). Sets in fall 3NO were primarily completed at depths <183 m, with only two sets completed deeper, and therefore are considered representative of the top of the Grand Bank only. Paired data are insufficient in number and spatial extent to yield conversions for stocks/taxa that have a significant portion of their distribution on the southern slope of the Grand Bank (e.g., White Hake, Silver Hake, Spiny dogfish).

Spring: Spring data were collected in Div. 3N and Subdiv. 3Ps. Sets in 3Ps (N = 25) were all <183 m. Sets in 3N covered a broad depth range, but sample size is too small to be representative (N = 12). Due to these limitations, the paired data collected is insufficient to accurately estimate conversion factors.

Special case: Yellowtail Flounder

Given its limited distribution (spatially and by depth; see Maddock Parsons et al. (2021) for more details), along with limited variation in habitat type (generally sandy to gravelly bank habitat), a special case has been identified for Yellowtail Flounder (*Myxopsetta ferruginea*). For this species only, paired sets have been combined from the fall and spring of 2022 to estimate conversion factors for use in Div. 3LNOPs.

Table 3. Summary of paired data availability and application to Northwest Atlantic Fisheries Organization (NAFO) Divisions and Canadian Coast Guard Ship (CCGS) Alfred Needler or CCGS Teleost.

Season	Vessels	Division(s)	Notes	Application
Spring	<i>Needler</i>	3Ps	Insufficient data for conversions. Small sample size combined with severe truncation of depth and habitat complexity sampled.	None.
Spring	<i>Needler</i>	3LNO	Insufficient data for conversions. Small sample size, severe truncation of depth and habitat complexity sampled on the Grand Bank	None.
Fall	<i>Needler</i>	3KLNO	Sample size dominated by Div. 3K, stations in Div. 3NO included to capture variation on top of the Grand Bank.	Div. 3KL. Application to Grand Bank stocks/EPU is limited. Species specific investigations of distribution (depth, temperature, etc.) relative to location of paired tows are required to justify

Season	Vessels	Division(s)	Notes	Application
				application of conversion factors beyond Div. 3KL. Consideration should also be given to growth rates, size distribution of the stock in question, etc. across the area.
Fall	<i>Teleost</i>	2HJ3KL	Representative across the range of normal survey conditions to 1,000 m. No sampling 1,000–1,500 m. Conversion factors are not estimated here for species considered to notably extend into these deep waters.	2HJ3K + 3L deep-water* for <1,000 m
Spring & Fall	<i>Needler</i>	3LNOPs	Special case given limited distribution of the species largely overlaps with the limited distribution of the sets.	Yellowtail Flounder only.

*Deep water for 3L is greater than 750 m.

4. RESULTS AND DISCUSSION

4.1. PRESENTATION OF CONVERSION FACTORS

The results of the various analyses for the numerous taxa covered in this report are simply too voluminous to interpret in detail. Instead, we aimed to provide detailed figures and tables (Table 6–Table 11) that describe the results, support decisions for the application of conversion factors, and provide some interpretation of results only for key harvested species and species of conservation concern.

Appendix 1 contains results for all taxa where data allowed the estimation of conversions via length-disaggregated modeling.

Appendix 2 presents results for all taxa where conversions were estimated with size-aggregated (abundance, biomass) methods.

Throughout analysis of both vessel pairings, estimates for several groups were provided however the taxa groupings used were concluded to be too broad for application and require further review. These include:

- Other skates – 91 (*Amblyraja* spp., *Rajella* spp., *Malacoraja* spp., *Leucoraja erinaceus*, *Raja fyllae*, and *Dipturus laevis*)
- Non Pandalid Shrimp – 8,020 (*Dichelopandalus* sp., *Aristaeopsis* sp., *Gennadas* spp., *Eusergestes* sp., *Pasiphaea* spp., *Eualus* spp., *Spirontocaris* spp., *Acanthephyra* spp., *Benthesicymus* sp., *Nematocarcinus* spp., *Parapasiphae* sp., *Robustosergia* sp., *Lebbeus* spp., *Atlantopandalus* sp., *Sclerocrangon* spp., *Sabinea* spp., *Pontophilus* sp., *Argis* sp., *Stereomastis* sp., *Munida* spp.)
- Sea Cucumbers – 8,290 (Holothuroidea)

-
- Sea stars – 8,390 (Crinoidea and Asteroidea)
 - Sea Urchin and Sand Dollars – 8,360 (Echinoidea)
 - Eels – 359 (Anguilliformes)

Additionally, for some groupings where a conversion factor was accepted, further work may still be conducted to further refine groupings to see if individual species can be assessed.

4.1.1. Fall Conversions – CCGS *Teleost* (Div. 2HJ3KL)

Length disaggregated analysis (Table 6 and Appendix 1) was completed for nine species where each species occurred in the minimum 25 sets recommended for analysis (Table 9). An additional five taxa met the minimum set number for length-disaggregated analyses, but data were deemed insufficient for length-based modelling due to small catch sizes within sets:

- Toad crab – 8,216 (*Hyas* spp.)
- Striped Shrimp – 8,112 (*Pandalus montagui*)
- Wrymouth – 721 (*Cryptacanthodes maculatus*)
- Common Lumpfish – 849 (*Cyclopterus lumpus*)
- Northern Wolffish – 699 (*Anarhichas denticulatus*)

Size aggregated analysis (Table 10 and Appendix 2) was conducted on all species/taxa groupings caught by at least one vessel in 15 sets, however the following were deemed to have insufficient data to consider the analysis valid:

- Amphipods – 6,980 (Amphipoda)
- Euphausiids – 7,991 (Euphausiacea)
- Spiny Crab – 8,196 (*Lithodes* sp., *Neolithodes* sp.)
- Sessile Tunicates – 8,680 (Tunicata)
- Longfin Hake – 444 (*Phycis chesteri*)
- Common Lumpfish – 849 (*Cyclopterus lumpus*)
- Coral, NS – 8,900
- Snake Blenny – 716 (*Lumpenus lumpretaeformis*)
- Wrymouth – 721 (*Cryptacanthodes maculatus*)

A number of species are not considered in the present analysis for *Teleost* conversions (despite being present in the minimum required sets for respective analyses) as further data input is needed from deeper depths (>1,000 m, planned for fall 2023) to properly assess conversion factors. These species include:

- Greenland Halibut – 892 (*Reinhardtius hippoglossoides*)
- Black Dogfish – 27 (*Centroscyllium fabricii*)
- Goitre Blacksmelt – 202 (*Bathylagus euryops*)
- Viperfishes – 207 (*Chauliodus* spp.)
- Boa Dragonfish – 230 (*Stomias boa ferox*)

-
- Lanternfishes – 272 (*Myctophidae*)
 - Barracudinas – 316 (*Paralepididae*)
 - Tapirfish – 386 (*Notacanthus* sp. & *Macdonaldia* sp.)
 - Blue Hake – 432 (*Antimora rostrata*)
 - Roughhead Grenadier – 474 (*Macrourus berglax*)
 - Grenadiers – 470 (*Macrouridae* except *Macrourus berglax*)

Depending on number of sets achieved in fall 2023, the grenadiers grouping may be further divided to individual species should the sample size of those species be sufficient for modelling efforts, and sample size for other species not listed here may become sufficient to estimate conversions.

4.1.1.1. American Plaice (*Hippoglossoides platessoides*)

American Plaice were caught in 172 sets with a length range from 4–60 cm. The best model selected for conversion factor estimation was BI1 with no significant length effect. CIs overlapped with equal catchability for entirety of the model, thus no conversion factor is required for American Plaice between the *Teleost* and new vessels. Results from size aggregated analysis agree with the conclusion that no conversion factor is required.

4.1.1.2. Atlantic Cod (*Gadus morhua*)

In the *Teleost* comparative fishing data set, there were very few sets with a depth <150 m due to limited allocation and trouble finding good fishing bottom in the shallow strata (Figure 14). This depth gap in the data set is expected to disproportionately impact and contribute to limited sample size for small Atlantic Cod since their distribution tends to favour these shallower depths. It was decided that this data gap was significant enough to impact conversion factor analysis and thus further comparative fishing with sets at depths <150 m is planned for 2023 to attempt to fill this gap. In the interim, the data from fall 2021 and 2022 was evaluated for the 20–98 cm length range to provide a preliminary conversion estimate until the shallow depth gap can be filled. There were 171 paired sets with cod in this length range, and the best model selected was BB1, with no significant length effect. The resulting conversion factor estimation resulted in a complete overlap of CIs with one, and thus no conversion factor is required for Atlantic Cod between the *Teleost* and new vessels for >20 cm individuals.

4.1.1.3. Thorny Skate (*Amblyraja radiata*)

Thorny Skate were present in 177 sets with a length range of 8–77 cm. The best model selected was BB1 with no significant length effect. The resulting conversion factor estimation had a complete overlap of CIs with equal catchability, and thus no conversion factor is required for Thorny Skate between the *Teleost* and new vessels. Results from size aggregated analysis agree with the conclusion that no conversion is required.

4.1.1.4. Witch Flounder (*Glyptocephalus cynoglossus*)

Witch Flounder were caught in 142 sets with a length range of 6–58 cm used in analysis. Model selection by BIC resulted in a non-significant length model (BI1) to be selected, however the AIC analysis did not agree with this and BI3 had the lowest AIC. Based on the length composition comparison between the *Teleost* and *Cabot/Cartier*, and the improved residual fit of BI3 compared to BI1, the decision was made to implement a conversion factor from the length based conversion factor estimates from BI3. In the size aggregated analysis, a significant conversion on abundance, but not biomass, was found, further supporting the implementation of a length-based conversion.

4.1.1.5. Striped Wolffish (*Anarhichas lupus*)

Striped Wolffish were caught in 73 sets with a length range of 6–113 cm. The best model selected was BI1 with no significant length effect. The resulting conversion factor estimation resulted in a complete overlap of CIs with equal catchability, and thus no conversion factor is required for Striped Wolffish between the *Teleost* and new vessels. Results from size aggregated analysis agree with the conclusion that no conversion is required.

4.1.1.6. Spotted Wolffish (*Anarhichas minor*)

Spotted Wolffish were caught in 92 sets with a length range of 7–108 cm. Model selection determined BI0 was the best model fit for conversion factor estimation, with no length or station effect, and a significant conversion. Size-aggregated analysis supports the need for a conversion but also suggests there may be a hidden length effect not detectable with the current amount of data since the conversion on abundance was significant, but biomass was not. The conversion from length disaggregated analysis has been accepted, however may be re-evaluated once further data is collected from deeper depths in 2023.

4.1.1.7. Redfish (*Sebastes mentella* & *S. fasciatus*)

Redfish were caught in 187 sets with a length range of 5–57 cm. One set was removed from analysis due to an abnormally high catch that was causing convergence issues with all models that included a random station effect. With the removal of this one set, the best model selected was BB1 with no length effect and no significant conversion. Size aggregated analysis agreed with this conclusion with no significant conversion for abundance, however a significant conversion was found for biomass, though this was likely driven by a few larger catches and not representative of the average redfish catch weights.

4.1.1.8. Snow Crab (*Chionoecetes opilio*)

As observed with Atlantic Cod, the *Teleost* comparative fishing data set has limited data in shallow strata, with no sets <150 m, which could disproportionately impact sample size of small Snow Crab as well since they tend to favour shallower depths. It was determined this data gap was significant enough for Snow Crab (Figure 15) that development of a full width range conversion factor would need to wait until further data inputs from 2023 were available. For the present data, a conversion factor has been determined for crabs with a carapace width from 40–138 mm. At this width range, Snow Crab were present in 101 sets and the best model selected was BI1. Though no size effect was found, a significant difference in relative catchability between vessels was found and a conversion factor is required for Snow Crab >40 mm.

4.1.1.9. Northern Shrimp (*Pandalus borealis*)

Northern Shrimp were caught in 174 sets and the 2.5–97.5 percentile length range assessed was 130–255 mm. The best model selected was BI4 with a significant length/station interaction effect. Size aggregated analysis agreed with the conclusion that a length based conversion is appropriate as a significant conversion of abundance was found, but not for biomass.

4.1.2. Spring Conversions – CCGS *Alfred Needler* (Div. 3Ps)

Data are insufficient to compute conversion factors for Subdivision 3Ps. There were only 25 successful paired tows, and these were limited in spatial and depth distribution (all <183 m).

4.1.3. Spring Conversions – CCGS *Alfred Needler* (Div. 3LNO)

Data are insufficient to compute conversion factors for Div. 3LNO in Spring. There were only twelve successful paired tows, and these were limited in space (Div. 3N only).

4.1.4. Fall Conversions – CCGS *Alfred Needler* (For Use in Div. 3KL)

Length disaggregated analysis (Table 8, Table 9, and Appendix 1) was conducted on 15 species where each species occurred in the minimum 25 sets recommended for analysis. Of those species, the following were deemed to have insufficient data for length-based conversion modelling:

- Striped Shrimp – 8,112 (*Pandalus montagui*)
- Striped Wolffish – 700 (*Anarhichas lupus*)
- Spotted Wolffish – 701 (*Anarhichas minor*)
- Wrymouth – 700 (*Cryptacanthodes maculatus*)
- Toad crab – 8,217 (*Hyas* spp.)

Size-aggregated (Table 11 and Appendix 2) analysis was conducted on all taxa (single species or grouping) caught by at least one vessel in 15 sets, however minimum set number does not guarantee a conversion can be estimated. A number of taxa were deemed to have insufficient data to consider the analysis valid despite meeting the minimum set requirement. These include:

- Amphipods – 6,980 (Amphipoda)
- Tunicates – 8,680 (Tunicata)
- Grenadiers – 470 (*Macrouridae* except *Macrourus berglax*)
- Snake Blenny – 716 (*Lumpenus lumpretaeformis*)
- Sea Raven – 809 (*Hemitripteris americanus*)
- Common Lumpfish – 849 (*Cyclopterus lumpus*)
- Cephalopods, Other – 4,545 (Cephalopoda)
- Polychaetes – 4,950 (Polychaeta)
- Comb-Jelly – 2,250 (Ctenophora)
- Soft Corals – 8,904
- Bryozoan – 9,992 (Bryozoa)
- White Hake (common) – 447 (*Urophycis tenuis*)
- Silver Hake – 449 (*Merluccius bilinearis*)

4.1.4.1. American Plaice (*Hippoglossoides platessoides*)

American Plaice were present in 98 paired sets and the length range assessed was 7–63 cm between the *Needler* and *Cabot* and model B13 was selected as the best model with a significant length effect. Though conversions from the size aggregated analysis are not significant, the length dependence of the conversion is evident based on the results of the length disaggregated analysis and thus the most appropriate conversion factor to implement.

4.1.4.2. Atlantic Cod (*Gadus morhua*)

Atlantic Cod were present in 94 paired sets and the length range assessed was 5–100 cm. Model B11 was selected as the best model fit, which indicated no significant effect of length on the catch between the two vessels. Additionally, the CIs of the estimated conversion overlap

with an equal conversion between vessels for the entirety of the function and thus no conversion is required for Atlantic Cod between the *Needler* and *Cabot*. Results from the catch aggregated analysis agree with both abundance and biomass resulting in a non-significant conversion factor estimate.

4.1.4.3. Thorny Skate (*Amblyraja radiata*)

Thorny Skate were caught in 93 paired sets with a length range of 10–93 cm. Model B11 was selected as best model fit with no significant length effect, and no conversion required. This is consistent with the results assessing abundance and biomass, also indicating no conversion factor required.

4.1.4.4. Witch Flounder (*Glyptocephalus cynoglossus*)

Witch Flounder were caught in 79 sets with a length range of 8–57 cm used in analysis. Model selection by BIC resulted in a non-significant length model (BB1) to be selected, however the AIC analysis did not agree with BB4 and BB5 (both length significant). Based on the length composition comparison between the *Needler* and *Cabot*, and the improved residual fit of BB4 compared to BB1, the decision was made to implement a conversion factor from the length based estimates of BB4.

4.1.4.5. Roughhead Grenadier (*Macrourus berglax*)

Roughhead Grenadier were present in 33 sets in 3K only, with a length range of 15–320 mm. Model selection for BIC and AIC agreed that B11 was the best model for conversion factor estimation, and no conversion factor is recommended for Roughhead Grenadier for the *Needler* and *Cabot*. Size aggregated analysis agrees with this conclusion.

4.1.4.6. Greenland Halibut (*Reinhardtius hippoglossoides*)

Greenland Halibut were caught in 79 sets and a length range of 6–93 cm was assessed. The model selected as best was BB1 which resulted in a constant conversion with no significant length effect. With the CIs overlapping an equal constant catch efficiency between both vessels, no conversion factor is required between the *Needler* and *Cabot*. Size aggregated analysis agrees with this conclusion.

4.1.4.7. Redfish (*Sebastes mentella* and *S. faciatus*)

Redfish were caught in 78 paired sets with a length range of 5–62 cm. During sensitivity tests, the removal of the 1 and 99 percentile lengths resulted in a completely different model shape, with numerous “wiggles” that were deemed biologically inaccurate. To assess this, the number of knots specified in the smooth construct of the models was reduced from 10 to five, to evaluate whether the observed wiggles were a result of improper fitting, or accurate to the length effect present for the catchability of redfish (Figure 12). The reduction to five knots reduced the wiggles and resulted in consistent model behaviour to the full length range at 10 knots. As a result, the decision was made to use the full length range size disaggregated analysis. The final model selected was BB4 with a significant length effect resulting in a conversion to be applied by length. Size aggregated analysis agreed with the conclusion that length of redfish impacted catchability as a significant conversion for abundance was found, but not for biomass.

4.1.4.8. Snow Crab (*Chionoecetes opilio*)

Snow Crab were caught in 72 sets with a carapace width range of 7–139 mm. A length-based model was selected (BB5) with a conversion factor to be applied by width. The size aggregated analysis also agree with this conclusion as a significant conversion is required on both

abundance and biomass, though the final conversion to be applied will be from the length-disaggregated analysis.

4.1.4.9. Northern Shrimp (*Pandalus borealis*)

Northern Shrimp were caught in 68 sets and the 2.5–97.5 percentile length range assessed was 105–255 mm. Both AIC and BIC agreed that the best model to select was BB5 with a significant length effect. Size aggregated analysis resulted in a significant conversion for biomass only, and not abundance, which is not necessarily consistent with the length-based analysis, however the aggregated analysis assesses all data in contrast to the length-disaggregated analysis where a reduced length range was used.

4.1.5. Fall Conversions – CCGS *Alfred Needler* (Grand Bank Stocks, 3LNO)

Consideration was given to running conversions using sets from 3LNO only (fall *Needler* pairs, excluding 3K) to best represent the conditions on the Grand Bank. However, data are limited in 3LNO in the fall, with 27 paired tows completed. Stations were also restricted in space and depth, with all but two sets occurring <183 m on top of the Bank. This sample size met the minimum criteria to run the models for six species, however, the data were considered insufficient given the limited sample size, spatial scope, and shallow depth range.

These data are not considered broadly applicable as they do not represent the normal range of survey conditions on the Grand Bank. Notably, the slope edges were not sampled, and relative catchability in waters deeper than 183 m can not be estimated with only two sets completed at those deeper depths. The sets however fully overlapped with the typical distribution of Yellowtail Flounder, and therefore the use of the data for only Yellowtail Flounder was examined (see below).

Given the difference in conditions between the Northeast Newfoundland shelf and the Grand Bank, the application of the 3KL fall conversions (see Section 4.1.4) to Grand Bank stocks/with the Grand Bank EPU is considered limited. Species specific investigations of distribution (depth, temperature, etc.) relative to location of paired tows are required to justify application of a conversion factor beyond Div. 3KL. Consideration should also be given to various parameters (i.e., growth rates, size distribution of the stock in question, etc.) across the area.

4.1.6. Special Case – Yellowtail Flounder

Size-disaggregated conversion factors for the *Needler* time series were estimated for Yellowtail Flounder for application in Div. 3LNOPs Spring and 3LNO Fall by combining data across both seasons. A length-dependent conversion is evident, and residuals do not indicate a significant impact of season within the conversion factor estimation. Therefore, a conversion is required for both spring and fall *Needler* series, to be applied by length, for Yellowtail Flounder. Exploration of conversions for fall alone were generally consistent with those from seasons combined. Data were insufficient to estimate spring-only conversions.

4.2. DIVERSITY AND COMMUNITY COMPOSITION

All results for this section are presented in **Appendix 3**.

Richness was significantly lower in the paired sets with the *Needler* than the paired sets with the *Teleost* (Figure A3–1; full: $\chi^2 = 32.6$, $p < 0.001$, fish: $\chi^2 = 27.4$, $p < 0.001$) and did not differ between the new vs old vessel when accounting for station. Alternatively, Shannon-Weaver diversity did not differ between *Teleost* vs *Needler* pairs but there was a significant difference between old vs new vessels when accounting for variation between stations (Figure A3–2; full: $\chi^2 = 12.3$, $p < 0.001$, fish: $\chi^2 = 6.17$, $p = 0.013$), with lower diversity observed in sets from the

older vessels, i.e., *Needler* and *Teleost*. Similarly, Pielou's evenness did not differ between *Teleost vs Needler* pairs, but did differ between old vs new vessels when accounting for variation between stations (Figure A3–3; full: $\chi^2 = 8.94$, $p = 0.002$, fish: $\chi^2 = 6.60$, $p = 0.010$), with lower evenness in sets from the older vessels. The interaction between vessel and pair group was not significant in any models so was removed.

Final results of the nMDS for full community and fish communities had stress of 0.15 and 0.13, respectively. In both analyses there was high correlations on Sheppard stress plots ($R^2 > 0.88$ in all cases). There was a high level of overlap of sets within nMDS plots for both full and fish communities (Figure A3–4, Figure A3–5). In both cases there was a group of sets that clustered together within the *Needler-Cabot* pairs along the nMDS2 axis with all pairs (from both *Needler* and *Cabot*) being found in the cluster together. Despite visually appearing to be similar based on nMDS, in the case of both the full and fish communities there is a significant difference in the interaction term between vessel and pair group (full: $F = 3.84$, $p < 0.001$, fish: $F = 3.82$, $p < 0.001$) but it explained very little of the variation (full: $R^2 = 0.005$, fish: $R^2 = 0.005$). As expected there was a significant difference between stations (full: $F = 1.38$, $p < 0.001$, fish: $F = 1.42$, $p > 0.001$) that also explained the majority of the variation in community composition (full: $R^2 = 0.56$, fish: $R^2 = 0.56$). Many species contributed to the variation in biological community between new and old vessel comparisons for both the full and fish community (Figure A3–6). More than 21 species had a significant difference in all comparisons.

Differences in richness between *Teleost vs Needler* paired sets is likely a result of areas and communities being sampled. Similarity in richness within paired sets suggests that there is not a widespread issue with species detectability at the taxonomic level that current species are being identified to on the vessels at the moment. This analysis removed extremely rare species (less than 7 observation over 533 sets), so this may be a problem for extremely rare species, or species that are currently being grouped at a taxonomic level (e.g., corals).

The differences in diversity and evenness are being driven by different catch weights for species, and support the need for conversion factors. At the time of the analysis, conversion factors were not available to see if corrected catch weights would result in similar diversity and evenness within pairs. This is something that can be explored in the future. The subtle differences in measures of diversity highlight the need for caution when exploring all measure of diversity that span the transition in vessels, and should be considered in analyses.

Community composition, similar to outcomes for measures of diversity, were similar but did display significant differences. Variation within paired sets were generally less than the variation amongst all sets (Figure A3–4, Figure A3–5). Many of the paired sets overlapped on each other, thereby making interpretation of the nMDS difficult. Clusters of sets were notable in the first two dimensions, but all sets within pairs were in the same cluster suggesting that a similar community was being sampled. Though Figure A3–4, Figure A3–5 showed similar community composition, statistical analysis of the distance matrix revealed significant differences in the community between *Teleost* and *Needler* pairs and old and new vessels. These differences were statistically significant but subtle and explain little in the observed variation, and were driven by multiple species (Figure A3–6). It should be noted that the species that differed significantly between pairs were not always the most common and different species were driving the pattern between the *Teleost* pairs vs *Needler*. This could be the result of different areas being targeted by the *Needler vs Teleost* or some species being more sensitive to the differences in the trawl configuration on *Needler vs Teleost*. Much of the variation was explained by the difference in station. This was expected since multiple areas with different community compositions were targeted during comparative fishing to ensure conversion factor analysis could be completed for as many species as possible. Similar to measures of diversity, analysis of community composition needs to be considered across the entire span of the transition period

between new and old vessels, to ensure ecosystem indicators remain consistent across vessel changes. The emphasis of comparative fishing to date has been on developing conversion factors for single species. Future analyses should strive to incorporate further community structure assessment to ensure accurate representation of rarer species that are important to ecosystem status, but may not be caught frequently enough to assess catchability comparisons as a single species.

4.3. BENTHIC HABITAT VARIABLES

All results for this section are presented in **Appendix 3**.

Final solutions for the nMDS looking at benthic habitat variables had a stress of 0.056 and 0.078 for analysis that included all sets and analysis that removed sets with no benthic substrate information, respectively. In both analyses, there were high correlations on Sheppard stress plots ($R^2 > 0.98$ in all cases). There was a high level of overlap between most paired sets across all dimensions (Figure A3–7), though there was a significant difference in the interaction term between vessel and pair group within the analysis when substrate type was removed. Nonetheless, the interaction did not explain much variation in the distance matrices in either analysis (set rm: $R^2 = 0.002$, $F = 1.86$, $p = 0.11$ var rm: $R^2 = 0.004$, $F = 4.40$, $p = 0.007$) with most of the variation explained by station (set rm: $R^2 = 0.59$, $F = 1.51$, $p = 0.01$, var rm: $R^2 = 0.64$, $F = 2.04$, $p = 0.01$). The benthic variables of trawls during 2021 and 2022 within the *Teleost* and *Cartier/Cabot* overlapped (Figure A3–8) though were significantly different (set rm: $R^2 = 0.11$, $F = 46.8$, $p = 0.001$, var rm: $R^2 = 0.11$, $F = 46.1$, $p = 0.001$). In all cases, the differences were driven by the majority of benthic habitat variables as opposed to a limited number of them (Figure A3–12).

Paired sets sampled nearly identical benthic habitats with a high level of overlap of all points on the nMDS plots (Figure A3–7, Figure A3–11). The few sets with low overlap are likely the result of spatial mismatch in driving variables from spatiotemporal models and not reflective of real differences in habitat. The majority of the variation in habitat was between paired sets.

Similar benthic habitat was sampled in 2021 and 2022 by the *Teleost*, although it was not identical (Figure A3–8). The range of all benthic variables overlapped between the years (Figure A3–13). The overlap in range of all variables, coupled with overlap within the nMDS plots suggest that these two years can be combined as these were sampling areas that shared similar benthic habitat, albeit not identical.

5. CONCLUSIONS

- The data obtained in 2021–22 are sufficient to reliably test for differences in relative catch efficiency between vessels and to estimate conversion factors and length-dependent conversion factor functions for the CCGS *Teleost* fall series, and for a portion of taxa and areas within the CCGS *Alfred Needler* fall series.
- Comparative fishing data are insufficient to determine conversion factors for the Spring CCGS *Alfred Needler* time series, and for the *Needler* time series on the Grand Bank (Div. 3LNO).
- For the CCGS *Teleost*, conversion factors were defined for 14 taxa including 2 with significant length effects, 18 taxa showed no significant difference in relative catchability, and 9 evaluated taxa had insufficient data to determine if a conversion factor is appropriate.
- For the CCGS *Alfred Needler*, conversion factors were defined for 15 taxa including 6 with significant length effects, 17 taxa showed no significant difference in relative catchability,

and 12 evaluated taxa had insufficient data to determine if a conversion factor is appropriate.

- In general, the trawl geometry and performance of the CCGS *Alfred Needler* showed considerable differences when compared to that of the other three vessels. The standard and modified Campelen trawl geometry were very comparable among and between the *Teleost* and the new vessels, *Cabot*, and *Cartier*, with often small differences in average towing speeds and tow duration.
- Analysis of benthic variables of the comparative fishing sets indicate that both the CCGS *Alfred Needler* and CCGS *Teleost* comparative data is representative of the typical survey area sampled for which the conversion factors are applicable (3KL, and 2HJ3K + 3L deep respectively, <1,000 m), though there was a reduced range of depth, slope and terrain ruggedness in the areas sampled by CCGS *Teleost*, as a result of the missing deep and shelf edge sets.
- Further work is needed to fill in identified data gaps in the CCGS *Teleost* data with deep (>1,000 m) and shallow (<150 m) sets and is planned for the 2023 comparative fishing program. Additionally, further conversion factors may be developed for different groupings and species depending on the availability of length-based data.
- Analysis of community structure and diversity indicates that both vessel pairs were fishing the same communities when conducting paired sets, and the differences detected in species diversity and evenness within catches supports the need for conversion factor analysis between the vessels.

6. ACKNOWLEDGEMENTS

The Comparative Fishing program could not have been undertaken without the massive effort, sacrifice, and dedication from sea-going staff and shore support! Thanks also to all CCG crew aboard these vessels, without whom fishing operations would not be possible.

Authorship note: beyond the leads S. Trueman & L. Wheeland, authors are listed alphabetically.

7. REFERENCES CITED

- Assis, J., Tyberghein, L., Bosh, S., Verbruggen, H., Serrão, E. A., and De Clerck, O. 2017. [Bio-ORACLE v2.0: Extending marine data layers for bioclimatic modelling](#). *Global Ecol. Biogeogr.* 27(3): 227–284.
- Benoît, H.P., and Swain, D.P. 2003. [Accounting for length- and depth-dependent diel variation in catchability of fish and invertebrates in an annual bottom-trawl survey](#). *ICES J. Mar. Sci.* 60(6): 1298–1317.
- Benoît, H.P., Yin, Y., and Bourdages, H. 2024. [Results of Comparative Fishing Between the CCGS *Teleost* and CCGS *John Cabot* in the Estuary and Northern Gulf of St. Lawrence in 2021 and 2022](#). *DFO Can. Sci. Advis. Sec. Res. Doc.* 2024/007. xvii + 229 p.
- Brooks, M.E., Kristensen, K., van Benthem, K.J., Magnusson, A., Berg, C.W., Nielsen, A., Skaug, H.J., Mächler, M., and Bolker, B.M. 2017. glmmTMB balances speed and flexibility among packages for zero-inflated generalized linear mixed modeling. *R Journal.* 9(2): 378–400.
- Dunn, P.K., and Smyth, G.K. 1996. [Randomized Quantile Residuals](#). *J. Comput. Graph. Stat.* 5(3): 236–244.

-
- Dunn, P.K., and Smyth, G.K. 2005. [Series evaluation of Tweedie exponential dispersion model densities](#). *Statist. Comput.* 15: 267–280.
- GEBCO Compilation Group. 2023. GEBCO 2023 Grid.
- Green, P.J., and Silverman, B.W. 1993. [Nonparametric Regression and Generalized Linear Models: A roughness penalty approach \(1st ed.\)](#). Chapman and Hall/CRC.
- Hartig, F. 2022. DHARMs: Residual diagnostics for hierarchical (multi-level/mixed) regression models. R package version 0.4.1.
- Hastie, T., Tibshirani, R., and Friedman, J., 2009. *The Elements of Statistical Learning: Data Mining, Inference, and Prediction*. Springer Science and Business Media.
- Kristensen, K., Nielsen, A., Berg, C.W., Skaug, H., and Bell, B.M. 2016. TMB: Automatic Differentiation and Laplace Approximation. *J. Stat. Softw.* 70(5): 1–21.
- Miller, T.J. 2013. [A comparison of hierarchical models for relative catch efficiency based on paired-gear data for US Northwest Atlantic fish stocks](#). *Can. J. Fish. Aquat. Sci.* 70(9): 1306–1316.
- Maddock Parsons, D., Rideout, R., and Rogers, R. 2021. Divisions 3LNO Yellowtail Flounder (*Limanda ferruginea*) in the 2018-2020 Canadian Stratified Bottom Trawl Surveys. Serial No. N7187. NAFO SCR Doc. 21/019. 36 p.
- Oksanen, J., Simpson, G., Blanchet, F., Kindt, R., Legendre, P., Minchin, P., O'Hara, R., Solymos, P., Stevens, M., Szoecs, E., Wagner, H., Barbour, M., Bedward, M., Bolker, B., Borcard, D., Carvalho, G., Chirico, M., De Caceres, M., Durand, S., Evangelista, H., FitzJohn, R., Friendly, M., Furneaux, B., Hannigan, G., Hill, M., Lahti, L., McGlenn, D., Ouellette, M., Ribeiro Cunha, E., Smith, T., Stier, A., Ter Braak, C., and Weedon, J. 2022. *Vegan: Community Ecology Package*. R package version 2.6.4.
- Pepin, P., Higdon, J., Koen-Alonso, M., Fogarty, M., and Ollerhead, N. 2014. Application of ecoregion analysis to the identification of Ecosystem Production Units (EPUs) in the NAFO Convention Area. Serial No. N6412. NAFO SCR Doc. 14/069. 13 p.
- R Core Team. 2021. *R: A language and environment for statistical computing*. R Foundation for Statistical Computing, Vienna, Austria.
- Thorson, J.T., and Minto, C. 2015. [Mixed effects: a unifying framework for statistical modelling in fisheries biology](#). *ICES J. Mar. Sci.* 72(5): 1245–1256.
- Tyberghein, L., Verbruggen, H., Pauly, K., Troupin, C., Mineur, F., and De Clerck, O. 2012. [Bio-ORACLE: a global environmental dataset for marine species distribution modelling](#). *Global Ecol. Biogeogr.* 21(2): 272–281.
- Verbyla, A.P., Cullis, B.R., Kenward, M.G, and Welham, S.J. 1999. The Analysis of Designed Experiments and Longitudinal Data by Using Smoothing Splines. *J. Roy. Stat. Soc. Ser. C Appl. Stat.* 48(3): 269–311.
- Walbridge, S., Slocum, N., Pobuda, M., and Wright, D.J. 2018. [Unified Geomorphological Analysis Workflows with Benthic Terrain Modeler](#). *Geosciences.* 8(3): 94.
- Wheeland, L., Skanes, K., Trueman, S. 2024. Summary of Comparative Fishing Data Collected in Newfoundland & Labrador from 2021 - 2022. *Can. Tech. Rep. Fish. Aquat. Sci.* 3579: iv + 132 p.
- Wood, S.N. 2000. [Modelling and Smoothing Parameter Estimation With Multiple Quadratic Penalties](#). *J. Royal Statist. Soc. Ser. B: Stat. Methodol.* 62(2): 413–428.
-

-
- Wood, S.N. 2011. [Fast Stable Restricted Maximum Likelihood and Marginal Likelihood Estimation of Semiparametric Generalized Linear Models](#). J. Royal Statist. Soc. Ser. B: Stat. Methodol. 73(1): 3–36.
- Wood, S.N. 2017. Generalized additive models: An introduction with R, 2nd ed. Chapman and Hall/CRC Press. 496 p.
- Yin, Y. and Benoît, H.P. 2022. A Comprehensive Simulation Study of A Class of Analysis Methods for Paired-Tow Comparative Fishing Experiments. Can. Tech. Rep. Fish. Aquat. Sci. 3466: vi + 99 p.

8. FIGURES

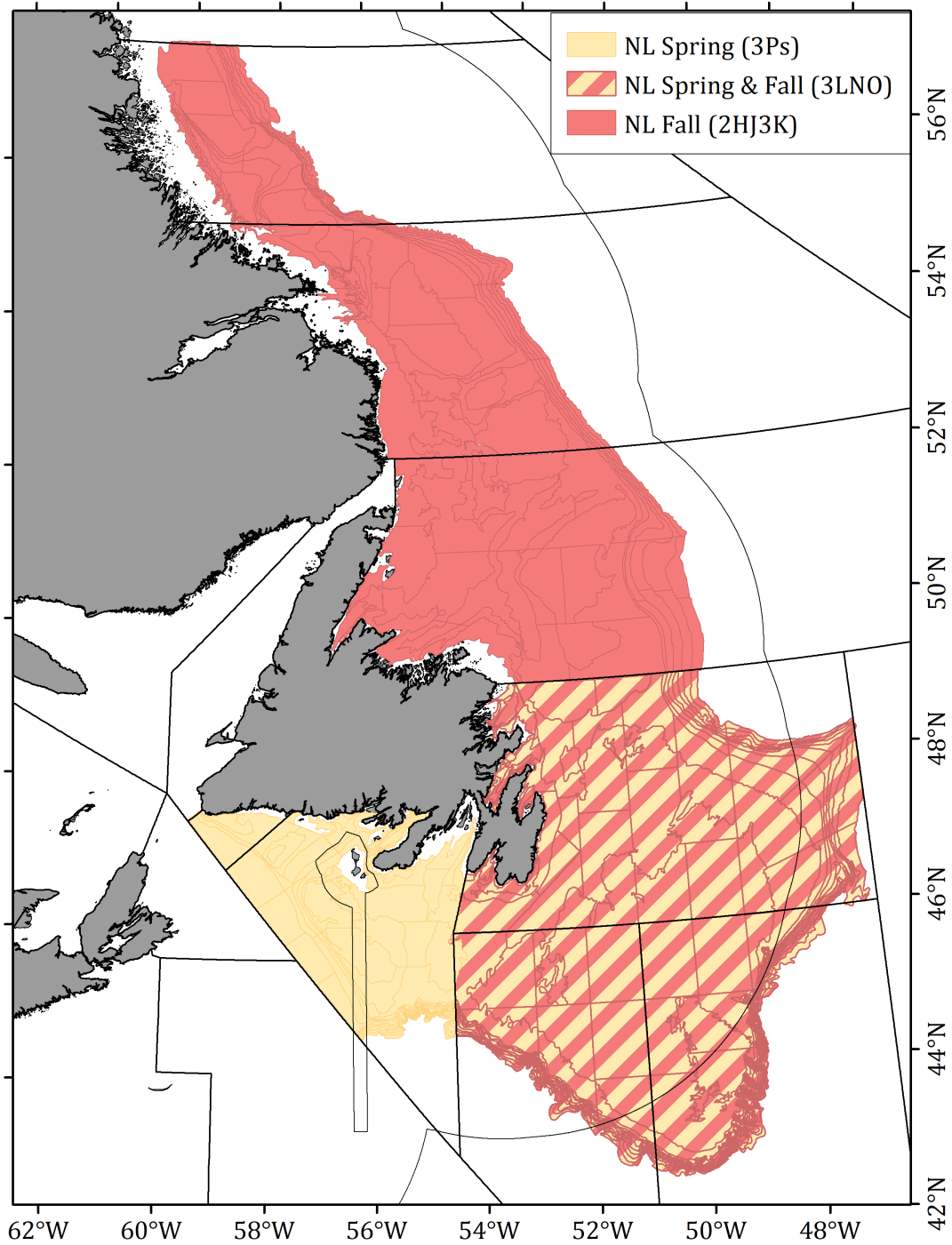


Figure 2. Newfoundland and Labrador Multispecies survey areas. Annually there is a spring survey (NAFO Div. 3LNOPs) and fall survey (NAFO Div. 2HJ3KLNO).

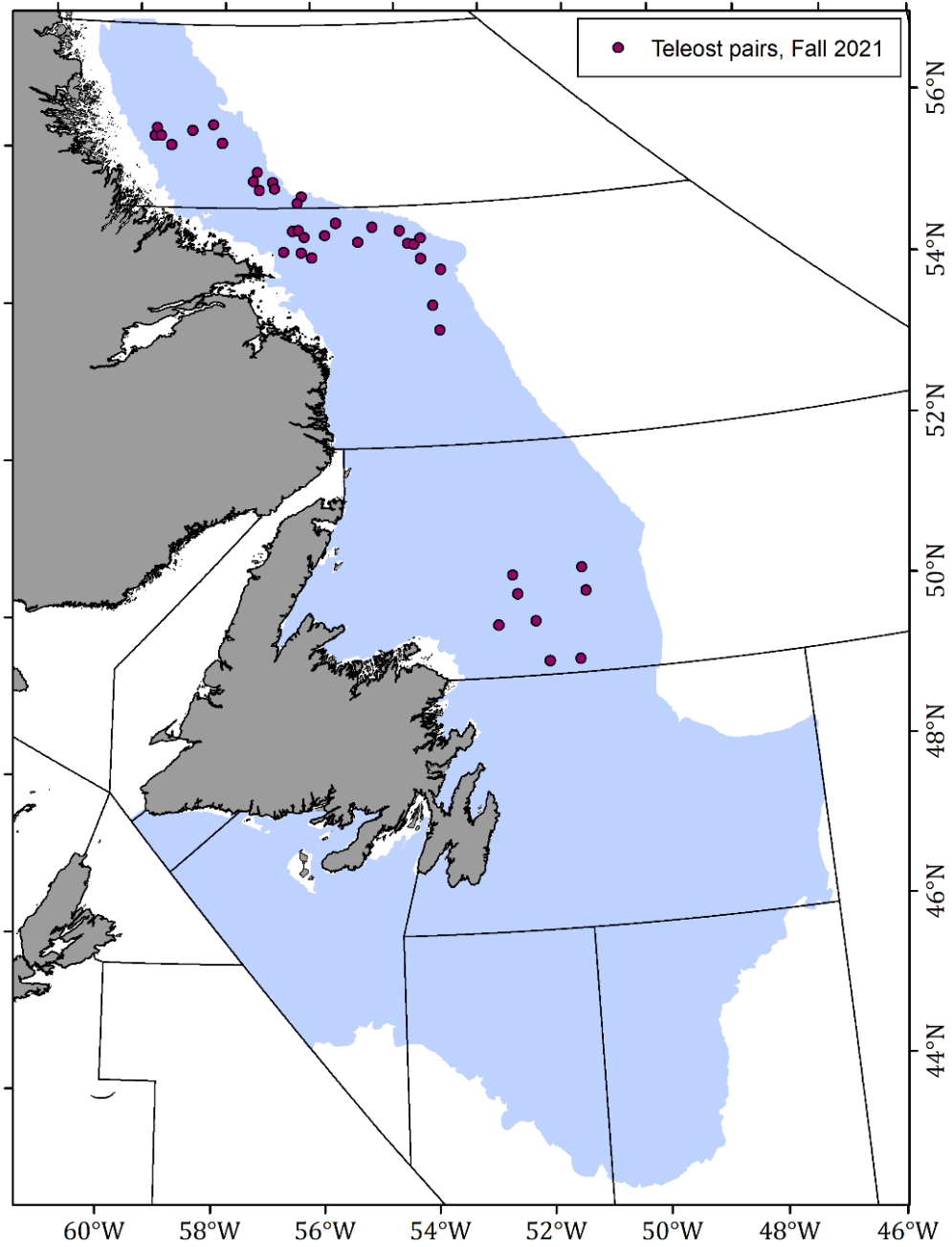


Figure 3. Paired tow locations between the CCGS Teleost and CCGS Capt. Jacques Cartier during the fall 2021 comparative fishing program.

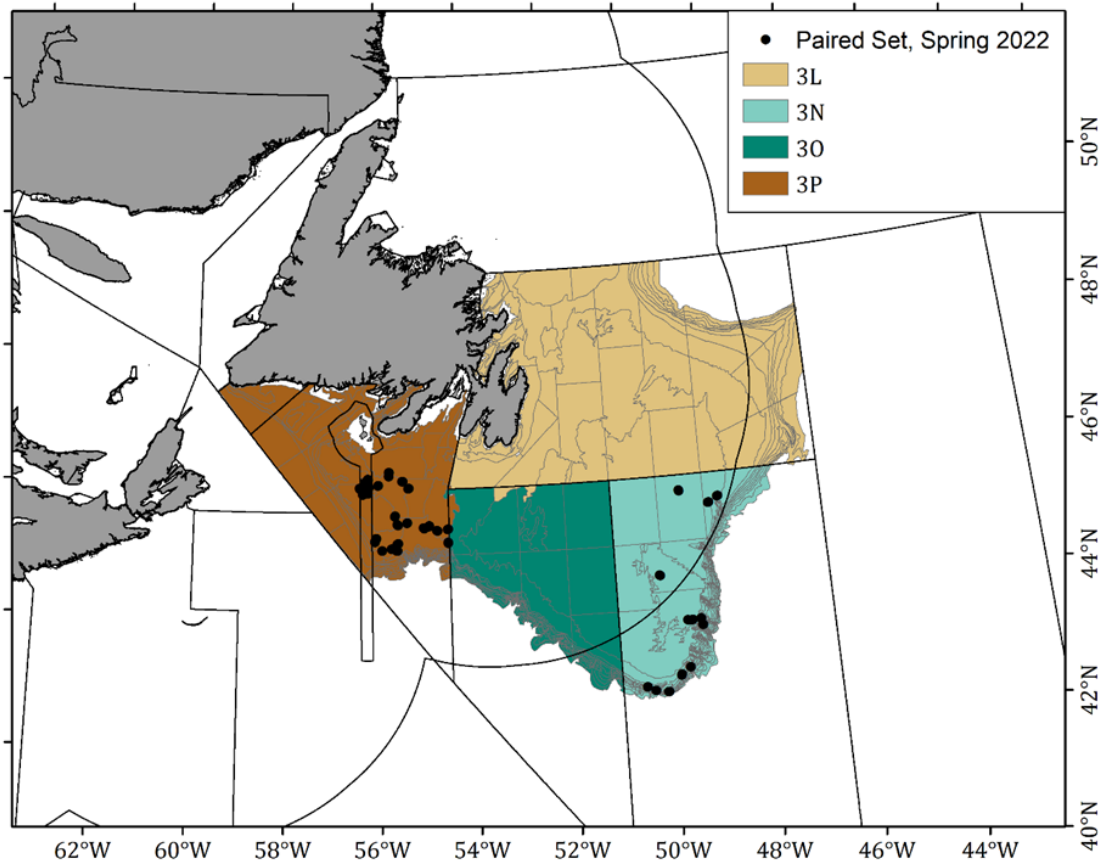


Figure 4. Paired tow locations between the CCGS Alfred Needler and CCGS John Cabot during the spring 2022 comparative fishing program.

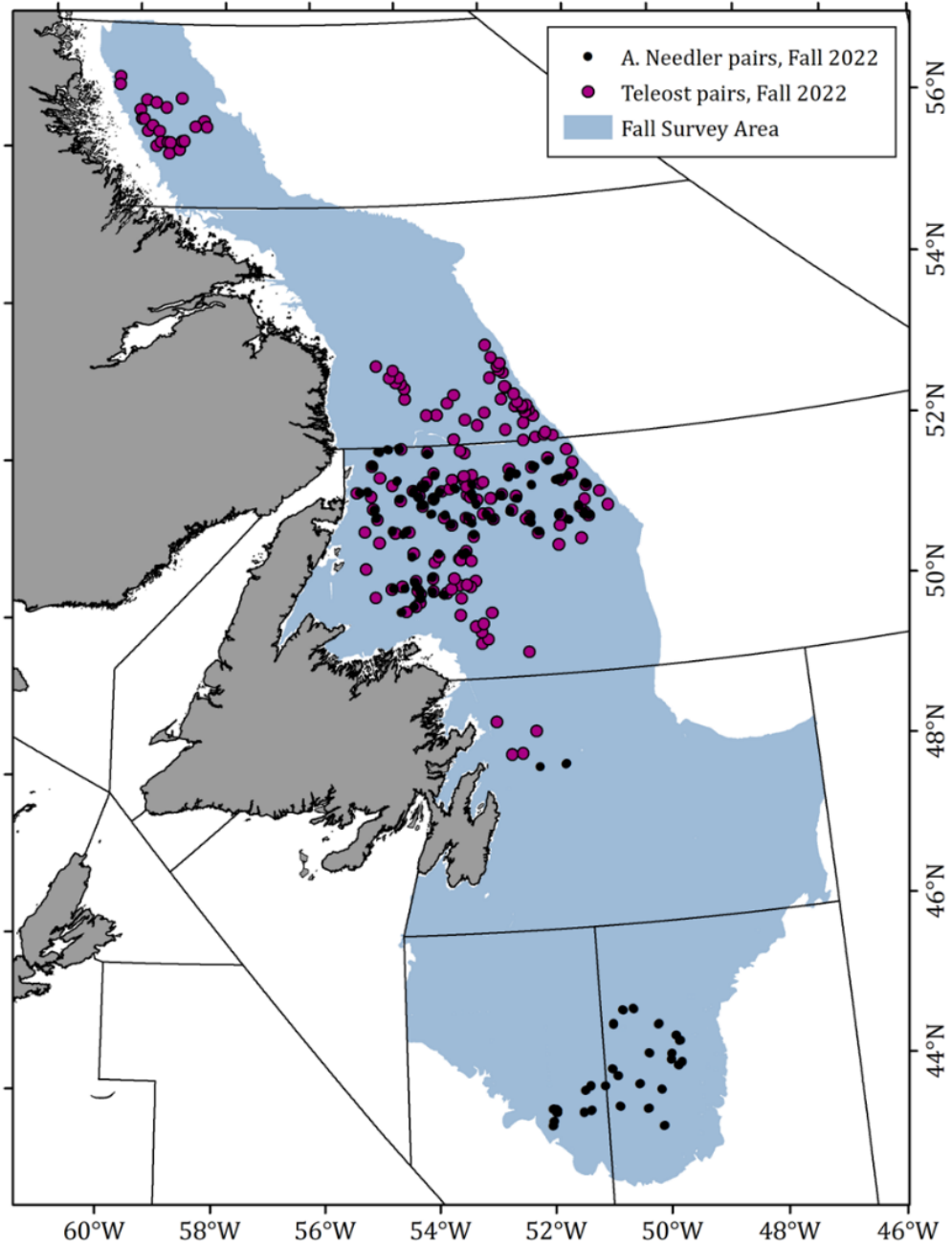


Figure 5. Paired tow locations between the CCGS Teleost and CCGS John Cabot/Capt. Jacques Cartier, and the CCGS Alfred Needler and CCGS John Cabot, during the fall 2022 comparative fishing program.

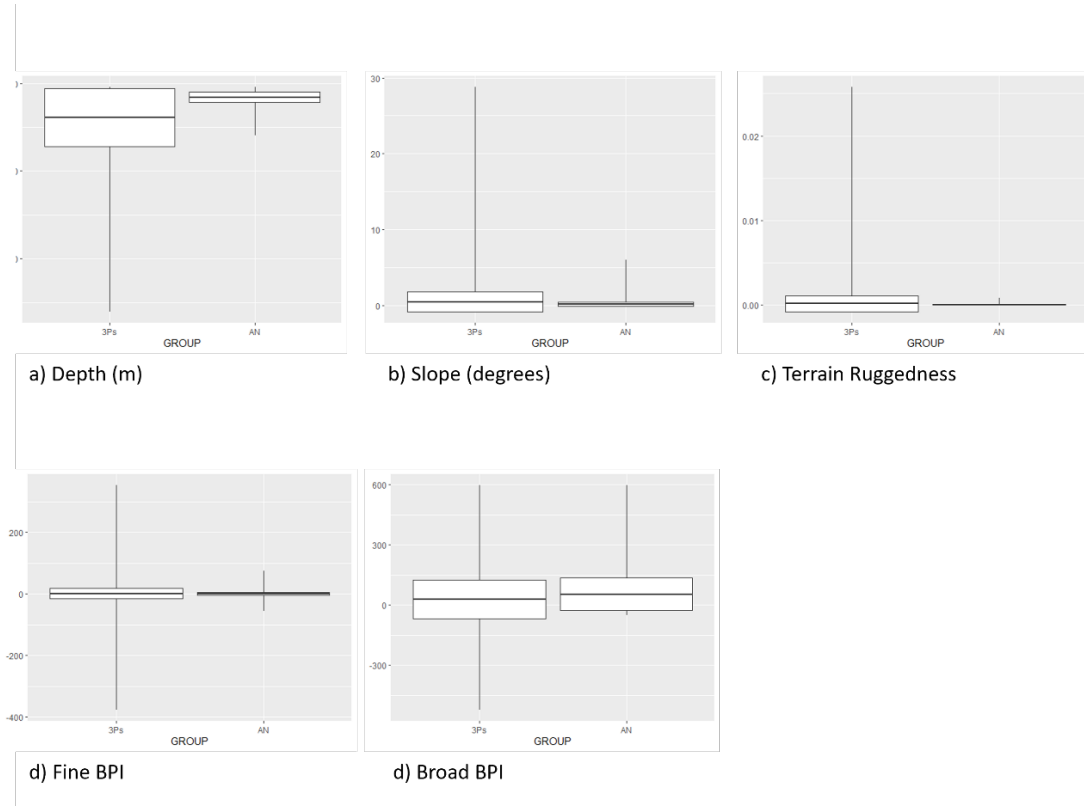
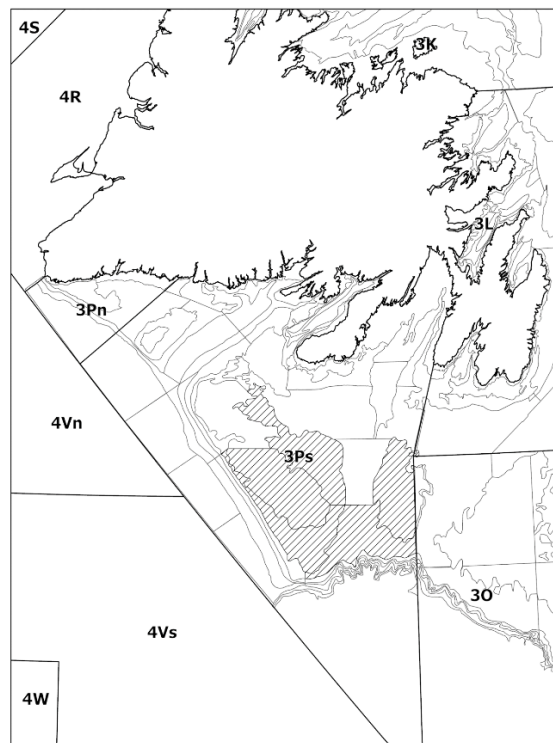


Figure 6. Left: Spring survey strata within NAFO Div. 3Ps; hashed areas indicate strata with ≥ 2 successful comparative fishing sets with the CCGS Alfred Needler in spring 2022. Right: Comparison of the summary statistics for seabed terrain attributes calculated for the full survey areas (3Ps) and for strata where comparative fishing was completed with the CCGS Alfred Needler (AN).

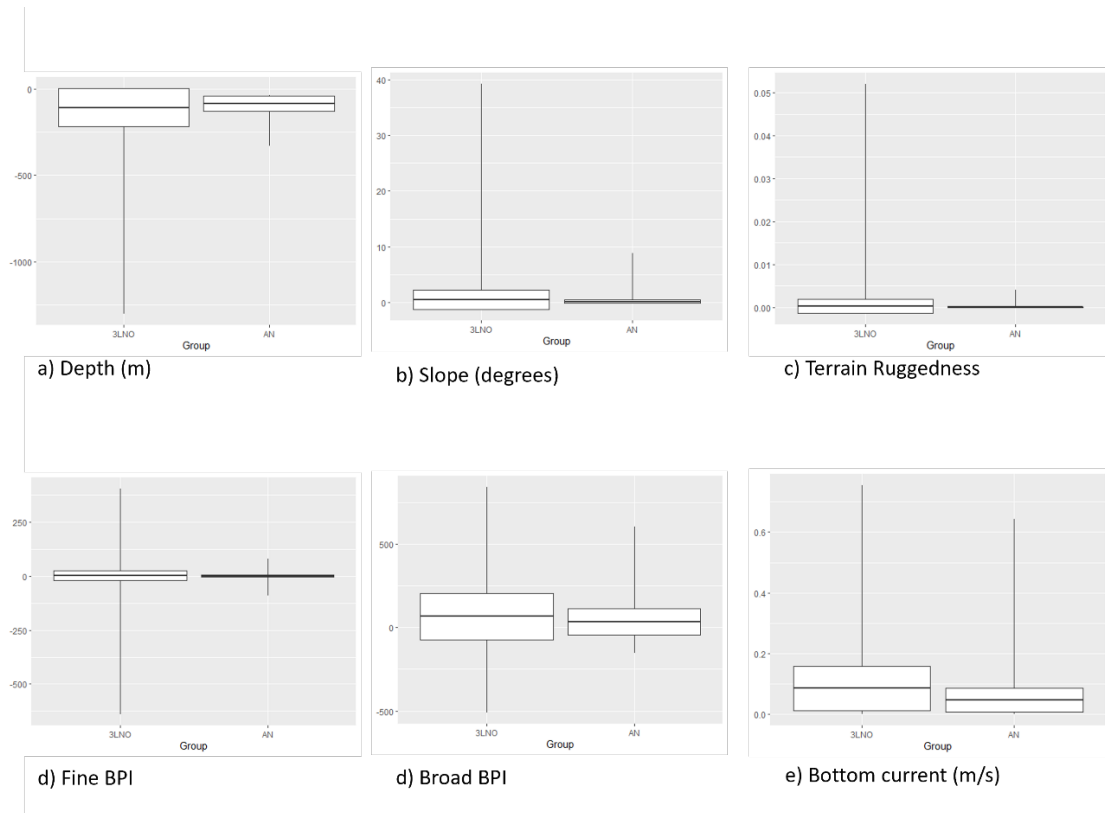
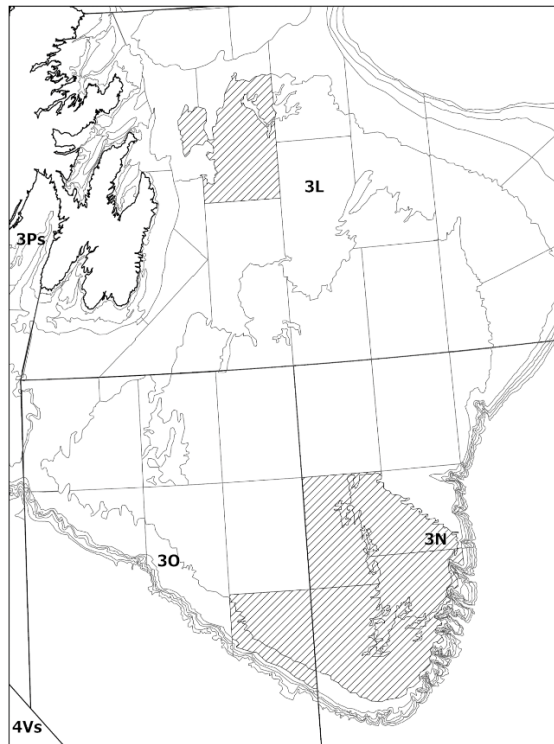


Figure 7. Left: Fall survey strata within NAFO Div. 3LNO; hashed areas indicate strata with ≥ 2 successful comparative fishing sets with the CCGS Alfred Needler in fall 2022. Right: Comparison of the summary statistics for seabed terrain attributes calculated for the full survey areas (3LNO) and for strata where comparative fishing was completed with the CCGS Alfred Needler (AN).

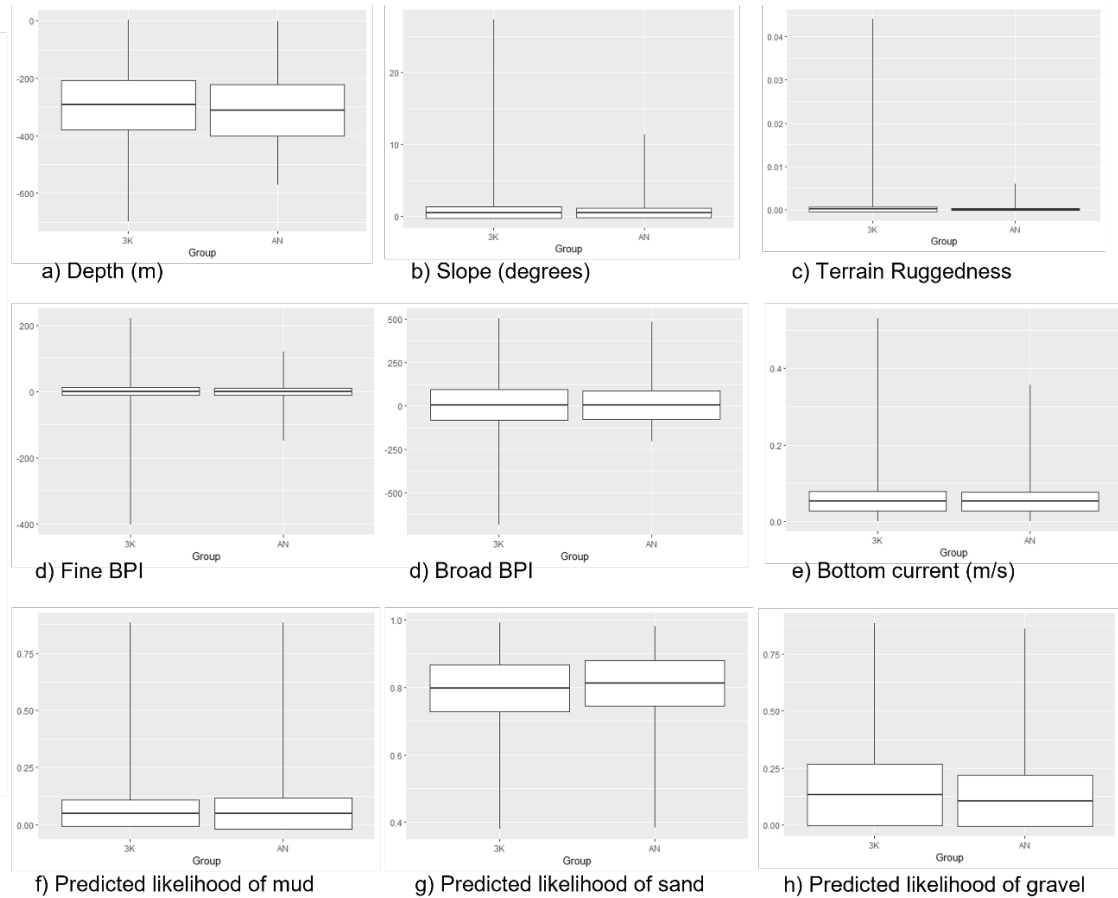
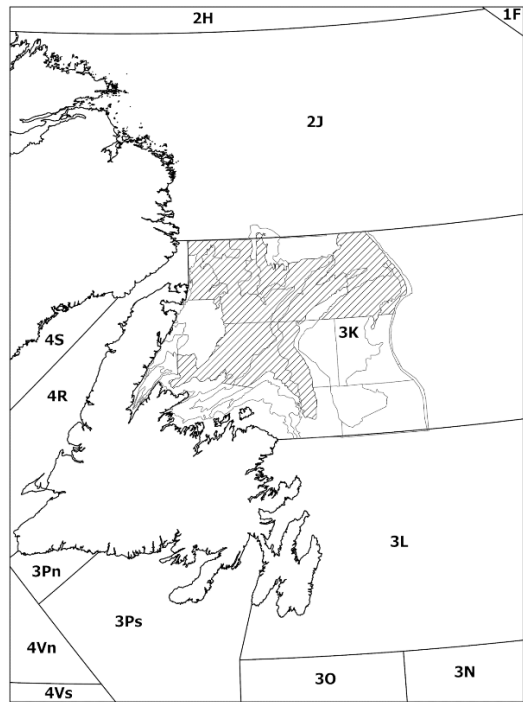


Figure 8. Left: Fall survey strata within NAFO Div. 3K; hashed areas indicate strata with ≥ 2 successful comparative fishing sets with the CCGS Alfred Needler in fall 2022. Right: Comparison of the summary statistics for seabed terrain attributes calculated for the full survey areas (3K) and for strata where comparative fishing was completed with the CCGS Alfred Needler (AN).

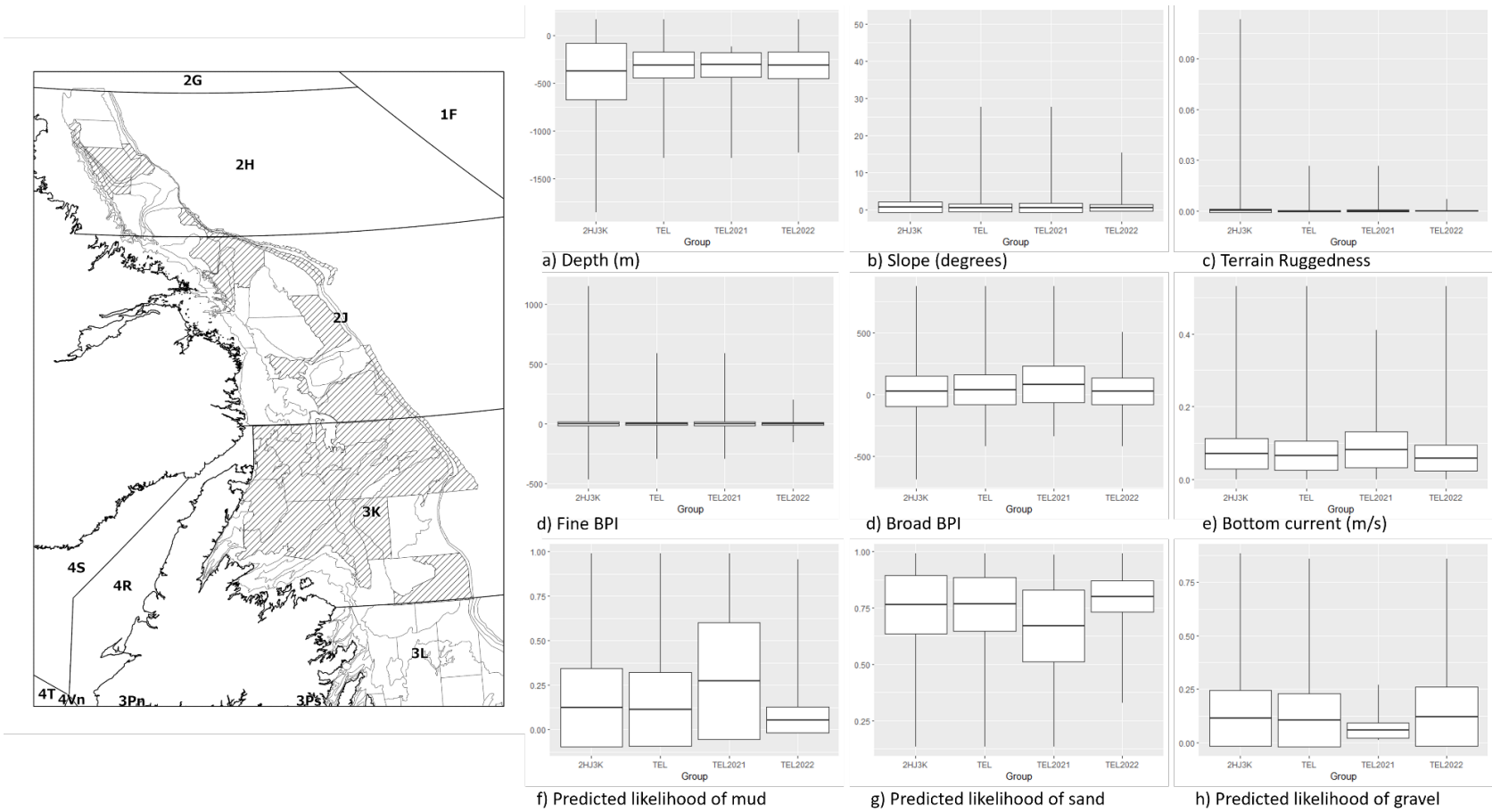


Figure 9. Left: Fall survey strata within NAFO Div. 2HJ3K; hashed areas indicate strata with ≥ 2 successful comparative fishing sets per season with the CCGS Teleost in fall 2021 and 2022. Right: Comparison of the summary statistics for seabed terrain attributes calculated for the full survey areas (2HJ3K) and for strata where comparative fishing was completed with the CCGS Teleost (TEL).

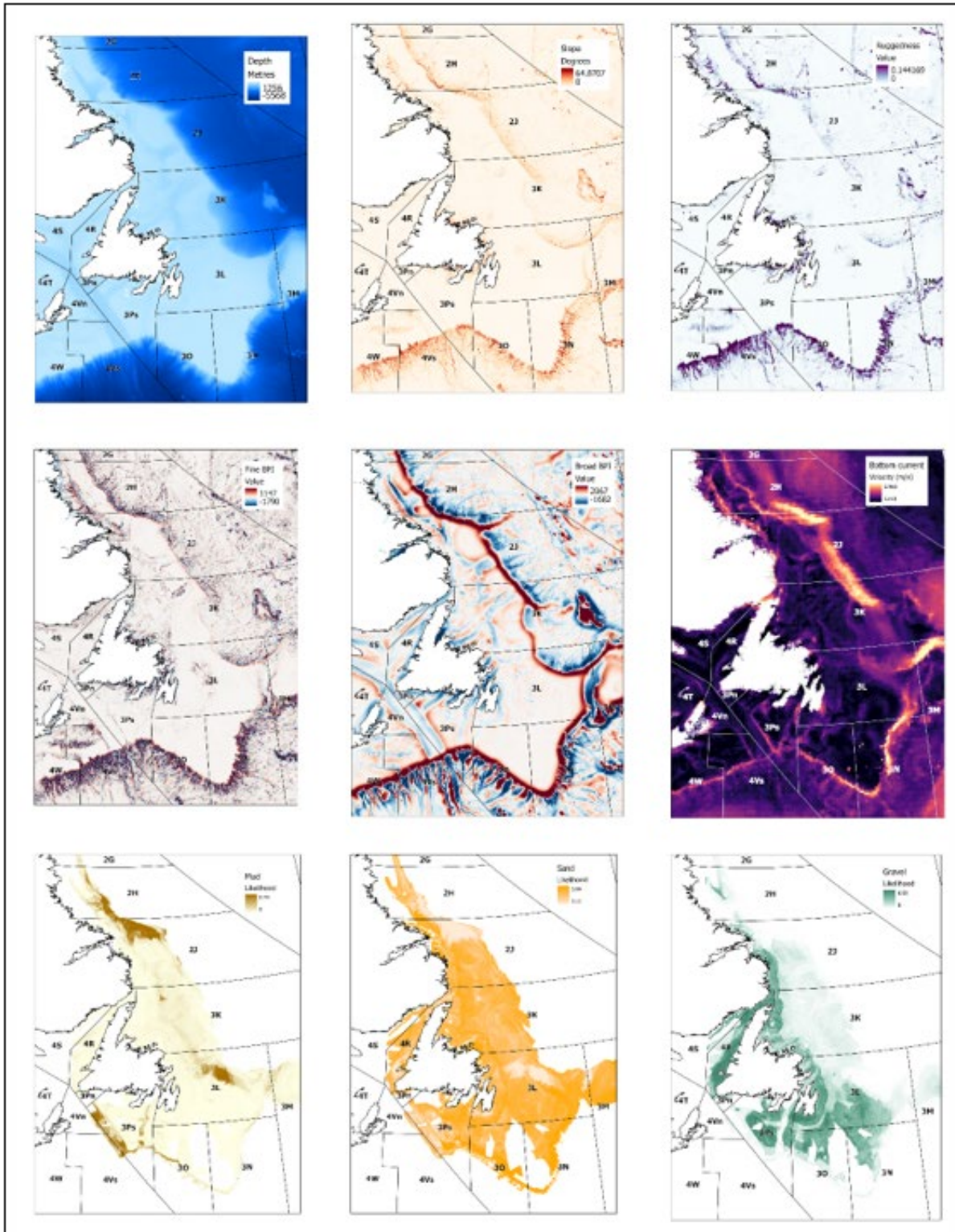


Figure 10. Terrain attributes included in the comparison of the annual survey area characteristics to the completed comparative fishing areas; from left to right: bathymetry, slope, terrain ruggedness, fine benthic position index, broad benthic position index, bottom current velocity, predicted distribution of mud, predicted distribution of sand, and predicted distribution of gravel.

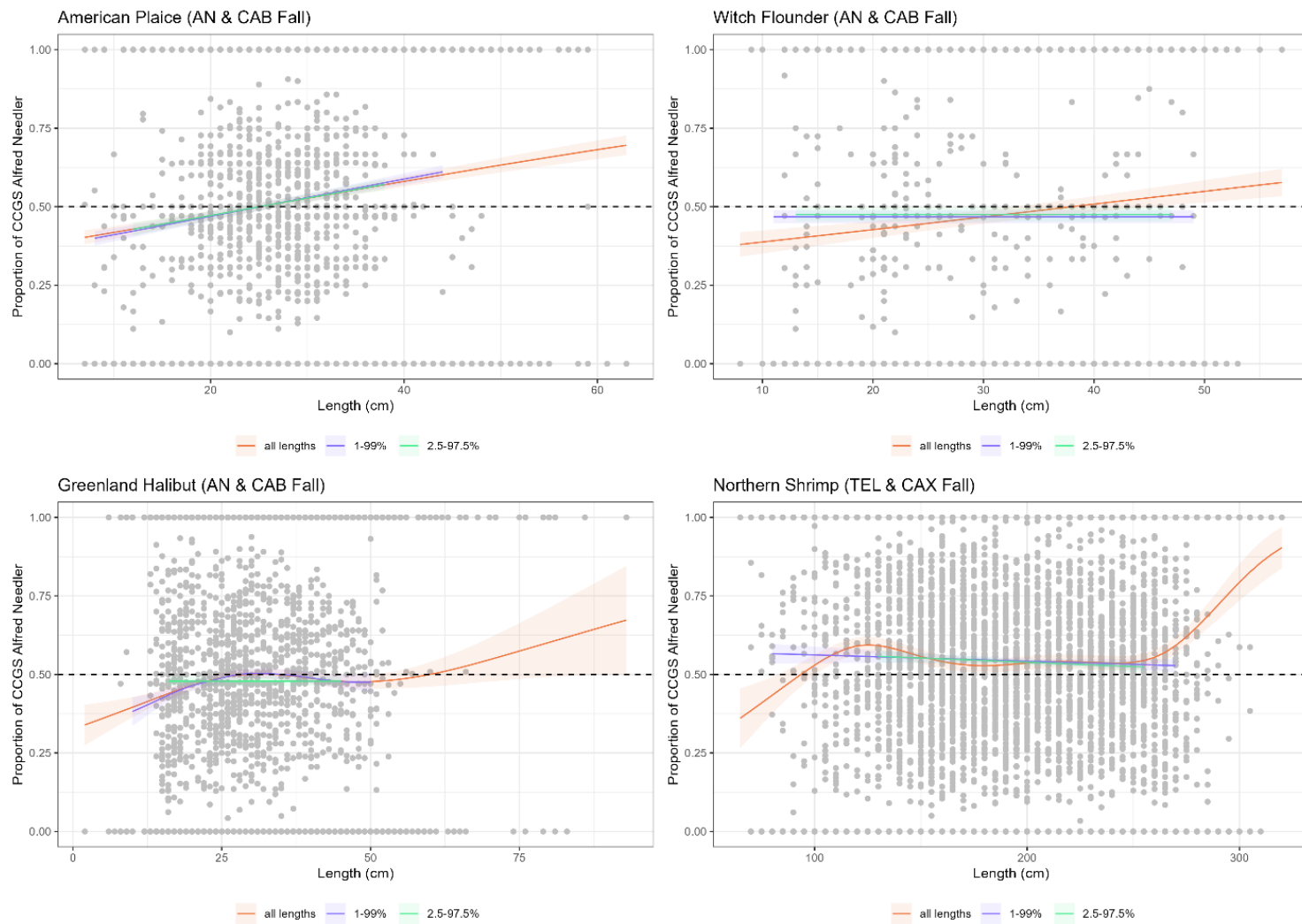


Figure 11. Four examples of length tail sensitivity testing showing model fit to all data (orange), with 1% tails removed at each end, and with 2.5% tails removed at each end (green).

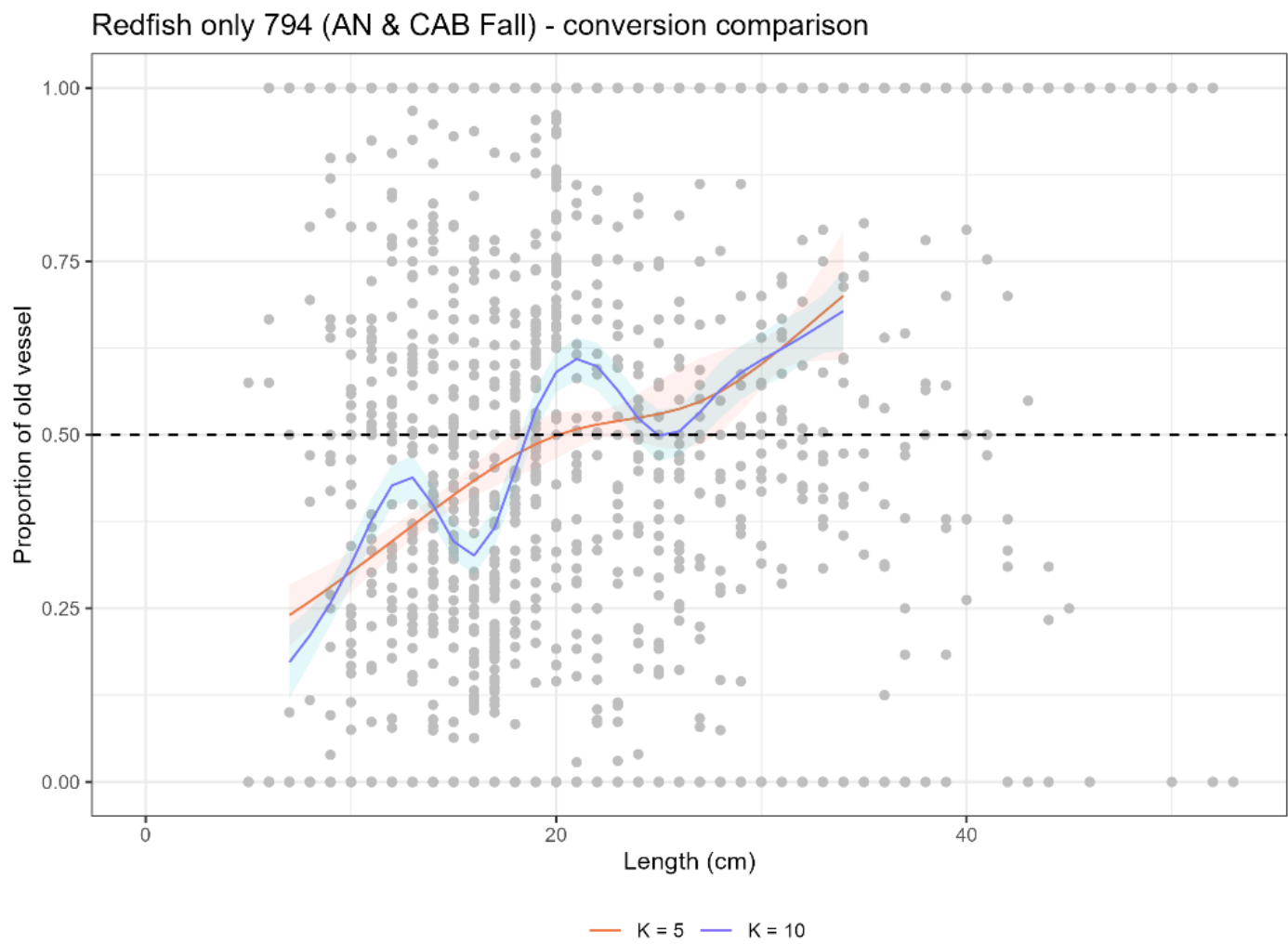


Figure 12. Tests of sensitivity to the maximum number of knots specified in model fitting for redfish (1–99 percentile lengths) with $k = 5$ and $k = 10$.

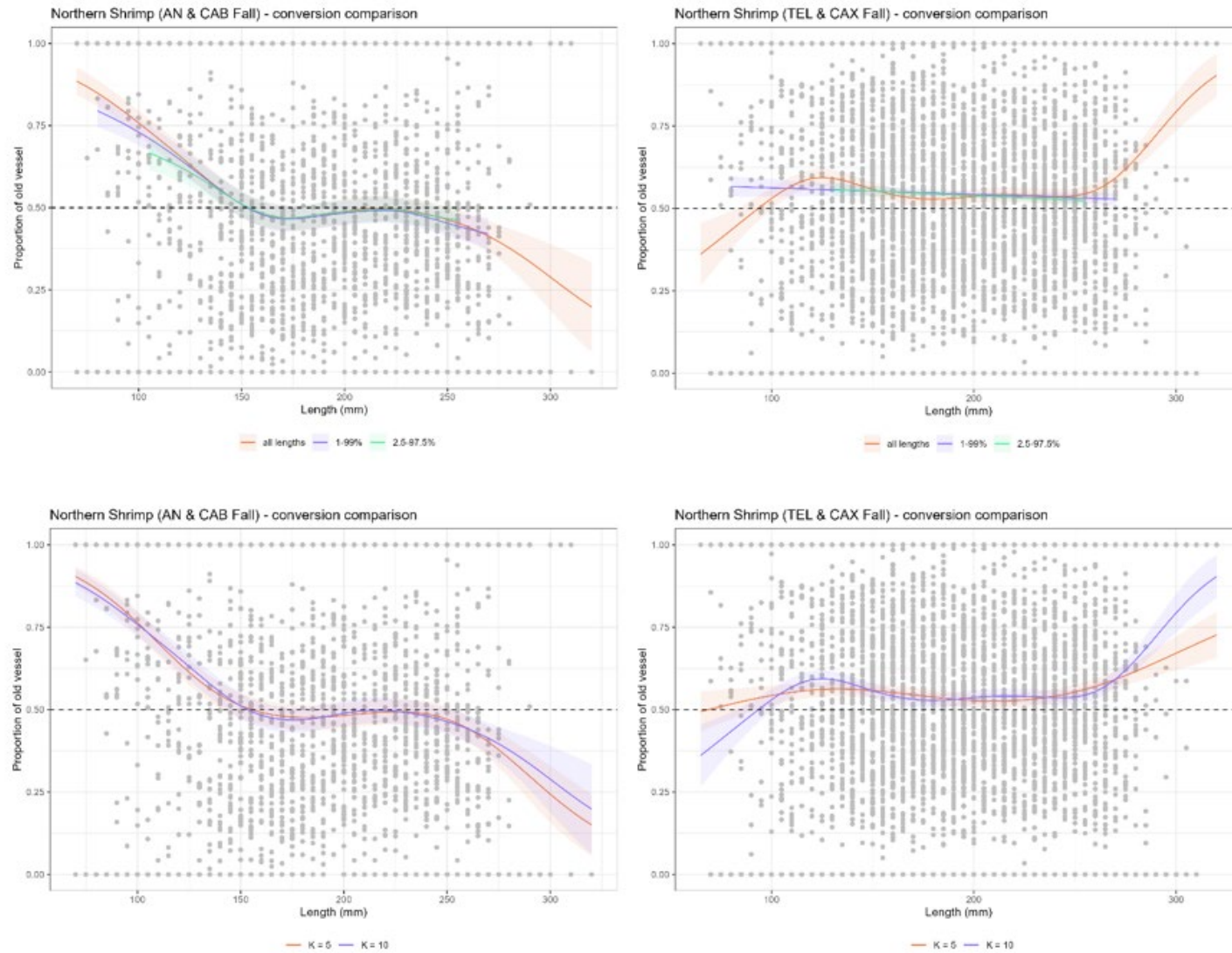


Figure 13. Tests of model sensitivity to length tails and knot specification for Northern Shrimp for CCGS Alfred Needler & CCGS John Cabot (left) and CCGS Teleost & CCGS John Cabot/Capt. Jacques Cartier (right). The knot comparison is shown here on the full length range.

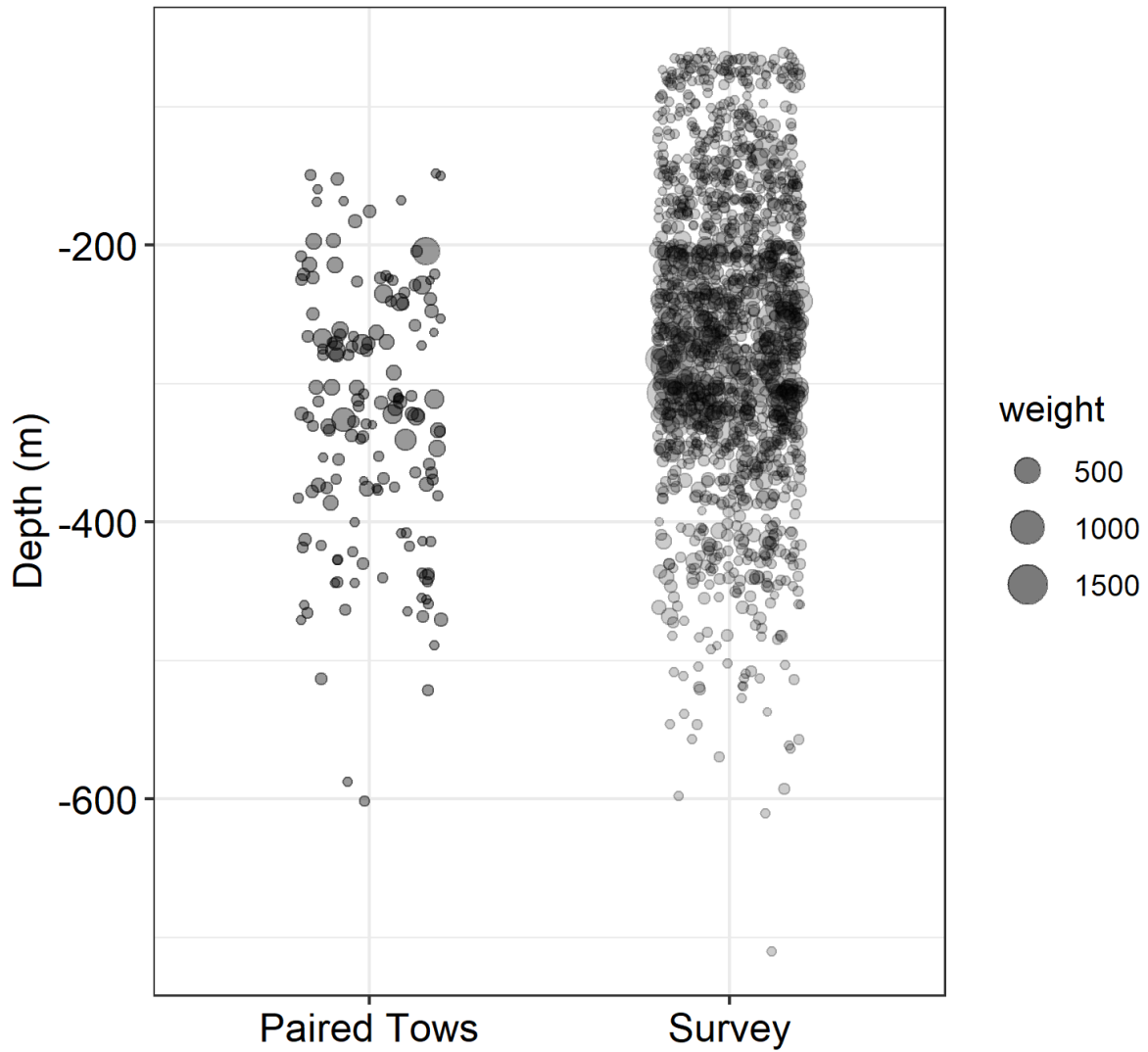


Figure 14. Comparison of depth range for catch of Atlantic Cod (*Gadus morhua*) during the comparative fishing program (paired tows), and during the typical fall survey of 2HJ3KL sampled by the CCGS Teleost for 2016 onwards (survey), where circle size is proportional to catch weight (kg).

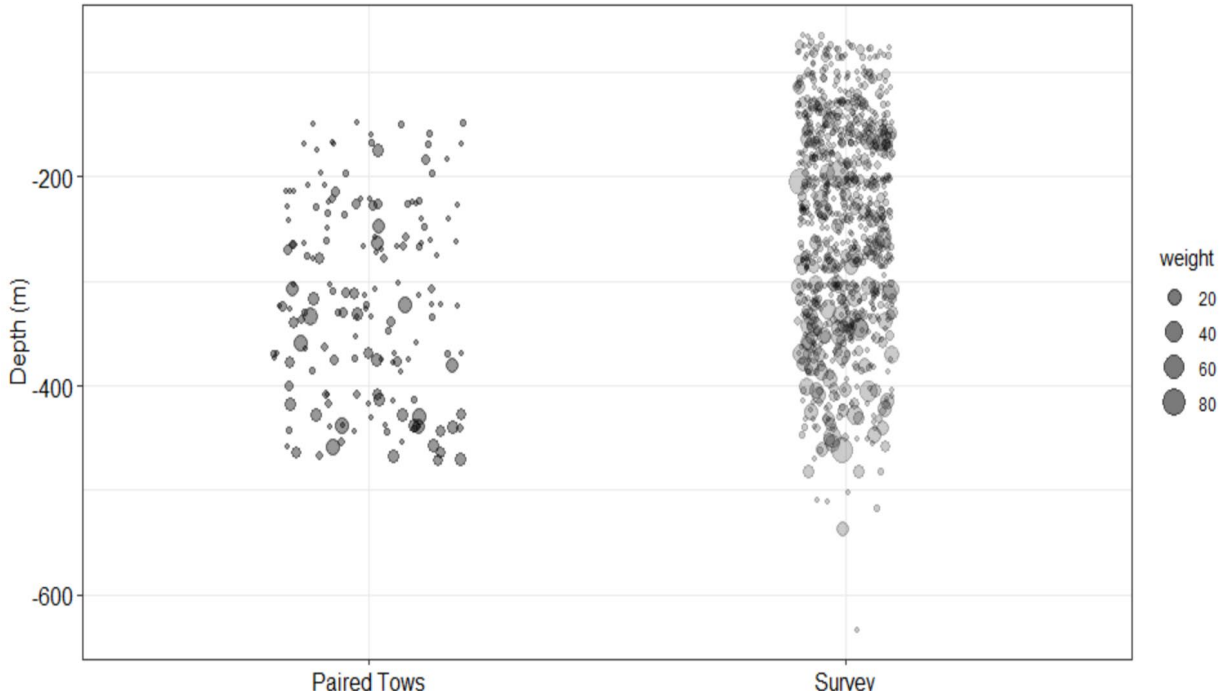


Figure 15. Comparison of depth range for catch of Snow Crab (*Chionoecetes opilio*) for during the comparative fishing program (paired tows), and during the typical fall survey of 2HJ3KL sampled by the CCGS Teleost for 2016 onwards (survey), where circle size is proportional to catch weight (kg).

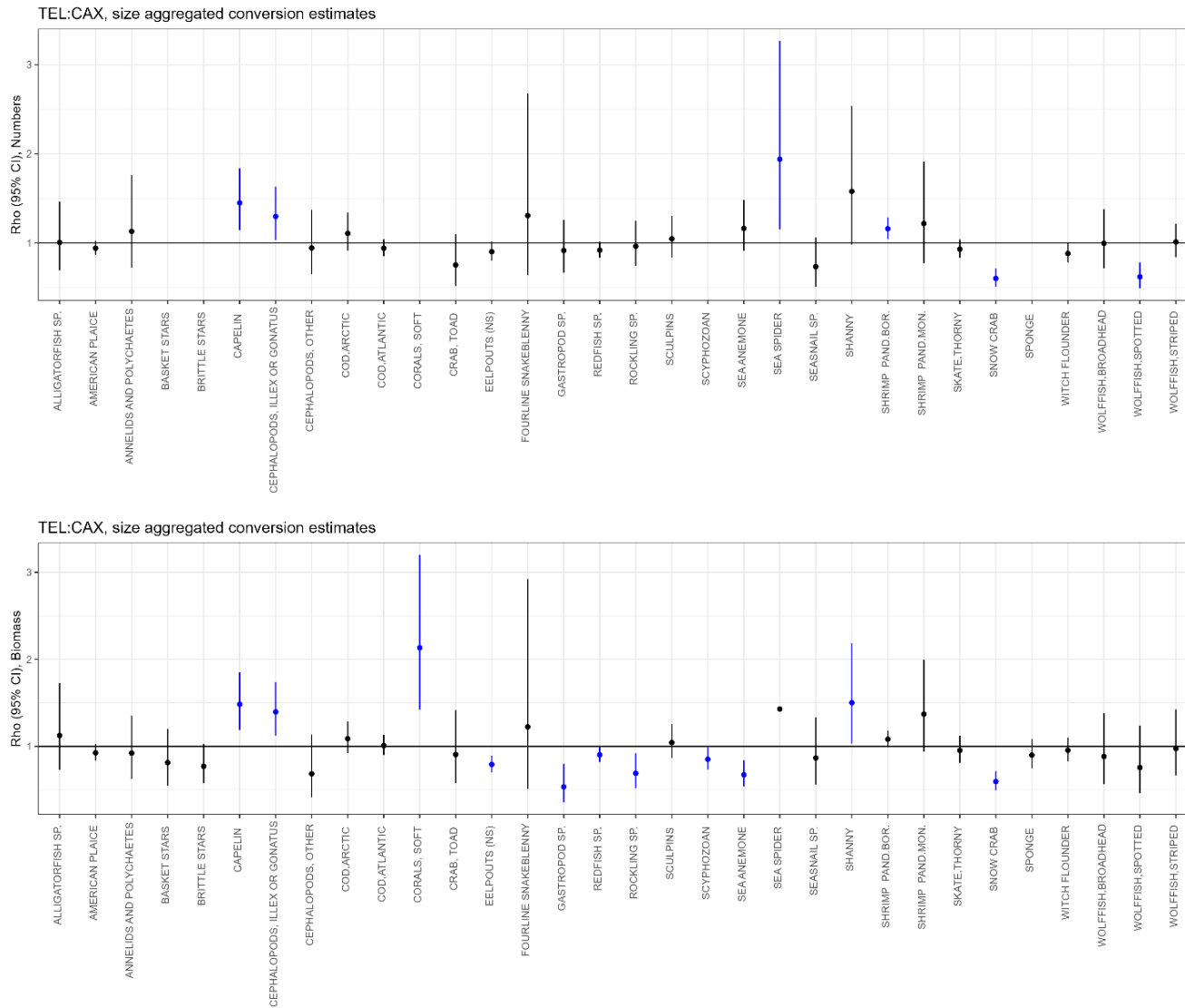


Figure 16. Summary of Rho estimates (+/- 95% CI) for numbers and biomass (weights) from size-aggregated analyses. Significant conversions are shown in blue. The horizontal black line indicates parity in catches between vessels. Taxa for which data are considered insufficient have been removed.

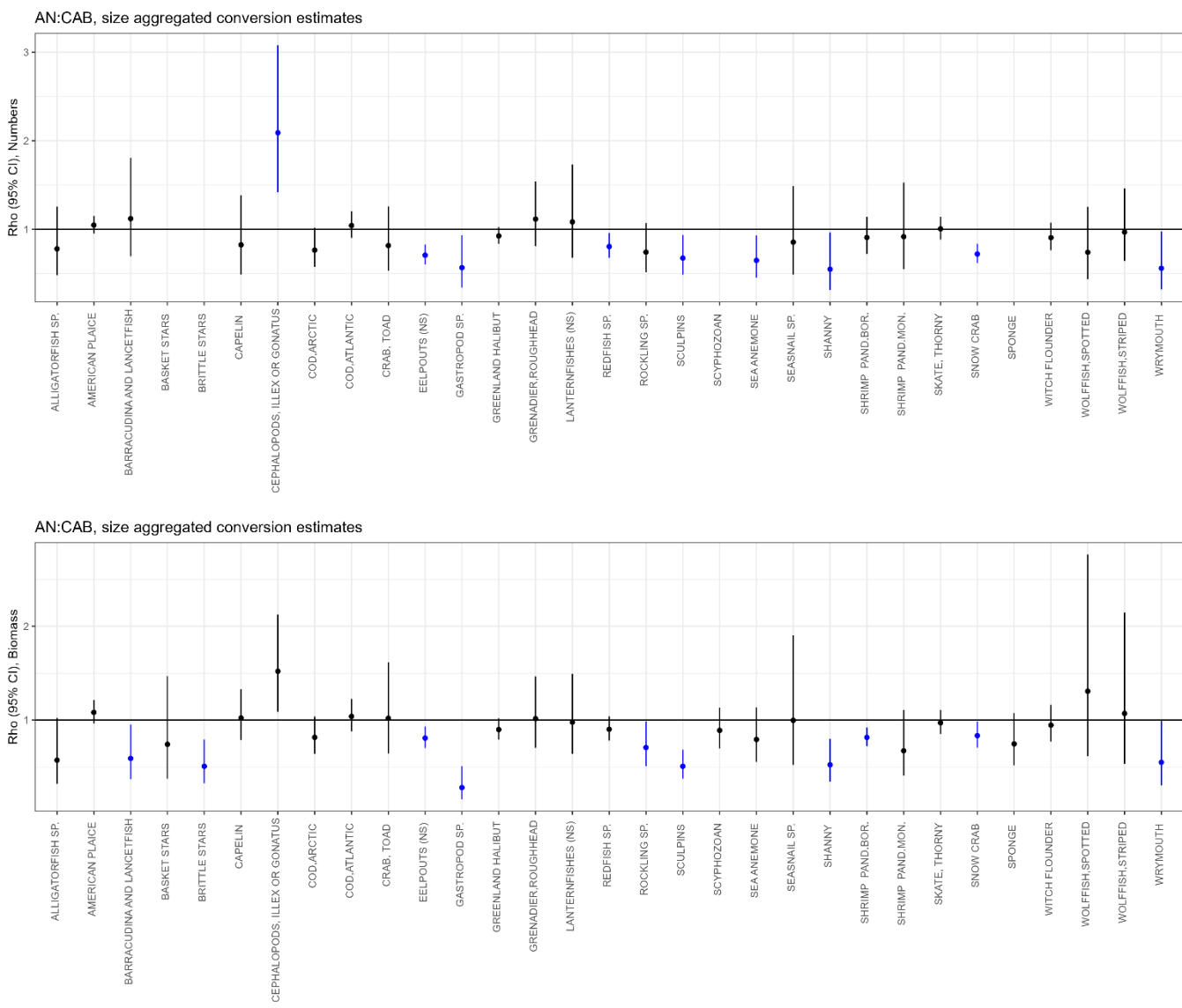


Figure 17. Summary of Rho estimates (+/- 95% CI) for numbers and biomass from size-aggregated analyses. Significant conversions are shown in blue. The horizontal black line indicates parity in catches between vessels. Taxa for which data are considered insufficient have been removed.

9. TABLES

Table 4. A set of binomial models with various assumptions for the length effect and station effect in the relative catch efficiency. A smoothing length effect can be considered, and the station effect can be added to the intercept, without interaction with the length effect, or added to both the intercept and smoother to allow for interaction between the two effects.

Model	$\log(\rho)$	Length Effect	Station Effect
BI0	β_0	constant	not considered
BI1	$\beta_0 + \delta_{0,i}$	constant	intercept
BI2	$X_f^T \beta_f + X_r^T \mathbf{b}$	smoothing	not considered
BI3	$X_f^T \beta_f + X_r^T \mathbf{b} + \delta_{0,i}$	smoothing	intercept
BI4	$X_f^T (\beta_f + \delta_i) + X_r^T (\mathbf{b} + \epsilon_i)$	smoothing	intercept, smoother

Table 5. A set of beta-binomial models with various assumptions for the length effect and station effect in the relative catch efficiency, and the length effect on the variance parameter. A smoothing length effect can be considered in both the conversion factor and the variance parameter. A possible station effect can be added to the intercept, without interaction with the length effect, or added to both the intercept and the smoother to allow for interaction between the two effects.

Model	$\log(\rho)$	$\log(\phi)$	Length Effects	Station Effect
BB0	β_0	γ_0	constant/constant	not considered
BB1	$\beta_0 + \delta_{0,i}$	γ_0	constant/constant	intercept
BB2	$X_f^T \beta_f + X_r^T \mathbf{b}$	γ_0	smoothing/constant	not considered
BB3	$X_f^T \beta_f + X_r^T \mathbf{b}$	$X_f^T \gamma + X_r^T \mathbf{g}$	smoothing/smoothing	not considered
BB4	$X_f^T \beta_f + X_r^T \mathbf{b} + \delta_{0,i}$	γ_0	smoothing/constant	intercept
BB5	$X_f^T \beta_f + X_r^T \mathbf{b} + \delta_{0,i}$	$X_f^T \gamma + X_r^T \mathbf{g}$	smoothing/smoothing	intercept
BB6	$X_f^T (\beta_f + \delta_i) + X_r^T (\mathbf{b} + \epsilon_i)$	γ_0	smoothing/constant	intercept, smoother
BB7	$X_f^T (\beta_f + \delta_i) + X_r^T (\mathbf{b} + \epsilon_i)$	$X_f^T \gamma + X_r^T \mathbf{g}$	smoothing/smoothing	intercept, smoother

Table 6. Relative evidence for length-disaggregated binomial and beta-binomial models for the CCGS Teleost and CCGS John Cabot/Capt. Jacques Cartier comparative fishing analysis based on the Akaike Information Criterion (AIC) and the Bayesian Information Criterion (BIC) and delta (Δ) values compared to lowest AIC/BIC per species. Entries with ‘-’ indicate models that did not converge. BB6 did not converge for any species and is not included in the table.

Value	Species	BI0	BI1	BI2	BI3	BI4	BB0	BB1	BB2	BB3	BB4	BB5
AIC	American Plaice	5,674	5,421	5,667	5,424	-	5,572	5,418	5,574	5,570	5,422	-
Δ AIC	American Plaice	256	3	250	7	-	154	0	156	152	4	-
BIC	American Plaice	5,681	5,435	5,689	5,453	-	5,586	5,439	5,603	5,613	5,458	-
Δ BIC	American Plaice	246	0	254	18	-	152	5	168	178	23	-
AIC	Atlantic Cod	7,391	7,019	7,393	7,019	-	7,248	7,003	7,252	7,254	7,003	7,004
Δ AIC	Atlantic Cod	389	16	391	16	-	246	0	249	251	1	1
BIC	Atlantic Cod	7,399	7,034	7,416	7,049	-	7,263	7,025	7,282	7,299	7,041	7,056
Δ BIC	Atlantic Cod	374	9	391	24	-	238	0	257	274	16	31
AIC	Northern Shrimp	23,602	20,170	23,585	20,167	17,931	18,649	-	18,646	18,597	-	-
Δ AIC	Northern Shrimp	5,671	2,239	5,654	2,236	0	718	-	715	667	-	-
BIC	Northern Shrimp	23,608	20,183	23,604	20,192	17,976	18,661	-	18,672	18,636	-	-
Δ BIC	Northern Shrimp	5,632	2,207	5,628	2,217	0	686	-	696	660	-	-
AIC	Redfish	18,801	14,489	18,774	14,466	-	14,093	13,416	14,093	14,083	-	-
Δ AIC	Redfish	5,385	1,073	5,358	1,050	-	677	0	677	667	-	-
BIC	Redfish	18,809	14,504	18,796	14,495	-	14,107	13,438	14,122	14,127	-	-
Δ BIC	Redfish	5,371	1,066	5,358	1,057	-	669	0	684	689	-	-
AIC	Snow Crab	4,467	4,033	4,435	4,025	-	4,368	4,027	4,350	4,321	4,020	4,018
Δ AIC	Snow Crab	449	15	417	7	-	351	10	333	303	3	0
BIC	Snow Crab	4,474	4,047	4,456	4,054	-	4,383	4,049	4,379	4,364	4,056	4,068
Δ BIC	Snow Crab	427	0	409	6	-	336	2	332	317	9	21
AIC	Spotted Wolffish	537	538	540	541	-	538	540	541	-	-	-
Δ AIC	Spotted Wolffish	0	1	3	3	-	1	2	3	-	-	-
BIC	Spotted Wolffish	545	553	562	569	-	553	561	570	-	-	-
Δ BIC	Spotted Wolffish	0	8	17	25	-	8	16	25	-	-	-
AIC	Striped Wolffish	1,315	1,303	1,319	1,305	-	1,313	1,304	1,316	-	1,307	-
Δ AIC	Striped Wolffish	12	0	16	3	-	10	1	13	-	4	-
BIC	Striped Wolffish	1,322	1,317	1,340	1,333	-	1,327	1,325	1,344	-	1,342	-
Δ BIC	Striped Wolffish	5	0	23	17	-	10	8	27	-	25	-
AIC	Thorny Skate	2,570	2,549	2,564	2,550	-	2,524	2,516	2,526	2,527	2,517	2,519
Δ AIC	Thorny Skate	55	34	48	34	-	9	0	10	12	2	3
BIC	Thorny Skate	2,578	2,564	2,586	2,579	-	2,539	2,538	2,555	2,572	2,554	2,571
Δ BIC	Thorny Skate	40	26	48	41	-	1	0	17	34	16	33
AIC	Witch Flounder	3,462	3,253	3,407	3,243	3,354	3,369	3,252	3,350	-	-	-
Δ AIC	Witch Flounder	219	10	164	0	111	126	9	107	-	-	-
BIC	Witch Flounder	3,469	3,267	3,428	3,271	3,402	3,383	3,273	3,378	-	-	-

Value	Species	BI0	BI1	BI2	BI3	BI4	BB0	BB1	BB2	BB3	BB4	BB5
ΔBIC	Witch Flounder	202	0	161	4	135	116	6	111	-	-	-

Table 7. Relative evidence for length-disaggregated binomial and beta-binomial models for the CCGS Alfred Needler and CCGS John Cabot comparative fishing analysis based on the Akaike Information Criterion (AIC) and the Bayesian Information Criterion (BIC) and delta (Δ) values compared to lowest AIC/BIC per species. Entries with ‘-’ indicate models that did not converge. BB6 did not converge for any species and is not included in the table.

Value	Species	BI0	BI1	BI2	BI3	BI4	BB0	BB1	BB2	BB3	BB4	BB5
AIC	American Plaice	4,488	4,316	4,445	4,287	-	4,392	4,307	4,366	4,365	4,281	-
ΔAIC	American Plaice	208	35	165	7	-	111	27	85	84	0	-
BIC	American Plaice	4,495	4,329	4,465	4,314	-	4,405	4,327	4,392	4,405	4,314	-
ΔBIC	American Plaice	181	15	152	0	-	91	14	79	91	0	-
AIC	Atlantic Cod	3,909	3,680	3,911	3,681	-	3,830	3,675	3,832	3,833	-	-
ΔAIC	Atlantic Cod	234	5	236	6	-	156	0	158	158	-	-
BIC	Atlantic Cod	3,916	3,694	3,932	3,709	-	3,845	3,696	3,861	3,875	-	-
ΔBIC	Atlantic Cod	222	0	238	15	-	150	2	167	181	-	-
AIC	Greenland Halibut	7,194	6,824	7,179	6,816	-	6,619	6,510	6,613	6,602	-	-
ΔAIC	Greenland Halibut	684	314	668	306	-	108	0	103	92	-	-
BIC	Greenland Halibut	7,201	6,838	7,199	6,843	-	6,633	6,531	6,641	6,643	-	-
ΔBIC	Greenland Halibut	670	307	668	312	-	102	0	110	112	-	-
AIC	Northern Shrimp	12,848	11,428	12,650	11,252	-	9,600	9,244	9,577	9,467	9,217	9,116
ΔAIC	Northern Shrimp	3,732	2,312	3,534	2,136	-	484	128	461	351	100	0
BIC	Northern Shrimp	12,854	11,439	12,667	11,274	-	9,611	9,261	9,599	9,501	9,245	9,156
ΔBIC	Northern Shrimp	3,698	2,283	3,511	2,119	-	456	106	444	345	89	0
AIC	Redfish	8,860	7,609	8,506	6,990	-	6,014	5,867	5,859	5,862	5,691	5,693
ΔAIC	Redfish	3,169	1,918	2,815	1,299	-	323	176	168	171	0	3
BIC	Redfish	8,866	7,622	8,525	7,015	-	6,026	5,886	5,885	5,900	5,723	5,738
ΔBIC	Redfish	3,143	1,899	2,802	1,292	-	303	163	162	177	0	15
AIC	Roughhead Grenadier	708	689	707	691	-	706	691	707	-	693	-
ΔAIC	Roughhead Grenadier	18	0	18	2	-	17	2	17	-	4	-
BIC	Roughhead Grenadier	713	701	724	713	-	718	708	729	-	721	-
ΔBIC	Roughhead Grenadier	13	0	23	13	-	17	8	29	-	21	-
AIC	Snow Crab	4,626	4,460	4,590	4,440	-	4,548	4,428	4,515	4,498	4,408	4,387
ΔAIC	Snow Crab	239	73	203	53	-	161	41	128	111	21	0
BIC	Snow Crab	4,633	4,474	4,611	4,469	-	4,562	4,450	4,543	4,541	4,444	4,437
ΔBIC	Snow Crab	196	37	174	32	-	125	12	106	104	6	0
AIC	Thorny Skate	2,522	2,489	2,526	2,491	-	2,510	2,487	2,514	-	-	-
ΔAIC	Thorny Skate	35	2	39	4	-	23	0	27	-	-	-
BIC	Thorny Skate	2,529	2,503	2,547	2,519	-	2,524	2,508	2,542	-	-	-
ΔBIC	Thorny Skate	27	0	44	16	-	21	5	39	-	-	-

Value	Species	BI0	BI1	BI2	BI3	BI4	BB0	BB1	BB2	BB3	BB4	BB5
AIC	Witch Flounder	1,662	1,584	1,657	1,579	-	1,566	1,548	1,564	1,562	1,544	1,545
Δ AIC	Witch Flounder	118	40	112	34	-	22	3	19	17	0	0
BIC	Witch Flounder	1,669	1,597	1,676	1,604	-	1,579	1,567	1,589	1,600	1,576	1,589
Δ BIC	Witch Flounder	102	30	109	37	-	12	0	22	33	9	22
AIC	Yellowtail Flounder	4,687	4,048	4,612	3,992	-	4,171	3,876	4,137	4,113	3,844	3,828
Δ AIC	Yellowtail Flounder	859	220	7,84	164	-	344	49	309	286	16	0
BIC	Yellowtail Flounder	4,692	4,060	4,629	4,015	-	4,183	3,894	4,160	4,148	3,873	3,868
Δ BIC	Yellowtail Flounder	824	191	761	147	-	315	26	292	280	5	0

Table 8. P-values associated with tests for a smooth effect of depth, a smooth effect of time of day, and fixed effects of day/night, year, partner vessel (CCGS Teleost pairs only) and season (Yellowtail Flounder only) on the normalized quantile residuals from the length-disaggregated selected best model. Values <0.01 are indicated in bold. '-' indicates this effect does not apply for the given model.

Vessel pair	Common Name	s(Depth)	s(Time)	Day/ night	Year	Partner Vessel	Season
TEL/CAX	American Plaice	0.18	0.39	0.76	0.17	0.95	-
TEL/CAX	Atlantic Cod	0.82	0.87	0.84	0.53	0.67	-
TEL/CAX	Thorny Skate	0.27	0.20	0.11	0.05	0.14	-
TEL/CAX	Witch Flounder	0.86	0.99	0.51	0.43	0.51	-
TEL/CAX	Redfish	0.92	0.45	0.63	0.18	0.64	-
TEL/CAX	Snow Crab	0.22	0.48	0.77	0.21	0.61	-
TEL/CAX	Northern Shrimp	0.46	0.15	0.83	0.61	0.80	-
TEL/CAX	Striped Wolffish	0.27	0.61	0.64	0.02	0.24	-
TEL/CAX	Spotted Wolffish	0.08	0.26	0.15	0.31	0.24	-
AN/CAB	American Plaice	0.83	0.75	0.78	-	-	-
AN/CAB	Atlantic Cod	0.56	0.89	0.98	-	-	-
AN/CAB	Roughhead Grenadier	0.55	0.85	0.44	-	-	-
AN/CAB	Snow Crab	0.95	0.56	0.91	-	-	-
AN/CAB	Thorny Skate	0.45	0.52	0.90	-	-	-
AN/CAB	Witch Flounder	0.77	0.60	0.61	-	-	-
AN/CAB	Yellowtail Flounder	0.40	0.75	0.60	-	-	0.86
AN/CAB	Redfish	0.50	0.10	0.06	-	-	-
AN/CAB	Northern Shrimp	0.24	0.30	0.97	-	-	-

Vessel pair	Common Name	s(Depth)	s(Time)	Day/ night	Year	Partner Vessel	Season
AN/CAB	Greenland Halibut	0.82	0.57	0.97	-	-	-

Table 9. Summary of recommendations for species for which length-disaggregated conversion factor models were applied. For species where length was not determined to be significant, $\rho \pm$ standard error (SE) estimates are provided here. Values shaded in grey represent a non-significant conversion where the 95% CIs overlap with a constant conversion between vessels, and no conversion factor is recommended for these species. For the species where a length based conversion was found, the percentiles at which a constant conversion is to be applied is also provided. Full conversion factor tables by length can be found in Appendix 1, and corresponding table numbers are provided.

Vessels	Species	Determination	Details	Rho	SE Rho	Percentile Lengths
TEL:CAX	American Plaice (889)	No conversion needed	n/a	0.93	0.04	-
TEL:CAX	Atlantic Cod (438)	No conversion needed	n/a	0.94	0.05	Only applicable for >20 cm
TEL:CAX	Thorny Skate (90)	No conversion needed	n/a	0.94	0.05	-
TEL:CAX	Witch Flounder (889)	Conversion required	Length-based	Appendix 1, Table 1		10, 54 cm (0.5–99.5 percentile)
TEL:CAX	Striped Wolffish (700)	No conversion needed	n/a	1.01	0.09	-
TEL:CAX	Spotted Wolffish (701)	Conversion required	Length not significant	0.65	0.06	-
TEL:CAX	Redfish (794)	No conversion needed	n/a	0.86	0.07	-
TEL:CAX	Snow Crab (8,213)	Conversion required	Length not significant	0.54	0.06	Only applicable for >40 mm
TEL:CAX	Northern Shrimp (8,111)	Conversion required	Length-based	Appendix 1, Table 2		130, 255 mm (2.5–97.5 percentile)
AN:CAB	American Plaice (889)	Conversion required	Length-based	Appendix 1, Table 3		8, 48 cm (0.5–99.5 percentile)
AN:CAB	Atlantic Cod (438)	No conversion needed	n/a	1.06	0.08	-
AN:CAB	Thorny Skate (90)	No conversion needed	n/a	1.01	0.07	-
AN:CAB	Witch Flounder (889)	Conversion required	Length significant	Appendix 1, Table 4		12, 52 cm (0.5–99.5 percentile)
AN:CAB	Roughead Grenadier (474)	No conversion needed	n/a	1.13	0.20	-
AN:CAB	Greenland Halibut (892)	No conversion needed	n/a	0.91	0.05	-
AN:CAB	Redfish (794)	Conversion required	Length-based	Appendix 1, Table 5		8, 38 cm (0.5–99.5 percentile)
AN:CAB	Snow Crab (8,213)	Conversion required	Length-based	Appendix 1, Table 6		11, 126 mm (0.5–99.5 percentile)
AN:CAB	Northern Shrimp (8,111)	Conversion required	Length-based	Appendix 1, Table 7		105, 255 mm (2.5–97.5 percentile)
AN:CAB	Yellowtail Flounder (891)	Conversion required	Length-based	Appendix 1, Table 8		8, 53 cm (0.5–99.5 percentile)

Table 10. Relative evidence for size-aggregated binomial and beta-binomial models for CCGS Teleost and CCGS John Cabot/Capt. Jacques Cartier fall catch counts based on Akaike's Information Criterion (AIC) and the Bayesian Information Criterion (BIC) values, and estimates of the conversion factor Rho, and approximate 95% CIs, for catches in numbers and in weights for taxa for which length-disaggregated analyses were also undertaken. Recall that a single model was used for catch weights and thus AIC and BIC values are not shown. Entries with '-' indicate models that did not converge.

Species	Code	BI1 (AIC)	BB0 (AIC)	BB1 (AIC)	BI1 (BIC)	BB0 (BIC)	BB1 (BIC)	Model Selected	Rho (CI), numbers	p-value, numbers	Rho (CI), weights	p-value, weights	Recommendation
Thorny Skate (<i>Amblyraja radiata</i>)	90	689.21	689.11	691.08	695.56	695.46	700.6	BB0	0.93 (0.83–1.04)	0.20	0.95 (0.81–1.12)	0.57	Apply results from length-disaggregated conversion (Table 9)
Capelin (<i>Mallotus villosus</i>)	187	916.66	909.92	910.62	921.66	914.91	918.12	BB0	1.45 (1.14–1.84)	<0.01	1.48 (1.19–1.85)	<0.01	abundance and biomass conversion
Atlantic Cod (<i>Gadus morhua</i>)	438	967.3	965.47	967.2	973.58	971.75	976.62	BB0	0.94 (0.85–1.04)	0.23	1.01 (0.9–1.13)	0.89	Apply results from length-disaggregated conversion (Table 9)
Longfin Hake (<i>Urophycis chesteri</i>)	444	51.54	49.63	51.62	53.53	51.63	54.6	BB0	1.15 (0.51–2.6)	0.73	0.95 (0.42–2.19)	0.91	insufficient data
Arctic Cod (<i>Boreogadus saida</i>)	451	1,000.26	989.63	989.84	1,005.85	995.23	998.23	BB0	1.11 (0.91–1.34)	0.30	1.09 (0.92–1.28)	0.32	no conversion
Rocklings (<i>Gaidropsarus</i> spp, <i>Enchelyopus</i> spp.)	453	426.46	421.64	423.63	431.82	427.01	431.68	BB0	0.96 (0.74–1.25)	0.77	0.69 (0.52–0.92)	0.01	biomass conversion
Broadhead Wolffish (<i>Anarhichas denticulatus</i>)	699	159.76	159.46	161.46	164.34	164.04	168.33	BB0	0.99 (0.72–1.38)	0.97	0.88 (0.56–1.38)	0.58	no conversion
Striped Wolffish (<i>Anarhichas lupus</i>)	700	303.01	302.76	304.76	307.59	307.34	311.63	BB0	1.01 (0.84–1.21)	0.91	0.97 (0.67–1.42)	0.89	Apply results from length-disaggregated conversion (Table 9)
Spotted Wolffish (<i>Anarhichas minor</i>)	701	224.06	223.95	225.94	229.1	228.99	233.51	BB0	0.62 (0.49–0.78)	<0.01	0.76 (0.46–1.24)	0.27	Apply results from length-disaggregated conversion (Table 9)
Fourline Snakeblenny (<i>Eumesogrammus praecisus</i>)	711	82.01	79.07	80.96	84	81.06	83.95	BB0	1.31 (0.64–2.68)	0.46	1.22 (0.51–2.92)	0.65	no conversion
Snake Blenny (<i>Lumpenus lumpretaeformis</i>)	716	89.31	88.68	90.63	91.4	90.77	93.76	BB0	1.7 (0.77–3.75)	0.19	1.59 (0.66–3.82)	0.30	Insufficient data

Species	Code	B1 (AIC)	BB0 (AIC)	BB1 (AIC)	B1 (BIC)	BB0 (BIC)	BB1 (BIC)	Model Selected	Rho (CI), numbers	p-value, numbers	Rho (CI), weights	p-value, weights	Recommendation
Shanny (<i>Leptoclinus maculatus</i>)	717	252.56	247.29	248.48	255.89	250.61	253.47	BB0	1.58 (0.98–2.54)	0.06	1.5 (1.03–2.19)	0.03	Abundance and biomass conversion
Wrymouth (<i>Cryptacanthodes maculatus</i>)	721	79.99	79.65	81.65	82.98	82.64	86.14	BB0	0.67 (0.39–1.13)	0.13	0.72 (0.43–1.18)	0.19	insufficient data
Eelpouts (<i>Zoarcidae</i>)	726	1,087.82	1,085.72	1,087.71	1,094.22	1,092.12	1,097.3	BB0	0.9 (0.8–1.01)	0.08	0.79 (0.7–0.89)	<0.01	Abundance and biomass conversion
Redfish (<i>Sebastes mentella</i> and <i>S. faciatius</i>)	794	2,090.6	2,080.1	2,079.8	2,097.03	2,086.6	2,089.5	BB0	0.92 (0.83–1.01)	0.07	0.88 (0.80–0.96)	0.01	Apply results from length-disaggregated conversion (Table 9)
Sculpins (<i>Cottoidea</i> spp.)	810	1,020.02	1,003.9	1,004.05	1,026.03	1,009.9	1,013.06	BB0	1.05 (0.84–1.3)	0.69	1.04 (0.87–1.26)	0.65	no conversion
Alligatorfish (<i>Agonus</i> spp., <i>Eumicrotremus</i> spp.)	836	387.41	375.03	376.89	392.15	379.77	383.99	BB0	1.01 (0.69–1.46)	0.98	1.12 (0.73–1.73)	0.59	no conversion
Common Lumpfish (<i>Cyclopterus lumpus</i>)	849	58.6	58.6	NA	61.71	61.71	NA	BB0	1.67 (1.02–2.75)	0.04	1.49 (0.89–2.5)	0.13	insufficient data
Snailfishes (<i>Liparidae</i>)	853	352.74	340.79	342.75	357.7	345.75	350.19	BB0	0.73 (0.51–1.06)	0.10	0.87 (0.56–1.34)	0.52	no conversion
American Plaice (<i>Hippoglossoides platessoides</i>)	889	911.25	910.38	912.3	917.54	916.68	921.74	BB0	0.94 (0.86–1.03)	0.17	0.92 (0.84–1.02)	0.13	Apply results from length-disaggregated conversion (Table 9)
Witch Flounder (<i>Glyptocephalus cynoglossus</i>)	890	668.23	667.67	669.67	674.14	673.58	678.53	BB0	0.88 (0.78–0.99)	0.04	0.95 (0.83–1.1)	0.51	Apply results from length-disaggregated conversion (Table 9)
Sea anemones (<i>Actinaria</i>)	2,165	757.97	745.39	746.91	763.98	751.4	755.92	BB0	1.16 (0.91–1.48)	0.23	0.67 (0.54–0.84)	<0.01	biomass conversion
Gastropods (<i>Gastropoda</i>)	3,175	476.09	461.32	463.14	481.53	466.76	471.3	BB0	0.92 (0.66–1.26)	0.59	0.53 (0.36–0.8)	<0.01	biomass conversion
Cephalopods (Cephalopoda excluding <i>Illex</i> sp. and <i>Gonatus</i> spp.)	4,545	270.44	264.01	265.97	275.07	268.65	272.92	BB0	0.94 (0.65–1.37)	0.76	0.68 (0.41–1.14)	0.14	no conversion
Squid (<i>Illex</i> sp. and <i>Gonatus</i> spp.)	4,753	836.43	827.92	829.59	842.5	833.98	838.68	BB0	1.3 (1.03–1.63)	0.03	1.4 (1.12–1.74)	<0.01	abundance and biomass conversion

Species	Code	B1 (AIC)	BB0 (AIC)	BB1 (AIC)	B1 (BIC)	BB0 (BIC)	BB1 (BIC)	Model Selected	Rho (CI), numbers	p-value, numbers	Rho (CI), weights	p-value, weights	Recommendation
Polychaetes (Polychaeta)	4,950	240.97	230.73	232.7	245.47	235.22	239.44	BB0	1.13 (0.72–1.76)	0.59	0.92 (0.63–1.36)	0.68	no conversion
Sea Spider (Pycnogonida)	5,951	186.19	181.37	183.33	189.8	184.99	188.75	BB0	1.94 (1.15–3.26)	0.01	-	-	Abundance conversion. Biomass conversion cannot be determined.
Amphipods (Amphipoda)	6,930	296.3	286.59	288.49	300.42	290.71	294.67	BB0	0.97 (0.62–1.52)	0.9	1.79 (1.34–2.38)	<0.01	insufficient data
Northern Shrimp (<i>Pandalus borealis</i>)	8,111	2,619.32	2,608.08	2,606.88	2,625.64	2,614.4	2,616.36	BB0	1.16 (1.04–1.29)	0.01	1.08 (0.99–1.18)	0.07	Apply results from length-disaggregated conversion (Table 9)
Striped Shrimp (<i>Pandalus montagui</i>)	8,112	437.5	427.04	425.55	441.2	430.74	431.1	BB0	1.22 (0.77–1.91)	0.39	1.37 (0.94–2)	0.10	no conversion
Spiny Crab (<i>Lithodes</i> sp., <i>Neolithodes</i> sp.)	8,196	30.12	30.12	32.12	31.66	31.66	34.43	BB0	0.52 (0.24–1.13)	0.10	0.36 (0.15–0.83)	0.02	insufficient data
Snow Crab (<i>Chionoecetes opilio</i>)	8,213	756.21	752.51	754.28	761.88	758.18	762.79	BB0	0.6 (0.51–0.71)	<0.01	0.59 (0.49–0.71)	<0.01	Apply results from length-disaggregated conversion (Table 9)
Toad crab (<i>Hyas</i> spp.)	8,216	177.37	176.09	178.09	181.2	179.92	183.83	BB0	0.75 (0.52–1.1)	0.14	0.9 (0.58–1.42)	0.66	no conversion
Sessile Tunicates (Tunicata)	8,680	33.53	37.86	39.85	36.9	41.24	44.92	B1	0 (0–0)	<0.01	1.19 (0.64–2.23)	0.58	insufficient data
Sponge (Porifera)	1,101	-	-	-	-	-	-	-	-	-	0.9 (0.75–1.08)	0.27	no conversion
Jellyfish (Scyphozoa)	2,040	-	-	-	-	-	-	-	-	-	0.85 (0.73–0.99)	0.03	biomass conversion
Euphausiids (Euphausiacea)	7,991	-	-	-	-	-	-	-	-	-	2.35 (1.45–3.83)	<0.01	Insufficient data
Brittle stars (Ophiuroidea except <i>Gorgonocephalus</i> spp.)	8,530	-	-	-	-	-	-	-	-	-	0.77 (0.58–1.03)	0.08	no conversion
Basket stars (<i>Gorgonocephalus</i> spp.)	8,540	-	-	-	-	-	-	-	-	-	0.81 (0.55–1.2)	0.30	no conversion
Corals, NS	8,900	-	-	-	-	-	-	-	-	-	0.2 (0.07–0.6)	<0.01	insufficient data
Soft Corals	8,904	-	-	-	-	-	-	-	-	-	2.13 (1.42–3.2)	<0.01	biomass conversion

Table 11. Relative evidence for size-aggregated binomial and beta-binomial models for the CCGS Alfred Needler and CCGS John Cabot Fall catch counts based on Akaike's Information Criterion (AIC) and the Bayesian Information Criterion (BIC) values, and estimates of the conversion factor ρ , and approximate 95% CIs, for catches in numbers and in weights for taxa for which length-disaggregated analyses were also undertaken. Recall that a single model was used for catch weights and thus AIC and BIC values are not shown. Entries with '-' indicate models that did not converge.

Species	Code	BI1 (AIC)	BB0 (AIC)	BB1 (AIC)	BI1 (BIC)	BB0 (BIC)	BB1 (BIC)	Model Selected	Rho (CI), numbers	p-value, numbers	Rho (CI), weights	p-value, weights	Recommendation
Thorny Skate (<i>Amblyraja radiata</i>)	90	432.55	432.42	434.42	437.6	437.47	441.99	BB0	1.01 (0.88–1.14)	0.93	0.97 (0.85–1.11)	0.67	Apply results from length-disaggregated conversion (Table 9)
Capelin (<i>Mallotus villosus</i>)	187	519.33	505.08	502.24	523.23	508.98	508.09	BB1	0.82 (0.49–1.38)	0.47	1.02 (0.79–1.33)	0.87	no conversion
Lanternfishes (<i>Myctophidae</i>)	272	222.8	220.62	222.3	225.39	223.21	226.19	BB0	1.08 (0.68–1.73)	0.74	0.98 (0.64–1.49)	0.92	no conversion
Barracudinas (<i>Paralepididae</i>)	316	212.67	210.18	212.1	216.15	213.66	217.31	BB0	1.12 (0.69–1.81)	0.64	0.59 (0.37–0.95)	0.03	biomass conversion, no conclusion for abundance
Atlantic Cod (<i>Gadus morhua</i>)	438	532.13	531.77	533.77	537.2	536.84	541.37	BB0	1.04 (0.9–1.21)	0.57	1.04 (0.88–1.23)	0.64	Apply results from length-disaggregated conversion (Table 9)
White Hake (<i>Urophycis tenuis</i>)	447	63.18	63.17	65.17	64.72	64.71	67.49	BB0	1.07 (0.7–1.63)	0.75	1.08 (0.52–2.26)	0.84	insufficient data
Silver Hake (<i>Merluccius bilinearis</i>)	449	127.94	127.99	129.99	130.3	130.34	133.52	B1	0.82 (0.63–1.06)	0.13	0.89 (0.69–1.15)	0.37	insufficient data
Arctic Cod (<i>Boreogadus saida</i>)	451	578.48	567.65	566.72	582.83	572	573.24	BB0	0.77 (0.58–1.02)	0.06	0.82 (0.64–1.04)	0.10	no conversion
Rockling Spp. (<i>Gaidropsarus</i> spp., <i>Enchelyopus</i> spp.)	453	155.26	154.06	156.04	159.09	157.89	161.78	BB0	0.74 (0.51–1.07)	0.11	0.71 (0.51–0.99)	0.04	biomass conversion
Grenadiers (<i>Macrouridae</i> except <i>Macrourus berglax</i>)	470	73.1	72.62	74.61	75.09	74.61	77.6	BB0	0.98 (0.55–1.76)	0.95	0.79 (0.45–1.37)	0.4	insufficient data
Roughhead Grenadier (<i>Macrourus berglax</i>)	474	151.7	151.06	152.96	154.69	154.05	157.45	BB0	1.12 (0.81–1.54)	0.50	1.02 (0.7–1.46)	0.93	no conversion
Striped Wolffish (<i>Anarhichas lupus</i>)	700	136.33	134.91	136.91	139.66	138.23	141.9	BB0	0.97 (0.64–1.46)	0.88	1.07 (0.53–2.15)	0.85	Apply results from length-disaggregated conversion (Table 9)

Species	Code	BI1 (AIC)	BB0 (AIC)	BB1 (AIC)	BI1 (BIC)	BB0 (BIC)	BB1 (BIC)	Model Selected	Rho (CI), numbers	p-value, numbers	Rho (CI), weights	p-value, weights	Recommendation
Spotted Wolffish (<i>Anarhichas minor</i>)	701	71.6	71.13	73.13	74.65	74.18	77.71	BB0	0.74 (0.44–1.25)	0.26	1.31 (0.62-2.77)	0.48	no conversion
Snake Blenny (<i>Lumpenus lumpretaeformis</i>)	716	65.32	63.69	65.69	66.74	65.11	67.82	BB0	1.29 (0.55–3.05)	0.56	0.69 (0.25-1.89)	0.47	data insufficient
Shanny (<i>Leptoclinus maculatus</i>)	717	150.77	147.92	149.67	153.28	150.44	153.45	BB0	0.55 (0.31–0.96)	0.04	0.52 (0.34-0.8)	<0.01	abundance and biomass conversion
Wrymouth (<i>Cryptacanthodes maculatus</i>)	721	73.29	72.57	74.55	75.88	75.16	78.44	BB0	0.56 (0.32–0.98)	0.04	0.55 (0.31-0.99)	0.05	abundance and biomass conversion
Eelpouts (<i>Zoarcidae</i>)	726	483.14	479.58	481.37	487.78	484.22	488.33	BB0	0.71 (0.6–0.83)	<0.01	0.81 (0.7-0.93)	<0.01	abundance and biomass conversion
Redfish (<i>Sebastes mentella</i> and <i>S. faciatus</i>)	794	824.23	819.46	820.36	828.91	824.15	827.39	BB0	0.81 (0.68–0.96)	0.01	0.9 (0.78-1.04)	0.15	Apply results from length-disaggregated conversion (Table 9)
Sea Raven (<i>Hemitripterus americanus</i>)	809	44.79	44.78	46.78	46.33	46.33	49.1	BB0	0.73 (0.25–2.11)	0.57	0.52 (0.21-1.27)	0.15	insufficient data
Sculpins (<i>Cottoidea</i>)	810	460.86	452.85	454.65	465.6	457.59	461.76	BB0	0.68 (0.49–0.94)	0.02	0.51 (0.38-0.69)	<0.01	abundance and biomass conversion
Alligatorfish (<i>Agonus</i> sp., <i>Eumicrotremus</i> sp.)	836	240.42	233.29	235.23	244.12	236.99	240.78	BB0	0.78 (0.48–1.26)	0.31	0.57 (0.32-1.02)	0.06	no conversion
Common Lumpfish (<i>Cyclopterus lumpus</i>)	849	38.62	38.62	40.62	40.29	40.29	43.12	BB0	1.21 (0.62–2.35)	0.58	1.28 (0.57-2.91)	0.55	insufficient data
Snailfishes (<i>Liparidae</i>)	853	116.33	112.36	114.36	119.44	115.47	119.03	BB0	0.85 (0.49–1.49)	0.58	1 (0.52-1.9)	0.99	no conversion
American Plaice (<i>Hippoglossoides platessoides</i>)	889	614.67	614.25	616.24	619.82	619.4	623.97	BB0	1.05 (0.95–1.15)	0.33	1.08 (0.96-1.21)	0.18	Apply results from length-disaggregated conversion (Table 9)
Witch Flounder (<i>Glyptocephalus cynoglossus</i>)	890	347.64	346.95	348.94	352.35	351.66	356.01	BB0	0.91 (0.76–1.08)	0.26	0.95 (0.77-1.16)	0.6	Apply results from length-disaggregated conversion (Table 9)
Yellowtail Flounder (<i>Myxopsetta ferruginea</i>)	891	419.19	413.53	414.11	422.8	417.14	419.53	BB0	1.27 (1.02–1.58)	0.03	1.27 (1.02 -1.58)	0.03	Apply results from length-disaggregated conversion (Table 9)

Species	Code	BI1 (AIC)	BB0 (AIC)	BB1 (AIC)	BI1 (BIC)	BB0 (BIC)	BB1 (BIC)	Model Selected	Rho (CI), numbers	p-value, numbers	Rho (CI), weights	p-value, weights	Recommendation
Greenland Halibut (<i>Reinhardtius hippoglossoides</i>)	892	631.24	631.06	632.97	635.95	635.77	640.04	BB0	0.93 (0.84–1.02)	0.13	0.9 (0.79-1.02)	0.1	Apply results from length-disaggregated conversion (Table 9)
Sea anemones (Actinaria)	2,165	341.87	335.51	337.14	346.16	339.79	343.57	BB0	0.65 (0.45–0.93)	0.02	0.79 (0.55-1.14)	0.21	abundance conversion
Cephalopods (Cephalopoda excluding <i>Illex</i> sp. and <i>Gonatus</i> spp.)	4,545	51.35	53.27	55.27	53.34	55.26	58.26	B1	1155.24 (3.57–373914.1)	0.02	0.78 (0.38-1.6)	0.43	insufficient data
Squid (<i>Illex</i> sp. and <i>Gonatus</i> spp.)	4,753	271.85	268.93	270.71	275.87	272.95	276.73	BB0	2.09 (1.42–3.08)	<0.01	1.52 (1.09-2.12)	0.01	abundance and biomass conversion
Polychaetes (Polychaeta)	4,950	91.02	86.76	88.76	93.95	89.69	93.15	BB0	0.75 (0.38–1.48)	0.4	0.46 (0.25-0.85)	0.01	insufficient data
Amphipods (Amphipoda)	6,930	76.45	75.58	77.58	79.44	78.58	82.07	BB0	1.15 (0.54–2.45)	0.72	-	-	insufficient data
Northern Shrimp (<i>Pandalus borealis</i>)	8,111	1,158.8	1,137.1	1,129.8	1,163.2	1,141.5	1,136.4	BB1	0.91 (0.72–1.14)	0.41	0.82 (0.72-0.92)	<0.01	Apply results from length-disaggregated conversion (Table 9)
Striped Shrimp (<i>Pandalus montagui</i>)	8,112	312.79	306.37	306.92	315.96	309.53	311.67	BB0	0.92 (0.55–1.53)	0.74	0.67 (0.41-1.11)	0.12	no conversion
Snow Crab (<i>Chionoecetes opilio</i>)	8,213	464.45	464.44	466.44	468.98	468.97	473.23	BB0	0.72 (0.62–0.84)	<0.01	0.83 (0.71-0.99)	0.03	Apply results from length-disaggregated conversion (Table 9)
Toad crab (<i>Hyas</i> spp.)	8,216	168.77	164.08	166.01	172.59	167.9	171.75	BB0	0.82 (0.53–1.26)	0.36	1.02 (0.64-1.61)	0.93	no conversion
Gastropods (Gastropoda)	3,175	198.5207	193.1609	195.15	202.263	196.90	200.76	BB0	0.57 (0.34–0.93)	0.03	0.28 (0.16-0.51)	<0.01	Abundance and biomass conversion
Sessile tunicates (Tunicata)	8,680	45.5	49.11	51.11	48.16	51.77	55.1	B1	48364.42 (192.87–12128074.3)	<0.01	0.41 (0.19-0.87)	0.02	insufficient data
Sponge (Porifera)	1,101	-	-	-	-	-	-	-	-	-	0.75 (0.52-1.07)	0.12	no conversion
Jellyfish (Scyphozoa)	2,040	-	-	-	-	-	-	-	-	-	0.89 (0.7-1.13)	0.35	no conversion
Brittle stars (Ophiuroidea except <i>Gorgonocephalus</i> spp)	8,530	-	-	-	-	-	-	-	-	-	0.51 (0.33-0.79)	<0.01	biomass conversion

Species	Code	BI1 (AIC)	BB0 (AIC)	BB1 (AIC)	BI1 (BIC)	BB0 (BIC)	BB1 (BIC)	Model Selected	Rho (CI), numbers	p-value, numbers	Rho (CI), weights	p-value, weights	Recommendation
Basket stars (<i>Gorgonocephalus</i> spp.)	8,540	-	-	-	-	-	-	-	-	-	0.74 (0.38-1.47)	0.39	no conversion
Soft Corals	8,904	-	-	-	-	-	-	-	-	-	2.05 (0.83-5.1)	0.12	insufficient data
Bryozoan (Bryozoa)	9,992	-	-	-	-	-	-	-	-	-	2.3 (0.93-5.66)	0.07	insufficient data

APPENDIX 1: LENGTH-BASED CONVERSIONS

FIGURES

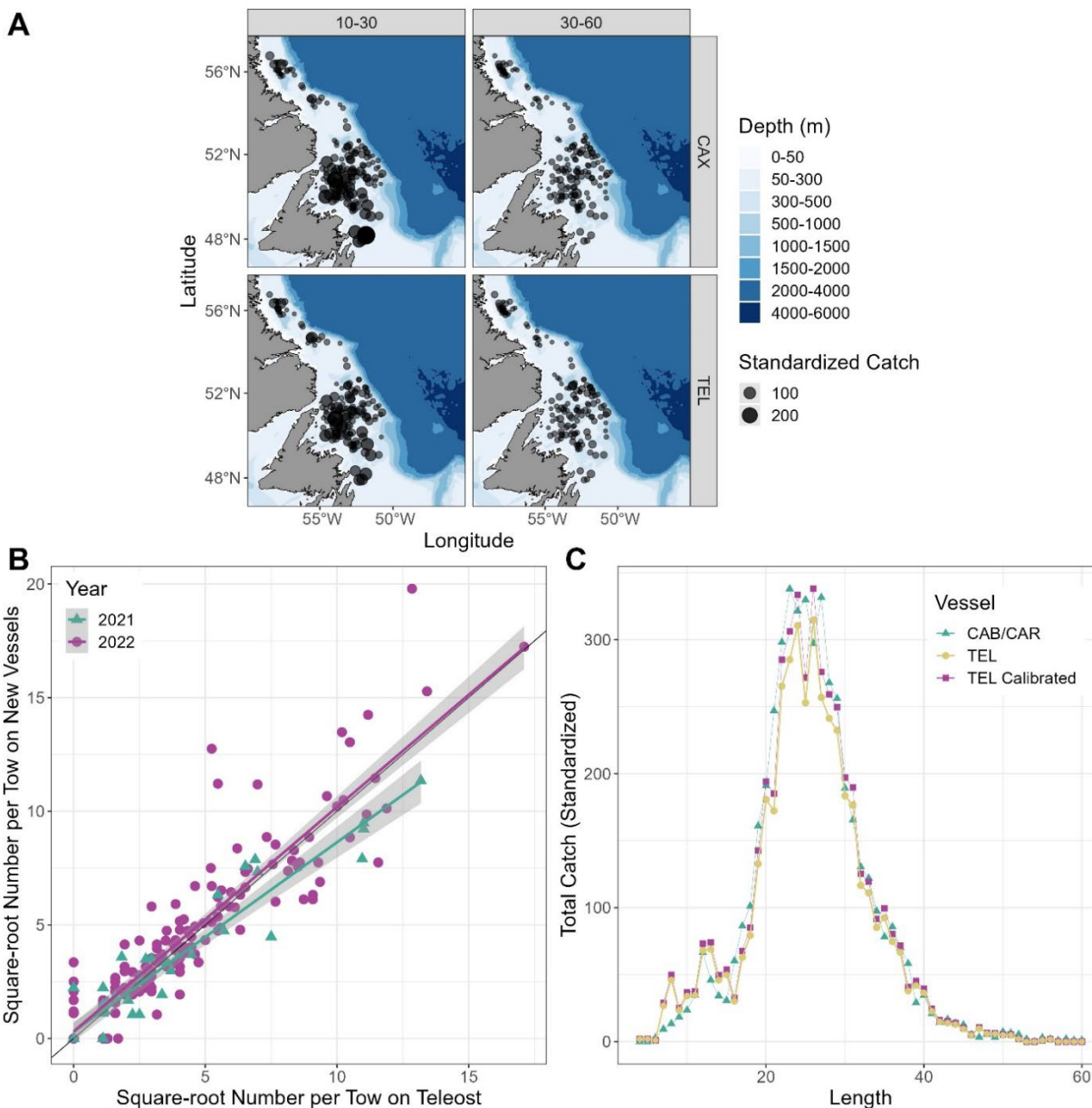


Figure A1–1. Results for length-disaggregated comparative fishing analyses for American Plaice (*Hippoglossoides platessoides*), between the CCGS Teleost and CCGS John Cabot/Capt. Jacques Cartier for Fall 2HJ3K + 3L deep. (A) map of catches by length group (length in cm specified in top panel) by the CCGS John Cabot/Capt. Jacques Cartier (top) and the CCGS Teleost (bottom) in comparative fishing sets, where circle size is proportional catch weight (B) Biplot of the square-root of CCGS John Cabot & Capt. Jacques Cartier catch numbers against the square-root of CCGS Teleost catch numbers, showing 2021 and 2022. (C) Total length frequencies for catches made by the CCGS Teleost (yellow), by the CCGS John Cabot/Capt. Jacques Cartier (green), and Teleost catches with the conversion factor applied (purple).

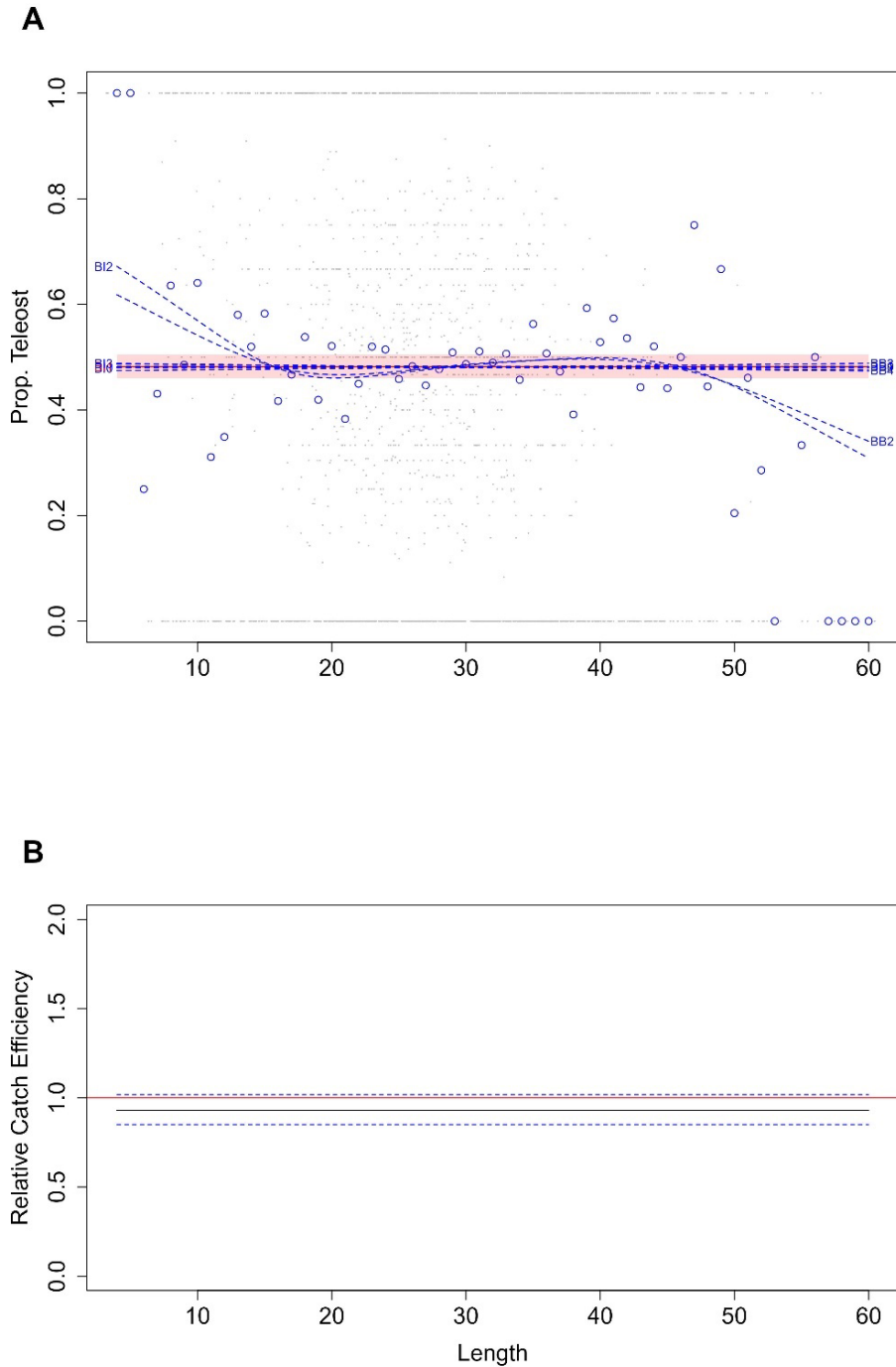


Figure A1–2. American Plaice (*Hippoglossoides platessoides*) conversion factor, between the CCGS Teleost and CCGS John Cabot/Capt. Jacques Cartier for Fall 2HJ3K + 3L deep. (A) Estimated length-specific catch proportion functions, $\text{logit}(p_{Ai}(l))$, for each converged model, with the selected model plotted using a red line along with its approximate 95% CI (shaded area), as well as the length class-specific mean empirical proportion of total catch in a pair made by the CCGS Teleost (blue dots). (B) Estimated relative catch efficiency (conversion factor) function from the best model (black line) with 95% CI (dashed blue lines). The horizontal red line indicates equivalent efficiency between vessels.

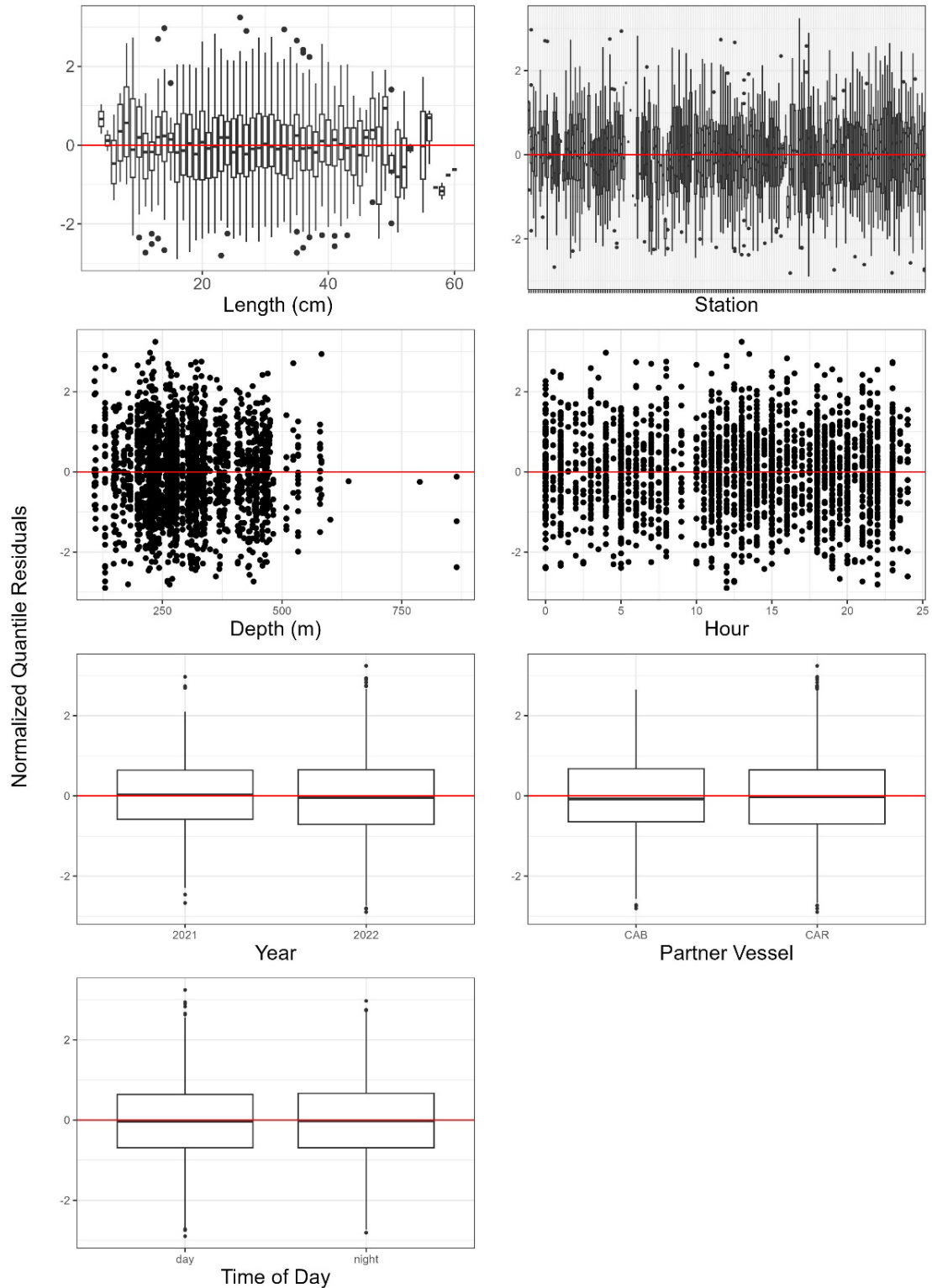


Figure A1–3. Normalized quantile residuals for as a function of length, station, depth, hour, year, partner vessel, and diel period for American Plaice (*Hippoglossoides platessoides*), best model selected (BI1) for length disaggregated conversion factor analysis for the CCGS Teleost, and CCGS John Cabot/Capt. Jacques Cartier for Fall 2HJ3K + 3L deep.

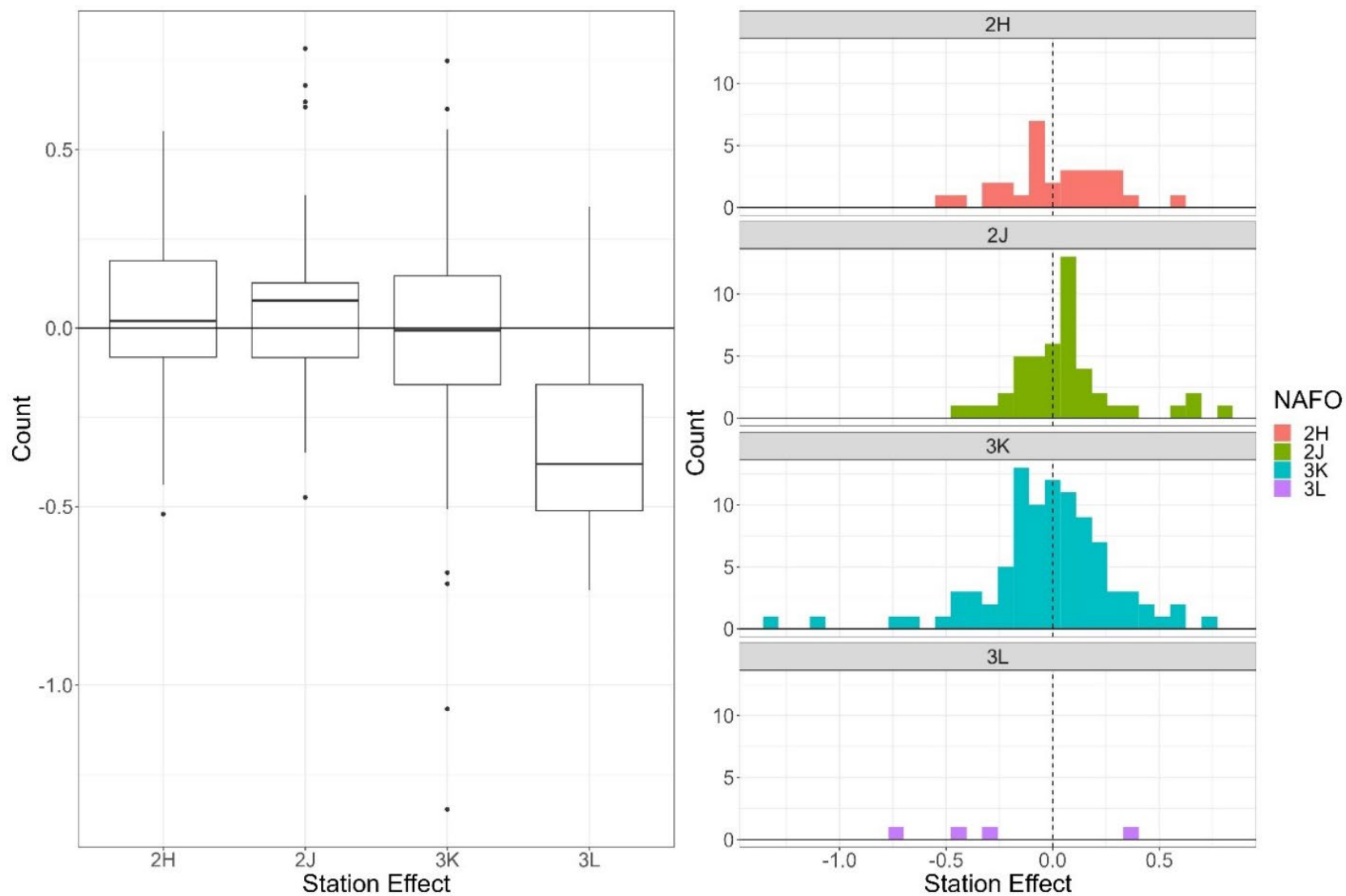


Figure A1–4. Boxplot (left) and histogram (right) of station effect by NAFO Division for best model (B11) selected for American Plaice (*Hippoglossoides platessoides*) conversion factor analysis of CCGS Teleost and CCGS John Cabot/Capt. Jacques Cartier in Fall 2HJ3K + 3L deep.

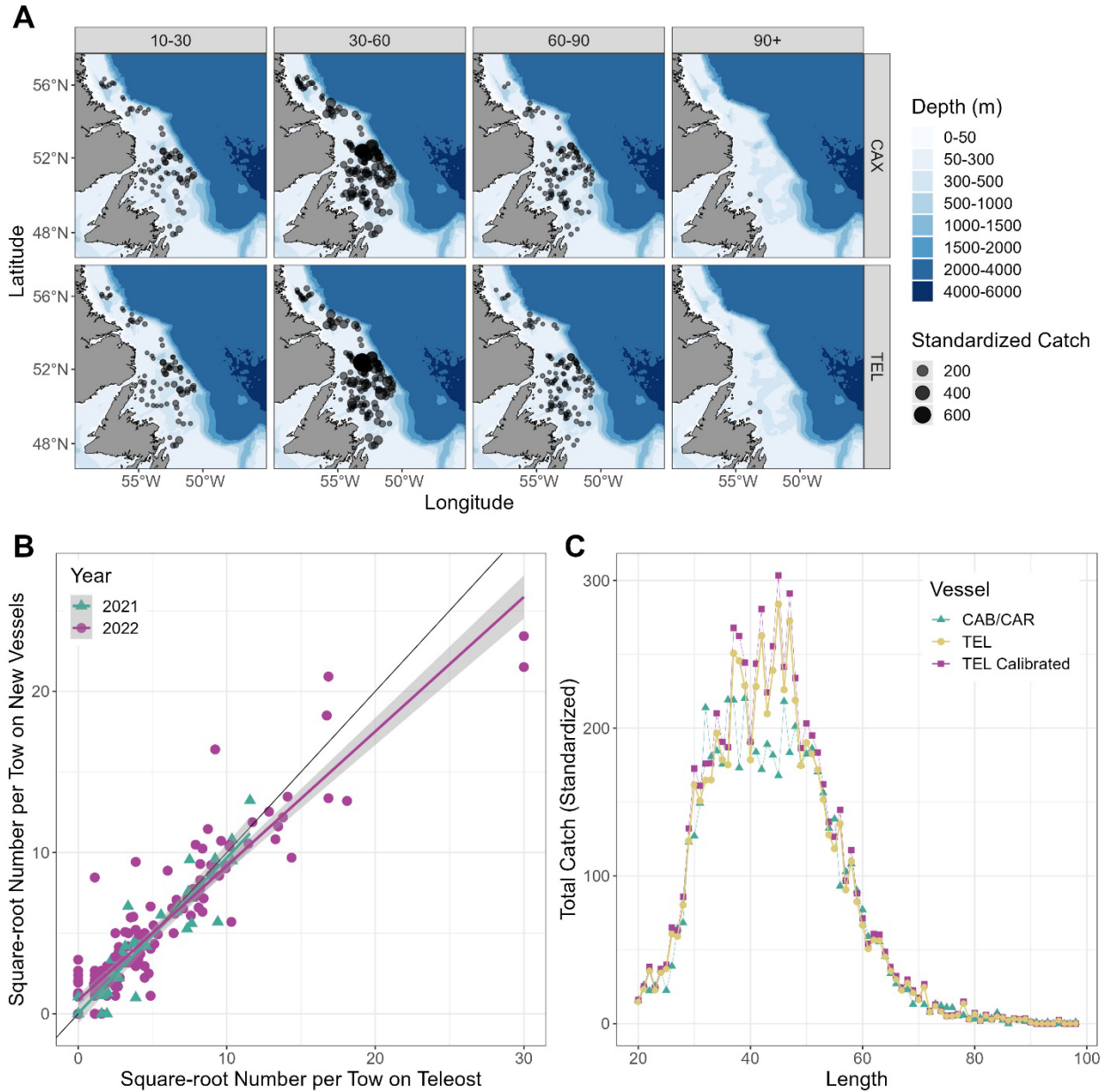


Figure A1–5. Results for length-disaggregated comparative fishing analyses for Atlantic Cod (*Gadus morhua*) >20 cm, between the CCGS Teleost and CCGS John Cabot/Capt. Jacques Cartier for Fall 2HJ3K + 3L deep. (A) map of catches by length group (length in cm specified in top panel) by the CCGS John Cabot/Capt. Jacques Cartier (top) and the CCGS Teleost (bottom) in comparative fishing sets, where circle size is proportional catch weight (B) Biplot of the square-root of CCGS John Cabot & Capt. Jacques Cartier catch numbers against the square-root of CCGS Teleost catch numbers, showing 2021 and 2022. (C) Total length frequencies for catches made by the CCGS Teleost (yellow), by the CCGS John Cabot/Capt. Jacques Cartier (green), and CCGS Teleost catches with the conversion factor applied (purple).

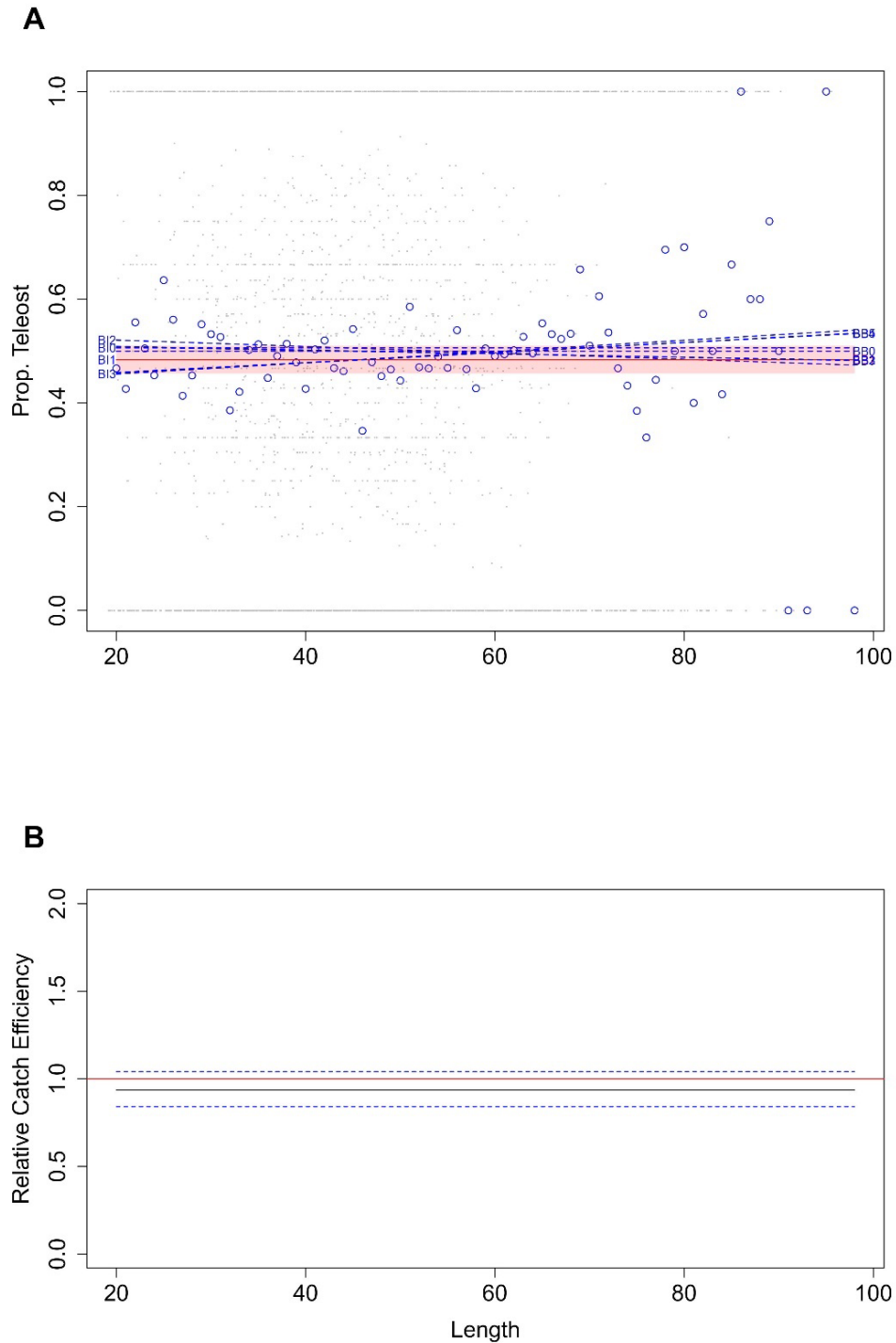


Figure A1–6. Atlantic Cod (*Gadus morhua*) >20 cm conversion factor, between the CCGS Teleost and CCGS John Cabot/Capt. Jacques Cartier for Fall 2HJ3K + 3L deep. (A) Estimated length-specific catch proportion functions, $\text{logit}(p_{Ai}(l))$, for each converged model, with the selected model plotted using a red line along with its approximate 95% CI (shaded area), as well as the length class-specific mean empirical proportion of total catch in a pair made by the CCGS Teleost (blue dots). (B) Estimated relative catch efficiency (conversion factor) function from the best model (black line) with 95% CI (dashed blue lines). The horizontal red line indicates equivalent efficiency between vessels.

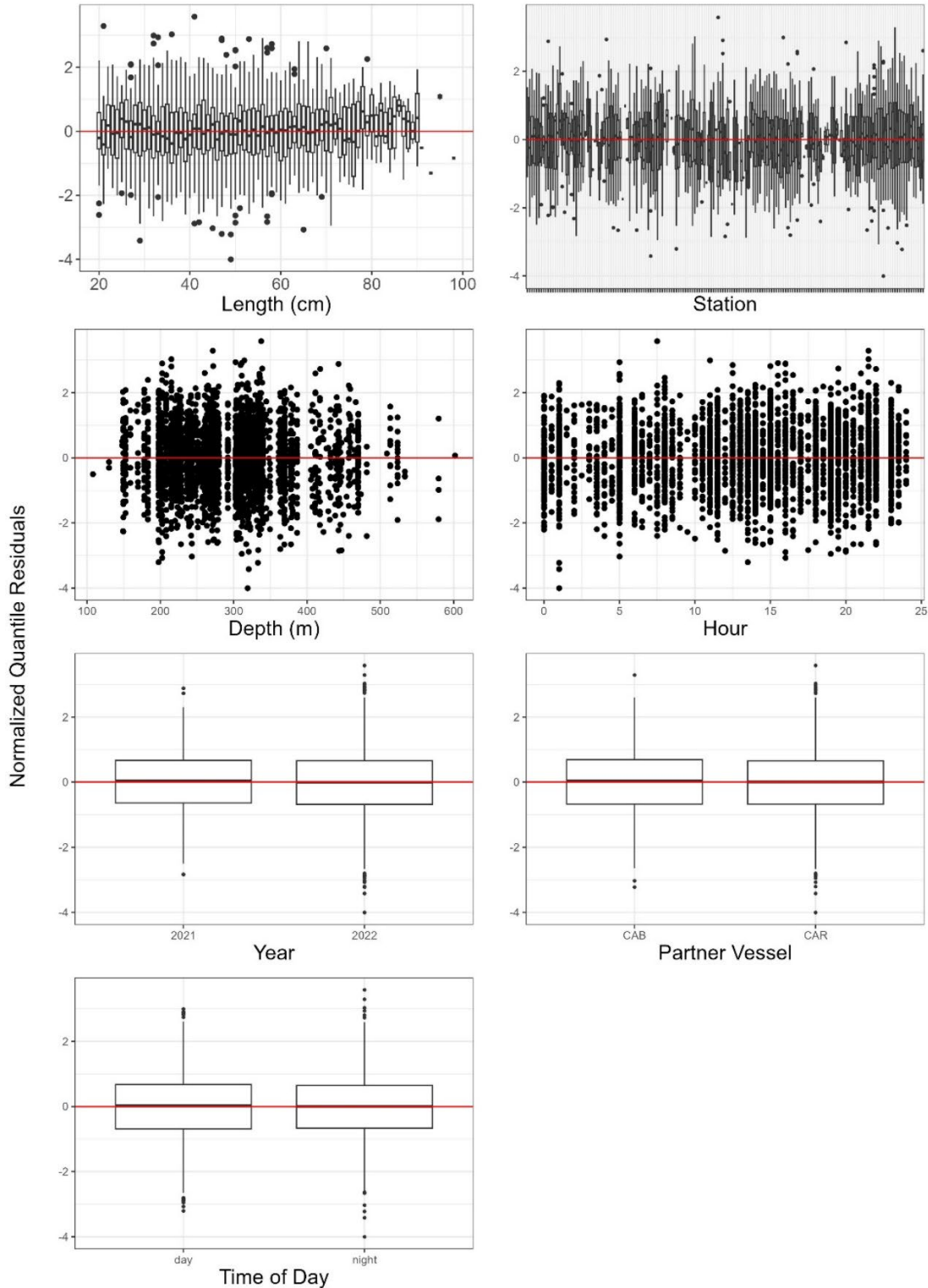


Figure A1–7. Normalized quantile residuals for as a function of length, station, depth, hour, year, partner vessel, and diel period for Atlantic Cod (*Gadus morhua*), >20 cm, best model selected (BB1) for length disaggregated conversion factor analysis for the CCGS Teleost, and CCGS John Cabot/Capt. Jacques Cartier for Fall 2HJ3K + 3L deep.

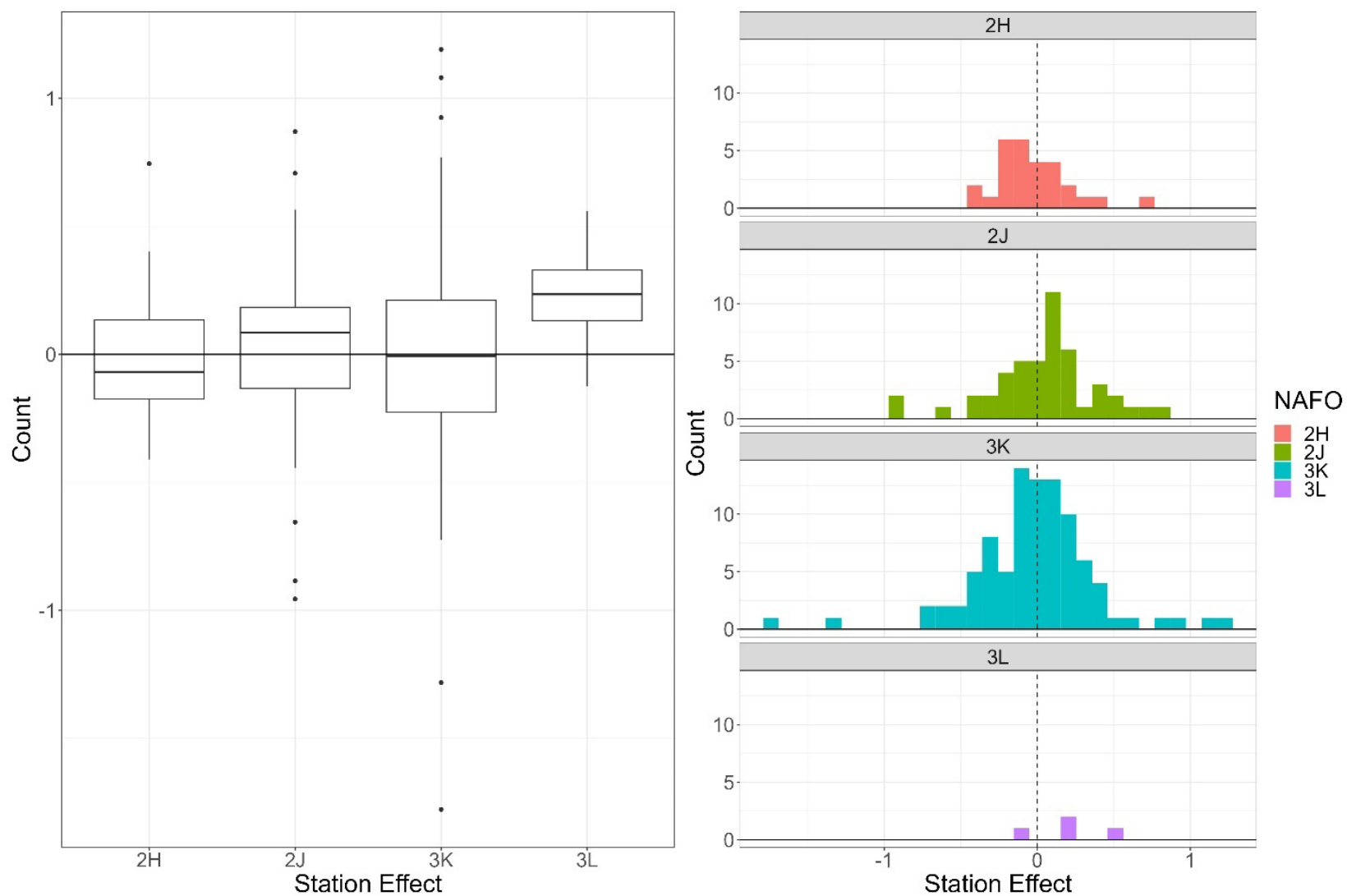


Figure A1–8. Boxplot (left) and histogram (right) of station effect by NAFO division for best model (BB1) selected for Atlantic Cod (*Gadus morhua*) >20 cm conversion factor analysis of CCGS Teleost and CCGS John Cabot/Capt. Jacques Cartier in Fall 2HJ3K + 3L deep.

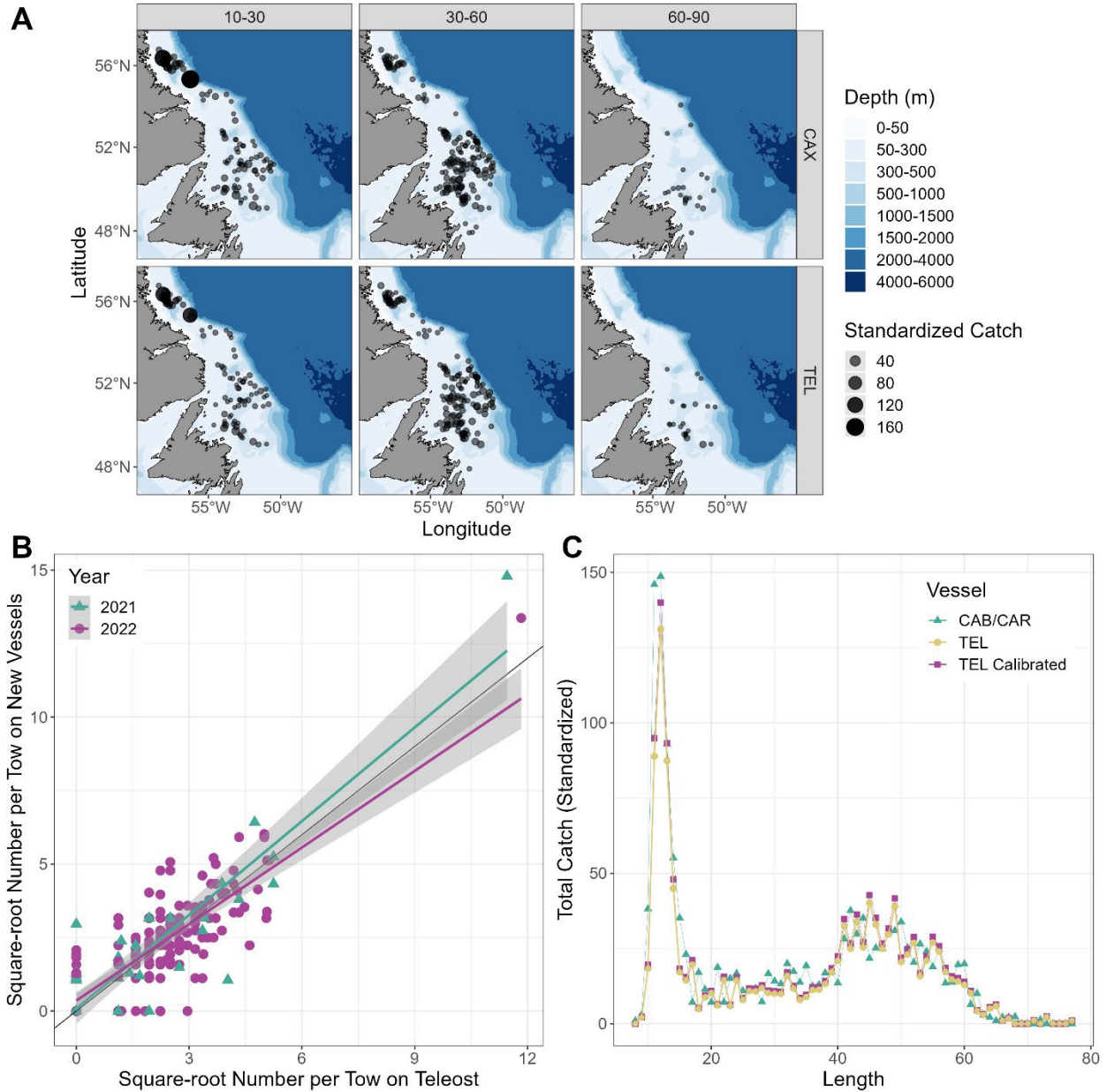


Figure A1–9. Results for length-disaggregated comparative fishing analyses for Thorny Skate (*Amblyraja radiata*), between the CCGS Teleost and CCGS John Cabot/Capt. Jacques Cartier for Fall 2HJ3K + 3L deep. (A) map of catches by length group (length in cm specified in top panel) by the CCGS John Cabot/Capt. Jacques Cartier (top) and the CCGS Teleost (bottom) in comparative fishing sets, where circle size is proportional catch weight (B) Biplot of the square-root of CCGS John Cabot & CCGS Capt. Jacques Cartier catch numbers against the square-root of Teleost catch numbers, showing 2021 and 2022. (C) Total length frequencies for catches made by the CCGS Teleost (yellow), by the Cabot/Cartier (green), and Teleost catches with the conversion factor applied (purple).

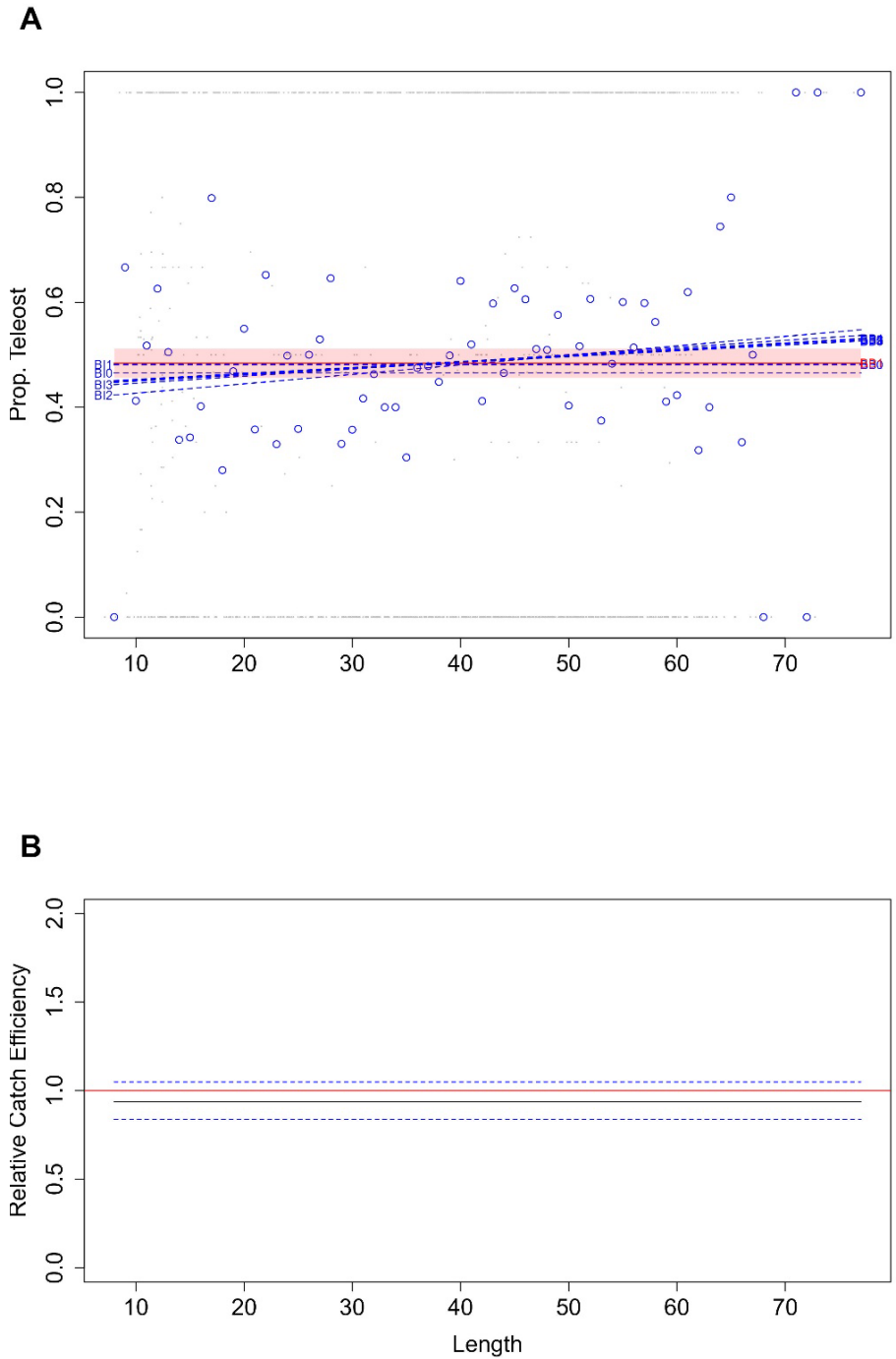


Figure A1–10. Thorny Skate (*Amblyraja radiata*) conversion factor, between the CCGS Teleost and CCGS John Cabot/Capt. Jacques Cartier for Fall 2HJ3K + 3L deep. (A) Estimated length-specific catch proportion functions, $\text{logit}(p_{Ai}(l))$, for each converged model, with the selected model plotted using a red line along with its approximate 95%CI (shaded area), as well as the length class-specific mean empirical proportion of total catch in a pair made by the CCGS Teleost (blue dots). (B) Estimated relative catch efficiency (conversion factor) function from the best model (black line) with 95% CI (dashed blue lines). The horizontal red line indicates equivalent efficiency between vessels.

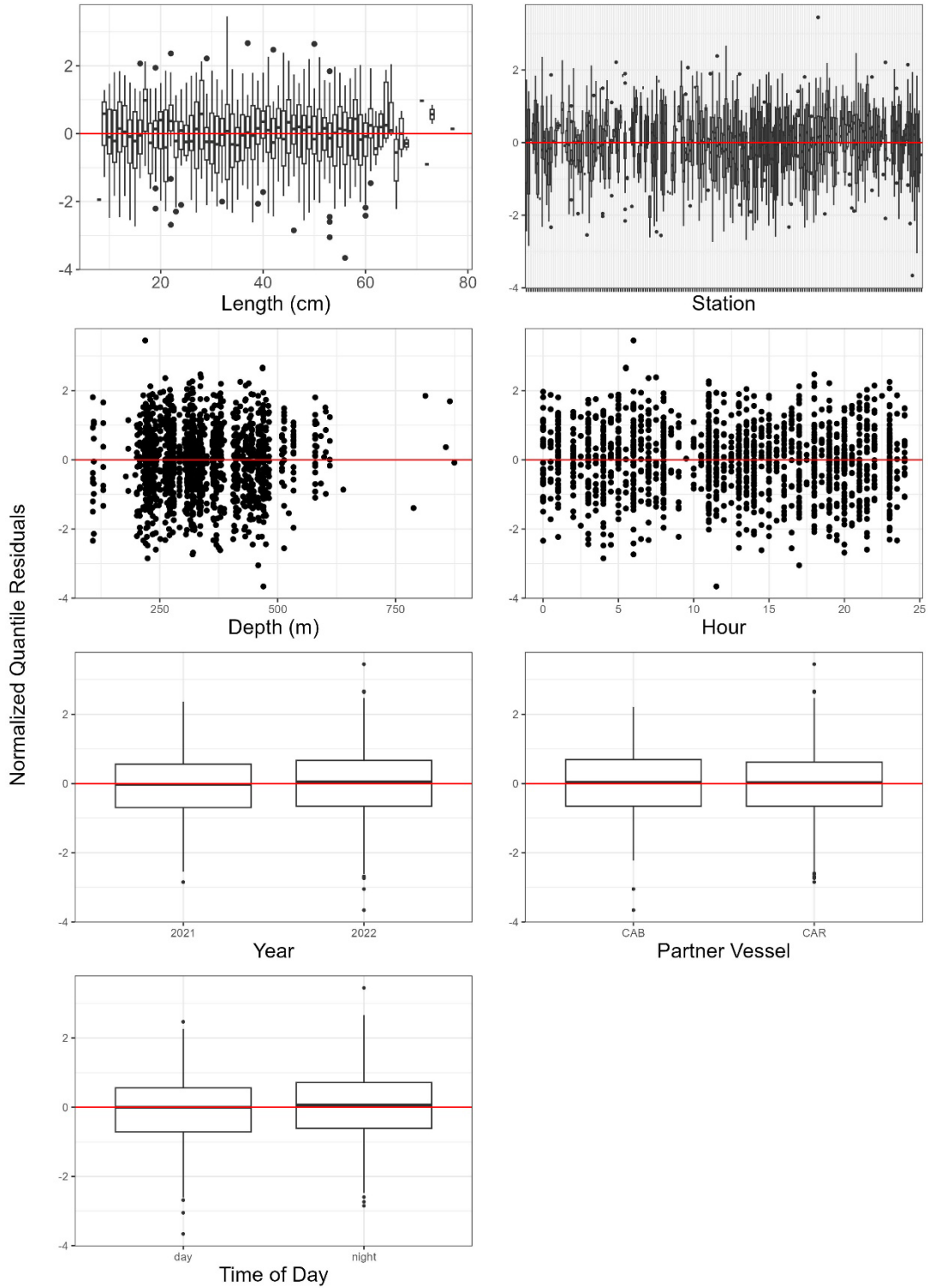


Figure A1–11. Normalized quantile residuals for as a function of length, station, depth, hour, year, partner vessel, and diel period for Thorny Skate (*Amblyraja radiata*), best model selected (BB1) for length disaggregated conversion factor analysis for the CCGS Teleost, and CCGS John Cabot/Capt. Jacques Cartier for Fall 2HJ3K + 3L deep.

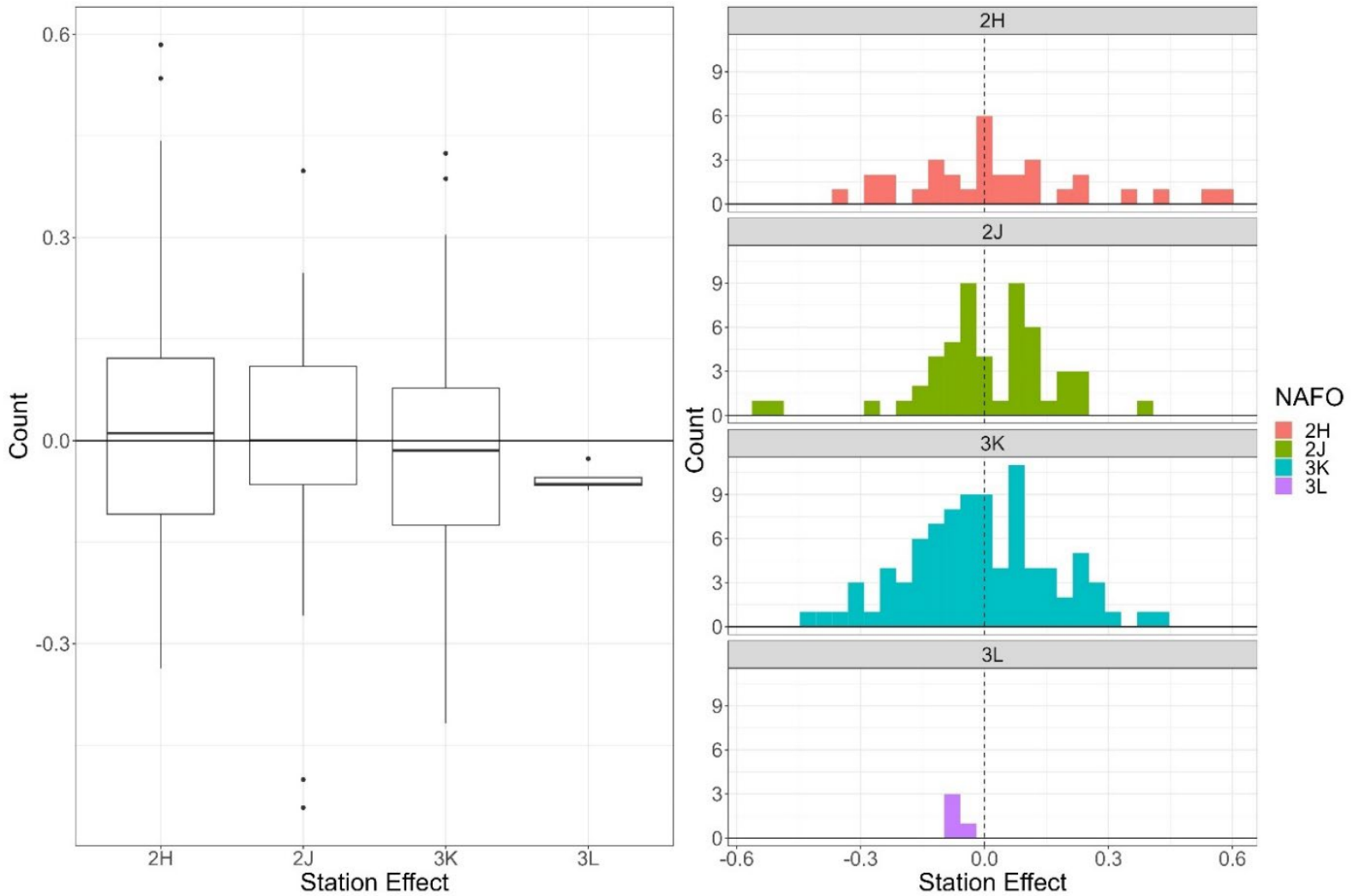


Figure A1-12. Boxplot (left) and histogram (right) of station effect by NAFO Division for best model (BB1) selected for Thorny Skate (*Amblyraja radiata*) conversion factor analysis of CCGS Teleost and CCGS John Cabot/Capt. Jacques Cartier in Fall 2HJ3K + 3L deep.

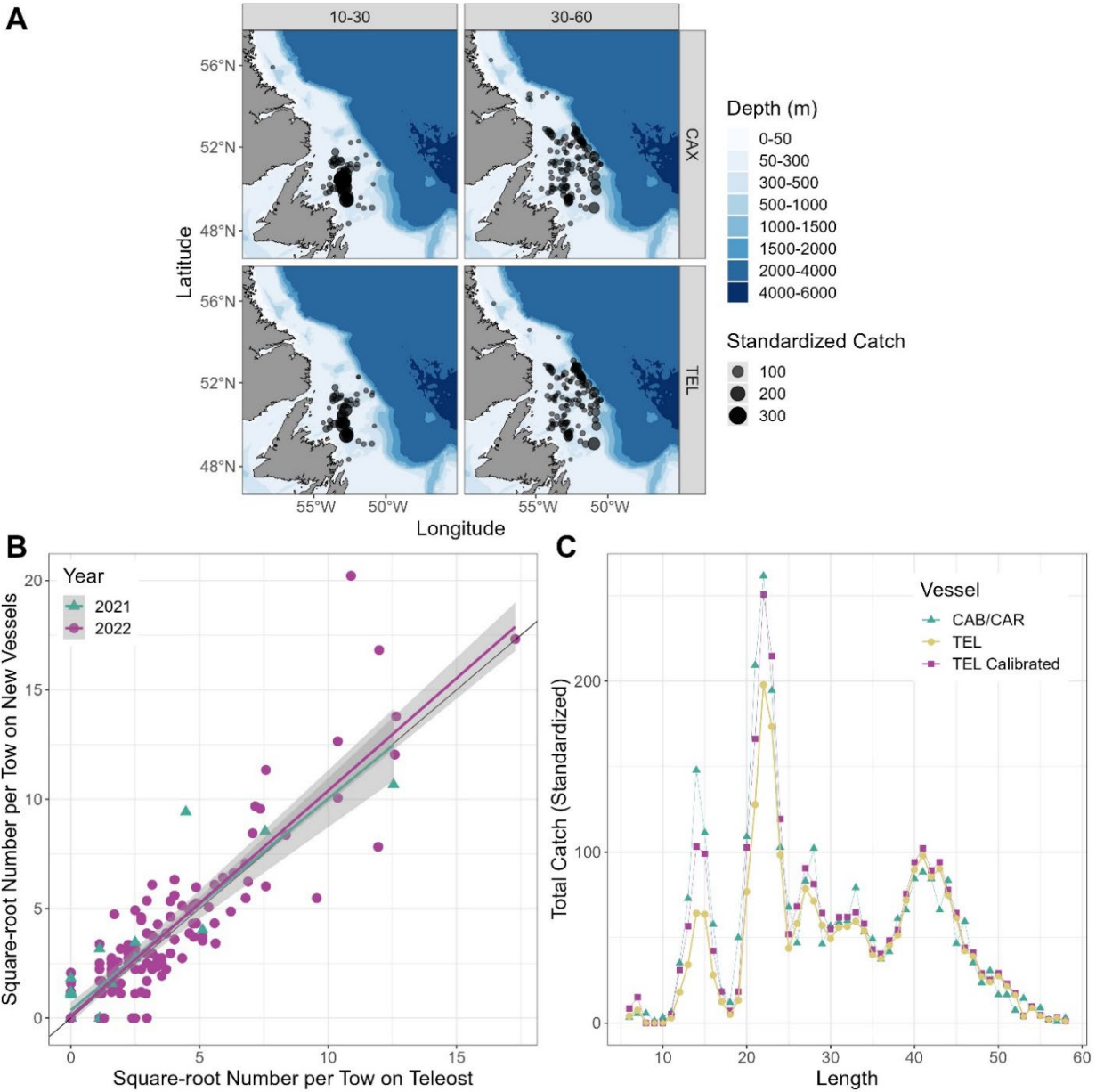


Figure A1–13. Results for length-disaggregated comparative fishing analyses for Witch Flounder (*Glyptocephalus cynoglossus*), between the CCGS Teleost and CCGS John Cabot/Capt. Jacques Cartier for Fall 2HJ3K + 3L deep. (A) map of catches by length group (length in cm specified in top panel) by the CCGS John Cabot/Capt. Jacques Cartier (top) and the CCGS Teleost (bottom) in comparative fishing sets, where circle size is proportional catch weight (B) Biplot of the square-root of CCGS John Cabot & CCGS Capt. Jacques Cartier catch numbers against the square-root of CCGS Teleost catch numbers, showing 2021 and 2022. (C) Total length frequencies for catches made by the CCGS Teleost (yellow), by the CCGS John Cabot/CCGS Capt. Jacques Cartier (green), and CCGS Teleost catches with the conversion factor applied (purple).

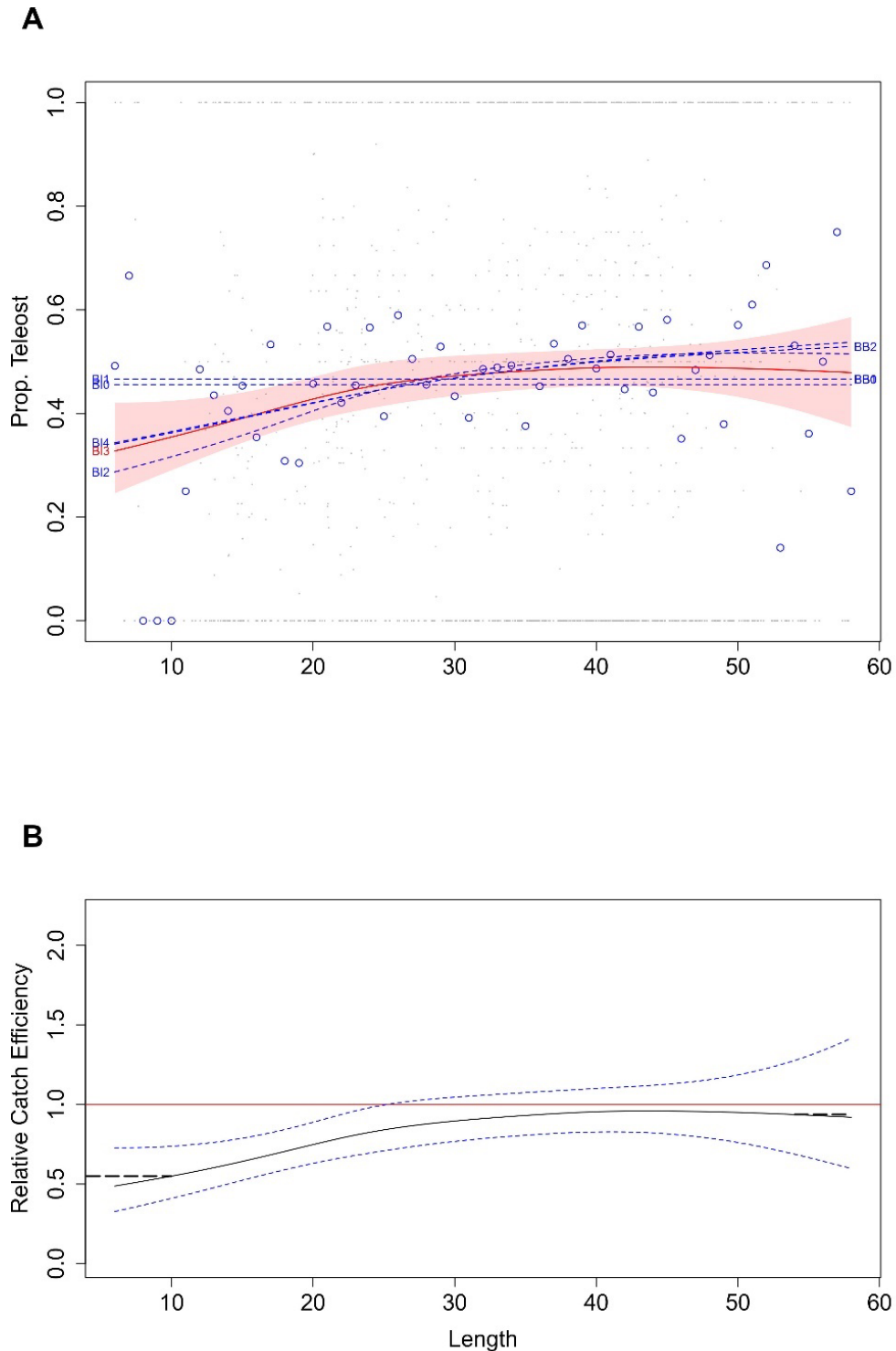


Figure A1–14. Witch Flounder (*Glyptocephalus cynoglossus*) conversion factor, between the CCGS Teleost and CCGS John Cabot/Capt. Jacques Cartier for Fall 2HJ3K + 3L deep. (A) Estimated length-specific catch proportion functions, $\text{logit}(p_{Ai}(l))$, for each converged model, with the selected model plotted using a red line along with its approximate 95% CI (shaded area), as well as the length class-specific mean empirical proportion of total catch in a pair made by the CCGS Teleost (blue dots). (B) Estimated relative catch efficiency (conversion factor) function from the best model (black line) with 95% CI (dashed blue lines). The horizontal red line indicates equivalent efficiency between vessels.

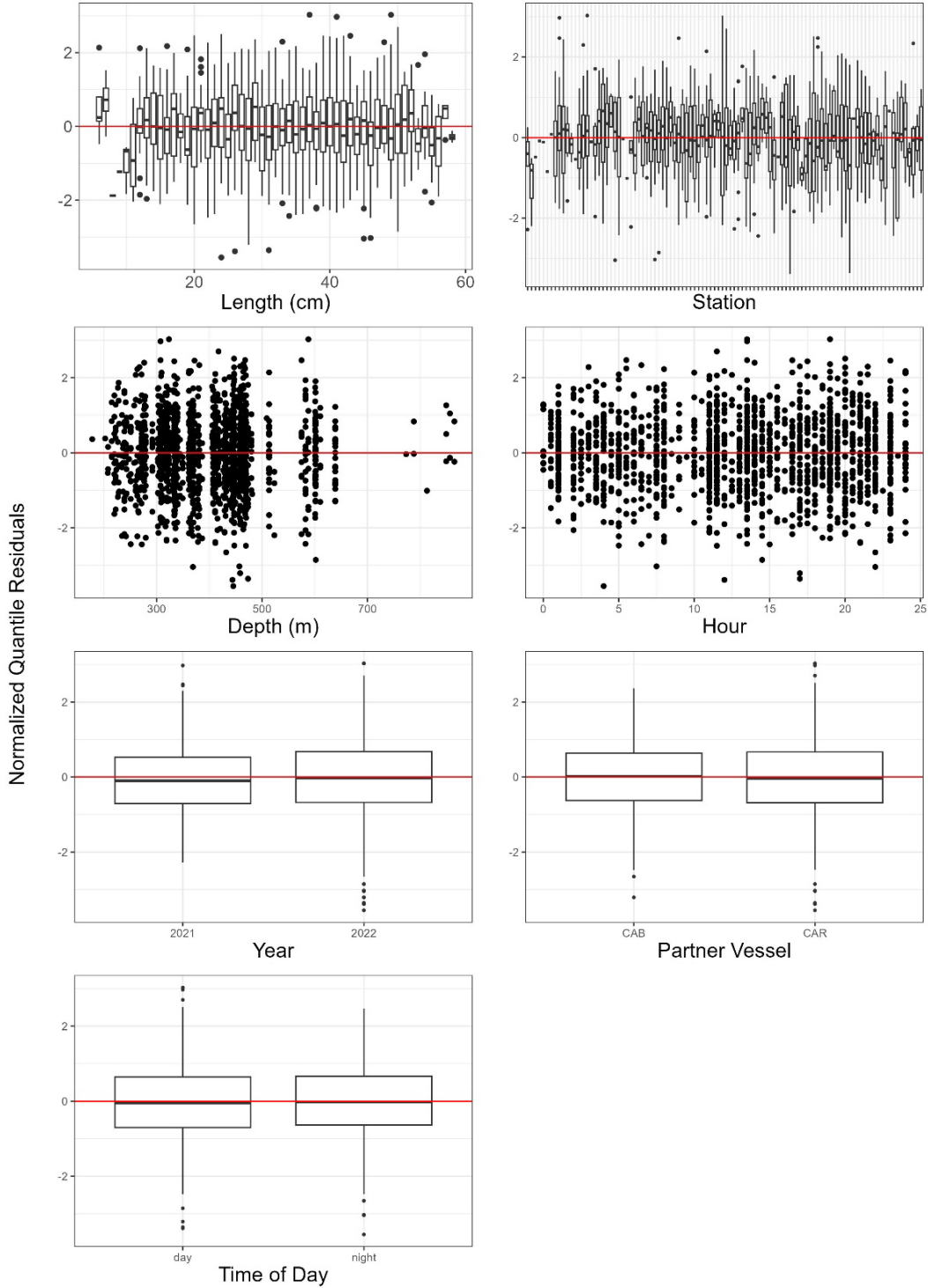


Figure A1-15. Normalized quantile residuals for as a function of length, station, depth, hour, year, partner vessel, and diel period for Witch Flounder (*Glyptocephalus cynoglossus*), best model selected (BI3) for length disaggregated conversion factor analysis for the CCGS Teleost, and CCGS John Cabot/Capt. Jacques Cartier for Fall 2HJ3K + 3L deep.

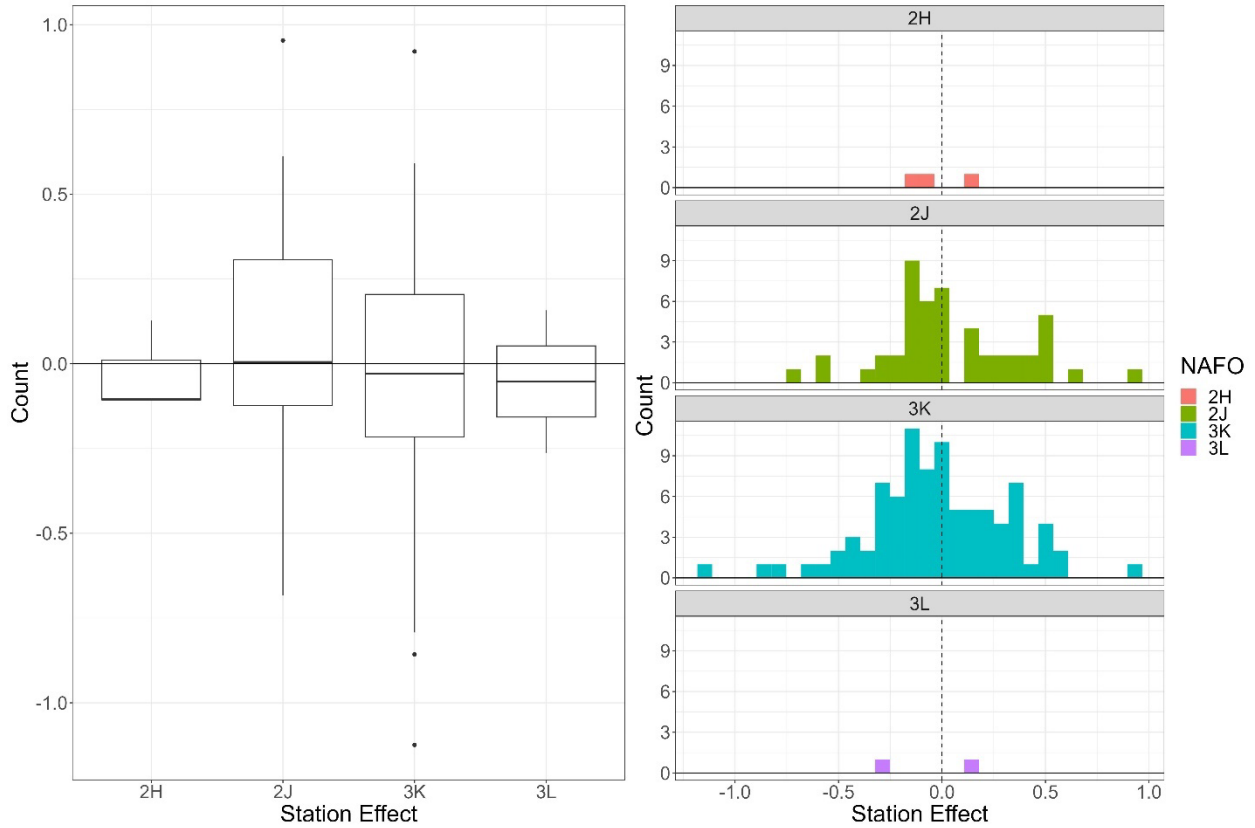


Figure A1–16. Boxplot (left) and histogram (right) of station effect by NAFO division for best model (BI3) selected for Witch Flounder (*Glyptocephalus cynoglossus*) conversion factor analysis of CCGS Teleost and CCGS John Cabot/Capt. Jacques Cartier in Fall 2HJ3K + 3L deep.

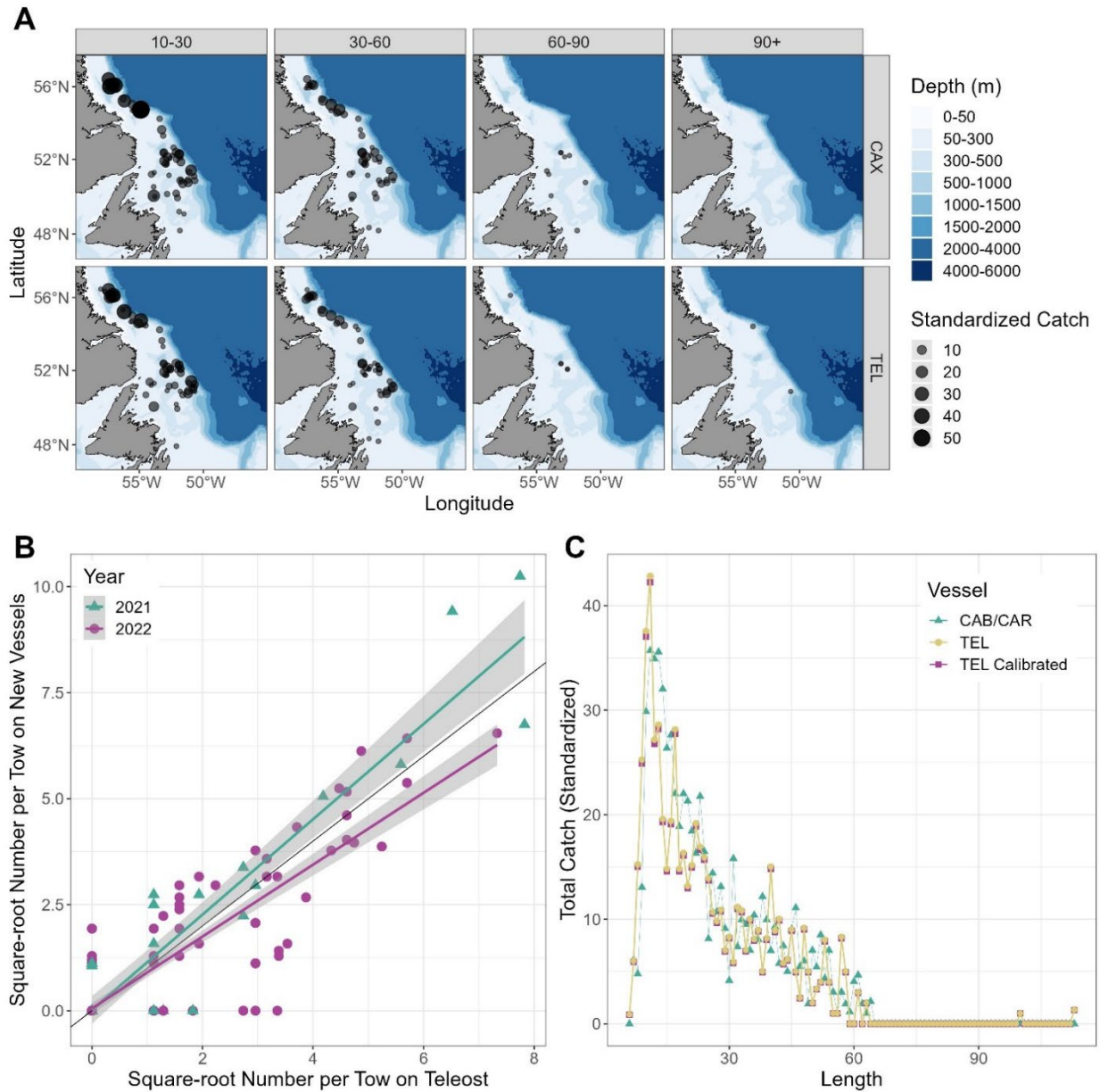


Figure A1–17. Results for length-disaggregated comparative fishing analyses for Striped Wolffish (*Anarhichas lupus*), between the CCGS Teleost and CCGS John Cabot/Capt. Jacques Cartier for Fall 2HJ3K + 3L deep. Data and results for length-disaggregated analyses. (A) map of catches by length group (length in cm specified in top panel) by the CCGS John Cabot/Capt. Jacques Cartier (top) and the CCGS Teleost (bottom) in comparative fishing sets, where circle size is proportional catch weight (B) Biplot of the square-root of CCGS John Cabot/Capt. Jacques Cartier catch numbers against the square-root of CCGS Teleost catch numbers, showing 2021 and 2022. (C) Total length frequencies for catches made by the CCGS Teleost (yellow), by the CCGS John Cabot/Capt. Jacques Cartier (green), and CCGS Teleost catches with the conversion factor applied (purple).

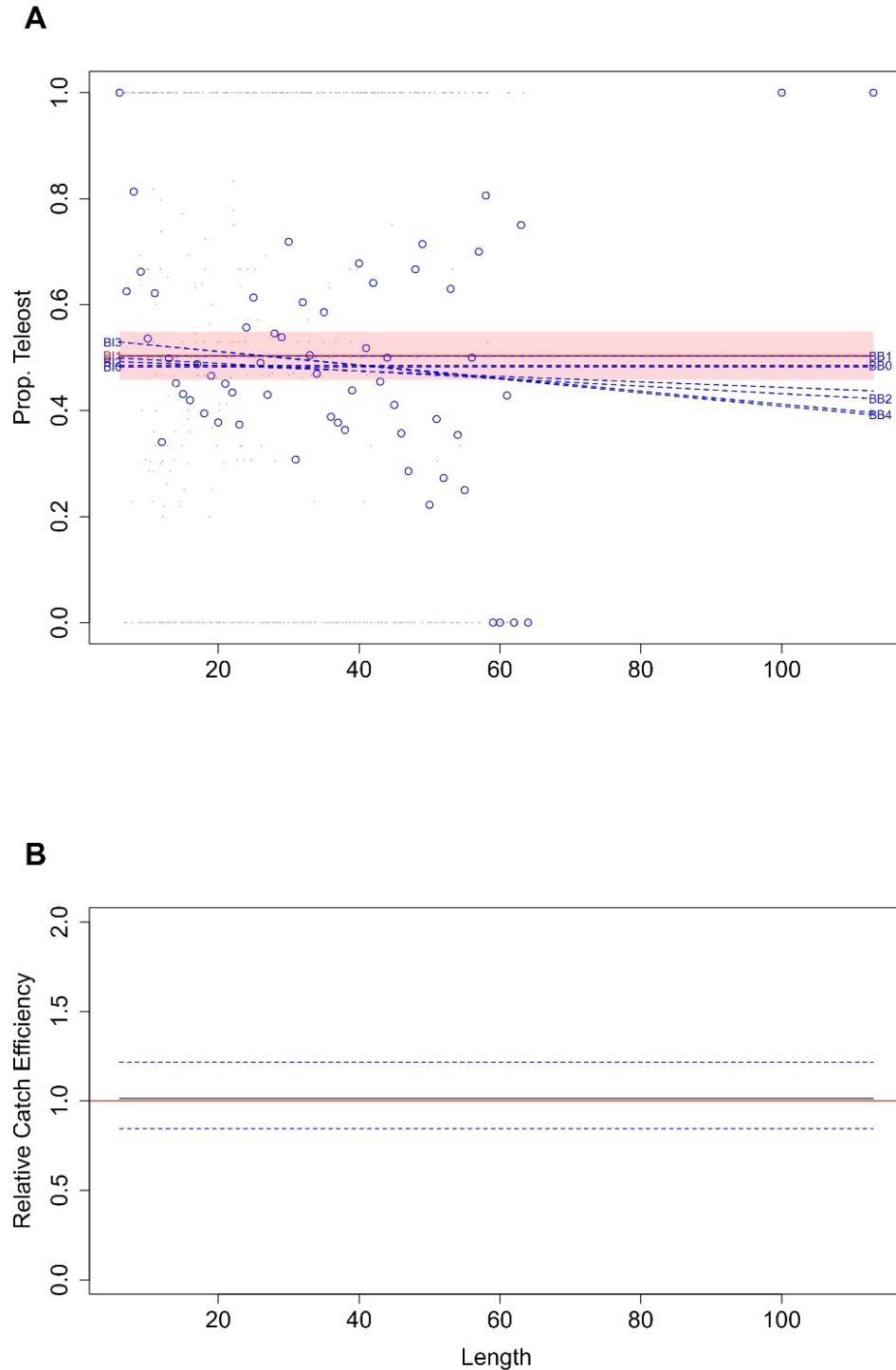


Figure A1-18. Striped Wolffish (*Anarhichas lupus*) conversion factor, between the CCGS Teleost and CCGS John Cabot/Capt. Jacques Cartier for Fall 2HJ3K + 3L deep. (A) Estimated length-specific catch proportion functions, $\text{logit}(p_{Ai}(l))$, for each converged model, with the selected model plotted using a red line along with its approximate 95% CI (shaded area), as well as the length class-specific mean empirical proportion of total catch in a pair made by the CCGS Teleost (blue dots). (B) Estimated relative catch efficiency (conversion factor) function from the best model (black line) with 95% CI (dashed blue lines). The horizontal red line indicates equivalent efficiency between vessels.

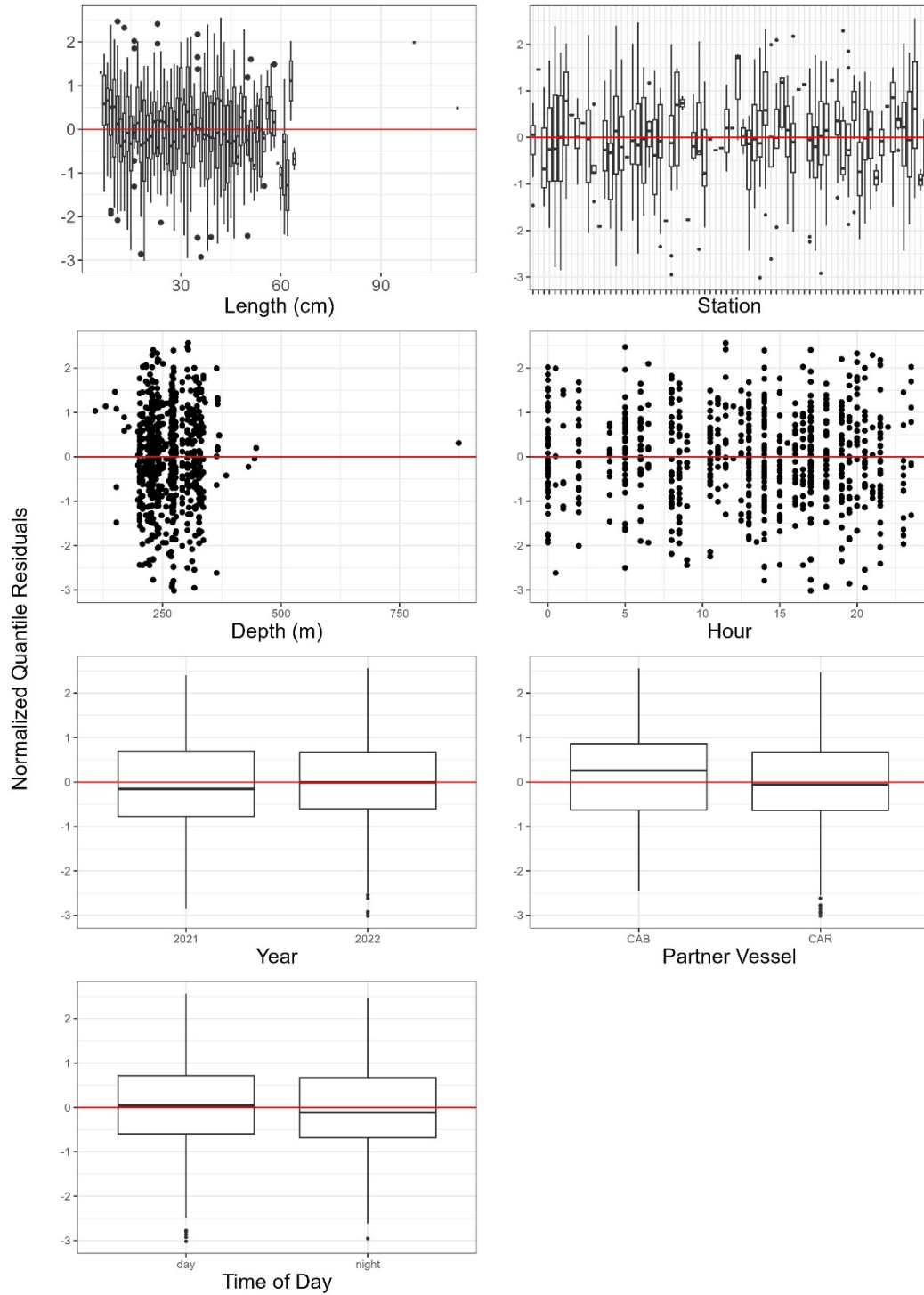


Figure A1-19. Normalized quantile residuals for as a function of length, station, depth, hour, year, partner vessel, and diel period for Striped Wolffish (*Anarhichas lupus*), best model selected (BI1) for length disaggregated conversion factor analysis for the CCGS Teleost, and CCGS John Cabot/Capt. Jacques Cartier for Fall 2HJ3K + 3L deep.

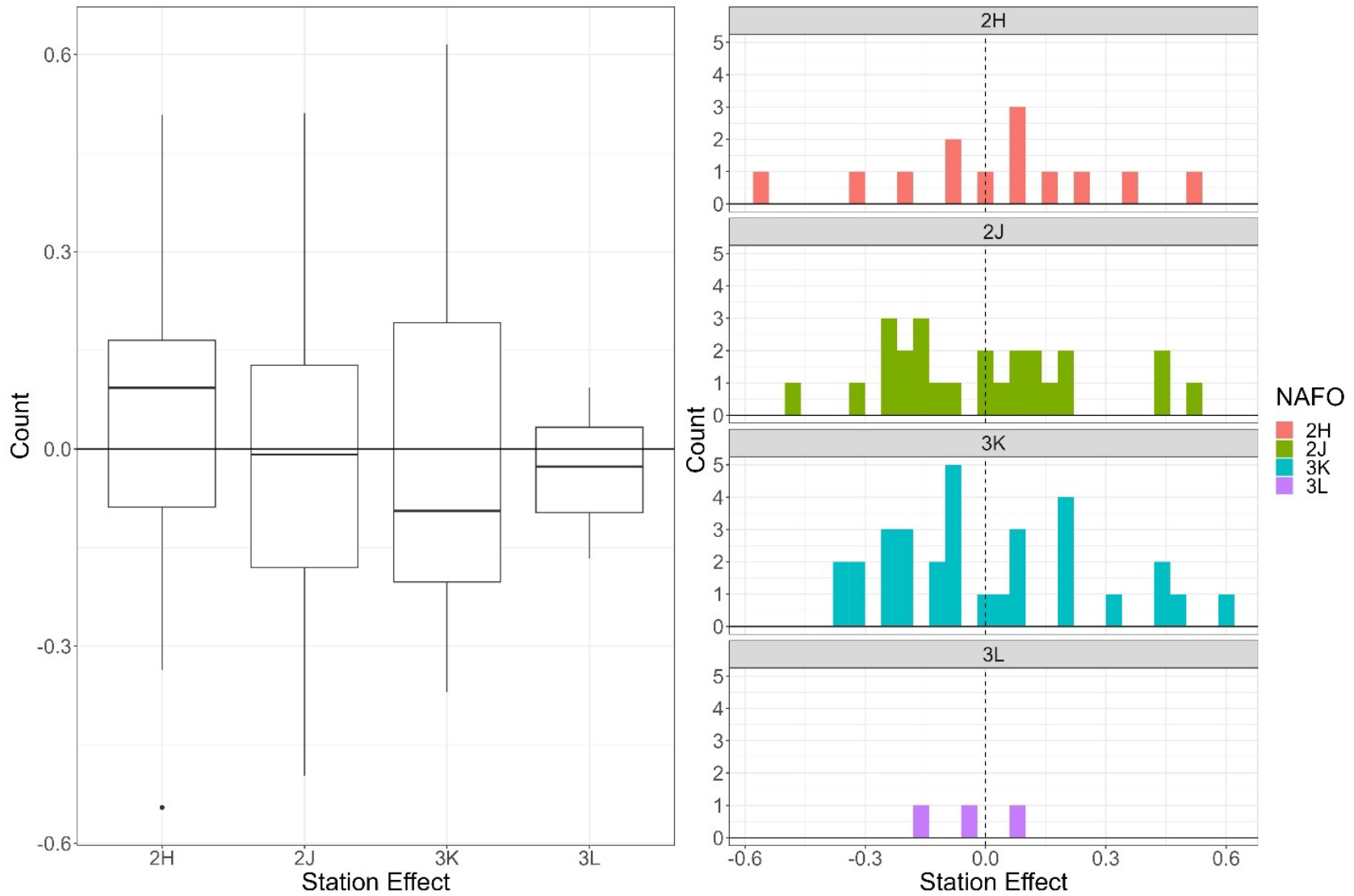


Figure A1–20. Boxplot (left) and histogram (right) of station effect by NAFO division for best model (B1) selected for Striped Wolffish (*Anarhichas lupus*), conversion factor analysis of CCGS Teleost and CCGS John Cabot/Capt. Jacques Cartier in Fall 2HJ3K + 3L deep.

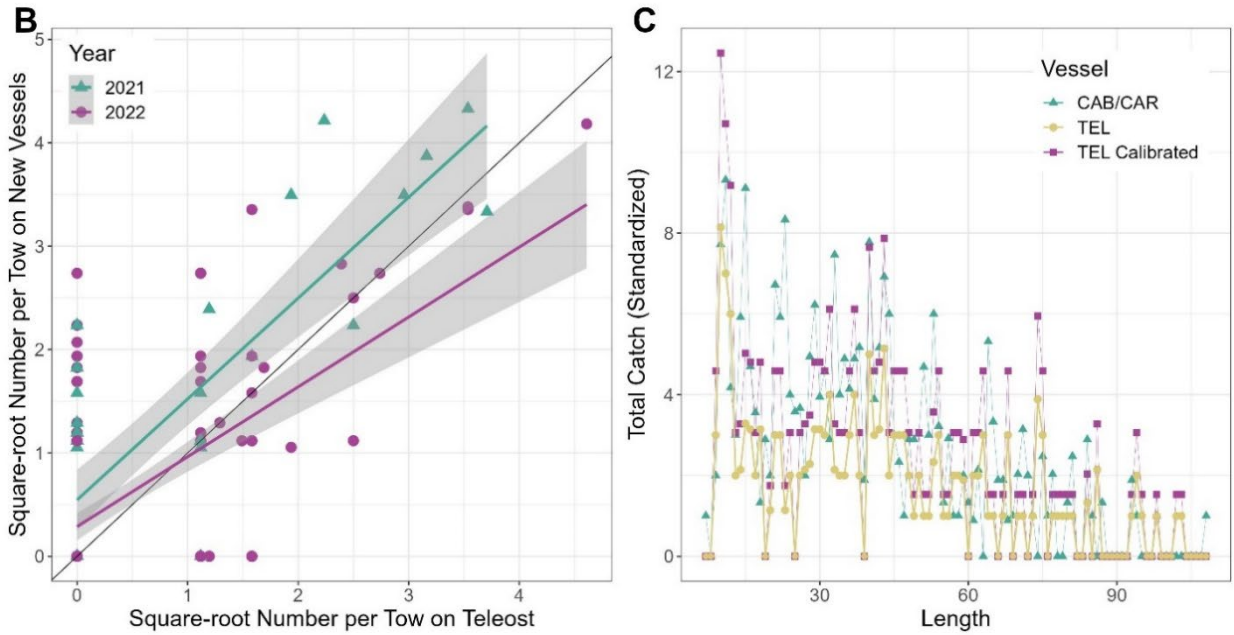
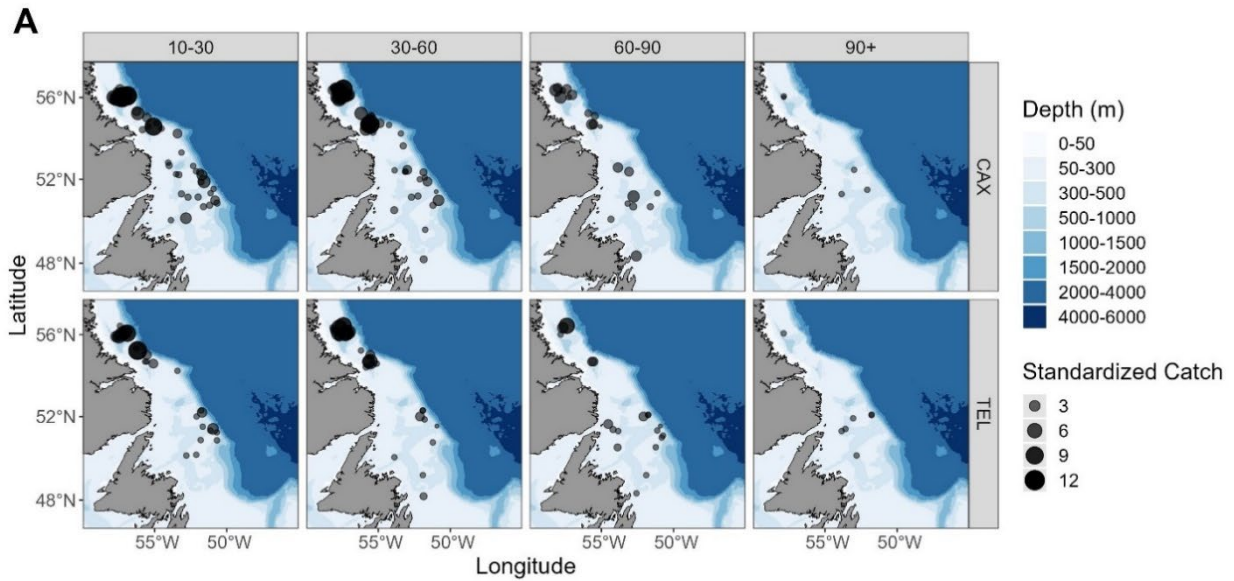


Figure A1–21. Results for length-disaggregated comparative fishing analyses for Spotted Wolffish (*Anarhichas minor*), between the CCGS Teleost and CCGS John Cabot/Capt. Jacques Cartier for Fall 2HJ3K + 3L deep. Data and results for length-disaggregated analyses. (A) map of catches by length group (length in cm specified in top panel) by the CCGS John Cabot/Capt. Jacques Cartier (top) and the CCGS Teleost (bottom) in comparative fishing sets, where circle size is proportional catch weight (B) Biplot of the square-root of Cabot & Cartier catch numbers against the square-root of Teleost catch numbers, showing 2021 and 2022. (C) Total length frequencies for catches made by the CCGS Teleost (yellow), by the Cabot/Cartier (green), and Teleost catches with the conversion factor applied (purple).

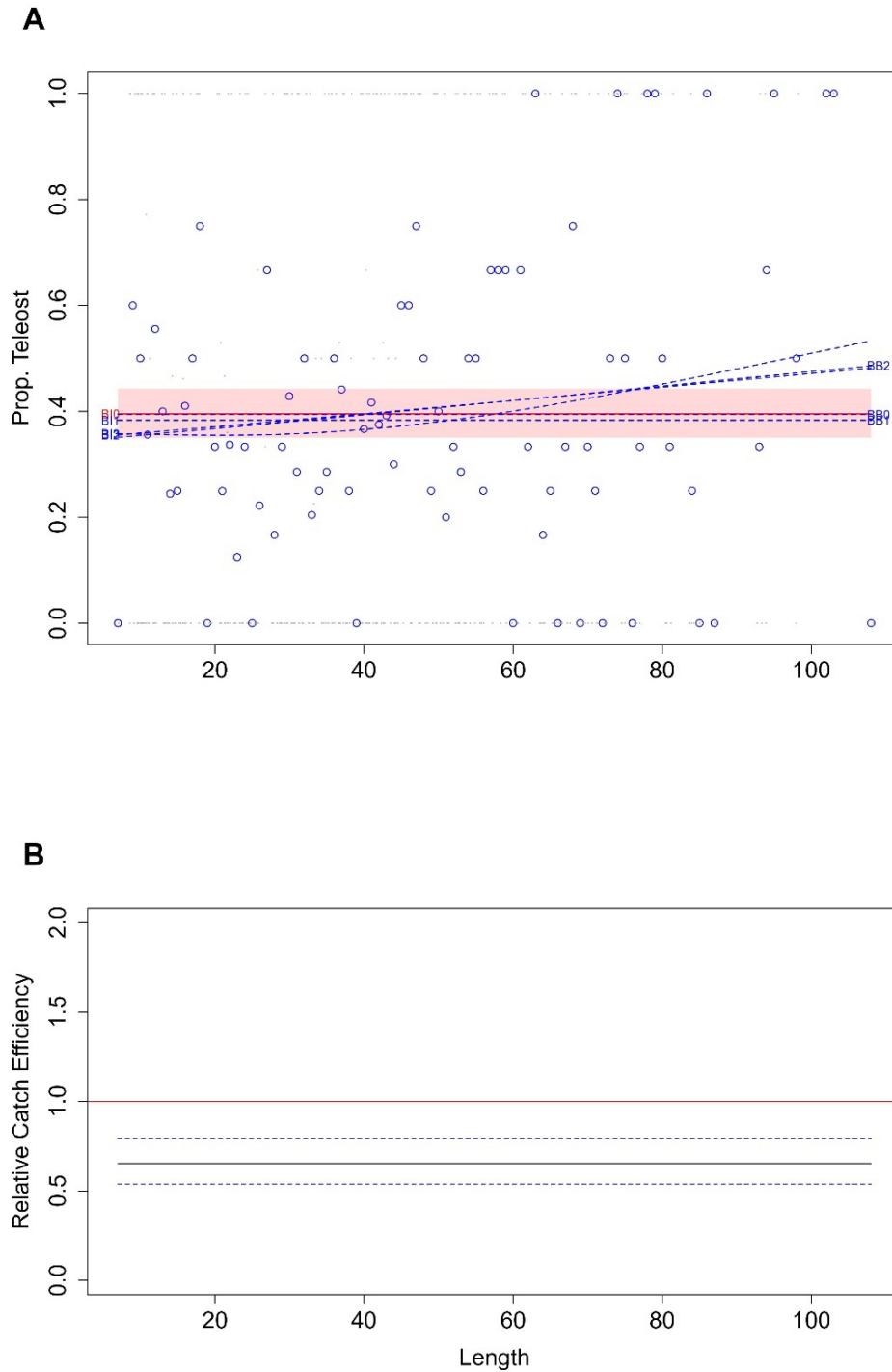


Figure A1–22. Spotted Wolffish (*Anarhichas minor*) conversion factor, between the CCGS Teleost and CCGS John Cabot/Capt. Jacques Cartier for Fall 2HJ3K + 3L deep. (A) Estimated length-specific catch proportion functions, $\text{logit}(p_{Ai}(l))$, for each converged model, with the selected model plotted using a red line along with its approximate 95% CI (shaded area), as well as the length class-specific mean empirical proportion of total catch in a pair made by the CCGS Teleost (blue dots). (B) Estimated relative catch efficiency (conversion factor) function from the best model (black line) with 95% CI (dashed blue lines). The horizontal red line indicates equivalent efficiency between vessels.

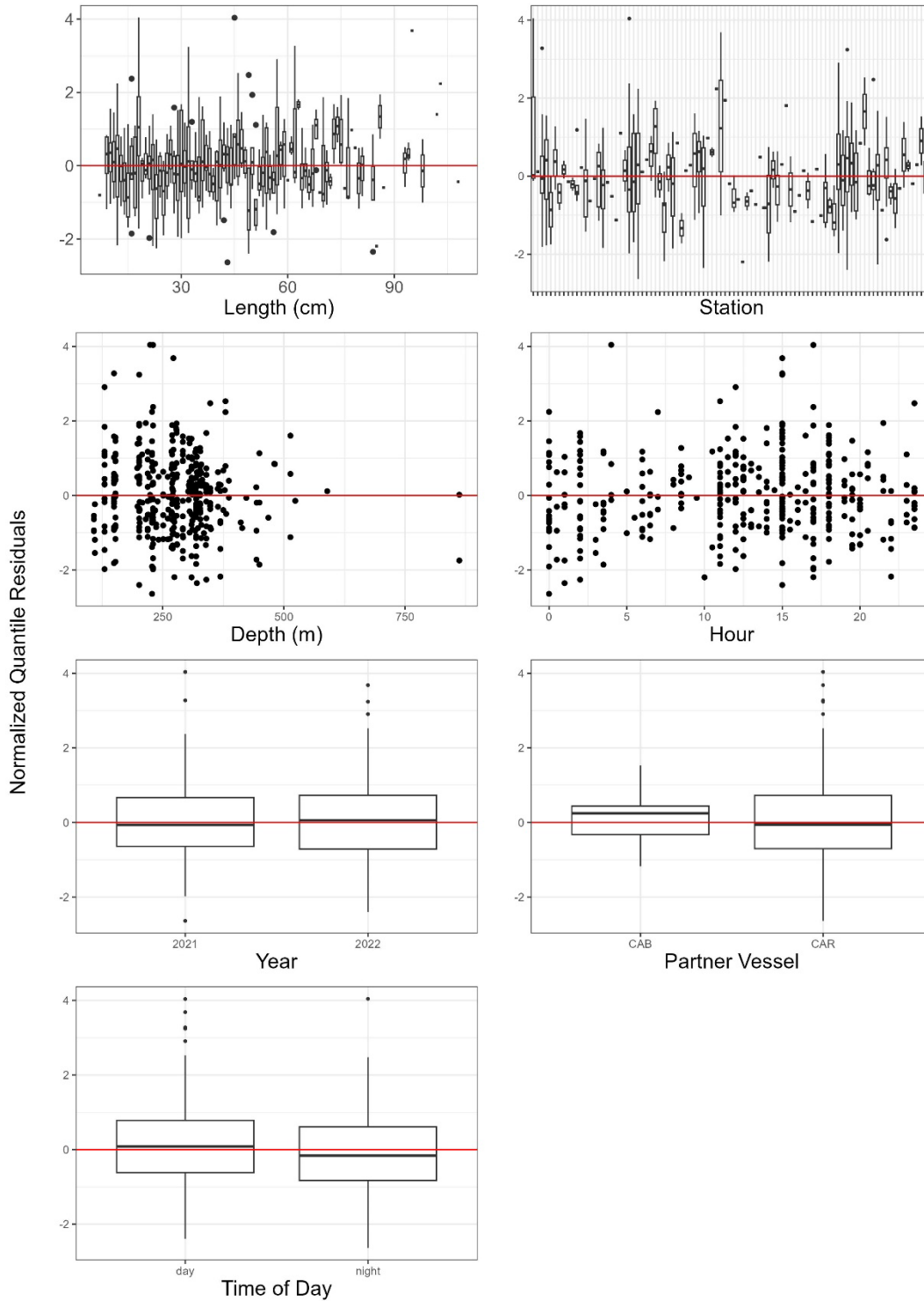


Figure A1–23. Normalized quantile residuals for as a function of length, station, depth, hour, year, partner vessel, and diel period for Spotted Wolffish (*Anarhichas minor*), best model selected (B10) for length disaggregated conversion factor analysis for the CCGS Teleost, and CCGS John Cabot/Capt. Jacques Cartier for Fall 2HJ3K + 3L deep.

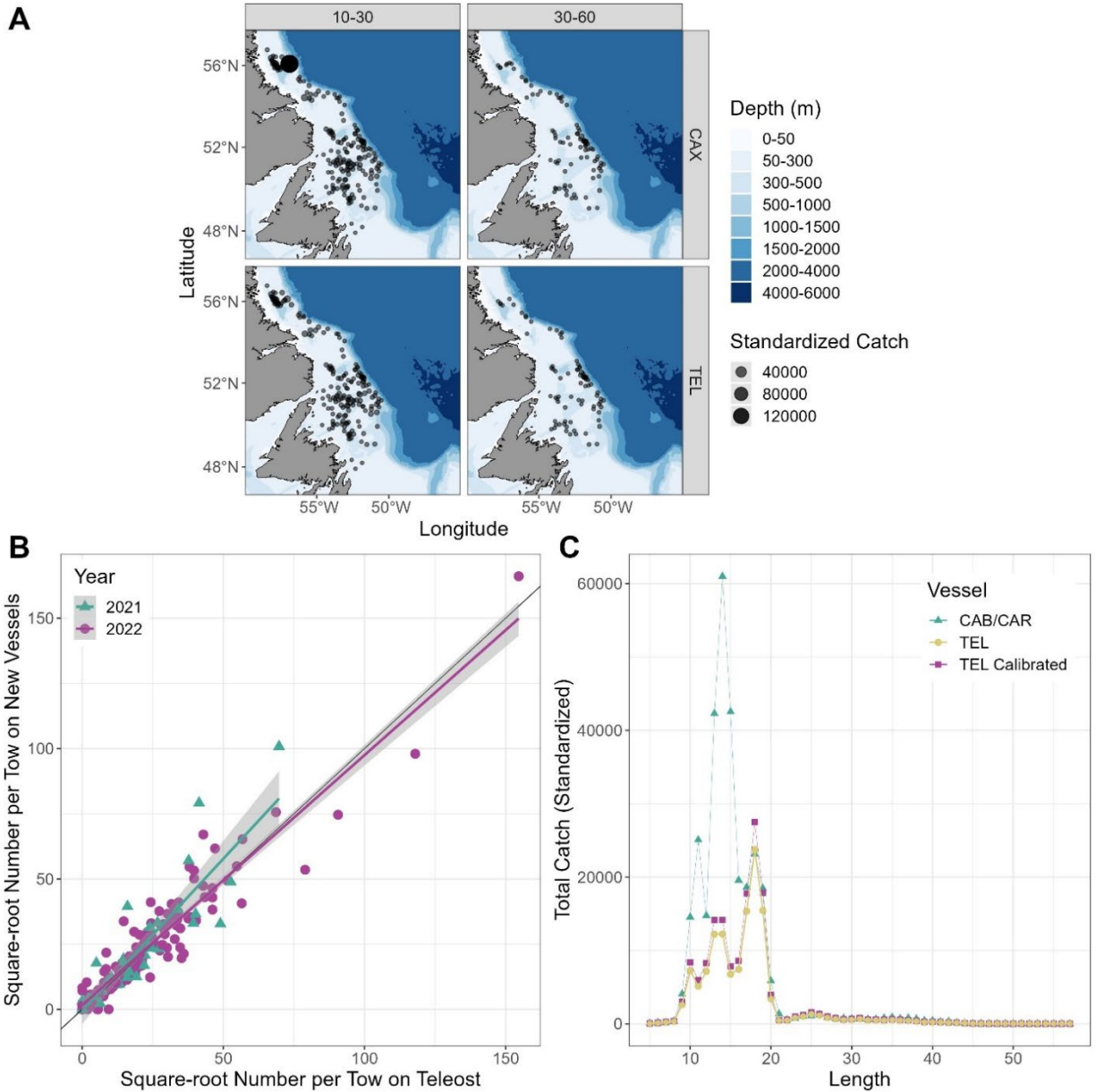


Figure A1–24. Results for length-disaggregated comparative fishing analyses for Redfish (*Sebastes mentella* + *S. fasciatus*) between the CCGS Teleost and CCGS John Cabot/Capt. Jacques Cartier for Fall 2HJ3K + 3L deep. Data and results for length-disaggregated analyses. (A) map of catches by length group (length in cm specified in top panel) by the CCGS John Cabot/Capt. Jacques Cartier (top) and the CCGS Teleost (bottom) in comparative fishing sets, where circle size is proportional catch weight (B) Biplot of the square-root of CCGS John Cabot/ Capt. Jacques Cartier catch numbers against the square-root of CCGS Teleost catch numbers, showing 2021 and 2022. (C) Total length frequencies for catches made by the CCGS Teleost (yellow), by the CCGS John Cabot/Capt. Jacques Cartier (green), and CCGS Teleost catches with the conversion factor applied (purple).

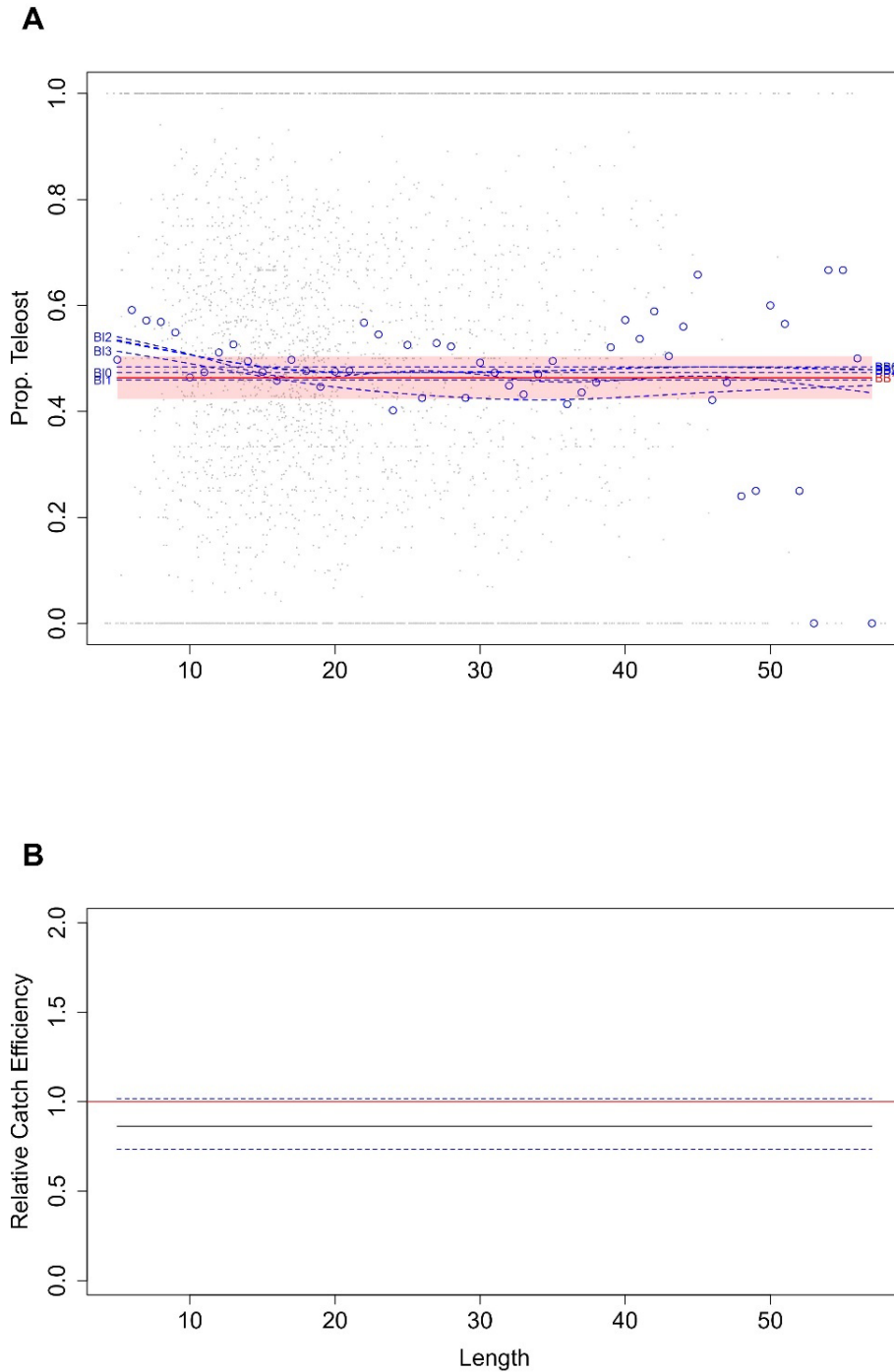


Figure A1–25. Redfish (*Sebastes mentella* + *S. fasciatus*) conversion factor, between the CCGS Teleost and CCGS John Cabot/Capt. Jacques Cartier for Fall 2HJ3K + 3L deep. (A) Estimated length-specific catch proportion functions, $\text{logit}(p_{Ai}(l))$, for each converged model, with the selected model plotted using a red line along with its approximate 95% CI (shaded area), as well as the length class-specific mean empirical proportion of total catch in a pair made by the CCGS Teleost (blue dots). (B) Estimated relative catch efficiency (conversion factor) function from the best model (black line) with 95% CI (dashed blue lines). The horizontal red line indicates equivalent efficiency between vessels.

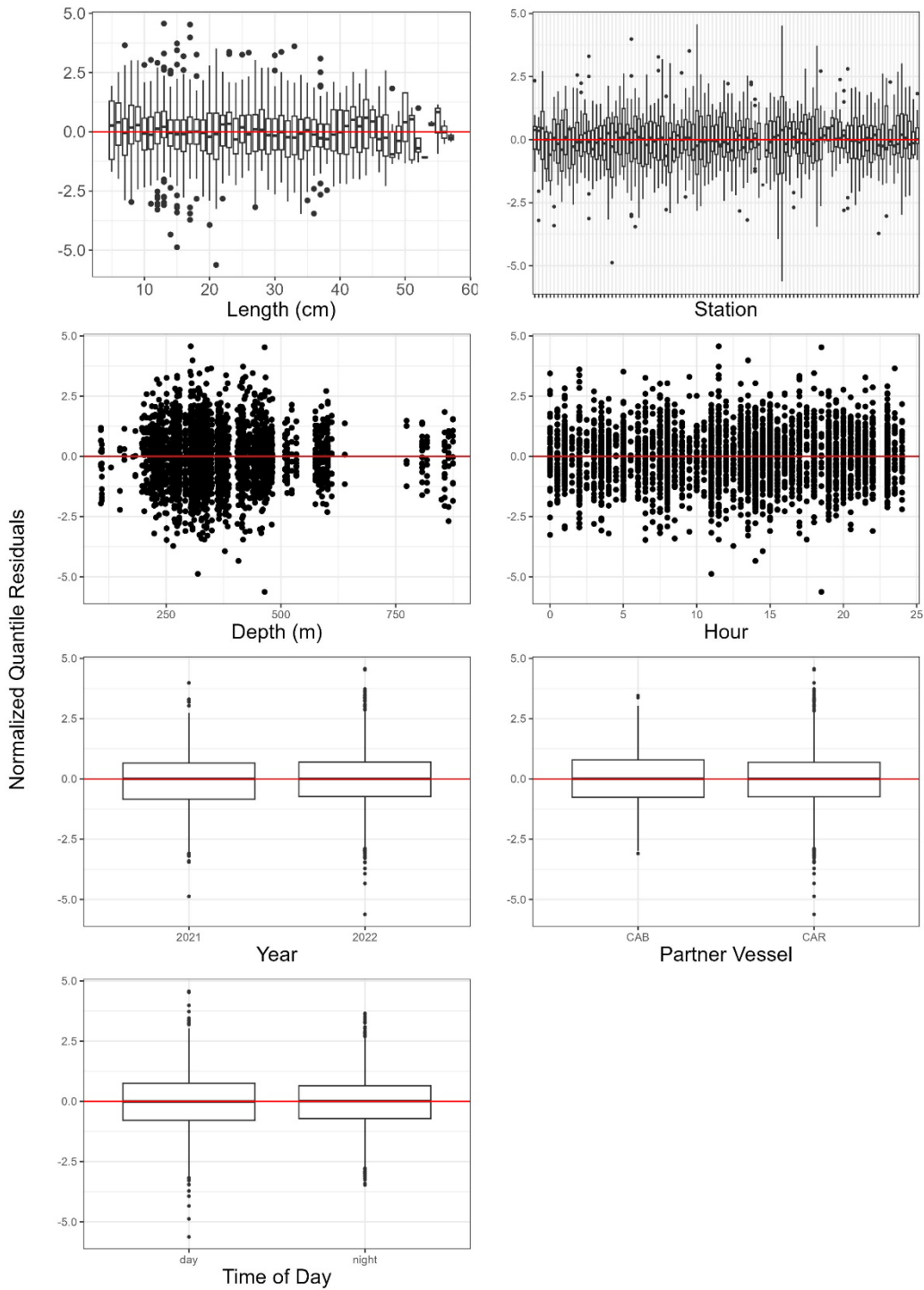


Figure A1–26. Normalized quantile residuals for as a function of length, station, depth, hour, year, partner vessel, and diel period for Redfish (*Sebastes mentella* + *S. fasciatus*), best model selected (BB1) for length disaggregated conversion factor analysis for the CCGS Teleost, and CCGS John Cabot/Capt. Jacques Cartier for Fall 2HJ3K + 3L deep.

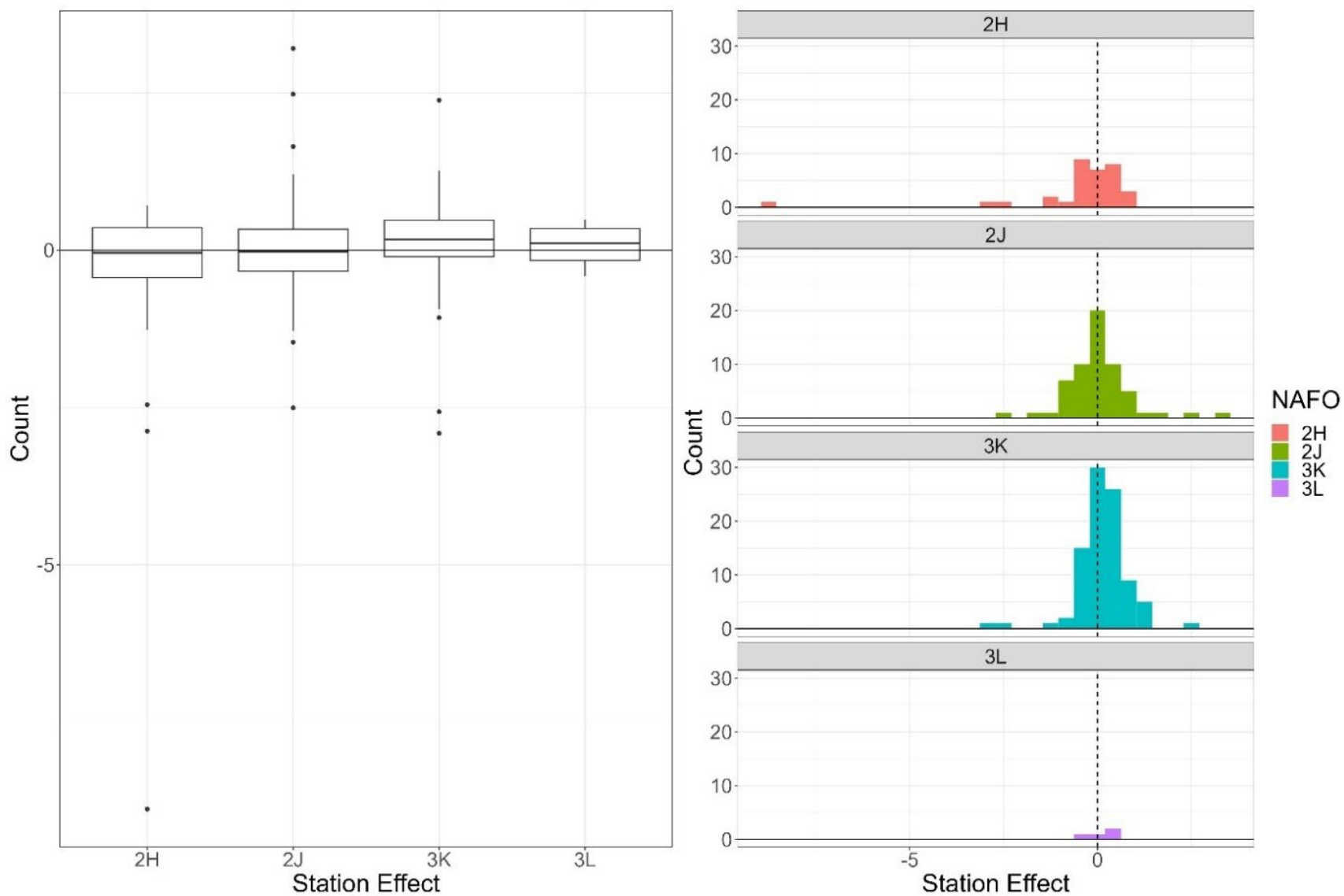


Figure A1-27. Boxplot (left) and histogram (right) of station effect by NAFO division for best model (BB1) selected for Redfish (*Sebastes mentella* + *S. fasciatus*), conversion factor analysis of CCGS Teleost and CCGS John Cabot/Capt. Jacques Cartier in Fall 2HJ3K + 3L deep.

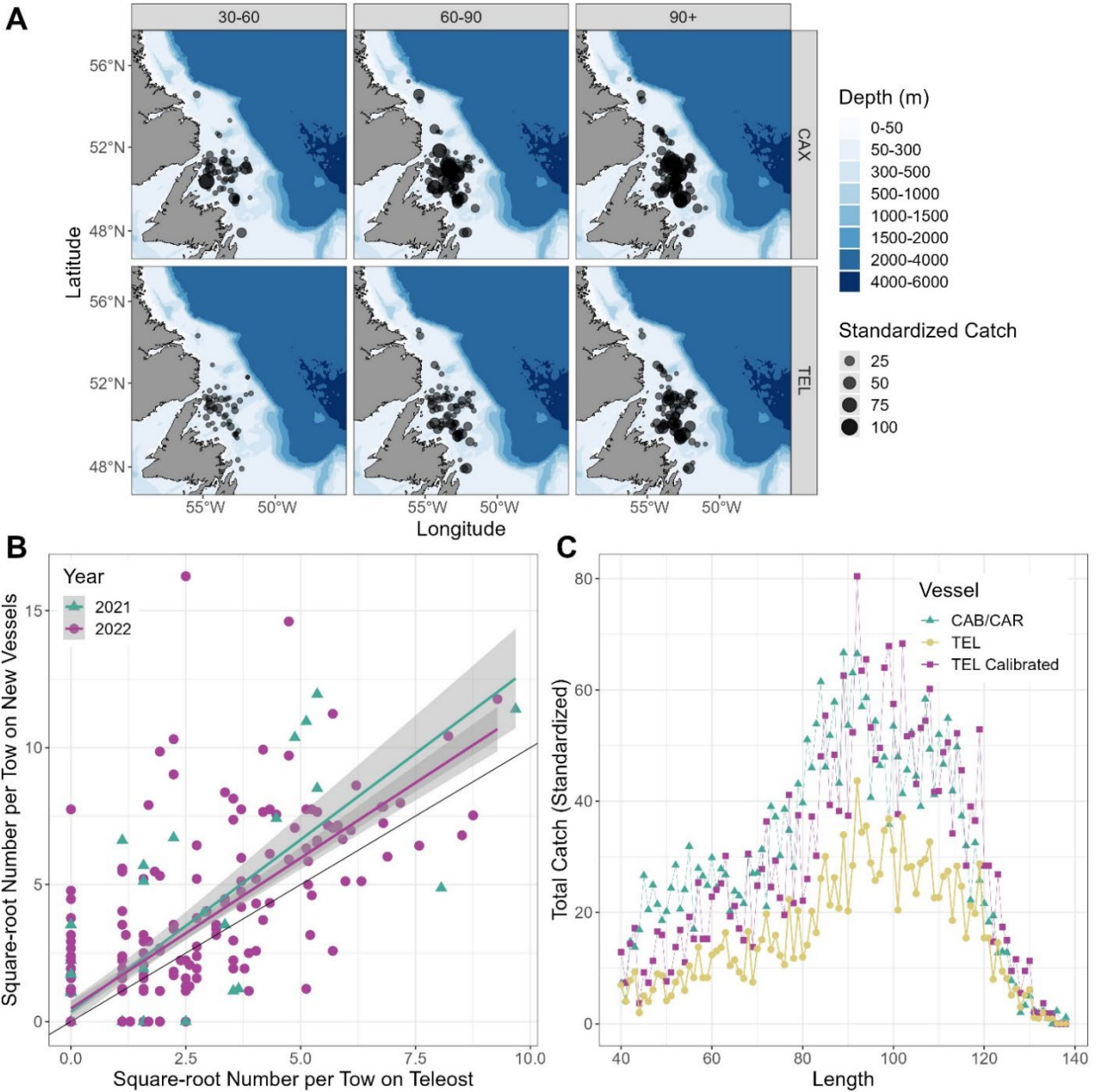


Figure A1–28. Results for length-disaggregated comparative fishing analyses for Snow Crab (*Chionoecetes opilio*), >40 mm, between the CCGS Teleost and CCGS John Cabot/Capt. Jacques Cartier for Fall 2HJ3K + 3L deep. Data and results for length-disaggregated analyses. (A) map of catches by length group (carapace width in mm specified in top panel) by the CCGS John Cabot/Capt. Jacques Cartier (top) and the CCGS Teleost (bottom) in comparative fishing sets, where circle size is proportional catch weight (B) Biplot of the square-root of Cabot & Cartier catch numbers against the square-root of Teleost catch numbers, showing 2021 and 2022. (C) Total length frequencies for catches made by the CCGS Teleost (yellow), by the Cabot/Cartier (green), and Teleost catches with the conversion factor applied (purple).

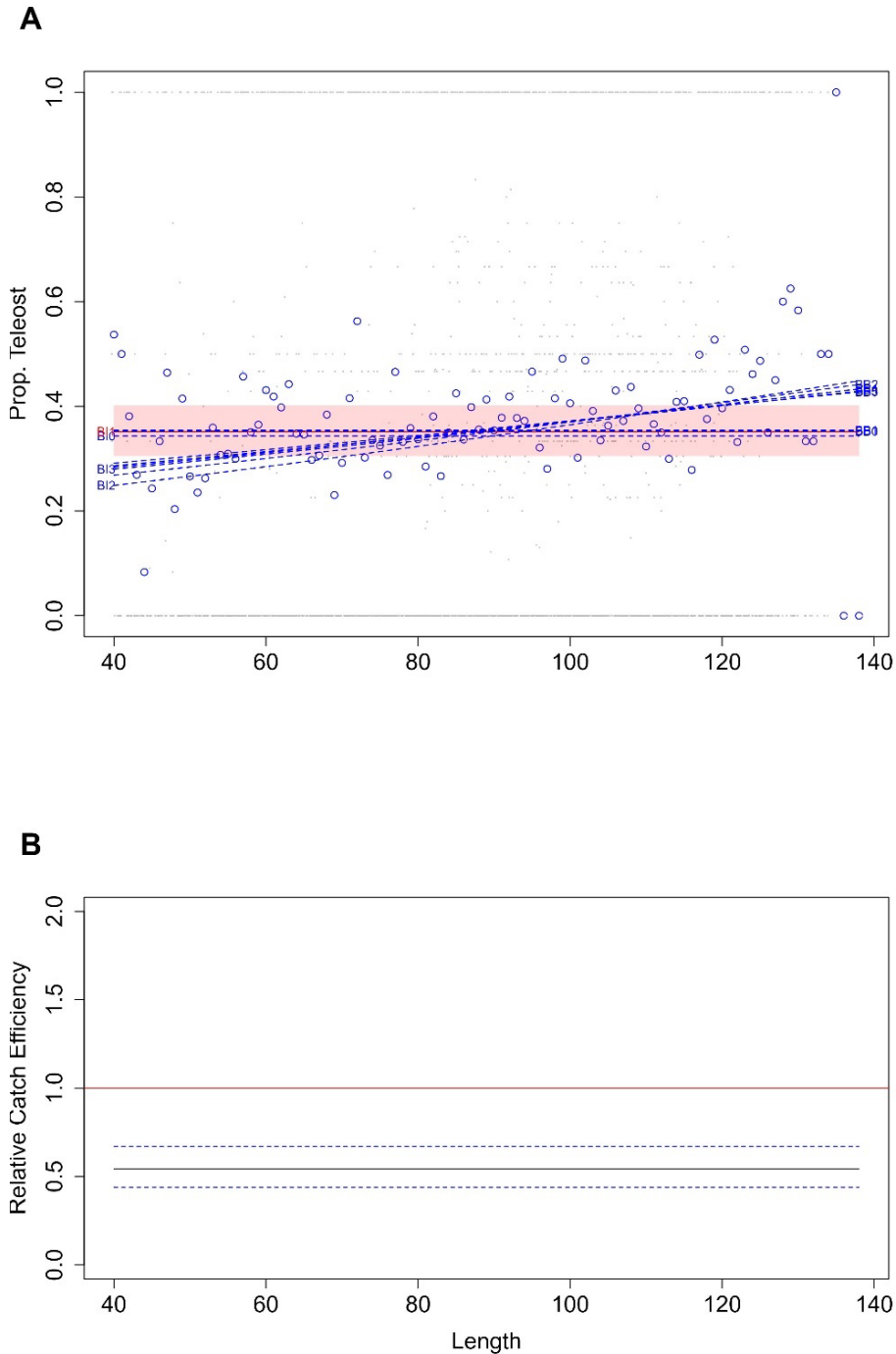


Figure A1–29. Snow Crab (*Chionoectes opilio*) >40 mm conversion factor, between the CCGS Teleost and CCGS John Cabot/Capt. Jacques Cartier for Fall 2HJ3K + 3L deep. (A) Estimated length-specific catch proportion functions, $\text{logit}(p_{Ai}(l))$, for each converged model, with the selected model plotted using a red line along with its approximate 95% CI (shaded area), as well as the length class-specific mean empirical proportion of total catch in a pair made by the CCGS Teleost (blue dots). (B) Estimated relative catch efficiency (conversion factor) function from the best model (black line) with 95% CI (dashed blue lines). The horizontal red line indicates equivalent efficiency between vessels. A constant conversion of $0.54 (\pm 0.06)$ to be applied.

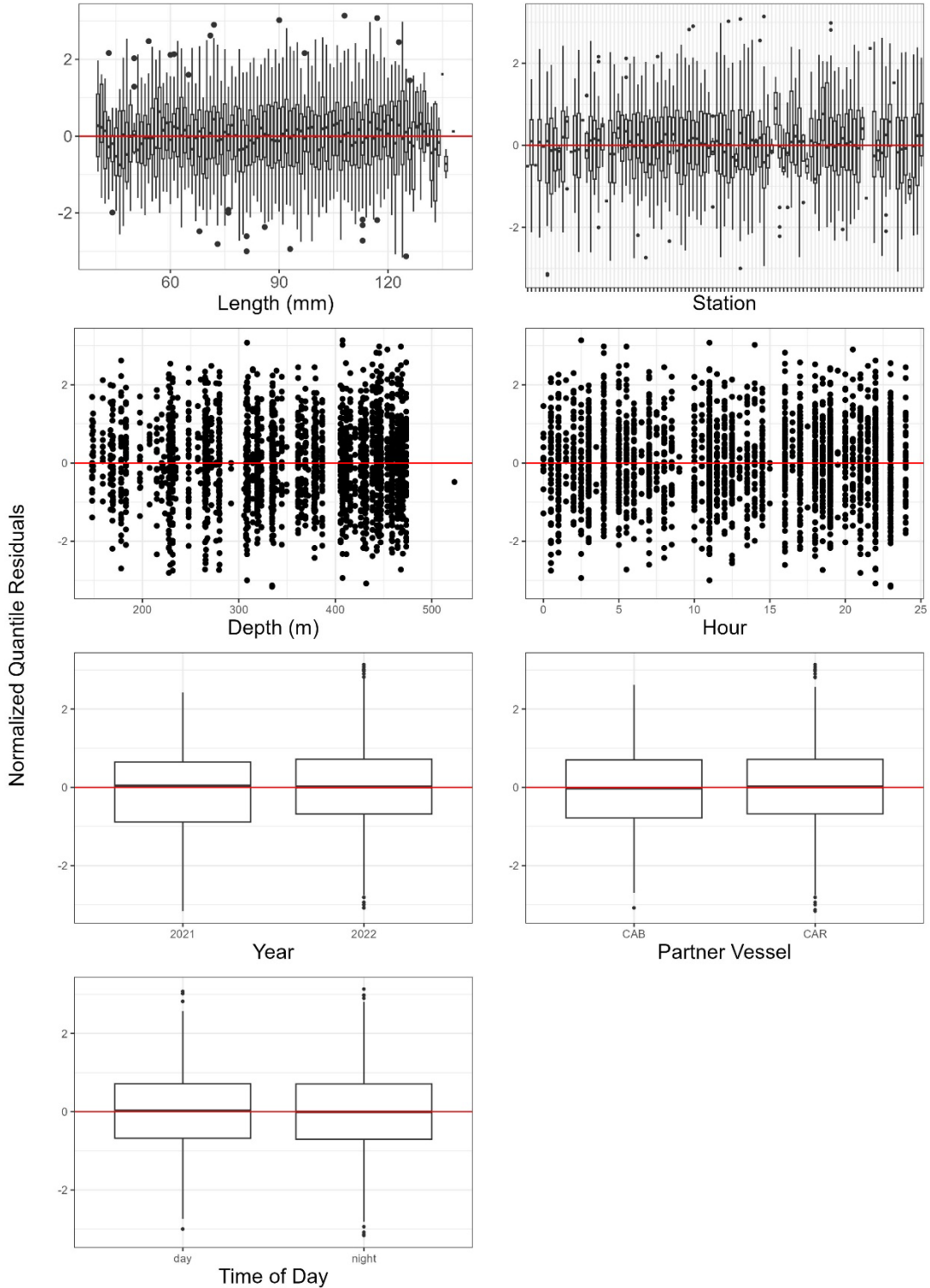


Figure A1–30. Normalized quantile residuals for as a function of length, station, depth, hour, year, partner vessel, and diel period for Snow Crab (*Chionoecetes opilio*), best model selected (B11) for length disaggregated conversion factor analysis for the CCGS Teleost, and CCGS John Cabot/Capt. Jacques Cartier for Fall 2HJ3K + 3L deep. Normalized quantile residuals for as a function of length, station, depth, hour, year, new vessel, and diel period.

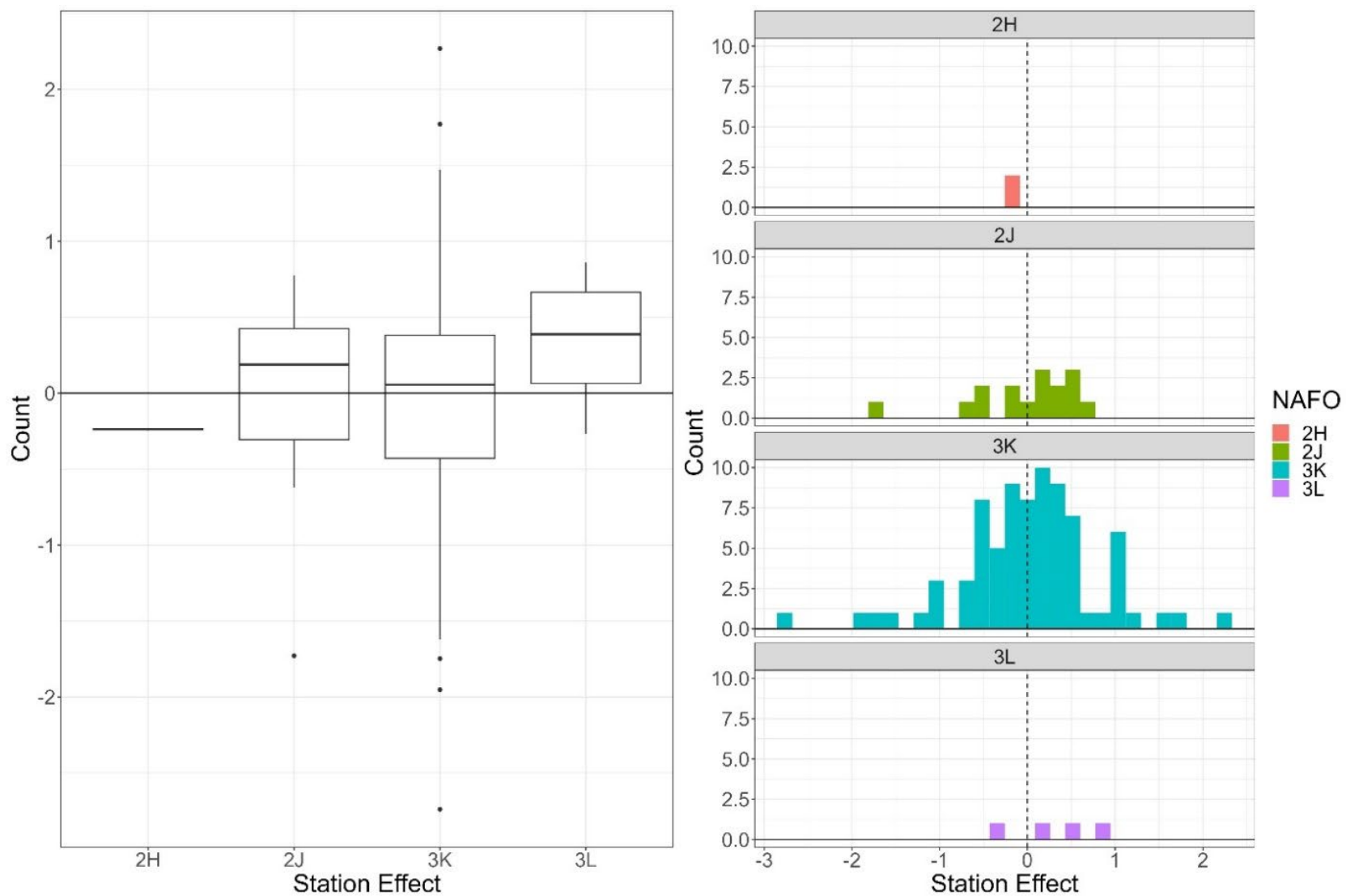


Figure A1-31. Boxplot (left) and histogram (right) of station effect by NAFO division for best model (BI1) selected for Snow Crab (*Chionoecetes opilio*) >40 mm, conversion factor analysis of CCGS Teleost and CCGS John Cabot/Capt. Jacques Cartier in Fall 2HJ3K + 3L deep.

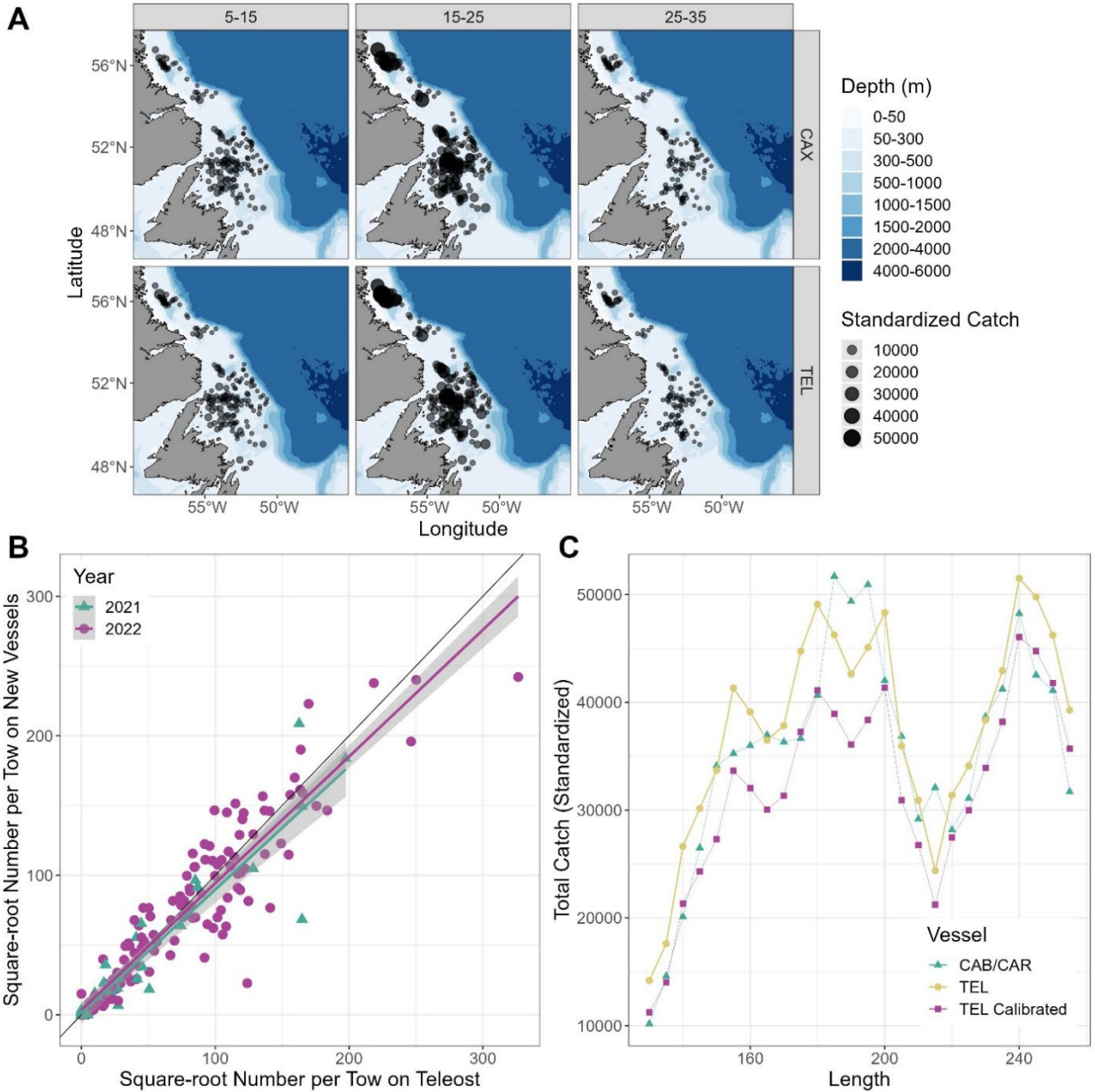


Figure A1–32. Results for length-disaggregated comparative fishing analyses for Northern Shrimp (*Pandalus borealis*), between the CCGS Teleost and CCGS John Cabot/Capt. Jacques Cartier for Fall 2HJ3K + 3L deep. Note, lengths have been trimmed to the 2.5 & 97.5 percentiles prior to model fit. Lengths are binned in 0.5 mm bins. Data and results for length-disaggregated analyses. (A) map of catches by length group (length in cm specified in top panel) by the CCGS John Cabot/Capt. Jacques Cartier (top) and the CCGS Teleost (bottom) in comparative fishing sets, where circle size is proportional catch weight (B) Biplot of the square-root of Cabot & Cartier catch numbers against the square-root of CCGS Teleost catch numbers, showing 2021 and 2022. (C) Total length frequencies (mm) for catches made by the CCGS Teleost (yellow), by the CCGS John Cabot/Capt. Jacques Cartier (green), and CCGS Teleost catches with the conversion factor applied (purple).

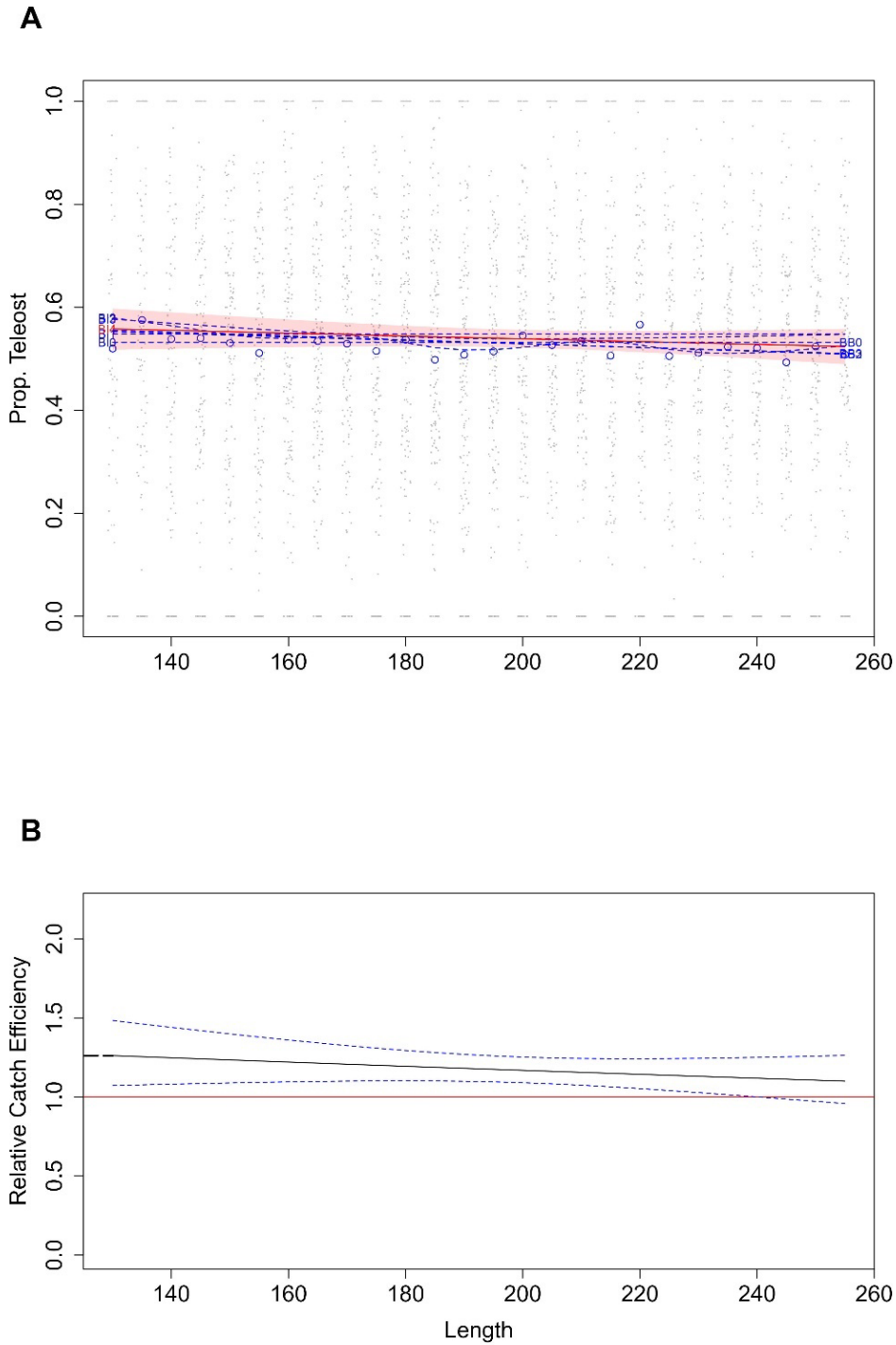


Figure A1–33. Northern Shrimp (*Pandalus borealis*) conversion factor, between the CCGS Teleost and CCGS John Cabot/Capt. Jacques Cartier for Fall 2HJ3K + 3L deep. Note, lengths have been trimmed to the 2.5 & 97.5 percentiles prior to model fit. Carapace lengths (mm) are binned in 0.5 mm intervals. (A) Estimated length-specific catch proportion functions, $\text{logit}(p_{Ai}(l))$, for each converged model, with the selected model plotted using a red line along with its approximate 95% CI (shaded area), as well as the length class-specific mean empirical proportion of total catch in a pair made by the CCGS Teleost (blue dots). (B) Estimated relative catch efficiency (conversion factor) function from the best model (black line) with 95% CI (dashed blue lines). The horizontal red line indicates equivalent efficiency between vessels.

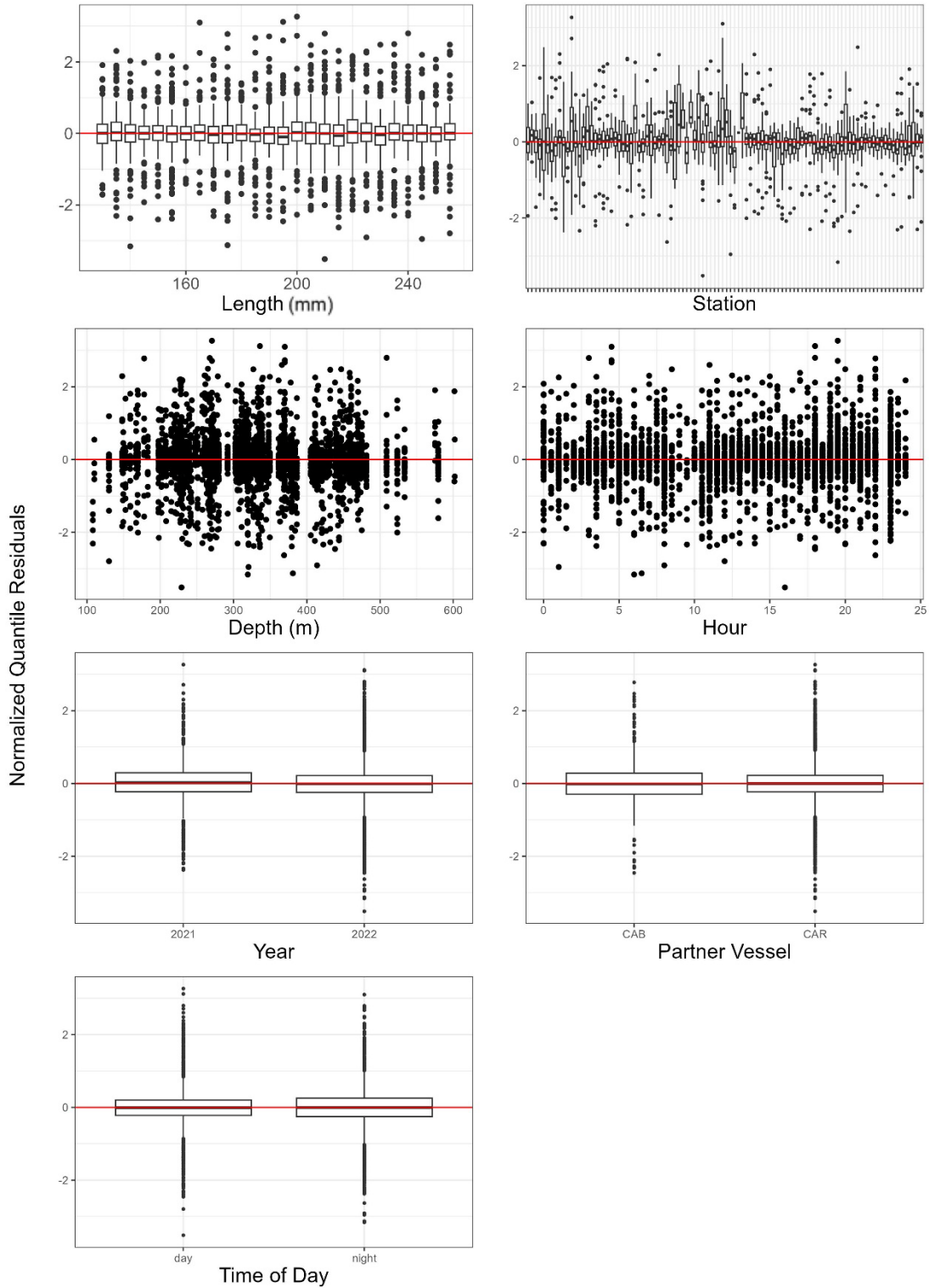
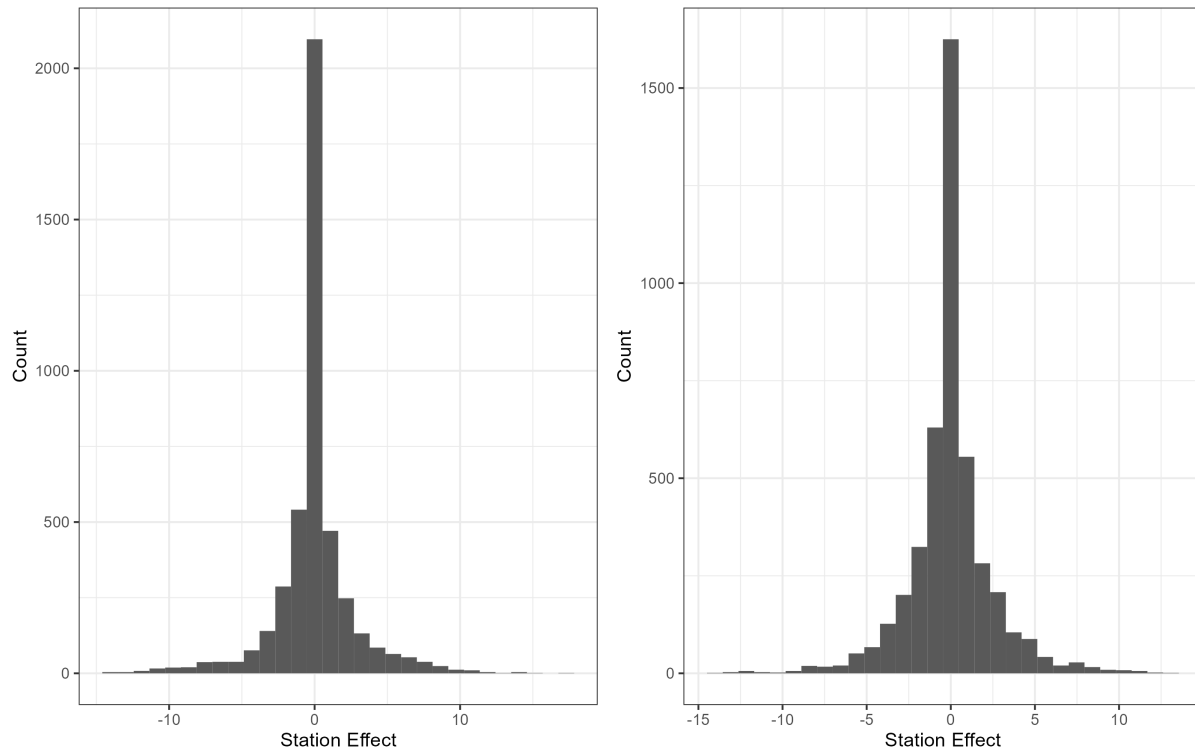


Figure A1–34. Normalized quantile residuals for as a function of length, station, depth, hour, year, partner vessel, and diel period for Northern Shrimp (*Pandalus borealis*), best model selected (BI4) for length disaggregated conversion factor analysis for the CCGS Teleost, and CCGS John Cabot/Capt. Jacques Cartier for Fall 2HJ3K + 3L deep. Note, lengths have been trimmed to the 2.5 & 97.5 percentiles prior to model fit and lengths are binned in 0.5 mm bins.



*Figure A1–35. Histogram of station effect on intercept (left) and smoother (right) for best model (BI4) selected for Northern Shrimp (*Pandalus borealis*), conversion factor analysis of CCGS Teleost and CCGS John Cabot/Capt. Jacques Cartier in Fall 2HJ3K + 3L deep.*

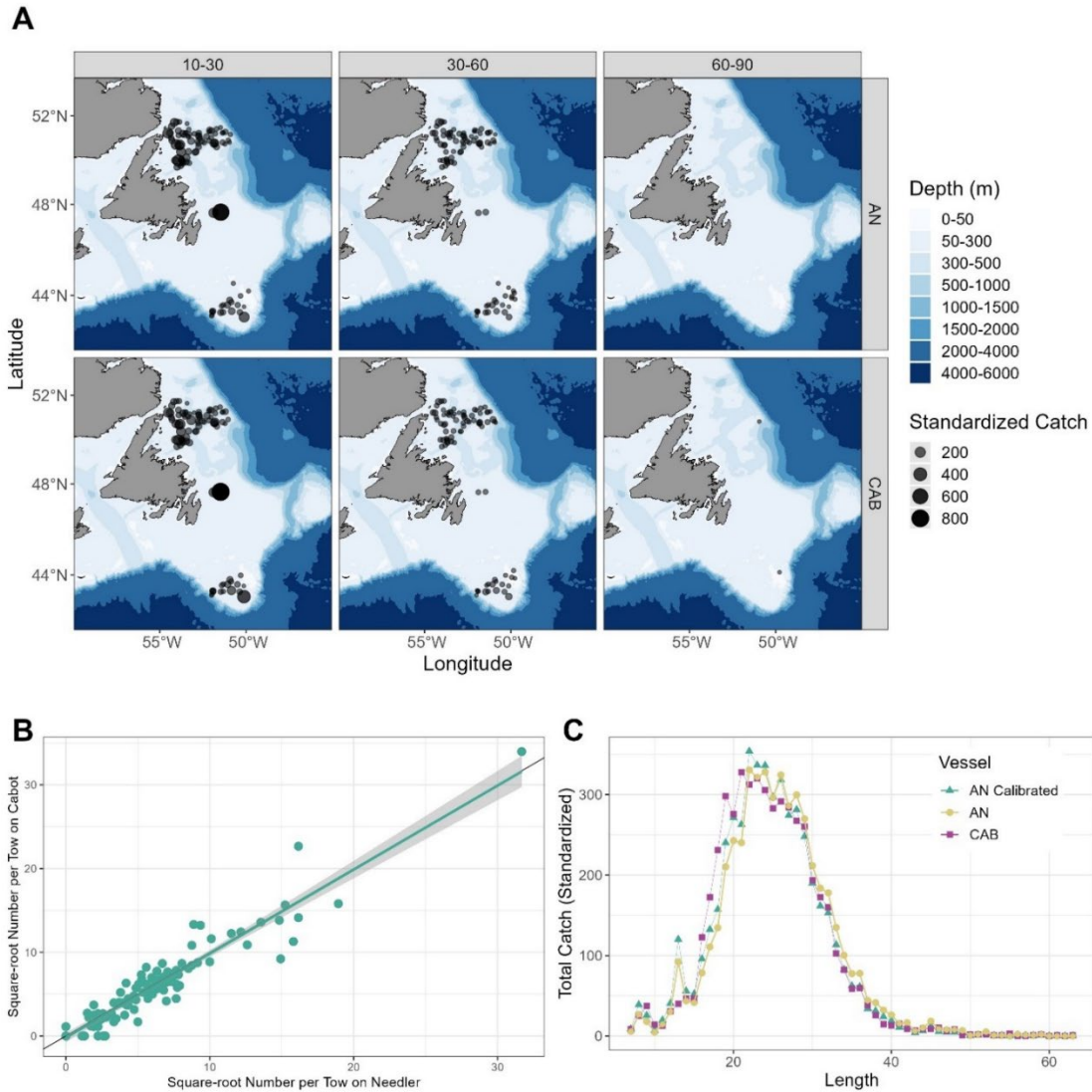


Figure A1–36. American Plaice (*Hippoglossoides platessoides*), for CCGS Alfred Needler and CCGS John Cabot Fall 3KL. Data and results for length-disaggregated analyses. (A) map of catches by length group (length in cm specified in top panel) by the CCGS Alfred Needler (top) and the CCGS John Cabot (bottom) in comparative fishing sets, where circle size is proportional catch weight (B) Biplot of the square-root of Cabot catch numbers against the square-root of Needler catch numbers. (C) Total length frequencies for catches made by the CCGS Alfred Needler (yellow), by the CCGS John Cabot (pink), and CCGS Alfred Needler catches with the conversion factor applied (green).

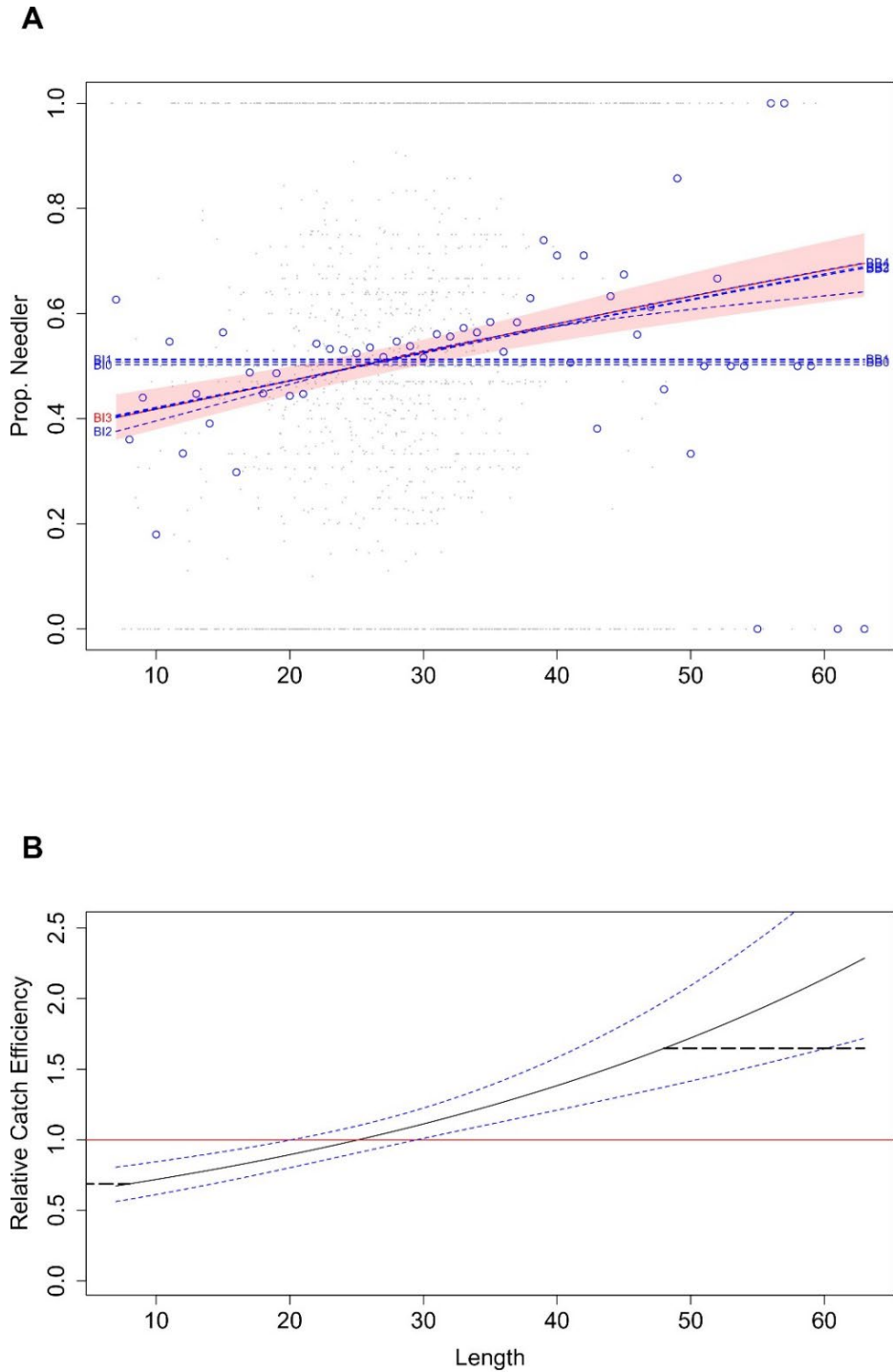


Figure A1–37. American Plaice (*Hippoglossoides platessoides*) conversion factor, for CCGS Alfred Needler and CCGS John Cabot Fall 3KL. (A) Estimated length-specific catch proportion functions, $\text{logit}(p_{Ai}(l))$, for each converged model, with the selected model plotted using a red line along with its approximate 95% CI (shaded area), as well as the length class-specific mean empirical proportion of total catch in a pair made by the CCGS Alfred Needler (blue dots). (B) Estimated relative catch efficiency (conversion factor) function from the best model (black line) with 95% CI (dashed blue lines). The horizontal red line indicates equivalent efficiency between vessels.

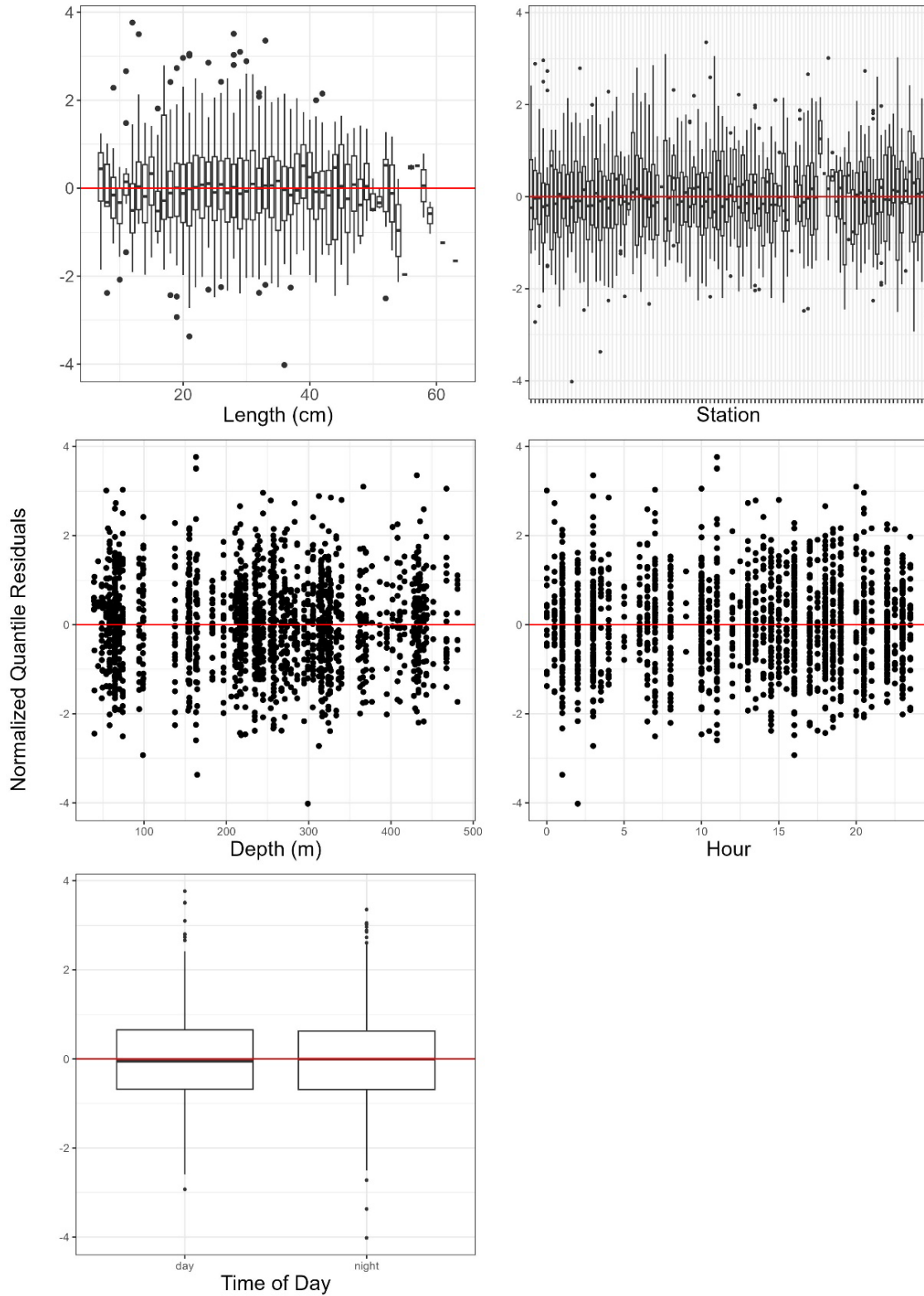


Figure A1–38. Normalized quantile residuals for as a function of length, station, depth, hour, and diel period for American Plaice (*Hippoglossoides platessoides*) best model selected (B13) for length disaggregated conversion factor analysis for the CCGS Alfred Needler, and CCGS John Cabot Fall 3KL.

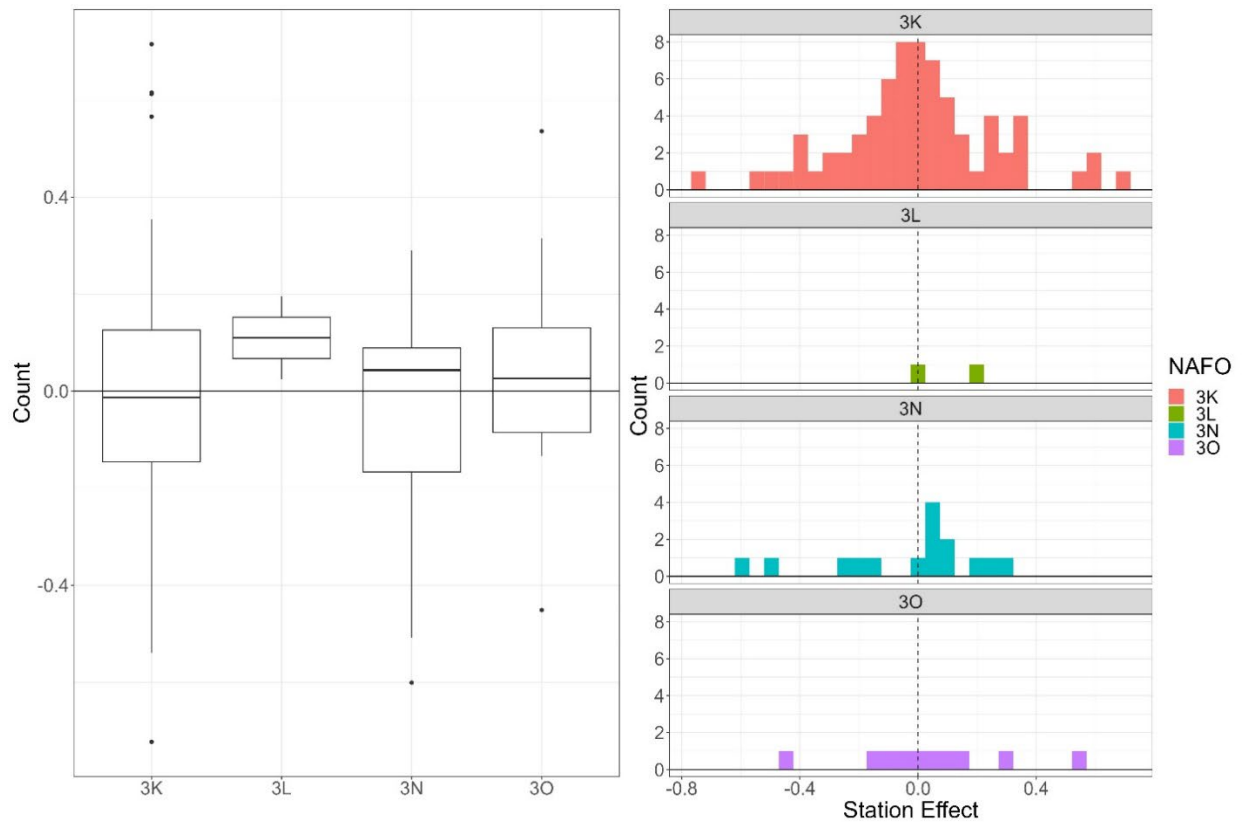


Figure A1–39. Boxplot (left) and histogram (right) of station effect by NAFO division for best model (B13) selected for American Plaice (*Hippoglossoides platessoides*) conversion factor analysis of CCGS Alfred Needler and CCGS John Cabot in Fall 3KL.

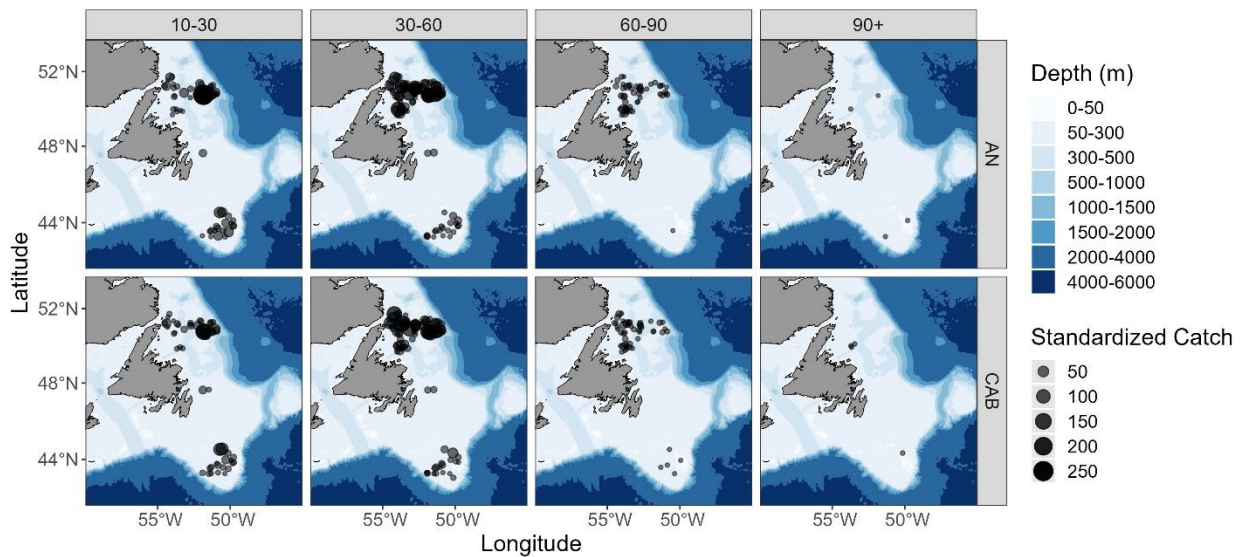
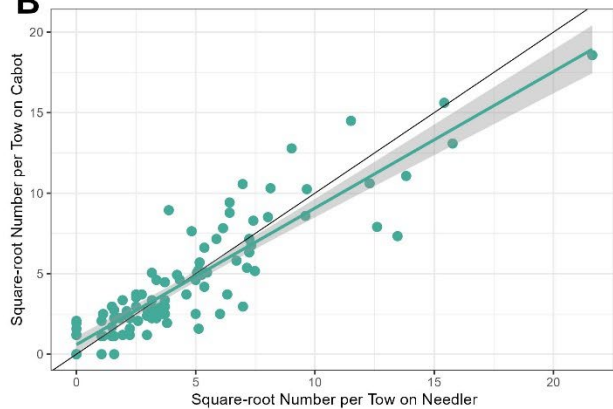
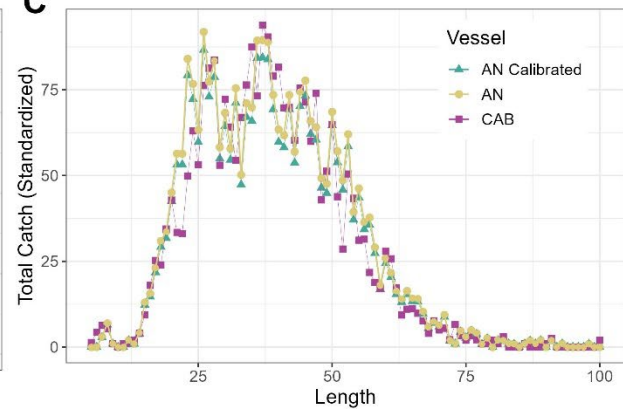
A**B****C**

Figure A1–40. Results for length-disaggregated comparative fishing analyses for Atlantic Cod, (*Gadus morhua*), between the CCGS Alfred Needler and CCGS John Cabot, for Fall 3KL. (A) map of catches by length group (length in cm specified in top panel) by the CCGS Alfred Needler (top) and the CCGS John Cabot (bottom) in comparative fishing sets, where circle size is proportional catch weight (B) Biplot of the square-root of Cabot catch numbers against the square-root of Needler catch numbers. (C) Total length frequencies for catches made by the CCGS Alfred Needler (yellow), by the CCGS John Cabot (pink), and Needler catches with the conversion factor applied (green).

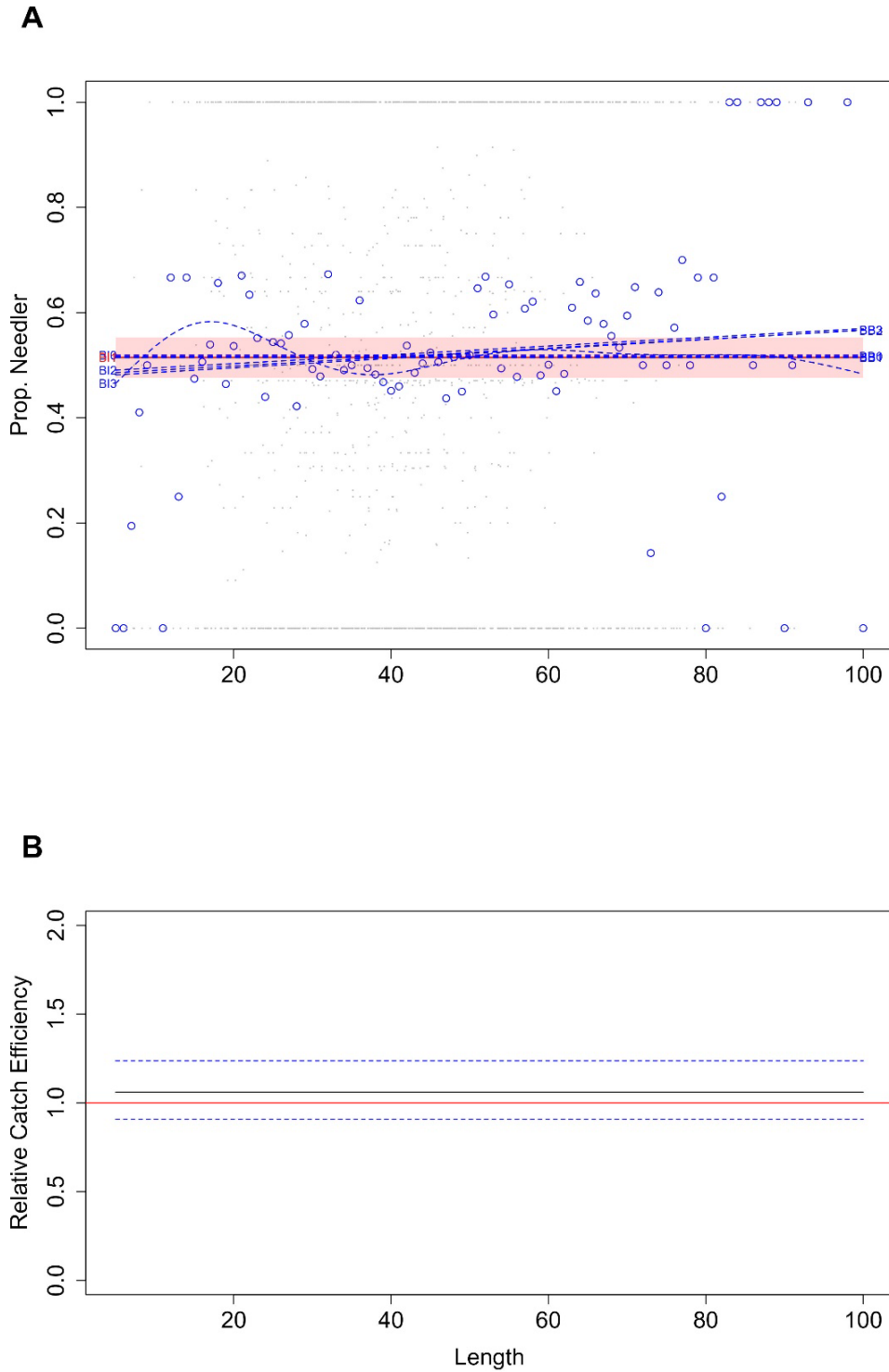


Figure A1–41. Atlantic Cod, (*Gadus morhua*) conversion factor, for CCGS Alfred Neebler and CCGS John Cabot Fall 3KL. (A) Estimated length-specific catch proportion functions, $\text{logit}(p_{Ai}(l))$, for each converged model, with the selected model (BI1) plotted using a red line along with its approximate 95% CI (shaded area), as well as the length class-specific mean empirical proportion of total catch in a pair made by the CCGS Alfred Neebler (blue dots). (B) Estimated relative catch efficiency (conversion factor) function from the best model (black line) with 95% CI (dashed blue lines). The horizontal red line indicates equivalent efficiency between vessels.

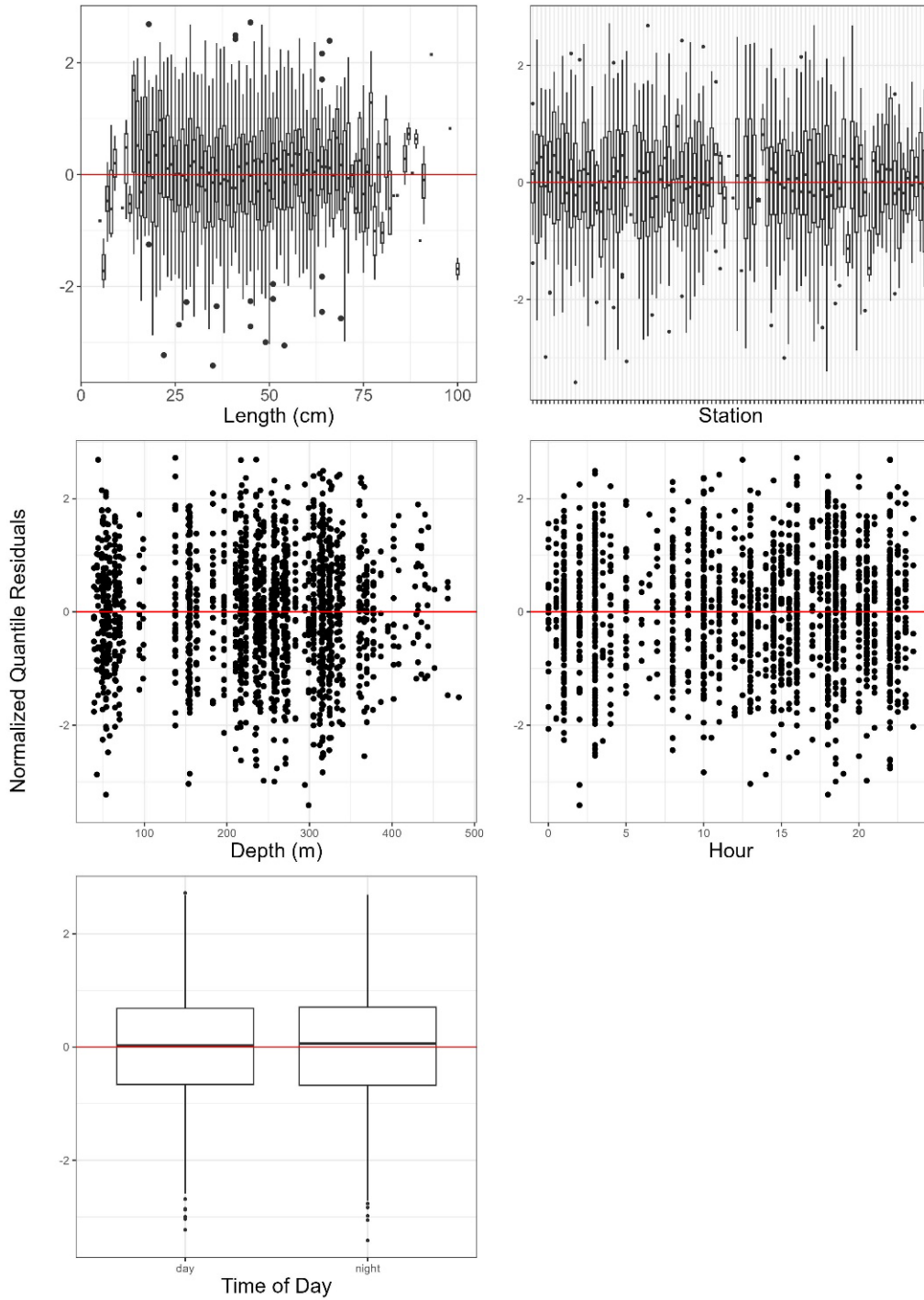


Figure A1–42. Normalized quantile residuals for as a function of length, station, depth, hour, and diel period for Atlantic Cod (*Gadus morhua*) best model selected (B11) for length disaggregated conversion factor analysis for the CCGS Alfred Needler, and CCGS John Cabot Fall 3KL.

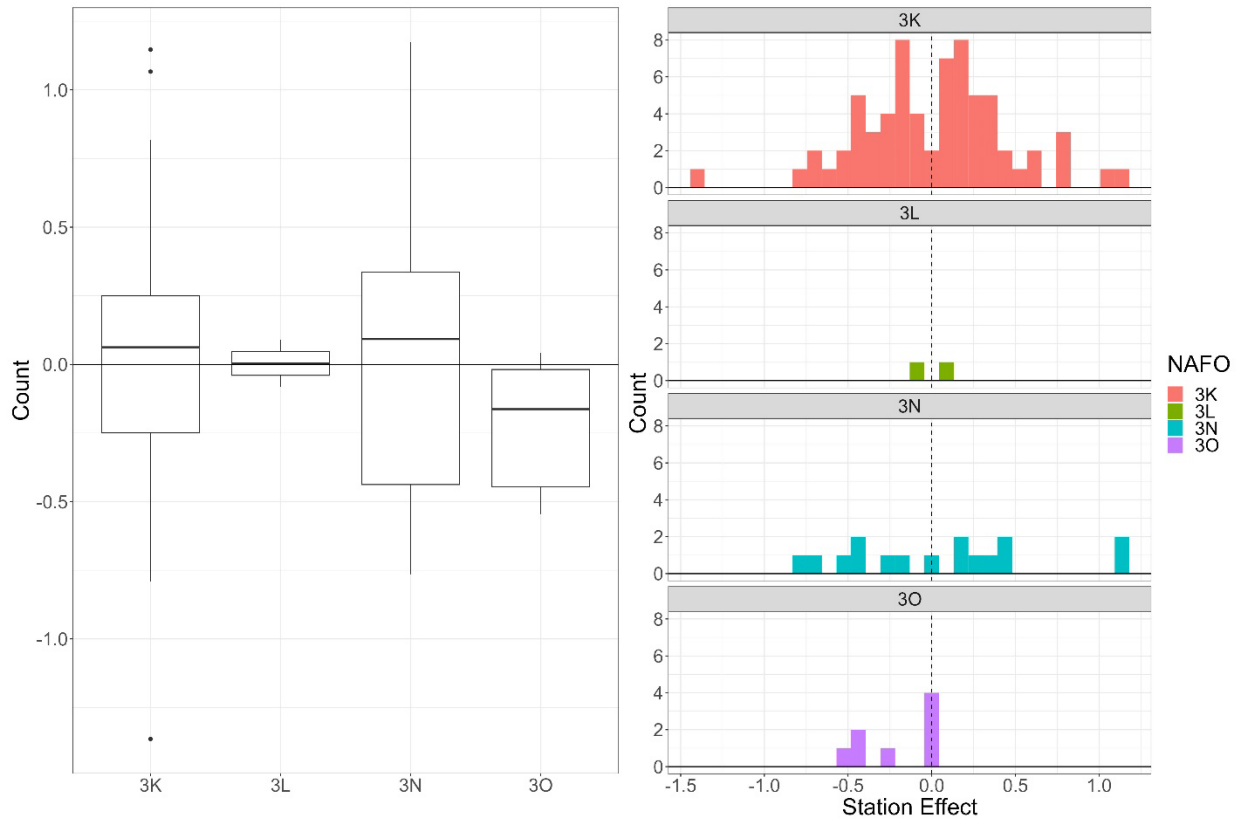
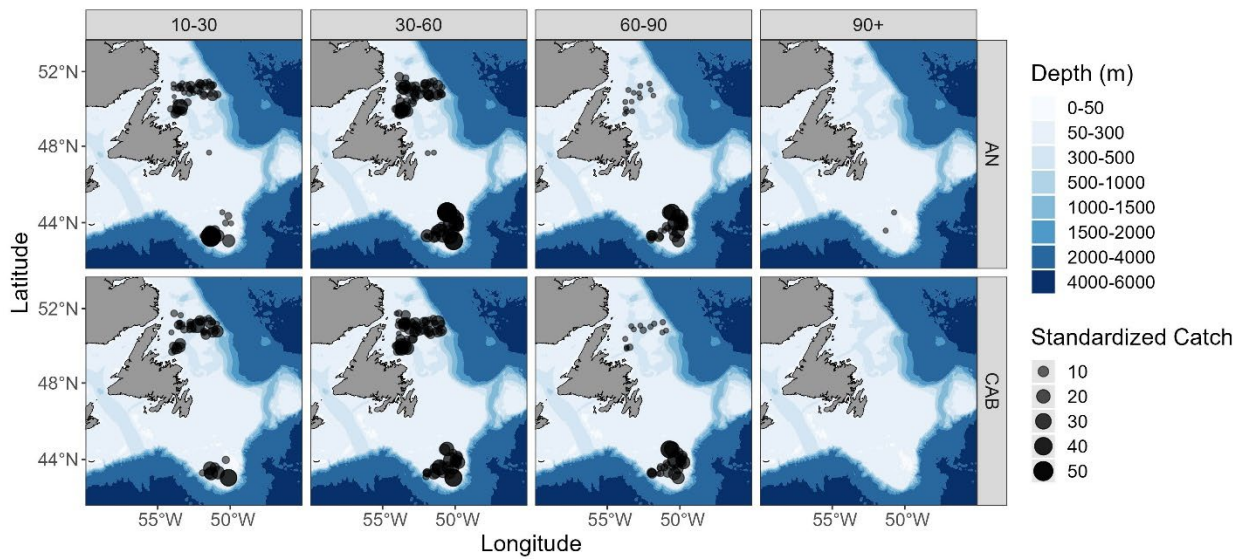
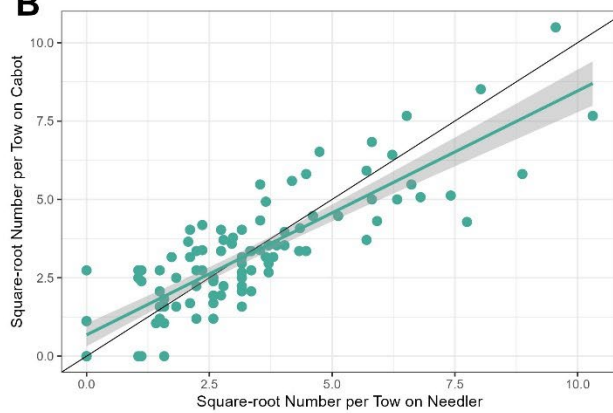


Figure A1–43. Boxplot (left) and histogram (right) of station effect by NAFO division for best model (B1) selected for Atlantic Cod (*Gadus morhua*) conversion factor analysis of CCGS Alfred Needler and CCGS John Cabot in Fall 3KL.

A



B



C

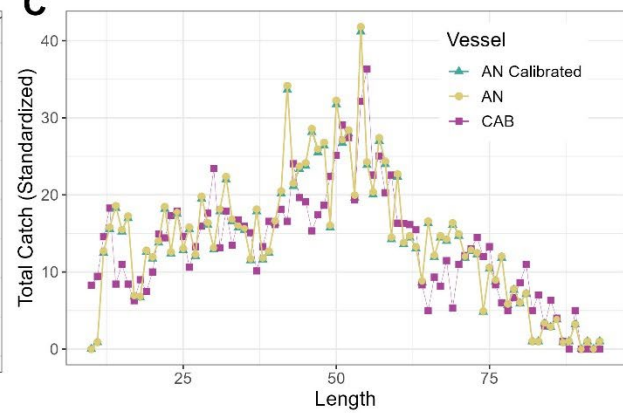


Figure A1–44. Data and results for length-disaggregated comparative fishing analyses for Thorny Skate (*Amblyraja radiata*), between then CCGS Alfred Needler and CCGS John Cabot for Fall 3KL. (A) map of catches by length group (length in cm specified in top panel) by the CCGS Alfred Needler (top) and the CCGS John Cabot (bottom) in comparative fishing sets, where circle size is proportional catch weight (B) Biplot of the square-root of CCGS John Cabot catch numbers against the square-root of Needler catch numbers. (C) Total length frequencies for catches made by the CCGS Alfred Needler (yellow), by the CCGS John Cabot (pink), and CCGS Alfred Needler catches with the conversion factor applied (green).

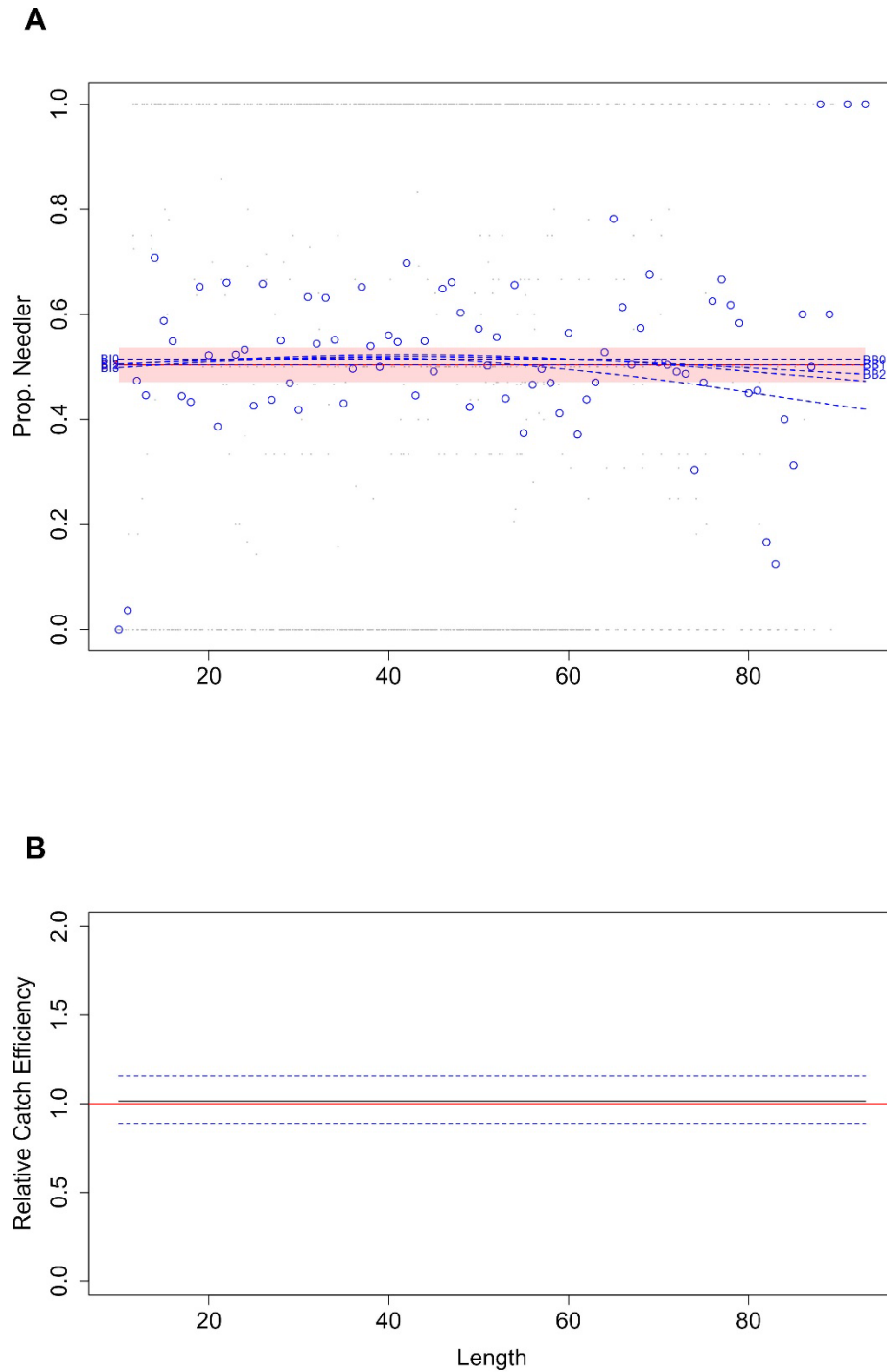


Figure A1–45. Thorny Skate (*Amblyraja radiata*) conversion factor, for CCGS Alfred Needler and CCGS John Cabot Fall 3KL. (A) Estimated length-specific catch proportion functions, $\text{logit}(p_{Ai}(l))$, for each converged model, with the selected model plotted using a red line along with its approximate 95% CI (shaded area), as well as the length class-specific mean empirical proportion of total catch in a pair made by the CCGS Alfred Needler (blue dots). (B) Estimated relative catch efficiency (conversion factor) function from the best model (black line) with 95% CI (dashed blue lines). The horizontal red line indicates equivalent efficiency between vessels.

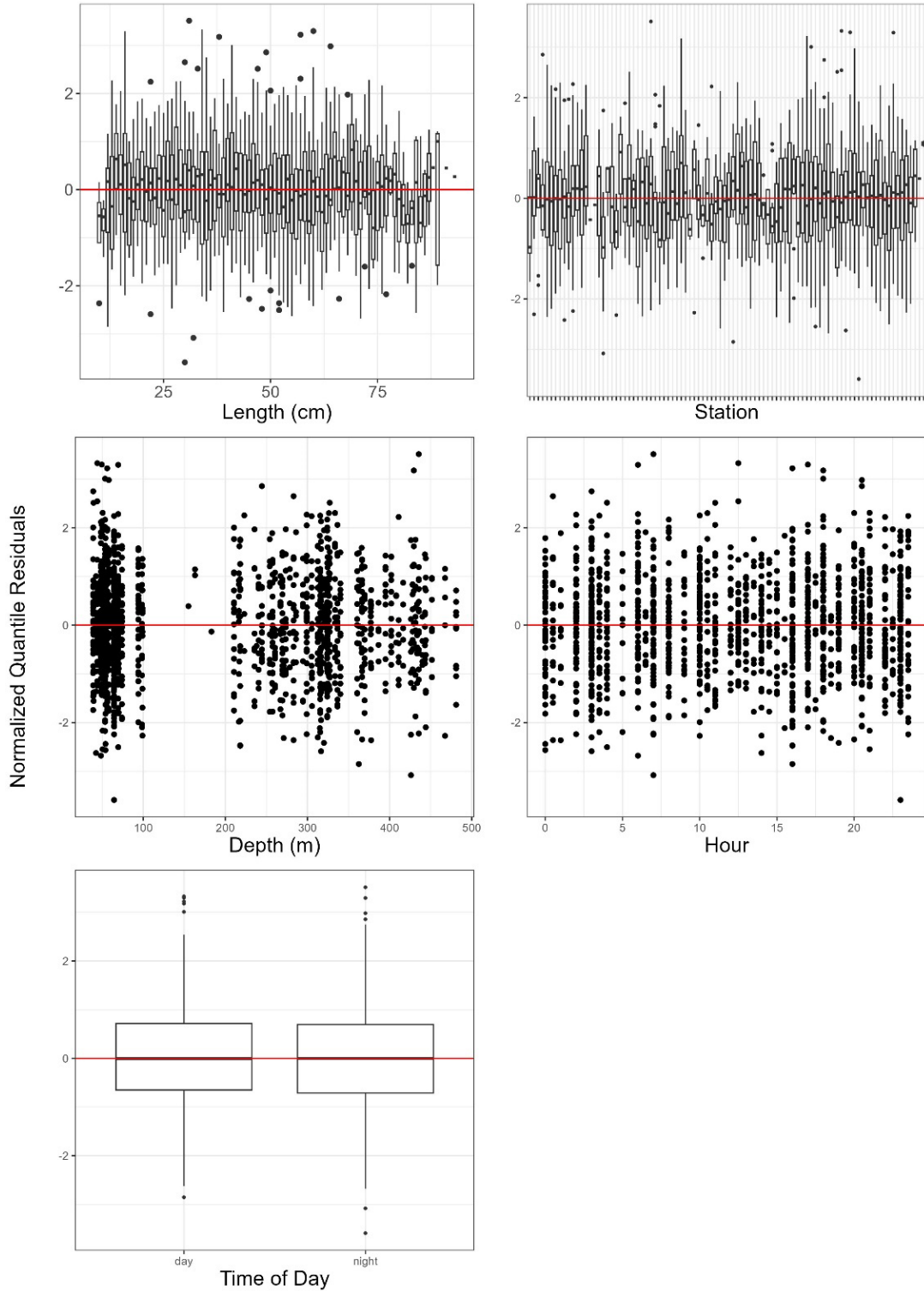


Figure A1–46. Normalized quantile residuals for *as* as a function of length, station, depth, hour, and diel period for Thorny Skate (*Amblyraja radiata*) best model selected (BI1) for length disaggregated conversion factor analysis for the CCGS Alfred Needler, and CCGS John Cabot Fall 3KL.

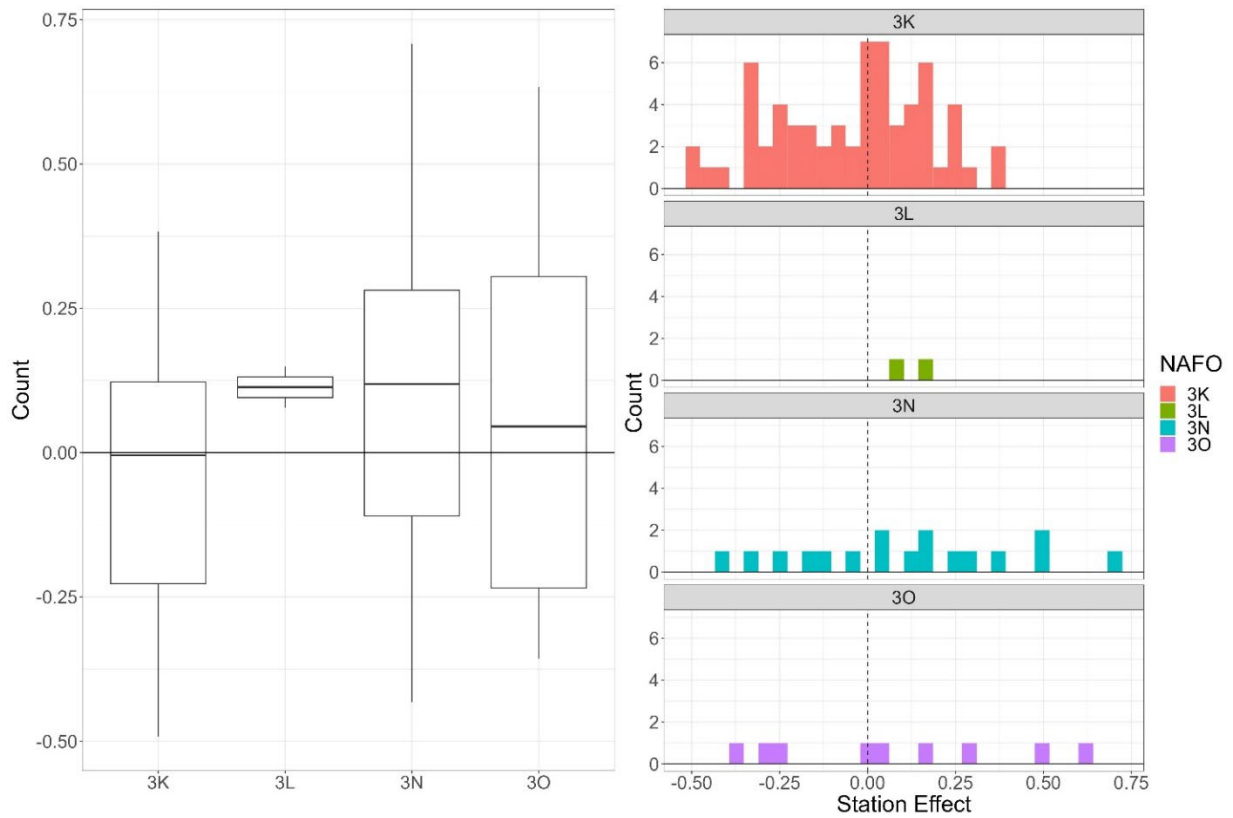


Figure A1–47. Boxplot (left) and histogram (right) of station effect by NAFO division for best model (BI1) selected for Thorny Skate (*Amblyraja radiata*) conversion factor analysis of CCGS Alfred Needler and CCGS John Cabot in Fall 3KL.

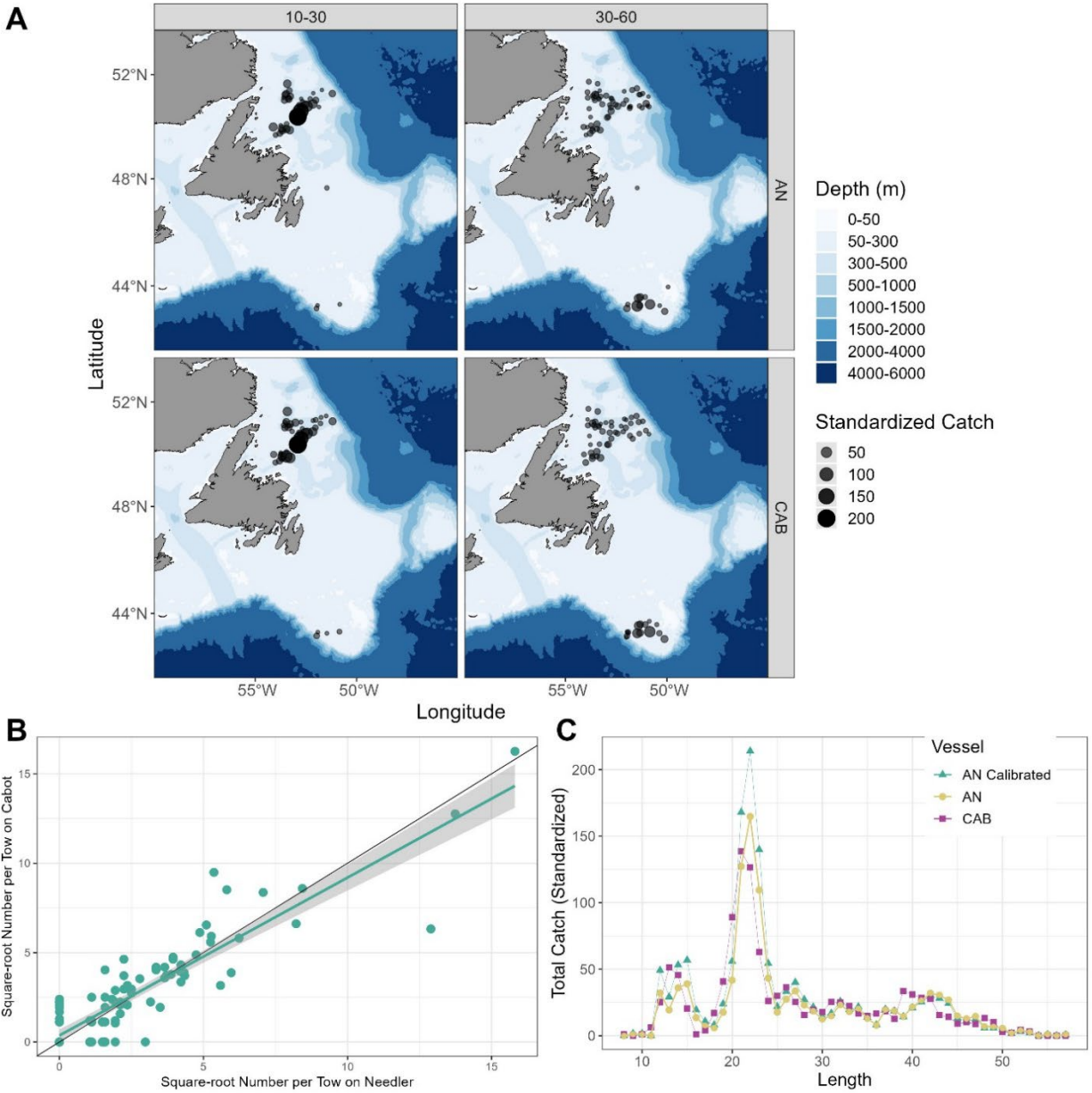


Figure A1–48. Results for length-disaggregated comparative fishing analyses for Witch Flounder (*Glyptocephalus cynoglossus*), between the CCGS Alfred Needler and CCGS John Cabot for Fall 3KL. (A) map of catches by length group (length in cm specified in top panel) by the CCGS Alfred Needler (top) and the CCGS John Cabot (bottom) in comparative fishing sets, where circle size is proportional catch weight (B) Biplot of the square-root of CCGS John Cabot catch numbers against the square-root of Needler catch numbers. (C) Total length frequencies for catches made by the CCGS Alfred Needler (yellow), by the CCGS John Cabot (pink), and Needler catches with the conversion factor applied (green).

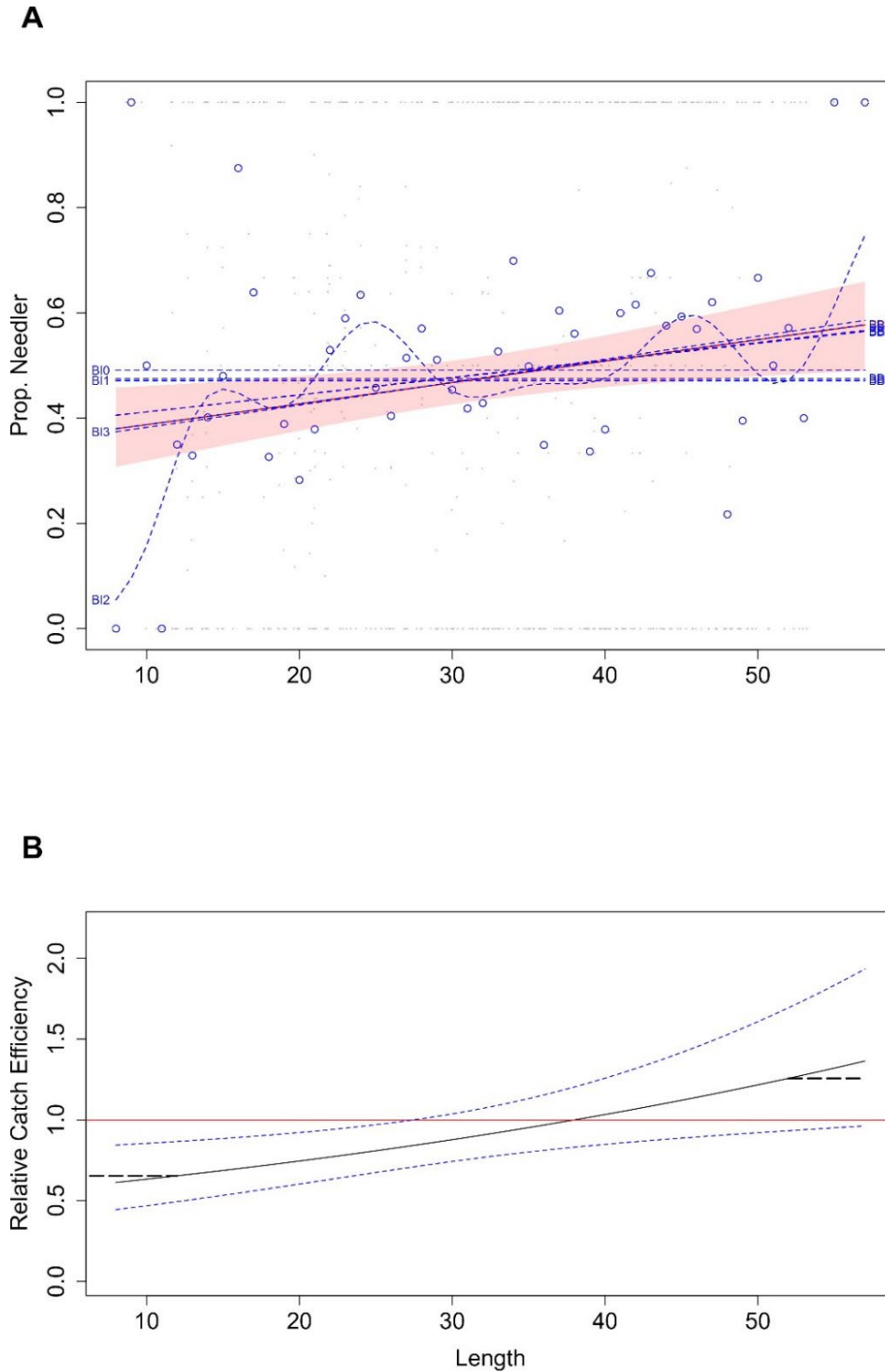


Figure A1–49. Witch Flounder (*Glyptocephalus cynoglossus*) conversion factor, for CCGS Alfred Needler and CCGS John Cabot Fall 3KL. (A) Estimated length-specific catch proportion functions, $\text{logit}(p_{Ai}(l))$, for each converged model, with the selected model plotted using a red line along with its approximate 95% CI (shaded area), as well as the length class-specific mean empirical proportion of total catch in a pair made by the CCGS Alfred Needler (blue dots). (B) Estimated relative catch efficiency (conversion factor) function from the best model (black line) with 95% CI (dashed blue lines). The horizontal red line indicates equivalent efficiency between vessels.

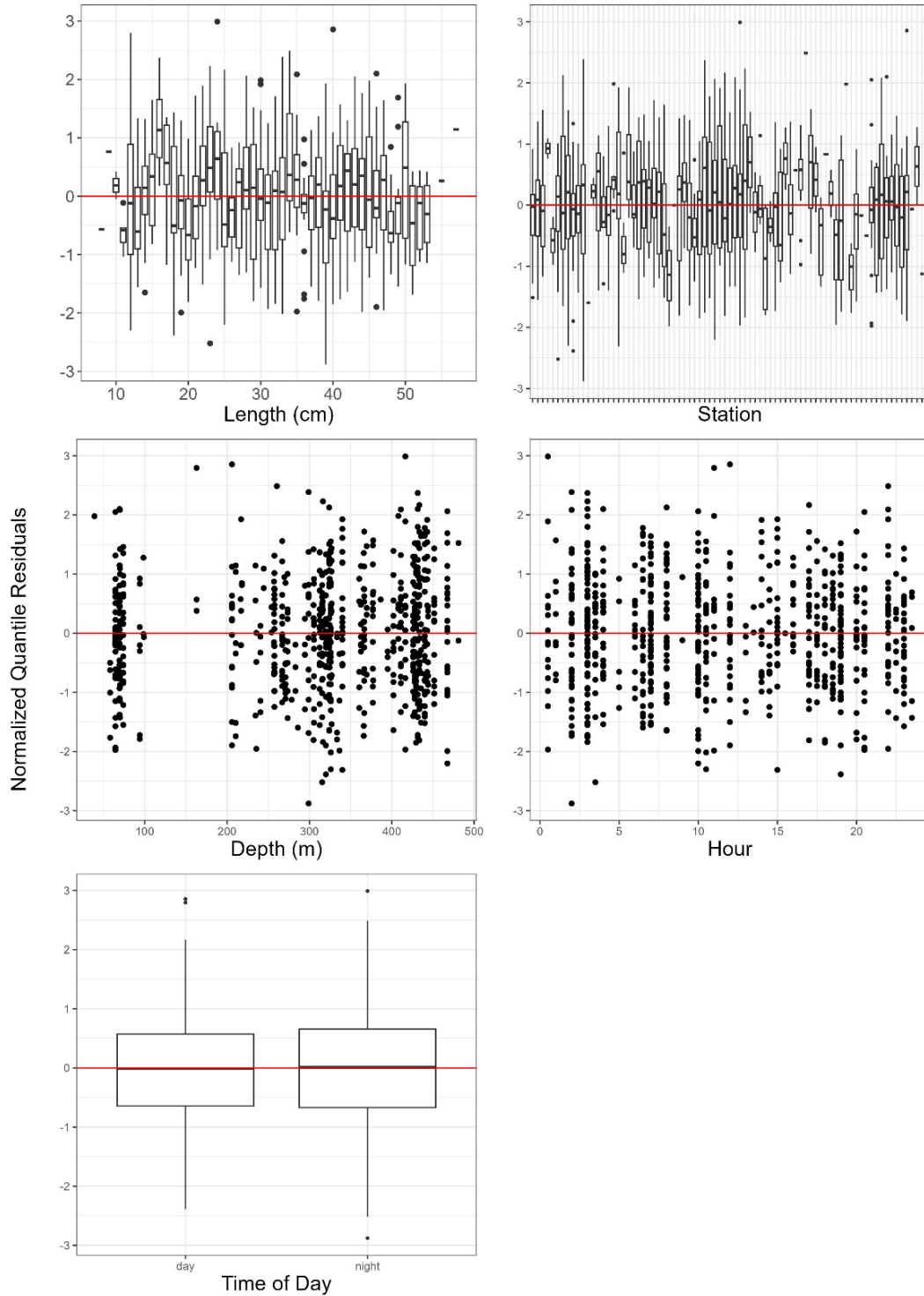


Figure A1–50. Normalized quantile residuals for as a function of length, station, depth, hour, and diel period for Witch Flounder (*Glyptocephalus cynoglossus*), best model selected (BB4) for length disaggregated conversion factor analysis for the CCGS Alfred Needler, and CCGS John Cabot Fall 3KL.

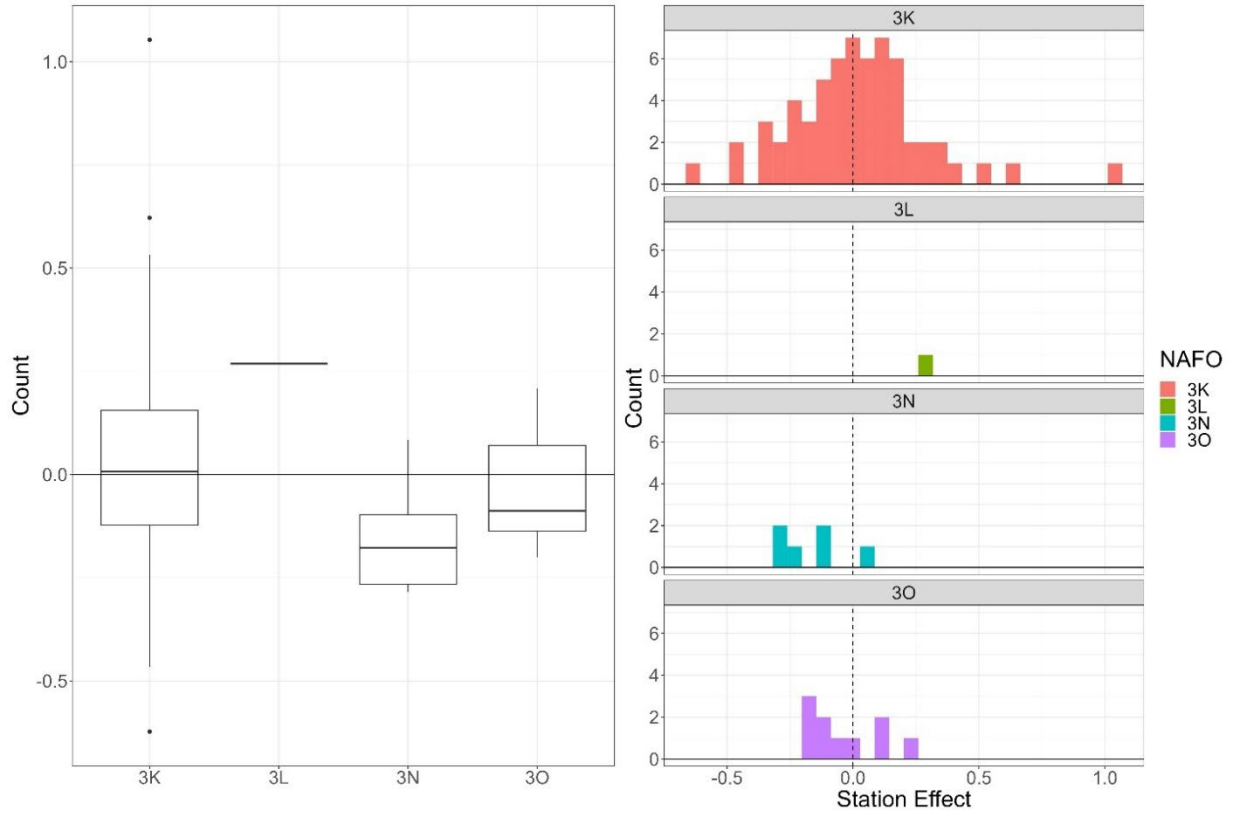


Figure A1–51. Boxplot (left) and histogram (right) of station effect by NAFO division for best model (BB4) selected for Witch Flounder (*Glyptocephalus cynoglossus*) conversion factor analysis of CCGS Alfred Needler and CCGS John Cabot in Fall 3KL.

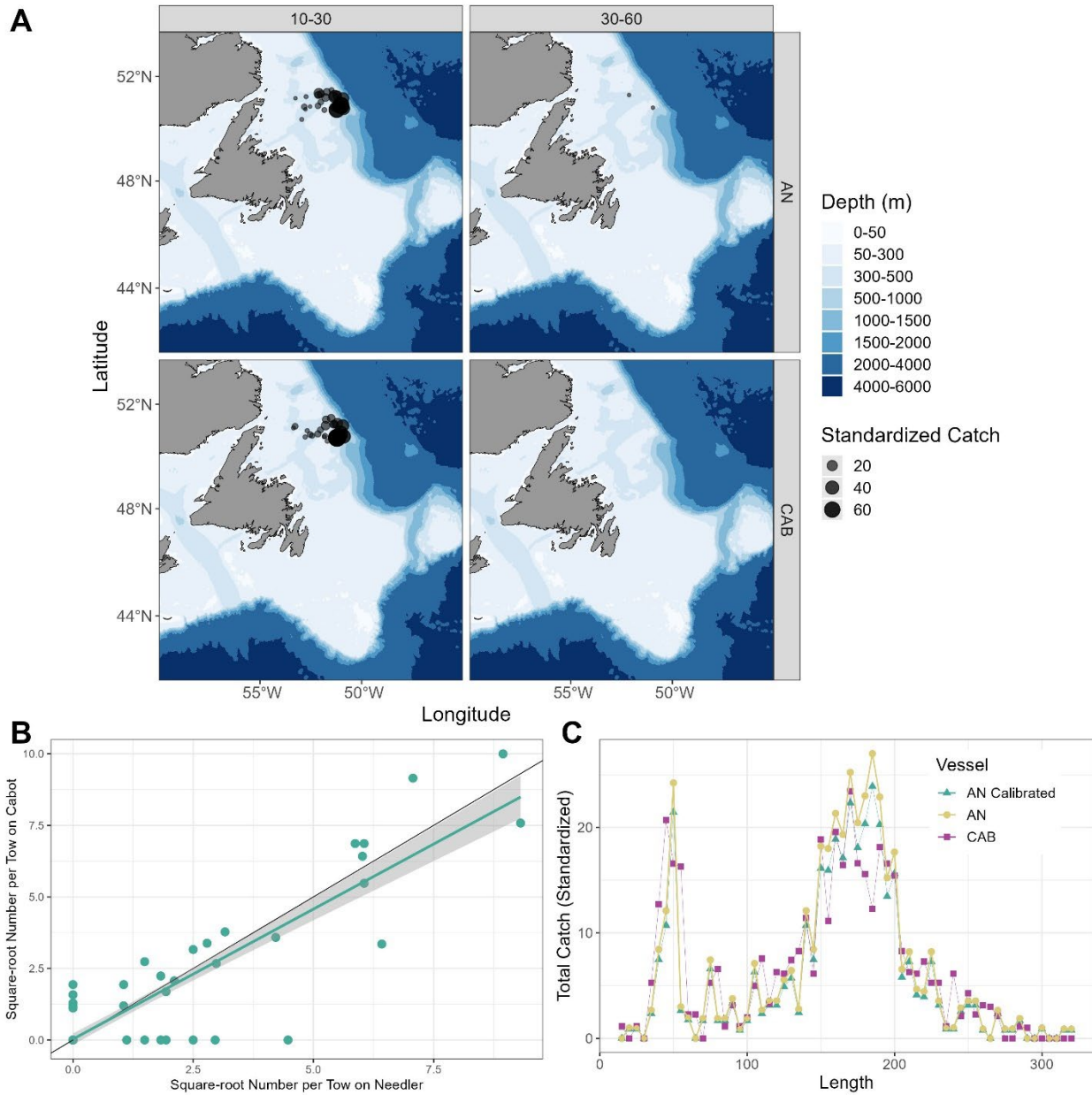


Figure A1-52. Results for length-disaggregated comparative fishing analyses for Roughhead Grenadier (*Macrourus berglax*), between the CCGS Alfred Needler and CCGS John Cabot for Fall 3KL. (A) map of catches by length group (length in cm specified in top panel) by the CCGS Alfred Needler (top) and the CCGS John Cabot (bottom) in comparative fishing sets, where circle size is proportional catch weight (B) Biplot of the square-root of CCGS John Cabot catch numbers against the square-root of CCGS Alfred Needler catch numbers. (C) Total length frequencies for catches made by the CCGS Alfred Needler (yellow), by the Cabot (pink), and Needler catches with the conversion factor applied (green).

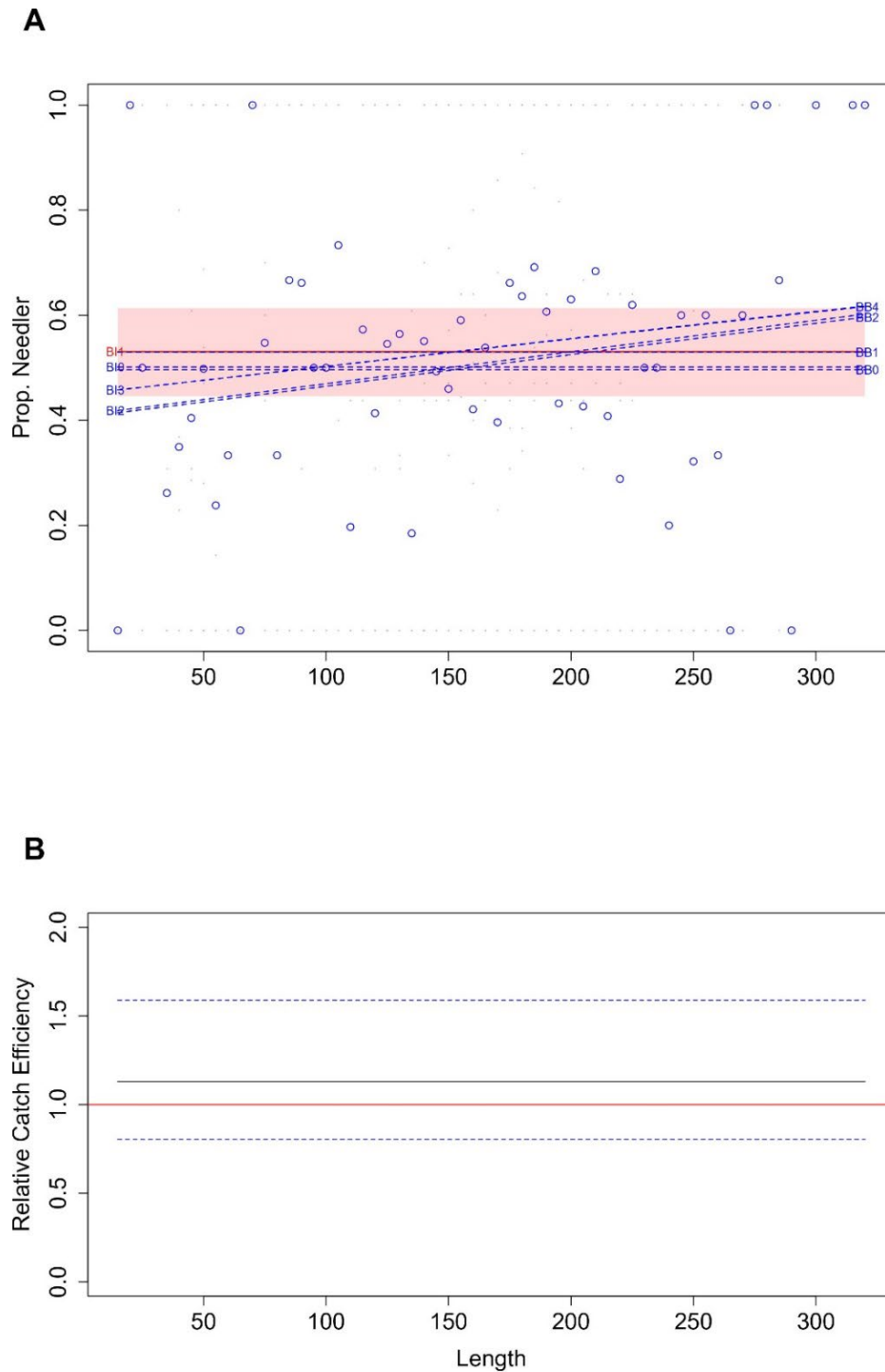


Figure A1–53. Roughhead Grenadier (*Macrourus berglax*) conversion factor, for CCGS Alfred Needler and CCGS John Cabot Fall 3KL. (A) Estimated length-specific catch proportion functions, $\text{logit}(p_{Ai}(l))$, for each converged model, with the selected model plotted using a red line along with its approximate 95% CI (shaded area), as well as the length class-specific mean empirical proportion of total catch in a pair made by the CCGS Alfred Needler (blue dots). (B) Estimated relative catch efficiency (conversion factor) function from the best model (black line) with 95% CI (dashed blue lines). The horizontal red line indicates equivalent efficiency between vessels.

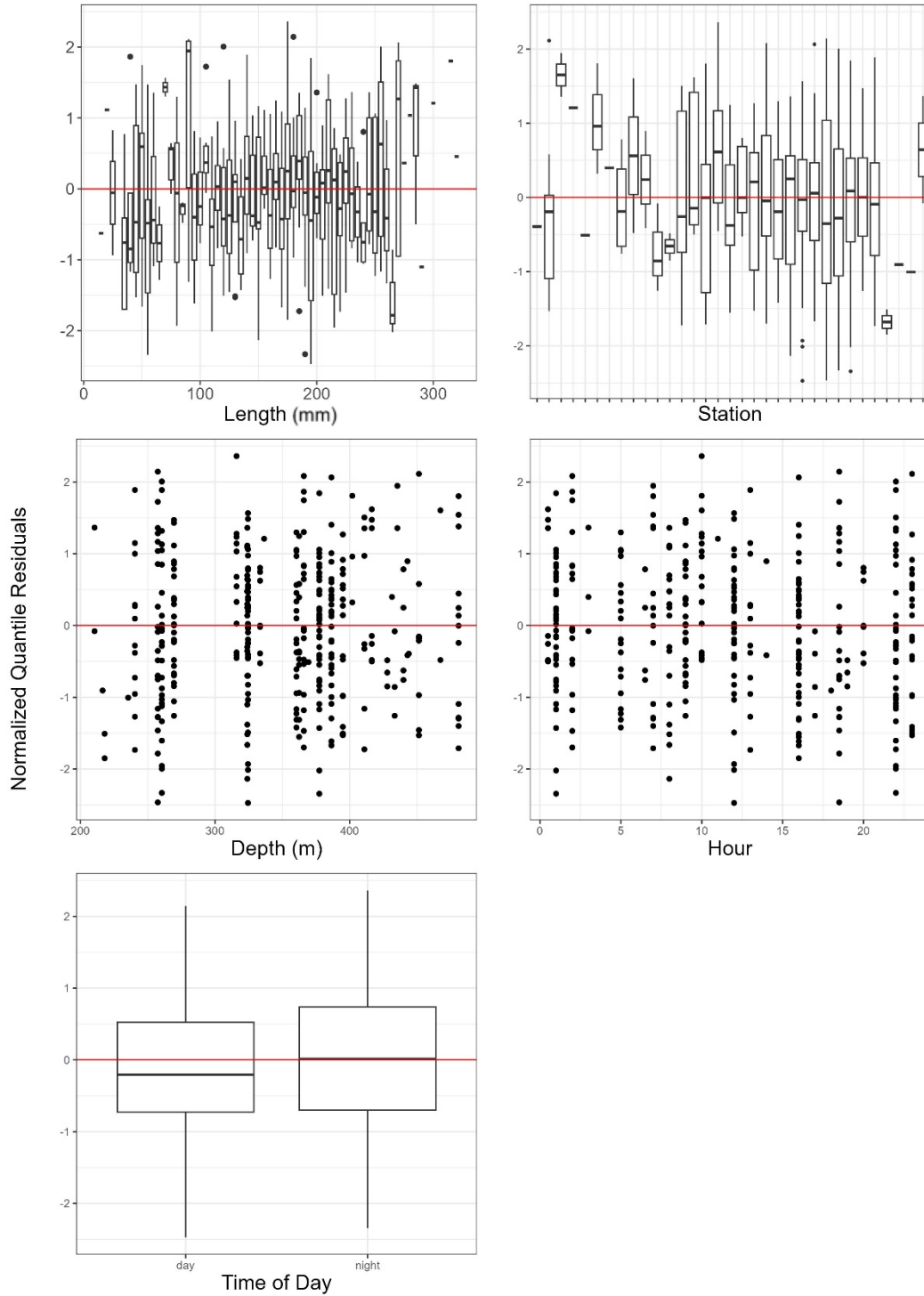


Figure A1–54. Normalized quantile residuals for as a function of length, station, depth, hour, and diel period for Roughhead Grenadier (*Macrourus berglax*), best model selected (BI1) for length disaggregated conversion factor analysis for the CCGS Alfred Needler, and CCGS John Cabot Fall 3KL.

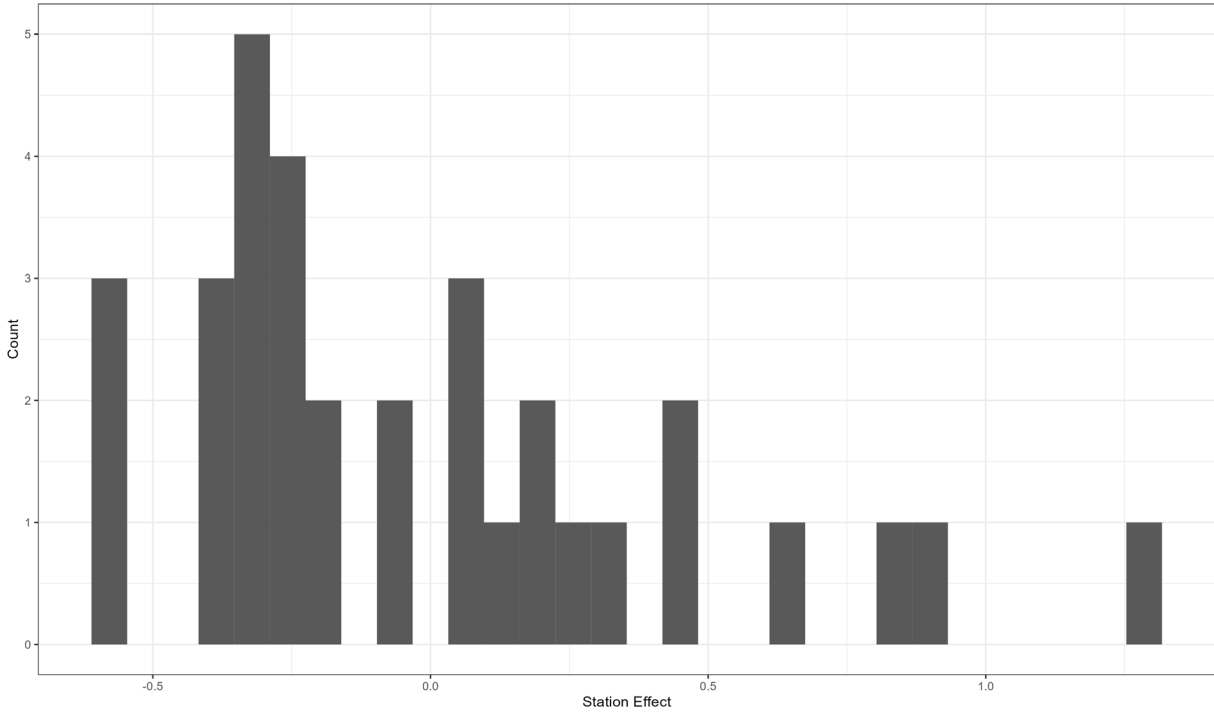


Figure A1–55. Histogram of station effect for best model (BI1) selected for Roughhead Grenadier (Macrourus berglax) conversion factor analysis of CCGS Alfred Needler and CCGS John Cabot in Fall 3KL. NAFO Division is not displayed here since all catches were within 3K.

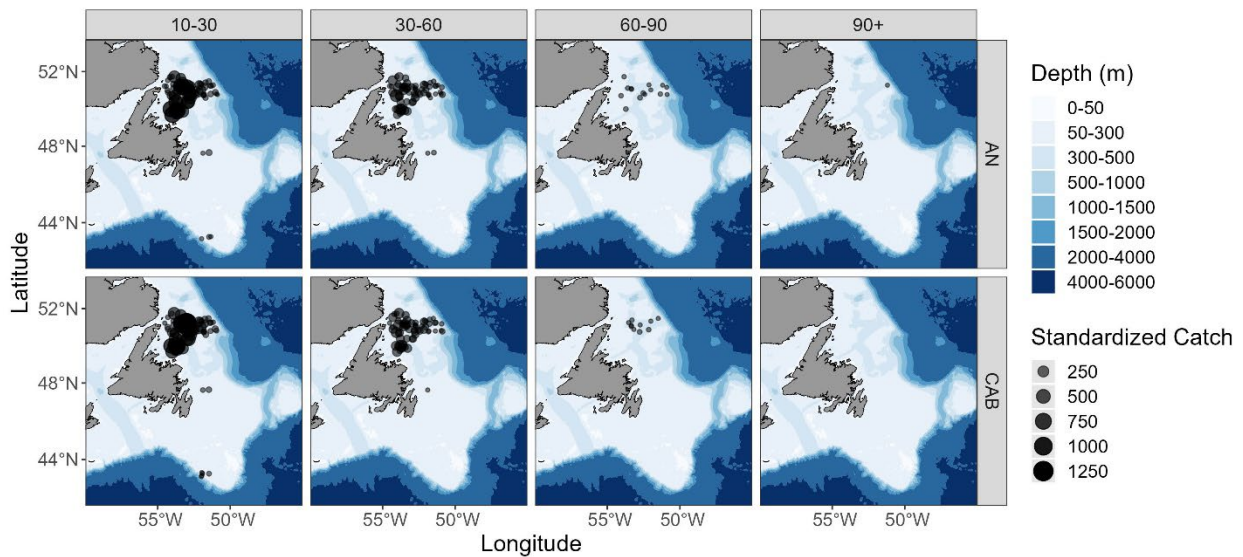
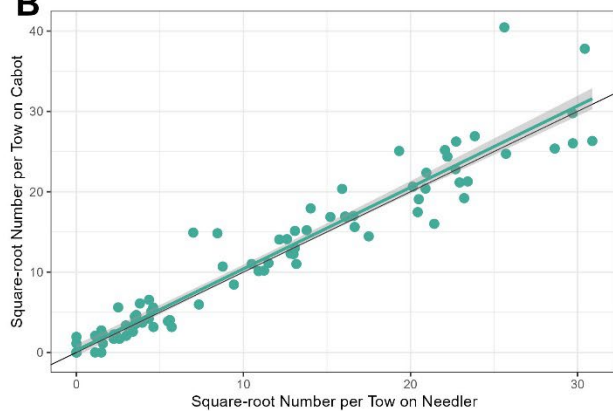
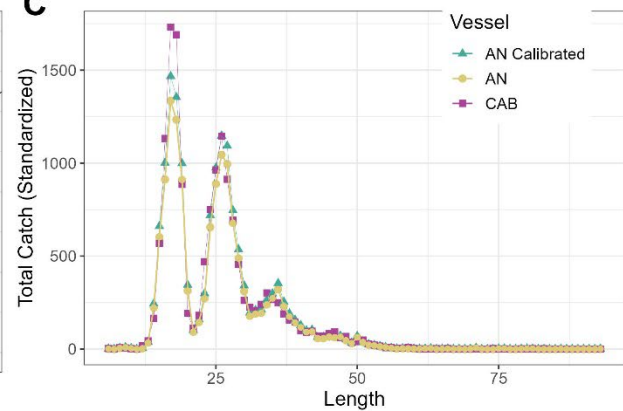
A**B****C**

Figure A1–56. Data and results for length-disaggregated comparative fishing analyses for Greenland Halibut (*Reinhardtius hippoglossoides*), between the CCGS Alfred Needler and CCGS John Cabot for Fall 3KL. (A) map of catches by length group (length in cm specified in top panel) by the CCGS Alfred Needler (top) and the CCGS John Cabot (bottom) in comparative fishing sets, where circle size is proportional catch weight (B) Biplot of the square-root of CCGS John Cabot catch numbers against the square-root of CCGS Alfred Needler catch numbers. (C) Total length frequencies for catches made by the CCGS Alfred Needler (yellow), by the CCGS John Cabot (pink), and Needler catches with the conversion factor applied (green).

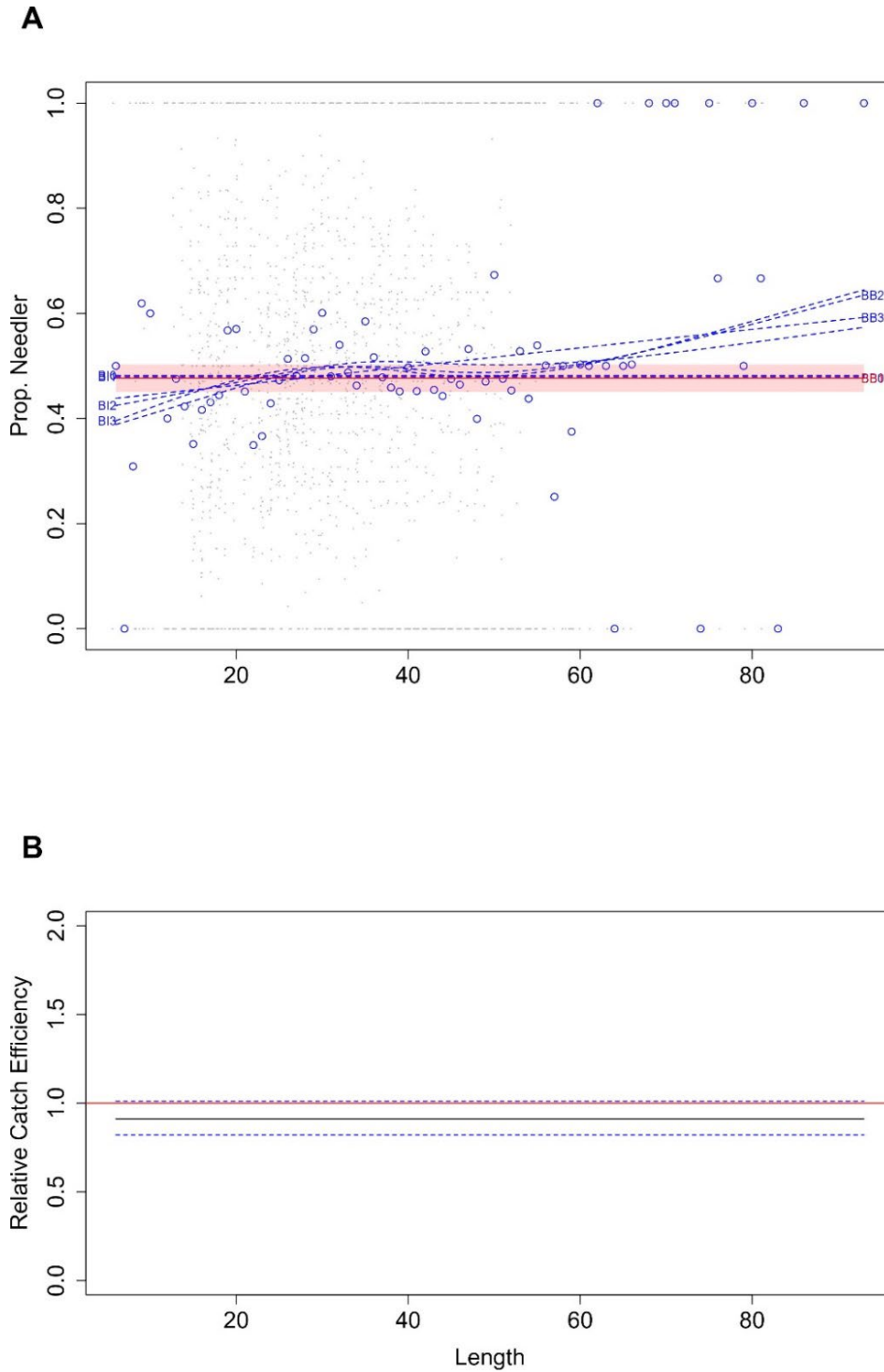


Figure A1–57. Greenland Halibut (*Reinhardtius hippoglossoides*) conversion factor, for CCGS Alfred Needler and CCGS John Cabot Fall 3KL. (A) Estimated length-specific catch proportion functions, $\text{logit}(p_{Ai}(l))$, for each converged model, with the selected model plotted using a red line along with its approximate 95% CI (shaded area), as well as the length class-specific mean empirical proportion of total catch in a pair made by the CCGS Alfred Needler (blue dots). (B) Estimated relative catch efficiency (conversion factor) function from the best model (black line) with 95% CI (dashed blue lines). The horizontal red line indicates equivalent efficiency between vessels.

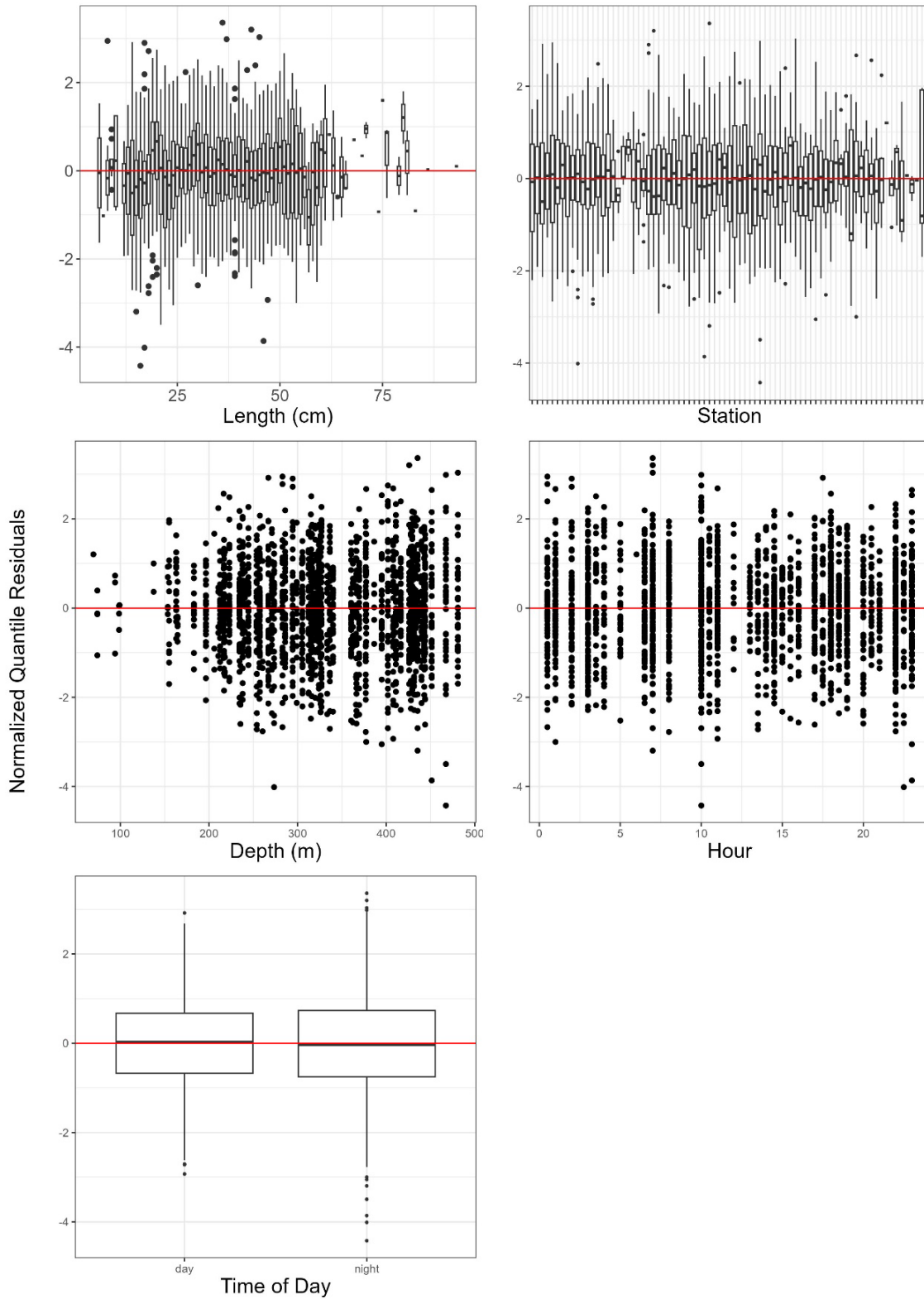


Figure A1–58. Normalized quantile residuals for as a function of length, station, depth, hour, and diel period for Greenland Halibut (*Reinhardtius hippoglossoides*), best model selected (BB1) for length disaggregated conversion factor analysis for the CCGS Alfred Needler, and CCGS John Cabot Fall 3KL.

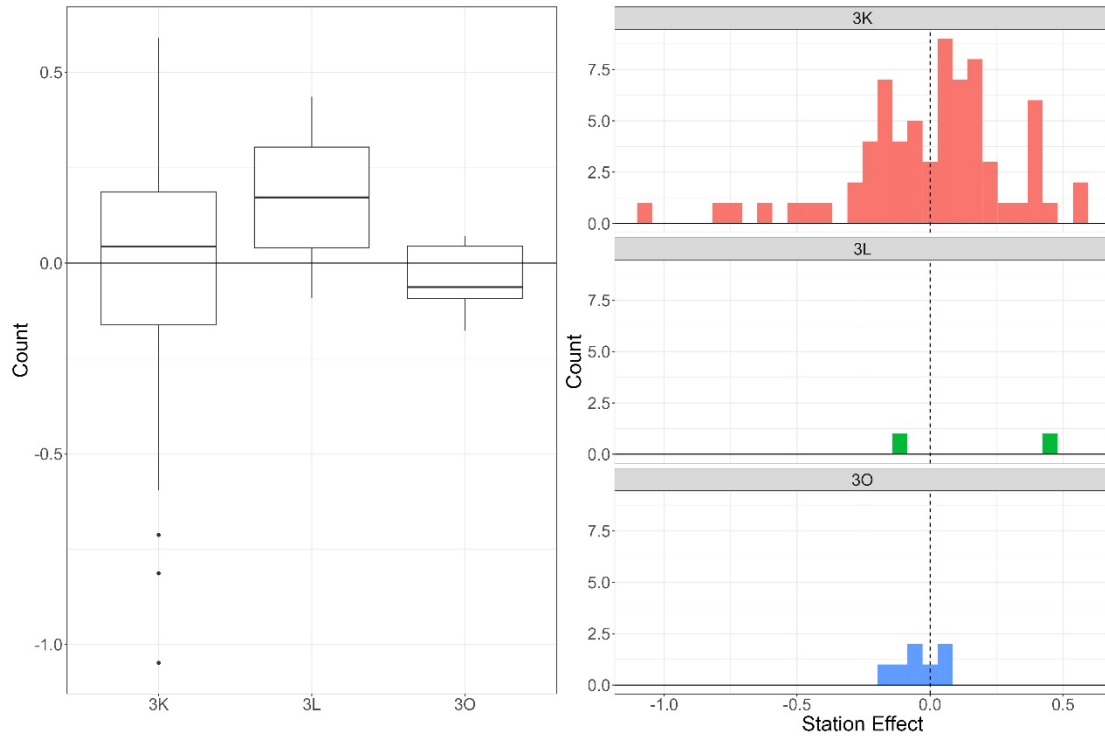


Figure A1–59. Boxplot (left) and histogram (right) of station effect by NAFO Division for best model (BB1) selected for Greenland Halibut (*Reinhardtius hippoglossoides*) conversion factor analysis of CCGS Alfred Needler and CCGS John Cabot in Fall 3KL.

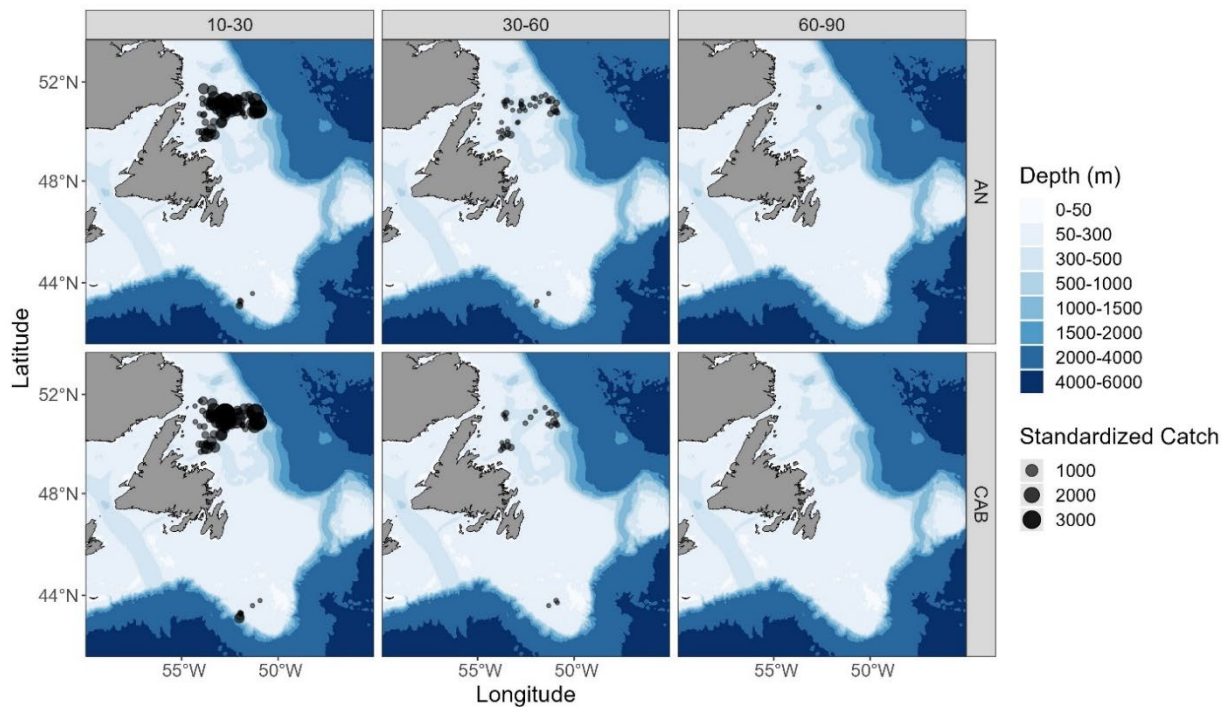
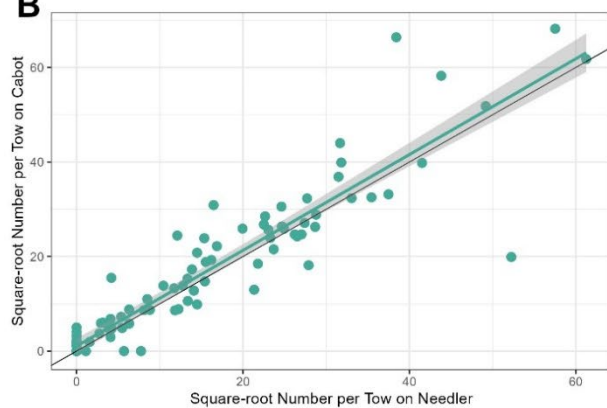
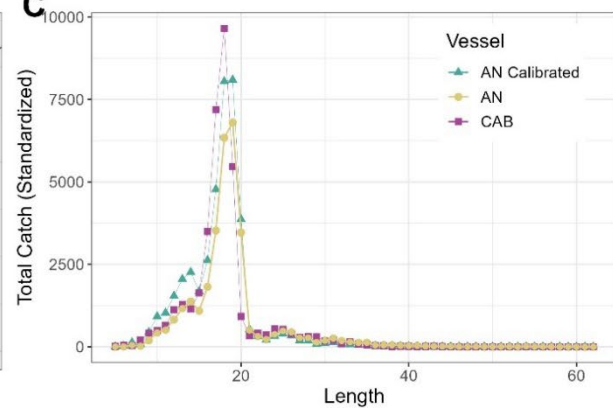
A**B****C**

Figure A1–60. Results for length-disaggregated comparative fishing analyses for Redfish (*Sebastes mentella* & *S. faciatus*), between the CCGS Alfred Needler and CCGS John Cabot for Fall 3KL. (A) map of catches by length group (length in cm specified in top panel) by the CCGS Alfred Needler (top) and the CCGS John Cabot (bottom) in comparative fishing sets, where circle size is proportional catch weight (B) Biplot of the square-root of CCGS John Cabot catch numbers against the square-root of CCGS Alfred Needler catch numbers. (C) Total length frequencies for catches made by the CCGS Alfred Needler (yellow), by the CCGS John Cabot (pink), and Needler catches with the conversion factor applied (green).

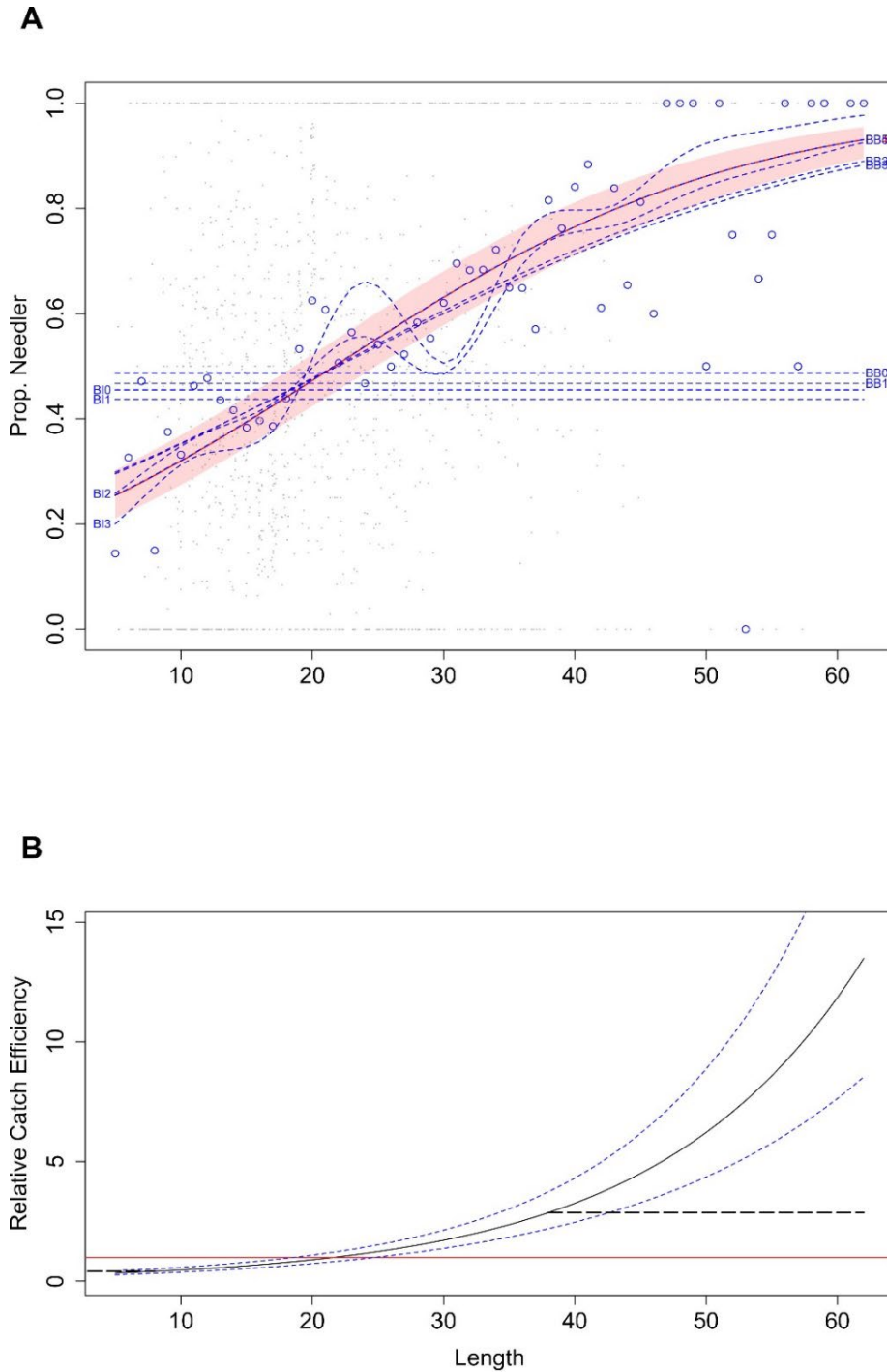


Figure A1–61. Redfish (*Sebastes mentella* & *S. faciatus*) conversion factor, for CCGS Alfred Needler and CCGS John Cabot Fall 3KL. (A) Estimated length-specific catch proportion functions, $\text{logit}(p_{Ai}(l))$, for each converged model, with the selected model plotted using a red line along with its approximate 95% CI (shaded area), as well as the length class-specific mean empirical proportion of total catch in a pair made by the CCGS Alfred Needler (blue dots). (B) Estimated relative catch efficiency (conversion factor) function from the best model (black line) with 95% CI (dashed blue lines). The horizontal red line indicates equivalent efficiency between vessels.

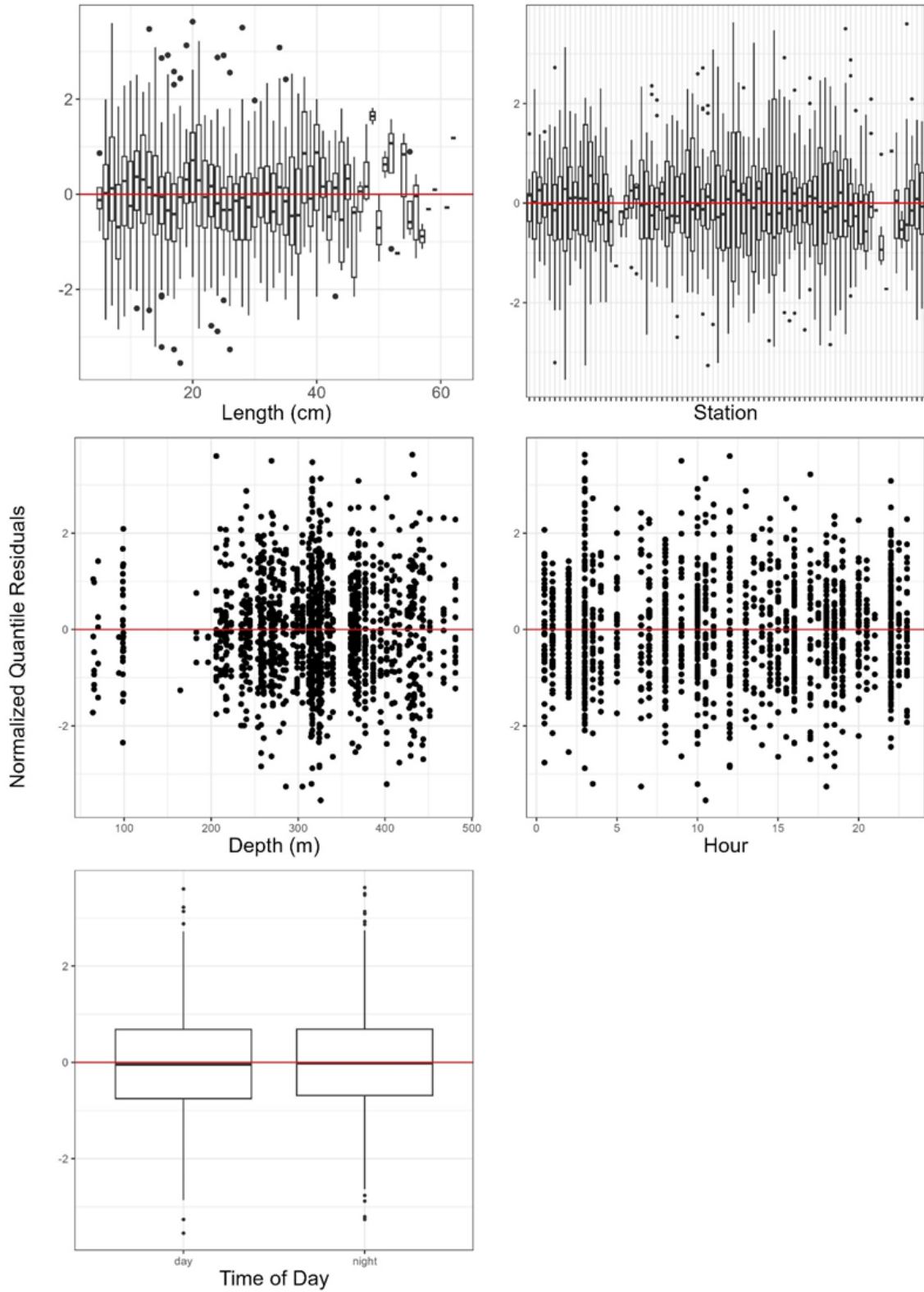


Figure A1–62. Normalized quantile residuals for as a function of length, station, depth, hour, and diel period for Redfish (*Sebastes mentella* & *S. faciatius*), best model selected (BB4) for length disaggregated conversion factor analysis for the CCGS Alfred Needler, and CCGS John Cabot Fall 3KL.

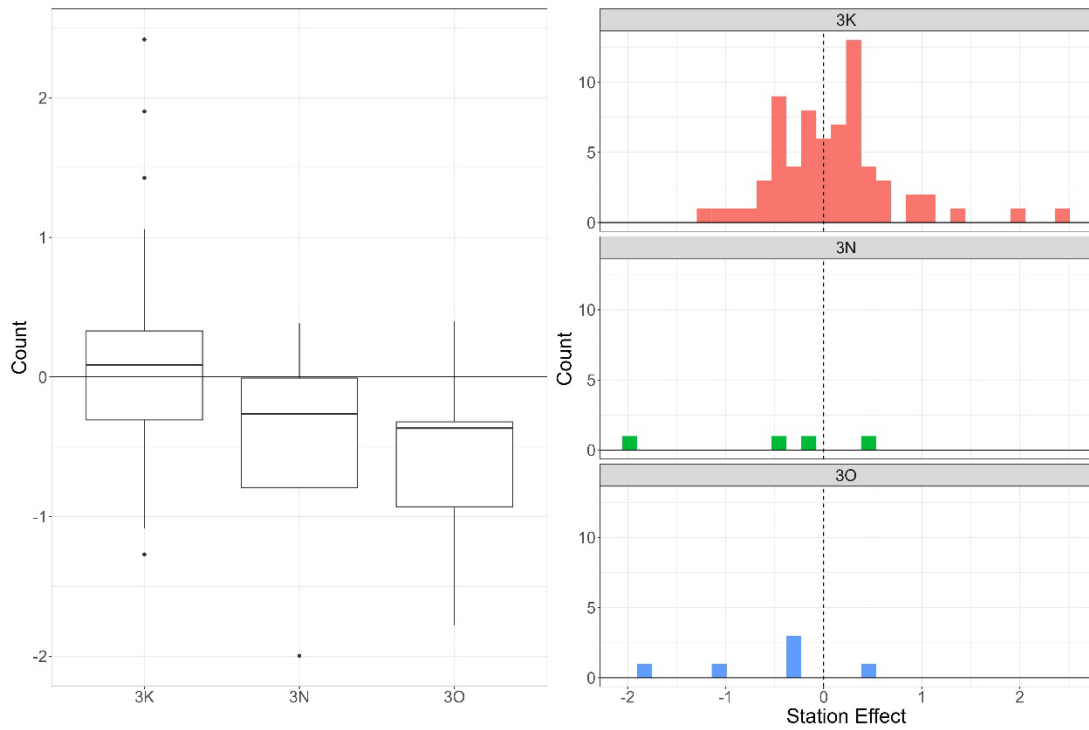


Figure A1–63. Boxplot (left) and histogram (right) of station effect by NAFO Division for best model (BB4) selected for Redfish (*Sebastes mentella* & *S. faciatus*) conversion factor analysis of CCGS Alfred Needler and CCGS John Cabot in Fall 3KL.

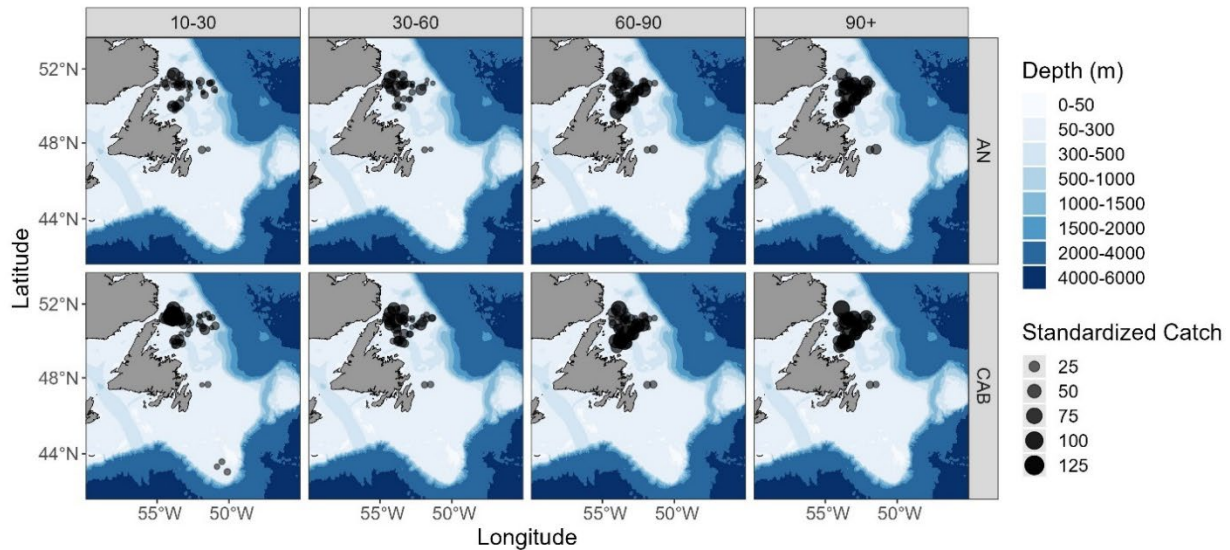
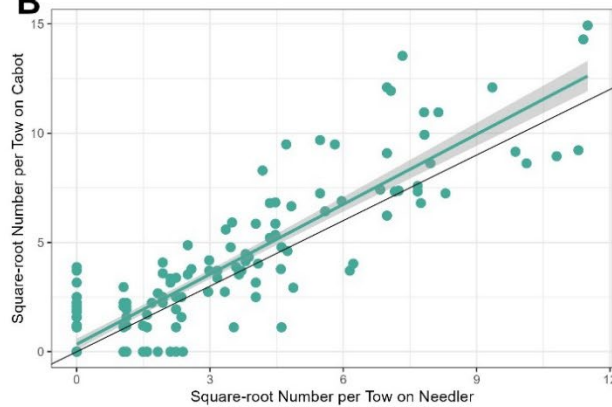
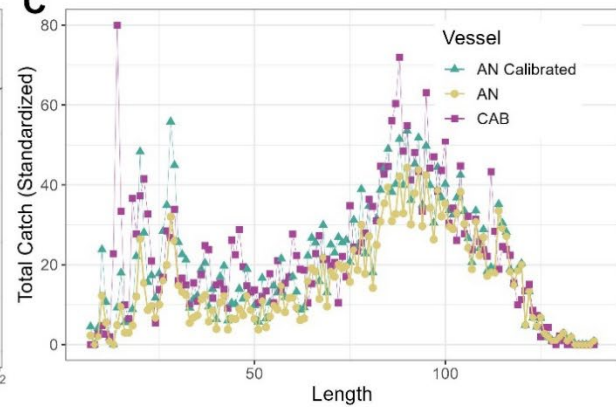
A**B****C**

Figure A1–64. Results for length-disaggregated comparative fishing analyses for Snow Crab (*Chionoecetes opilio*) between the CCGS Alfred Needler and CCGS John Cabot Fall 3KL. (A) map of catches by length group (length in mm specified in top panel) by the CCGS Alfred Needler (top) and the CCGS John Cabot (bottom) in comparative fishing sets, where circle size is proportional catch weight (B) Biplot of the square-root of CCGS John Cabot catch numbers against the square-root of CCGS Alfred Needler catch numbers. (C) Total length (mm) frequencies for catches made by the CCGS Alfred Needler (yellow), by the CCGS Cabot (pink), and CCGS Alfred Needler catches with the conversion factor applied (green).

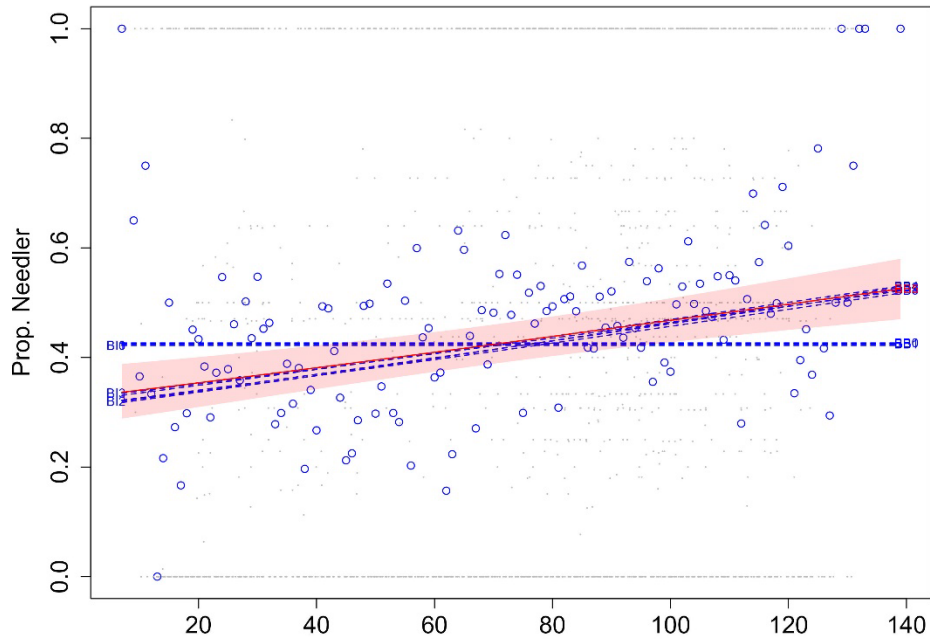
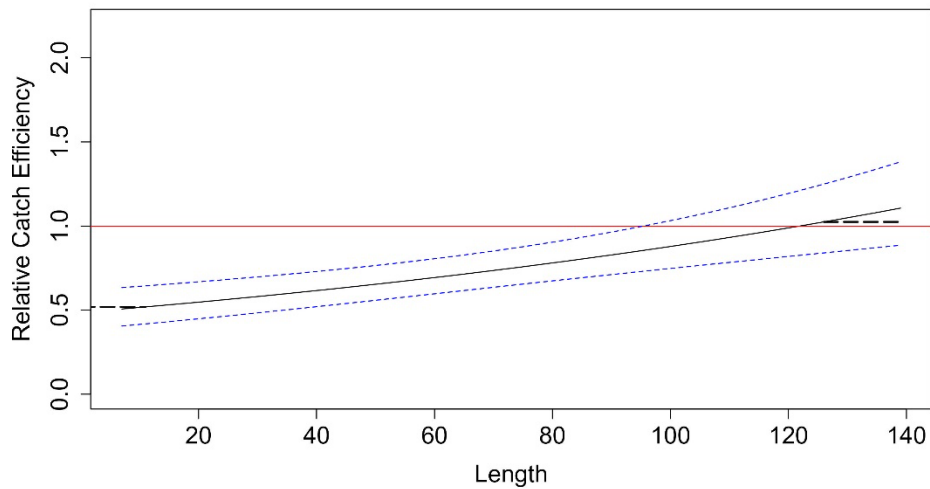
A**B**

Figure A1–65. Snow Crab (*Chionoecetes opilio*) conversion factor, for CCGS Alfred Needler and CCGS John Cabot Fall 3KL. (A) Estimated length-specific catch proportion functions, $\text{logit}(p_{Ai}(l))$, for each converged model, with the selected model plotted using a red line along with its approximate 95% CI (shaded area), as well as the length class-specific mean empirical proportion of total catch in a pair made by the CCGS Alfred Needler (blue dots). (B) Estimated relative catch efficiency (conversion factor) function from the best model (black line) with 95% CI (dashed blue lines). The horizontal red line indicates equivalent efficiency between vessels.

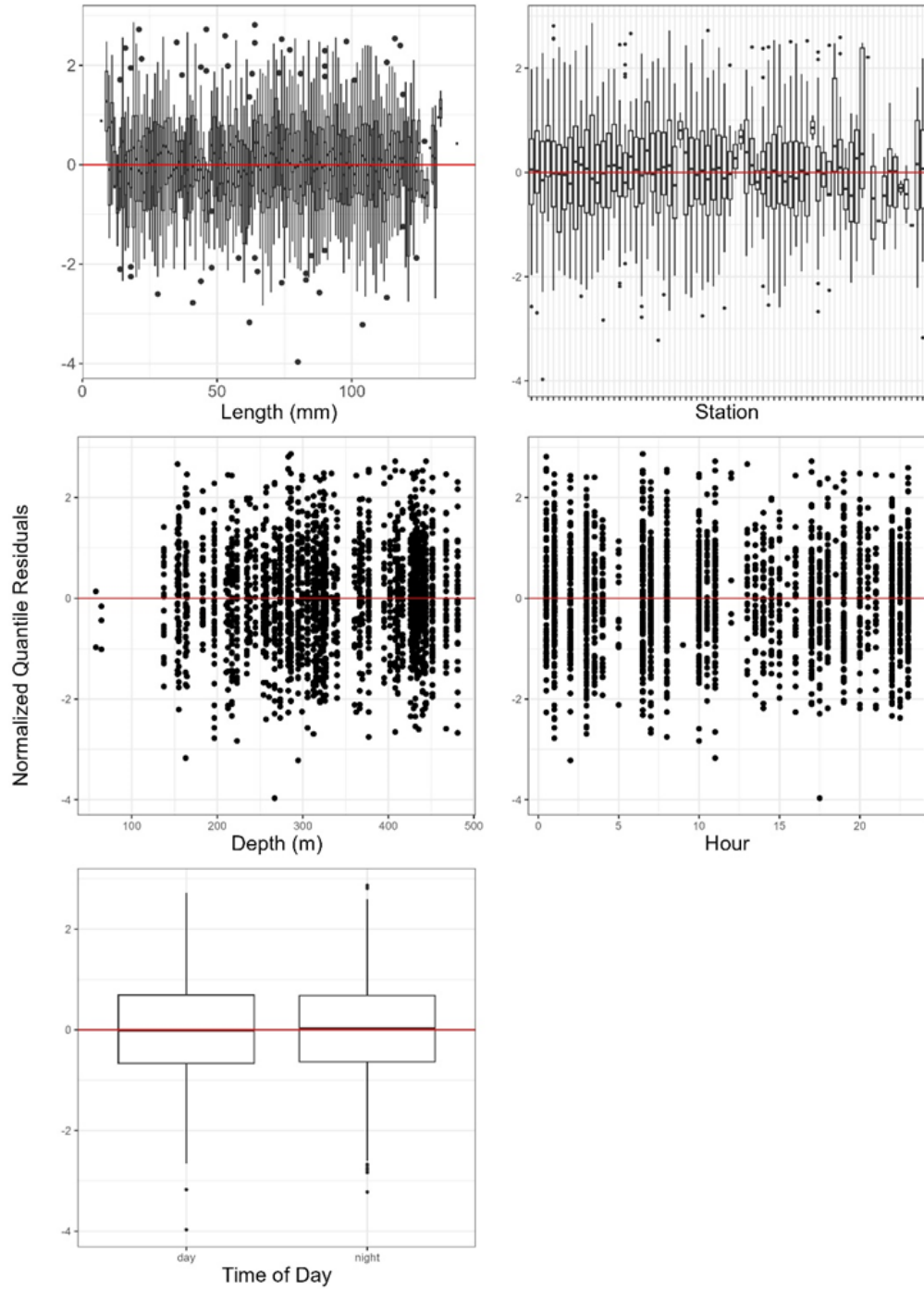


Figure A1–66. Normalized quantile residuals for as a function of length, station, depth, hour, and diel period for Snow Crab (*Chionoecetes opilio*), best model selected (BB4) for length (mm) disaggregated conversion factor analysis for the CCGS Alfred Needler, and CCGS John Cabot Fall 3KL.

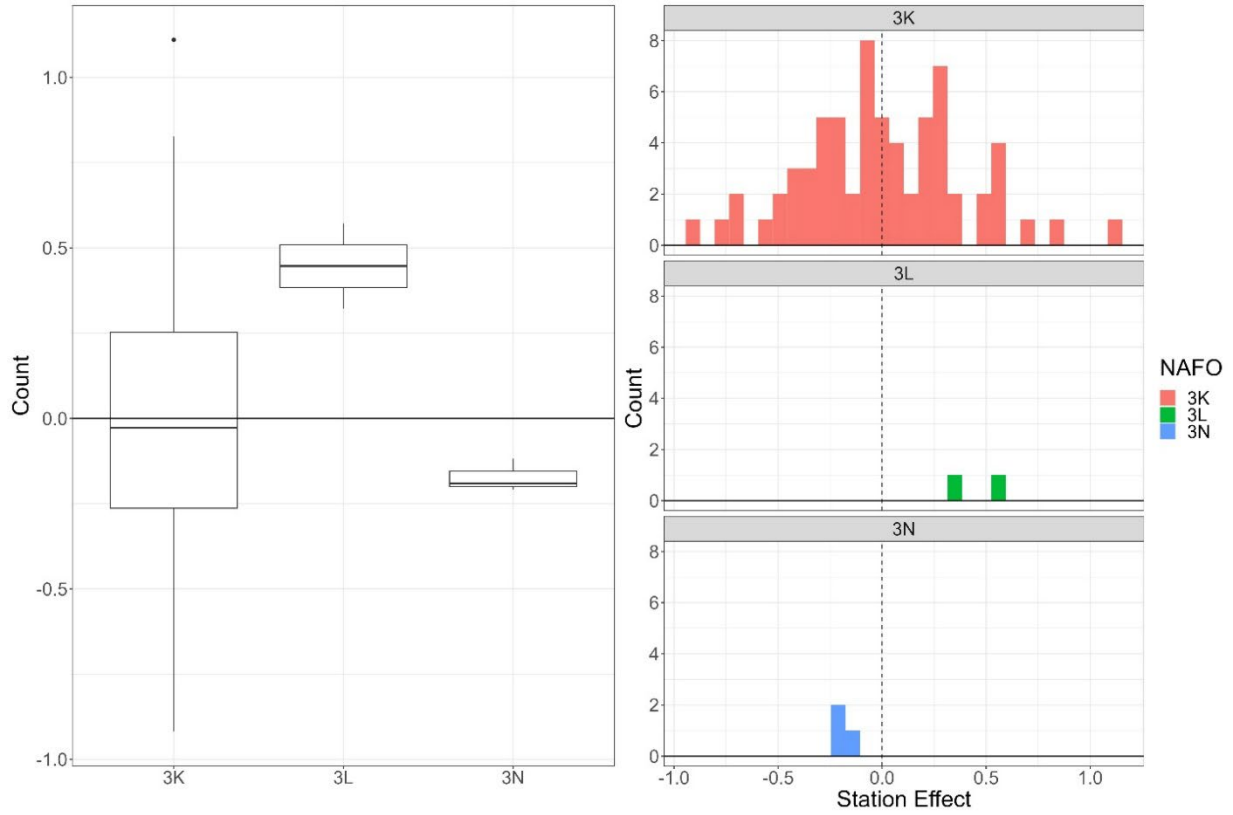


Figure A1–67. Boxplot (left) and histogram (right) of station effect by NAFO Division for best model (BB4) selected for Snow Crab (*Chionoecetes opilio*) conversion factor analysis of CCGS Alfred Needler and CCGS John Cabot in Fall 3KL.

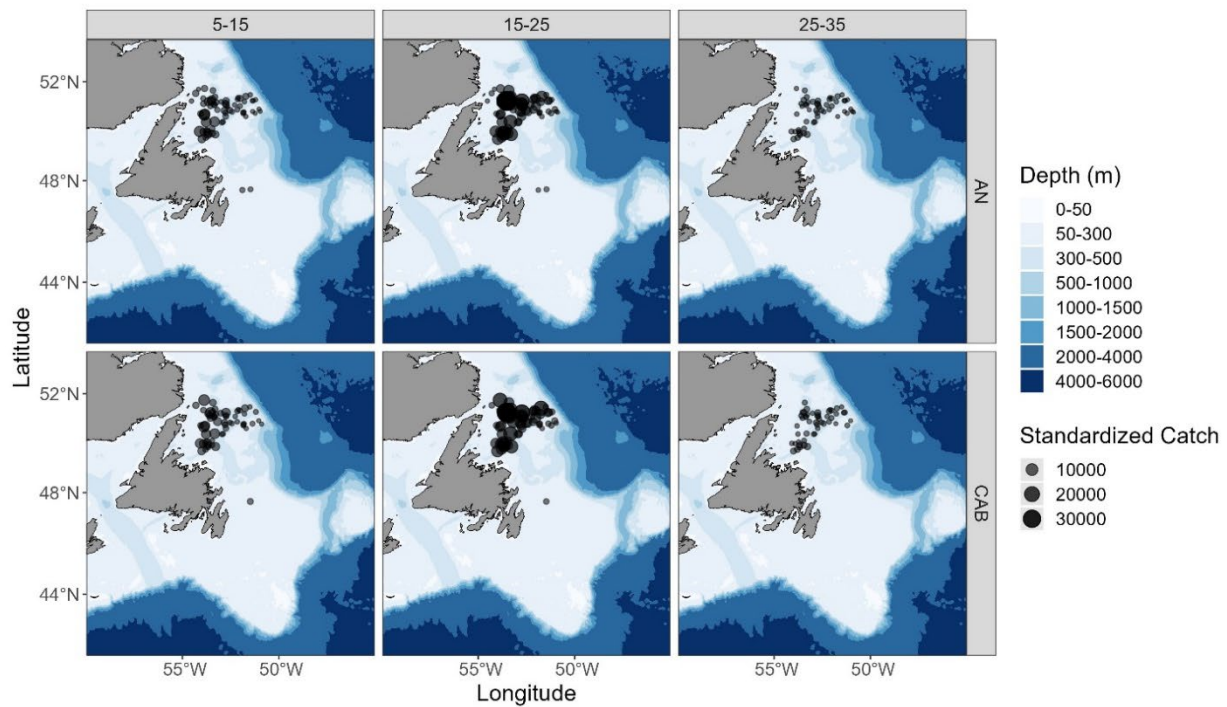
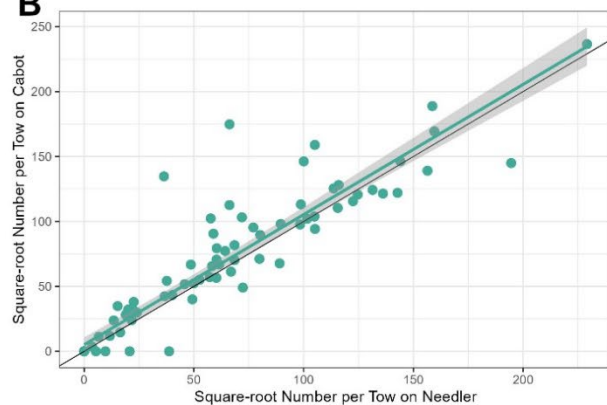
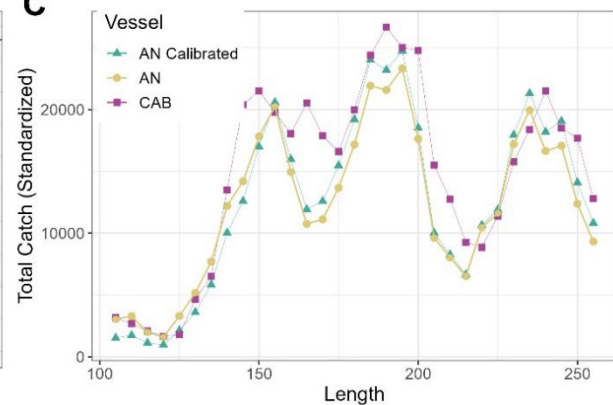
A**B****C**

Figure A1–68. Results for comparative fishing analysis for Northern Shrimp (*Pandalus borealis*), between the CCGS Alfred Needler and CCGS John Cabot for Fall 3KL. Note, lengths (mm) have been trimmed to the 2.5 & 97.5 percentiles prior to model fit. Lengths are binned in 0.5 mm bins. (A) map of catches by length group (length in cm specified in top panel) by the CCGS Alfred Needler (top) and the CCGS John Cabot (bottom) in comparative fishing sets, where circle size is proportional catch weight (B) Biplot of the square-root of CCGS John Cabot catch numbers against the square-root of Needler catch numbers. (C) Total length (mm) frequencies for catches made by the CCGS Alfred Needler (yellow), by the CCGS John Cabot (pink), and CCGS Alfred Needler catches with the conversion factor applied (green).

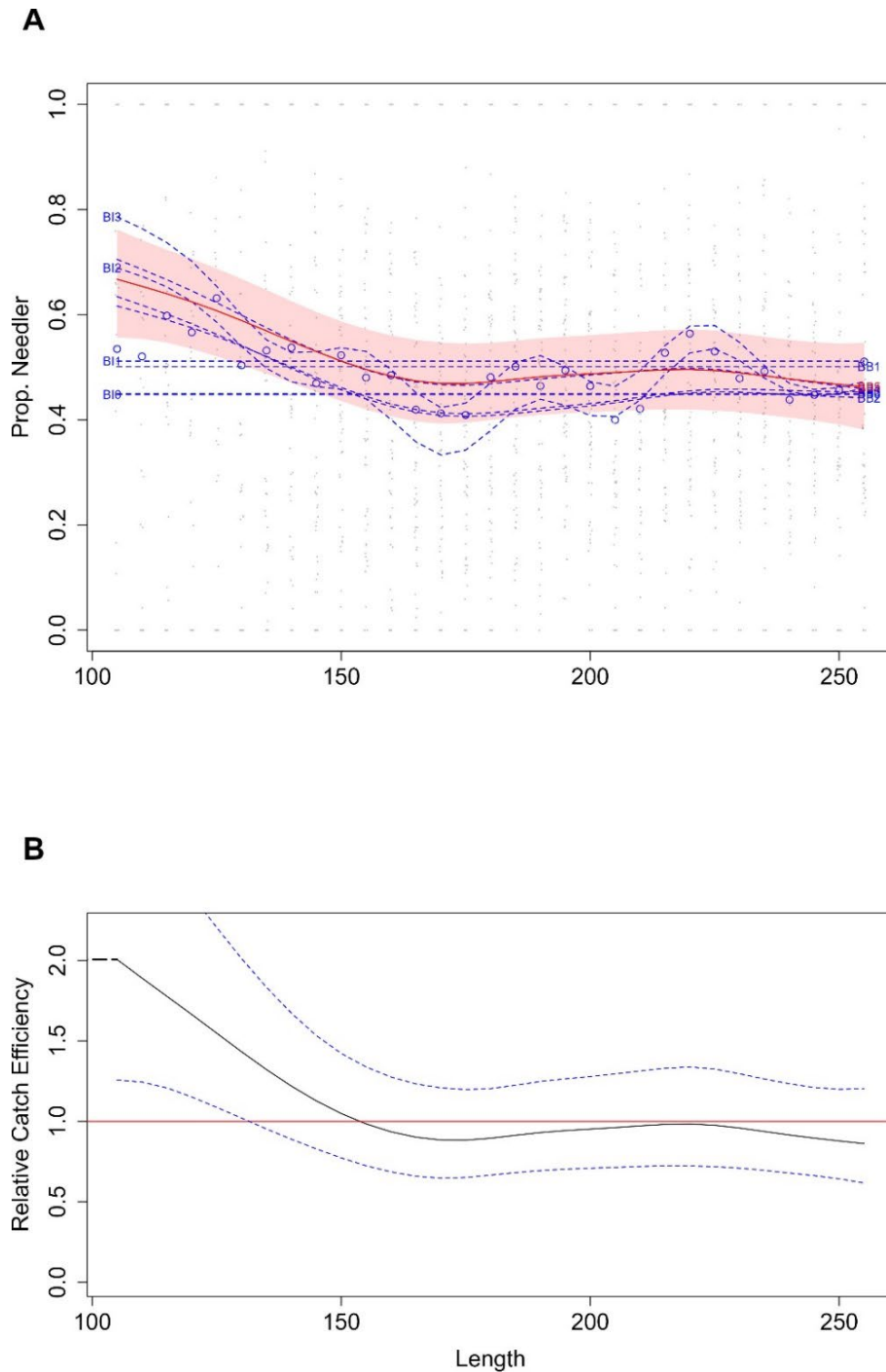


Figure A1–69. Northern Shrimp (*Pandalus borealis*) conversion factor, for CCGS Alfred Needler and CCGS John Cabot Fall 3KL. Note, lengths have been trimmed to the 2.5 & 97.5 percentiles prior to model fit. Lengths are binned in 0.5 mm bins. (A) Estimated length-specific catch proportion functions, $\text{logit}(p_{Ai}(l))$, for each converged model, with the selected model plotted using a red line along with its approximate 95% CI (shaded area), as well as the length class-specific mean empirical proportion of total catch in a pair made by the CCGS Alfred Needler (blue dots). (B) Estimated relative catch efficiency (conversion factor) function from the best model (black line) with 95% CI (dashed blue lines). The horizontal red line indicates equivalent efficiency between vessels.

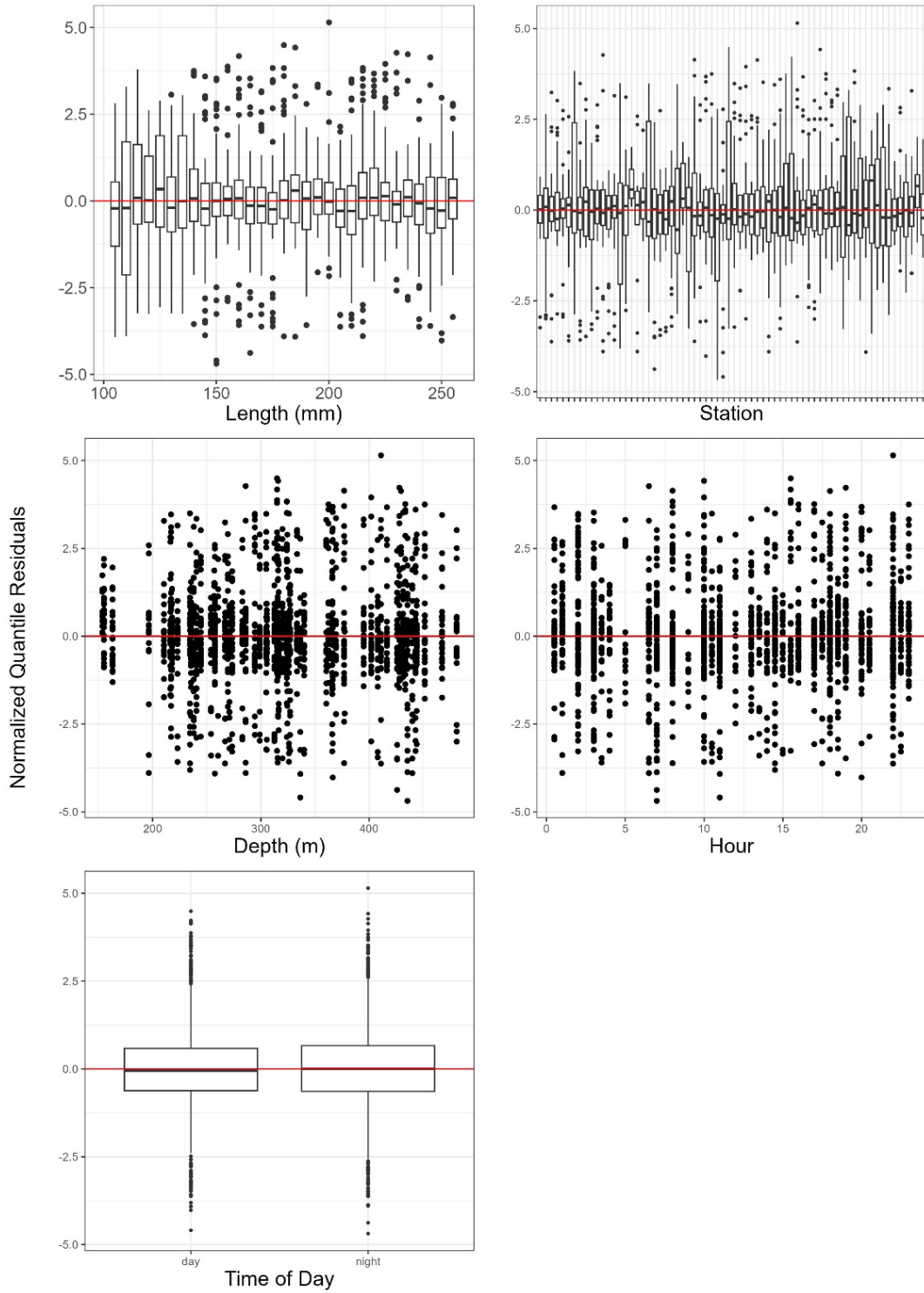


Figure A1–70. Northern Shrimp (*Pandalus borealis*), for CCGS Alfred Needler and CCGS John Cabot Fall 3KL. Note, lengths have been trimmed to the 2.5 & 97.5 percentiles prior to model fit. Lengths are binned in 0.5 mm bins. Normalized quantile residuals for as a function of length, station, depth, hour, and diel period.

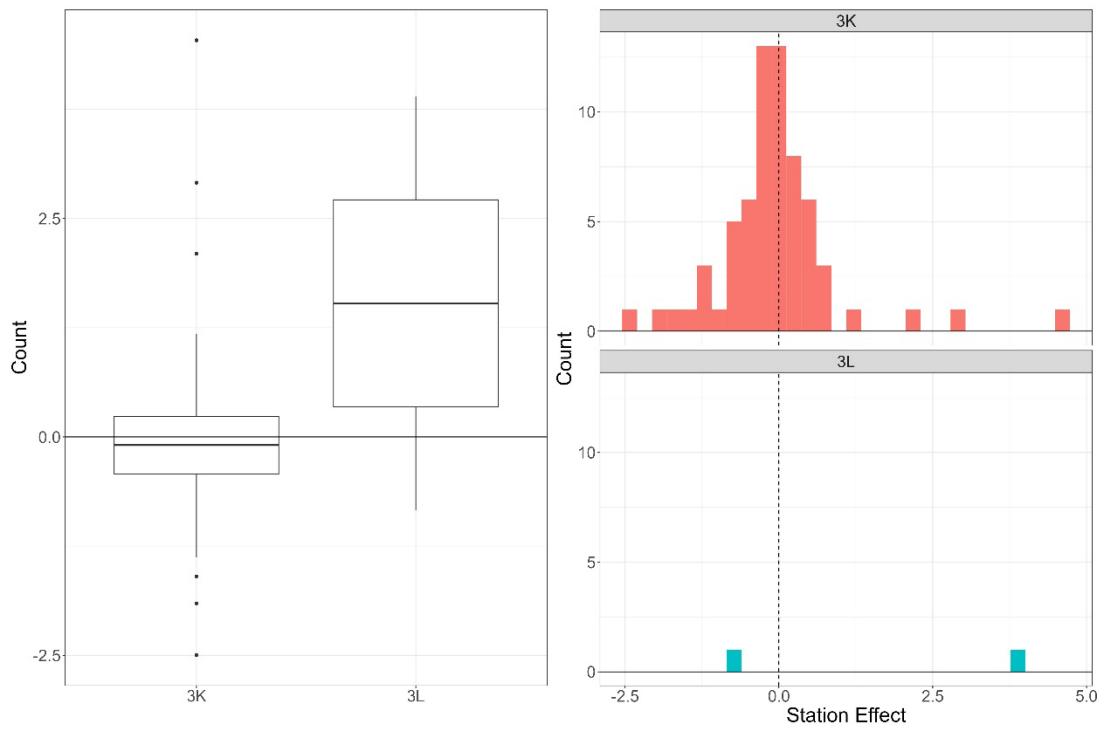


Figure A1–71. Boxplot (left) and histogram (right) of station effect by NAFO Division for best model (BB5) selected for Northern Shrimp (*Pandalus borealis*) conversion factor analysis of CCGS Alfred Needler and CCGS John Cabot in Fall 3KL.

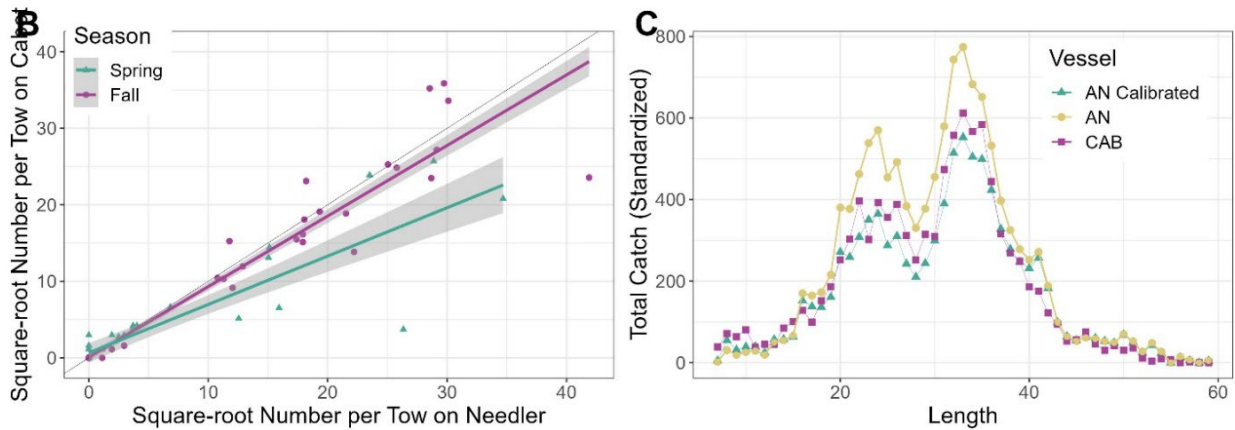
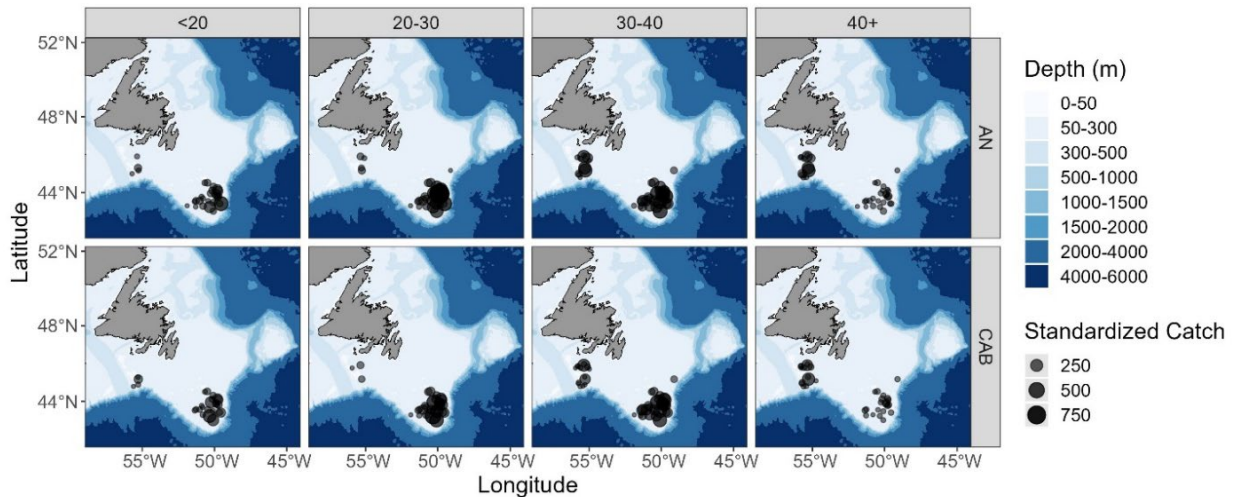
A

Figure A1–72. Results for length-disaggregated comparative fishing analyses for Yellowtail Flounder (*Myxopsetta ferruginea*), between the CCGS Alfred Needler and CCGS John Cabot for Fall 3LNO and Spring 3LNOPs. (A) map of catches by length group (length in cm specified in top panel) by the CCGS Alfred Needler (top) and the CCGS John Cabot (bottom) in comparative fishing sets, where circle size is proportional catch weight (B) Biplot of the square-root of CCGS John Cabot catch numbers against the square-root of CCGS Alfred Needler catch numbers showing spring (green) and fall (purple). (C) Total length frequencies for catches made by the CCGS Alfred Needler (yellow), by the CCGS John Cabot (pink), and Needler catches with the conversion factor applied (green).

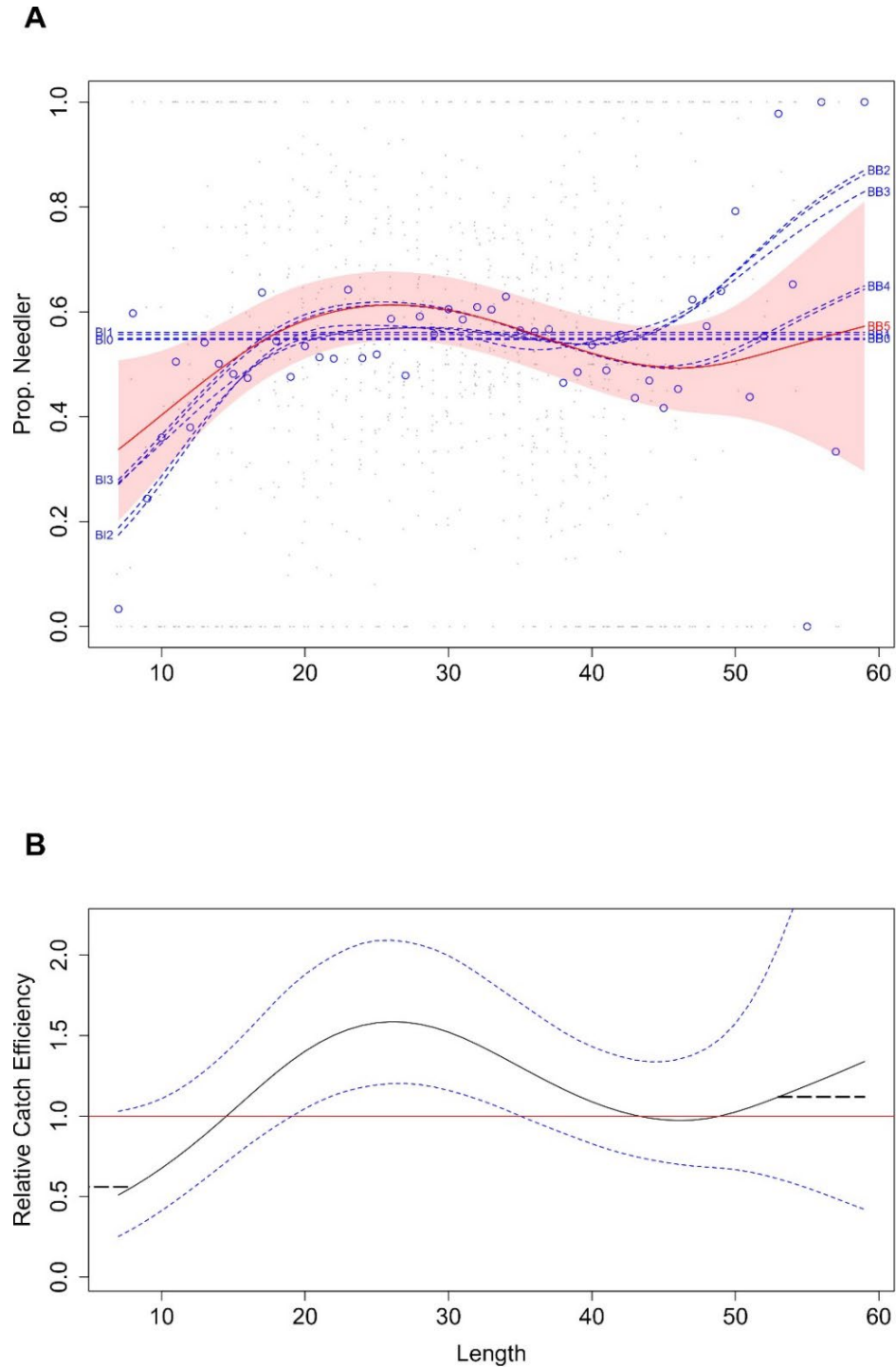


Figure A1–73. Yellowtail Flounder (*Myxopsetta ferruginea*) conversion factor, for CCGS Alfred Needler and CCGS John Cabot Fall 3LNO and Spring 3LNOPs. (A) Estimated length-specific catch proportion functions, $\text{logit}(p_{Ai}(l))$, for each converged model, with the selected model plotted using a red line along with its approximate 95% CI (shaded area), as well as the length class-specific mean empirical proportion of total catch in a pair made by the CCGS Alfred Needler (blue dots). (B) Estimated relative catch efficiency (conversion factor) function from the best model (black line) with 95% CI (dashed blue lines). The horizontal red line indicates equivalent efficiency between vessels.

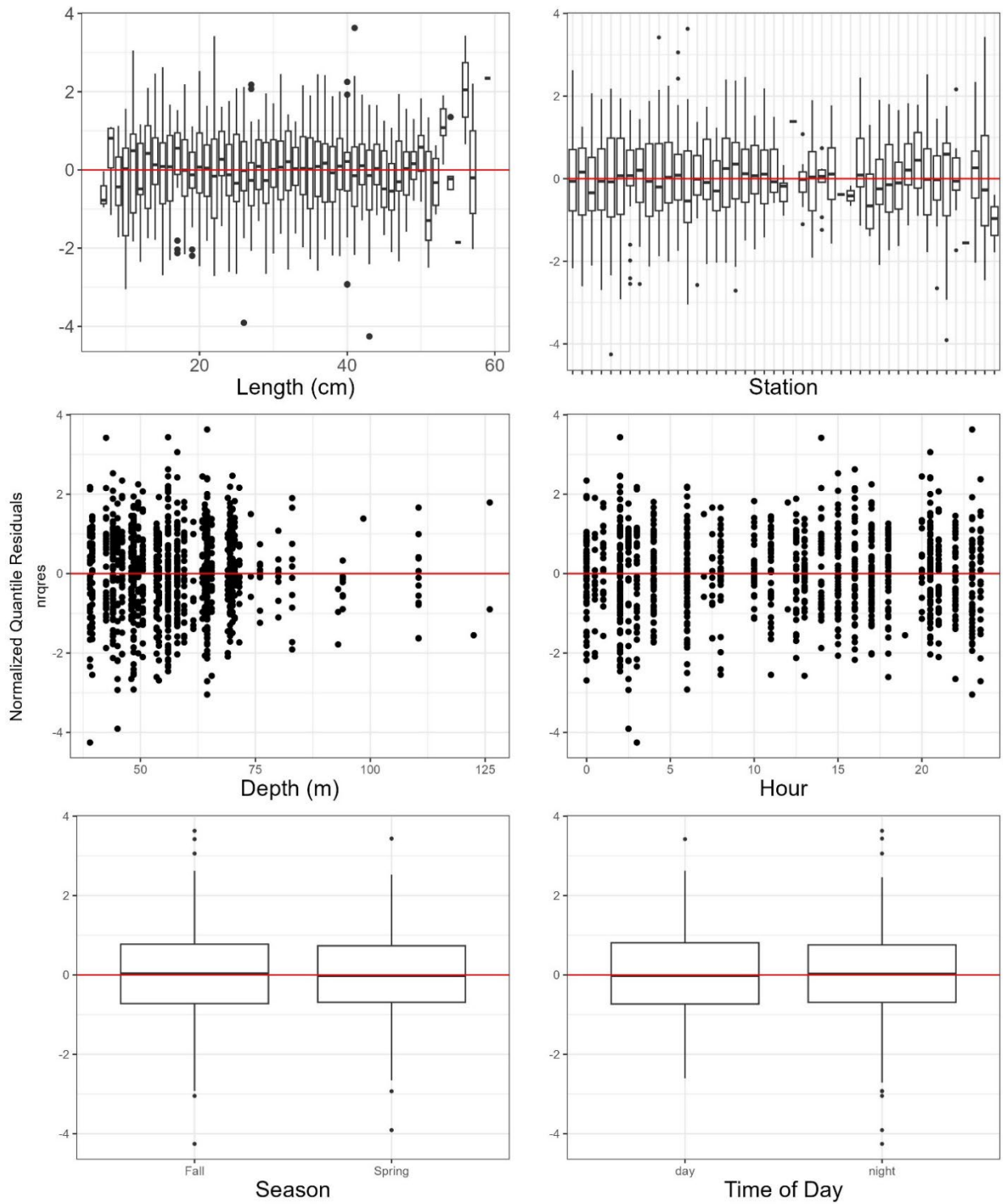


Figure A1–74. Yellowtail Flounder (*Myxopsetta ferruginea*), for CCGS Alfred Needler and CCGS John Cabot Fall 3LNO and Spring 3LNOPs. Normalized quantile residuals for as a function of length, station, depth, hour, and diel period.

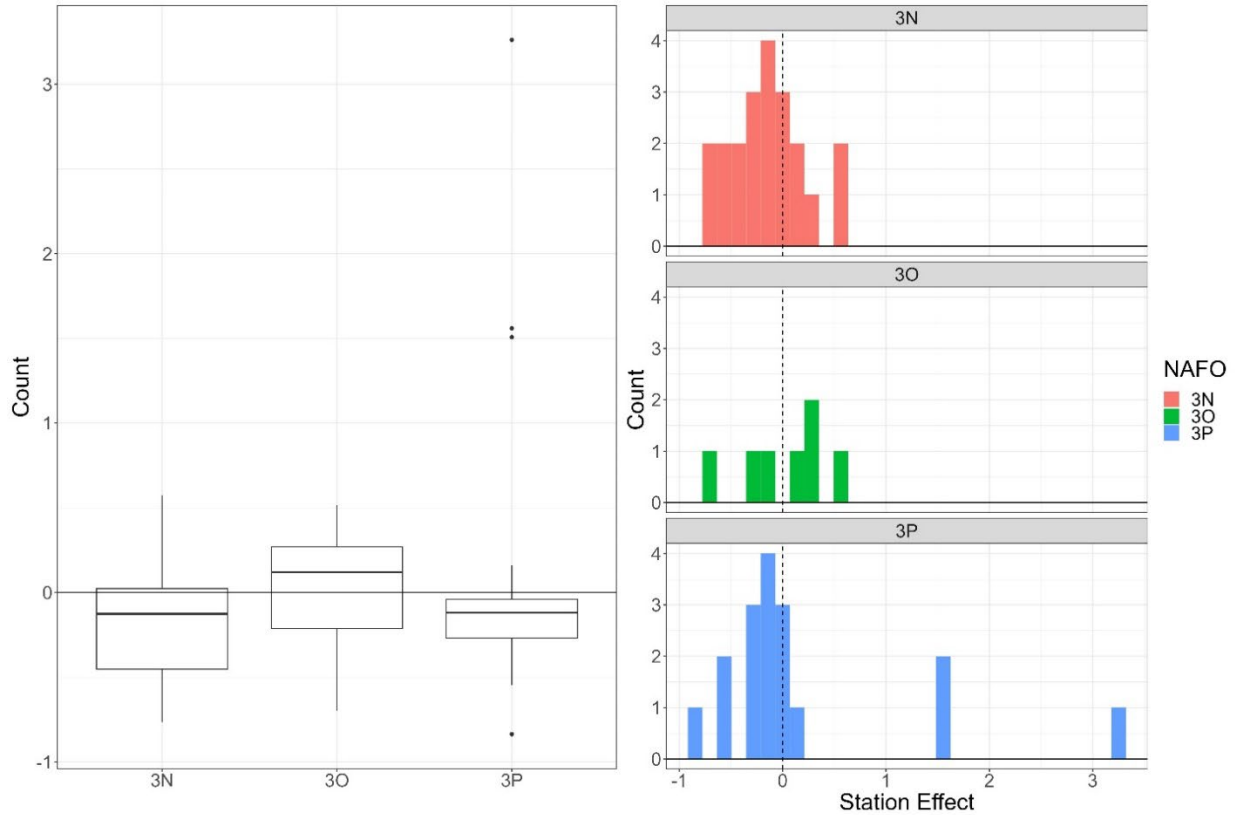


Figure A1-75. Boxplot (left) and histogram (right) of station effect by NAFO Division for best model (BB5) selected for Yellowtail Flounder (*Myxopsetta ferruginea*) conversion factor analysis of CCGS Alfred Needler and CCGS John Cabot for Fall 3LNO and Spring 3LNOPs.

TABLES

Table A1-1. Conversions (\pm Standard Error) required for Witch Flounder (*Glyptocephalus cynoglossus*) to be used for the CCGS Teleost, and CCGS John Cabot/Capt. Jacques Cartier for Fall 2HJ3K + 3L deep. Length (cm) range displayed is for the 0.5 and 99.5 percentile range, and conversions below 10 cm should be applied at 0.55 ± 0.08 and above 54 cm at 0.94 ± 0.15 .

Length	Conversion	SE
10	0.55	0.08
11	0.57	0.08
12	0.58	0.08
13	0.60	0.07
14	0.62	0.07
15	0.64	0.07
16	0.66	0.07
17	0.68	0.06
18	0.70	0.06
19	0.73	0.06
20	0.75	0.07
21	0.77	0.07
22	0.79	0.07
23	0.81	0.07
24	0.82	0.07
25	0.84	0.07

Length	Conversion	SE
26	0.85	0.07
27	0.87	0.07
28	0.88	0.07
29	0.89	0.07
30	0.90	0.07
31	0.90	0.07
32	0.91	0.07
33	0.92	0.07
34	0.92	0.07
35	0.93	0.07
36	0.94	0.07
37	0.94	0.07
38	0.95	0.07
39	0.95	0.07
40	0.95	0.07
41	0.96	0.07
42	0.96	0.07
43	0.96	0.07
44	0.96	0.08
45	0.96	0.08
46	0.96	0.08
47	0.96	0.09
48	0.95	0.09
49	0.95	0.10
50	0.95	0.11
51	0.95	0.12
52	0.94	0.13
53	0.94	0.14
54	0.94	0.15

*Table A1–2. Conversions (\pm Standard Error) required for Northern Shrimp (*Pandalus borealis*) to be used for CCGS Teleost, and CCGS John Cabot/Capt. Jacques Cartier for Fall 2HJ3K + 3L deep conversion. Length (mm) range displayed is for the 2.5 and 97.5 percentile range, and conversions below 130 mm should be applied at 1.26 ± 0.10 and above 255 mm at 1.10 ± 0.08 .*

Length	Conversion	SE
130	1.26	0.10
135	1.25	0.10
140	1.25	0.09
145	1.24	0.09
150	1.23	0.08
155	1.23	0.07
160	1.22	0.07
165	1.21	0.06
170	1.21	0.06
175	1.20	0.05
180	1.19	0.05
185	1.19	0.05
190	1.18	0.04
195	1.17	0.04
200	1.17	0.04

Length	Conversion	SE
205	1.16	0.04
210	1.16	0.04
215	1.15	0.05
220	1.14	0.05
225	1.14	0.05
230	1.13	0.06
235	1.12	0.06
240	1.12	0.06
245	1.11	0.07
250	1.11	0.07
255	1.10	0.08

*Table A1–3. Conversions (\pm Standard Error) required for American Plaice (*Hippoglossoides platessoides*) to be used for the CCGS Alfred Needler and CCGS John Cabot Fall 3KL conversion. Length (cm) range displayed is for the 0.5 and 99.5 percentile range, and conversions below 8 cm should be applied at 0.69 ± 0.06 and above 48 cm at 1.65 ± 0.15 .*

Length	Conversion	SE
8	0.69	0.06
9	0.70	0.06
10	0.72	0.06
11	0.73	0.06
12	0.75	0.06
13	0.77	0.06
14	0.78	0.06
15	0.80	0.05
16	0.82	0.05
17	0.84	0.05
18	0.86	0.05
19	0.87	0.05
20	0.89	0.05
21	0.91	0.05
22	0.93	0.05
23	0.95	0.05
24	0.98	0.05
25	1.00	0.05
26	1.02	0.05
27	1.04	0.05
28	1.06	0.05
29	1.09	0.05
30	1.11	0.05
31	1.14	0.06
32	1.16	0.06
33	1.19	0.06
34	1.21	0.07
35	1.24	0.07
36	1.27	0.07
37	1.30	0.08

Length	Conversion	SE
38	1.32	0.08
39	1.35	0.09
40	1.38	0.09
41	1.41	0.10
42	1.45	0.11
43	1.48	0.11
44	1.51	0.12
45	1.54	0.13
46	1.58	0.14
47	1.61	0.14
48	1.65	0.15

*Table A1–4. Conversions (\pm Standard Error) required for Witch Flounder (*Glyptocephalus cynoglossus*) to be used for the CCGS Alfred Needler and CCGS John Cabot Fall 3KL conversion. Length (cm) range displayed is for the 0.5 and 99.5 percentile range, and conversions below 12 cm should be applied at 0.65 ± 0.09 and above 52 cm at 1.26 ± 0.19 .*

Length	Conversion	SE
12	0.65	0.09
13	0.66	0.09
14	0.68	0.09
15	0.69	0.09
16	0.70	0.09
17	0.71	0.09
18	0.72	0.08
19	0.73	0.08
20	0.75	0.08
21	0.76	0.08
22	0.77	0.08
23	0.78	0.08
24	0.80	0.08
25	0.81	0.07
26	0.82	0.07
27	0.84	0.07
28	0.85	0.07
29	0.86	0.07
30	0.88	0.07
31	0.89	0.08
32	0.91	0.08
33	0.92	0.08
34	0.94	0.08
35	0.95	0.08
36	0.97	0.09
37	0.98	0.09
38	1.00	0.09
39	1.02	0.10
40	1.03	0.10
41	1.05	0.11
42	1.07	0.11

Length	Conversion	SE
43	1.09	0.12
44	1.10	0.13
45	1.12	0.13
46	1.14	0.14
47	1.16	0.15
48	1.18	0.16
49	1.20	0.16
50	1.22	0.17
51	1.24	0.18
52	1.26	0.19

*Table A1–5. Conversions (\pm Standard Error) required for Redfish (*Sebastes mentella* & *S. faciatus*) to be used for the CCGS Alfred Needler and CCGS John Cabot Fall 3KL conversion. Length (cm) range displayed is for the 0.5 and 99.5 percentile range, and conversions below 8 cm should be applied at 0.41 ± 0.05 and above 38 cm at 2.86 ± 0.39 .*

Length	Conversion	SE
8	0.41	0.05
9	0.44	0.05
10	0.47	0.05
11	0.50	0.05
12	0.53	0.06
13	0.57	0.06
14	0.61	0.06
15	0.65	0.07
16	0.69	0.07
17	0.74	0.07
18	0.79	0.08
19	0.84	0.08
20	0.90	0.09
21	0.96	0.10
22	1.02	0.10
23	1.09	0.11
24	1.16	0.12
25	1.24	0.13
26	1.32	0.14
27	1.41	0.15
28	1.50	0.16
29	1.60	0.18
30	1.71	0.19
31	1.82	0.21
32	1.94	0.23
33	2.07	0.25
34	2.21	0.27
35	2.36	0.30
36	2.52	0.33

Length	Conversion	SE
37	2.69	0.36
38	2.86	0.39

Table A1–6. Conversions (\pm Standard Error) required for Snow Crab (*Chionoecetes opilio*) to be used for the CCGS Alfred Needler and CCGS John Cabot Fall 3KL conversion. Width (mm) range displayed is for the 0.5 and 99.5 percentile range, and conversions below 11 mm should be applied at 0.52 ± 0.06 and above 126 mm at 1.02 ± 0.10 .

Carapace width	Conversion	SE
11	0.52	0.06
12	0.52	0.06
13	0.53	0.06
14	0.53	0.06
15	0.53	0.06
16	0.53	0.06
17	0.54	0.06
18	0.54	0.06
19	0.54	0.06
20	0.55	0.06
21	0.55	0.06
22	0.55	0.06
23	0.56	0.06
24	0.56	0.06
25	0.56	0.05
26	0.57	0.05
27	0.57	0.05
28	0.57	0.05
29	0.58	0.05
30	0.58	0.05
31	0.58	0.05
32	0.59	0.05
33	0.59	0.05
34	0.59	0.05
35	0.60	0.05
36	0.60	0.05
37	0.61	0.05
38	0.61	0.05
39	0.61	0.05
40	0.62	0.05
41	0.62	0.05
42	0.62	0.05
43	0.63	0.05
44	0.63	0.05
45	0.63	0.05
46	0.64	0.05
47	0.64	0.05
48	0.65	0.05
49	0.65	0.05
50	0.65	0.05
51	0.66	0.05
52	0.66	0.05

Carapace width	Conversion	SE
53	0.67	0.05
54	0.67	0.05
55	0.67	0.05
56	0.68	0.05
57	0.68	0.05
58	0.69	0.05
59	0.69	0.05
60	0.69	0.05
61	0.70	0.05
62	0.70	0.05
63	0.71	0.05
64	0.71	0.05
65	0.71	0.05
66	0.72	0.05
67	0.72	0.05
68	0.73	0.05
69	0.73	0.05
70	0.74	0.05
71	0.74	0.06
72	0.74	0.06
73	0.75	0.06
74	0.75	0.06
75	0.76	0.06
76	0.76	0.06
77	0.77	0.06
78	0.77	0.06
79	0.78	0.06
80	0.78	0.06
81	0.79	0.06
82	0.79	0.06
83	0.79	0.06
84	0.80	0.06
85	0.80	0.06
86	0.81	0.06
87	0.81	0.06
88	0.82	0.06
89	0.82	0.06
90	0.83	0.06
91	0.83	0.06
92	0.84	0.07
93	0.84	0.07
94	0.85	0.07
95	0.85	0.07
96	0.86	0.07
97	0.86	0.07
98	0.87	0.07
99	0.87	0.07
100	0.88	0.07
101	0.88	0.07
102	0.89	0.07
103	0.89	0.08
104	0.90	0.08

Carapace width	Conversion	SE
105	0.90	0.08
106	0.91	0.08
107	0.92	0.08
108	0.92	0.08
109	0.93	0.08
110	0.93	0.08
111	0.94	0.08
112	0.94	0.08
113	0.95	0.09
114	0.95	0.09
115	0.96	0.09
116	0.97	0.09
117	0.97	0.09
118	0.98	0.09
119	0.98	0.09
120	0.99	0.10
121	0.99	0.10
122	1.00	0.10
123	1.01	0.10
124	1.01	0.10
125	1.02	0.10
126	1.02	0.10

*Table A1–7. Conversions (\pm Standard Error) required for Northern Shrimp (*Pandalus borealis*) to be used for the CCGS Alfred Needler and CCGS John Cabot Fall 3KL conversion. Carapace length (mm) range displayed is for the 2.5 and 97.5 percentile range, and conversions below 105 mm should be applied at 2.01 ± 0.48 and above 250 mm at 0.88 ± 0.14 .*

Carapace length	Conversion	SE
105	2.01	0.48
110	1.89	0.40
115	1.78	0.35
120	1.66	0.31
125	1.55	0.28
130	1.43	0.25
135	1.32	0.22
140	1.22	0.20
145	1.13	0.18
150	1.05	0.16
155	0.98	0.15
160	0.94	0.15
165	0.90	0.14
170	0.88	0.14
175	0.88	0.14
180	0.90	0.14
185	0.91	0.14
190	0.93	0.14
195	0.94	0.14
200	0.95	0.14

Carapace length	Conversion	SE
205	0.96	0.15
210	0.97	0.15
215	0.98	0.15
220	0.98	0.15
225	0.98	0.15
230	0.96	0.15
235	0.94	0.14
240	0.92	0.14
245	0.90	0.14
250	0.88	0.14

*Table A1–8. Conversions (\pm Standard Error) required for Yellowtail Flounder (*Myxopsetta ferruginea*) to be used for the CCGS Alfred Needler and CCGS John Cabot Fall 3LNO and Spring 3LNOPs conversion. Length (cm) range displayed is for the 0.5 & 99.5 percentile range, and conversions below 8 cm should be applied at 0.56 ± 0.18 and above 53 cm at 1.12 ± 0.35 .*

Length	Conversion	SE
8	0.56	0.18
9	0.62	0.17
10	0.68	0.17
11	0.74	0.17
12	0.81	0.17
13	0.88	0.17
14	0.96	0.17
15	1.04	0.17
16	1.12	0.18
17	1.19	0.19
18	1.27	0.20
19	1.34	0.20
20	1.40	0.21
21	1.46	0.21
22	1.50	0.22
23	1.54	0.22
24	1.56	0.22
25	1.58	0.23
26	1.59	0.22
27	1.58	0.22
28	1.57	0.22
29	1.55	0.22
30	1.52	0.21
31	1.49	0.20
32	1.45	0.20
33	1.40	0.19
34	1.35	0.18
35	1.31	0.18
36	1.26	0.17
37	1.21	0.16
38	1.17	0.16
39	1.13	0.15
40	1.09	0.15
41	1.06	0.15

Length	Conversion	SE
42	1.03	0.15
43	1.00	0.15
44	0.99	0.15
45	0.98	0.16
46	0.97	0.16
47	0.97	0.17
48	0.98	0.18
49	1.00	0.20
50	1.02	0.22
51	1.05	0.26
52	1.08	0.30
53	1.12	0.35

APPENDIX 2: SIZE AGGREGATED CONVERSIONS

FIGURES

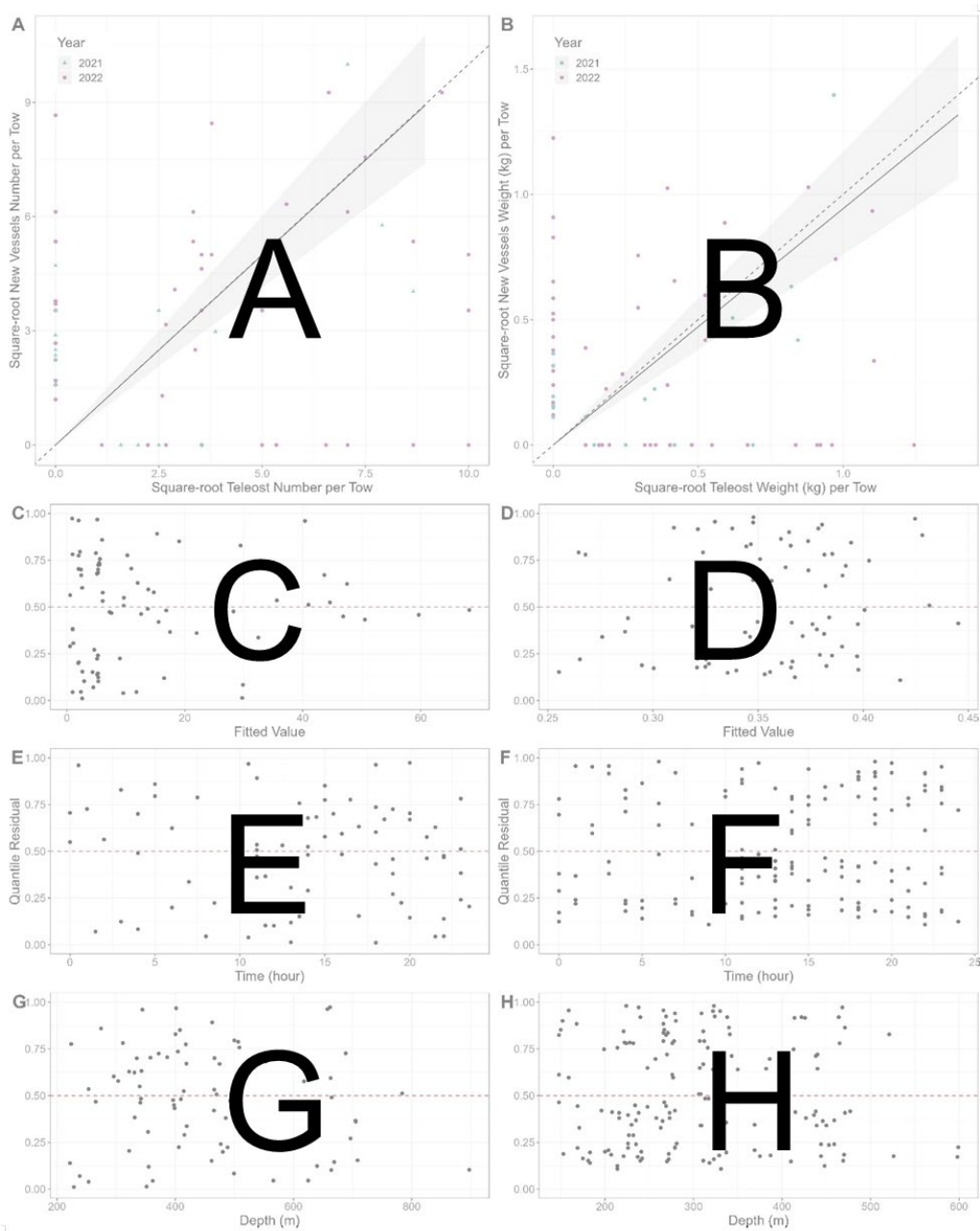


Figure A2–1. An outline for the interpretation of the figures presenting the data and results for taxa where size aggregated analyses was completed. Panel A is the biplot of the square-root of CCGS John Cabot and/or Capt. Jacques Cartier catch numbers against the square-root of CCGS Teleost or Needler catch numbers, where the solid black line and shaded interval show the estimated conversion and approximate 95%CI from the best size-aggregated model. Panel B is the same as A except for catch weights. Below A and B are the quantile residuals from the analysis of catch numbers, and weights plotted as a function of the fitted values (panels C and D respectively), time (panels E and F respectively), and depth (panels G and H respectively). Captions for the individual taxa figures only state the species and vessel pairing visualized in the figure.

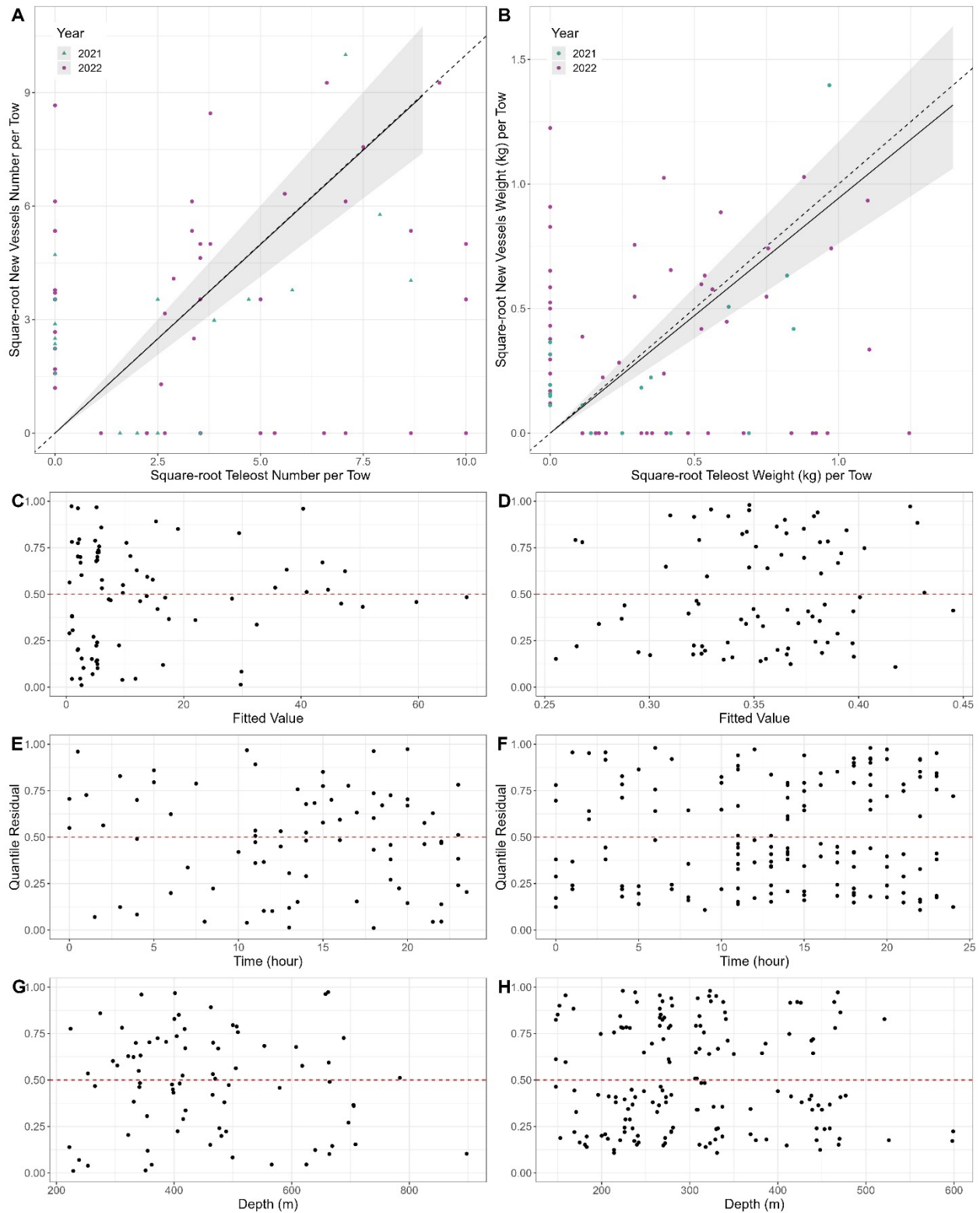


Figure A2–2. Results of size aggregated analysis for the CCGS Teleost and CCGS John Cabot/Capt. Jacques Cartier for catch of Alligatorfishes & Poachers (*Agonus* spp., *Eumicrotremus* spp.), fall 2HJ3K + 3L deep water.

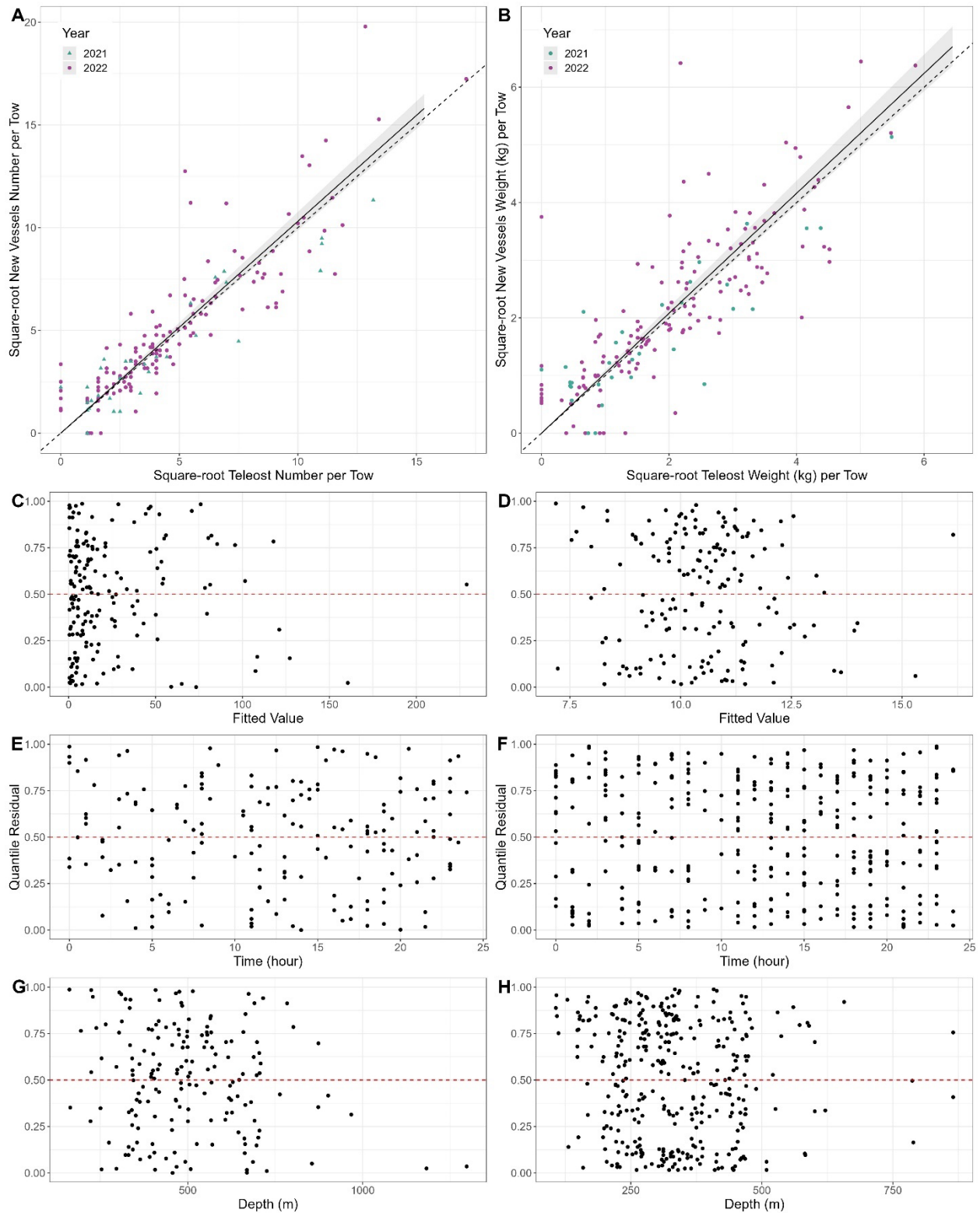


Figure A2-3. Results of size aggregated analysis for the CCGS Teleost and CCGS John Cabot/Capt. Jacques Cartier for catch of American Plaice (*Hippoglossoides platessoides*), fall 2HJ3K + 3L deep water.

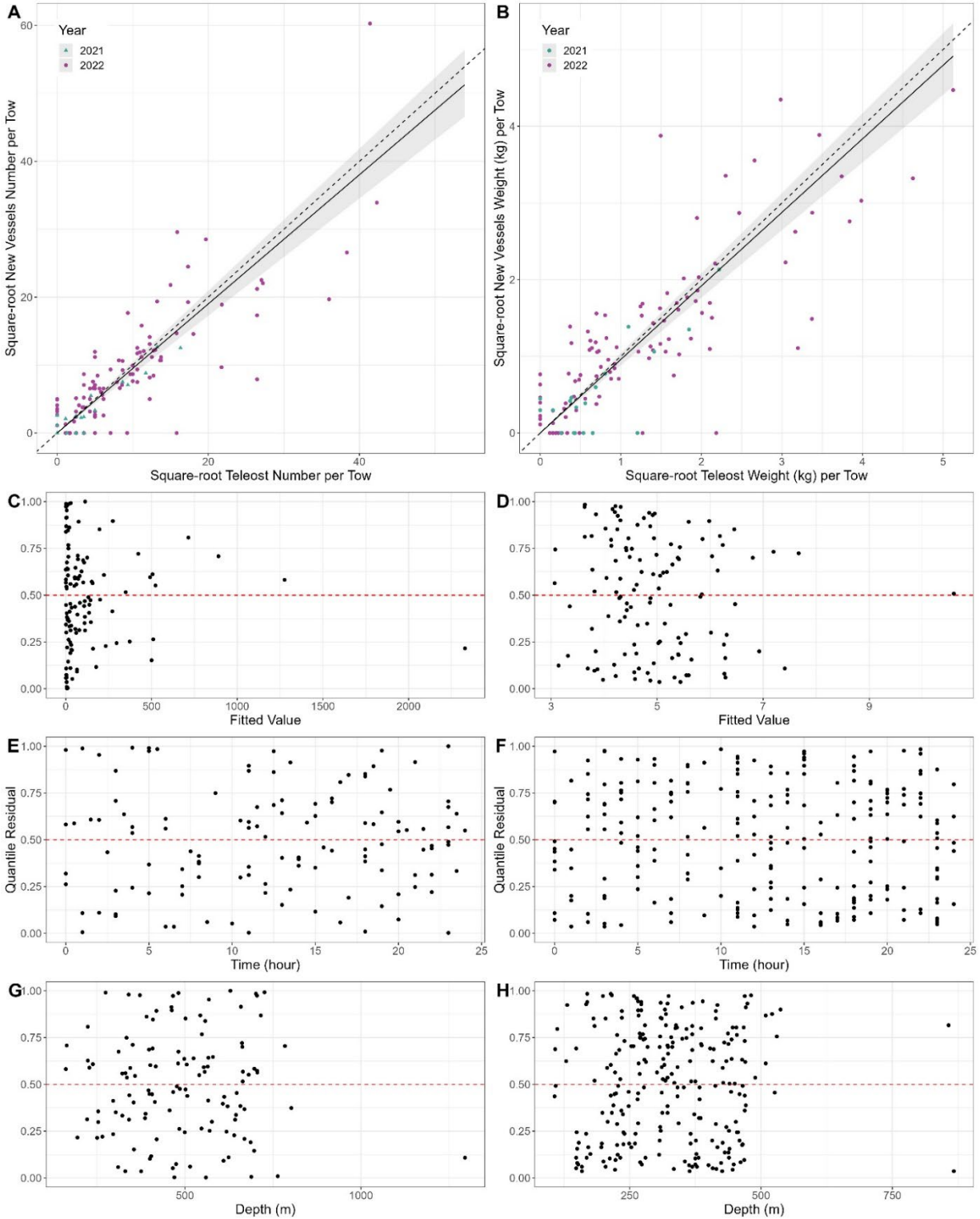


Figure A2-4. Results of size aggregated analysis for the CCGS Teleost and CCGS John Cabot/Capt. Jacques Cartier for catch of catch for Arctic cod (*Boreogadus saida*), fall 2HJ3K + 3L deep water.

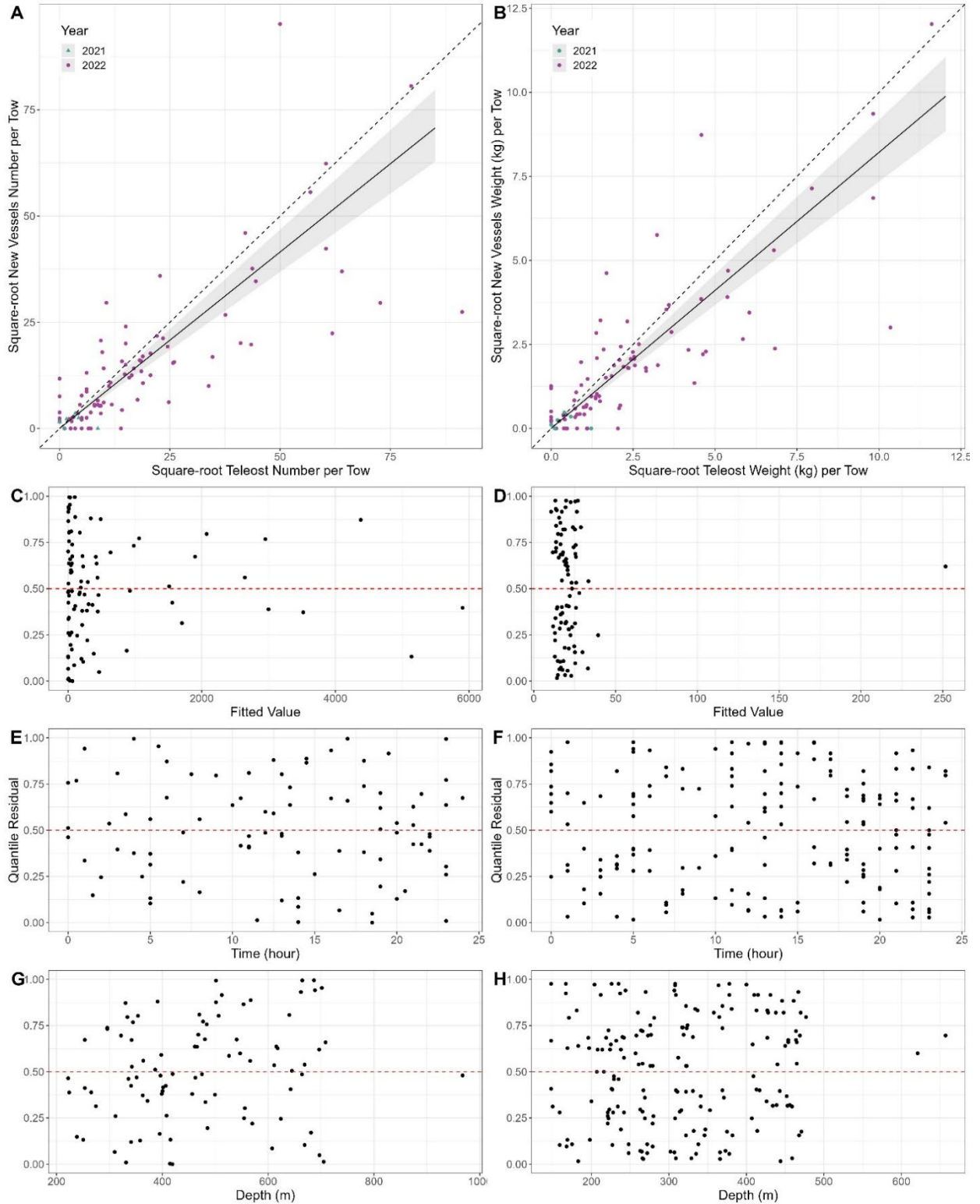


Figure A2-5. Results of size aggregated analysis for the CCGS Teleost and CCGS John Cabot/Capt. Jacques Cartier for catch of Capelin (*Mallotus villosus*), fall 2HJ3K + 3L deep water.

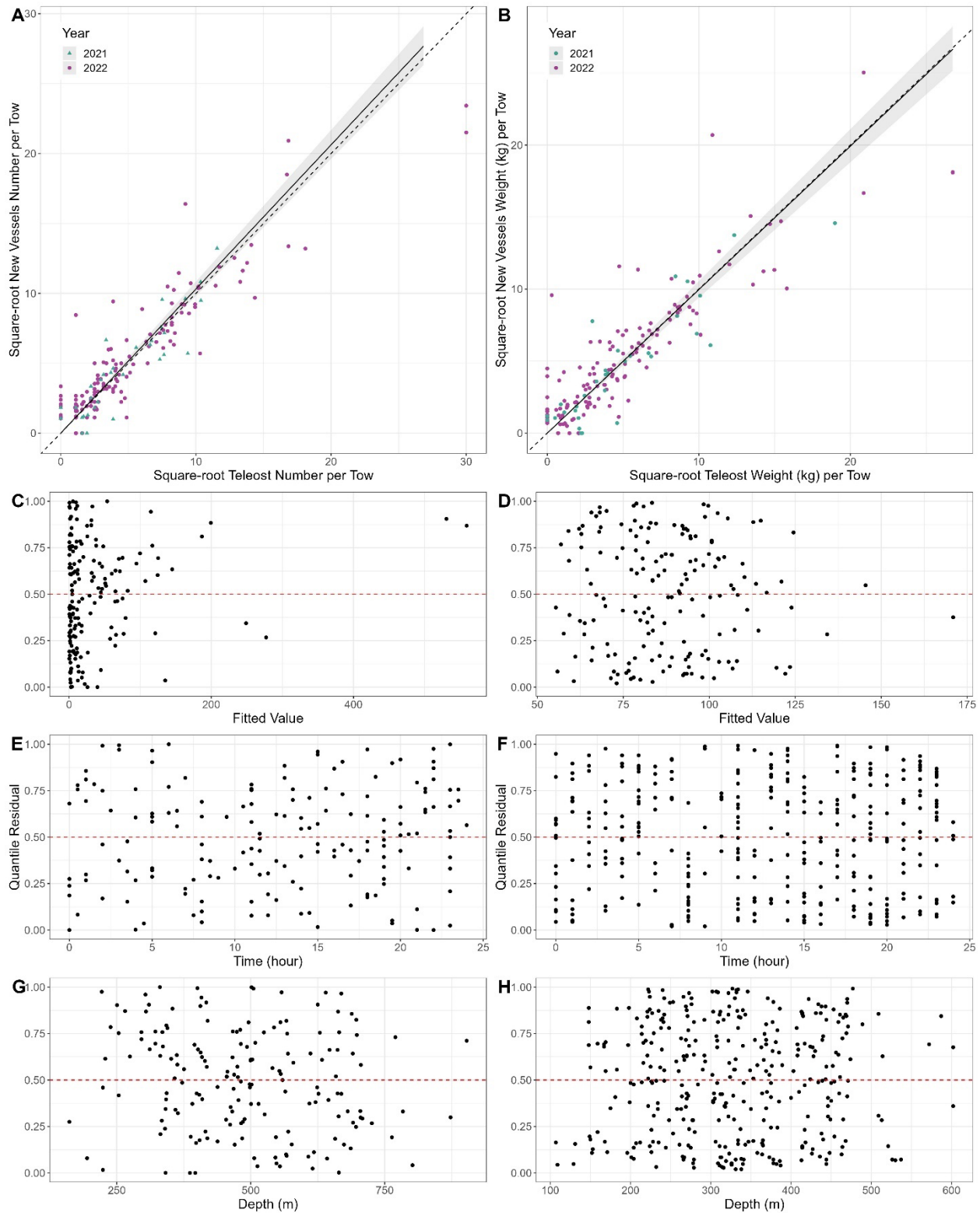


Figure A2-6. Results of size aggregated analysis for the CCGS Teleost and CCGS John Cabot/Capt. Jacques Cartier for catch of Atlantic Cod (*Gadus morhua*), fall 2HJ3K + 3L deep water.

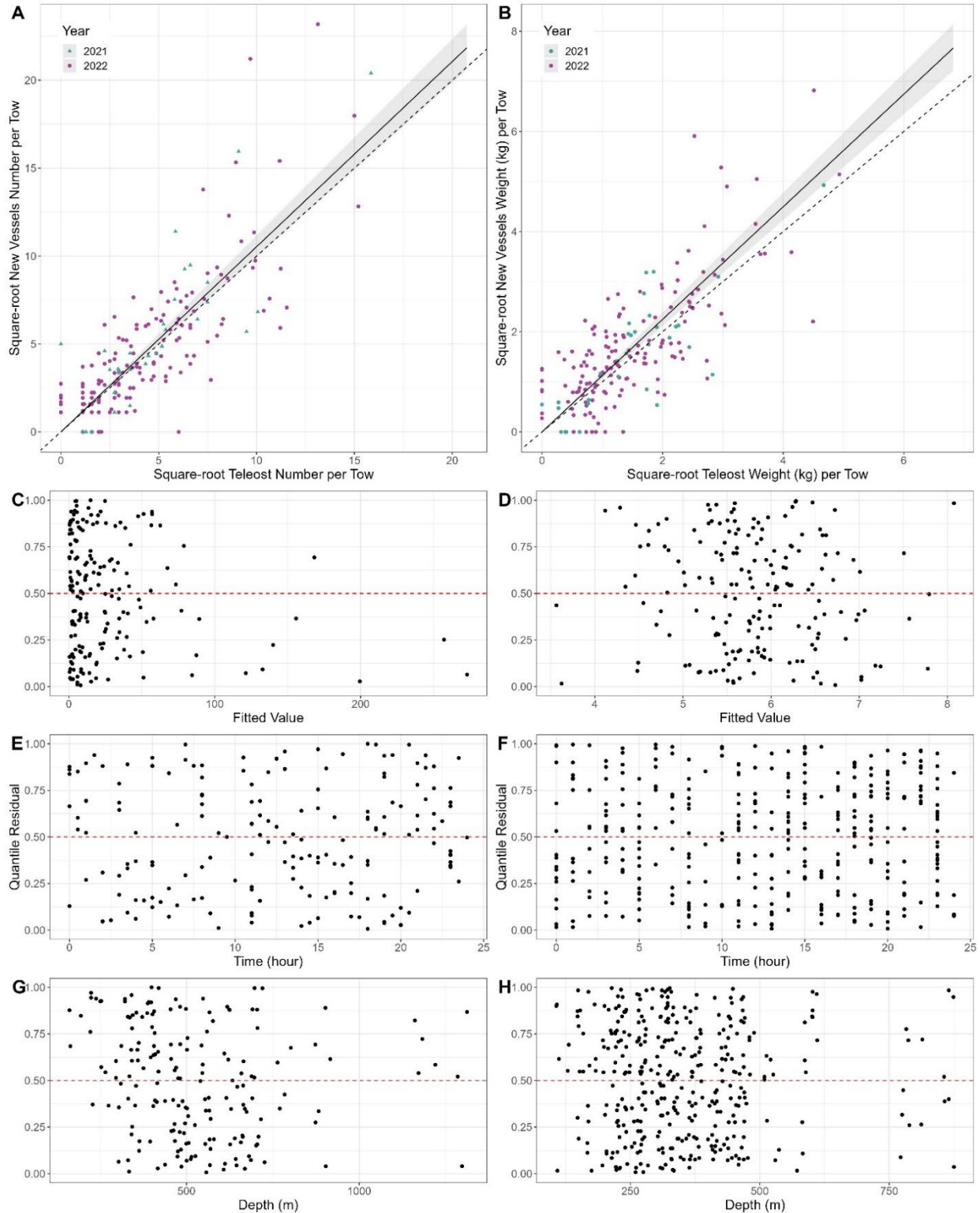


Figure A2-7. Results of size aggregated analysis for the CCGS Teleost and CCGS John Cabot/Capt. Jacques Cartier for catch of Eelpout (Zoarcidae), fall 2HJ3K + 3L deep water.

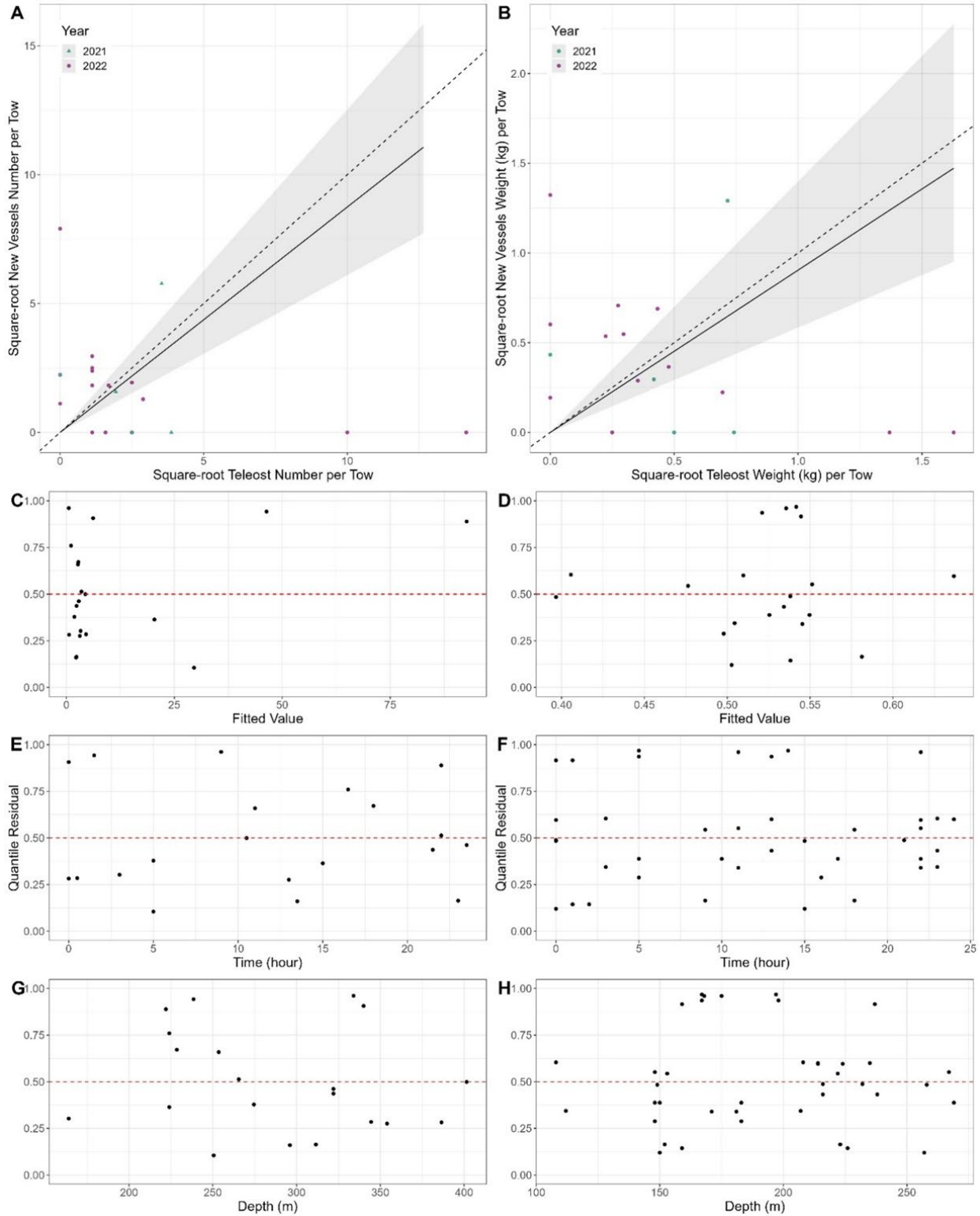


Figure A2-8. Results of size aggregated analysis for the CCGS Teleost and CCGS John Cabot/Capt. Jacques Cartier for catch of Fourline snakeblenny (*Eumesogrammus praecisus*), fall 2HJ3K + 3L deep water.

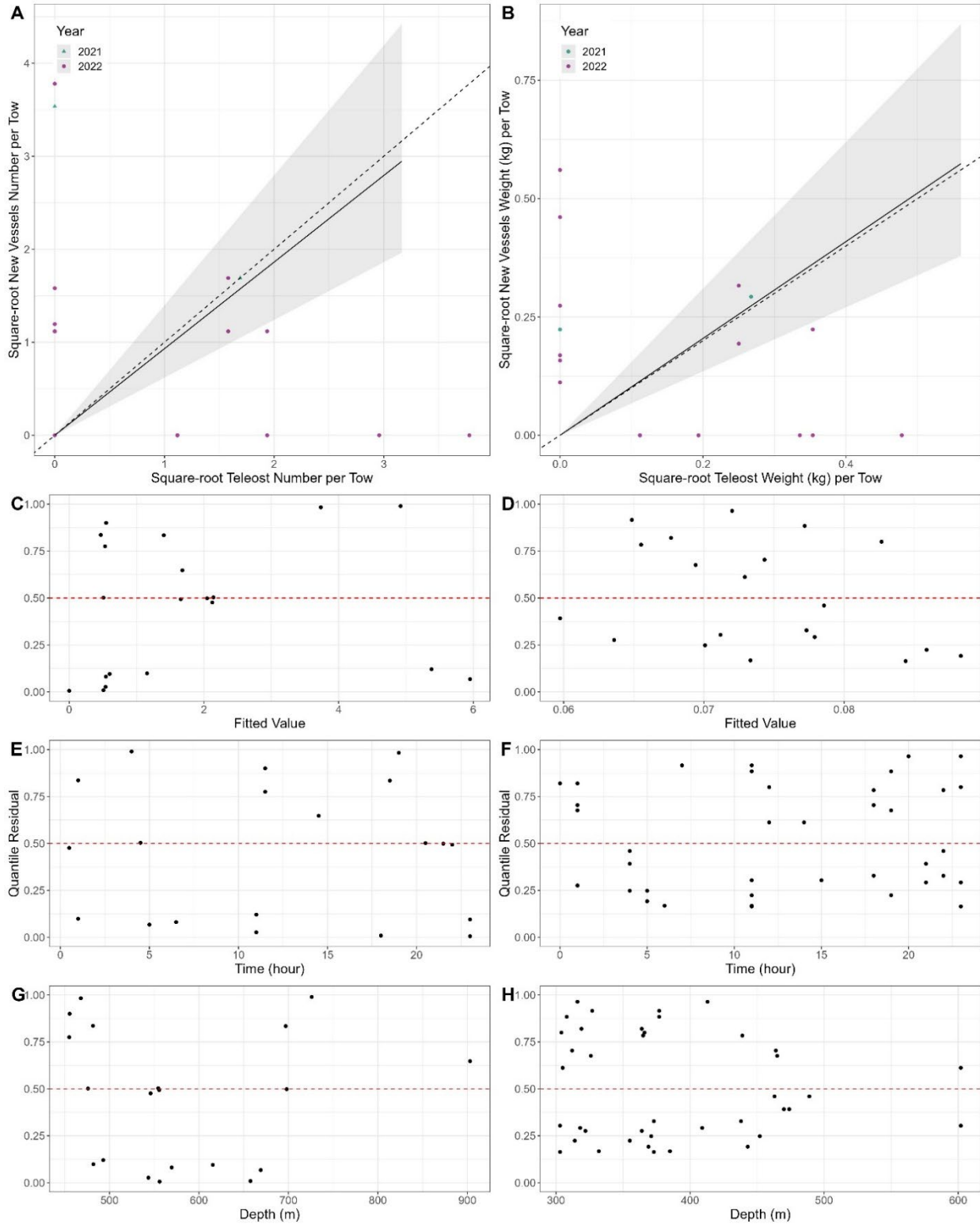


Figure A2-9. Results of size aggregated analysis for the CCGS Teleost and CCGS John Cabot/Capt. Jacques Cartier for catch of Longfin Hake (*Phycis chesteri*), fall 2HJ3K + 3L deep water. Data insufficient to determine if conversion is appropriate.

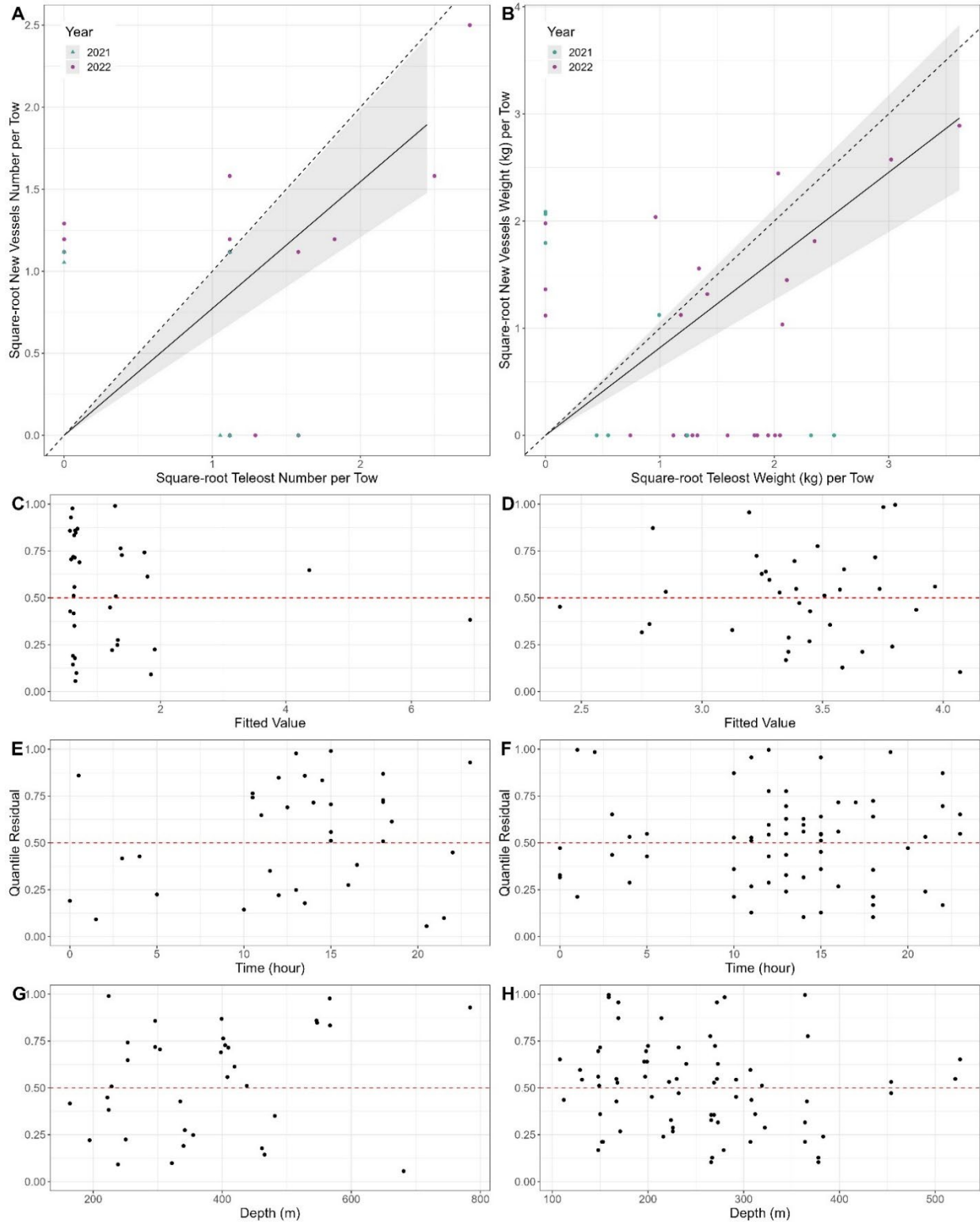


Figure A2-10. Results of size aggregated analysis for the CCGS Teleost and CCGS John Cabot/Capt. Jacques Cartier for catch of Common lumpfish (*Cyclopterus lumpus*), fall 2HJ3K + 3L deep water. Data insufficient to determine if conversion is appropriate.

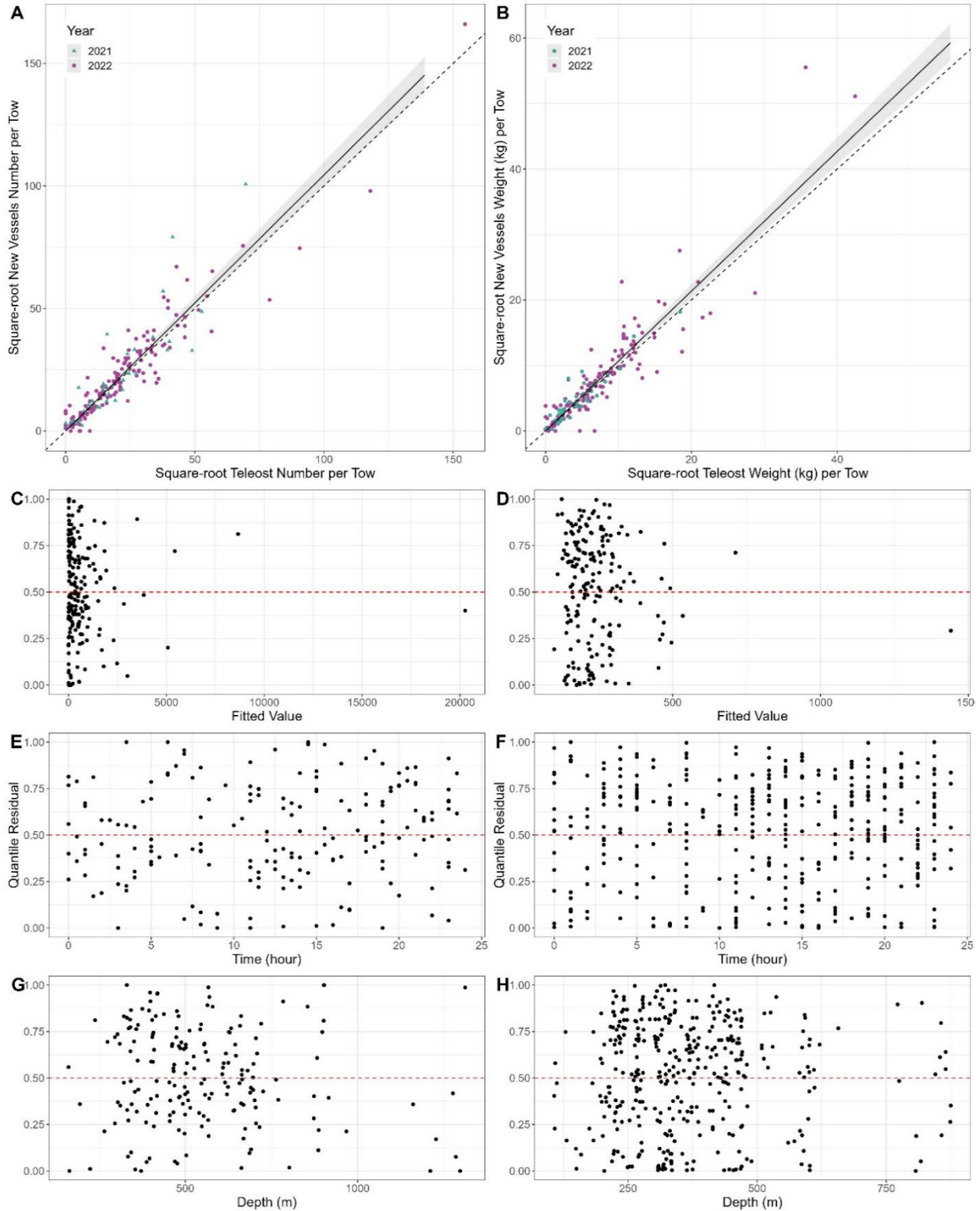


Figure A2-11. Results of size aggregated analysis for the CCGS Teleost and CCGS John Cabot/Capt. Jacques Cartier for catch of Redfishes (*Sebastes mentella*, *S. faciatus*), fall 2HJ3K + 3L deep water.

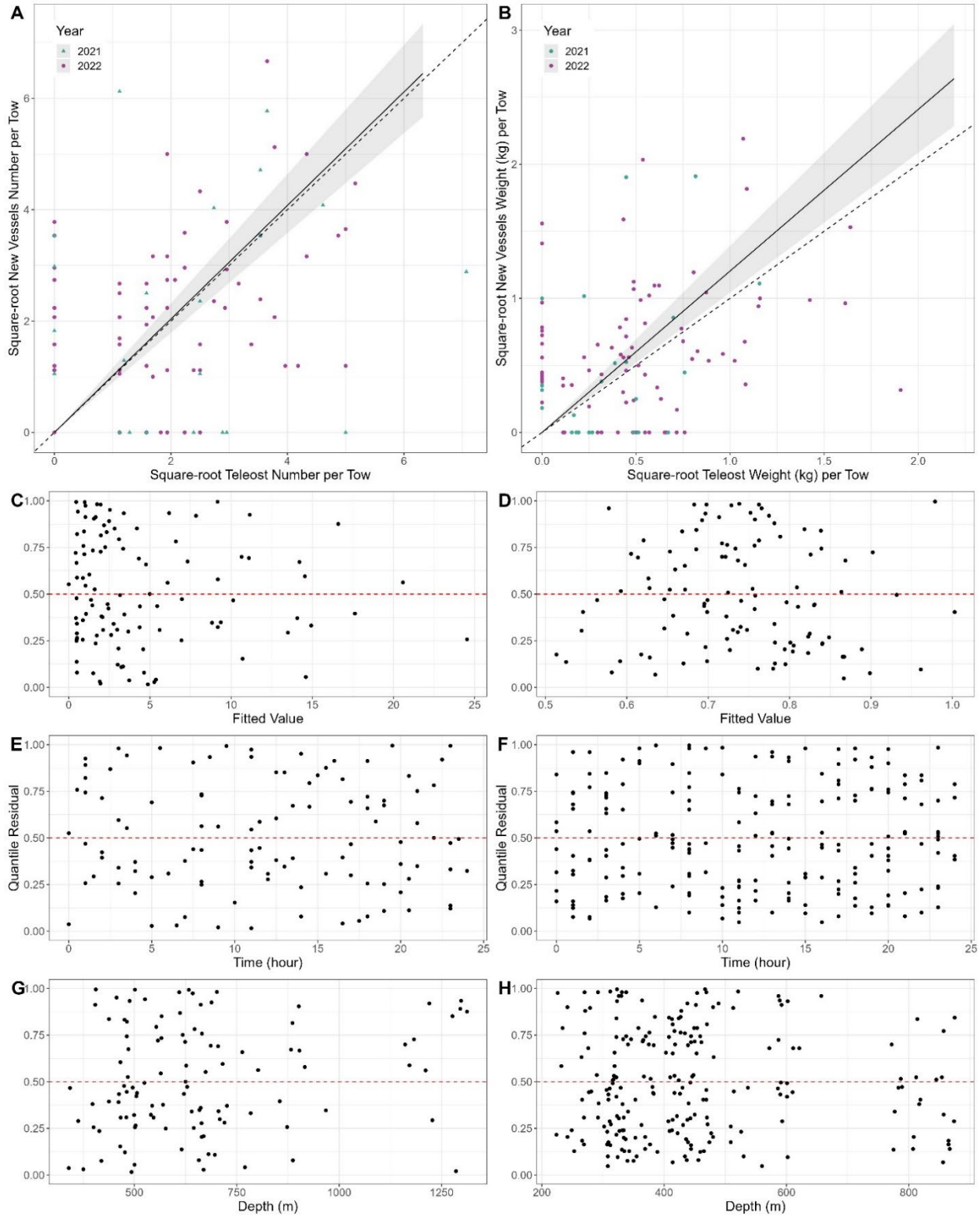


Figure A2-12. Results of size aggregated analysis for the CCGS Teleost and CCGS John Cabot/Capt. Jacques Cartier for catch of Rocklings (*Gaidropsarus* spp, *Enchelyopus* spp.), fall 2HJ3K + 3L deep water.

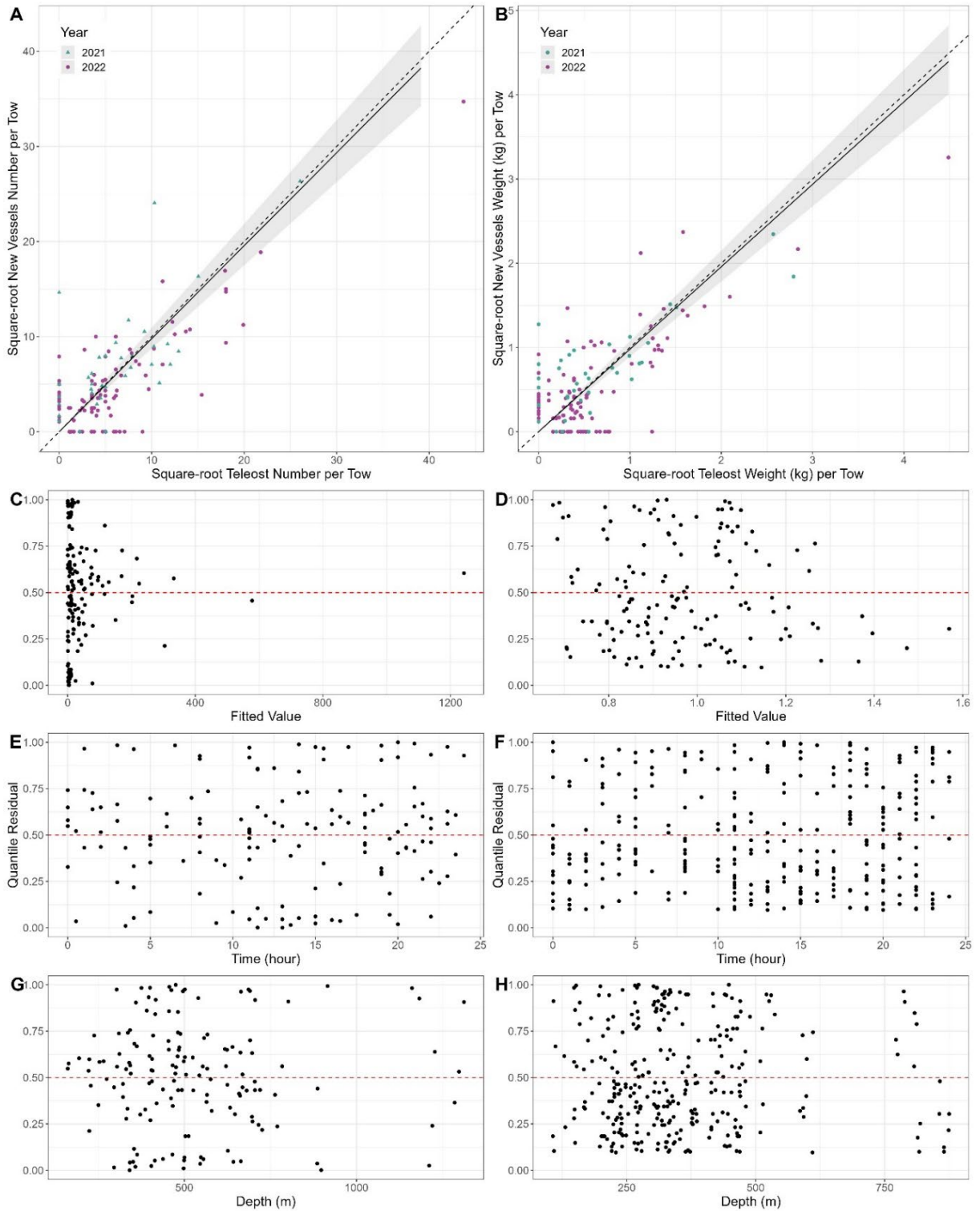


Figure A2–13. Results of size aggregated analysis for the CCGS Teleost and CCGS John Cabot/Capt. Jacques Cartier for catch of Sculpins (*Cottoidea*), fall 2HJ3K + 3L deep water.

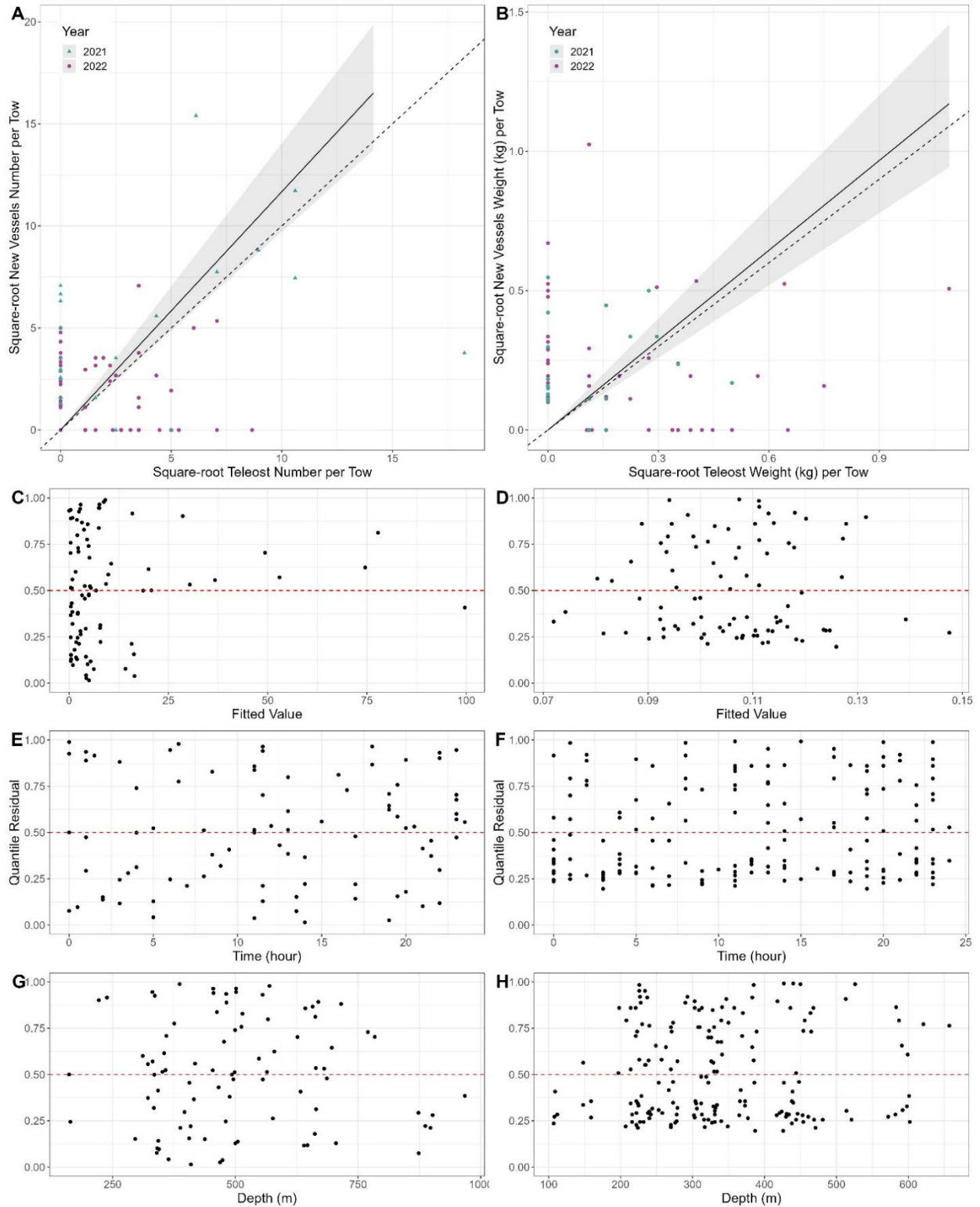


Figure A2-14. Results of size aggregated analysis for the CCGS Teleost and CCGS John Cabot/Capt. Jacques Cartier for catch of Snailfishes (*Liparidae*), fall 2HJ3K + 3L deep water.

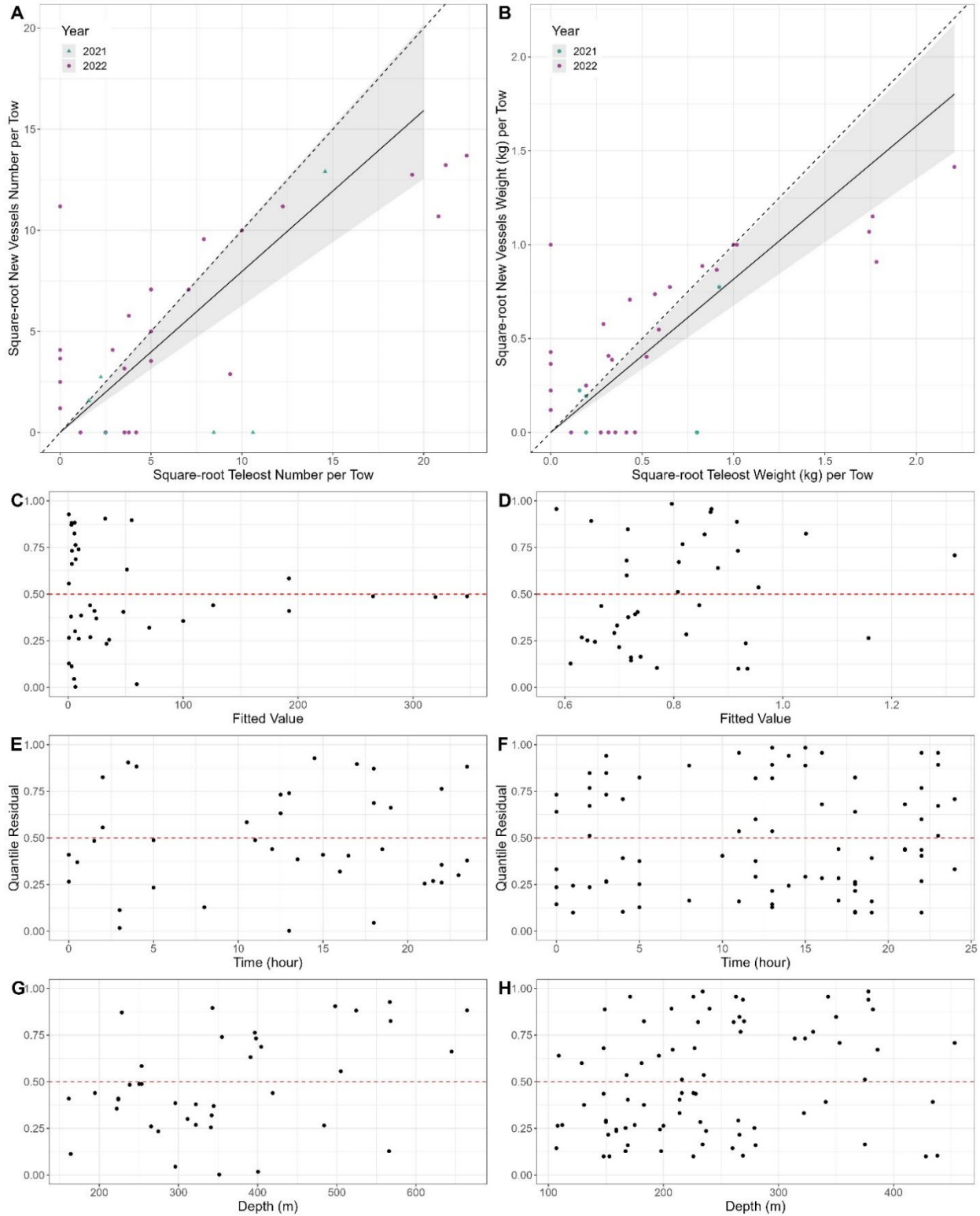


Figure A2-15. Results of size aggregated analysis for the CCGS Teleost and CCGS John Cabot/Capt. Jacques Cartier for catch of Shannies (*Leptoclinus maculatus*), fall 2HJ3K + 3L deep water.

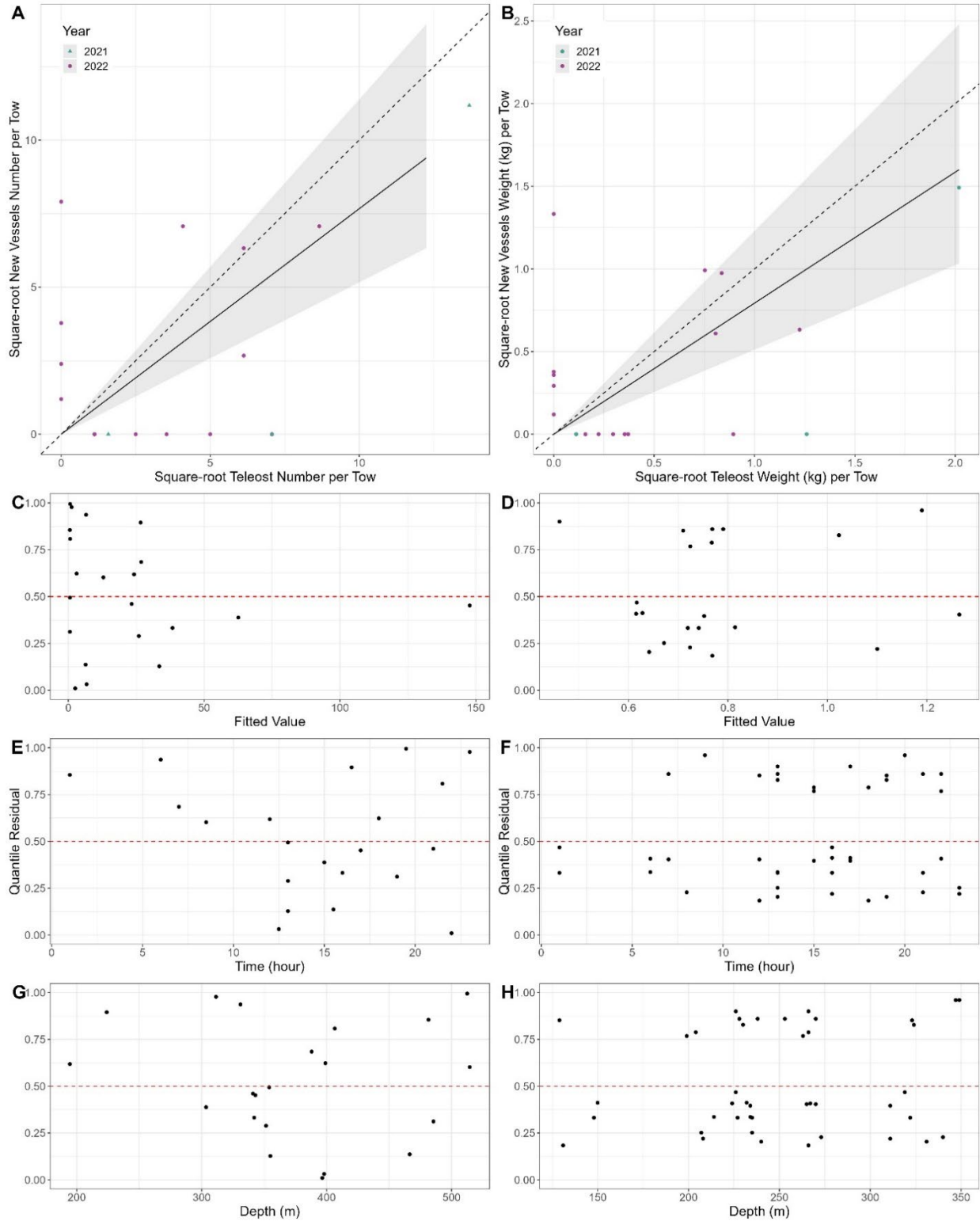


Figure A2-16. Results of size aggregated analysis for the CCGS Teleost and CCGS John Cabot/Capt. Jacques Cartier for catch of Snake blennies (*Lumpenus lumpretaeformis*), fall 2HJ3K + 3L deep water. Data insufficient to determine if conversion is appropriate.

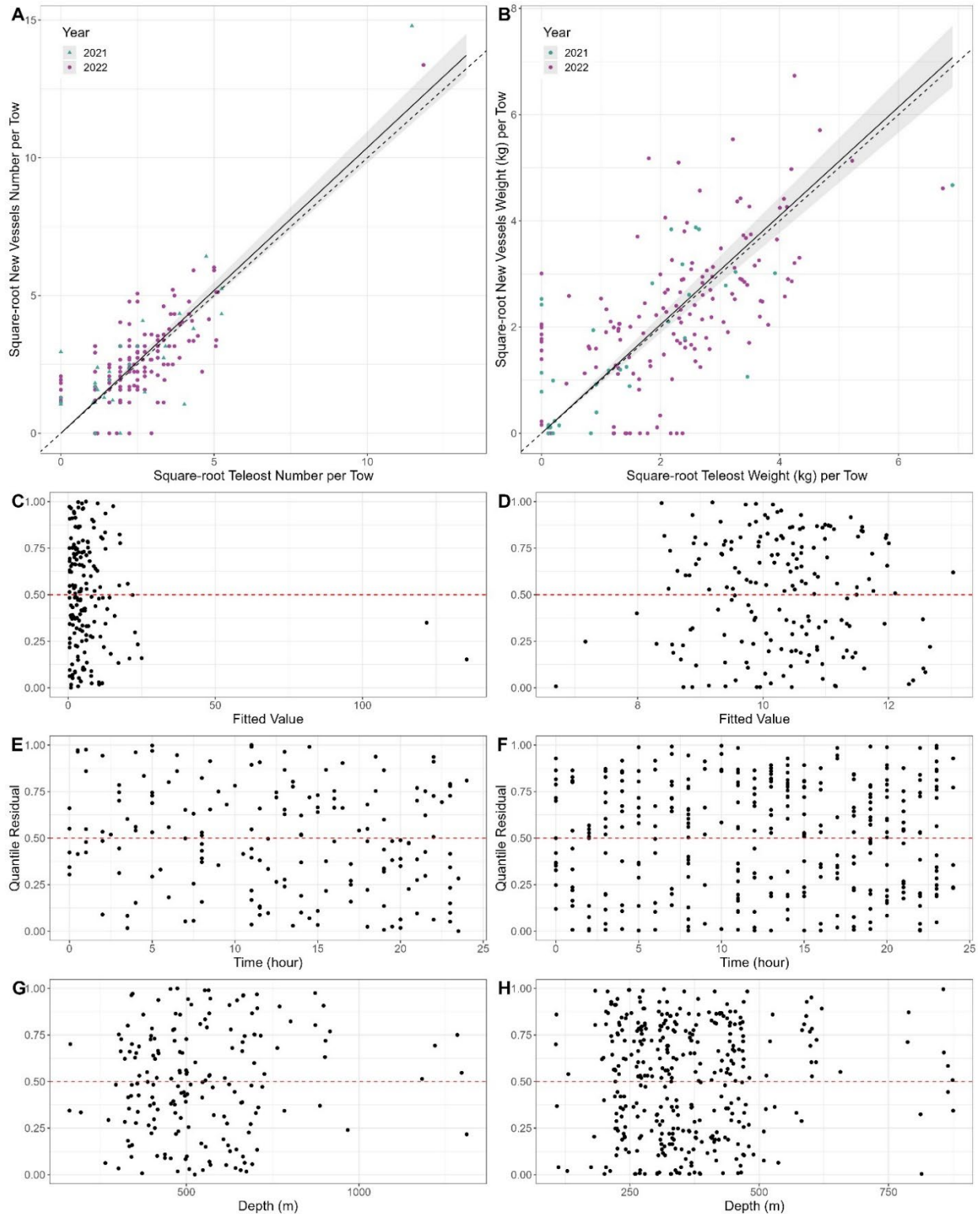


Figure A2-17. Results of size aggregated analysis for the CCGS Teleost and CCGS John Cabot/Capt. Jacques Cartier for catch of Thorny Skate (*Amblyraja radiata*), fall 2HJ3K + 3L deep water.

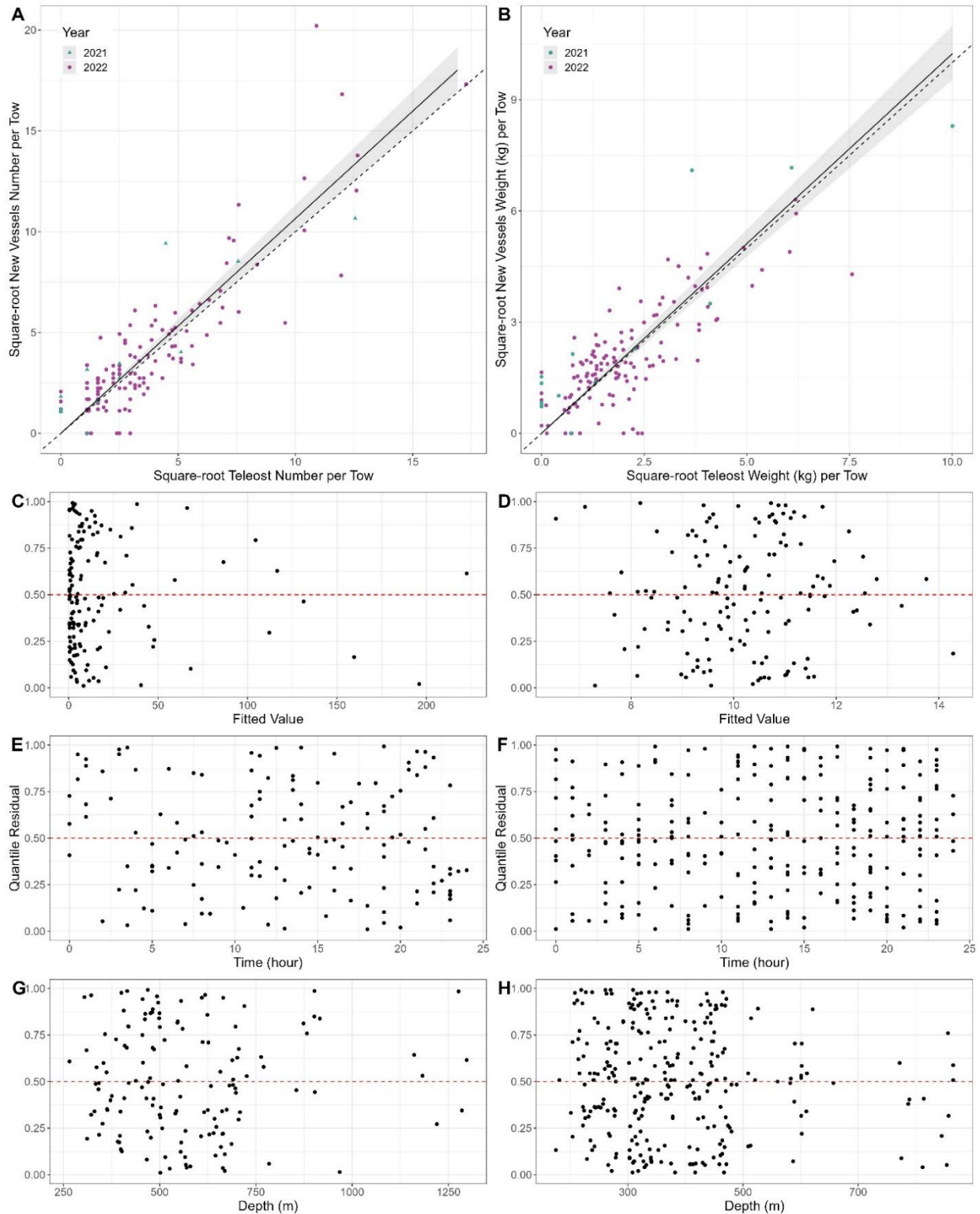


Figure A2-18. Results of size aggregated analysis for the CCGS Teleost and CCGS John Cabot/Capt. Jacques Cartier for catch of Witch Flounder (*Glyptocephalus cynoglossus*), fall 2HJ3K + 3L deep water.

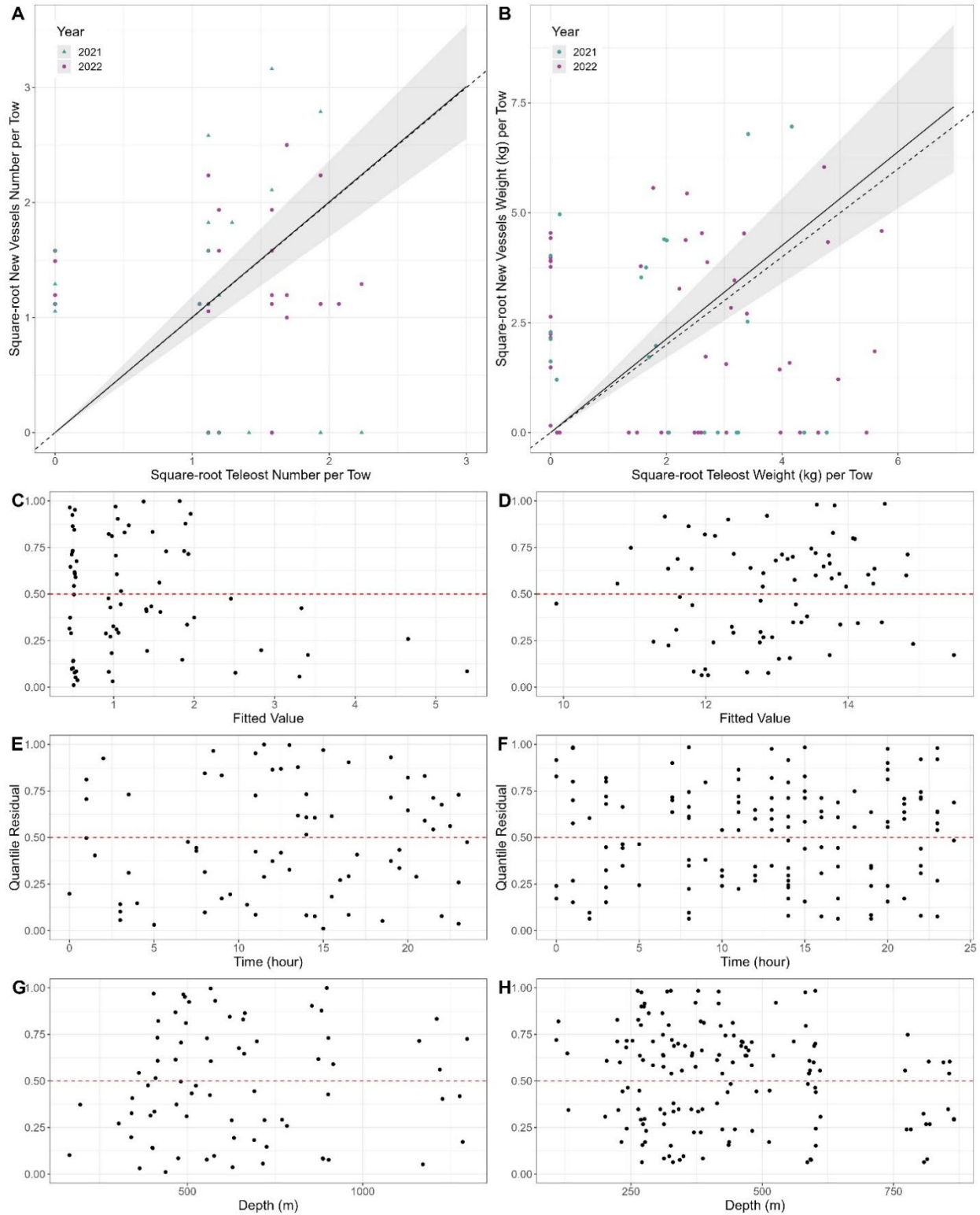


Figure A2-19. Results of size aggregated analysis for the CCGS Teleost and CCGS John Cabot/Capt. Jacques Cartier for catch of Broadhead (Northern) Wolffish (*Anarhichas denticulatus*), fall 2HJ3K + 3L deep water.

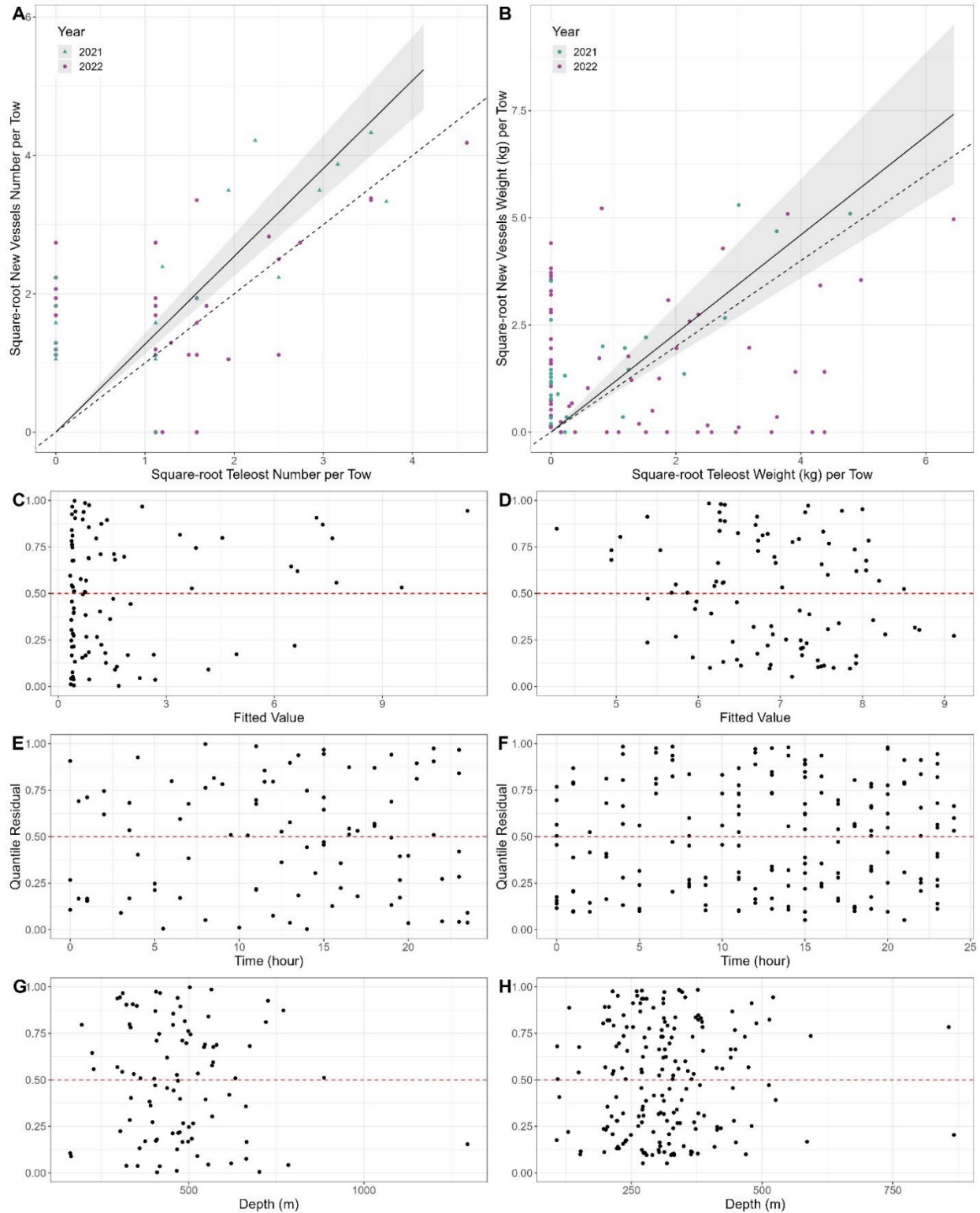


Figure A2–20. Results of size aggregated analysis for the CCGS Teleost and CCGS John Cabot/Capt. Jacques Cartier for catch of Spotted Wolffish (*Anarhichas minor*), fall 2HJ3K + 3L deep water.

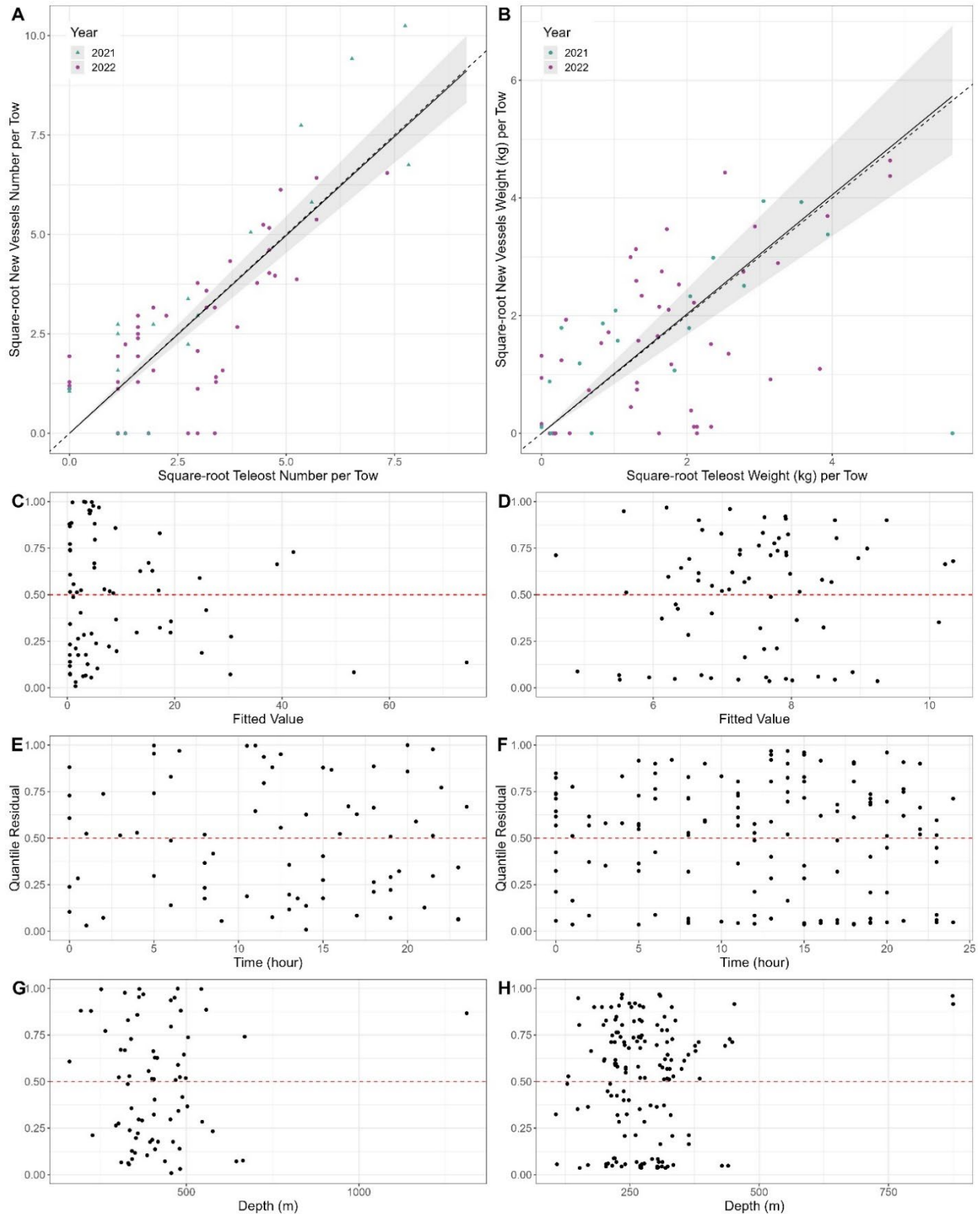


Figure A2-21. Results of size aggregated analysis for the CCGS Teleost and CCGS John Cabot/Capt. Jacques Cartier for catch of Striped Wolffish (*Anarhichas lupus*), fall 2HJ3K + 3L deep water.

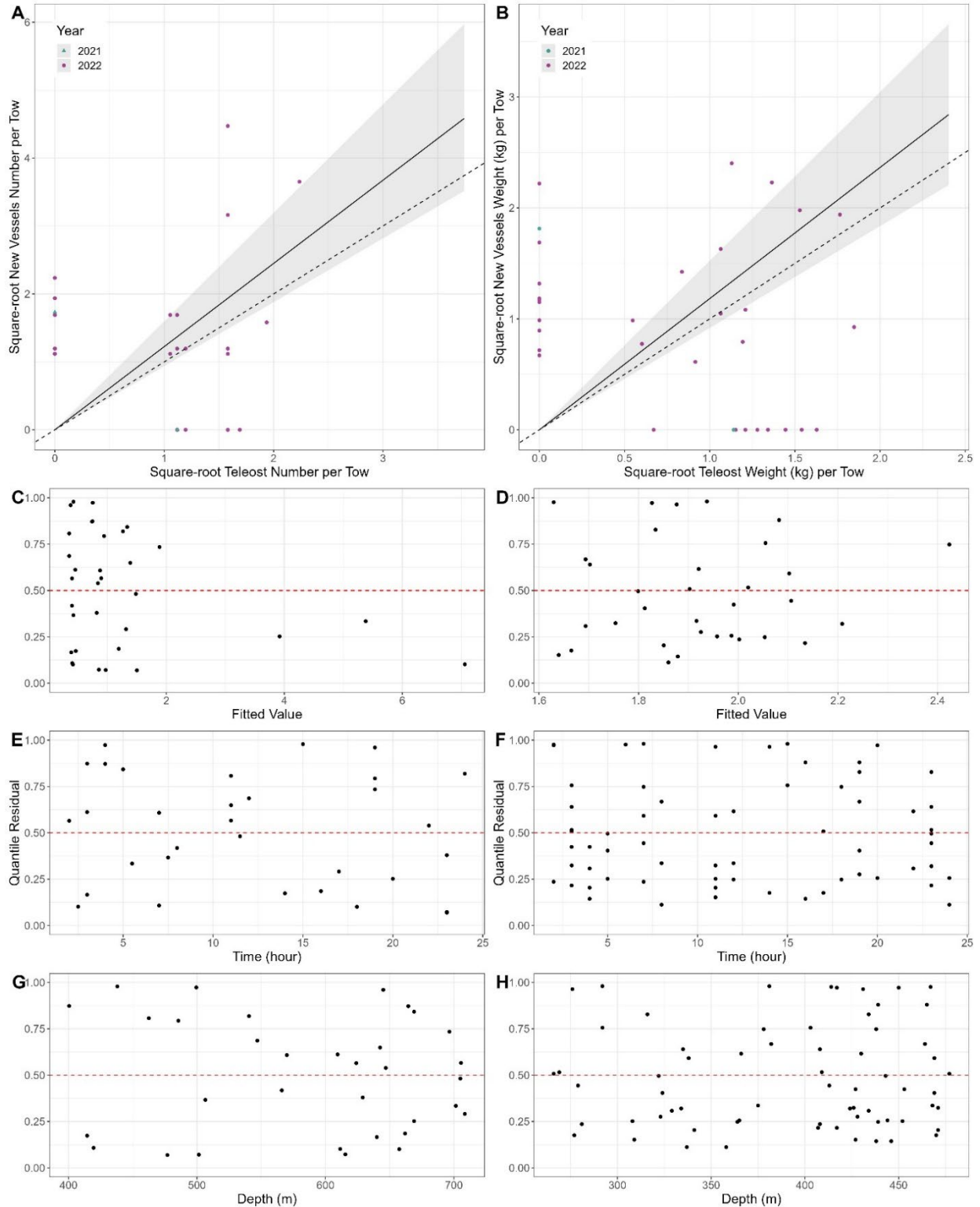


Figure A2-22. Results of size aggregated analysis for the CCGS Teleost and CCGS John Cabot/Capt. Jacques Cartier for catch of Wrymouth (*Cryptacanthodes maculatus*), fall 2HJ3K + 3L deep water. Data insufficient to determine if conversion is appropriate.

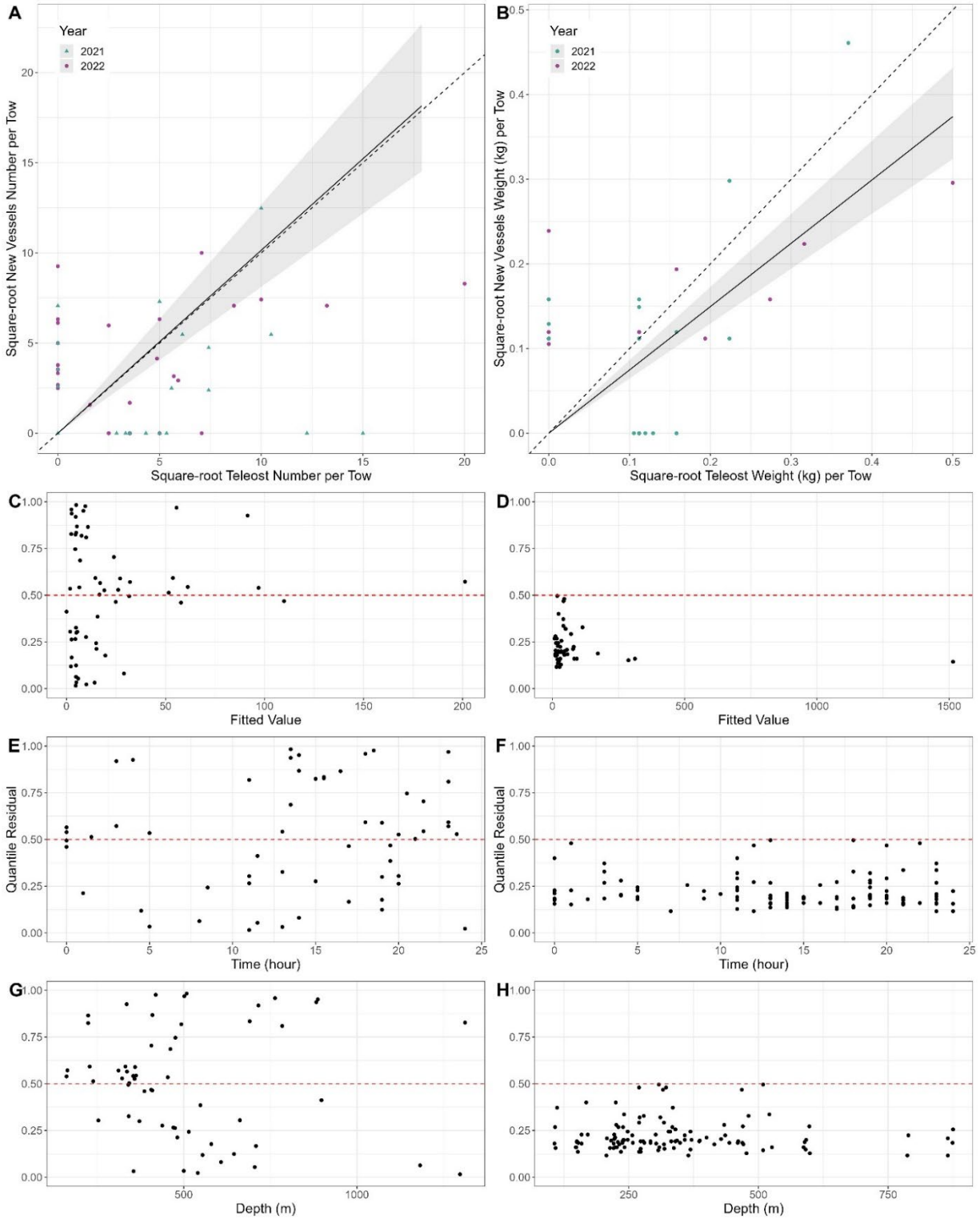


Figure A2-23. Results of size aggregated analysis for the CCGS Teleost and CCGS John Cabot/Capt. Jacques Cartier for catch of Amphipods (*Amphipoda*), fall 2HJ3K + 3L deep water. Residuals are suggesting a poor model fit, and data deemed inappropriate for determining conversion.

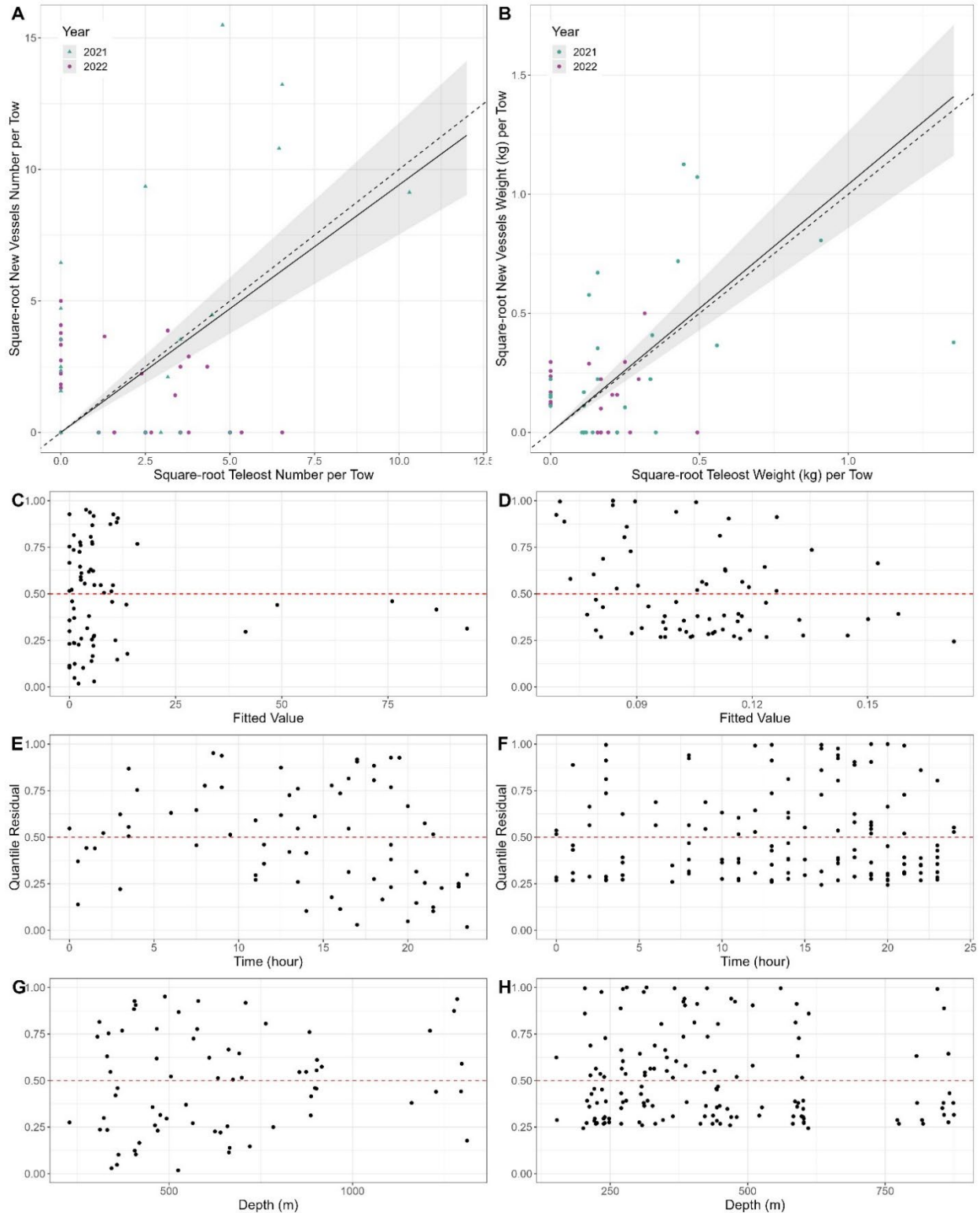


Figure A2-24. Results of size aggregated analysis for the CCGS Teleost and CCGS John Cabot/Capt. Jacques Cartier for catch of *Polychaetes* (*Polychaeta*), fall 2HJ3K + 3L deep water.

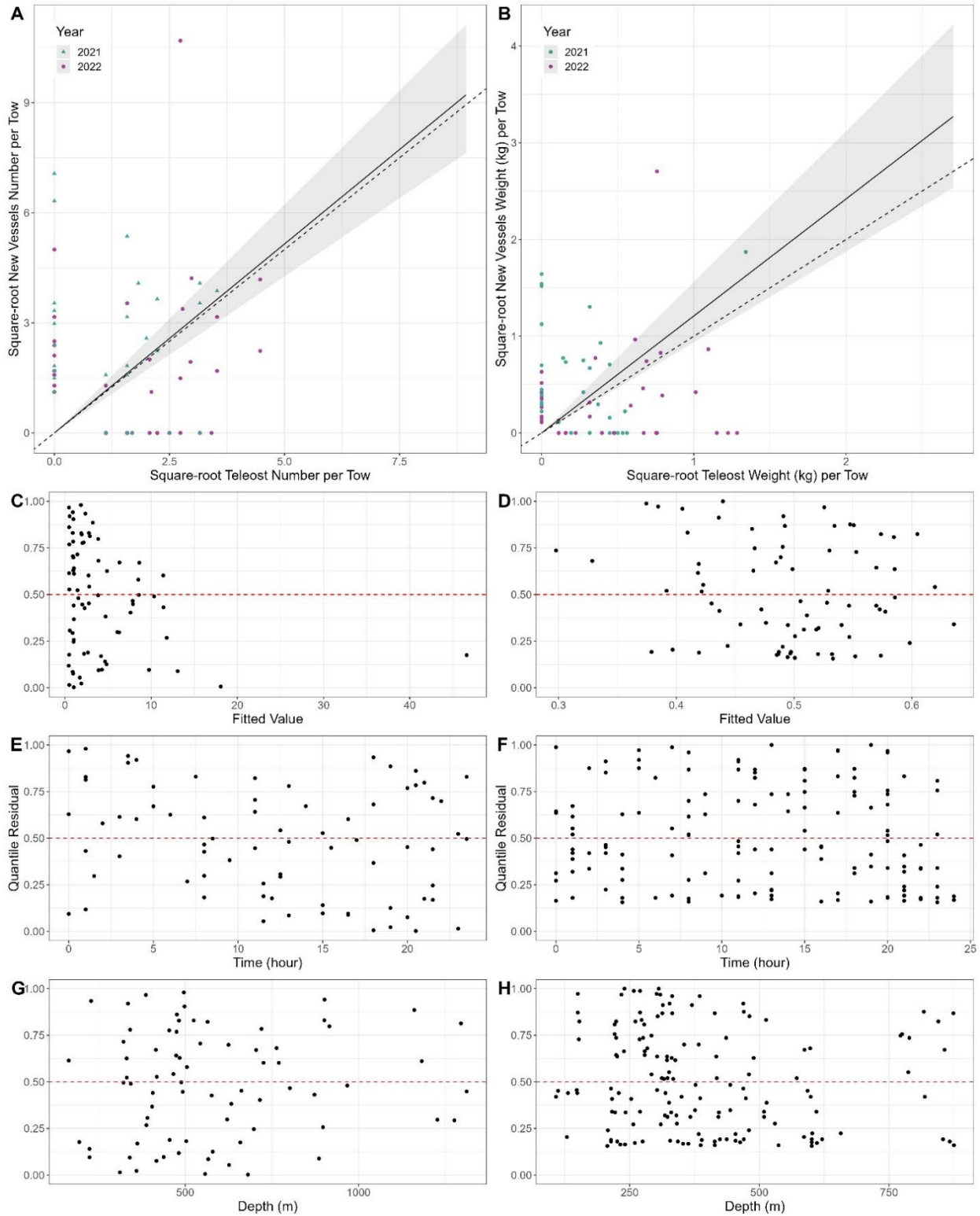


Figure A2–25. Results of size aggregated analysis for the CCGS Teleost and CCGS John Cabot/Capt. Jacques Cartier for catch of Cephalopods (*Cephalopoda*, excluding *Gonatus* sp. & *Illex* spp.), fall 2HJ3K + 3L deep water.

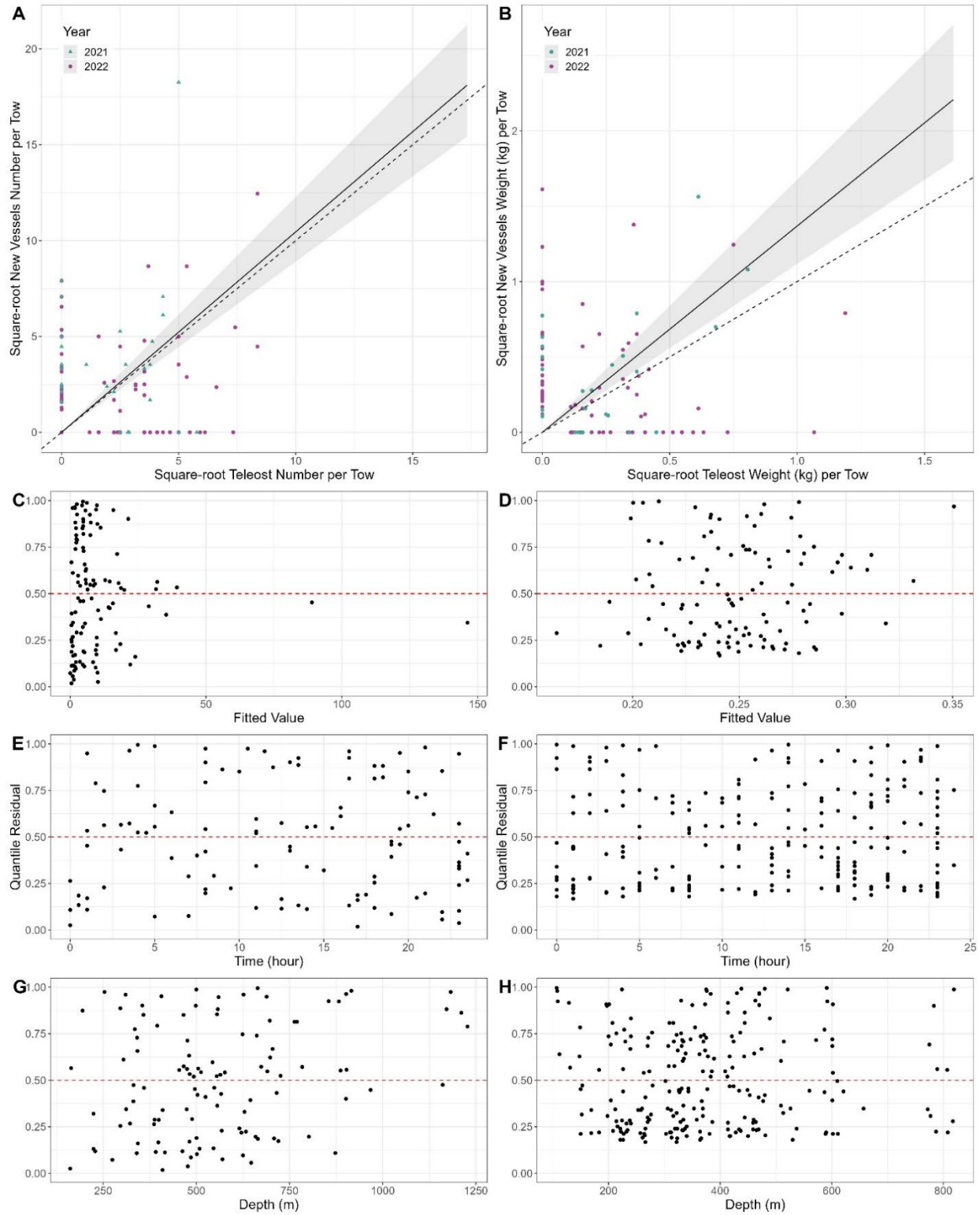


Figure A2-26. Results of size aggregated analysis for the CCGS Teleost and CCGS John Cabot/Capt. Jacques Cartier for catch of Gastropods (*Gastropoda*), fall 2HJ3K + 3L deep water.

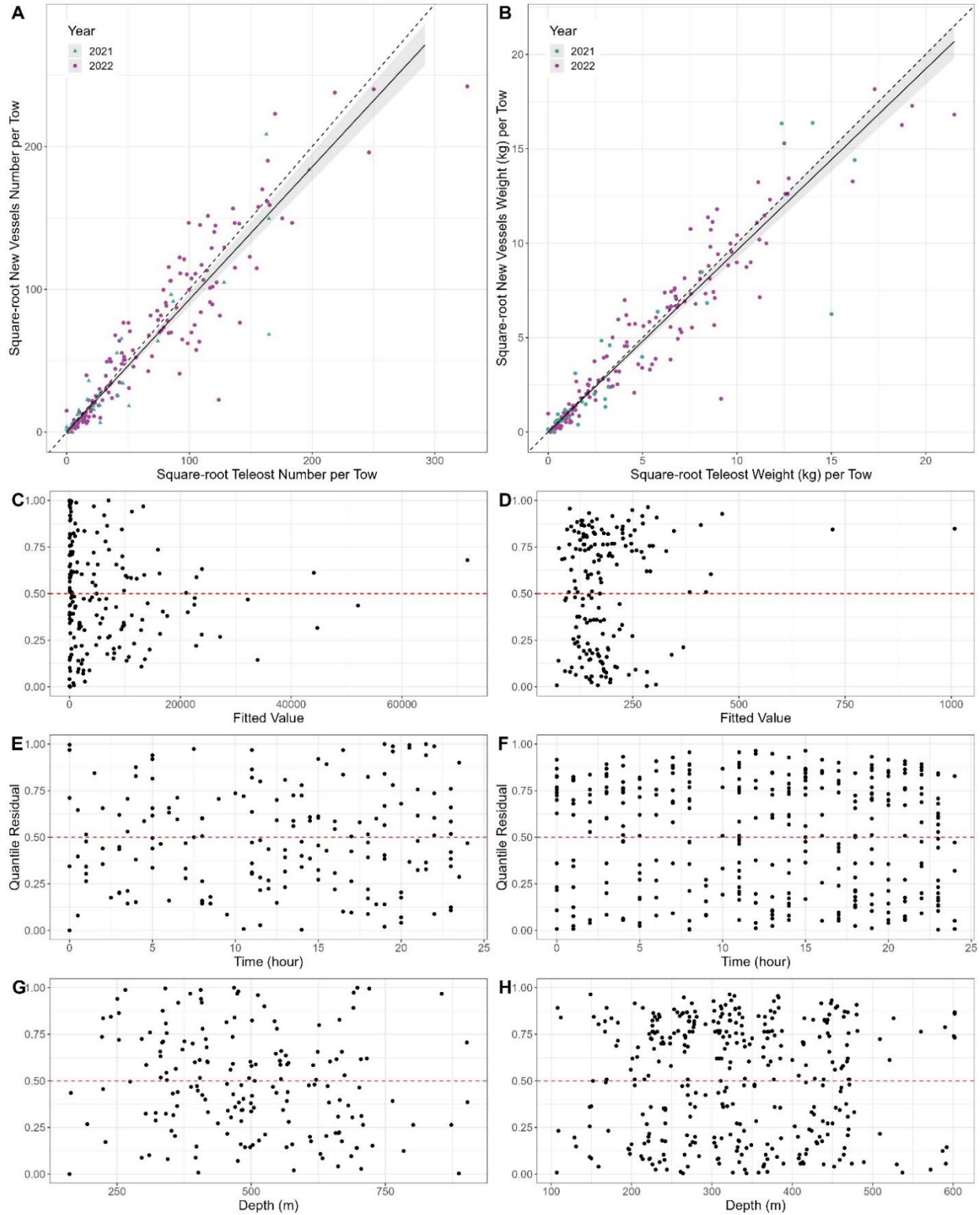


Figure A2-27. Results of size aggregated analysis for the CCGS Teleost and CCGS John Cabot/Capt. Jacques Cartier for catch of Northern Shrimp (*Pandalus borealis*), fall 2HJ3K + 3L deep water.

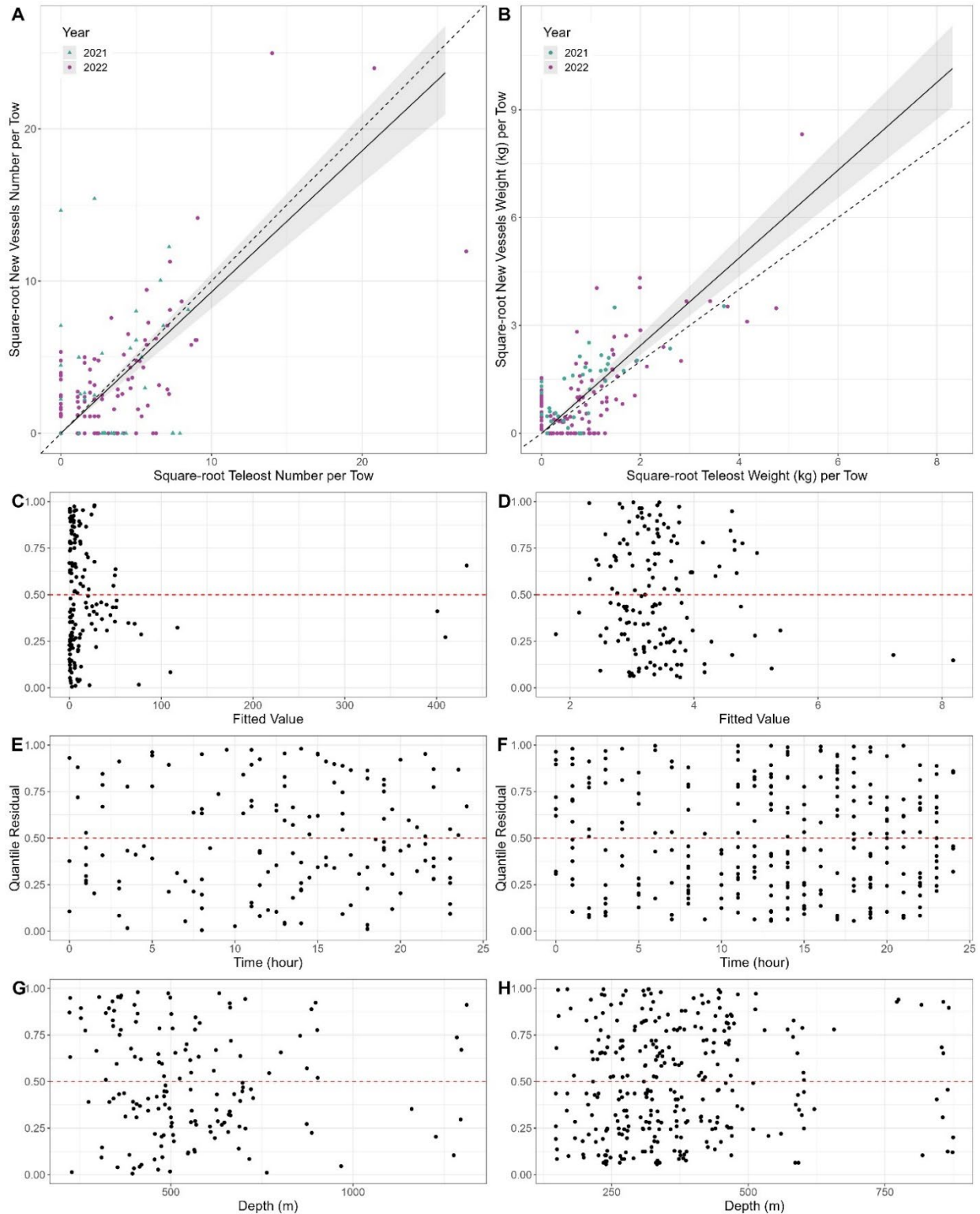


Figure A2-28. Results of size aggregated analysis for the CCGS Teleost and CCGS John Cabot/Capt. Jacques Cartier for catch of Sea anemones (*Actinaria*), fall 2HJ3K + 3L deep water.

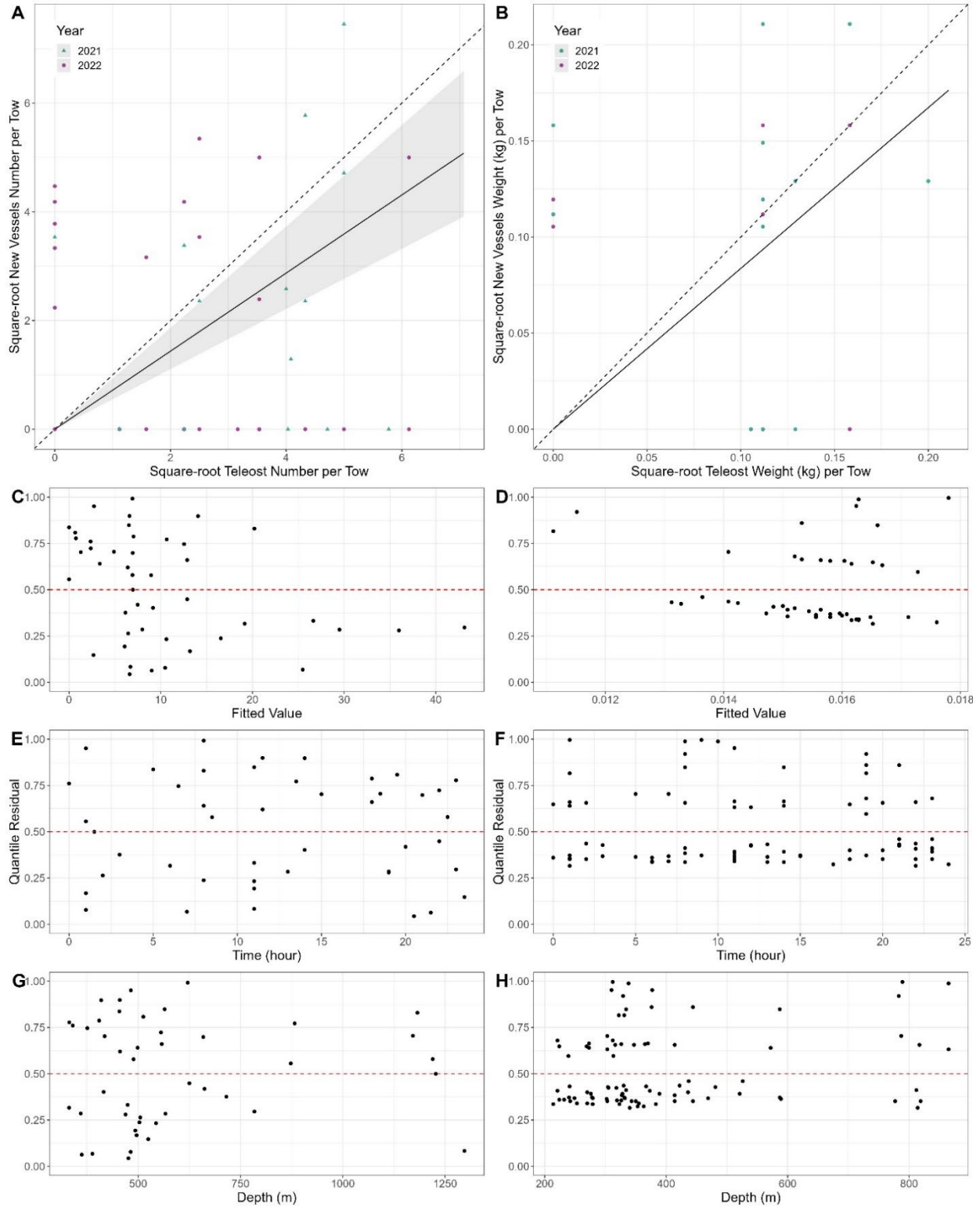


Figure A2-29. Results of size aggregated analysis for the CCGS Teleost and CCGS John Cabot/Capt. Jacques Cartier for catch of Sea spiders (*Pycnogonida*), fall 2HJ3K + 3L deep water. Biomass data is inappropriate for conversion analysis.

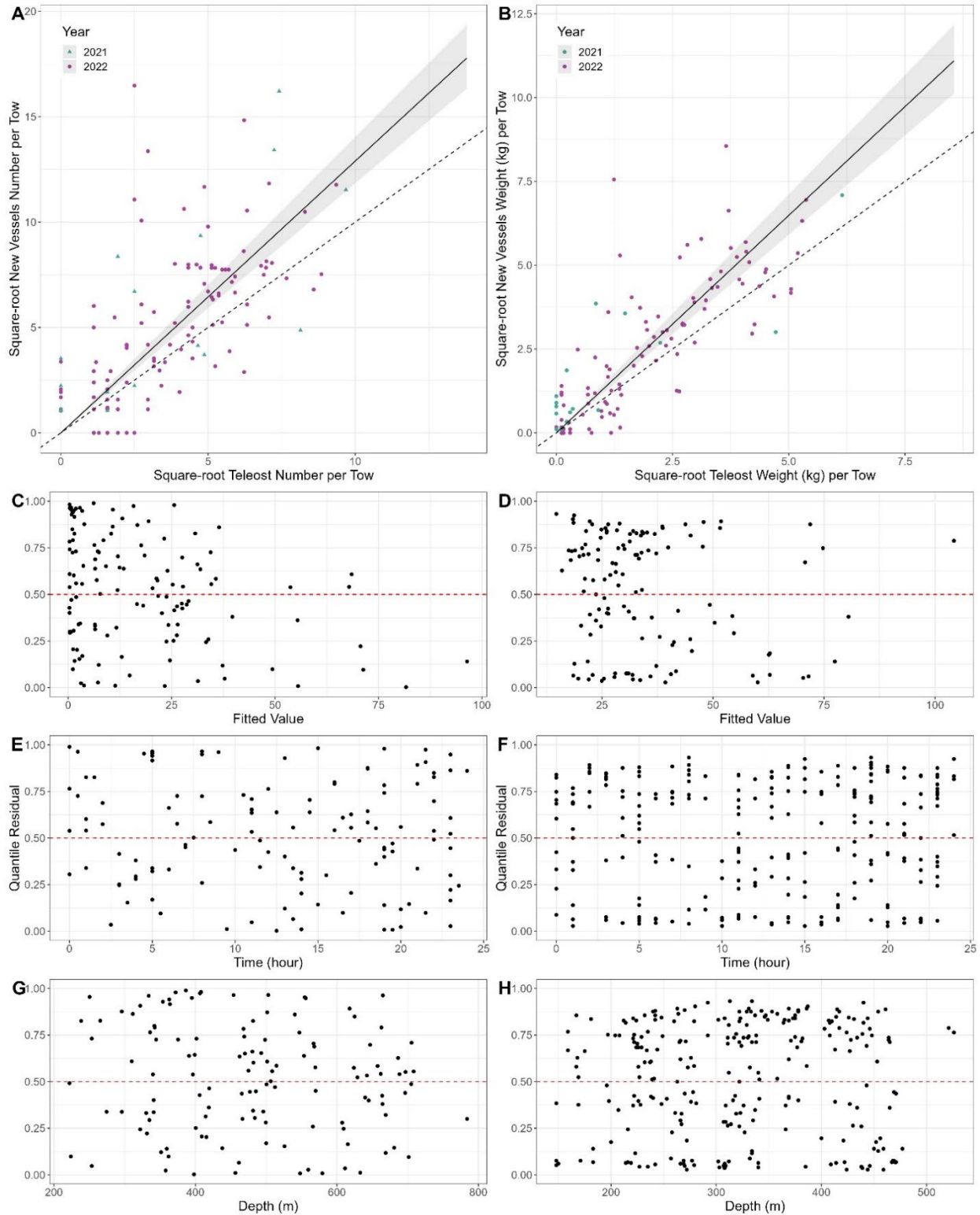


Figure A2-30. Results of size aggregated analysis for the CCGS Teleost and CCGS John Cabot/Capt. Jacques Cartier for catch of Snow Crab (*Chionoecetes opilio*), fall 2HJ3K + 3L deep water.

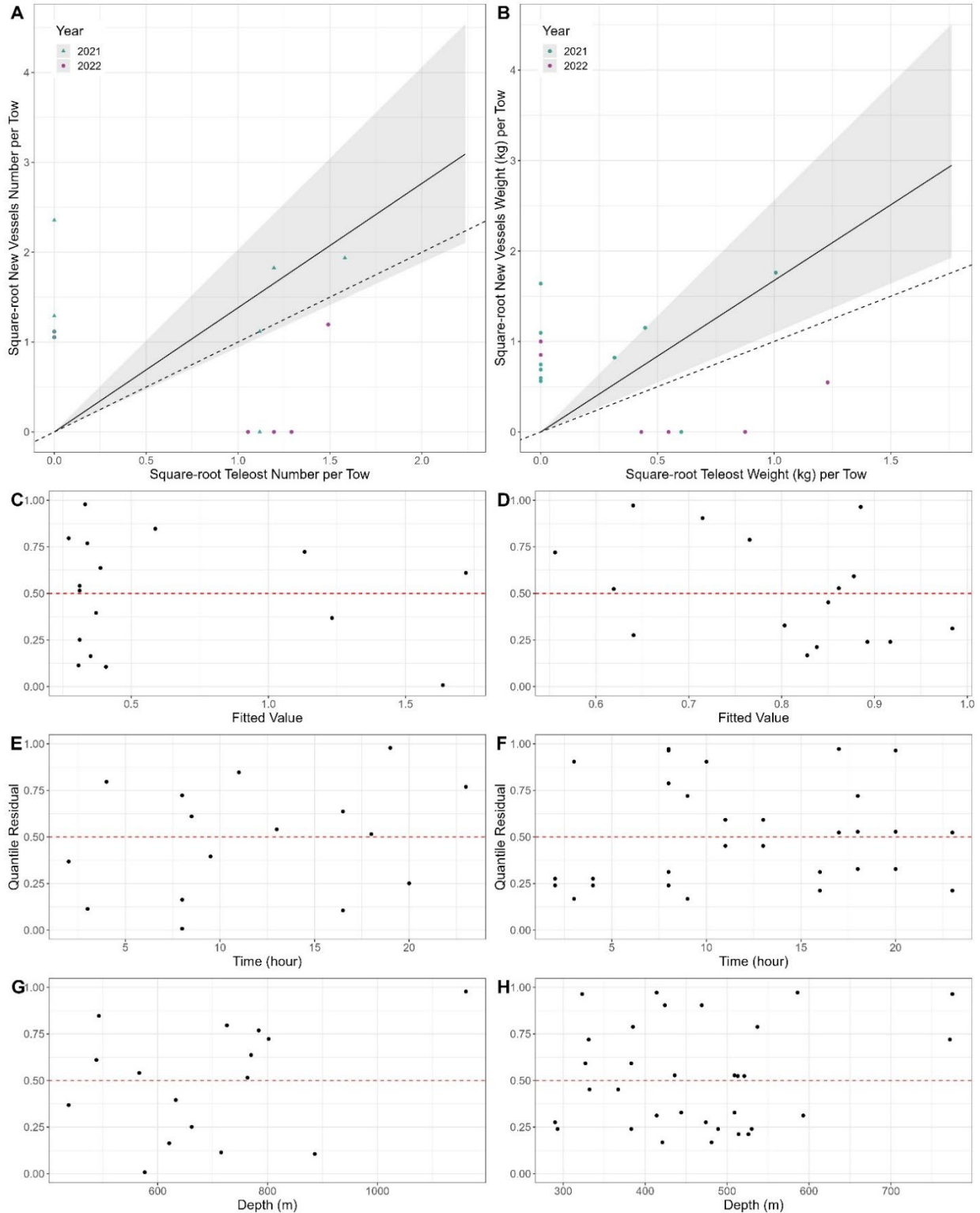


Figure A2-31. Results of size aggregated analysis for the CCGS Teleost and CCGS John Cabot/Capt. Jacques Cartier for catch of Spiny Crab (*Lithodes sp.*, *Neolithodes sp.*), fall 2HJ3K + 3L deep water. Data insufficient to determine if conversion is appropriate.

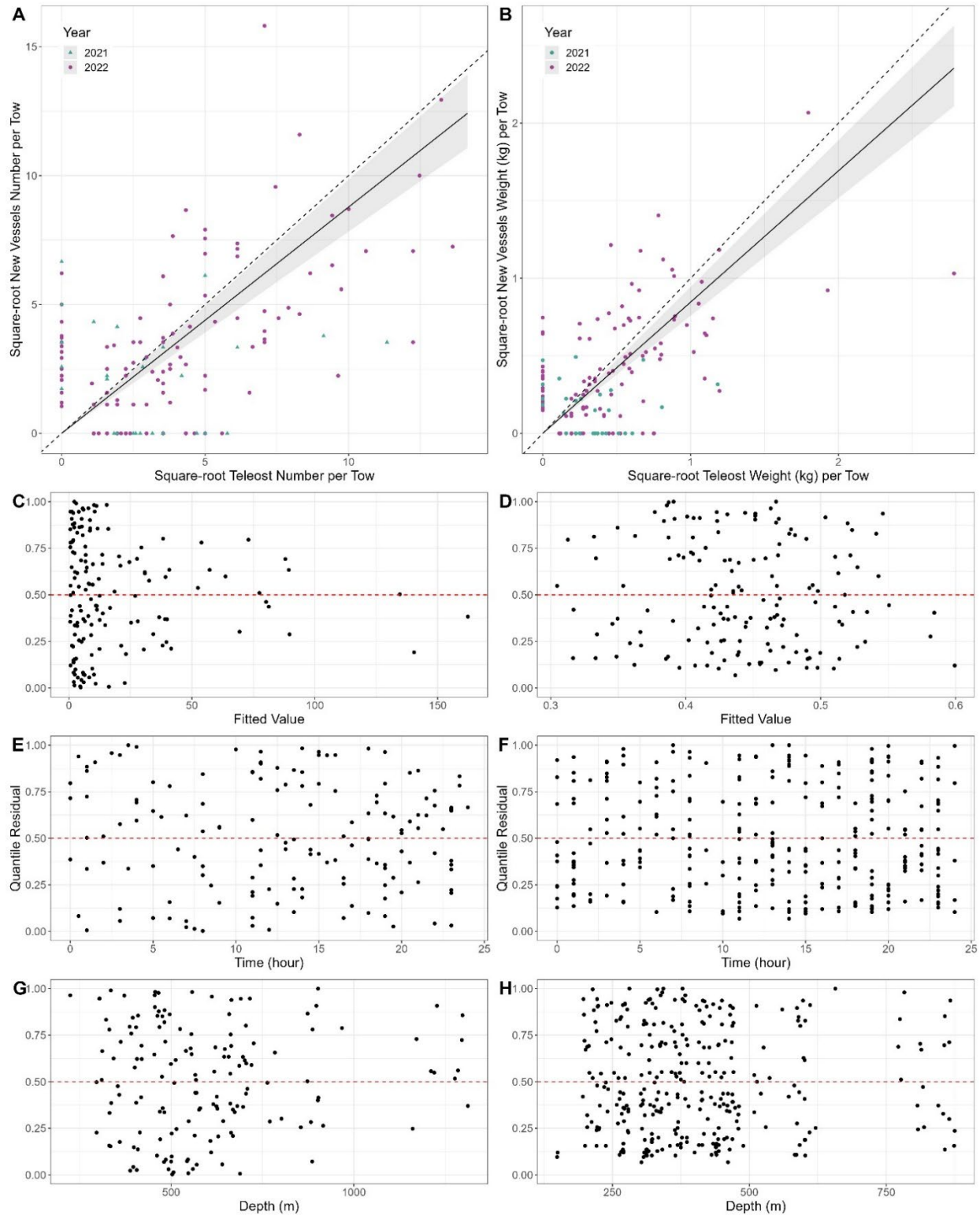


Figure A2-32. Results of size aggregated analysis for the CCGS Teleost and CCGS John Cabot/Capt. Jacques Cartier for catch of Squid (*Illex* spp. & *Gonatus* spp.), fall 2HJ3K + 3L deep water.

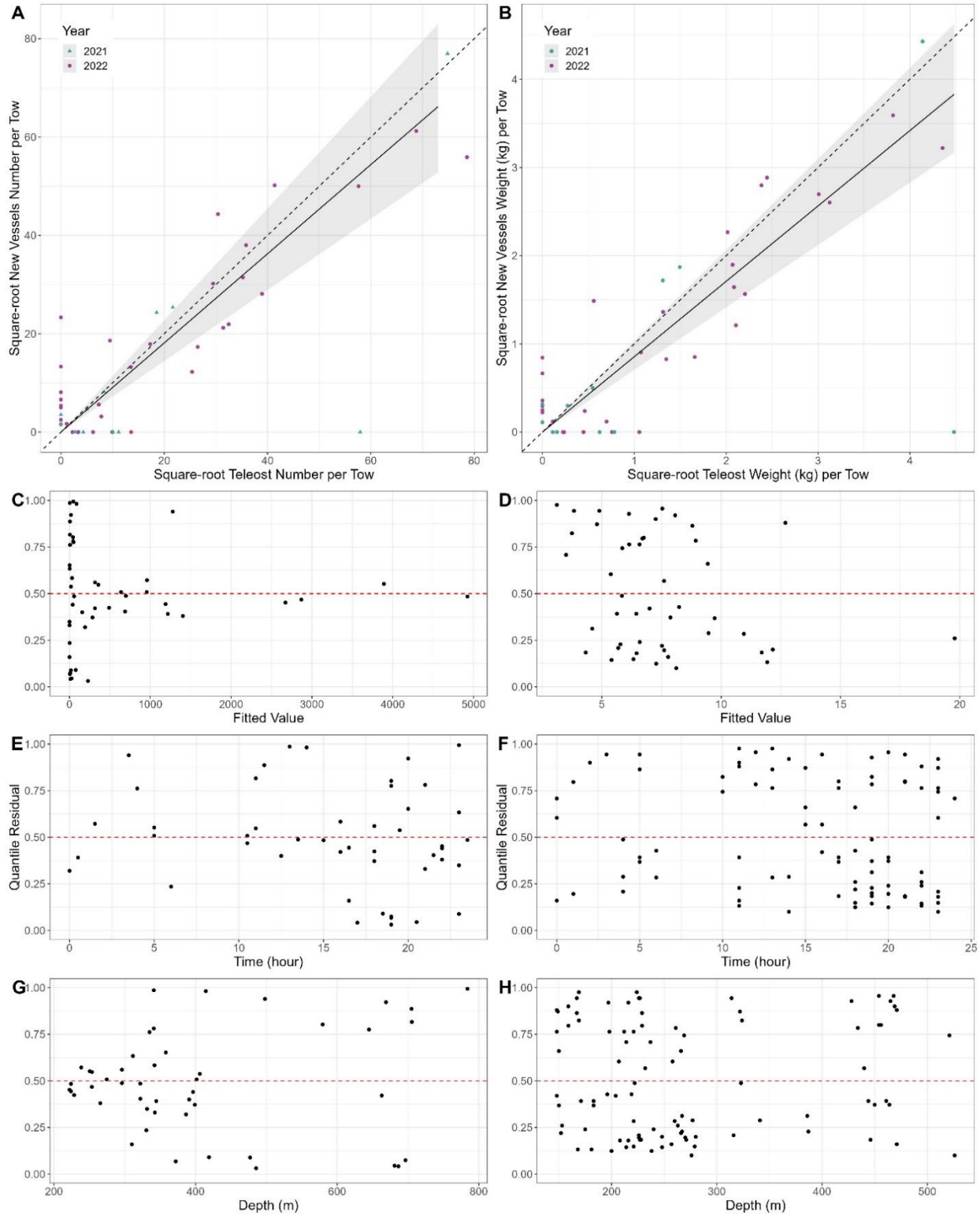


Figure A2-33. Results of size aggregated analysis for the CCGS Teleost and CCGS John Cabot/Capt. Jacques Cartier for catch of striped shrimp (*Pandalus monatgui*), fall 2HJ3K + 3L deep water.

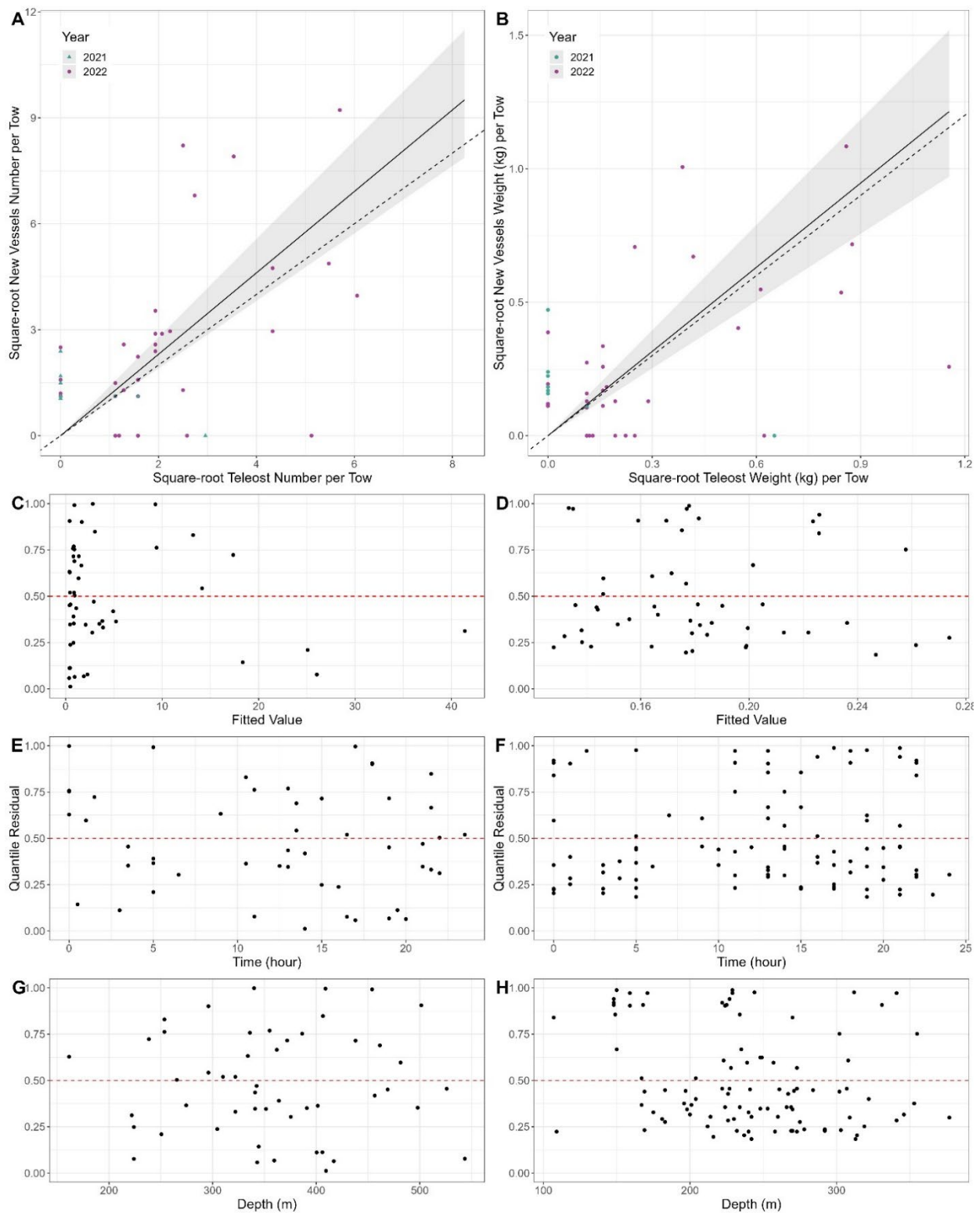


Figure A2–34. Results of size aggregated analysis for the CCGS Teleost and CCGS John Cabot/Capt. Jacques Cartier for catch of Toad crab (*Hyas spp.*), fall 2HJ3K + 3L deep water.

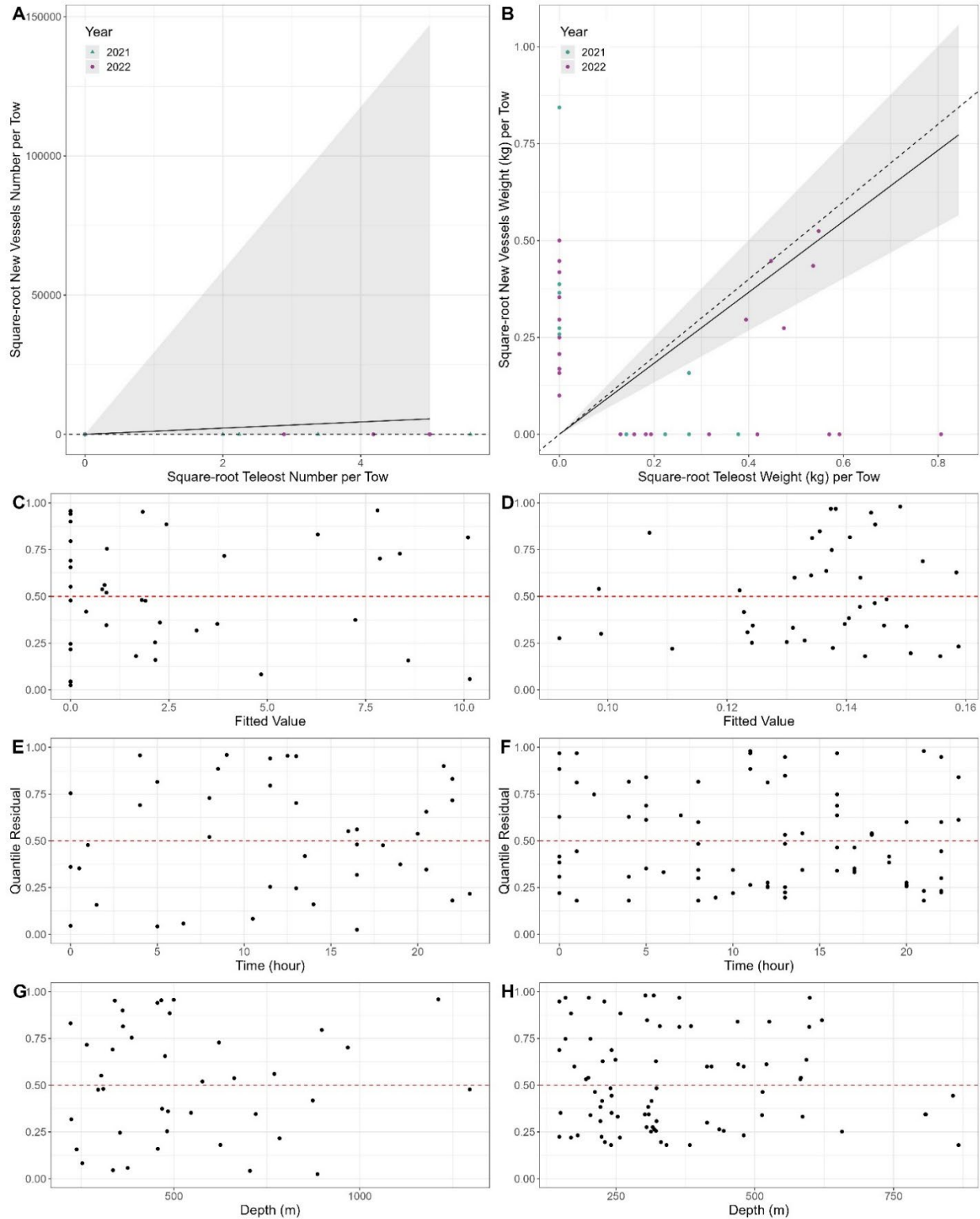


Figure A2–35. Results of size aggregated analysis for the CCGS Teleost and CCGS John Cabot/Capt. Jacques Cartier for catch of Sessile tunicates (*Tunicata*), fall 2HJ3K + 3L deep water. Data insufficient to determine if conversion is appropriate.

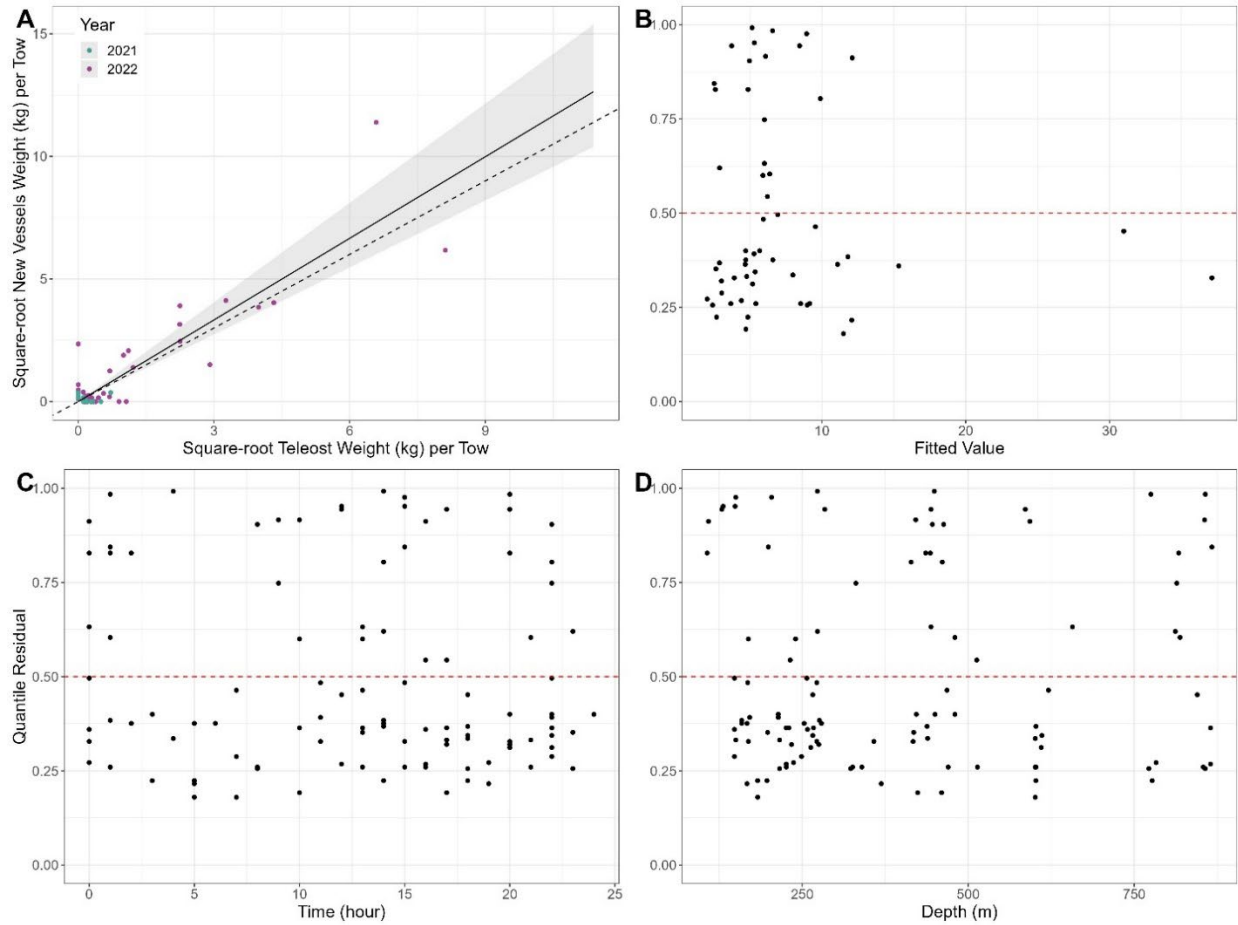


Figure A2-36. Results of size aggregated analysis for the CCGS Teleost and CCGS John Cabot/Capt. Jacques Cartier for catch of Basketstars (*Gorgonocephalus* spp.), fall 2HJ3K + 3L deep water.

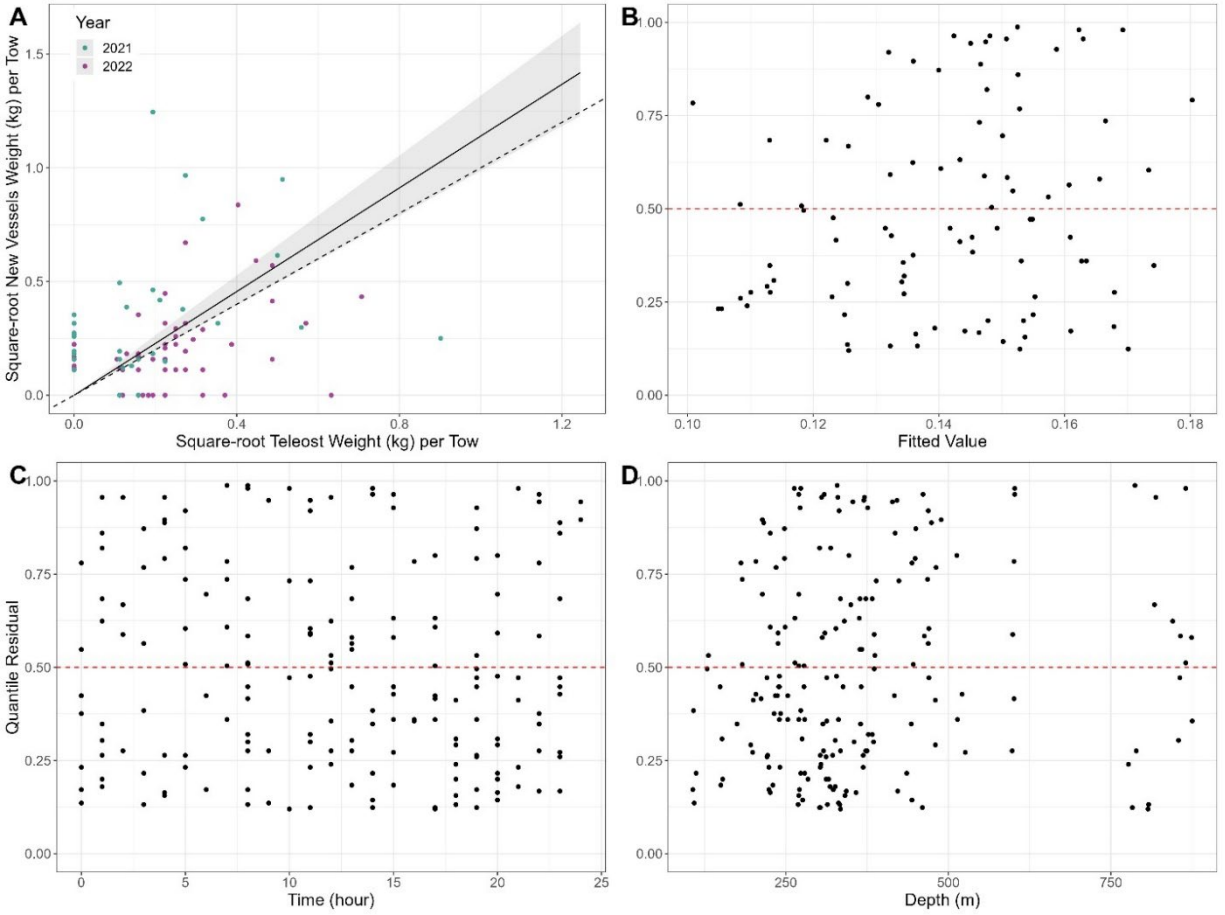


Figure A2–37. Results of size aggregated analysis for the CCGS Teleost and CCGS John Cabot/Capt. Jacques Cartier for catch of Brittle stars (*Ophiuroidea* except *Gorgonocephalus*), fall 2HJ3K + 3L deep water.

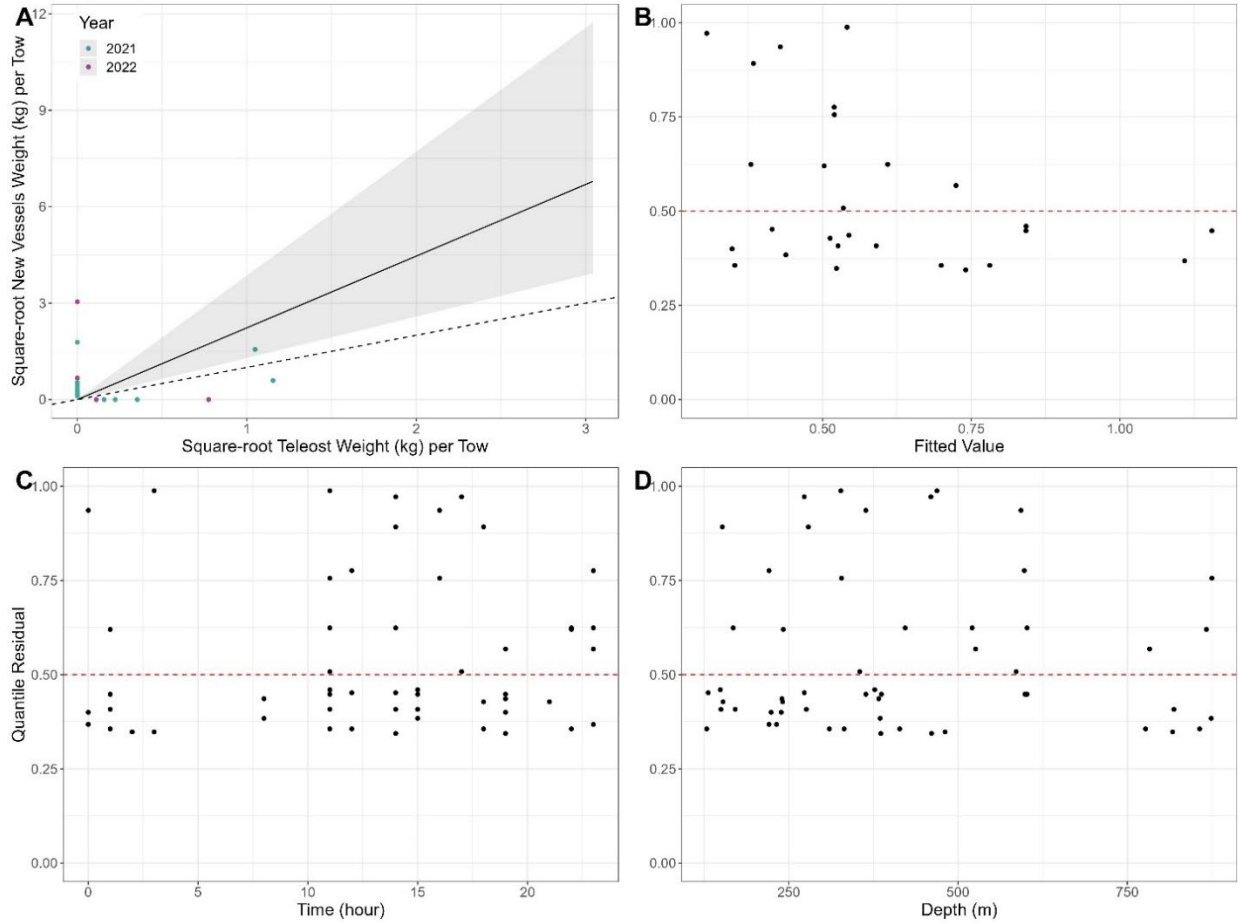


Figure A2-38. Results of size aggregated analysis for the CCGS Teleost and CCGS John Cabot/Capt. Jacques Cartier for catch of Corals n.s. (excludes soft coral), fall 2HJ3K + 3L deep water. Data insufficient to determine if conversions are appropriate.

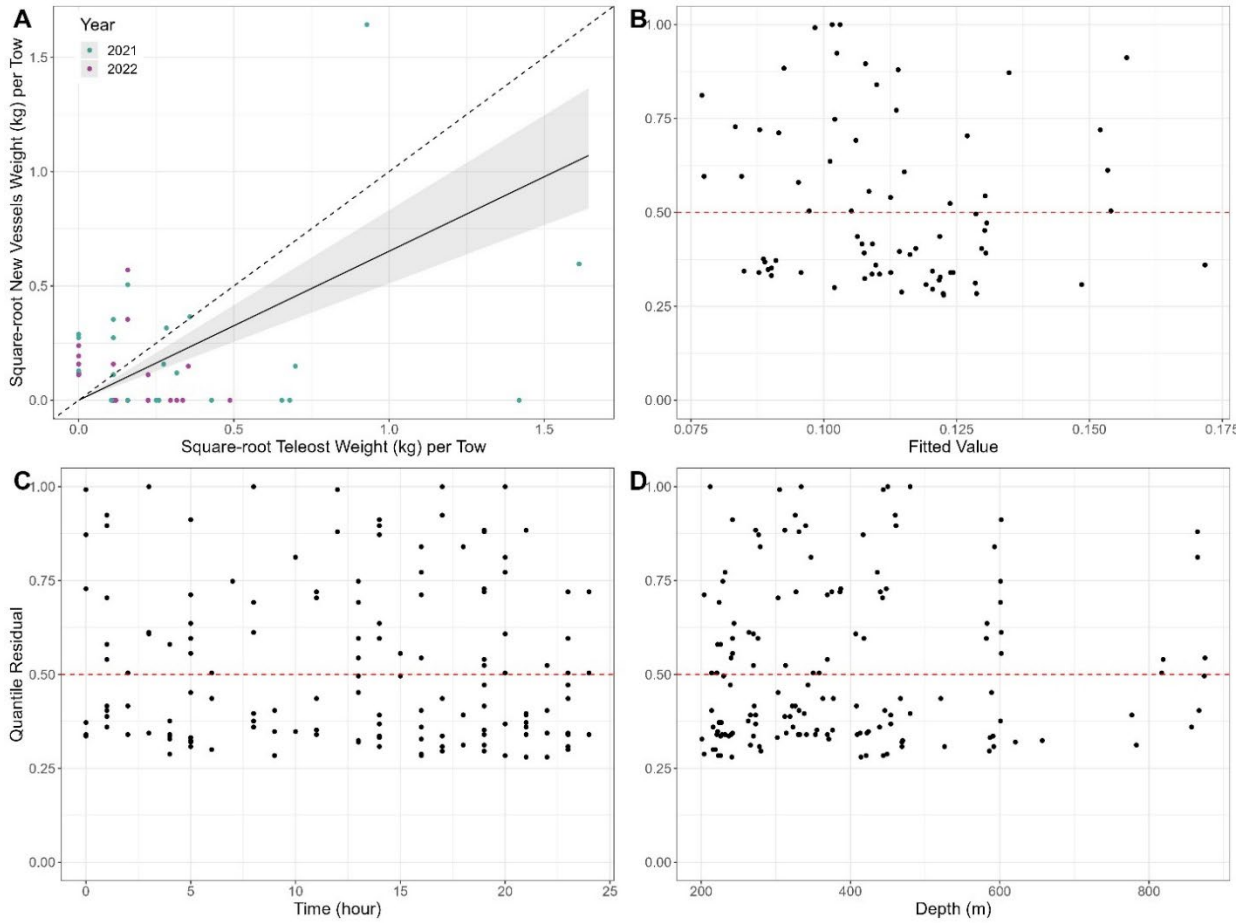


Figure A2-39. Results of size aggregated analysis for the CCGS Teleost and CCGS John Cabot/Capt. Jacques Cartier for catch of Euphausiids (Euphausiacea), fall 2HJ3K + 3L deep water. Data insufficient to determine if conversions are appropriate.

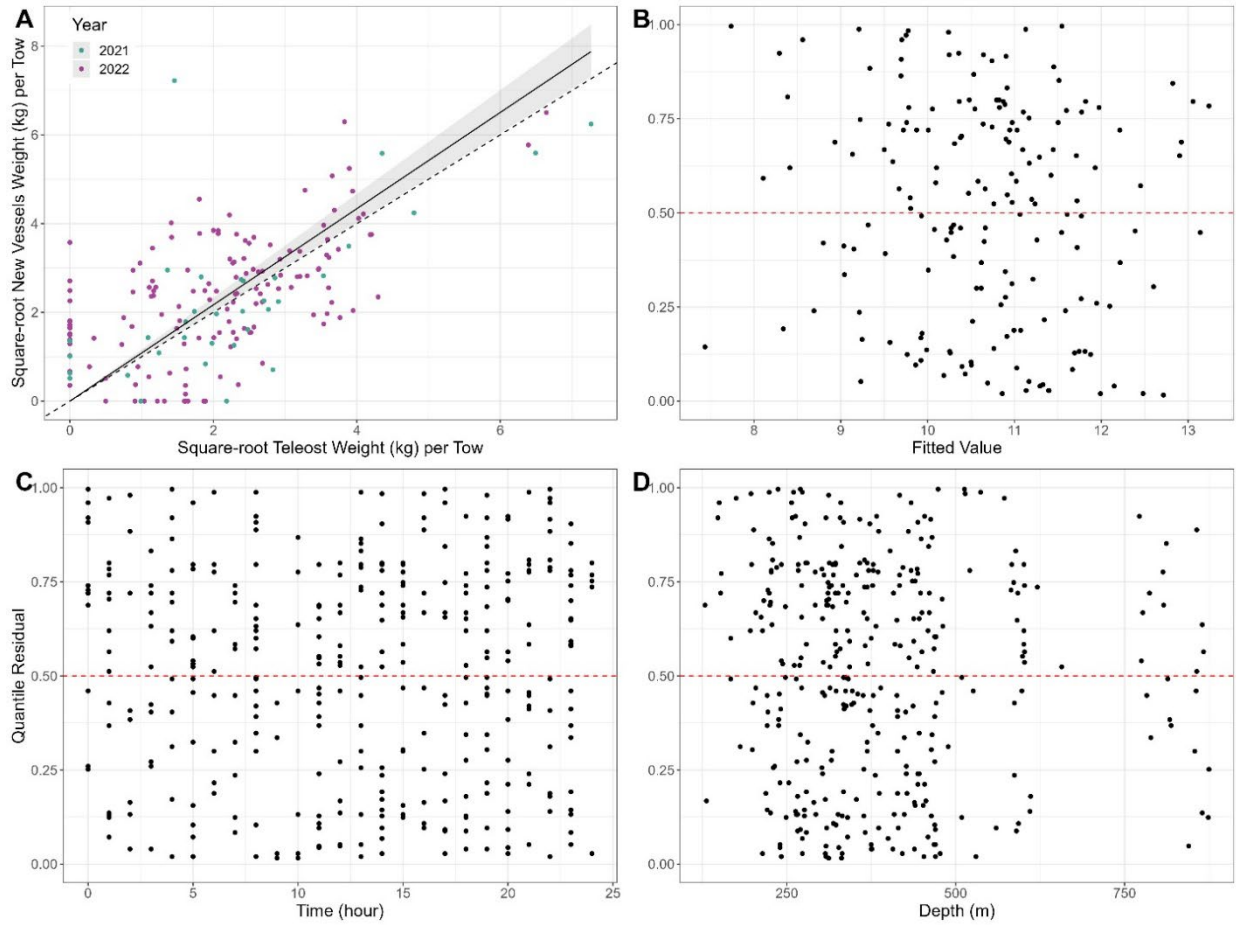


Figure A2-40. Results of size aggregated analysis for the CCGS Teleost and CCGS John Cabot/Capt. Jacques Cartier for catch of Jellyfishes (Scyphozoa), fall 2HJ3K + 3L deep water.

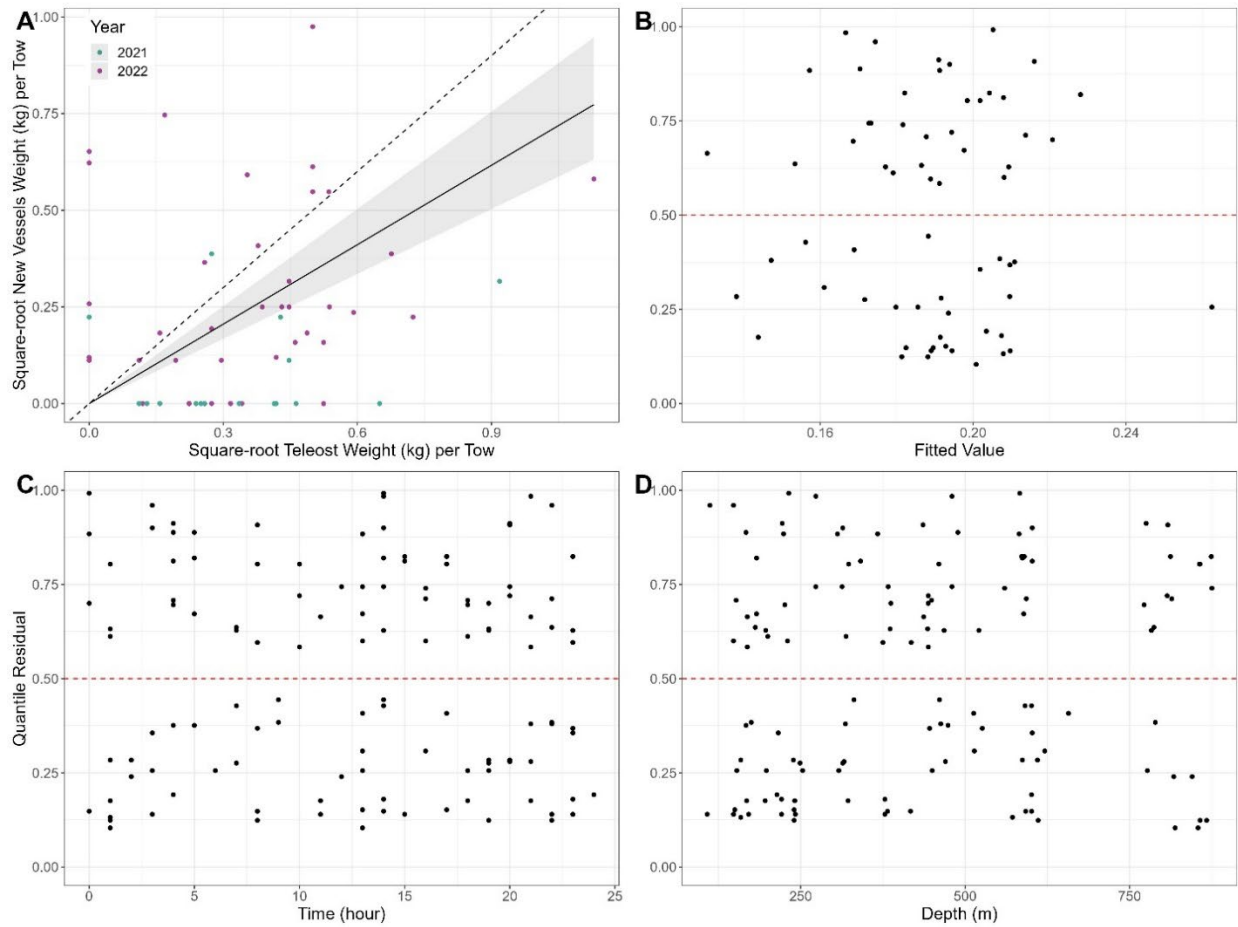


Figure A2-41. Results of size aggregated analysis for the CCGS Teleost and CCGS John Cabot/Capt. Jacques Cartier for catch of soft corals, fall 2HJ3K + 3L deep water.

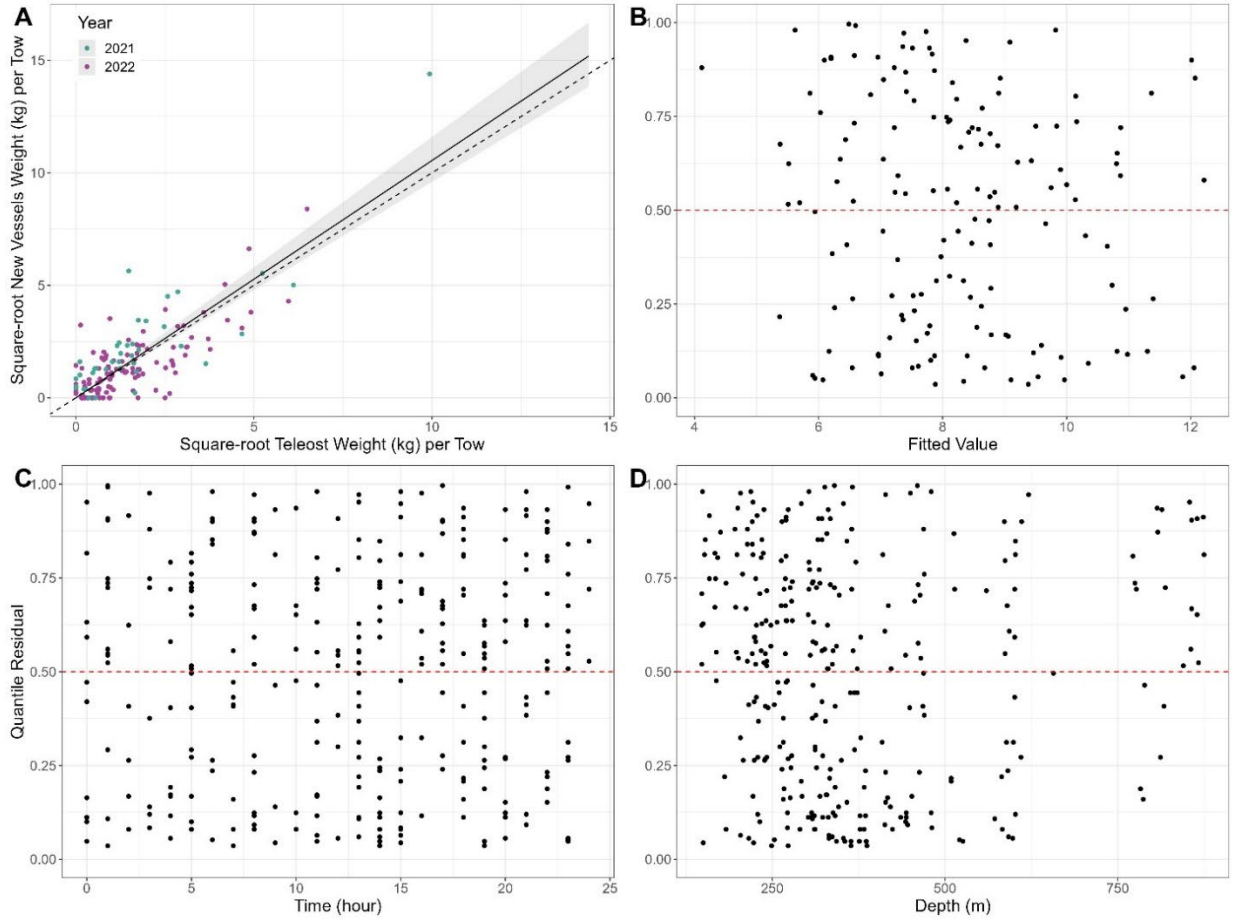


Figure A2-42. Results of size aggregated analysis for the CCGS Teleost and CCGS John Cabot/Capt. Jacques Cartier for catch of Sponge (*Porifera*), fall 2HJ3K + 3L deep water.

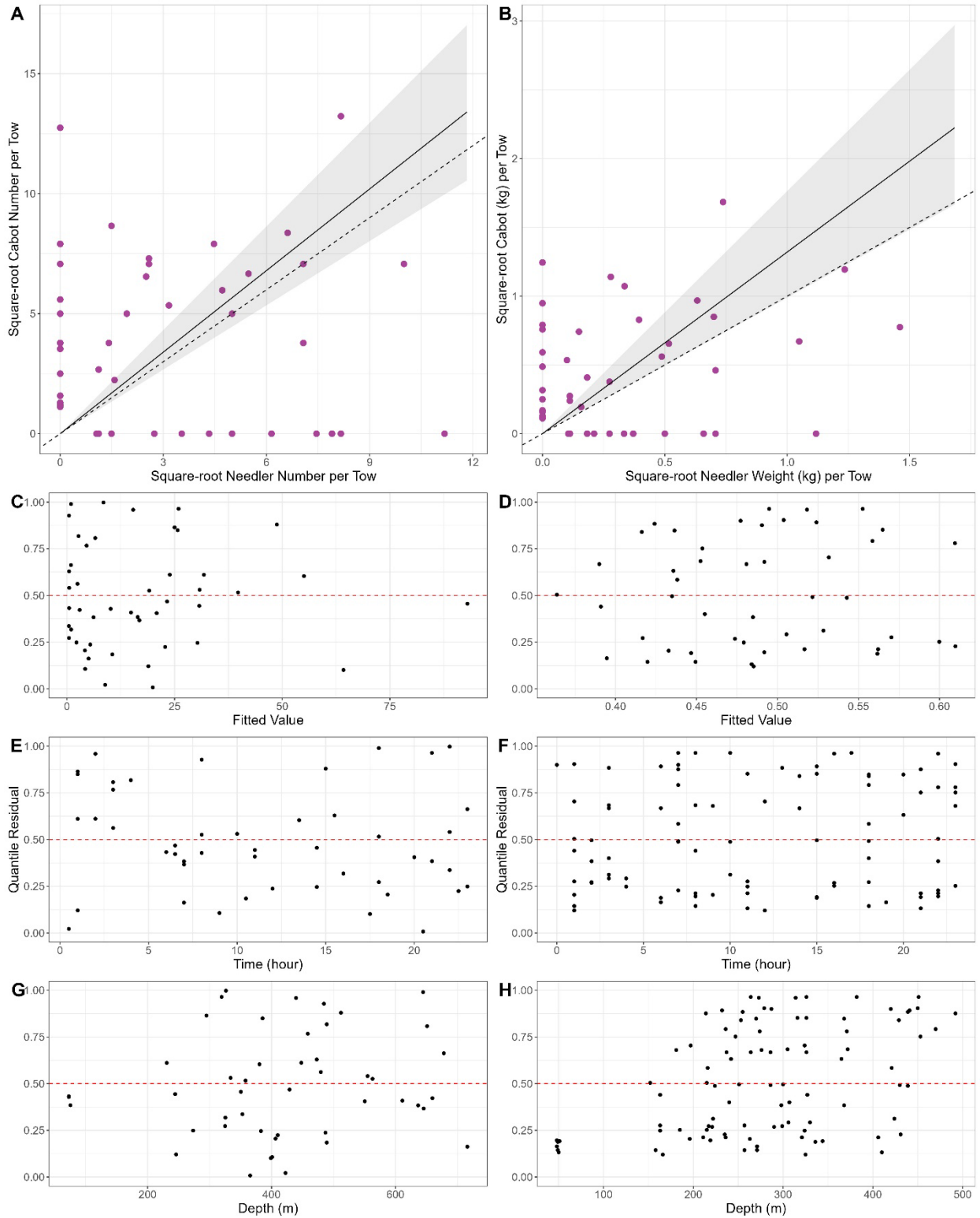


Figure A2-43. Results of size aggregated analysis for the CCGS Alfred Needler and CCGS John Cabot for catch of Alligatorfish (*Agonus* spp., *Eumicrotremus* spp), fall 3KL.

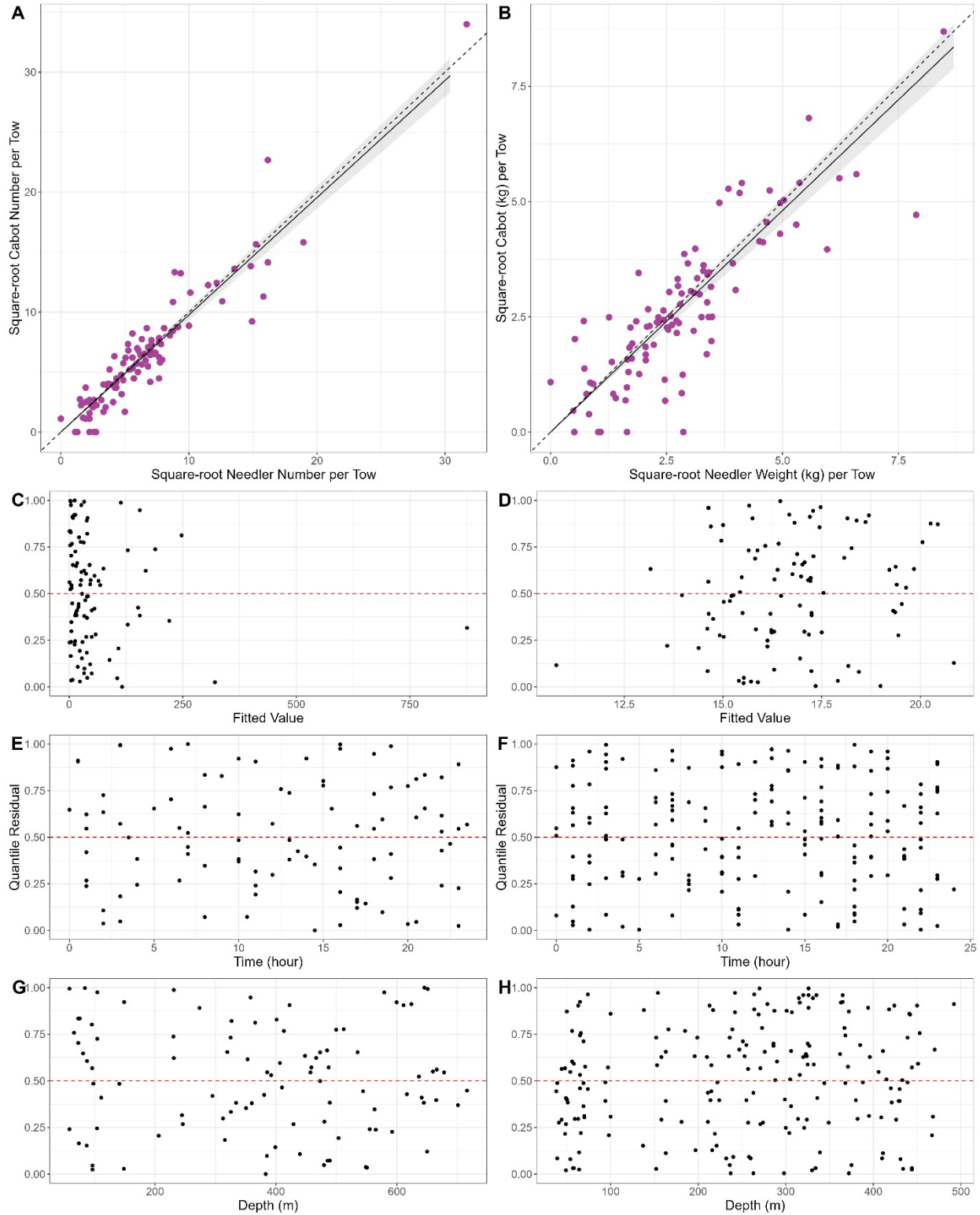


Figure A2-44. Results of size aggregated analysis for the CCGS Alfred Needler and CCGS John Cabot for catch of American Plaice (*Hippoglossoides platessoides*), fall 3KL.

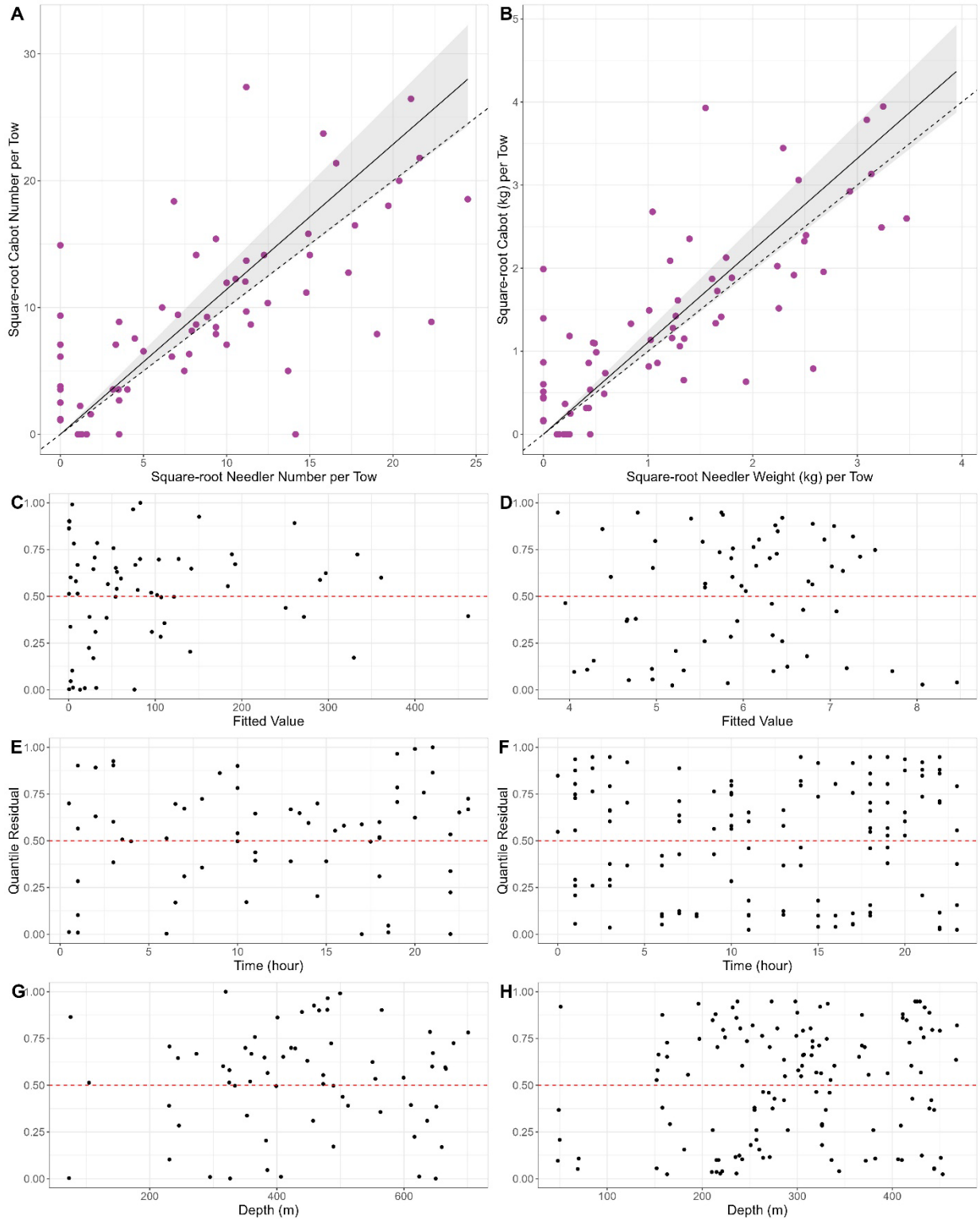


Figure A2-45. Results of size aggregated analysis for the CCGS Alfred Needler and CCGS John Cabot for catch of Arctic cod (*Boreogadus saida*), fall 3KL.

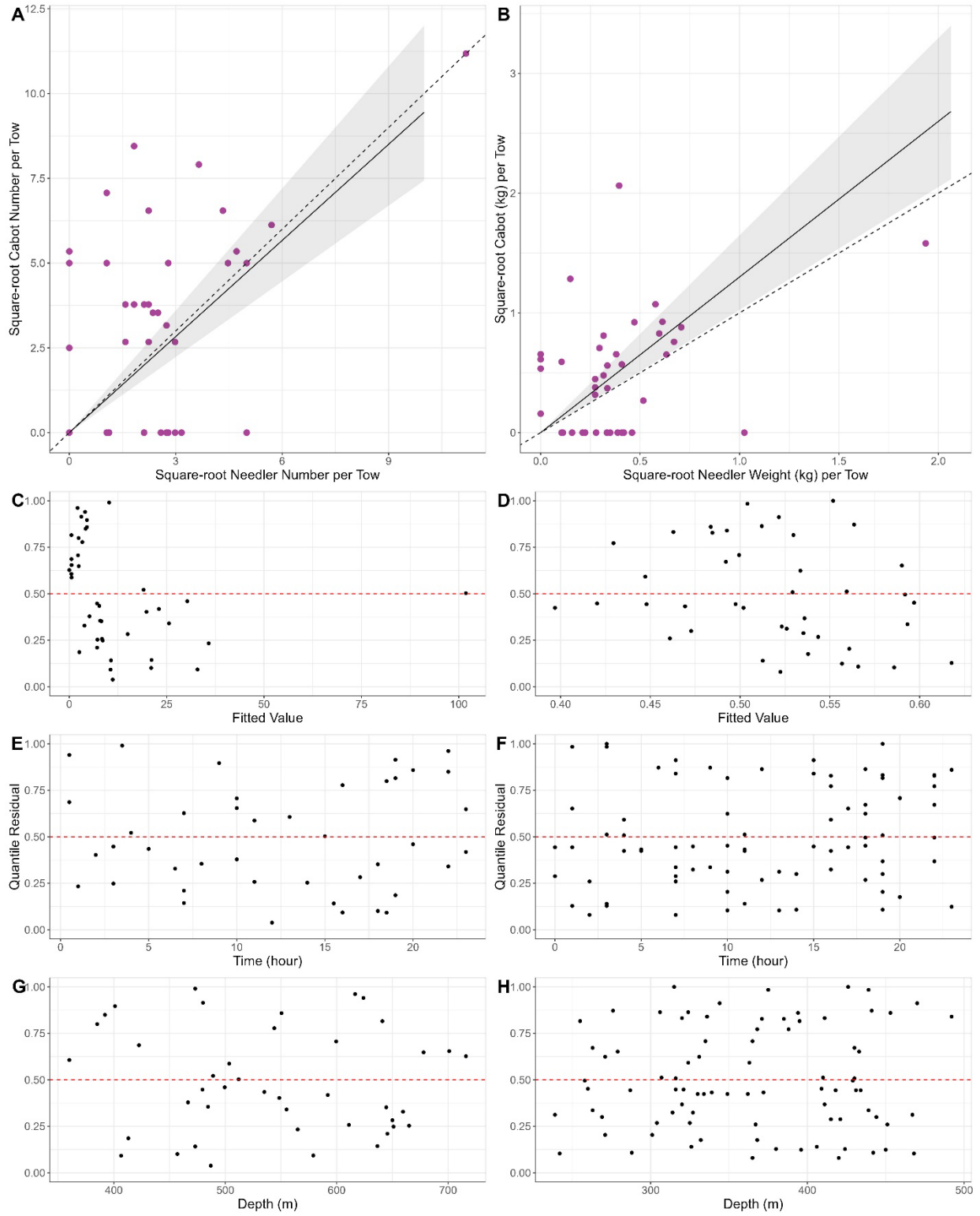


Figure A2-46. Results of size aggregated analysis for the CCGS Alfred Needler and CCGS John Cabot for catch of Barracudina and Lancetfish (*Paralepididae*), fall 3KL.

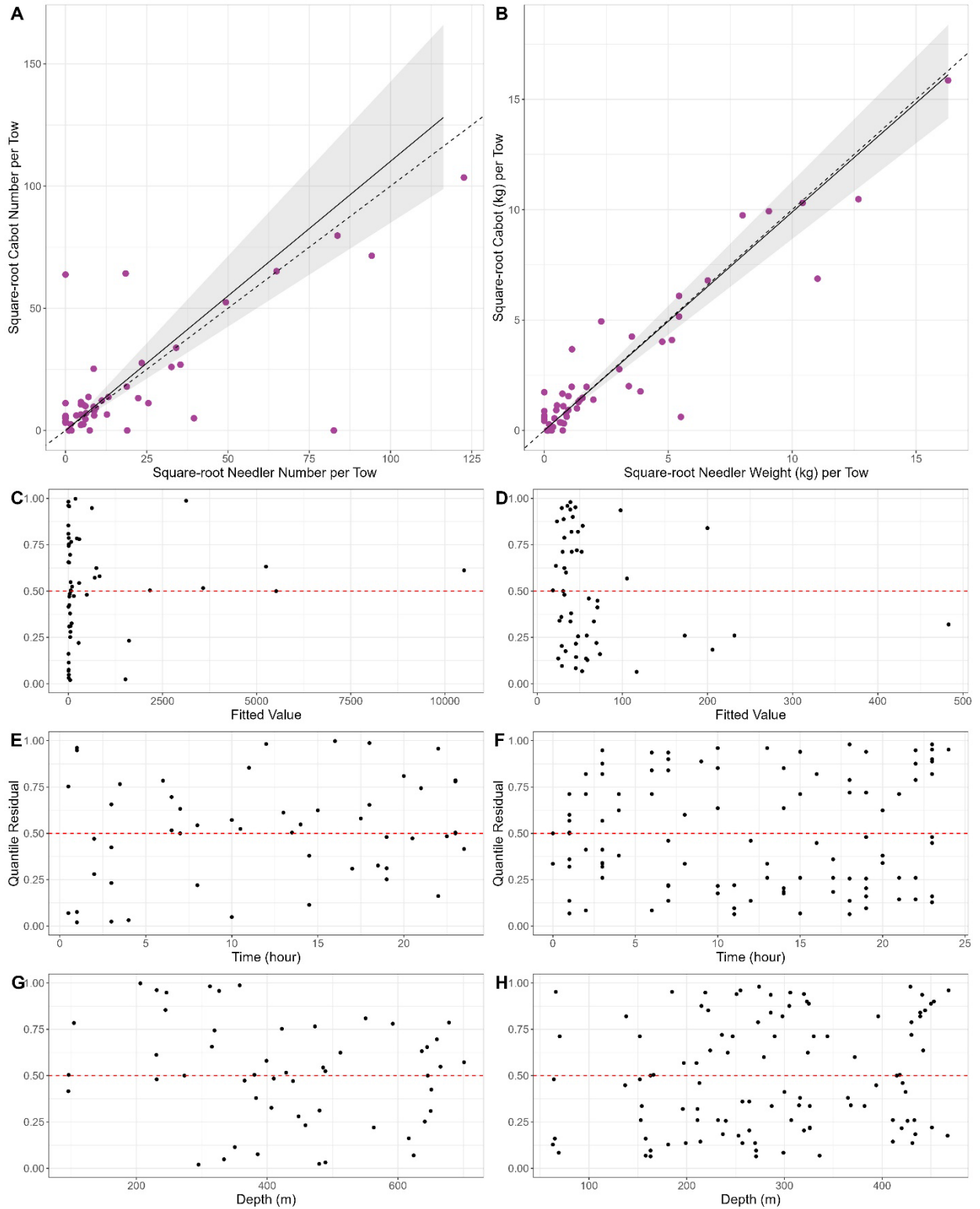


Figure A2-47. Results of size aggregated analysis for the CCGS Alfred Needler and CCGS John Cabot for catch of Capelin (*Mallotus villosus*), fall 3KL.

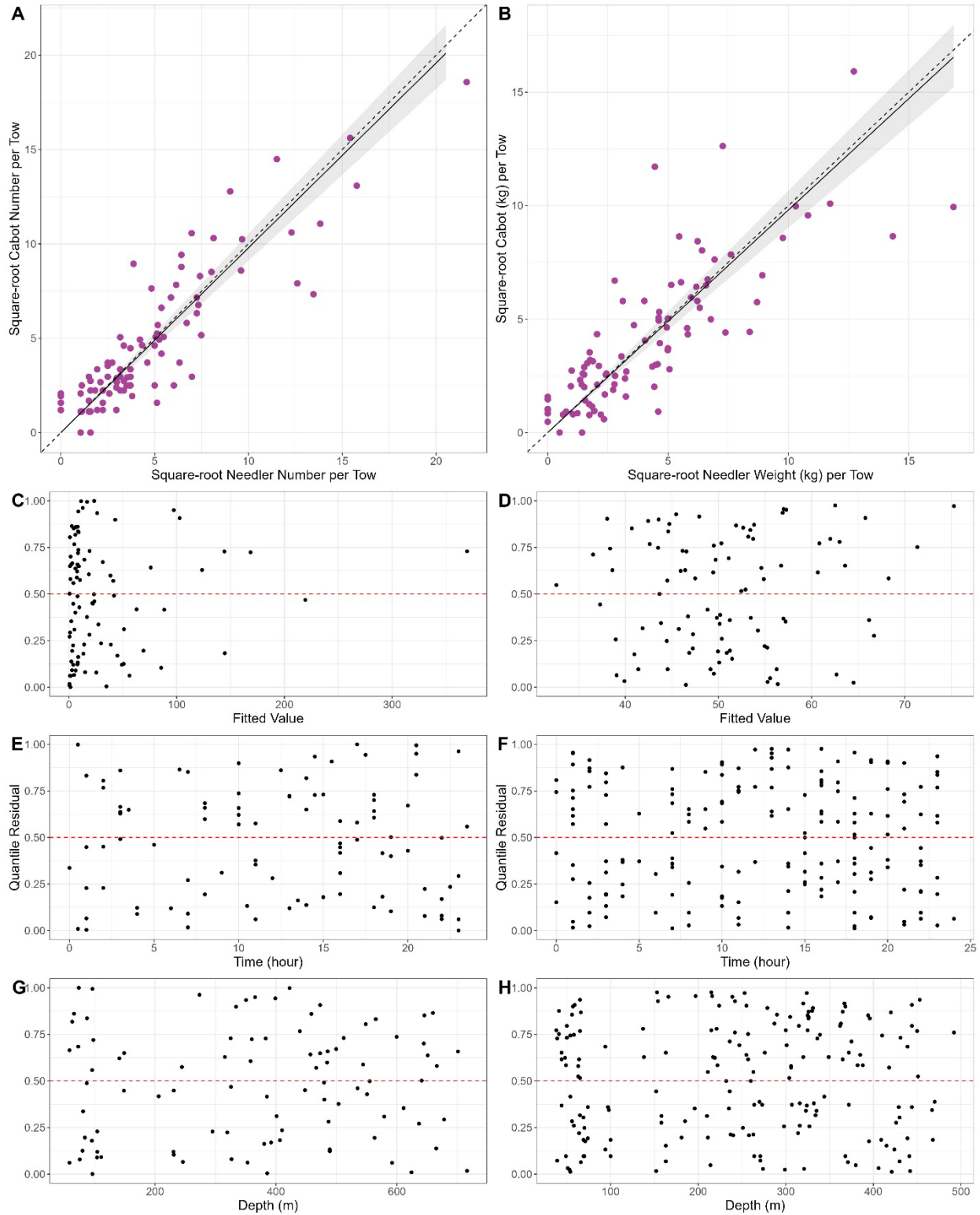


Figure A2-48. Results of size aggregated analysis for the CCGS Alfred Needler and CCGS John Cabot for catch of Atlantic Cod (*Gadus morhua*), fall 3KL.

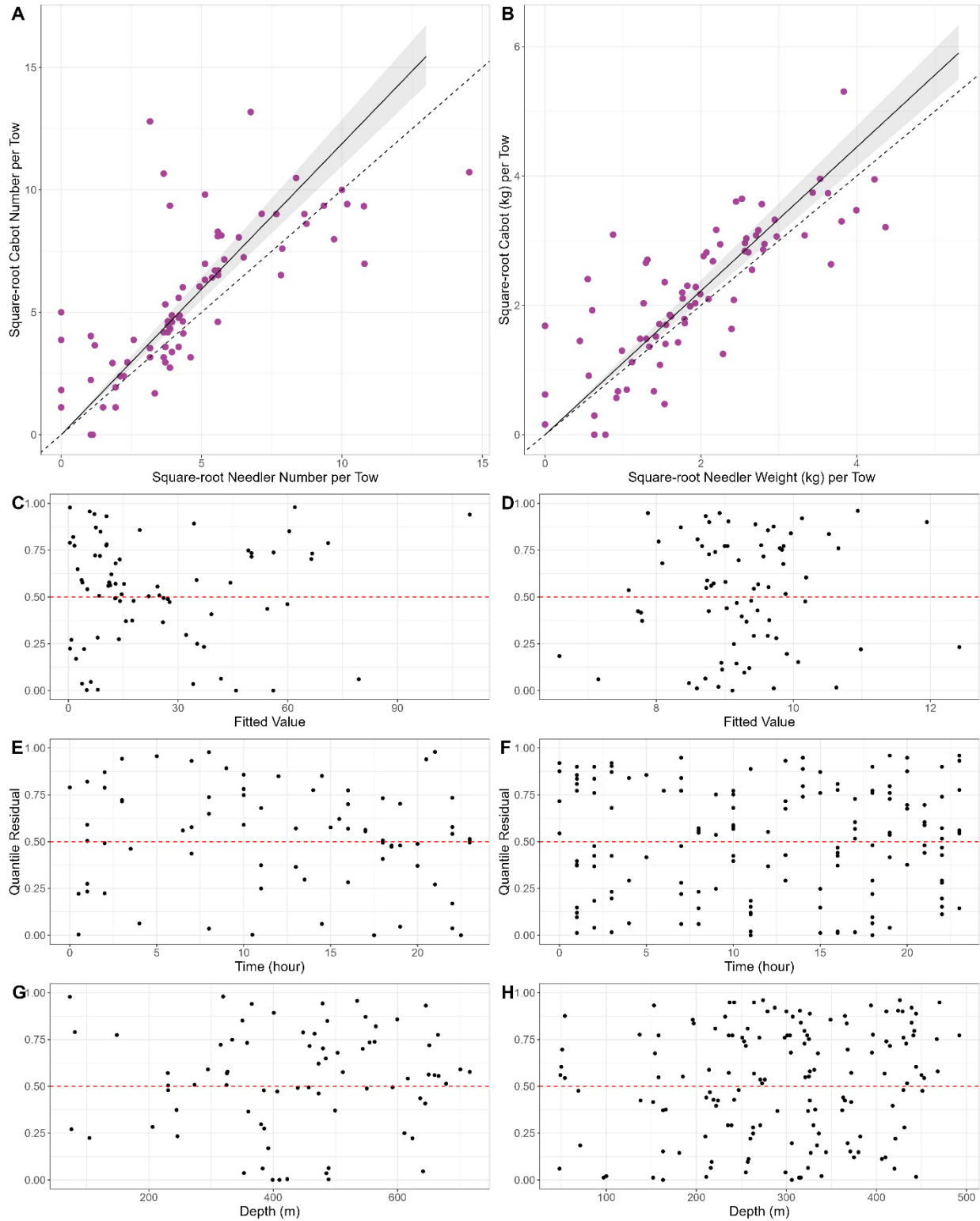


Figure A2-49. Results of size aggregated analysis for the CCGS Alfred Needler and CCGS John Cabot for catch of Eelpouts (Zoaridae), fall 3KL.

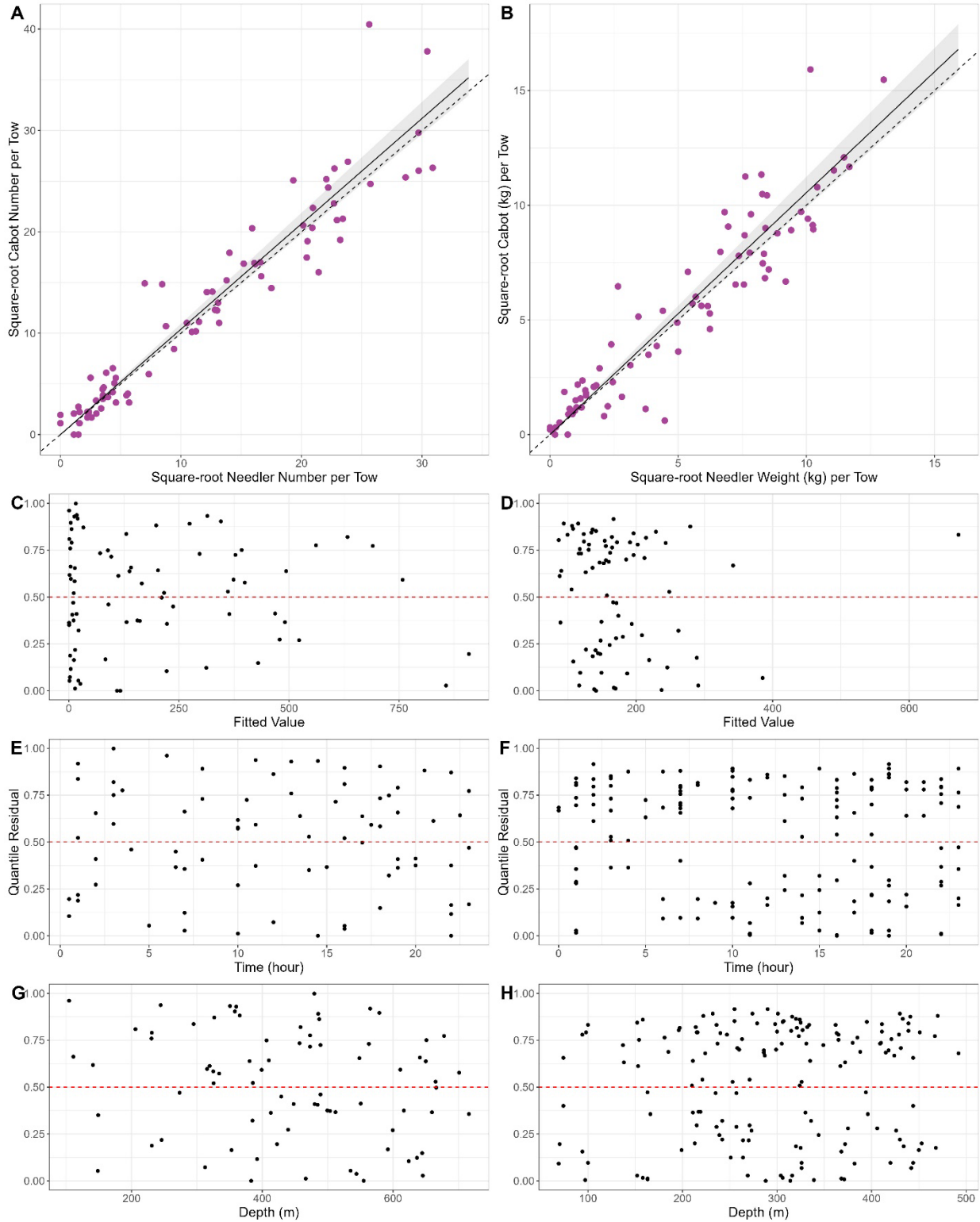


Figure A2-50. Results of size aggregated analysis for the CCGS Alfred Needler and CCGS John Cabot for catch of Greenland Halibut (*Reinhardtius hippoglossoides*), fall 3KL.

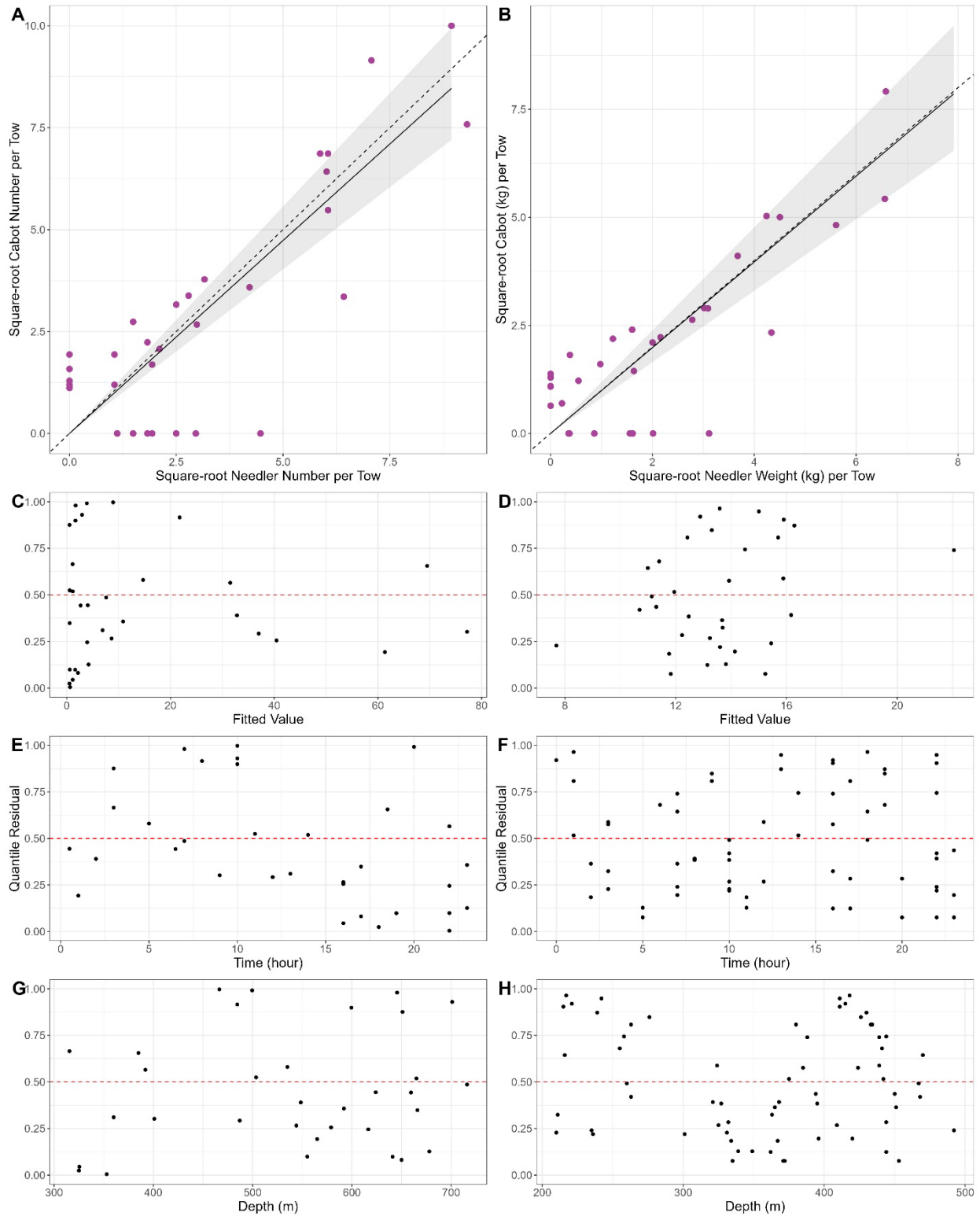


Figure A2-51. Results of size aggregated analysis for the CCGS Alfred Needler and CCGS John Cabot for catch of Roughead Grenadier (*Macrourus berglax*), fall 3KL.

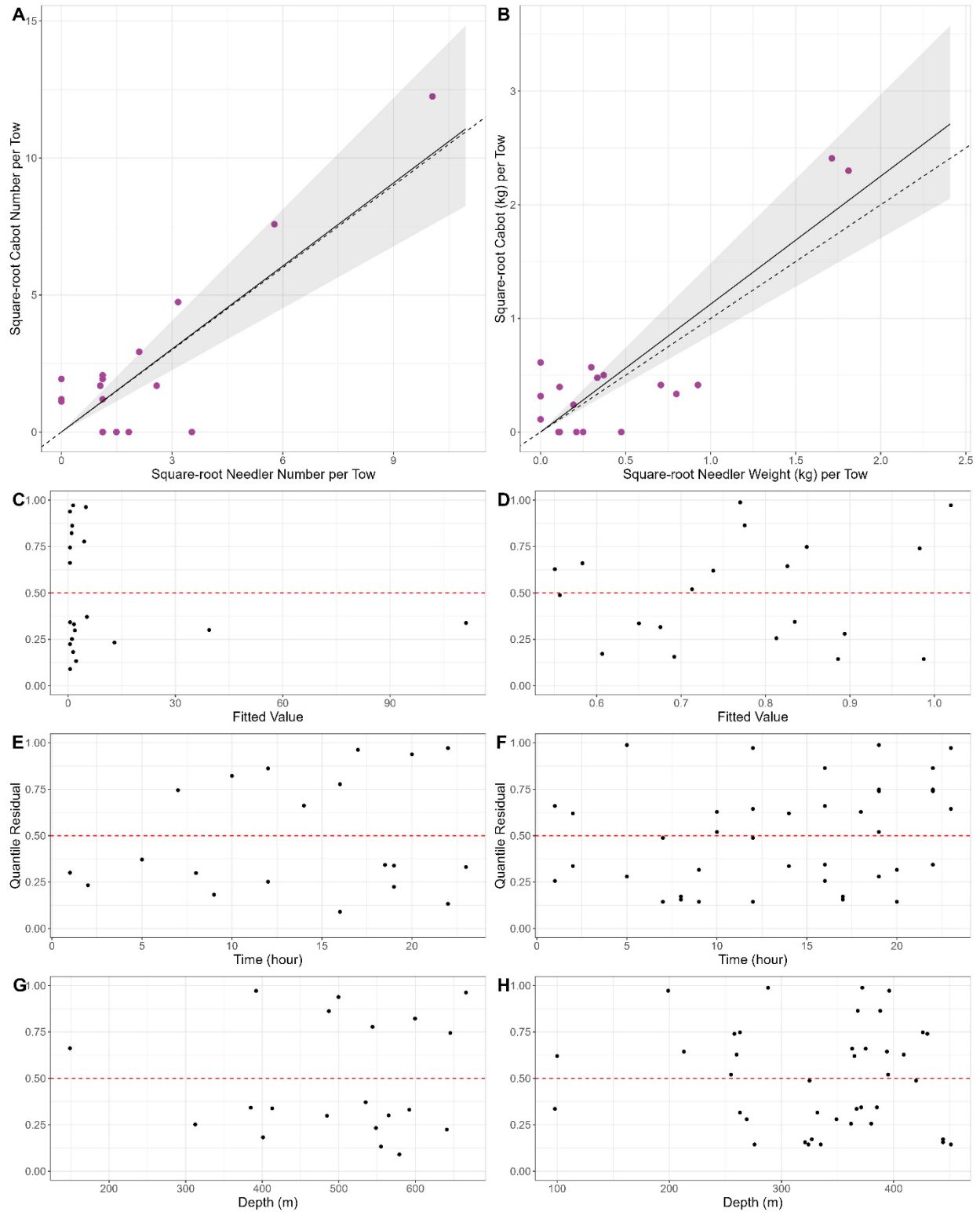


Figure A2-52. Results of size aggregated analysis for the CCGS Alfred Needler and CCGS John Cabot for catch of grenadier sp. (Macrouridae), fall 3KL.

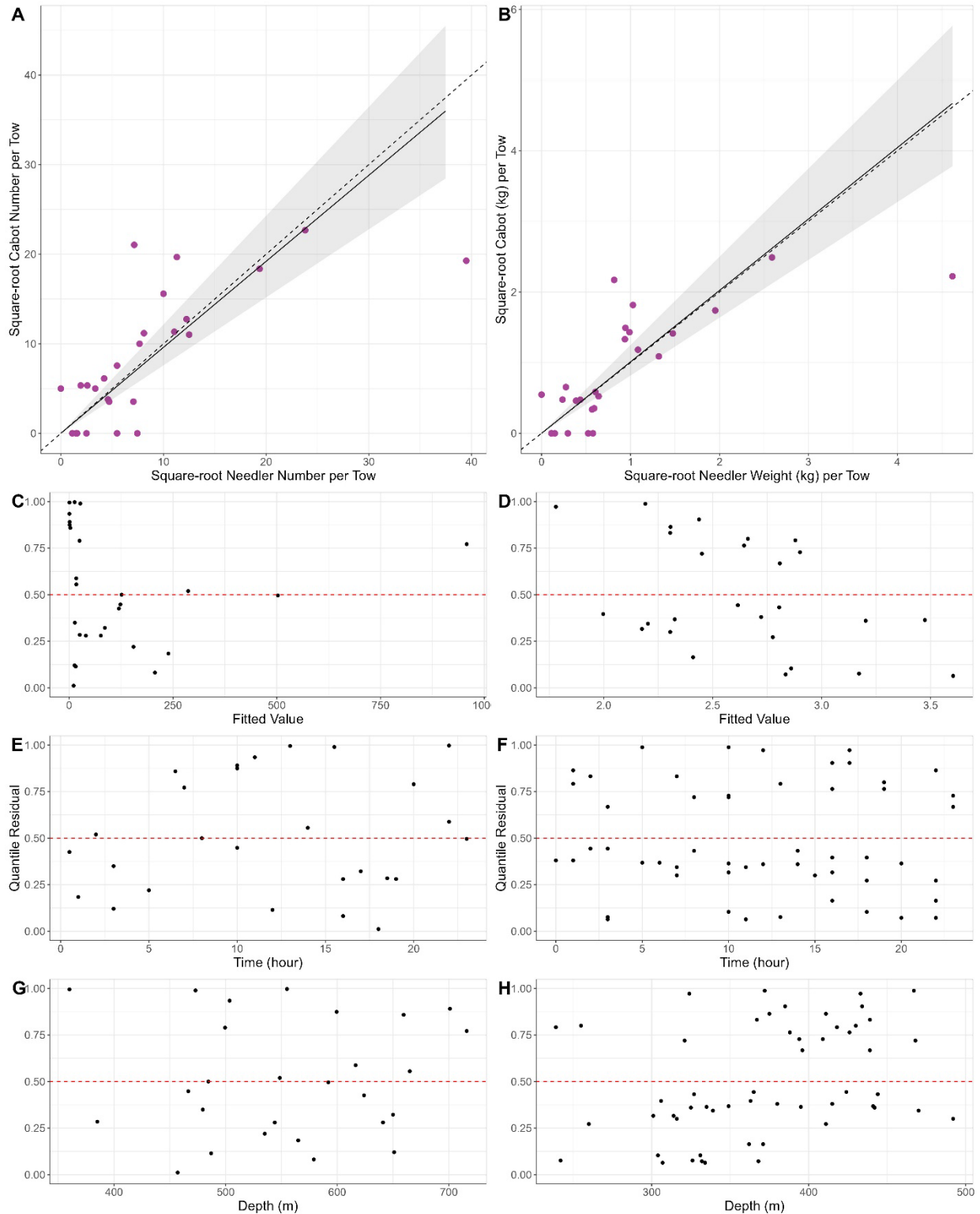


Figure A2-53. Results of size aggregated analysis for the CCGS Alfred Needler and CCGS John Cabot for catch of Lanternfishes (*Myctophidae*), fall 3KL.

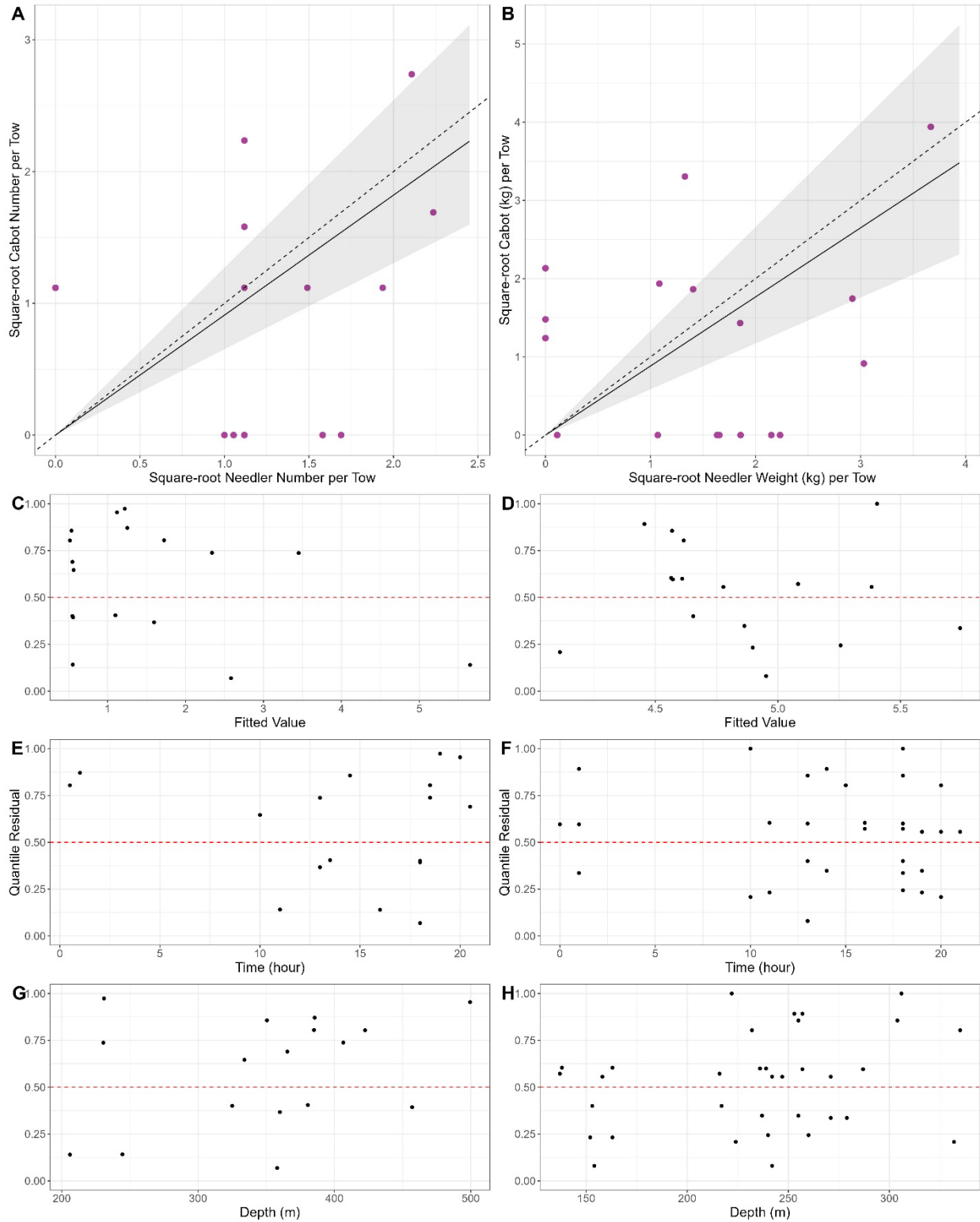


Figure A2-54. Results of size aggregated analysis for the CCGS Alfred Needler and CCGS John Cabot for catch of Common lumpfish (*Cyclopterus lumpus*), fall 3KL. Data insufficient to determine if conversion factor is appropriate.

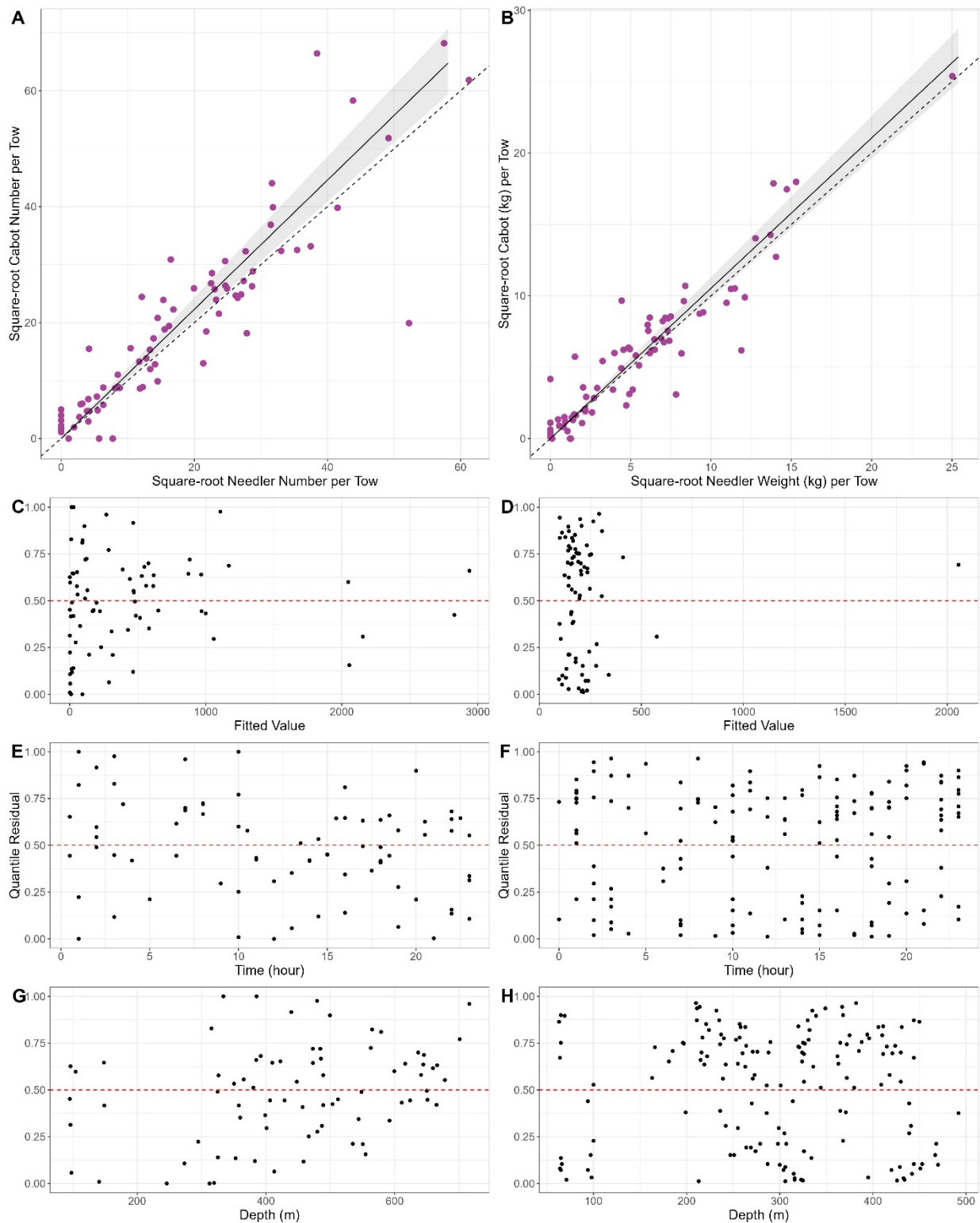


Figure A2-55. Results of size aggregated analysis for the CCGS Alfred Needler and CCGS John Cabot for catch of Redfish (*Sebastes mentalla* & *S. faciatius*), fall 3KL.

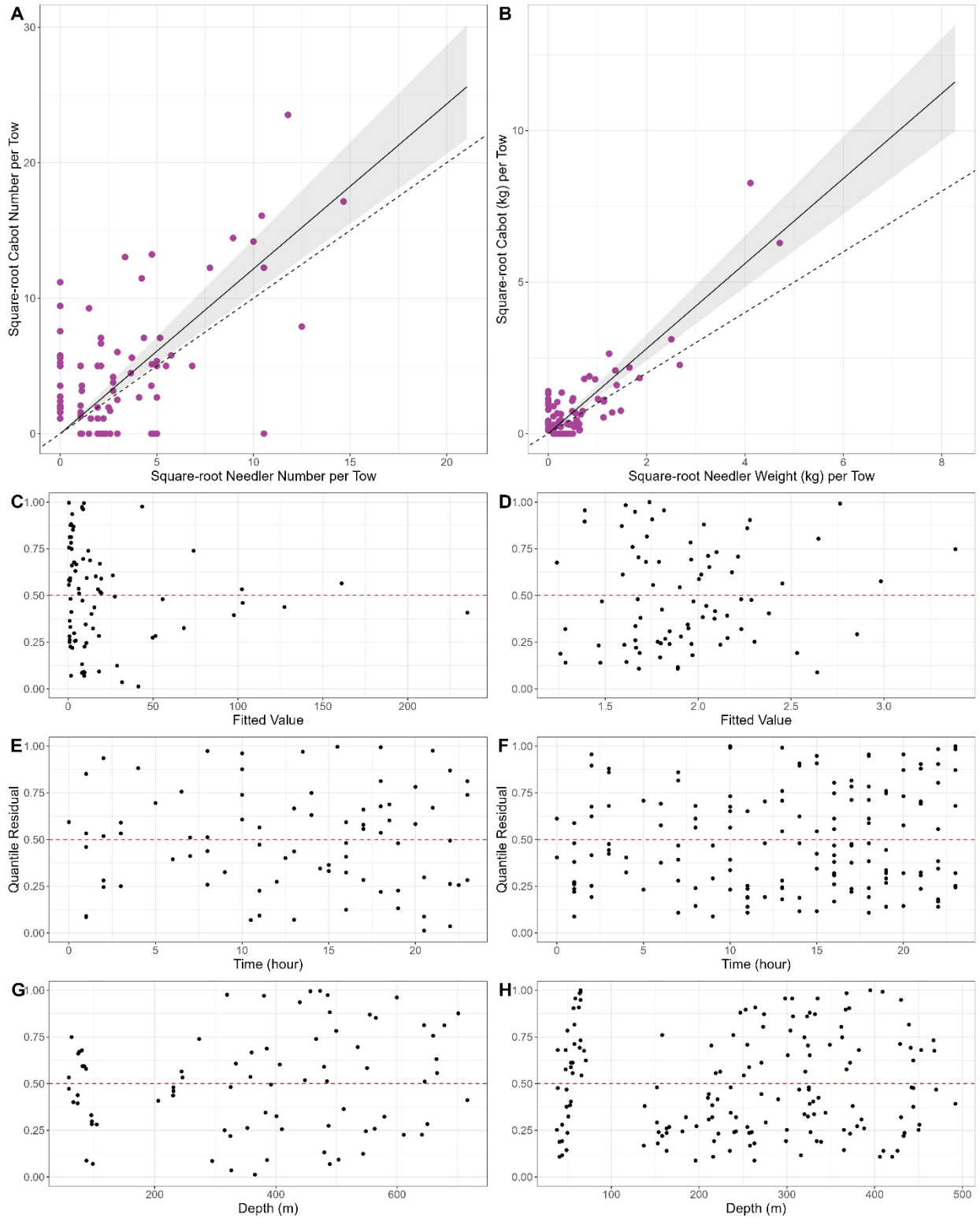


Figure A2-56. Results of size aggregated analysis for the CCGS Alfred Needler and CCGS John Cabot for catch of Sculpins (*Cottoidea*), fall 3KL.

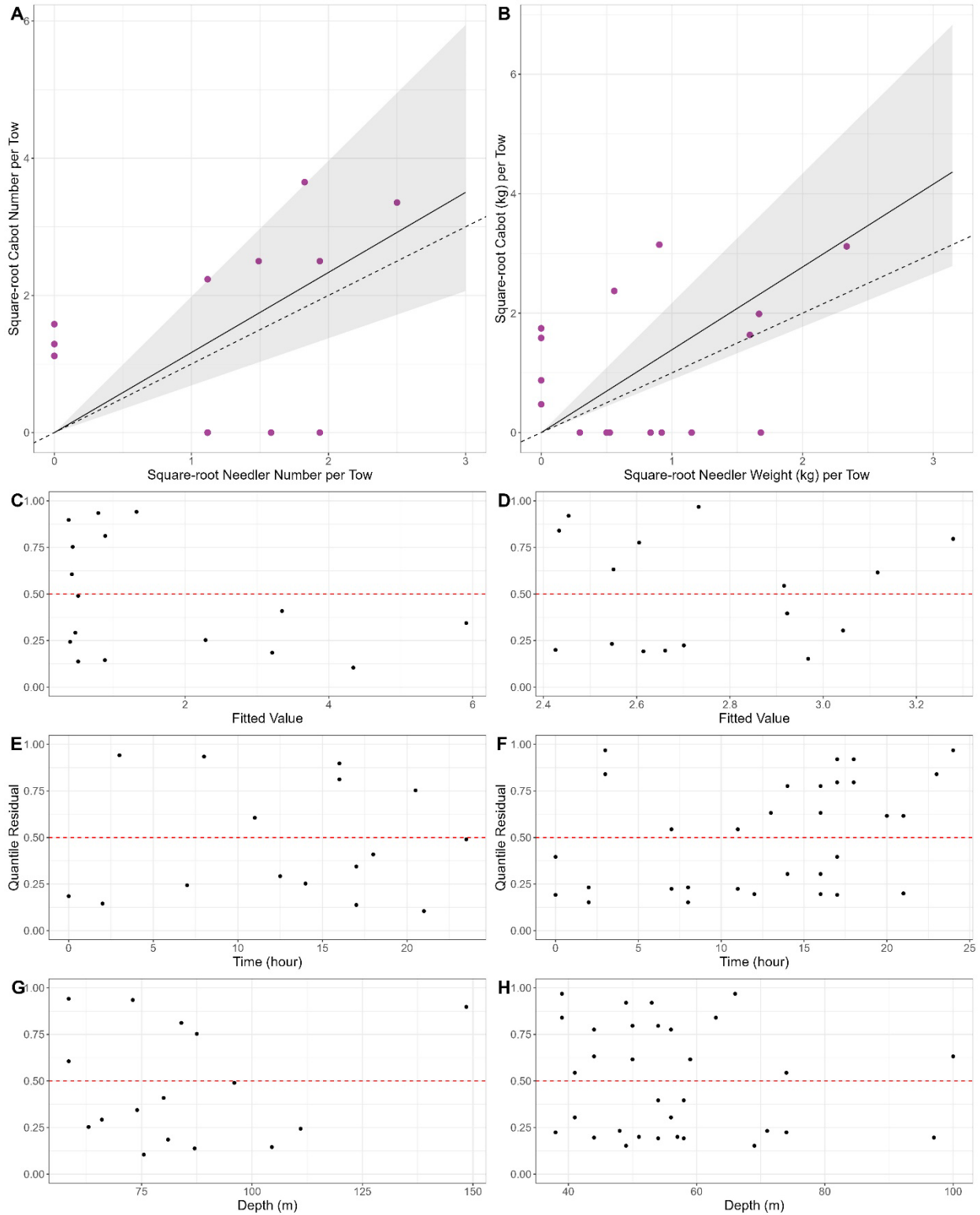


Figure A2-57. Results of size aggregated analysis for the CCGS Alfred Needler and CCGS John Cabot for catch of Sea raven (*Hemitripterus americanus*), fall 3KL. Data insufficient to determine if conversion is appropriate.

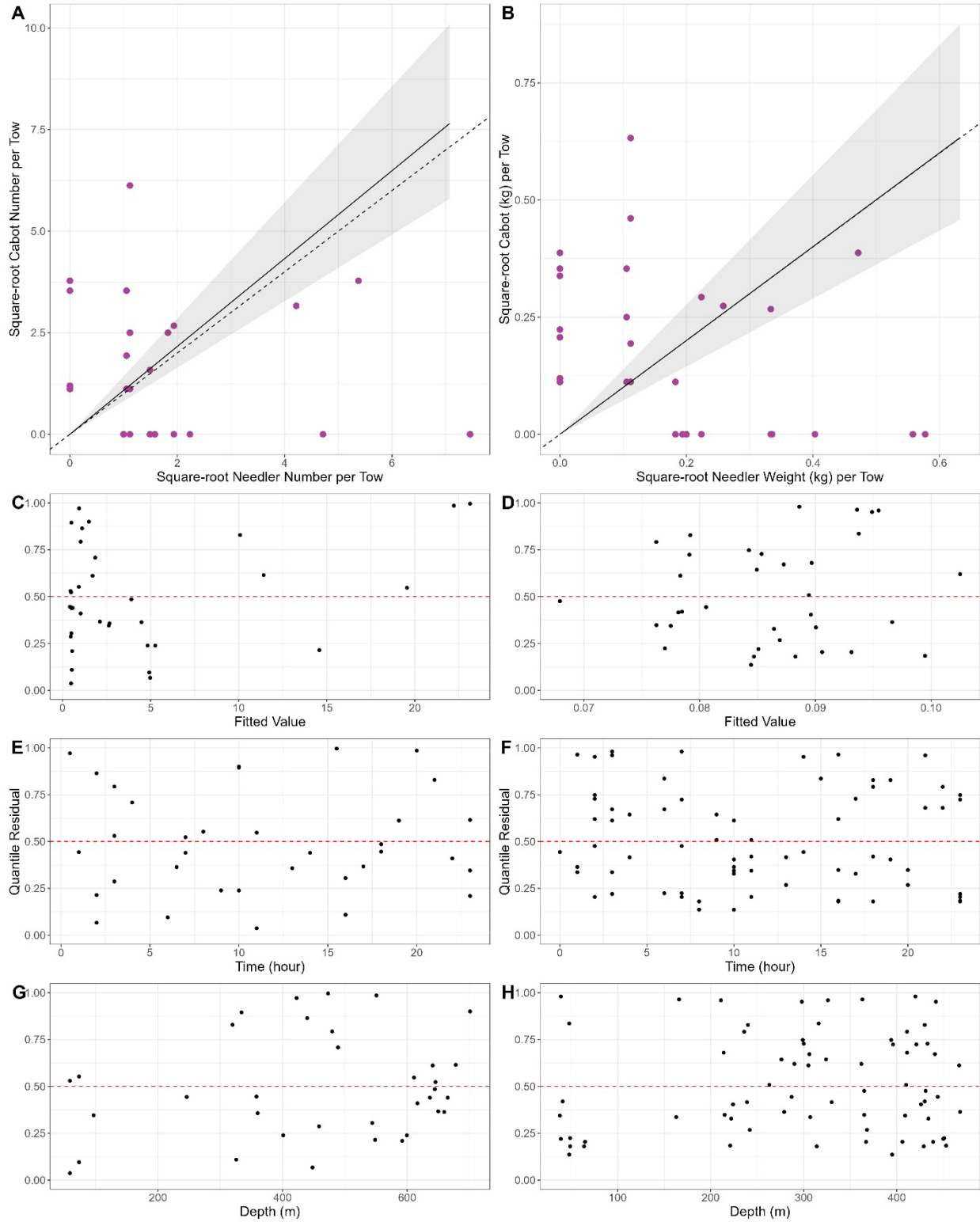


Figure A2-58. Results of size aggregated analysis for the CCGS Alfred Needler and CCGS John Cabot for catch of Snailfishes (*Liparidae*), fall 3KL.

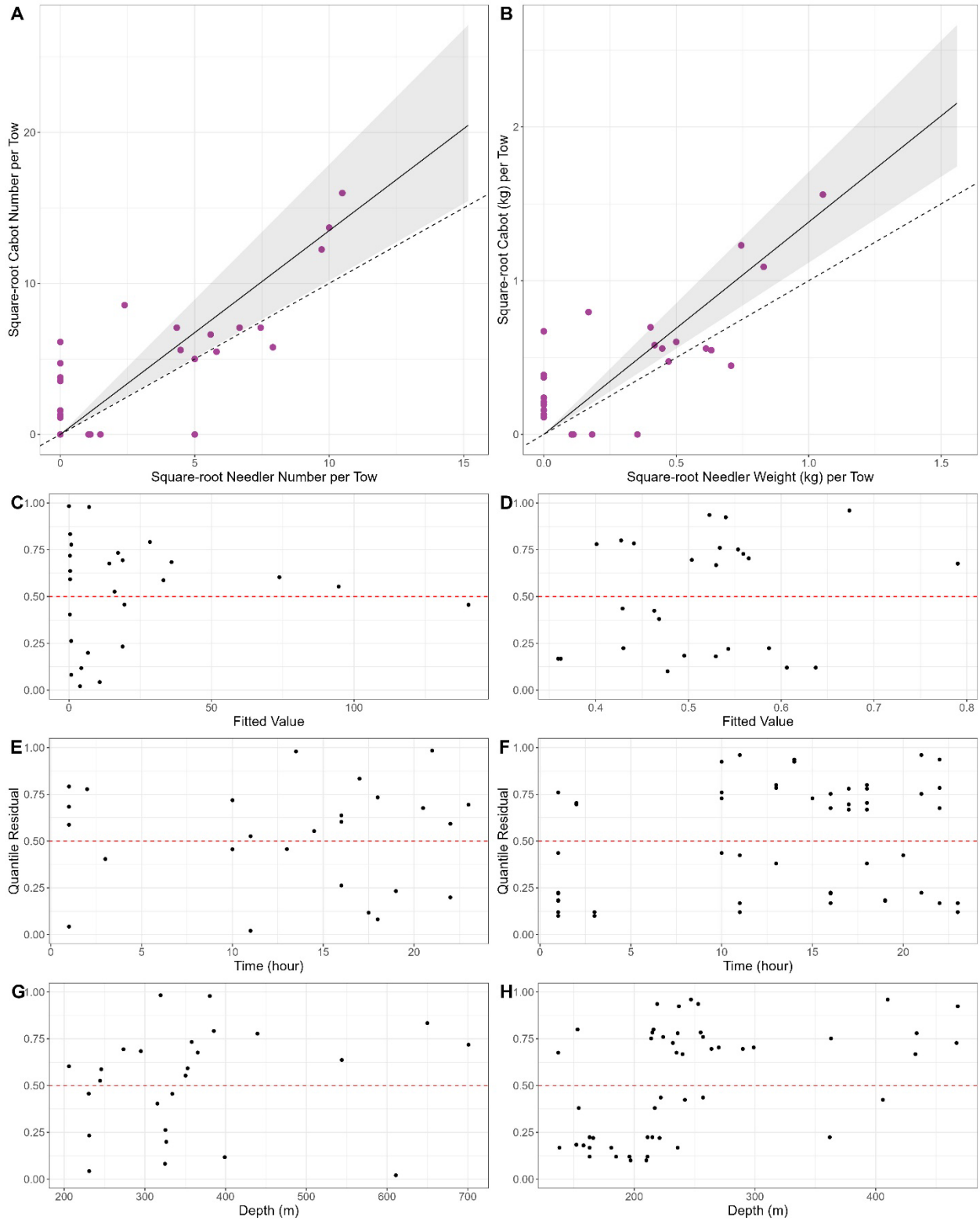


Figure A2-59. Results of size aggregated analysis for the CCGS Alfred Needler and CCGS John Cabot for catch of Shannies (*Leptoclinus maculatus*), fall 3KL.

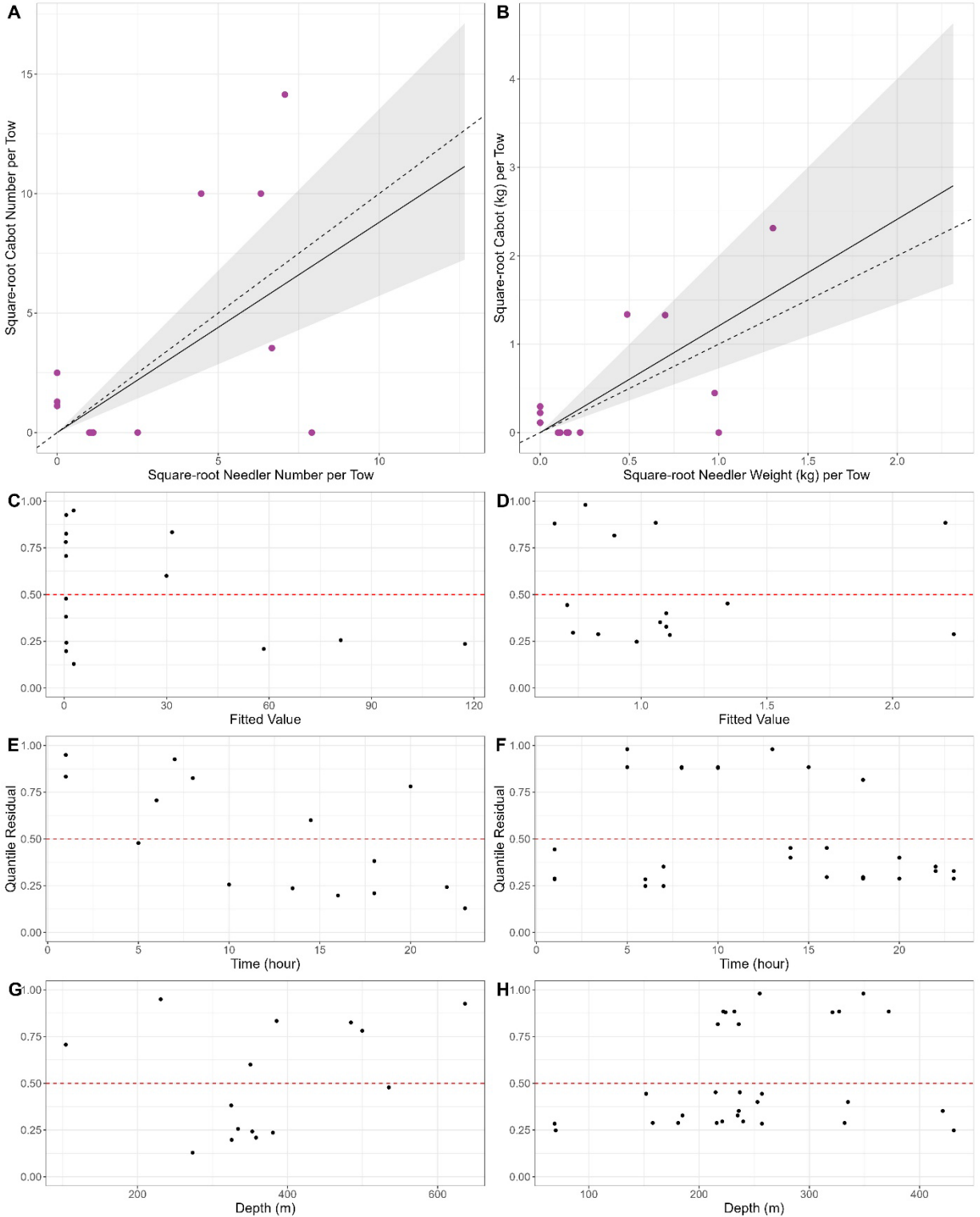


Figure A2-60. Results of size aggregated analysis for the CCGS Alfred Needler and CCGS John Cabot for catch of Snake blennies (*Lumpenus lumpretaeformis*), fall 3KL. Data insufficient to determine if conversion is appropriate.

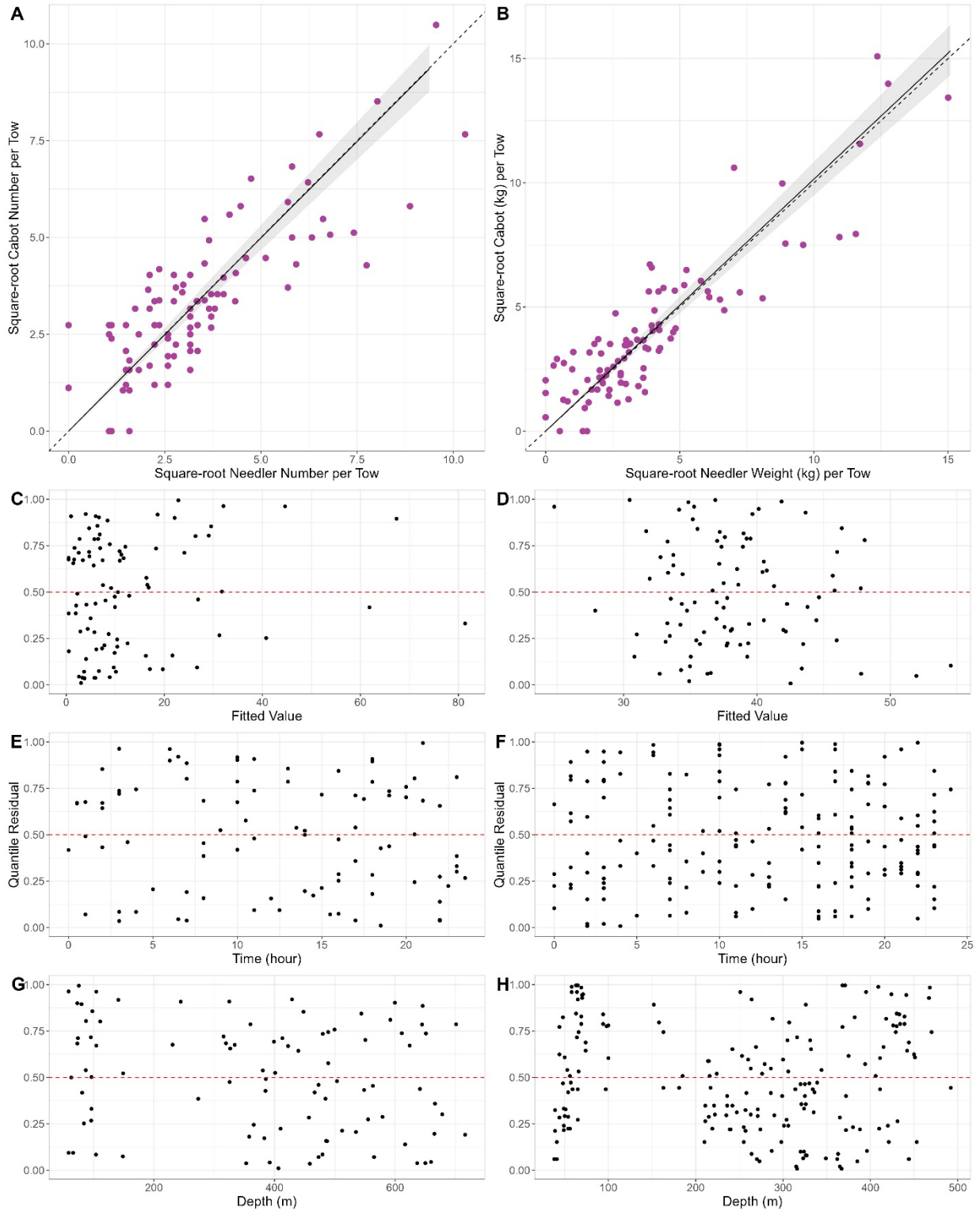


Figure A2-61. Results of size aggregated analysis for the CCGS Alfred Needler and CCGS John Cabot for catch of Thorny Skate (*Amblyraja radiata*), fall 3KL.

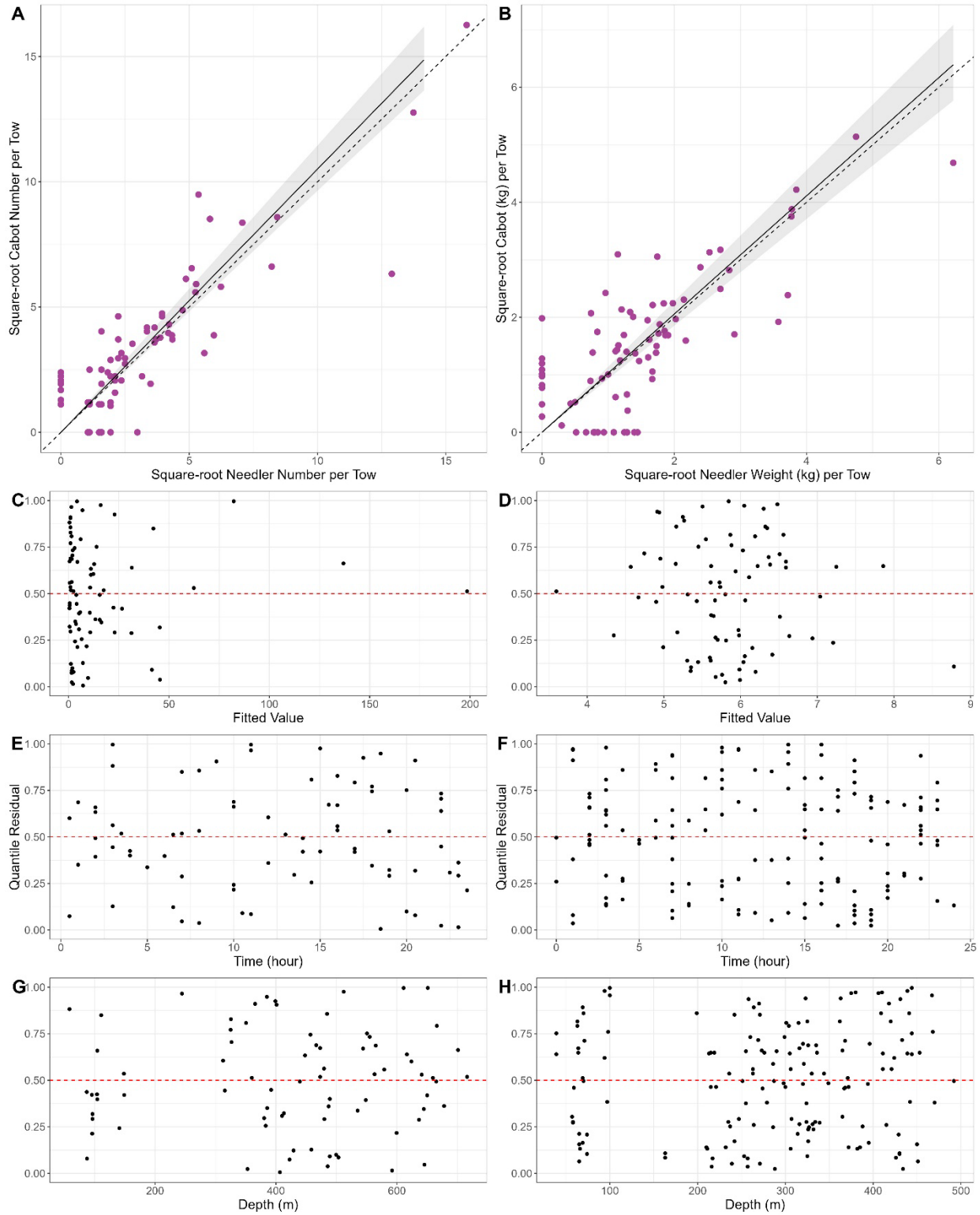


Figure A2-62. Results of size aggregated analysis for the CCGS Alfred Needler and CCGS John Cabot for catch of Witch Flounder (*Glyptocephalus cynoglossus*), fall 3KL.

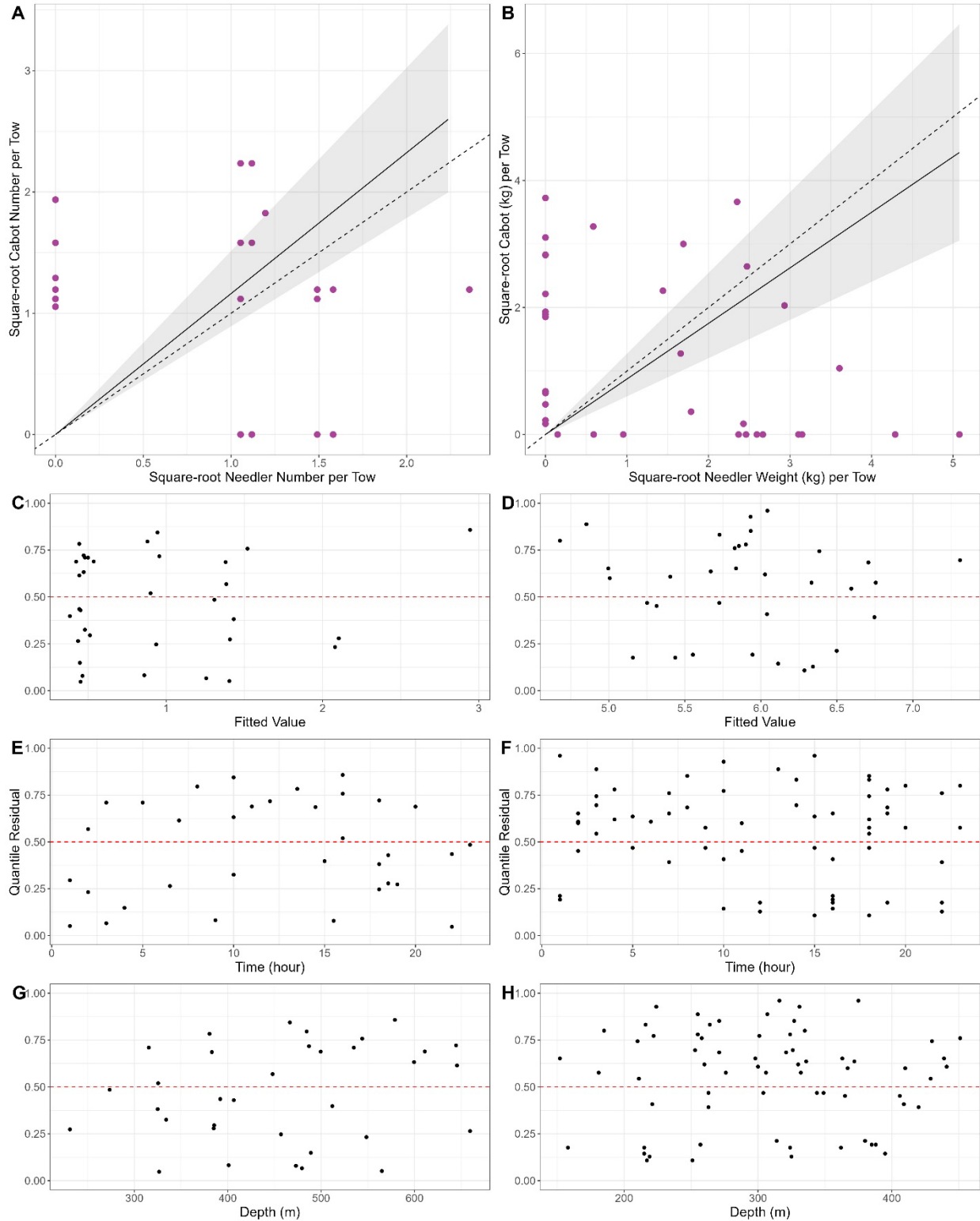


Figure A2-63. Results of size aggregated analysis for the CCGS Alfred Needler and CCGS John Cabot for catch of Spotted Wolffish (*Anarhichas minor*), fall 3KL.

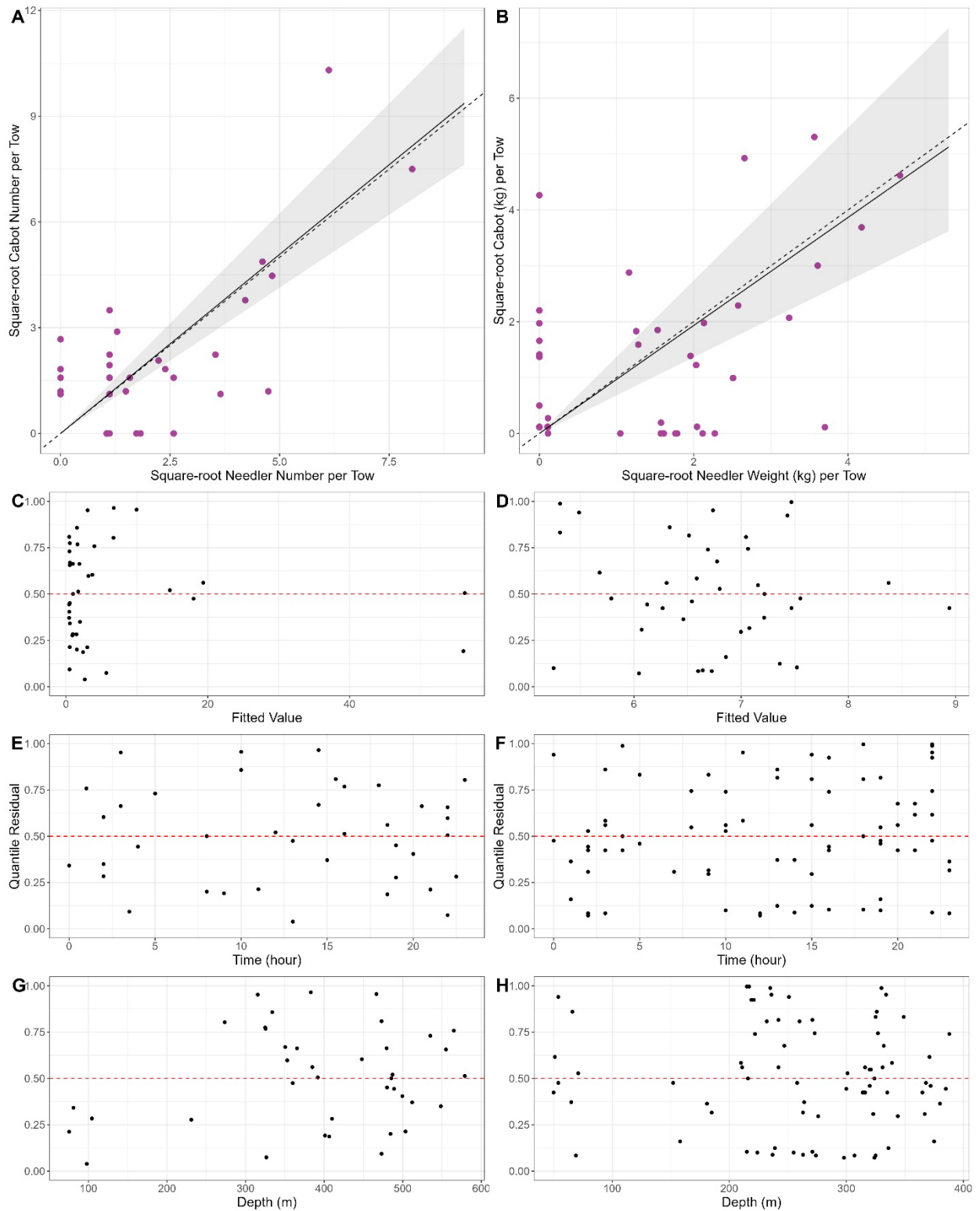


Figure A2-64. Results of size aggregated analysis for the CCGS Alfred Needler and CCGS John Cabot for catch of Striped Wolffish (*Anarhichas lupus*), fall 3KL.

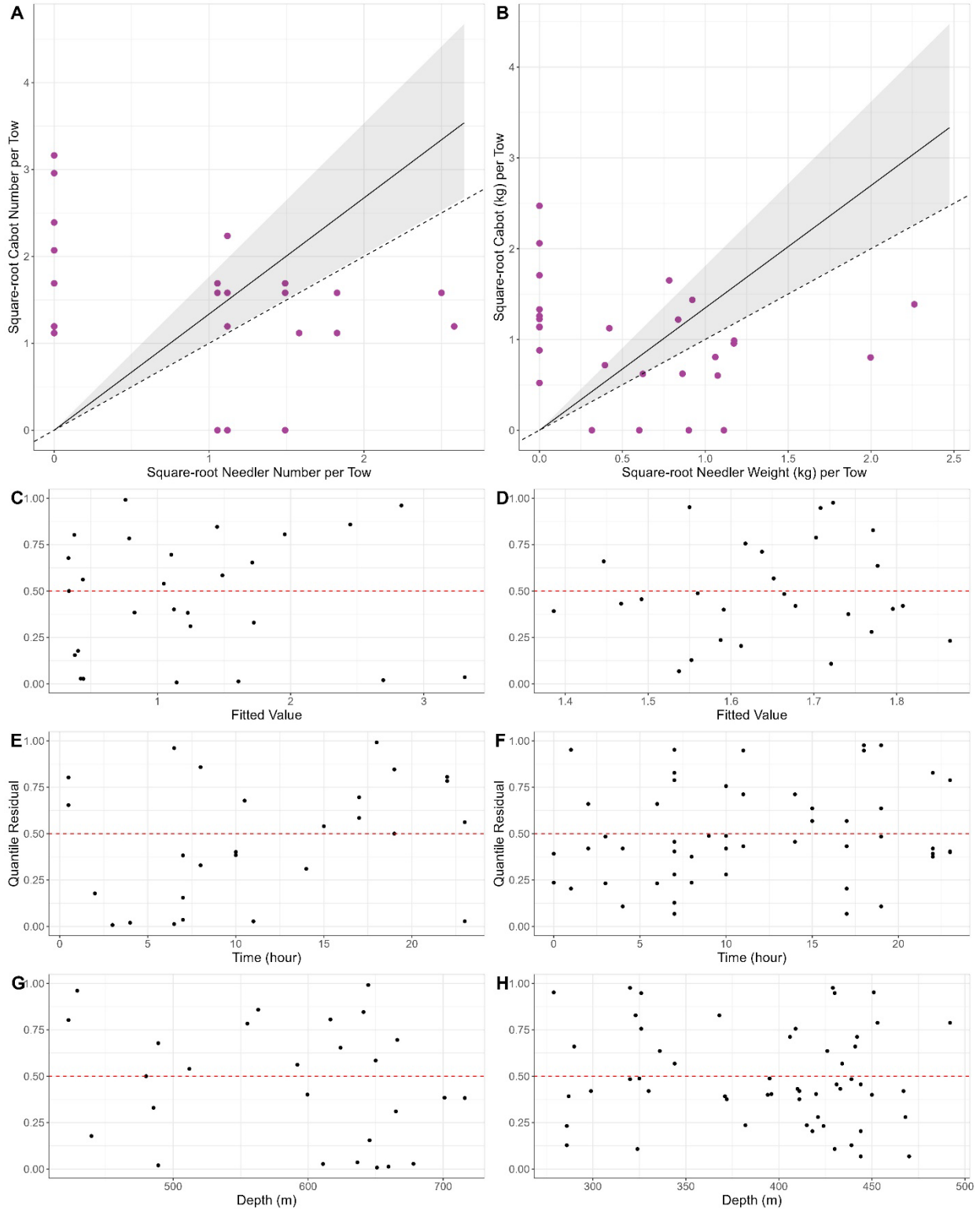


Figure A2-65. Results of size aggregated analysis for the CCGS Alfred Needler and CCGS John Cabot for catch of Wrymouth (*Cryptacanthodes maculatus*), fall 3KL.

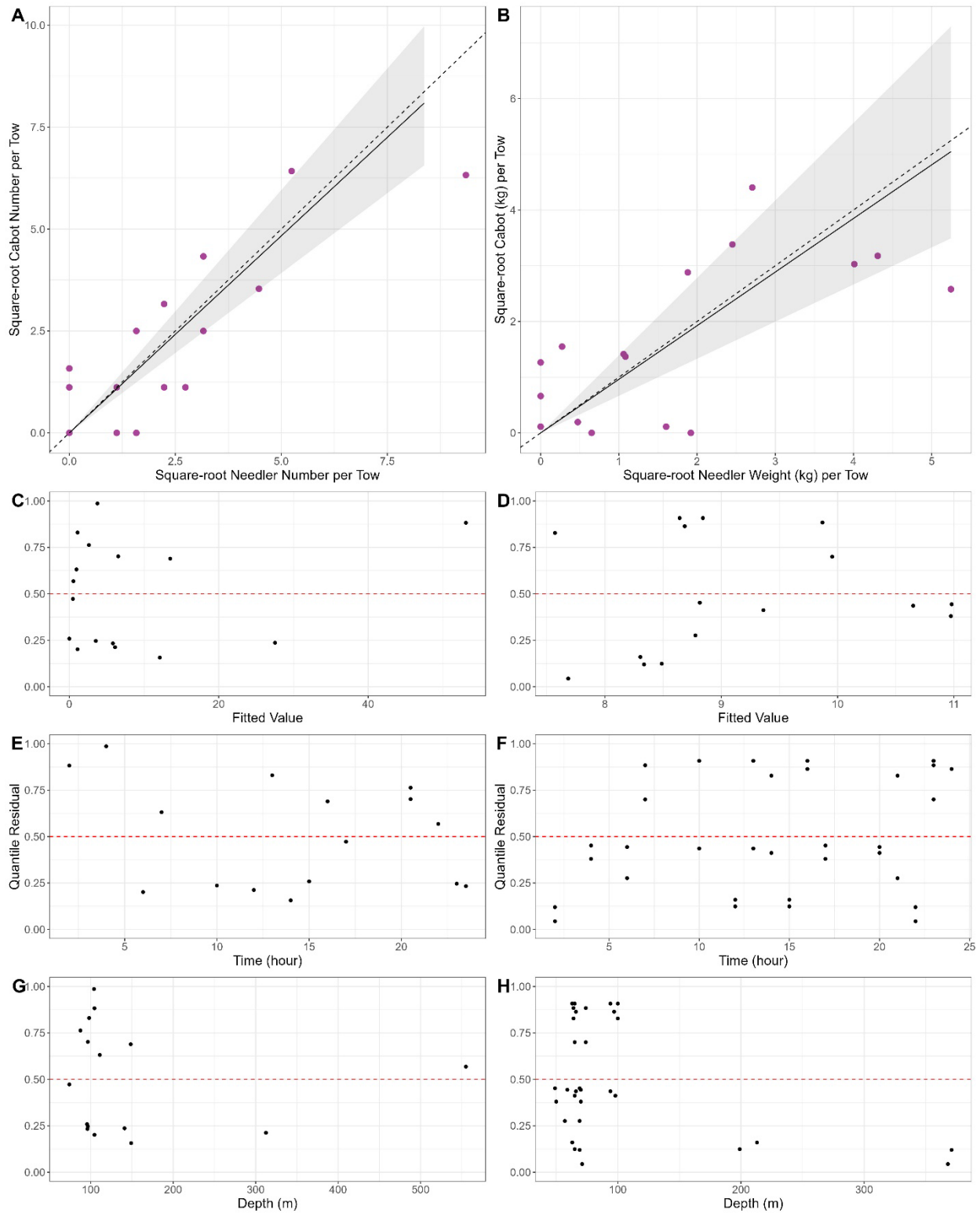


Figure A2-66. Results of size aggregated analysis for the CCGS Alfred Needler and CCGS John Cabot for catch of White Hake (*Urophycis tenuis*), fall 3KL. Data insufficient to determine if conversion is appropriate.

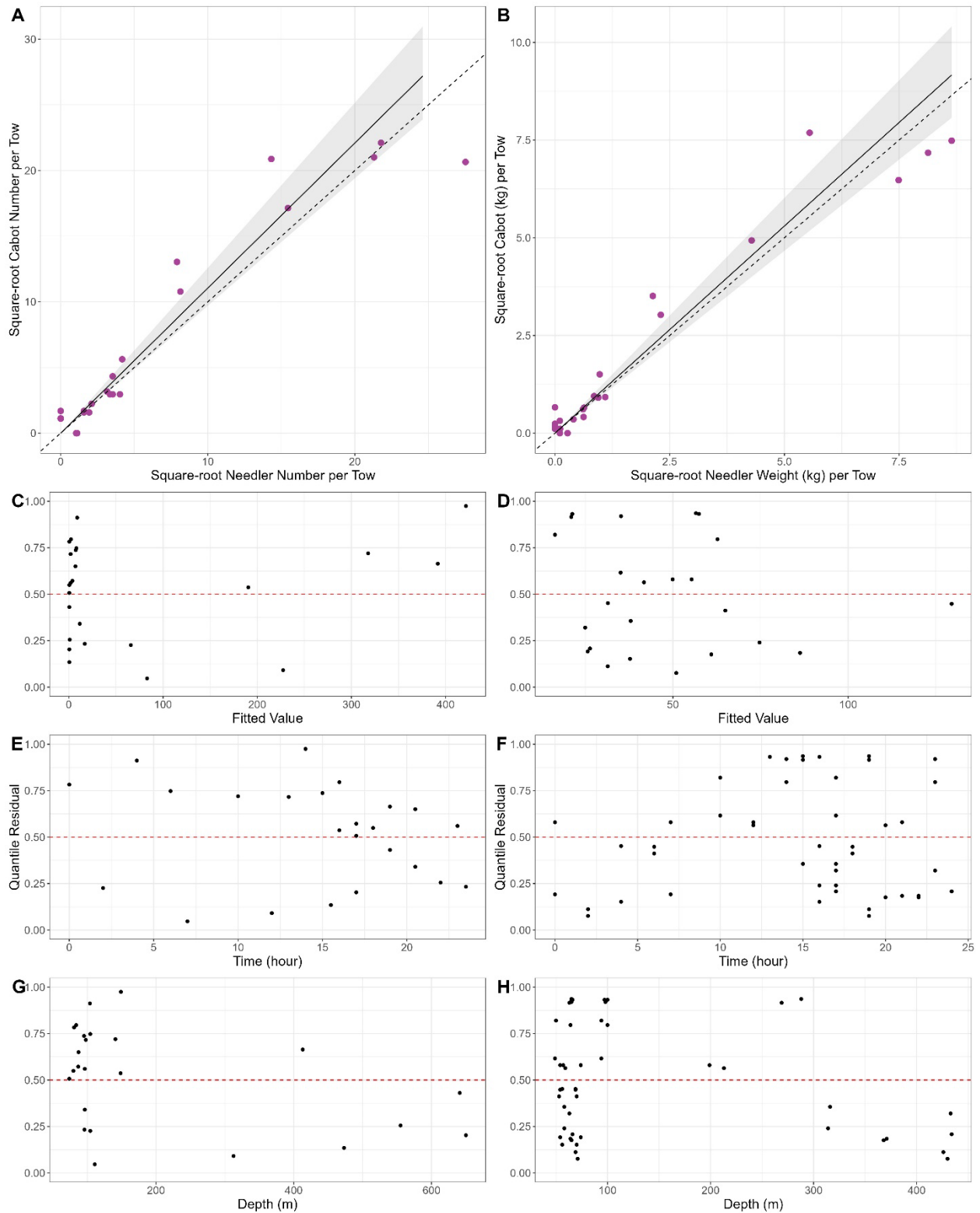


Figure A2-67. Results of size aggregated analysis for the CCGS Alfred Needler and CCGS John Cabot for catch of Silver Hake (*Merluccius bilinearis*), fall 3KL. Data insufficient to determine if conversion is appropriate.

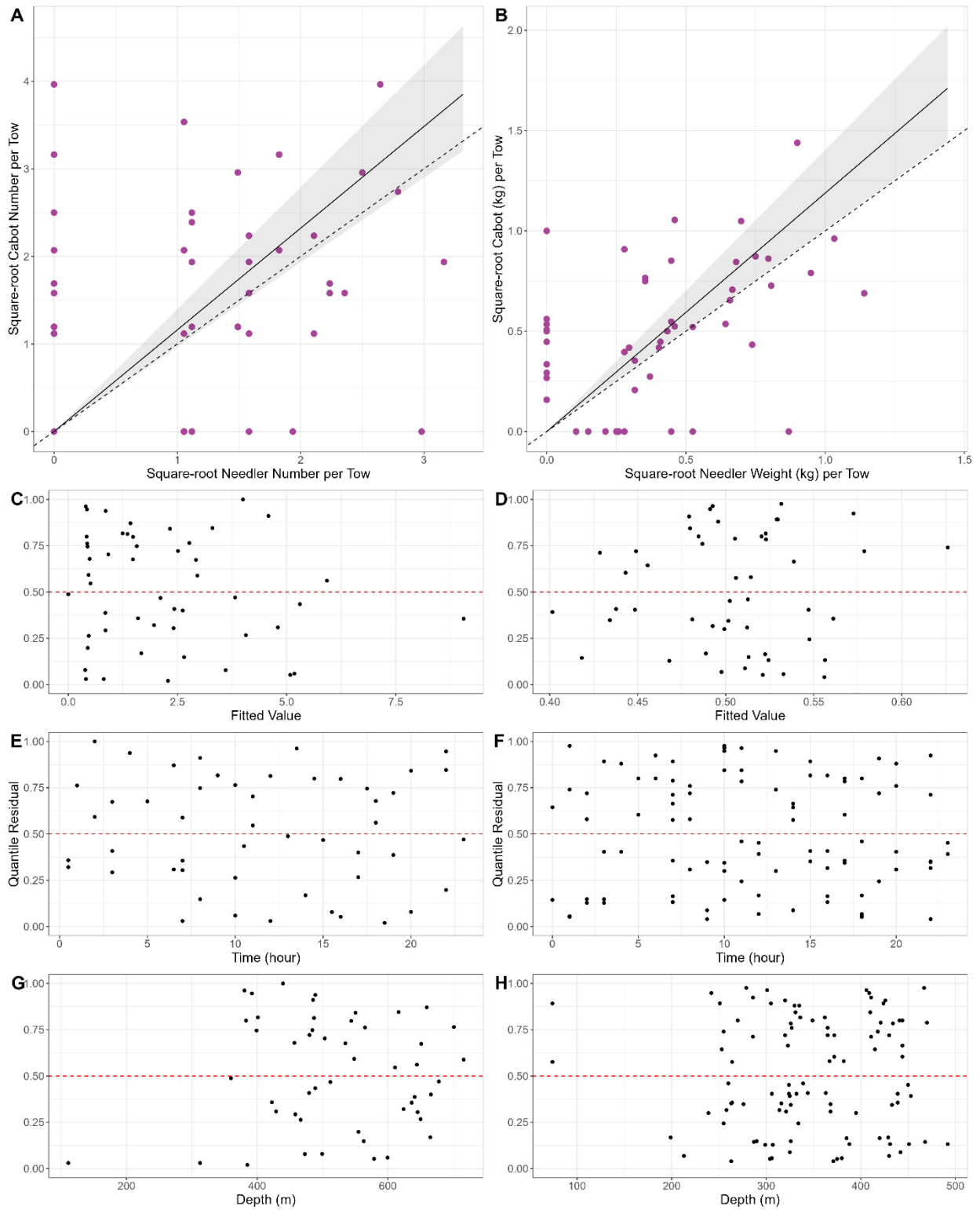


Figure A2-68. Results of size aggregated analysis for the CCGS Alfred Needler and CCGS John Cabot for catch of Rocklings (*Gaidropsarus* spp., *Enchelyopus* spp.), fall 3KL.

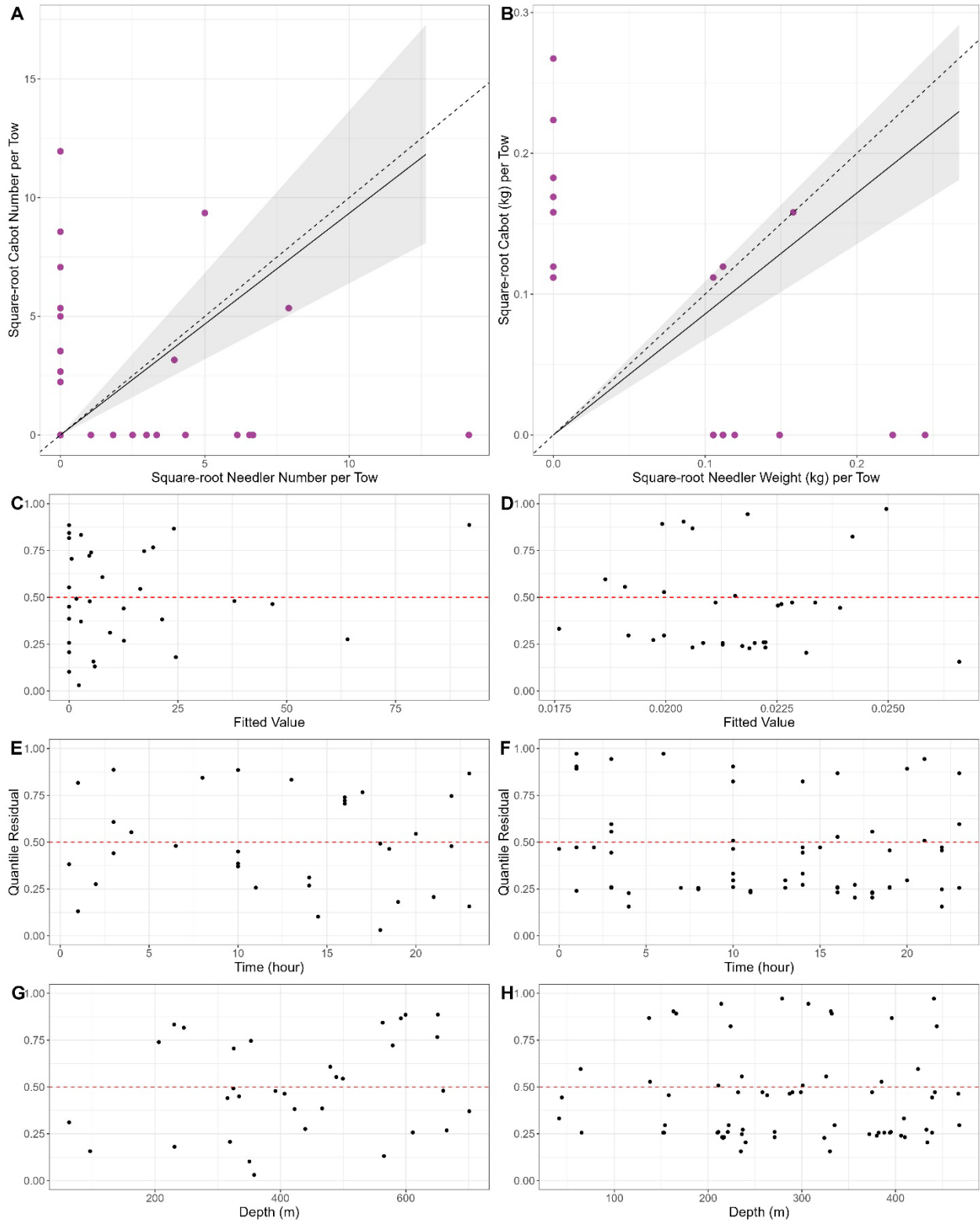


Figure A2-69. Results of size aggregated analysis for the CCGS Alfred Needler and CCGS John Cabot for catch of Amphipods (*Amphipoda*), fall 3KL. Data insufficient to determine if conversion is appropriate.

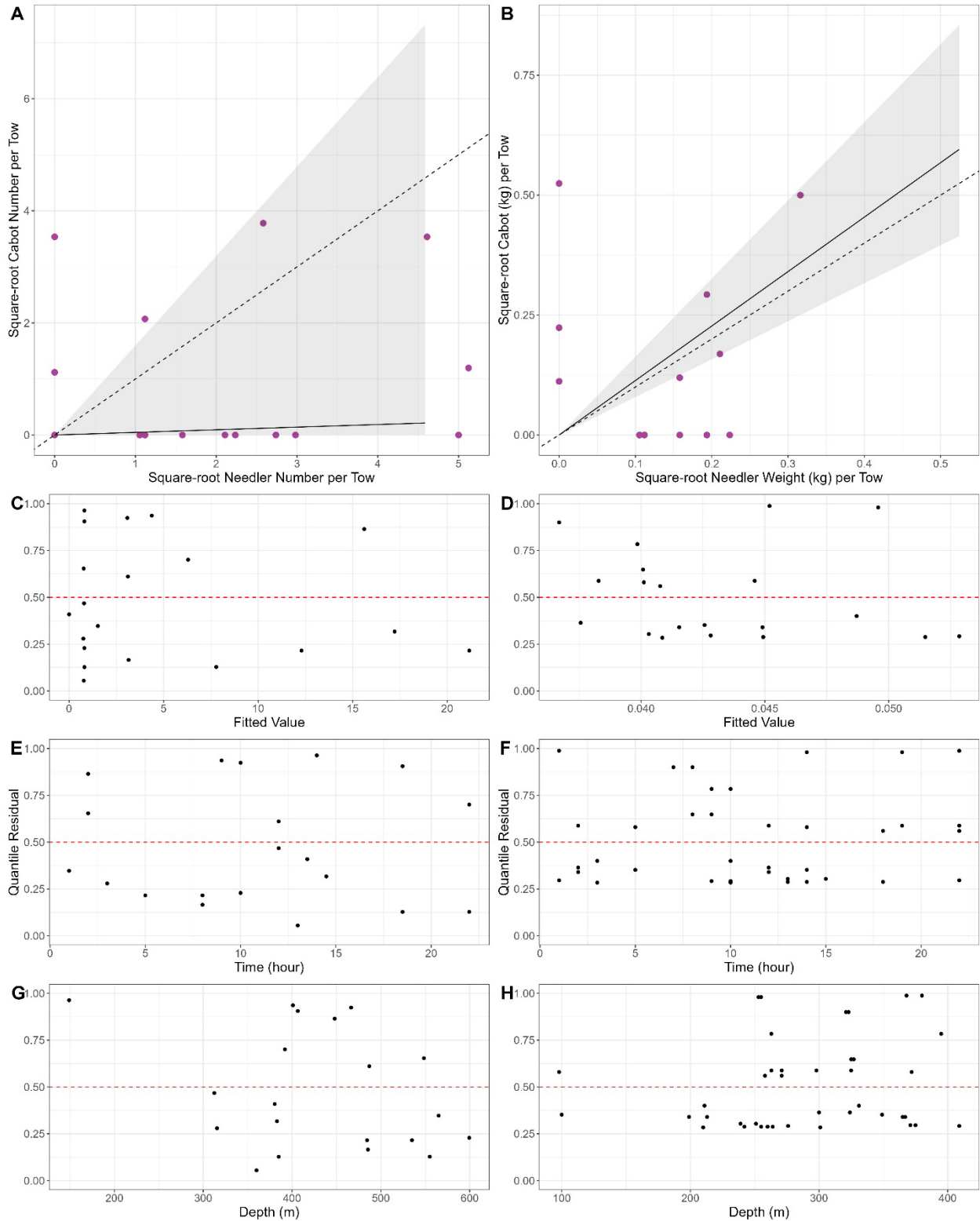


Figure A2-70. Results of size aggregated analysis for the CCGS Alfred Needler and CCGS John Cabot for catch of Cephalopods (Cephalopoda, excluding *Illex* spp., and *Gonatus* spp.), fall 3KL. Data insufficient to determine if conversion is appropriate.

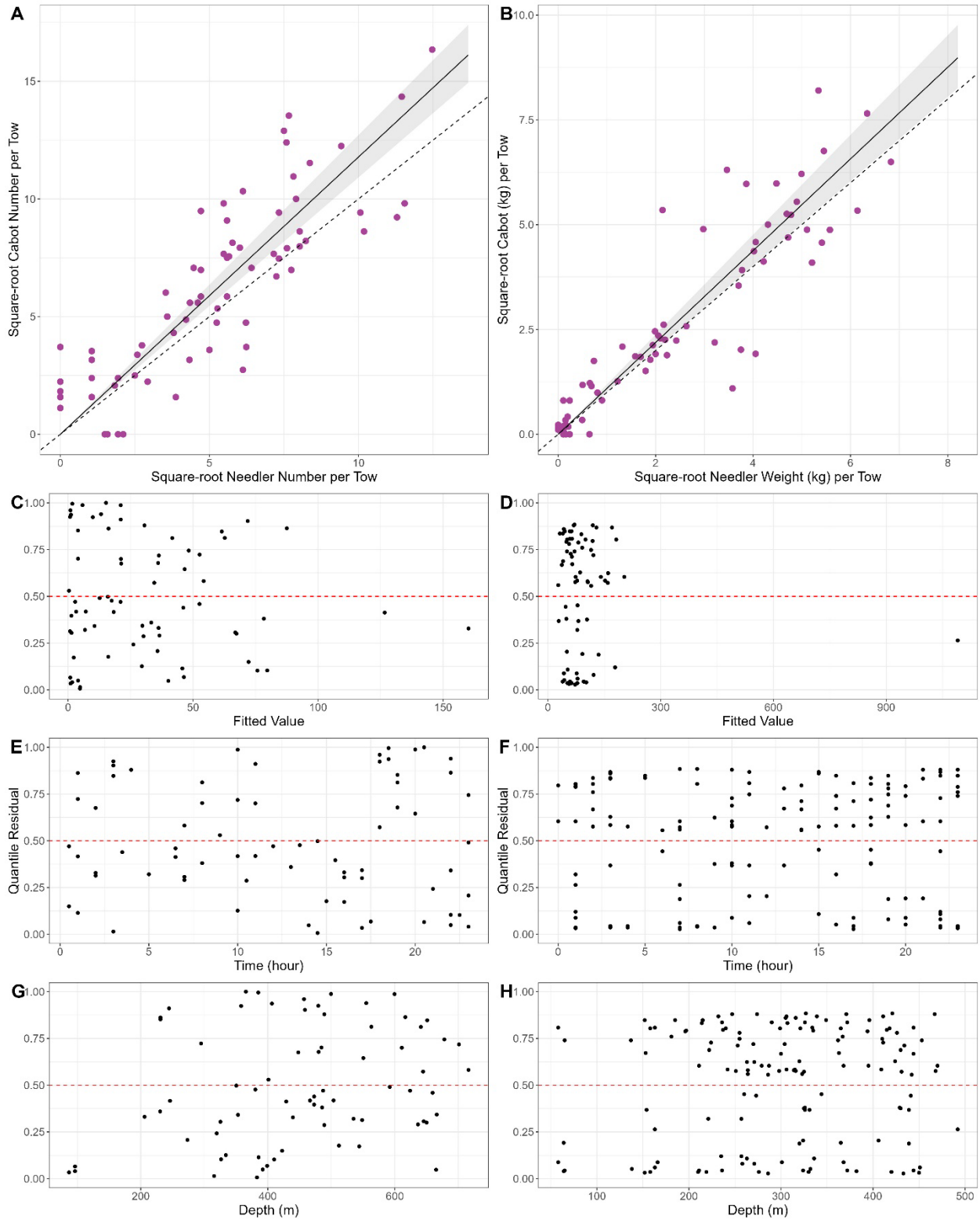


Figure A2-71. Results of size aggregated analysis for the CCGS Alfred Needler and CCGS John Cabot for catch of Snow Crab (*Chionoecetes opilio*), fall 3KL.

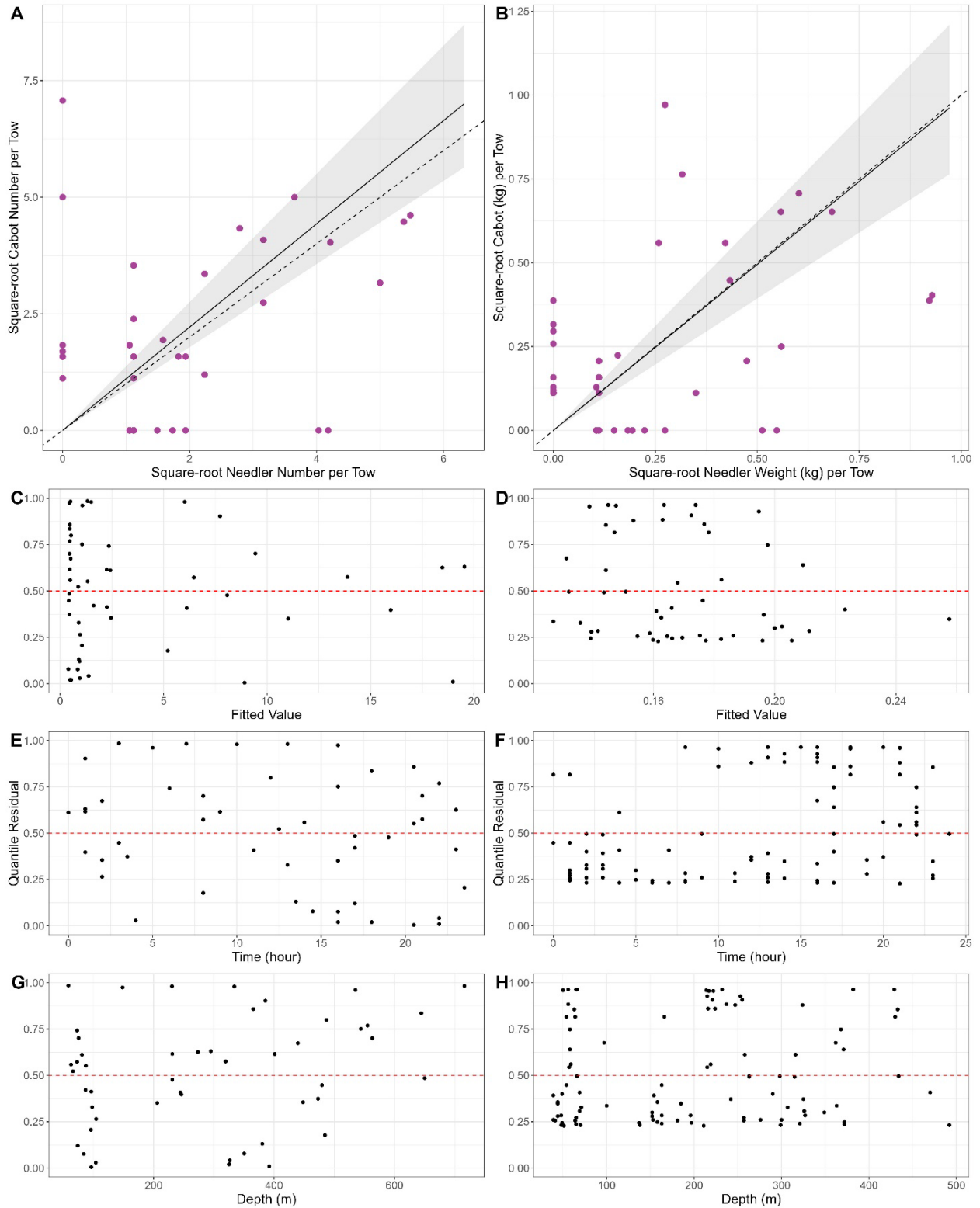


Figure A2-72. Results of size aggregated analysis for the CCGS Alfred Needler and CCGS John Cabot for catch of Toad crab (*Hyas* sp.), fall 3KL.

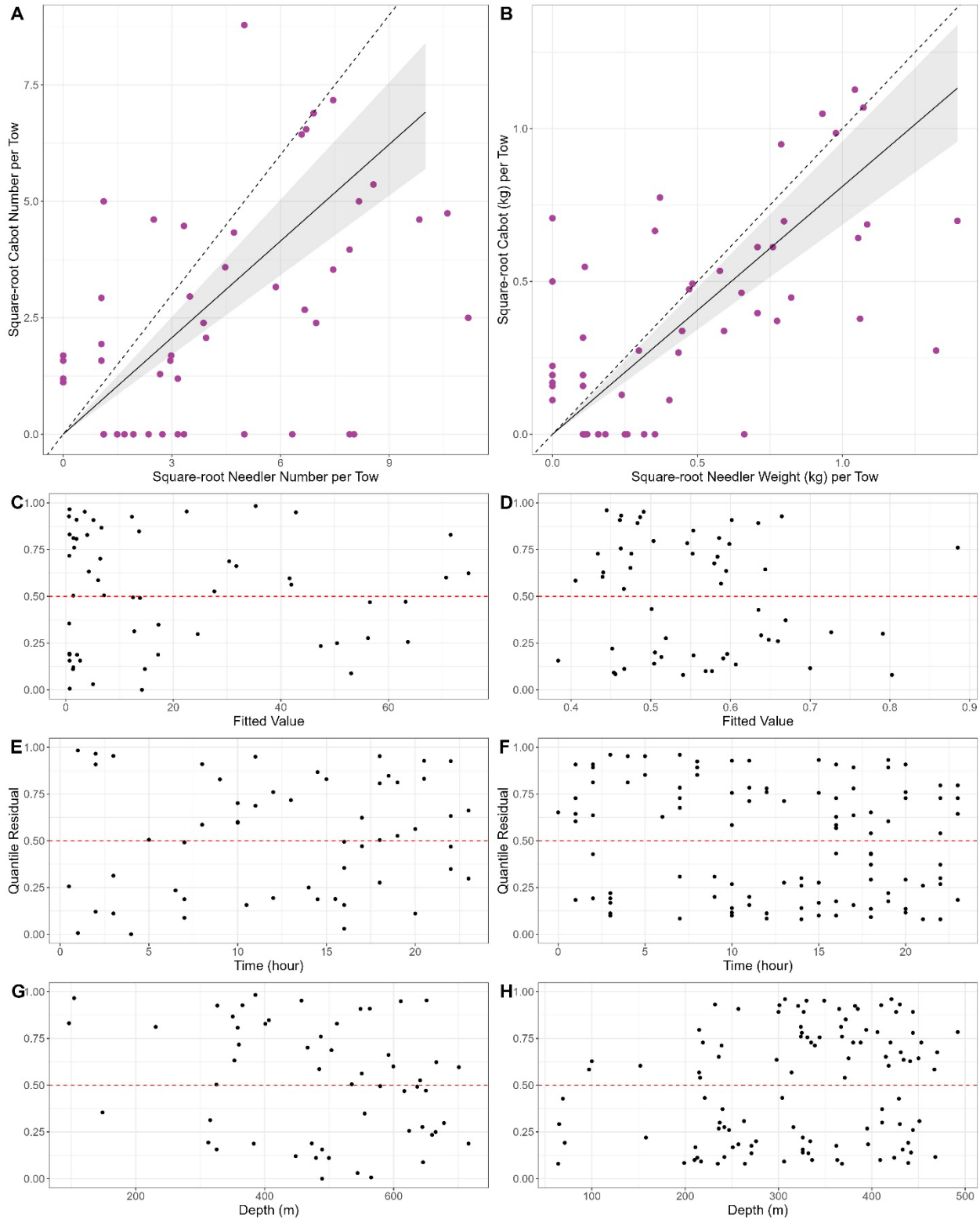


Figure A2-73. Results of size aggregated analysis for the CCGS Alfred Needler and CCGS John Cabot for catch of Squid (*Illex* spp. and *Gonatus* spp.), fall 3KL.

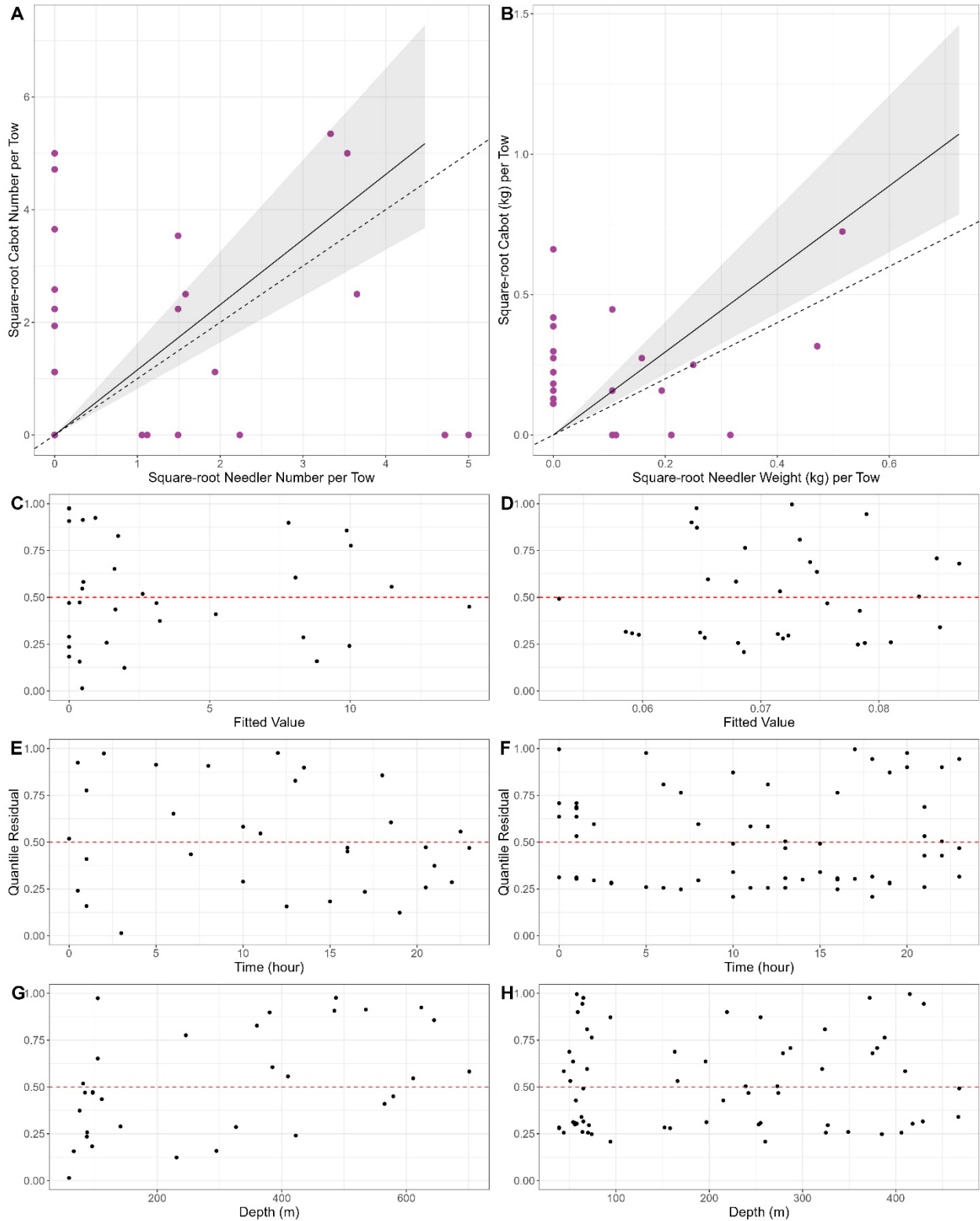


Figure A2-74. Results of size aggregated analysis for the CCGS Alfred Needler and CCGS John Cabot for catch of Polychaetes (*Polychaeta*), fall 3KL. Data insufficient to determine if conversion is appropriate.

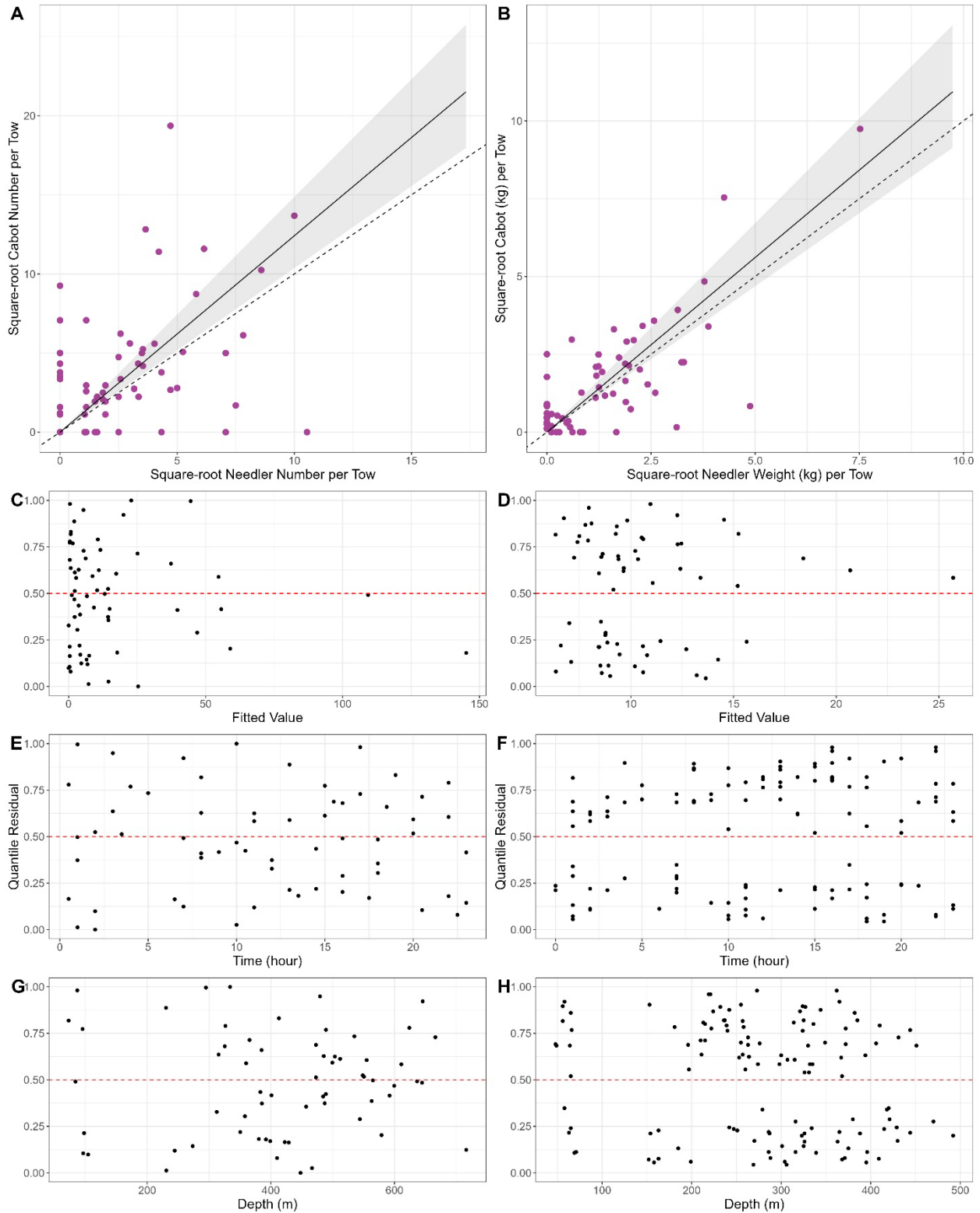


Figure A2-75. Results of size aggregated analysis for the CCGS Alfred Needler and CCGS John Cabot for catch of Sea anemones (*Actinaria*), fall 3KL.

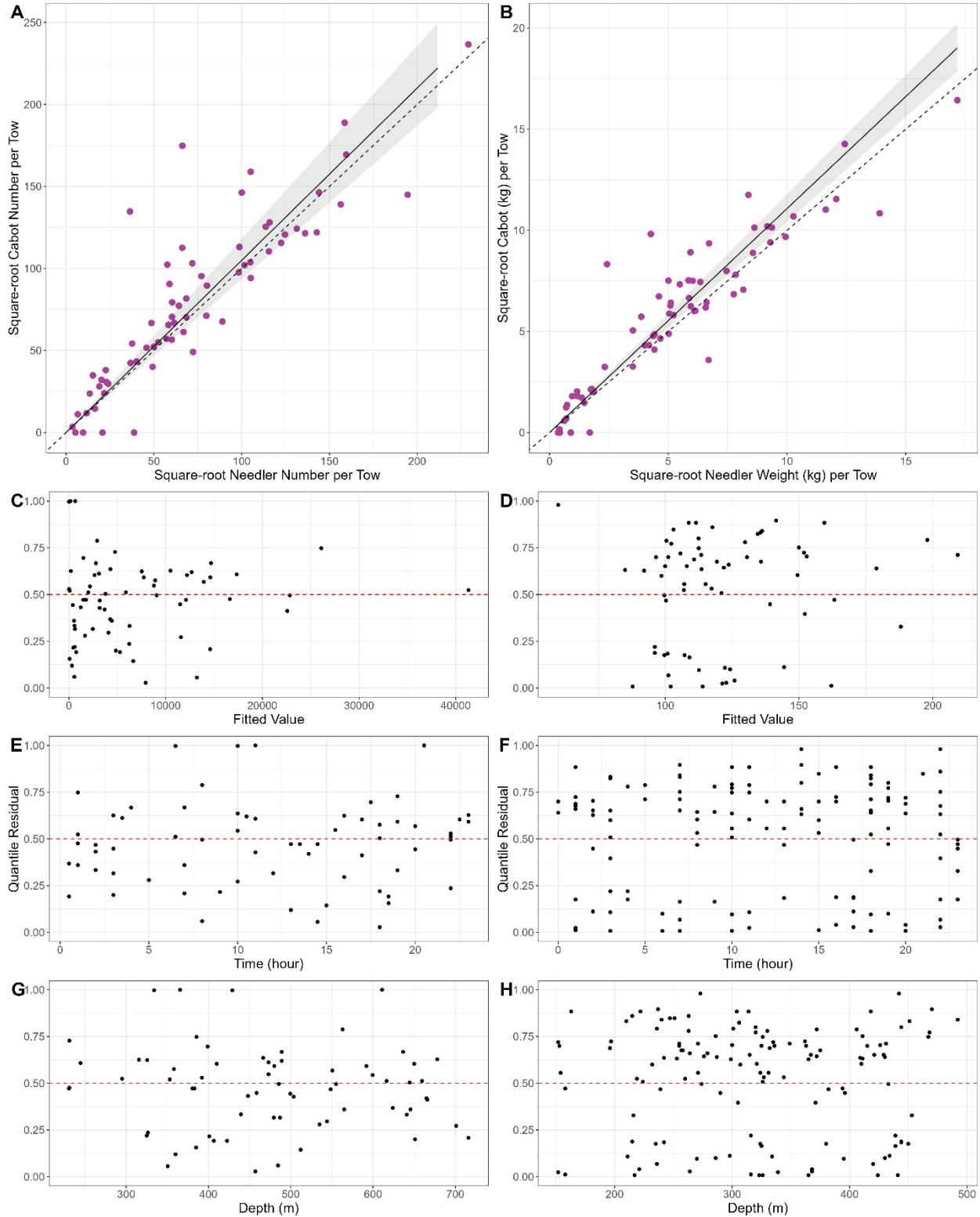


Figure A2-76. Results of size aggregated analysis for the CCGS Alfred Needler and CCGS John Cabot for catch of Northern Shrimp (*Pandalus borealis*), fall 3KL.

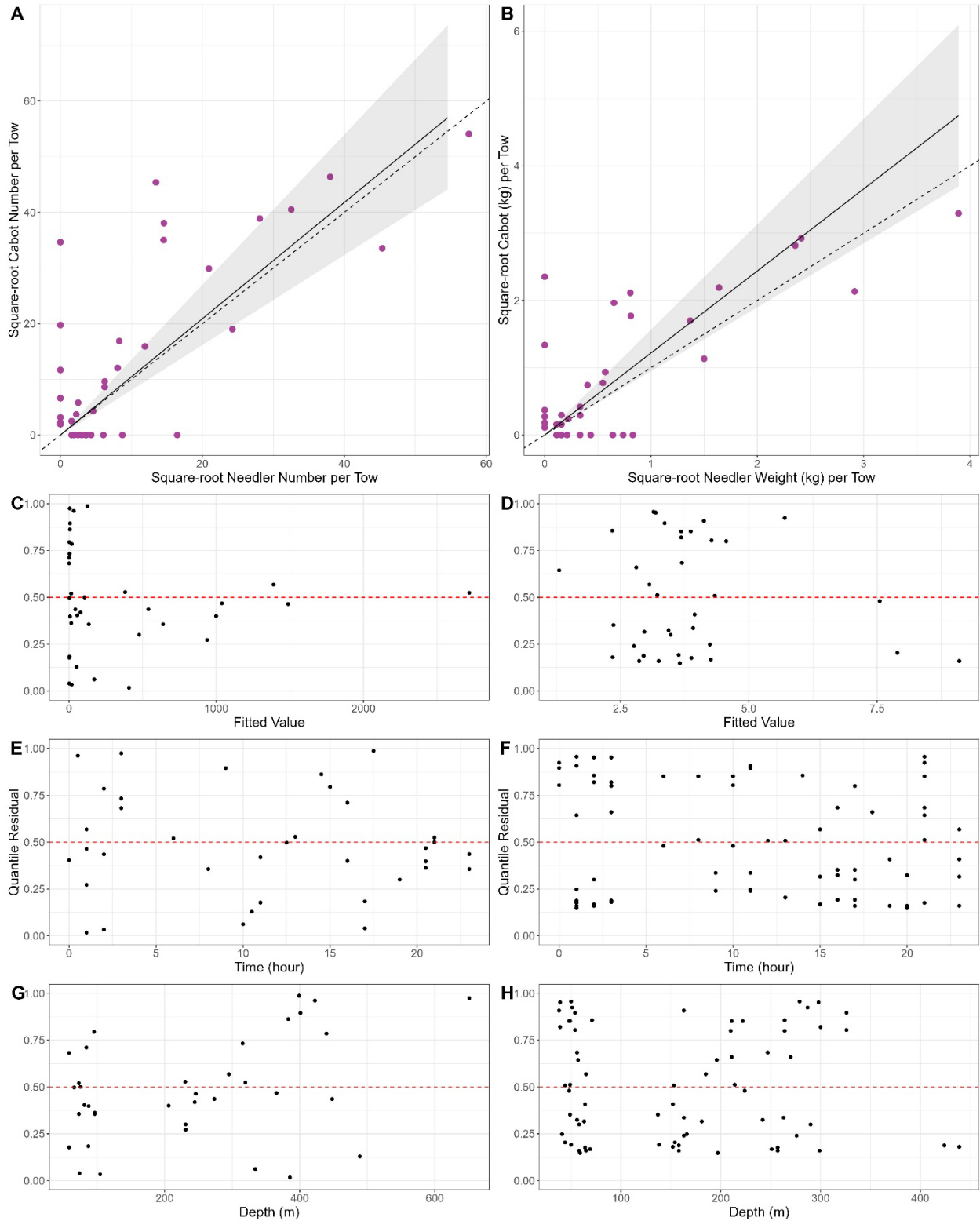


Figure A2-77. Results of size aggregated analysis for the CCGS Alfred Needler and CCGS John Cabot for catch of striped shrimp (*Pandalus montagui*), fall 3KL.

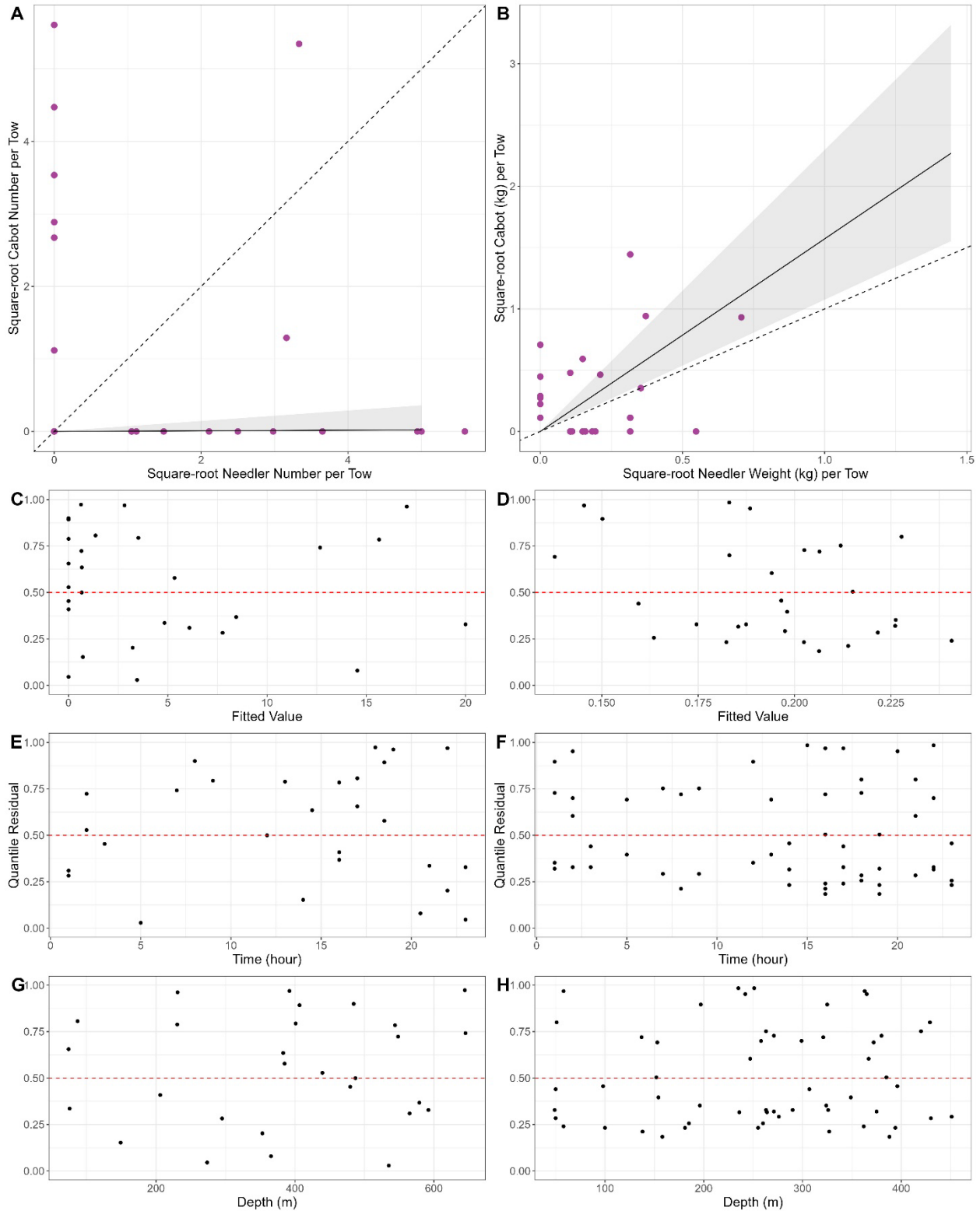


Figure A2-78. Results of size aggregated analysis for the CCGS Alfred Needler and CCGS John Cabot for catch of Sessile tunicates (*Tunicata*), fall 3KL. Data insufficient to determine if conversion is appropriate.

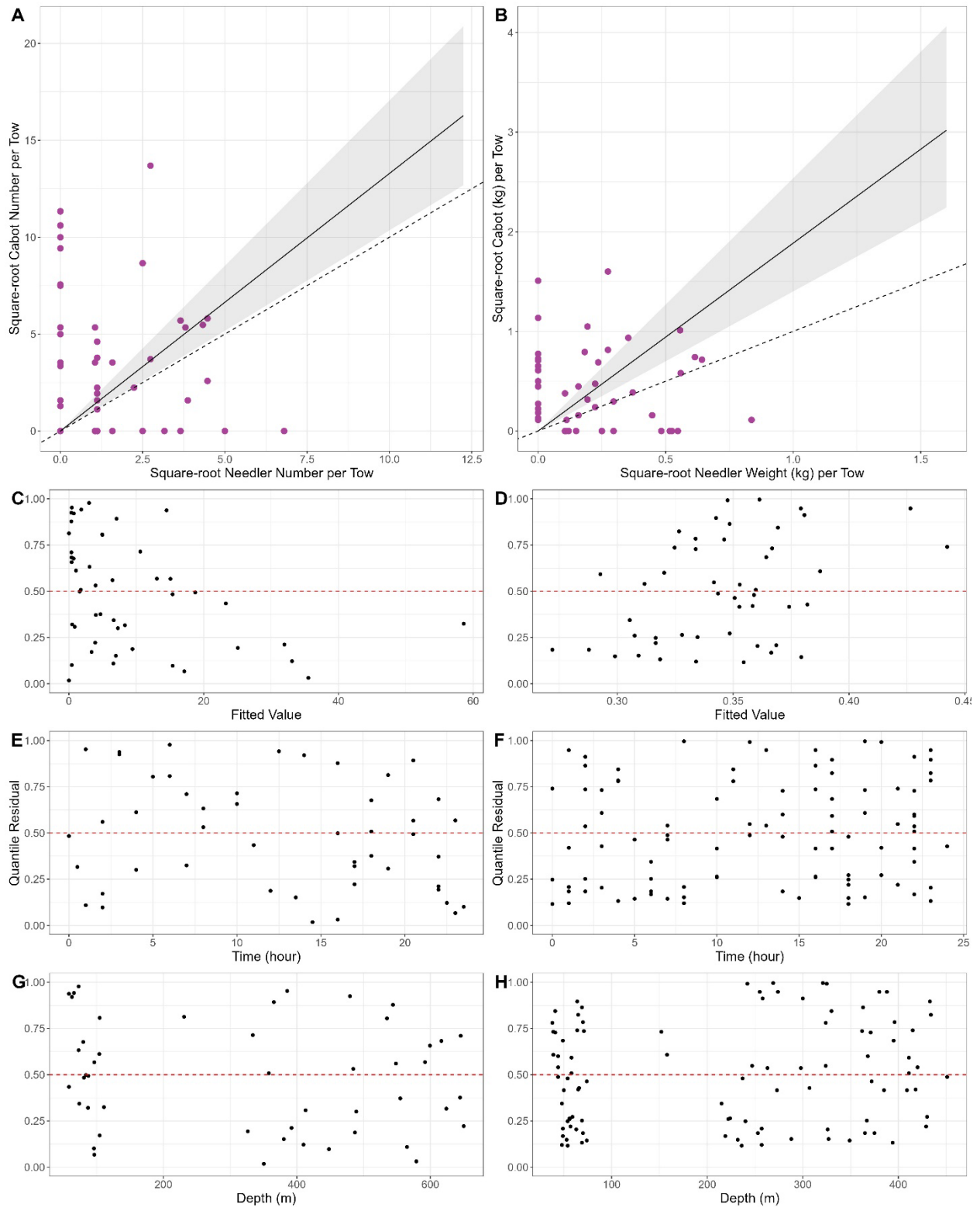


Figure A2-79. Results of size aggregated analysis for the CCGS Alfred Needler and CCGS John Cabot for catch of Gastropods (*Gastropoda*), fall 3KL.

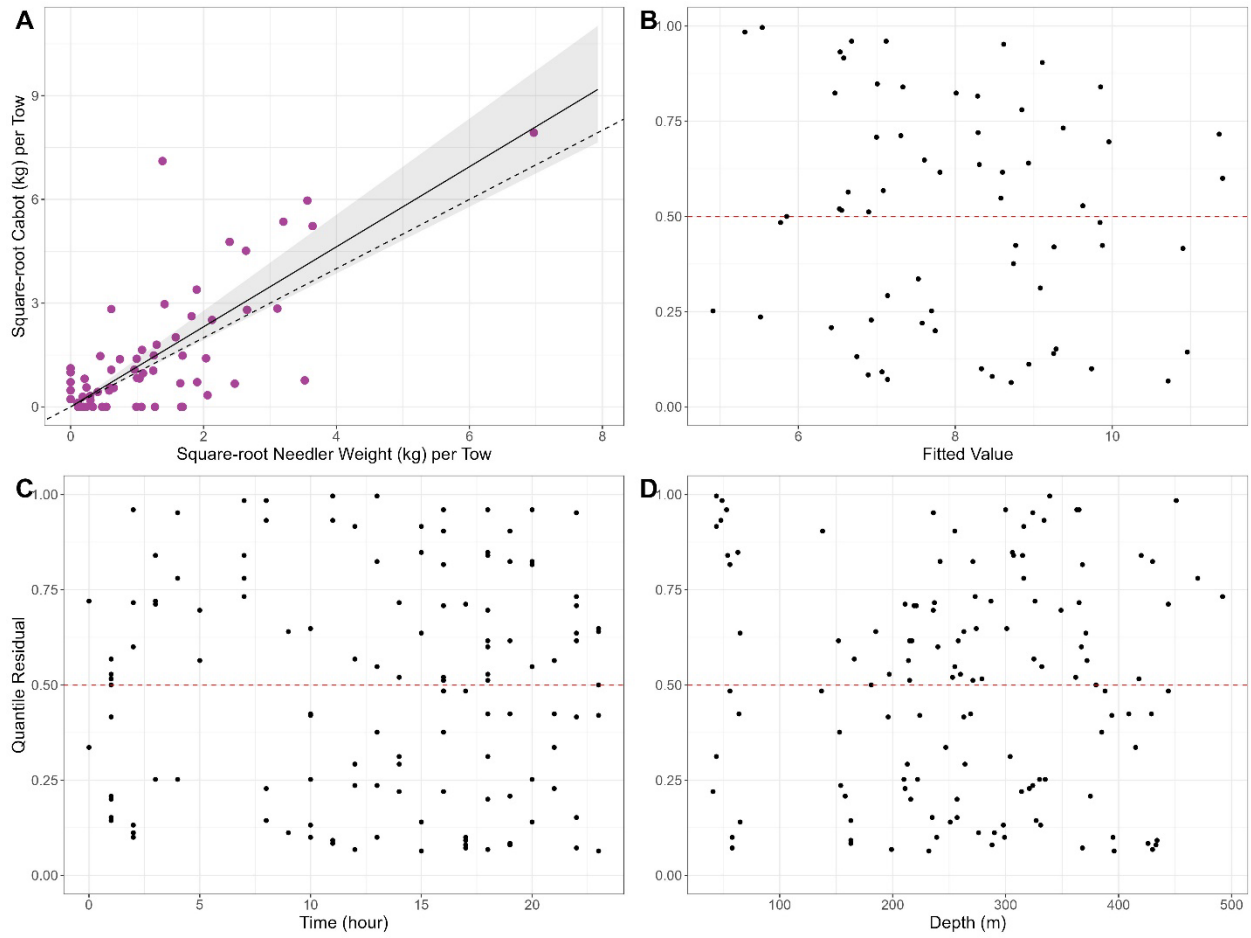


Figure A2–80. Results of size aggregated analysis for the CCGS Alfred Needler and CCGS John Cabot for catch of Sponge (*Porifera*), fall 3KL.

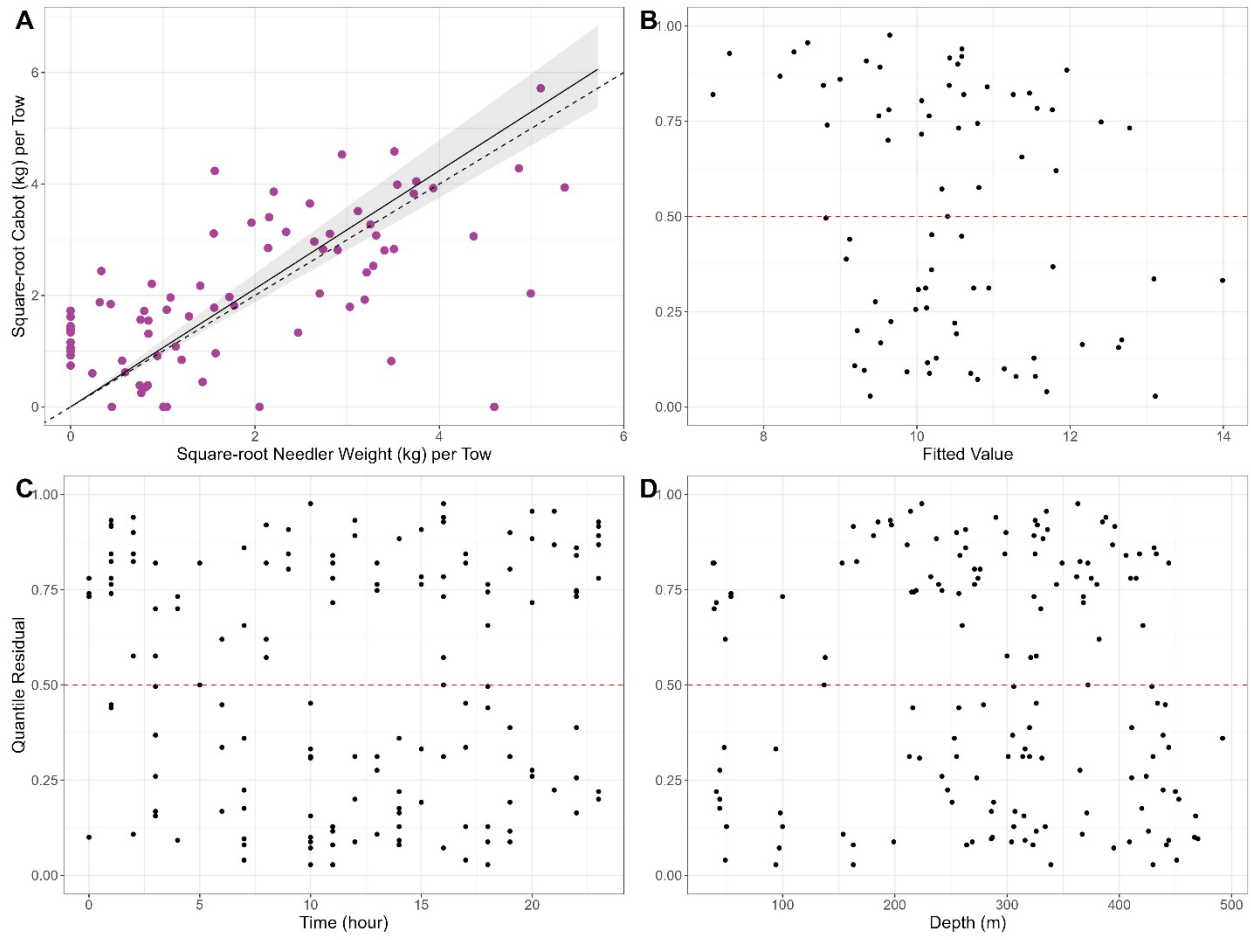


Figure A2-81. Results of size aggregated analysis for the CCGS Alfred Needler and CCGS John Cabot for catch of Jellyfish (Scyphozoa), fall 3KL.

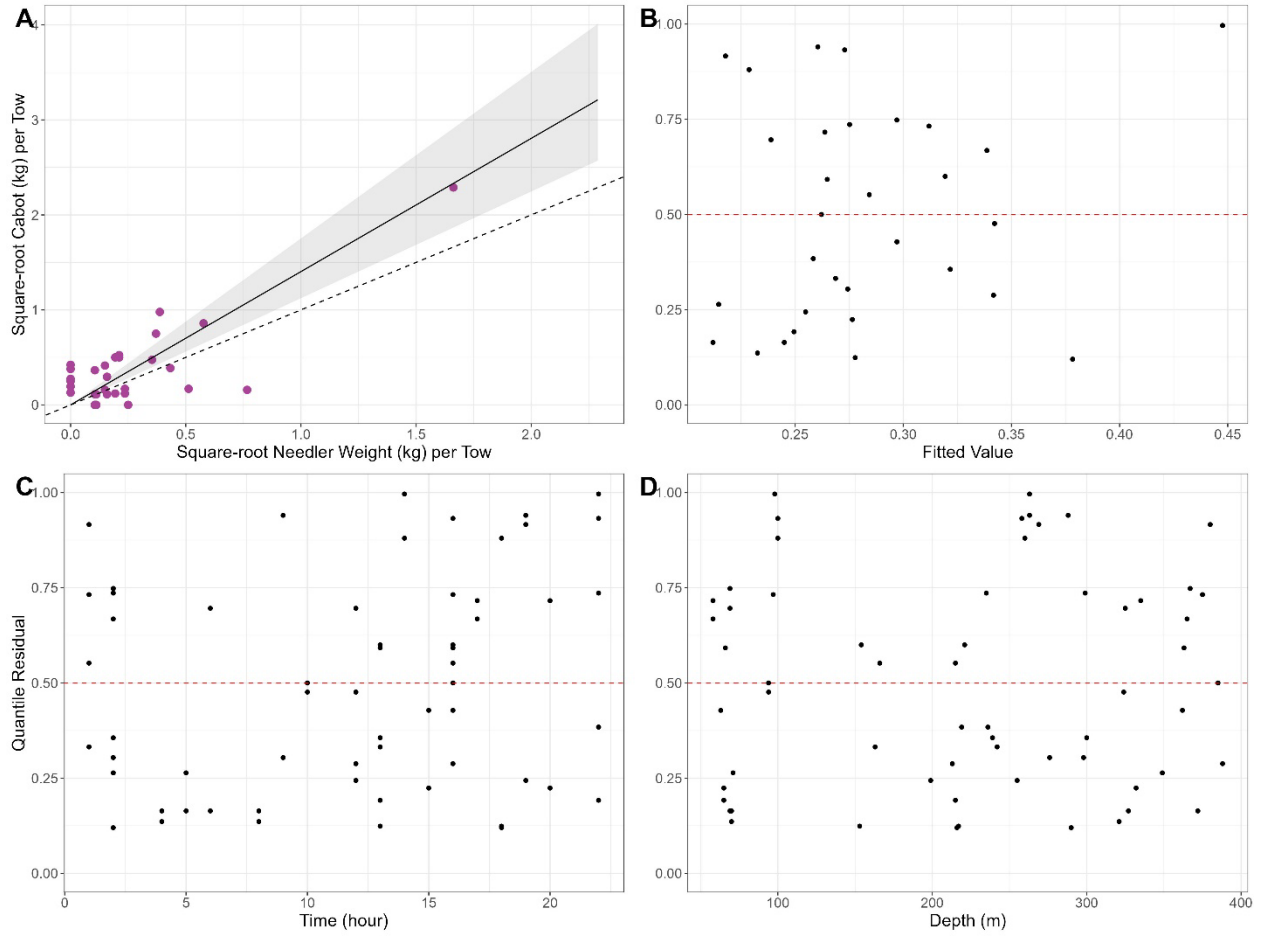


Figure A2-82. Results of size aggregated analysis for the CCGS Alfred Needler and CCGS John Cabot for catch of Brittlestars (*Ophiuroidea* except *Gorgonocephalus* spp), fall 3KL.

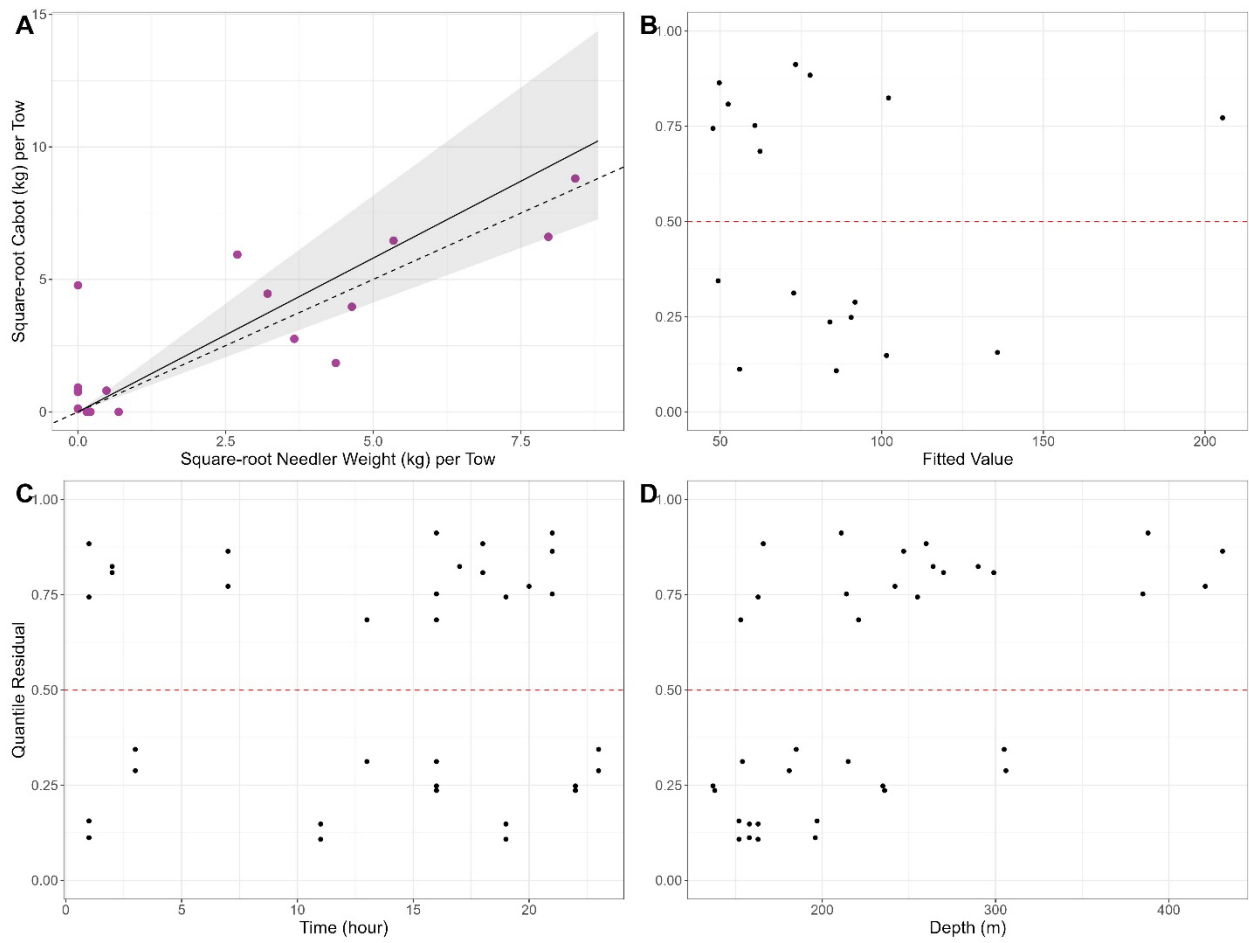


Figure A2-83. Results of size aggregated analysis for the CCGS Alfred Needler and CCGS John Cabot for catch of Basketstars (*Gorgonocephalus* spp.), fall 3KL.

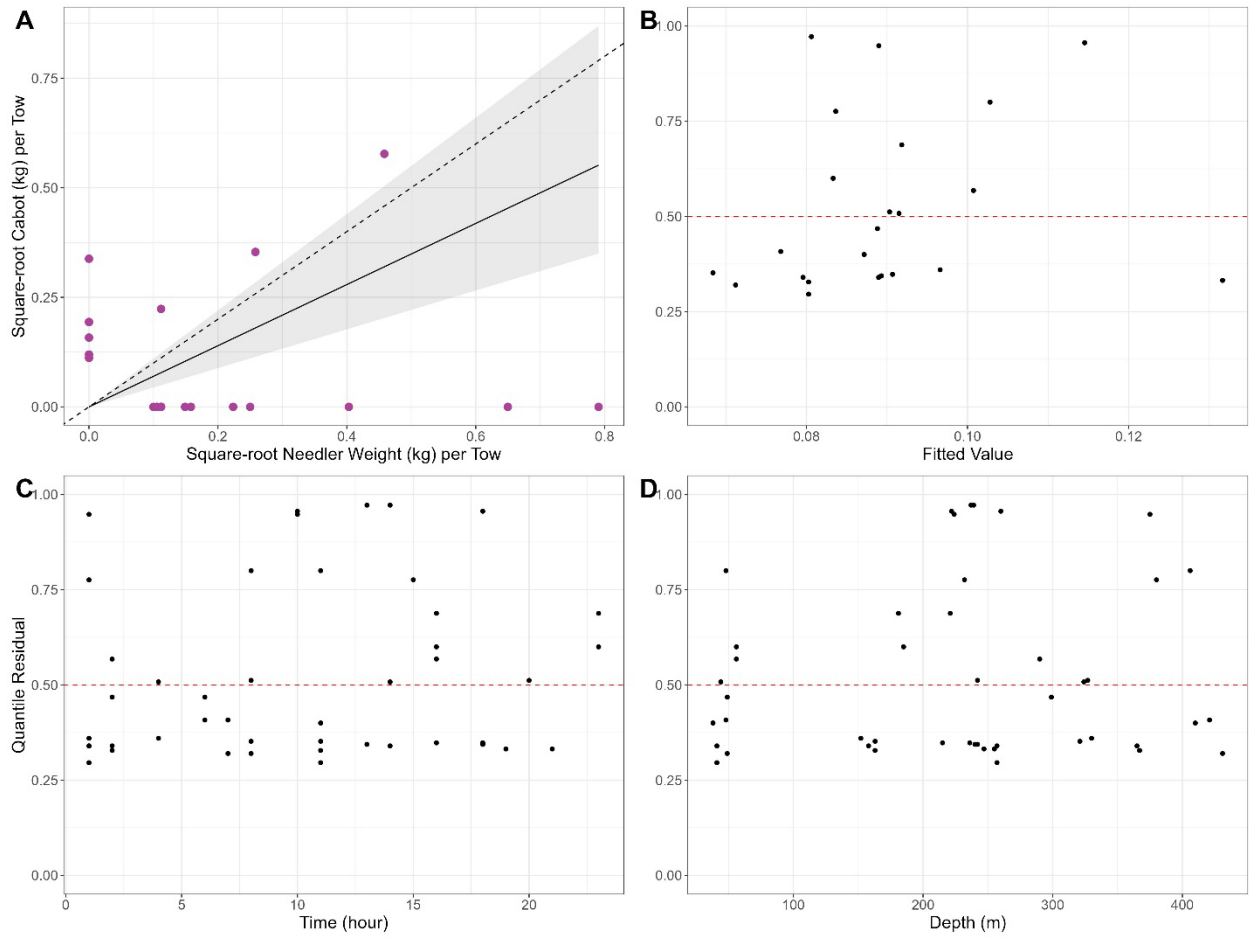


Figure A2-84. Results of size aggregated analysis for the CCGS Alfred Needler and CCGS John Cabot for catch of soft corals, fall 3KL. Data insufficient to determine if conversion is appropriate.

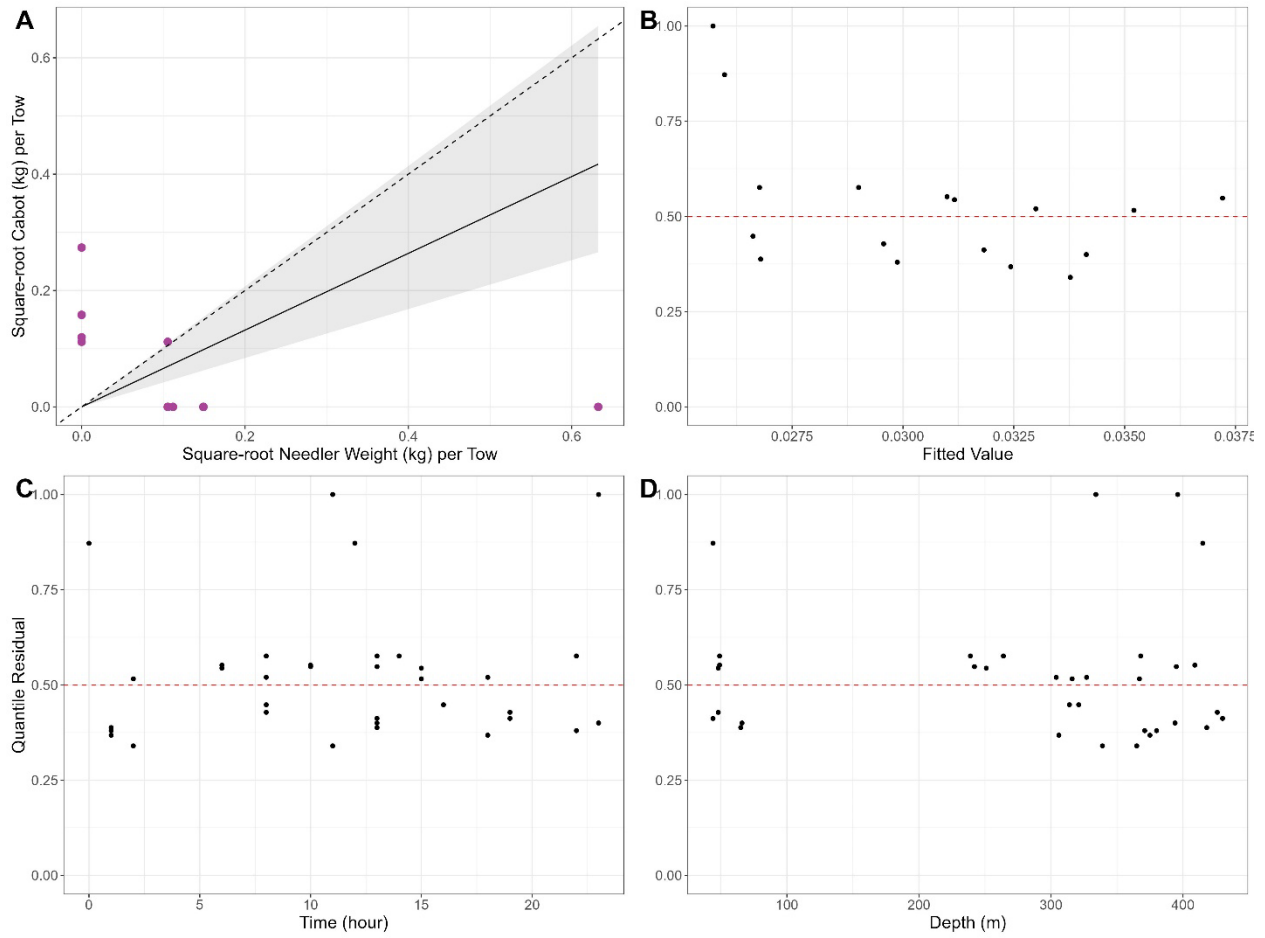


Figure A2-85. Results of size aggregated analysis for the CCGS Alfred Needler and CCGS John Cabot for catch of Bryozonans (Bryozoa), fall 3KL. Data insufficient to determine if conversion is appropriate.

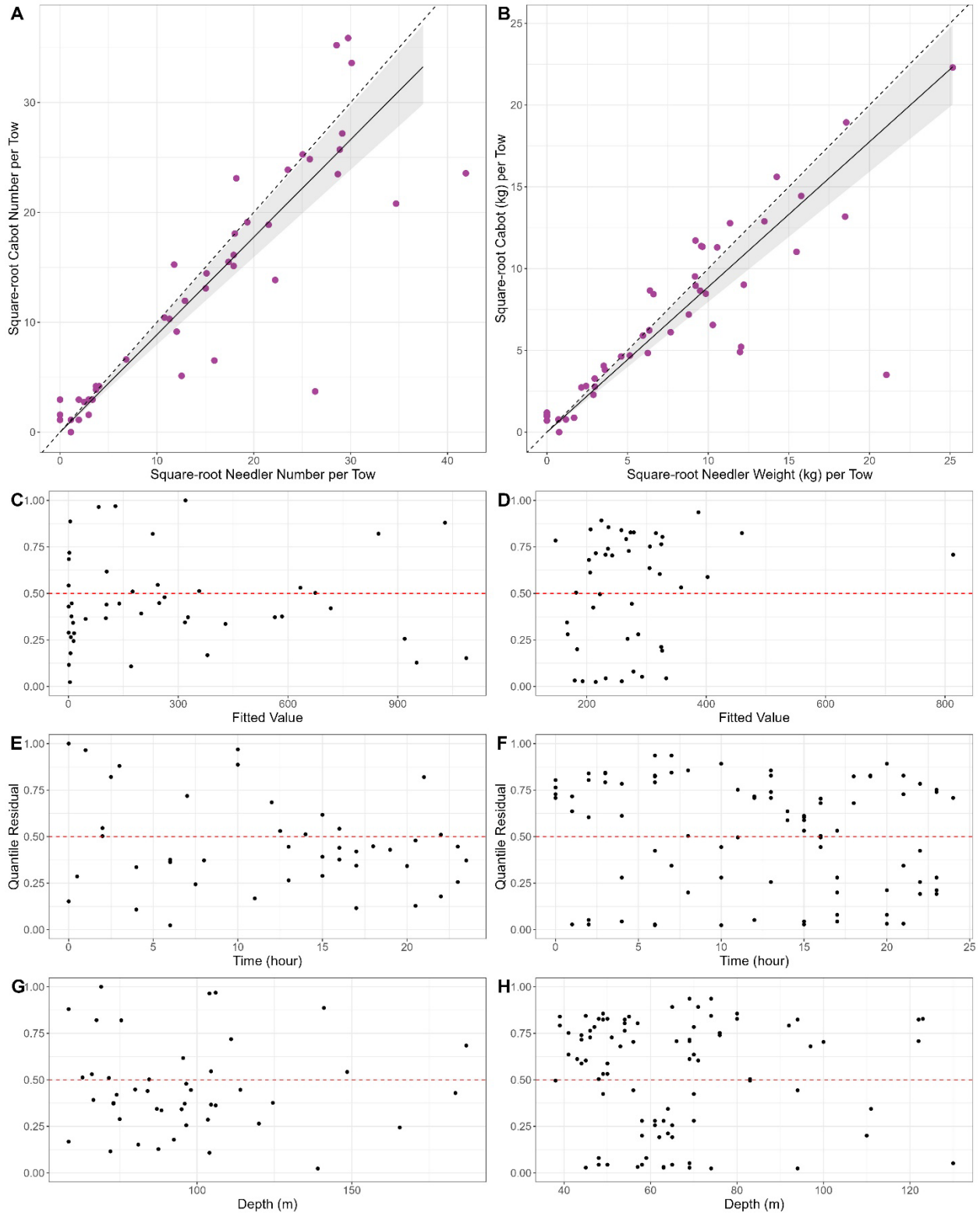


Figure A2-86. Results of size aggregated analysis for the CCGS Alfred Needler and CCGS John Cabot for catch of Yellowtail Flounder (*Myxopsetta ferruginea*), spring and fall 3LNOPs.

APPENDIX 3: DIVERSITY, COMMUNITY COMPOSITION, AND BENTHIC HABITAT IN COMPARATIVE SETS

FIGURES

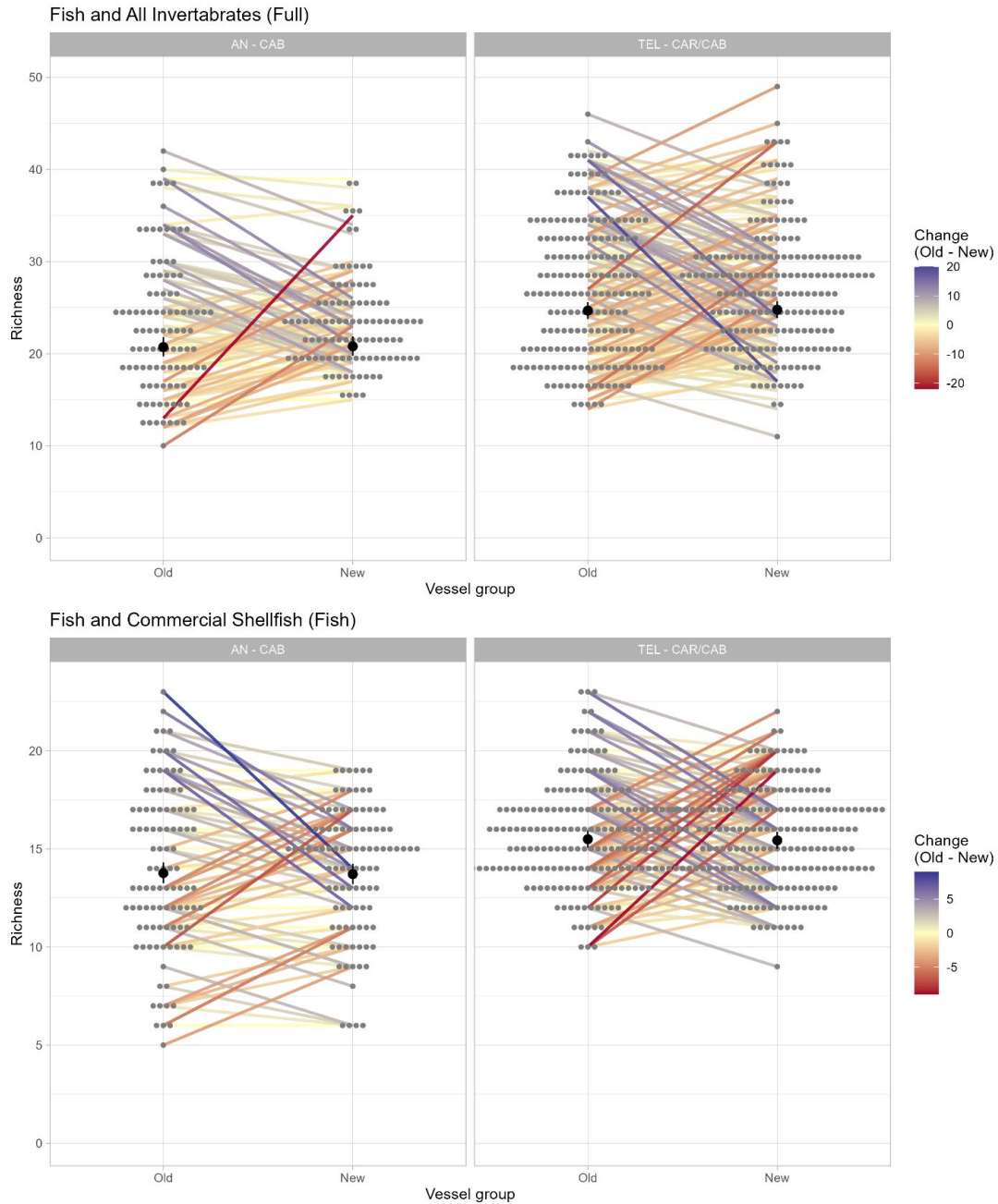


Figure A3–1. Observed richness in all sets summarized by vessel group (Old = CCGS Teleost and CCGS Alfred Needler, New = CCGS John Cabot and CCGS Capt. Jacques Cartier) and pair group (AN – CAB = Needler – Cabot pairs, TEL – CAR/CAB = Teleost – Cartier/Cabot pairs) in grey dots. Colored lines connect paired sets with the color and length reflecting the difference between the Old vessel vs New vessel. Longer higher intensity lines are larger difference between paired sets. The black dot with error bar is the model estimated parameter and 95% CI. Full community is the top panel with all fish and invertebrates, and bottom panel is the fish and commercial invertebrates only.

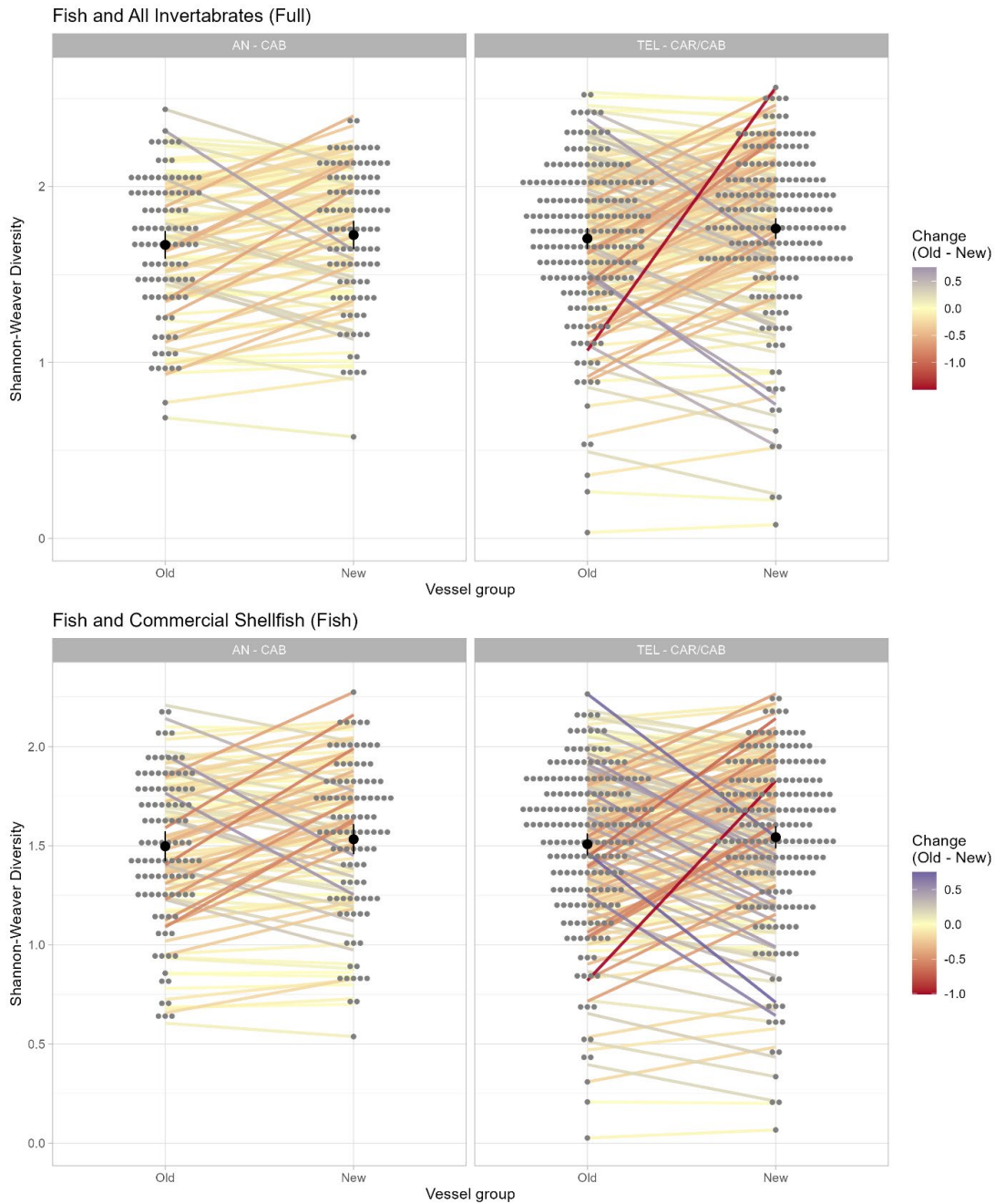


Figure A3–2. Observed Shannon-Weaver Diversity in all sets summarized by vessel group (Old = CCGS Teleost and CCGS Alfred Needler, New = CCGS John Cabot and CCGS Capt. Jacques Cartier) and pair group (AN – CAB = Needler – Cabot pairs, TEL – CAR/CAB = Teleost – Cartier/Cabot pairs) in grey dots. Colored lines connect paired sets with the color and length reflecting the difference between the Old vessel vs New vessel. Longer higher intensity lines are larger difference between paired sets. The black dot with error bar is the model estimated parameter and 95% CI. Full community is the top panel with all fish and invertebrates, and bottom panel is the fish and commercial invertebrates only.

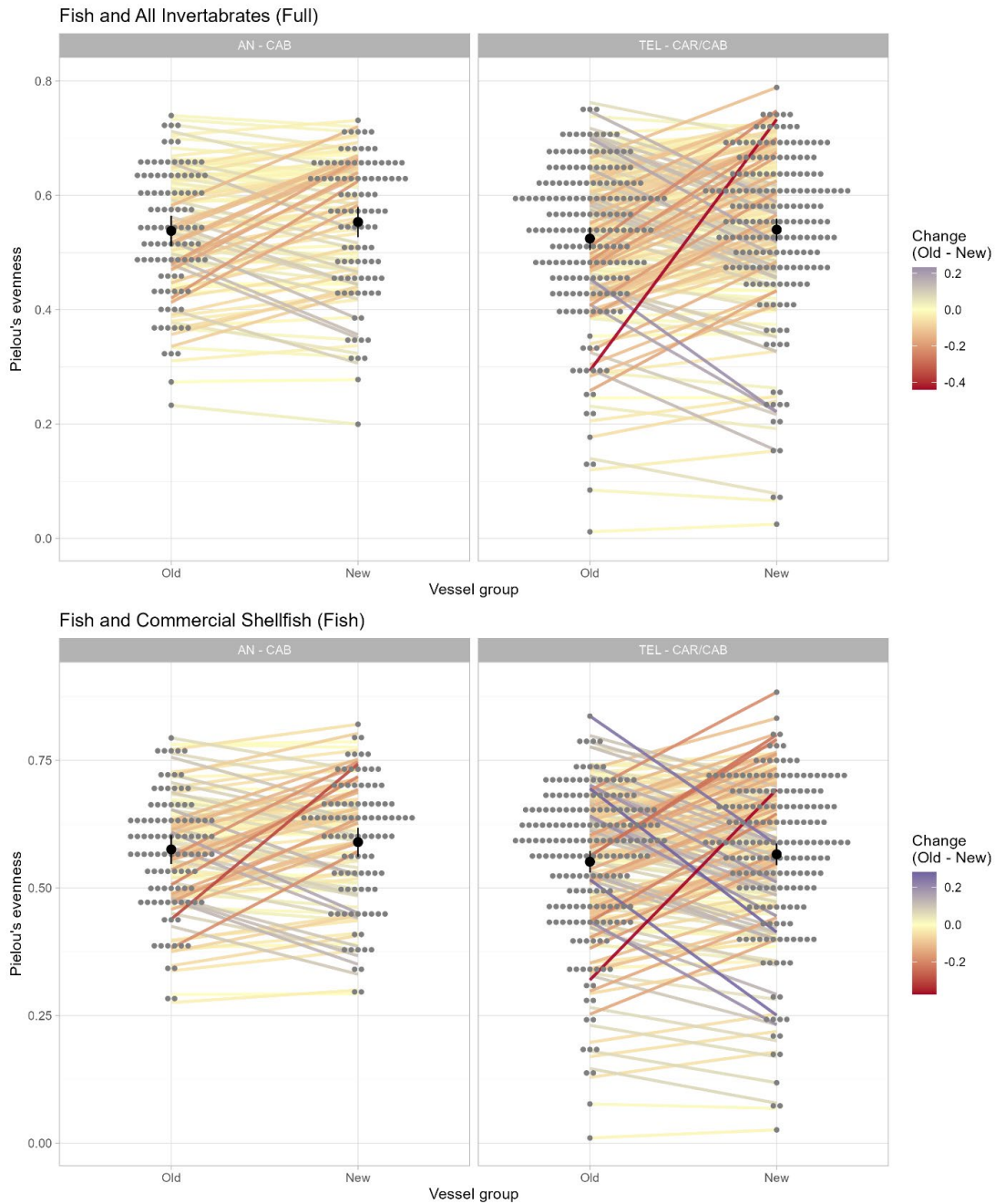


Figure A3–3. Observed Pielou’s evenness in all sets summarized by vessel group (Old = CCGS Teleost and CCGS Alfred Needler, New = CCGS John Cabot and CCGS Capt. Jacques Cartier) and pair group (AN – CAB = Needler – Cabot pairs, TEL – CAR/CAB = Teleost – Cartier/Cabot pairs) in grey dots. Colored lines connect paired sets with the color and length reflecting the difference between the Old vessel vs New vessel. Longer higher intensity lines are larger difference between paired sets. The black dot with error bar is the model estimated parameter and 95% CI. Full community is the top panel with all fish and invertebrates, and bottom panel is the fish and commercial invertebrates only.

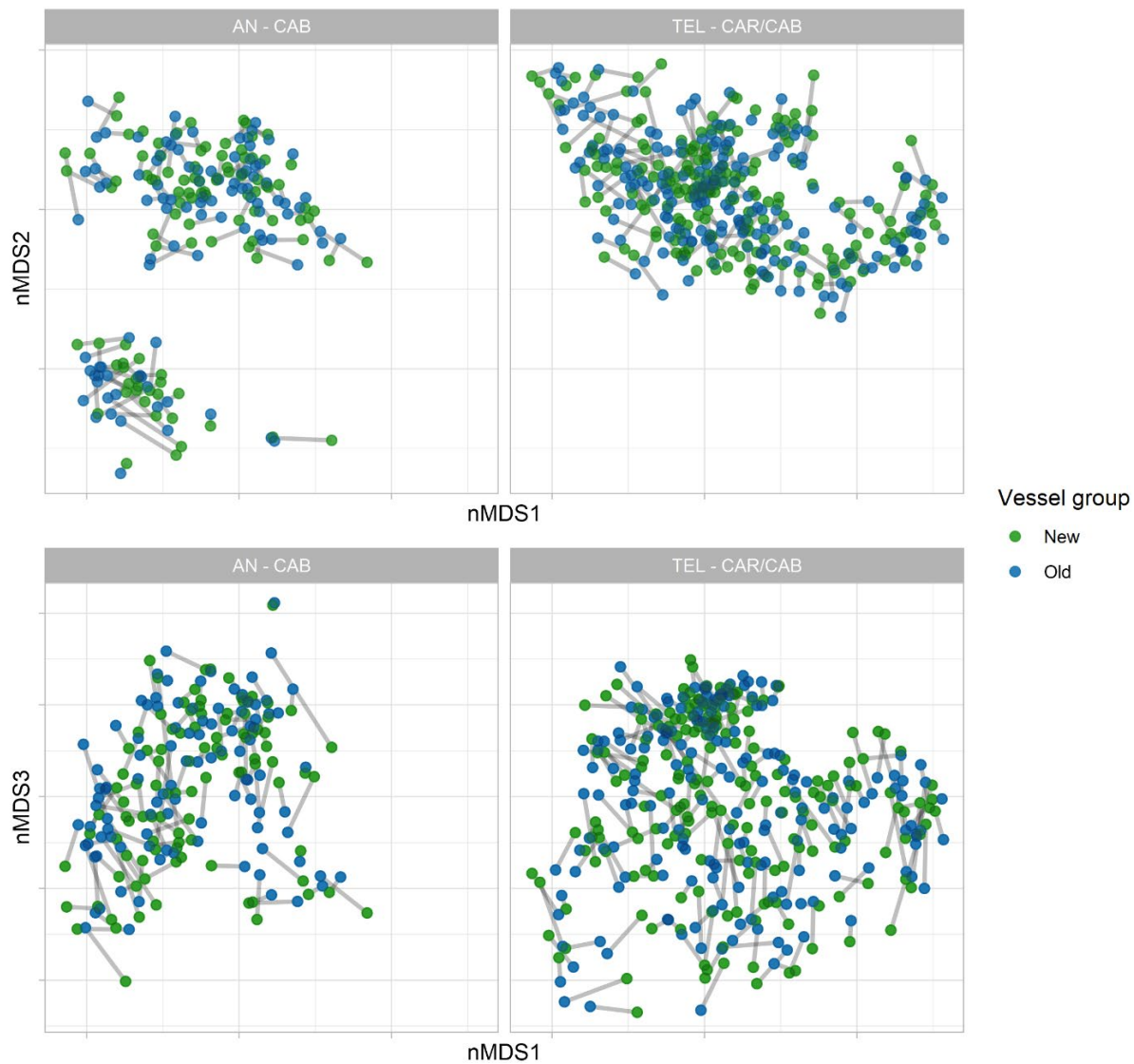


Figure A3–4. nMDS of full community with fish and all invertebrates. Color of the dots represents vessel group and grey line connecting the paired sets. CCGS Alfred Needler & CCGS John Cabot pairs on left and CCGS Teleost & CCGS John Cabot/Capt. Jacques Cartier pairs on right. Top panel is the first two dimensions and bottom panels the first and third dimensions.

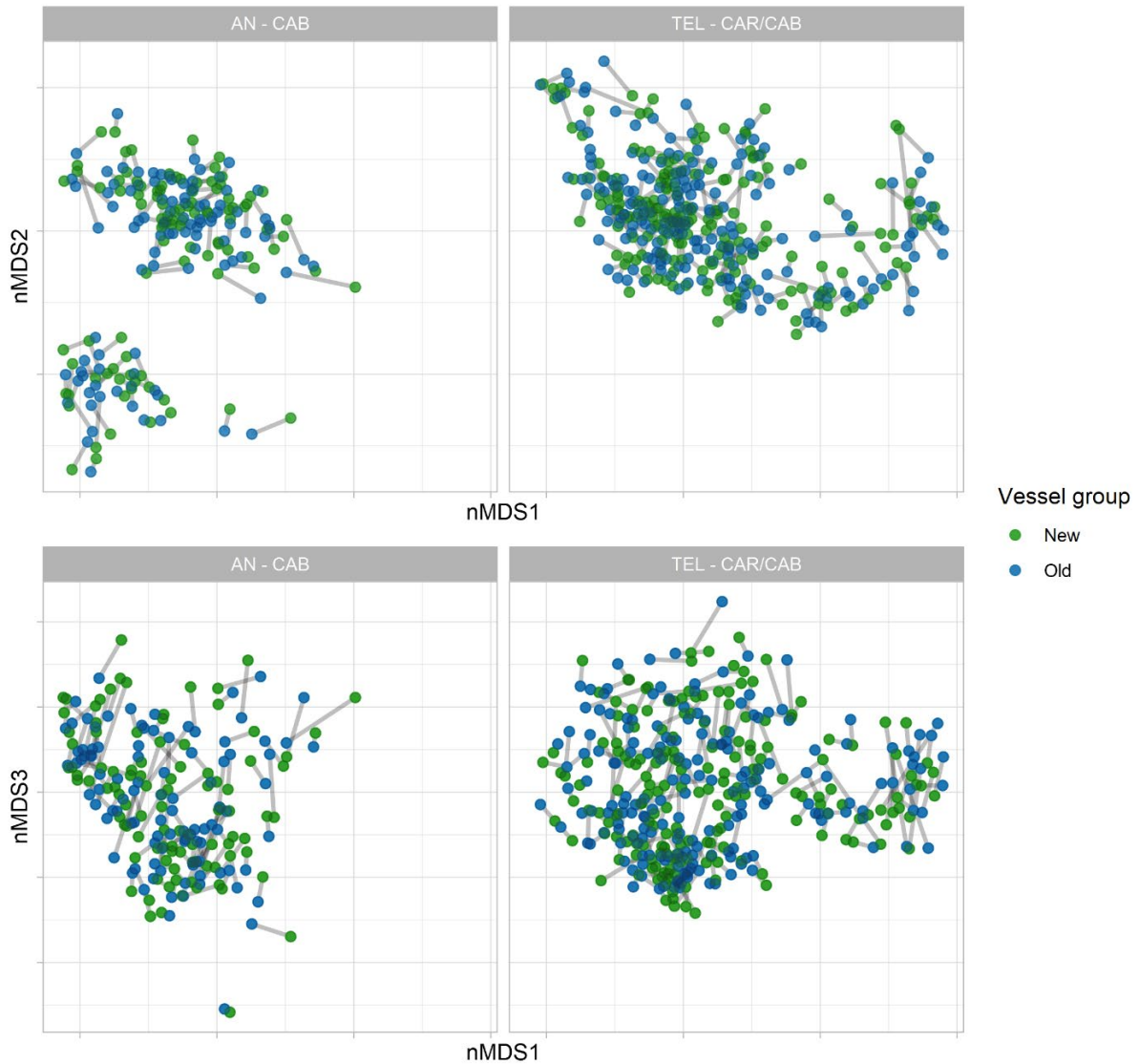


Figure A3–5. nMDS of fish community with all fish and commercial invertebrate species. Color of the dots represents vessel group and grey line connecting the paired sets. CCGS Alfred Needler & CCGS John Cabot pairs on left and CCGS Teleost & CCGS John Cabot/Capt. Jacques Cartier pairs on right. Top panel is the first two dimensions and bottom panels the first and third dimensions.

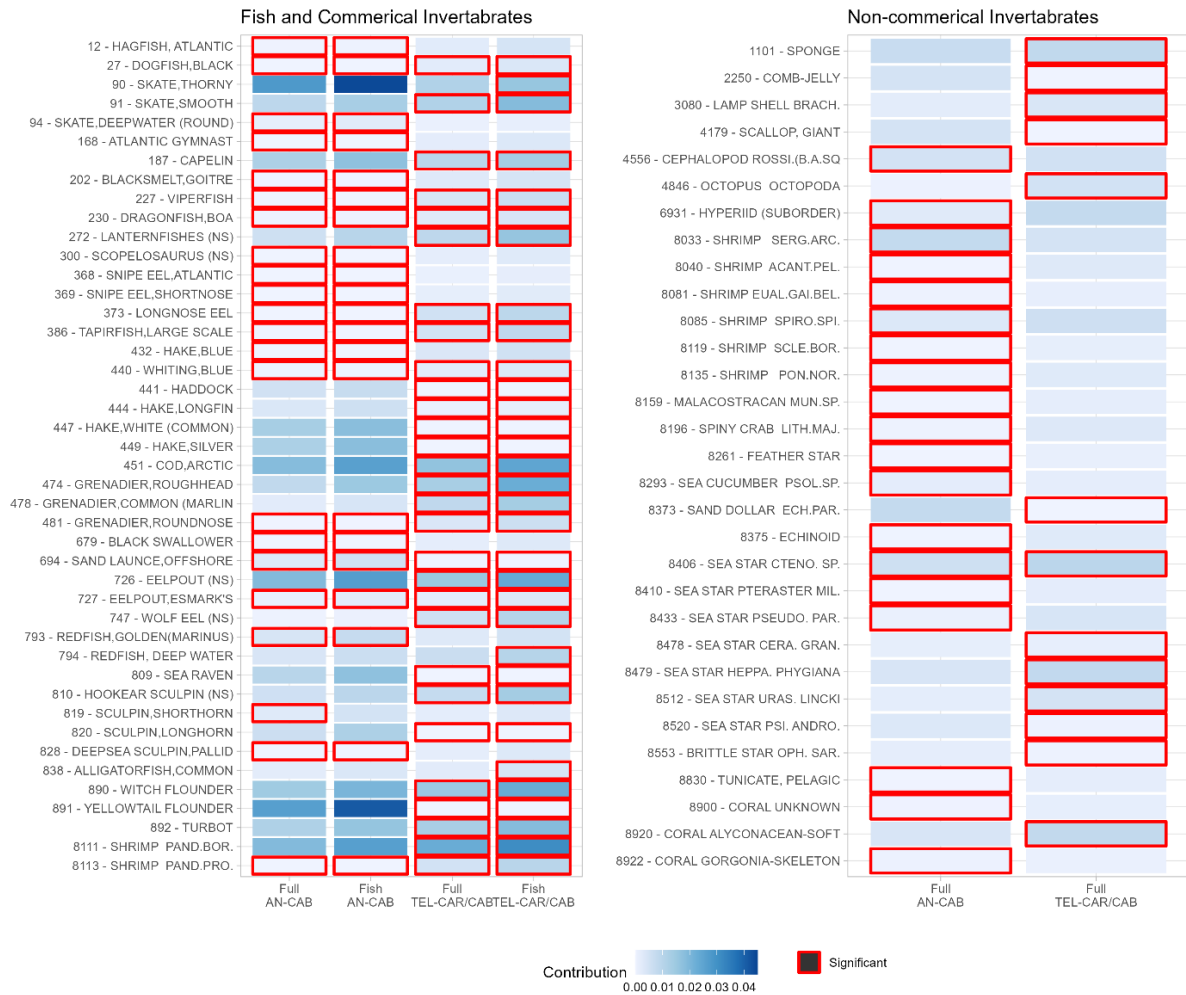


Figure A3–6. Contribution of species to distance matrix based on SIMPER analysis (intensity of color) with significant differences between old and new vessels highlighted in red. Only species that are significant in at least one comparison are presented.

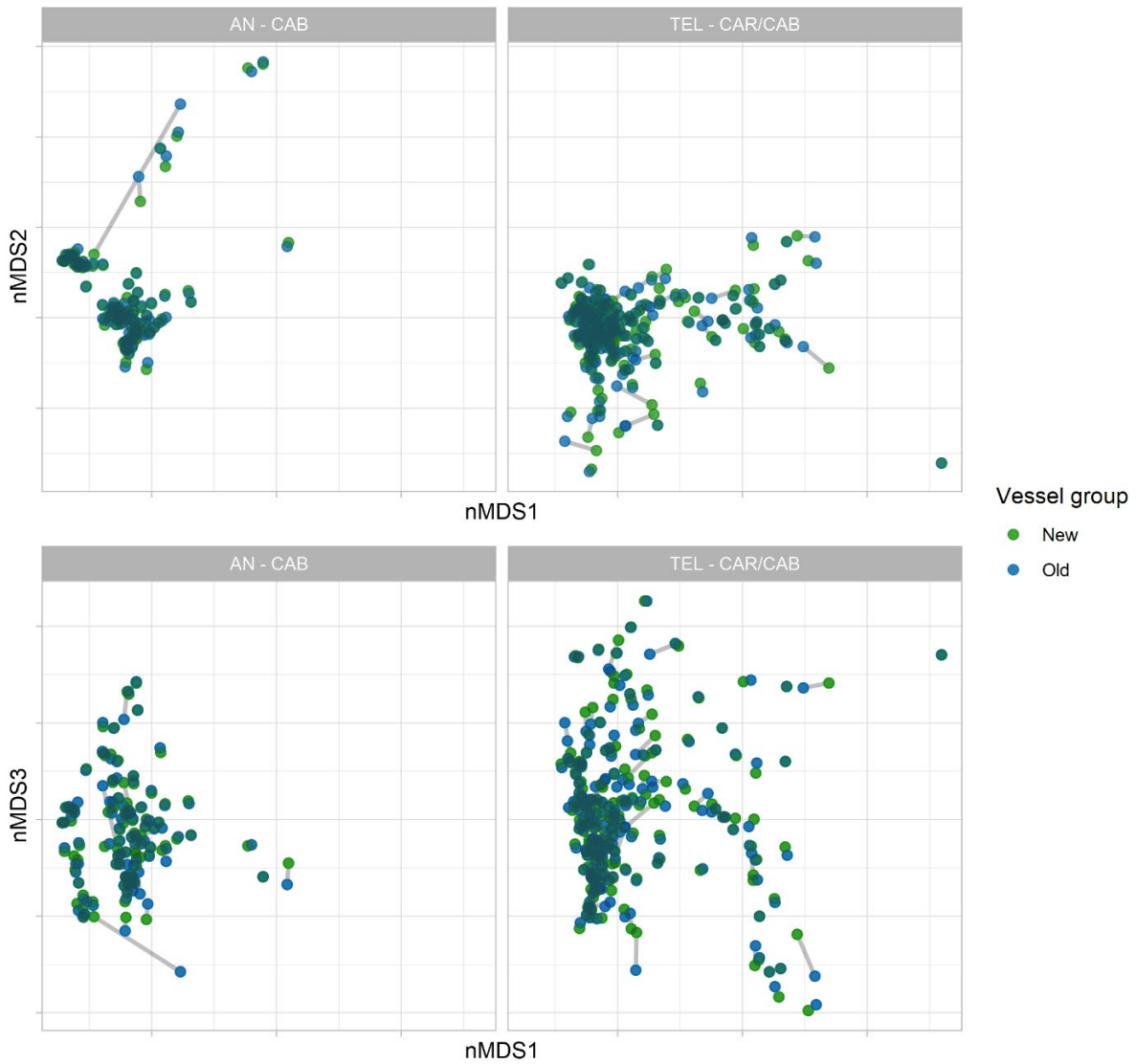


Figure A3–7. nMDS benthic habitat variables (with substrate type removed) for all sets. Color of the dots represents vessel group and grey line connecting the paired sets. CCGS Alfred Needler & CCGS John Cabot pairs on left and CCGS Teleost & CCGS John Cabot/Capt. Jacques Cartier pairs on right. Top panel is the first two dimensions and bottom panels the first and third dimensions.



Figure A3–8. nMDS benthic habitat variables with sets with missing substrate type removed (left) and with substrate type variables removed (right) for all CCGS Teleost & CCGS John Cabot/Capt. Jacques Cartier. Color of the dots represents year. Top panel is the first two dimensions and bottom panels the first and third dimensions.

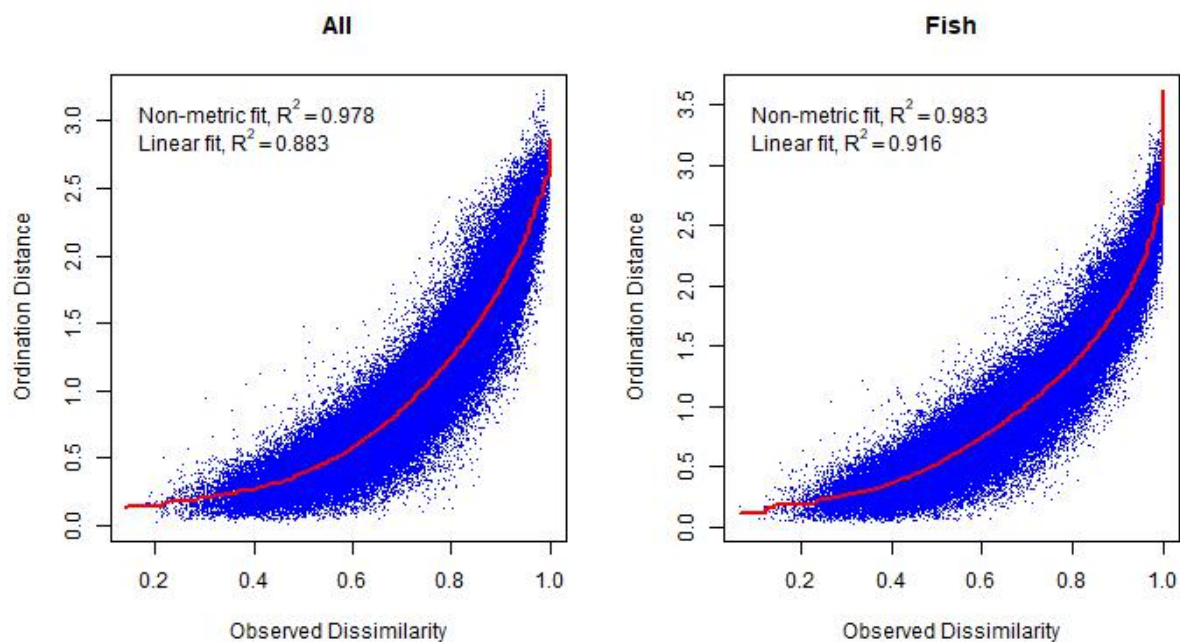


Figure A3–9. Sheppard stress plots for nMDS analysis of community with all species included (All) and just finfish and commercial shellfish (Fish).

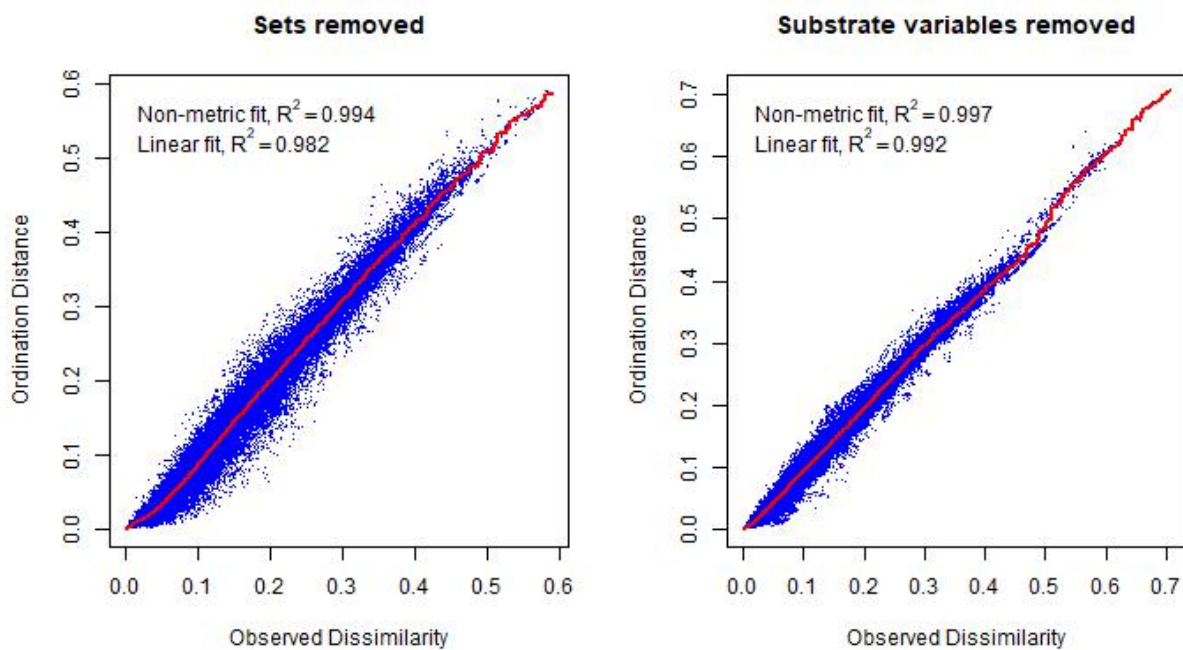


Figure A3–10. Sheppard stress plots for nMDS analysis of benthic habitat variables with sets that have missing data removed (sets removed) and benthic substrate variables removed (substrate variables removed).



Figure A3–11. nMDS benthic and oceanographic variables for sets that have substrate type data available. Color of the dots represents vessel group and grey line connecting the paired sets. CCGS Alfred Needler & CCGS John Cabot pairs on left and CCGS Teleost & CCGS John Cabot/Capt. Jacques Cartier pairs on right. Top panel is the first two dimensions and bottom panels the first and third dimensions.

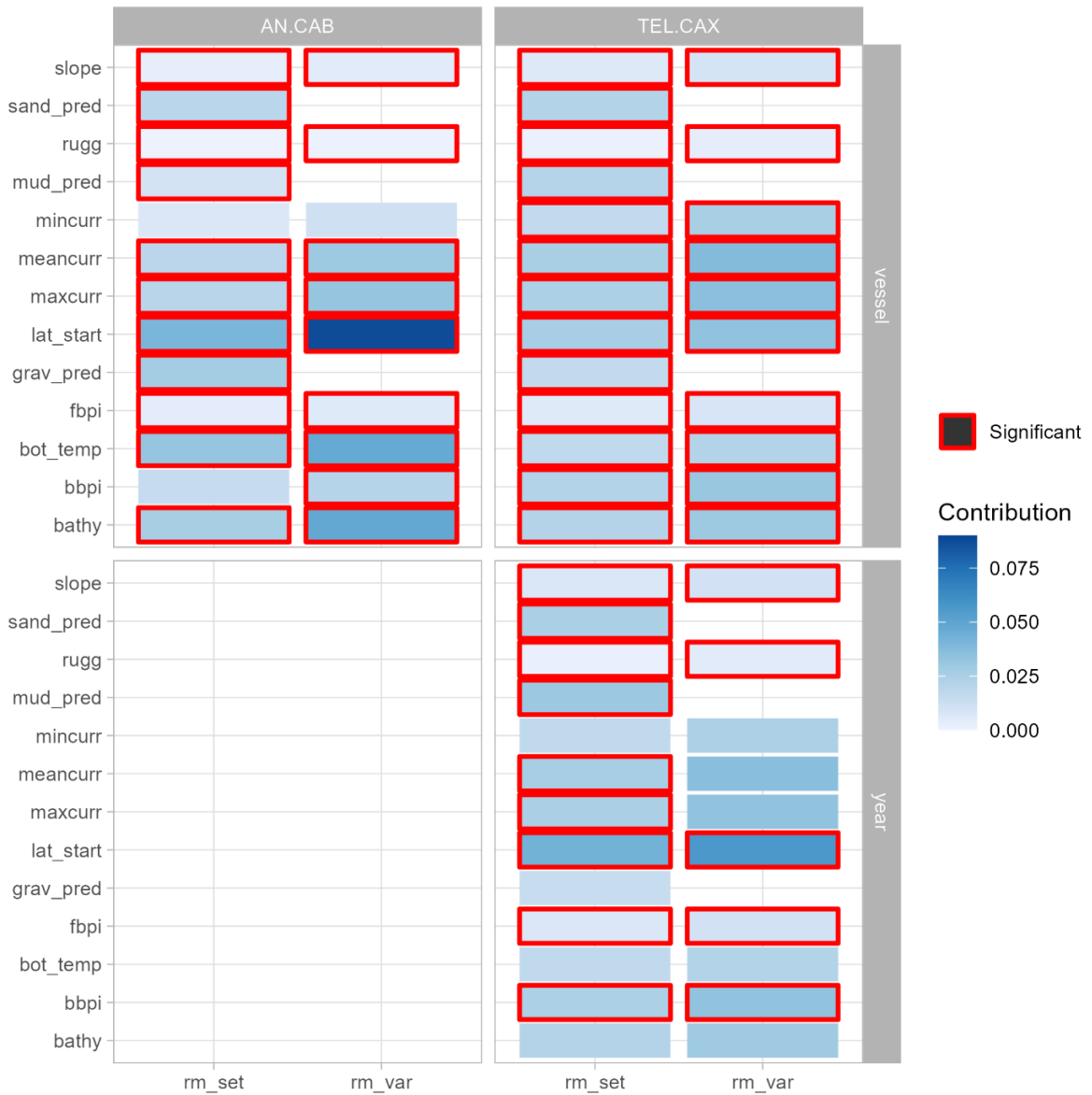


Figure A3–12. SIMPER results from all analysis for benthic habitat variables.

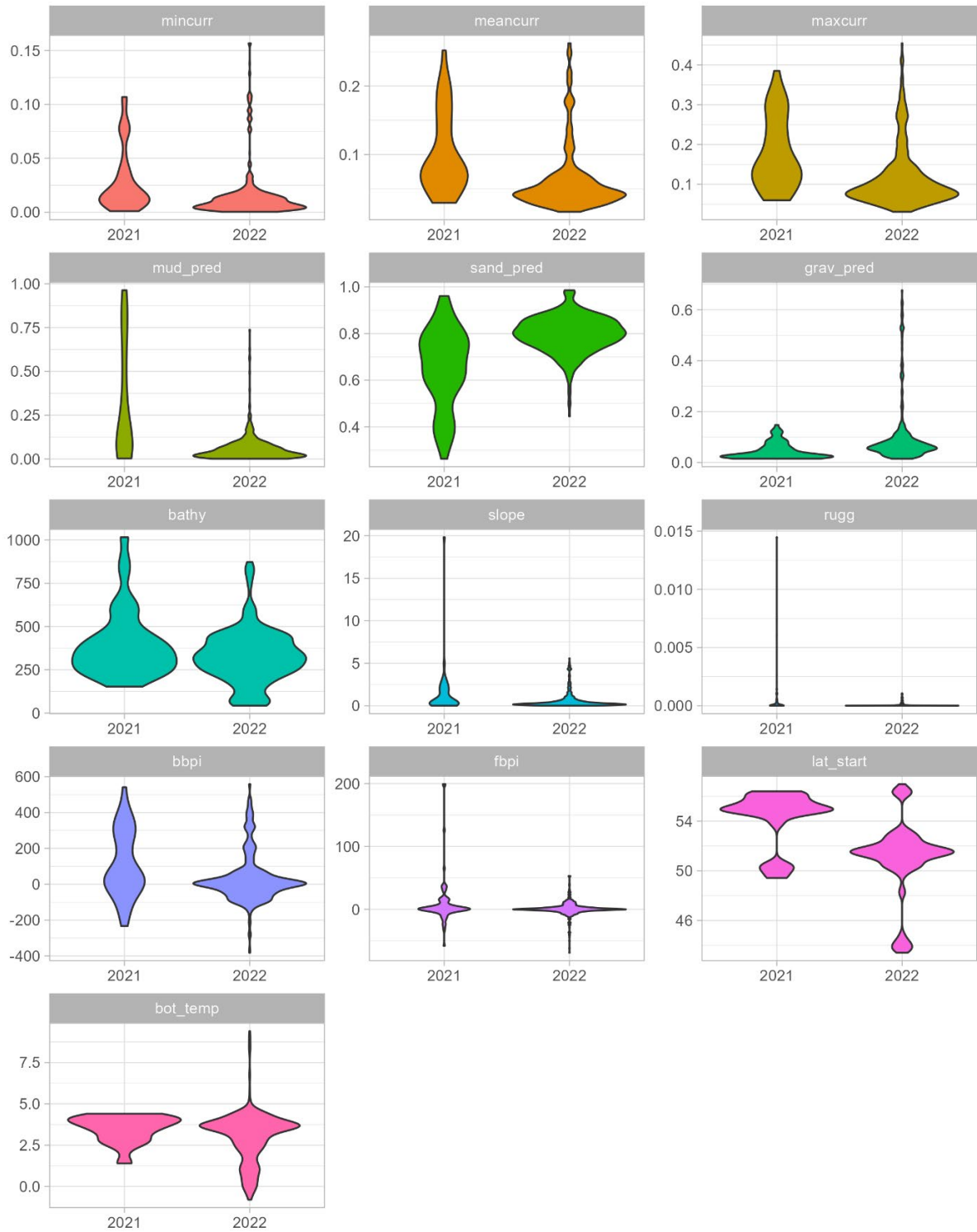


Figure A3–13. Distribution of benthic habitat variables in 2021 vs 2022 paired sets between CCGS Teleost and CCGS John Cabot/Capt. Jacques Cartier.